

World Journal of *Gastroenterology*

World J Gastroenterol 2018 April 28; 24(16): 1679-1824



REVIEW

- 1679 Beneficial effects of naringenin in liver diseases: Molecular mechanisms
Hernández-Aquino E, Muriel P
- 1708 Naturally occurring hepatitis B virus reverse transcriptase mutations related to potential antiviral drug resistance and liver disease progression
Choi YM, Lee SY, Kim BJ

MINIREVIEWS

- 1725 Nucleotide-binding oligomerization domain 1 and *Helicobacter pylori* infection: A review
Minaga K, Watanabe T, Kamata K, Asano N, Kudo M
- 1734 Diversion colitis and pouchitis: A mini-review
Tominaga K, Kamimura K, Takahashi K, Yokoyama J, Yamagiwa S, Terai S

ORIGINAL ARTICLE**Basic Study**

- 1748 Nonalcoholic steatohepatitis severity is defined by a failure in compensatory antioxidant capacity in the setting of mitochondrial dysfunction
Boland ML, Oldham S, Boland BB, Will S, Lapointe JM, Guionaud S, Rhodes CJ, Trevaskis JL
- 1766 Mucosa repair mechanisms of Tong-Xie-Yao-Fang mediated by CRH-R2 in murine, dextran sulfate sodium-induced colitis
Gong SS, Fan YH, Wang SY, Han QQ, Lv B, Xu Y, Chen X, He YE
- 1779 Sodium chloride exacerbates dextran sulfate sodium-induced colitis by tuning proinflammatory and antiinflammatory lamina propria mononuclear cells through p38/MAPK pathway in mice
Guo HX, Ye N, Yan P, Qiu MY, Zhang J, Shen ZG, He HY, Tian ZQ, Li HL, Li JT

Retrospective Cohort Study

- 1795 High tacrolimus intra-patient variability is associated with graft rejection, and *de novo* donor-specific antibodies occurrence after liver transplantation
Del Bello A, Congy-Jolivet N, Danjoux M, Muscari F, Lavayssière L, Esposito L, Hebral AL, Bellière J, Kamar N

Randomized Clinical Trial

- 1803 Papillary fistulotomy *vs* conventional cannulation for endoscopic biliary access: A prospective randomized trial
Furiya CK, Sakai P, Marinho FR, Otoch JP, Cheng S, Prudencio LL, de Moura EG, Artifon EL

META-ANALYSIS

- 1812 Compared efficacy of preservation solutions on the outcome of liver transplantation: Meta-analysis
Szilágyi ÁL, Mátrai P, Hegyi P, Tuboly E, Pécz D, Garami A, Solymár M, Pétervári E, Balaskó M, Veres G, Czopf L, Wobbe B, Szabó D, Wagner J, Hartmann P

Contents

World Journal of Gastroenterology

Volume 24 Number 16 April 28, 2018

ABOUT COVER

Editorial board member of *World Journal of Gastroenterology*, Shu-You Peng, FRCS (Gen Surg), FRCS (Hon), MD, Professor, Surgeon, General Surgery, The Second Affiliated Hospital, College of Medicine, Zhejiang University, Hangzhou 310009, Zhejiang Province, China

AIMS AND SCOPE

World Journal of Gastroenterology (*World J Gastroenterol*, *WJG*, print ISSN 1007-9327, online ISSN 2219-2840, DOI: 10.3748) is a peer-reviewed open access journal. *WJG* was established on October 1, 1995. It is published weekly on the 7th, 14th, 21st, and 28th each month. The *WJG* Editorial Board consists of 642 experts in gastroenterology and hepatology from 59 countries.

The primary task of *WJG* is to rapidly publish high-quality original articles, reviews, and commentaries in the fields of gastroenterology, hepatology, gastrointestinal endoscopy, gastrointestinal surgery, hepatobiliary surgery, gastrointestinal oncology, gastrointestinal radiation oncology, gastrointestinal imaging, gastrointestinal interventional therapy, gastrointestinal infectious diseases, gastrointestinal pharmacology, gastrointestinal pathophysiology, gastrointestinal pathology, evidence-based medicine in gastroenterology, pancreatology, gastrointestinal laboratory medicine, gastrointestinal molecular biology, gastrointestinal immunology, gastrointestinal microbiology, gastrointestinal genetics, gastrointestinal translational medicine, gastrointestinal diagnostics, and gastrointestinal therapeutics. *WJG* is dedicated to become an influential and prestigious journal in gastroenterology and hepatology, to promote the development of above disciplines, and to improve the diagnostic and therapeutic skill and expertise of clinicians.

INDEXING/ABSTRACTING

World Journal of Gastroenterology (*WJG*) is now indexed in Current Contents®/Clinical Medicine, Science Citation Index Expanded (also known as SciSearch®), Journal Citation Reports®, Index Medicus, MEDLINE, PubMed, PubMed Central and Directory of Open Access Journals. The 2017 edition of Journal Citation Reports® cites the 2016 impact factor for *WJG* as 3.365 (5-year impact factor: 3.176), ranking *WJG* as 29th among 79 journals in gastroenterology and hepatology (quartile in category Q2).

EDITORS FOR THIS ISSUE

Responsible Assistant Editor: Xiang Li
Responsible Electronic Editor: Yan Huang
Proofing Editor-in-Chief: Lian-Sheng Ma

Responsible Science Editor: Xue-Jiao Wang
Proofing Editorial Office Director: Ze-Mao Gong

NAME OF JOURNAL
World Journal of Gastroenterology

CA 90822, United States

PUBLICATION DATE

April 28, 2018

ISSN
ISSN 1007-9327 (print)
ISSN 2219-2840 (online)

EDITORIAL BOARD MEMBERS
All editorial board members resources online at <http://www.wjgnet.com/1007-9327/editorialboard.htm>

COPYRIGHT

© 2018 Baishideng Publishing Group Inc. Articles published by this Open-Access journal are distributed under the terms of the Creative Commons Attribution Non-commercial License, which permits use, distribution, and reproduction in any medium, provided the original work is properly cited, the use is non commercial and is otherwise in compliance with the license.

LAUNCH DATE
October 1, 1995

EDITORIAL OFFICE

SPECIAL STATEMENT

All articles published in journals owned by the Baishideng Publishing Group (BPG) represent the views and opinions of their authors, and not the views, opinions or policies of the BPG, except where otherwise explicitly indicated.

FREQUENCY

Weekly

Ze-Mao Gong, Director

INSTRUCTIONS TO AUTHORS

EDITORS-IN-CHIEF
Damian Garcia-Olmo, MD, PhD, Doctor, Professor, Surgeon, Department of Surgery, Universidad Autonoma de Madrid; Department of General Surgery, Fundacion Jimenez Diaz University Hospital, Madrid 28040, Spain

World Journal of Gastroenterology
Baishideng Publishing Group Inc
7901 Stoneridge Drive, Suite 501,
Pleasanton, CA 94588, USA
Telephone: +1-925-2238242
Fax: +1-925-2238243
E-mail: editorialoffice@wjgnet.com
Help Desk: <http://www.f6publishing.com/helpdesk>
<http://www.wjgnet.com>

Full instructions are available online at <http://www.wjgnet.com/bpg/gerinfo/204>

Stephen C Strom, PhD, Professor, Department of Laboratory Medicine, Division of Pathology, Karolinska Institutet, Stockholm 141-86, Sweden

PUBLISHER
Baishideng Publishing Group Inc
7901 Stoneridge Drive, Suite 501,
Pleasanton, CA 94588, USA
Telephone: +1-925-2238242
Fax: +1-925-2238243
E-mail: bpgoffice@wjgnet.com
Help Desk: <http://www.f6publishing.com/helpdesk>
<http://www.wjgnet.com>

ONLINE SUBMISSION
<http://www.f6publishing.com>



Beneficial effects of naringenin in liver diseases: Molecular mechanisms

Erika Hernández-Aquino, Pablo Muriel

Erika Hernández-Aquino, Pablo Muriel, Laboratory of Experimental Hepatology, Department of Pharmacology, Cinvestav-IPN, Mexico City 07000, Mexico

ORCID number: Erika Hernández-Aquino (0000-0003-4783-4240); Pablo Muriel (0000-0002-2236-6631).

Author contributions: All authors equally contributed to this paper with the conception and design of the study, the literature review and analysis, the drafting and critical revision and editing of the manuscript, and with their final approval of the final version.

Supported by National Council of Science and Technology (Conacyt) of Mexico, No. 253037.

Conflict-of-interest statement: The authors declare no conflicts of interest.

Open-Access: This article is an open-access article which was selected by an in-house editor and fully peer-reviewed by external reviewers. It is distributed in accordance with the Creative Commons Attribution Non Commercial (CC BY-NC 4.0) license, which permits others to distribute, remix, adapt, build upon this work non-commercially, and license their derivative works on different terms, provided the original work is properly cited and the use is non-commercial. See: <http://creativecommons.org/licenses/by-nc/4.0/>

Manuscript source: Invited manuscript

Correspondence to: Pablo Muriel, PhD, Research Scientist, Laboratory of Experimental Hepatology, Department of Pharmacology, Cinvestav-IPN, Av. Instituto Politécnico Nacional 2508, Apartado postal 14-740, Mexico City 07000, Mexico. pmuriel@cinvestav.mx

Telephone: +52-55-57473303
Fax: +52-55-57473394

Received: March 7, 2018

Peer-review started: March 8, 2018

First decision: March 29, 2018

Revised: April 4, 2018

Accepted: April 16, 2018

Article in press: April 16, 2018

Published online: April 28, 2018

Abstract

Liver diseases are caused by different etiological agents, mainly alcohol consumption, viruses, drug intoxication or malnutrition. Frequently, liver diseases are initiated by oxidative stress and inflammation that lead to the excessive production of extracellular matrix (ECM), followed by a progression to fibrosis, cirrhosis and hepatocellular carcinoma (HCC). It has been reported that some natural products display hepatoprotective properties. Naringenin is a flavonoid with antioxidant, antifibrogenic, anti-inflammatory and anticancer properties that is capable of preventing liver damage caused by different agents. The main protective effects of naringenin in liver diseases are the inhibition of oxidative stress, transforming growth factor (TGF- β) pathway and the prevention of the transdifferentiation of hepatic stellate cells (HSC), leading to decreased collagen synthesis. Other effects include the inhibition of the mitogen activated protein kinase (MAPK), toll-like receptor (TLR) and TGF- β non-canonical pathways, the inhibition of which further results in a strong reduction in ECM synthesis and deposition. In addition, naringenin has shown beneficial effects on nonalcoholic fatty liver disease (NAFLD) through the regulation of lipid metabolism, modulating the synthesis and oxidation of lipids and cholesterol. Moreover, naringenin protects from HCC, since it inhibits growth factors such as TGF- β and vascular endothelial growth factor (VEGF), inducing apoptosis and regulating MAPK pathways. Naringenin is safe and acts by targeting multiple proteins. However, it possesses low bioavailability and high intestinal metabolism. In this regard, formulations, such as nanoparticles or liposomes, have been developed to improve naringenin bioavailability. We conclude that naringenin should be considered in the future as an important candidate in the treatment of different liver

diseases.

Key words: Naringenin; Transforming growth factor; Liver; Fibrosis; MAPKs; CCl₄; Flavonoids; JNK; Hepatic stellate cells; Cirrhosis; Smads; α -SMA

© The Author(s) 2018. Published by Baishideng Publishing Group Inc. All rights reserved.

Core tip: Natural products such as flavonoids have been shown to display hepatoprotective properties. Naringenin possesses the ability to inhibit oxidative stress and inflammation and has anti-inflammatory and anticancer properties. Thus, naringenin should be considered in the future as an important candidate for the treatment of liver diseases.

Hernández-Aquino E, Muriel P. Beneficial effects of naringenin in liver diseases: Molecular mechanisms. *World J Gastroenterol* 2018; 24(16): 1679-1707 Available from: URL: <http://www.wjgnet.com/1007-9327/full/v24/i16/1679.htm> DOI: <http://dx.doi.org/10.3748/wjg.v24.i16.1679>

INTRODUCTION

Liver damage can be caused by alcohol intake, heavy metal intoxication, hepatitis virus infection, obstruction of the biliary tract or malnutrition. Chronic hepatic injury results in organ fibrosis characterized by an imbalance between the synthesis and degradation of extracellular matrix (ECM) derived from oxidative stress and inflammation during liver damage. After fibrosis, cirrhosis develops with tissue scars, the loss of parenchymal architecture, the disruption of hepatic blood flow and organ failure^[1,2]. The main causes of fibrosis globally are NAFLD (40%), hepatitis B virus (HBV) (30%), hepatitis C virus (HCV) (15%), and harmful alcohol consumption (11%)^[3]. The prevalence of cirrhosis is increasing; in 2010, 33% more people died from cirrhosis than in 1990^[4].

While the elimination of the causative agent may be the best option for some cirrhotic patients, in most cases, medical intervention is required. Therefore, pharmacological strategies should be developed to prevent or reverse hepatic damage. Researchers have developed multiple therapeutic strategies to combat this disease, including transforming growth factor- β (TGF- β) inhibitors^[5], antivirals^[6], cell-based therapies^[7], nanoparticles^[8], and natural products^[9-15].

Liver transplantation is an interesting option; unfortunately, the lack of sufficient donors and organ rejection restrict this surgical procedure. In recent years, the investigation on hepatoprotective properties of natural products has increased. Due to their molecular structure, many of them possess antioxidant properties and display anti-inflammatory and anticancer properties and are generally considered safe for human consumption. Among

the most studied natural compounds are silymarin, quercetin, and curcumin^[10,12,14], but recently, a flavonoid with very specific hepatoprotective properties has emerged: naringenin.

Naringenin has been studied in various *in vivo* and *in vitro* liver damage models, using hepatic damage agents such as carbon tetrachloride (CCl₄), alcohol, N-methyl-N-nitro-Nitroguanidine, lipopolysaccharide (LPS), and heavy metals, among others, displaying a good hepatoprotective activity due to its antioxidant capacity as well as its ability to inhibit inflammatory and profibrotic signaling pathways. However, despite the importance of naringenin in liver diseases, there is no detailed review of the effects of naringenin on hepatic pathologies.

Therefore, our objective was to document the effects of naringenin on liver diseases and to highlight the importance of this flavonoid in the therapeutic of pathologies of this organ.

LITERATURE SEARCH

A systematic literature search was conducted using PubMed, Scopus and EMBASE.

ABSORPTION, METABOLISM AND DISTRIBUTION OF NARINGENIN

Naringenin (4',5,7-trihydroxy flavanone) is a flavonoid, specifically a flavanone, and is the aglycone of naringin (naringenin-7-rhamnoglucoside)^[16]; naringenin can also be found as narirutin (naringenin- 7-O-rutinoside) or naringenin-glucoside (naringenin-7-O-glucoside), depending on the sugar motive (Figure 1)^[11].

This review is focused on the effects of naringenin (aglycone); the reader interested in glycosylated molecules is referred to another review^[11]. Because naringenin is found mostly in citrus fruits, natural intake occurs orally. Due to its chemical structure, naringenin is very lipophilic; thus, it is readily absorbed through the intestinal epithelium by passive diffusion into enterocytes. Once inside the intestinal cells, it can enter the general circulation by multidrug resistance-associated proteins (Mrp1) or can be transported by active efflux protein carriers P-glycoprotein (P-gp) and Mrp2 back to the intestinal lumen, out of the enterocytes, repeating the cycle^[17] (Figure 2).

On the other hand, small intestine, colonic epithelium, and liver metabolize naringenin *via* phase II conjugation by UDP-glucuronosyl transferase (UGT), sulfotransferase, and catechol-O-methyltransferase^[18-20]. Naringenin-glucuronides leave the cells by Mrp2 protein or pass into blood *via* breast cancer-resistant protein (Bcrp1)^[21]. Moreover, naringenin can be cleaved by β -glucuronidases (GUSB) located in tissues and liver^[22]. This deconjugation results in release of the aglycone, which in turn can be absorbed by passive transcellular diffusion or undergo efflux by Mrp2 and P-gp^[19]. Then,

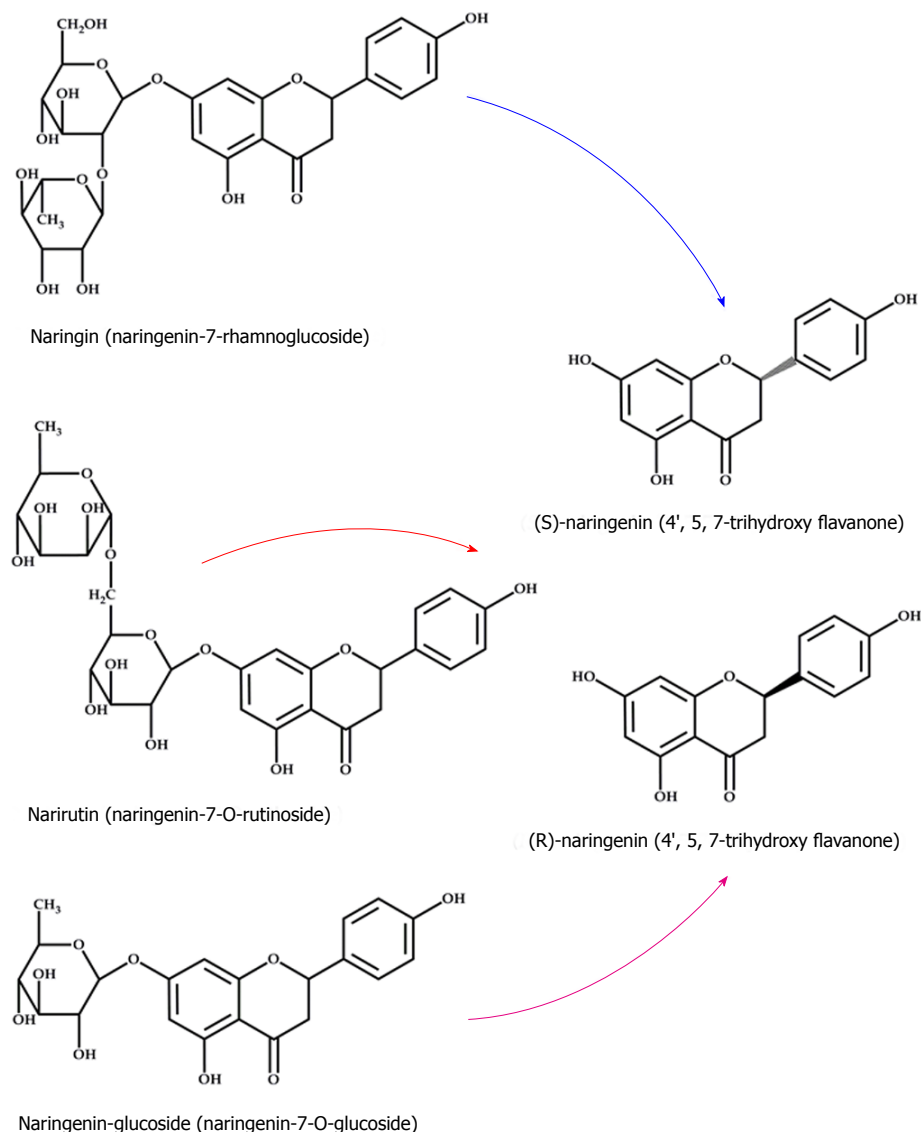


Figure 1 Chemical structure of naringenin, naringin, narirutin, and naringenin-glucoside. The flavonoid naringenin exists in two forms: Glycosylated (naringin, narirutin and naringenin-glucoside) and aglycone (naringenina). There are three types of naringenin glycosides depending of sugar moiety bound to the flavonoid: Naringin (rhamnose), narirutin (rutinose) and naringenin-glucoside (glucose); when the sugar moiety is cleaved by specific enzymes, the aglycone (naringenin) is released.

naringenin is metabolized in the lower intestine by *Streptococcus S-2*, *Lactobacillus L-2*, and *Bacteroides JY-6* to generate a series of low molecular weight aromatic acids^[11] (Figure 2).

With respect to naringenin distribution, it has been found in the stomach, small intestine, liver, kidney, trachea, lung, heart, fat, muscle, testis, ovary, spleen, brain, and urine^[20,23-25]. Furthermore, naringenin and its metabolites are bound to plasma proteins such as albumin^[26-28].

ANTIOXIDANT EFFECTS OF NARINGENIN, BEYOND THE STRUCTURE ACTIVITY RELATIONSHIP

Normally, flavonoid antioxidant activity has been attributed to the structure-activity relationship of flavonoids.

However, in addition to a direct antioxidant property by free radical scavenging activity, naringenin possesses the ability to induce the endogenous antioxidant system.

Classically, naringenin's antioxidant effect is due to its hydroxyl substituents (OH), which have high reactivity against reactive oxygen species (ROS) and reactive nitrogen species (RNS). In general, the antioxidant capacity of a given molecule increases in function with the number of OH radicals in the molecule, which, in the case of naringenin, is 3. Then, OH can donate its H to free radicals (R^{\bullet}), and later, naringenin can be stabilized by resonance^[29,30] (Figure 3). Within the typical structure of flavonoids, the B ring is very important because when OH groups are in the ring, flavonoids can stabilize hydroxyl (OH^{\bullet}), peroxy (ROO $^{\bullet}$), and peroxynitrite (ONOO $^{\bullet}$) radicals, producing a relatively stable flavonoid radical. On the other hand, 5-OH substitution and a 5,7-m-dihydroxy arrangement

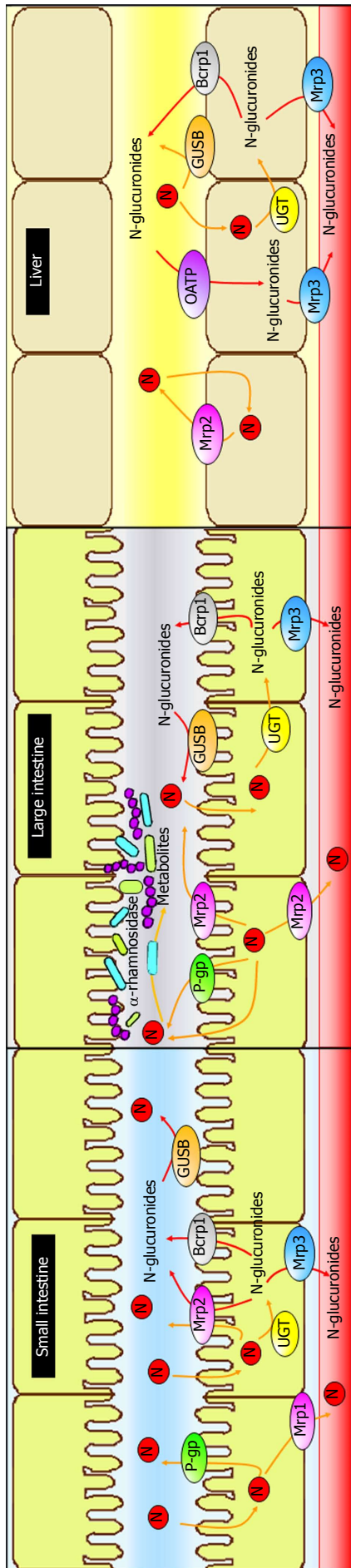


Figure 2 Absorption and metabolism of naringenin. Small intestine: Naringenin (N, orange arrows) is absorbed through the intestinal epithelium by passive diffusion into enterocytes; then, it can pass to general circulation by multidrug resistance associated proteins (Mrp1) or transported by active efflux protein carriers P-glycoprotein (P-gp) and Mfp2, back to the intestinal lumen, out of the enterocytes. Inside the enterocyte, naringenin is glucuronized by UDP-glucuronidases (GUSB), and after that, naringenin-glucuronides (red arrows) leave cells by Mrp2 protein or pass into blood via breast cancer-resistant protein (Bcrp1). Moreover, naringenin-glucuronides can be cleaved by β-glucuronidases (UGT), resulting in release of the aglycone. Large intestine: Naringenin undergoes same processes as in small intestine but also is highly metabolized by *Streptococcus S-2*, *Lactobacillus L-2*, and *Bacteroides JY-6* to generate a series of low molecular weight aromatic acids. Liver: Naringenin is highly conjugated to form naringenin-glucuronides, which allows it to pass into circulation. On the other hand, naringenin-glucuronides reach the liver from intestine and enter into hepatocytes via organic anion transporting protein-B (OATP), and then, they are transported by Mrp3 into the circulation.

in the A-ring is an important feature of naringenin that makes it an antioxidant and, at the same time, serves to stabilize the structure after donating H to the R[•]. Finally, the association between 5-OH and 4-oxo substituents contributes to the ability of naringenin to chelate compounds such as heavy metals^[29] (Figure 3).

An important phenomenon during liver damage is lipid peroxidation (LP); it can be defined as the abstraction of hydrogen from fatty acid that initiates a complex series of reactions that terminate in the complete disintegration of the polyunsaturated fatty acid (PUFA) molecules with the formation of aldehydes, such as malondialdehyde (MDA), other carbonyls, and alkanes. Liver: Naringenin is highly conjugated to form naringenin-glucuronides, which almost completely inhibits LP at the same dose. In this same study, a modest effect of naringenin (25 μmol/L) against LP induced by deleterious effects of LP^[31].

Naringenin trolox equivalent antioxidant activity is 1.53 mmol/L, which is a small value compared with that of quercetin, which is 4.7 mmol/L^[30]. In a model of nonenzymatic LP induction by ascorbic acid, naringenin showed 21%-44% inhibition of MDA formation in a dose-dependent manner; however, quercetin was able to prevent 70%-85% of the MDA formation at doses from 0.1 mmol/L to 4.0 mmol/L^[32]. During a di(phenyl)-(2,4,6-trinitrophenyl) iminoazanium (DPPH) assay, naringenin had an ID₅₀ of 225 μmol/L at 2 h, and the number of molecules of DPPH scavenged/naringenin molecule was 0.5, while the ID₅₀ of quercetin was 12.5 μmol/L of DPPH scavenged/quercetin molecule. In addition, naringenin showed a lower effect than quercetin in an LP model in liver and lung with an ID₅₀ of more than 1000 μmol/L and 35 μmol/L, respectively^[33]. Moreover, naringenin's effect on LP induced by iron-ascorbate in hepatic microsomes revealed that naringenin (5 μmol/L and 25 μmol/L) increases LP, unlike quercetin, which almost completely inhibited LP at the same dose. In this same study, a modest effect of naringenin (25 μmol/L) against LP induced by Fe³⁺-ADP/NADPH or TBH assay was observed. In contrast, naringenin strongly protected hepatocytes from TBH-cytotoxicity, suggesting that naringenin did not exert its cytoprotective effects through purely direct antioxidant mechanisms^[34].

Although several reports show that naringenin displays poor antioxidant capacity compared to other flavonoids such as quercetin, the results obtained in the 2,2'-azinobis-(3-ethylbenzothiazoline-6-sulfonic acid (ABTS) assay showed that naringenin had an IC₅₀ of 7.9 μmol/L, and when the determination of superoxide radical (O²) scavenger activity was performed by the nitro blue tetrazolium (NBT) method and the Xanthine oxidase/cytochrome c (CYPc) method, naringenin had an IC₅₀ of 94.7 and 4.4 μmol/L, respectively. Moreover, naringenin had an IC₅₀ of 1.06 and 1.55 μmol/L with EDTA and without EDTA on OH[•] scavenger activity, respectively; in addition, the IC₅₀

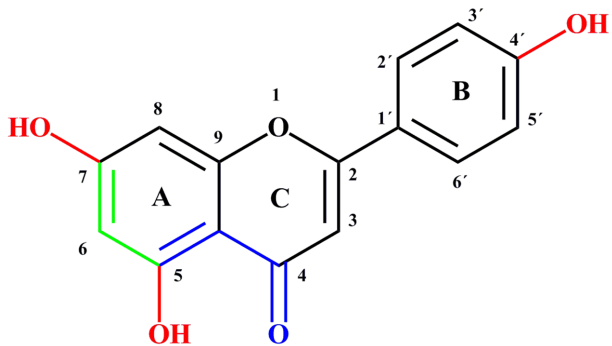


Figure 3 Naringenin antioxidant activity-structure relationship. In red: Hydroxyl substituents (OH) that have high reactivity against reactive oxygen species and reactive nitrogen species. In green: 5,7-*m*-dihydroxy arrangement in the A-ring serves to stabilize the structure after donating electrons to free radicals. In blue: The association between 5-OH and 4-oxo substituents contributes to the chelation of compounds such as heavy metals.

of naringenin on liver LP in the presence of HO[•] or OH[−] was 1.21 and 0.23 mmol/L, respectively^[35].

As seen, the antioxidant effect of naringenin can be considered ambiguous, and it may depend on the radical formed and the model used and the flavonoid concentration. Even though naringenin has fewer antioxidant functional groups than quercetin, it shows other properties due to its structure-activity relationship, as it has been reported that naringenin is able to accumulate in cell membranes^[36] and biomembranes^[37,38]. Interaction with membranes is favored because flavonoids form reversible bonds with the polar heads of the phospholipids^[39], and this interaction may be possible due to naringenin's solubility, since it is highly lipophilic because of its structure (Figure 4).

Interestingly, it has been shown that naringenin decreases membrane fluidity. Membrane fluidity is the relative motional freedom of the lipid molecules in the membrane bilayer, and naringenin accumulates in the membrane hydrophobic core, where it modifies lipid packing order leading to decreased membrane fluidity in a concentration-dependent manner. Therefore, by increasing the rigidity of membranes, naringenin can reduce the interaction between R[•] and lipids; as a result, LP may be attenuated^[38]. In conclusion, in addition to its antioxidant capacity, naringenin can block LP by reducing membrane fluidity^[40] (Figure 4).

Although antioxidant assays are important, *in vitro* and *in vivo* model systems offer much more information since normal functions of a complete system are preserved. Either by its antioxidant activity or by protection of lipid membranes, naringenin offers protection against ROS and other R[•] in *in vitro* and *in vivo* models. Naringenin protects against ROS in a model of neuronal damage, since it reduces their levels in neurons and decreases mitochondrial dysfunction and increases mitochondrial membrane potential^[41]. In addition, naringenin inhibits K⁺O₂-induced oxidative stress in a pain model in mice by inhibiting LP and O₂[•] production^[42]. On the other hand, naringenin exerts

antioxidant effects against paraquat-induced toxicity in human bronchial epithelial cells, since it decreases intracellular ROS generation^[43]. Moreover, this flavanone significantly decreased thiobarbituric acid reactive substances (TBARS) and improved membrane phospholipid composition in favor of n-3 PUFAs and the n-6/n-3 PUFAs ratio in the liver of old-aged Wistar rats^[44].

Naringenin has shown the ability of combating LP in many organs, tissues and cells, for example, in lung^[45], ankle joints (arthritis model)^[46], retina of streptozotocin-induced diabetic rats^[47], SH-SY5Y cells^[48], cardiomyoblast cells^[49], skin^[50], testis^[51] and, interestingly, in liver^[44,52,53]. It can be concluded that, in contrast to the results obtained in chemical antioxidant assays, the beneficial effects of naringenin against LP in systems involving living organisms or cells, the flavanone shows strong activity. This characteristic is very important for the treatment of hepatic diseases, since LP constitutes one of the main causative agents that triggers liver damage.

In the studies where a reduction in LP by naringenin was demonstrated, a relationship between reduced glutathione (GSH) and flavonoid levels is observed. In fact, it has been observed that naringenin improves GSH levels during oxidative stress^[44,47-52]. Improvement of GSH levels by naringenin is associated with the beneficial properties of this flavonoid on the liver because oxidative stress plays a causative role in hepatic disorders^[54].

The effect of naringenin on GSH levels deserves further explanation. GSH is a tripeptide (L-γ-glutamyl-L-cysteinyl-glycine) that serves several essential functions within the cell. The main functions of GSH are antioxidant, detoxification of oxygen-derived free radicals, thiol disulfide exchange and storage/transfer of cysteine. GSH is formed in two steps: in the first (rate-limiting) step, cysteine and glutamate form c-glutamyl cysteine by the enzyme glutamyl cysteinyl ligase (GCL); in the second step, GSH forms from c-glutamyl cysteine and glycine by GSH synthetase (GSS) catalysis^[55-57] (Figure 4). It has been observed that naringenin possesses the ability to increase total and mitochondrial GSH levels during hydrogen peroxide (H₂O₂)-induced liver damage^[48,49,51], as well total hepatic GSH^[52,58,59] and total GSH in other organs^[60,61]. These effects can be explained because naringenin increases the expression of the GCLC catalytic subunit and the GCL modulatory subunit at both the protein and mRNA levels^[60-62].

The tripeptide can directly scavenge R[•] or function as a co-substrate of the internal antioxidant system enzymes. For example, GSH is the co-substrate of glutathione peroxidase (GPx) in H₂O₂ reduction and of glutathione transferase (GST), which catalyzes xenobiotics biotransformation in the liver^[56,57]. In either case, GSH is oxidized to GSSG, which leads to consumption of GSH. Therefore, there are mechanisms in charge of maintaining the GSH/GSSG balance; for example, glutathione reductase (GR or GSR) is responsible of GSSG reduction to the disulfide form (GSH) at the

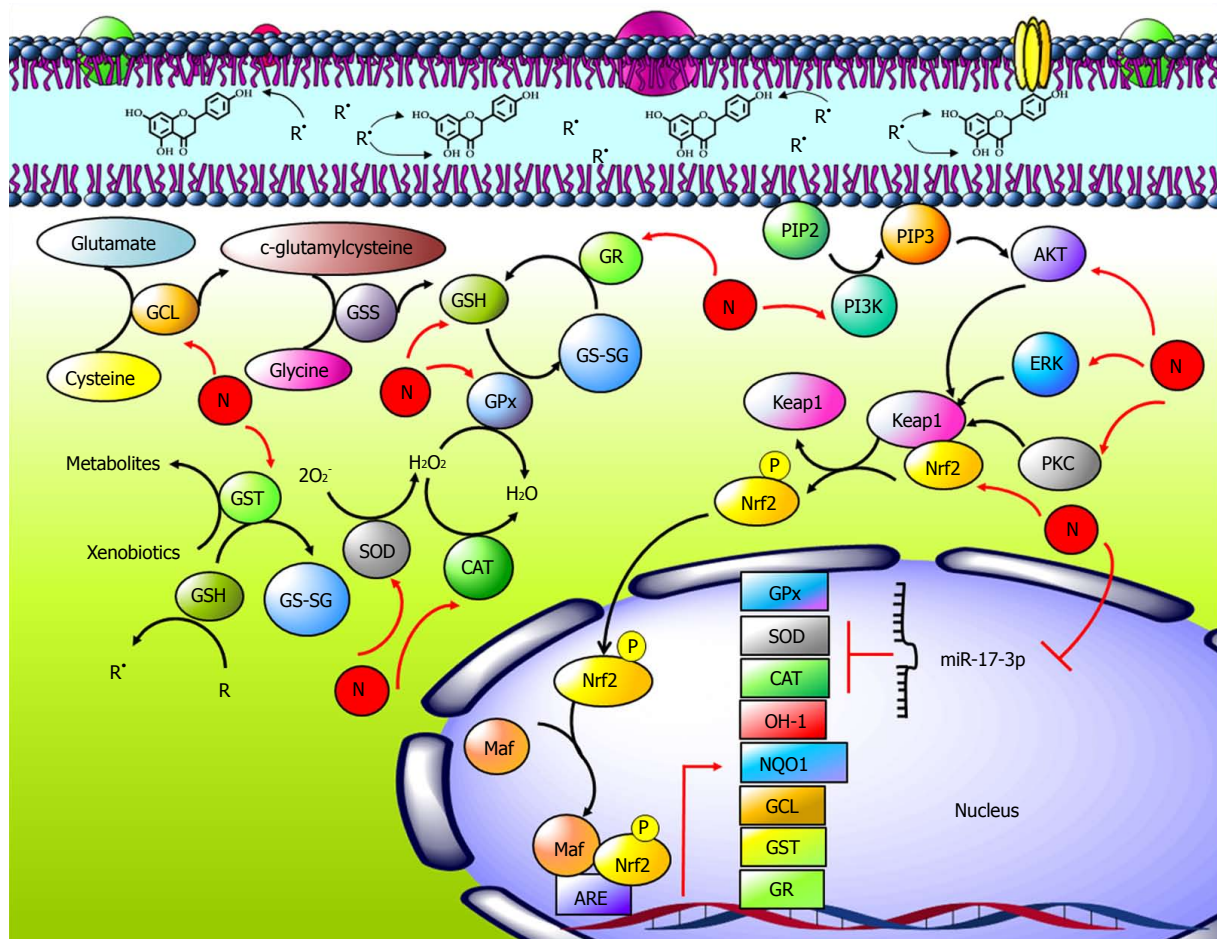


Figure 4 Antioxidant effects of naringenin. Naringenin (N) accumulates in cell membranes, where it provides rigidity to the lipid bilayer; naringenin can reduce the interaction between free radicals (R[·]) and the cell membrane, as well as reduce membrane phospholipid attack and prevent lipid peroxidation (LP). Glutathione (GSH) is formed when cysteine and glutamate form c-glutamyl cysteine by the enzyme glutamyl cysteinyl ligase (GCL); then, glycine and c-glutamyl cysteine form GSH by GSH synthetase (GSS). Naringenin increases GCLC protein and mRNA levels as well as GSH levels. Naringenin increases activity and protein and mRNA of superoxide dismutase (SOD), catalase (CAT), glutathione peroxidase (GPx), glutathione transferase (GST) and glutathione reductase (GR), enzymes that are part of the endogenous antioxidant system. Naringenin decreases the expression level of *miR-17-3p*; its targets genes are SOD and GPx. The nuclear factor-erythroid 2-related factor 2 (Nrf2) is an oxidative stress regulator; it stimulates antioxidant enzyme expression as well as heme oxygenase (OH-1) and NADPH quinone oxidoreductase (NQO1). Naringenin upregulates the Nrf2 pathway by increasing its activation, nucleus translocation, and protein and mRNA levels through PI3K/AKT, ERK and PKC.

expense of NADPH^[55-57]. It has been reported that naringenin increased the GSH/GSSG ratio^[59,61] by improving GR mRNA levels and activity in the liver^[44,63-66] and in other organs^[67,68] (Figure 4).

Naringenin can influence cellular antioxidant balance not only through its own chemical structure but also by inducing the cell antioxidant system. In this regard, it has been reported that naringenin upregulates important antioxidant enzymes, such as superoxide dismutase (SOD), catalase (CAT), GPx and GST.

SOD catalyzes the reaction in which O₂[·] is converted to H₂O₂, a more stable species but that at high concentrations is harmful to cells; in turn, CAT eliminates excess H₂O₂, generating water^[69]. Naringenin significantly increases SOD enzyme activity in different models of liver damage induced by oxidative stress^[44, 50, 52, 62-65, 67, 70-74]. This effect is associated with the ability of this flavonoid to increase enzyme protein levels in the liver and other organs^[58,59,68]. Naringenin can prevent

CAT activity decrement after damage to several tissues^[44,49,50,52,62-65,67,70-74] by increasing protein^[58,59,68] and mRNA levels^[43].

SOD and CAT, together with GPx and GST, are diminished during oxidative stress. It is worth noting that naringenin has been reported to upregulate these enzymes^[44,63-66] (Figure 4). There are some reports trying to explain the mechanism of naringenin to increase GPx activity. One report indicates that the flavanone produces an increment in GPx mRNA levels^[43], while others indicate that it increases the protein content^[58,59,68]. Another hypothesis postulates that during cell damage, GSH is almost depleted and, thus, cannot be utilized by GPx as a cofactor, leading to decreased enzyme activity; in this situation, naringenin acts by improving GSH levels and, as a consequence, enzyme activity^[44,49,50,52,63-65,71-74]. Further experiments are needed to clarify this point.

Naringenin preserves GST activity under prooxidant conditions associated with several illnesses^[49-51,63-65,70,72,74].

It has been demonstrated that the flavanone acts by increasing mRNA levels of GST^[61,63], which in turn induces the transduction of the corresponding functional protein^[68]. The specific action mechanism by which naringenin produces these effects remains to be elucidated (Figure 4).

As it has been previously described, naringenin has very important effects on endogenous antioxidant system enzymes, in contrast to its own weak antioxidant properties in comparison to those of other natural compounds, such as quercetin. This low antioxidant activity suggests that naringenin's effects are not only a result of its structural activity relationship but also due to other properties. In this regard, it is worth noting that naringenin influences microRNAs (miRNAs) and nuclear factor-erythroid 2 related factor 2 (Nrf2).

miRNAs are noncoding or nonmessenger RNAs that are approximately 22 nucleotides in length that regulate gene expression because they bind to target mRNA, inhibiting protein synthesis^[75]. *miR-17-3p* is involved in oxidative stress, and its targets are mRNAs coding for SOD and GPx, thereby preventing the expression of these proteins^[76]. Naringenin decreased the expression level of *miR-17-3p*, which is in agreement with increased levels of target mRNAs coding for SOD and GPx2^[77]. As noted, this reduction in *miR-17-3p* expression may be a mechanism by which naringenin modulates antioxidant enzymes; however, more research is needed on the role of naringenin in miRNA and its effect on the endogenous antioxidant system (Figure 4).

Nrf2 interacts with the actin binding protein, Kelch-like ECH associating protein 1 (Keap1), inactivating Nrf2 in the cytoplasm. Nrf2 must be released from Keap1 to be active. Its release can occur either by MAPK phosphorylation or by conformational changes in Keap1 due to ROS. Once free, Nrf2 translocates to the nucleus, where it forms a dimer with the musculo-aponeurotic fibrosarcoma (Maf) family proteins. Nrf2-Maf dimer is a transcription factor that binds to the antioxidant response element (ARE) sequence, resulting in transcriptional activation of detoxification proteins such as NADPH quinone oxidoreductase (NQO1), GST, and aldo-keto reductase (AKR), antioxidant enzymes such as thioredoxin (TXN1), thioredoxin reductase 1(TXNR), peroxiredoxin 1 (PRDX1), GPx, GCL, GR, CAT and SOD, and heme and iron metabolism proteins such as heme oxygenase (OH-1) and ferro chelatase (FECH)^[78-80] (Figure 4).

Interestingly, there are reports indicating that naringenin upregulates Nrf2 in various models. In a model of UVB irradiation-induced skin inflammation and oxidative damage in hairless mice, naringenin significantly increased *Nrf2* mRNA levels compared with those in the damaged group^[66]. Moreover, in a model of KO₂-induced inflammatory pain in mice, naringenin inhibited the KO₂-induced decrease in *Nrf2* mRNA expression^[42]. In addition, naringenin upregulated the mRNA expression of *Nrf2* in complete Freund's adjuvant-induced rats^[46],

and naringenin increased Nrf2 mRNA expression in a model of oxidative stress induced by H₂O₂^[49].

The induction of *Nrf2* mRNA may propitiate Nrf2 protein levels to increase. It has been reported that naringenin is capable of increasing Nrf2 protein levels in CCl₄-induced hepatic damage^[63]. In addition, the flavonoid protected SH-SY5Y cells against 6-OHDA neurotoxicity via Nrf2 because it improved the levels of this protein^[60]. Moreover, one mechanism to explain why naringenin prevented CCl₄-induced acute liver injury in mice is by preserving Nrf2 levels^[59]. In addition, naringenin improved intracellular Nrf2 levels in LPS-induced apoptosis of PC12 cells^[81] and reduced oxidative stress by increasing Nrf2 protein levels in neurons^[41].

Increased Nrf2 protein levels do not necessarily correlate with increases in Nrf2 activity. Nrf2 must dissociate from Keap1 to translocate to the nucleus and to induce proteins of the antioxidant system. Naringenin activates Nrf2 because it promotes its translocation from the cytoplasm to the nucleus^[43,61-63,82].

Phosphorylation of Nrf2 by extracellular signal-regulated protein kinase (ERK) triggers the dissociation of Nrf2-Keap1 and inhibits the reassociation of Nrf2-Keap1 complexes^[83,84]. Other important proteins involved in the activation of Nrf2 are 5' AMP-activated protein kinase (AMPK)^[85], phosphatidylinositol-3-kinase (PI3K/AKT), and protein kinase C (PKC)^[86]. Notably, it has been observed that naringenin upregulated phosphorylated ERK1/2, leading to nuclear translocation of Nrf2 in doxorubicin-induced toxicity in H9c2 cardiomyocytes^[62]. In another report, after treatment with 40 µg/mL of naringenin, nuclear Nrf2 increased at 0.25 h and remained elevated until 3 h after naringenin treatment to H9c2 cells^[82]. In addition, naringenin increased the phosphorylation levels of ERK1/2, PKC δ , and AKT, but this increase was prevented by chemical inhibitors of AKT (LY294002), ERK1/2 (PD98059), and PKC α (rottlerin), which suppressed Nrf2 activation induced by naringenin^[82]. These results suggest that the naringenin-induced activation of Nrf2 signaling may be mediated by the phosphorylation of ERK1/2, PKC δ , and AKT^[82] (Figure 4).

Nrf2 activation and its translocation to the nucleus lead to its union with Maf; Nrf2-Maf dimer, in turn, binds to ARE sequence, which results in transcriptional activation of detoxification and antioxidant proteins. Naringenin not only activates Nrf2 but also increases the mRNA and protein levels of target genes such as NQO1, GPx, GCL, GR, OH-1, and GST^[43,46,49,59-63,66,81,82,87]. To corroborate this effect, experiments have been carried out to silence Nrf2. A small interfering RNA (siRNA) study revealed that the knockdown of *Nrf2* can abrogate naringenin-mediated protection of the BEAS-2B cells from paraquat-induced cellular toxicity^[43]. Another report showed that naringenin fails to block 6-OHDA neurotoxicity if *Nrf2* siRNA is administered^[60]. Moreover, naringenin prevented mitochondrial depolarization is inhibited by *Nrf2* siRNA^[87]; in addition, the naringenin-

induced upregulation of GCL and HO-1 proteins was significantly inhibited by *Nrf2*-siRNA transfection in H9c2 cells^[82]. Finally, silencing of *Nrf2* suppressed naringenin-induced cytoprotection and mitochondrial protection in SH-SY5Y cells exposed to H₂O₂^[48] (Figure 4).

Due to the important regulatory effects of naringenin on endogenous antioxidant system, the flavonoid takes great importance as a possible hepatoprotector, since one of the main mechanisms of liver damage is oxidative stress^[54]. In addition, this antioxidant is different from others, since in addition to its direct effect as an antioxidant, it induces the expression of endogenous antioxidants.

NARINGENIN PREVENTS LIVER DAMAGE CAUSED BY ALCOHOL

Liver damage induced by excessive alcohol consumption is a worldwide problem^[3]. It has been reported that an intake of 80 g/day by men and 40 g/day by women between 10-20 years may lead to fibrosis^[88-90]. Therefore, it is important to find a drug that prevents or reverses the effects of alcohol abuse in the population.

Liver alcohol metabolism consists of the following steps: (1) In the cytosol, alcohol is converted into acetaldehyde by the enzyme alcohol dehydrogenase (ADH) using NAD⁺ to generate NADH; acetaldehyde is also formed in microsomes by CYP2E1 and in peroxisomes by CAT; and (2) In the mitochondria, acetaldehyde dehydrogenase (ALDH) transforms acetaldehyde to acetate^[91-93] (Figure 5). During these reactions, secondary harmful products to hepatocytes are generated; among the most important of these harmful products is MDA, which forms adducts with proteins and is also an important indicator of LP^[91-93]. Moreover, ROS, such as H₂O₂ and O₂[•], are generated during the metabolism of alcohol by CYP2E1. Additionally, alcohol metabolism induces fatty liver disease by increasing the NADH/NAD⁺ ratio. In general, these processes induce hepatocyte damage, leading to an inflammatory environment that activates endothelial cells, Kupffer cells and HSCs^[91-93].

The evidence indicates that naringin, the naringenin-glycoside, significantly lowered ethanol concentration in plasma in a dose-dependent manner^[94]. Ethanol administration resulted in higher ADH and lower ALDH activities, resulting in toxic acetaldehyde accumulation. Naringin increased the activities of both enzymes, resulting in efficient alcohol elimination *via* acetaldehyde and its conversion to acetate, preventing the accumulation of acetaldehyde, and resulting in the rapid clearance of alcohol from the serum^[94]. In agreement with these findings, naringenin administration to alcohol-treated rats increased ADH and ALDH enzyme activities^[70]. In addition, ethanol increased the activity of cytochrome CYP2E1, while this effect was reversed by naringenin^[70] (Figure 5).

Ethanol consumption modifies the phase I and phase II xenobiotic metabolism enzymes. During phase I metabolism, enzymes catalyze reactions of oxidation, reduction, and hydrolysis of xenobiotics to increase their polarity and improve their excretion. On the other hand, phase II reactions are glucuronidation, acetylation, S-methylation, and glutathione- or sulfo-conjugation of xenobiotics. These reactions are carried out on phase I products for their better excretion, since tissue damage occurs if the products of phase I are not eliminated by the enzymes of phase II^[95]. It has been reported that alcohol intake raises the activity of phase I enzymes such as CYP450, cytochrome b5, NADH-cytochrome b5 reductase and NADPH-CYP450 reductase. In contrast, ethanol injection decreases the activity of phase II enzymes such as GST and DT-diaphorase^[70,96]. Interestingly, naringenin was able to reverse these effects caused by alcohol in both types of enzymes, leading to efficient elimination of alcohol metabolism products and reestablishment of the NADH/NAD⁺ ratio^[70] (Figure 5).

Due to acetaldehyde accumulation during alcohol metabolism, oxidative stress is generated. This is characterized by LP, increased R[•] and endogenous antioxidant system dysfunction^[97]. During ethanol administration *in vivo*, significantly elevated levels of TBARS, lipid hydroperoxides (LOOH), conjugated dienes (CD), protein carbonyl content and significantly lowered activities of SOD, GPx, CAT, GR and GST, and lowered levels of GSH have been observed^[64,70,94].

As discussed above, naringenin displays antioxidant effects at different levels, and this was evident when the administration of naringin or naringenin prevented and reverted oxidative stress caused by ethanol, normalizing levels of TBARS, LOOH, CD, protein carbonyl content, antioxidant enzymes activity and GSH levels^[64,70,94] (Figure 5).

If oxidative stress is constant and the antioxidant system has failed, liver damage is generated; this liver damage is marked by increases in liver damage markers such as alkaline phosphatase (AP), aspartate aminotransferase (AST), alanine aminotransaminase (ALT), γ -glutamyl transferase (GGT) and lactate dehydrogenase (LDH) activities or by the elevation of serum bilirubins and aspartate levels. However, naringenin administration during ethanol-induced hepatic damage decreases the activity/levels of liver damage markers, demonstrating that naringenin protects hepatocytes against necrosis, cholestasis and membrane permeation^[64,70,98] (Figure 5).

After hepatocyte damage occurs, an inflammatory reaction is produced that is characterized by increases in cytokines and proteins that mediate the immune response. It has been reported that rats that received 20% ethanol equivalent to 6 g/kg body weight (bw) every day for a period of 60 days showed significantly elevated mRNA levels of tumor necrosis factor-alpha (TNF- α), interleukin-6 (IL-6), nuclear factor-kappa

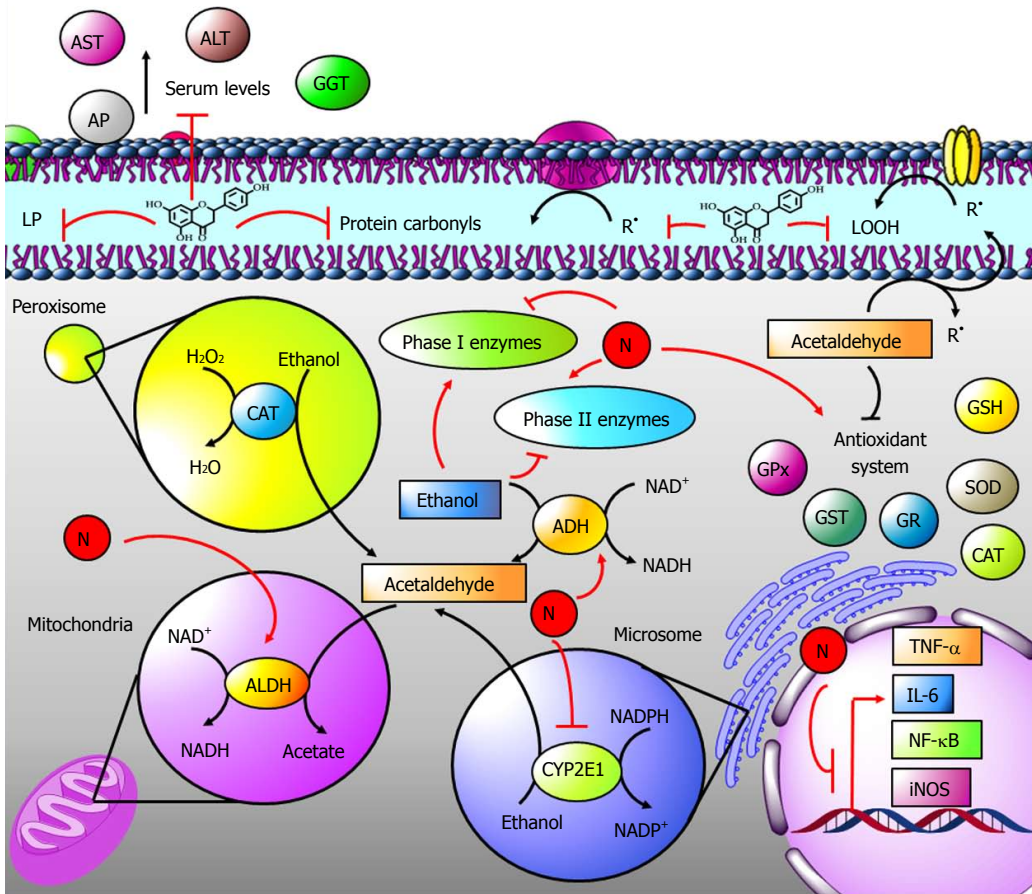


Figure 5 The role of naringenin in alcohol-induced liver damage. Alcohol metabolism: In the cytosol, alcohol is converted into acetaldehyde by alcohol dehydrogenase (ADH); it is also formed in microsomes by CYP2E1 and in peroxisomes by catalase (CAT). In mitochondria, acetaldehyde dehydrogenase (ALDH) transforms acetaldehyde to acetate. Ethanol elevates ADH and CYP2E1 activities but decreases ALDH activity, resulting in toxic acetaldehyde accumulation, free radical (R^{\cdot}) formation in the form of lipid hydroperoxides (LOOH) or protein carbonyls and resulting in the elevation of lipid peroxidation (LP). Naringenin (N) increases the activities of all those enzymes, which results in alcohol efficient elimination leading to endogenous antioxidant system restoration, oxidative stress prevention and balance of phase I and phase II xenobiotic metabolism enzymes. Naringenin also prevents increased levels of alkaline phosphatase (AP), aspartate aminotransferase (AST), alanine aminotransaminase (ALT), and γ -glutamyl transferase (GGT) as well as inflammation during alcohol-mediated liver damage.

B (NF- κ B), cyclooxygenase-2 (COX-2), macrophage inflammatory protein 2 (MIP-2) and CD14, as well as increased staining for inducible nitric oxide synthase (iNOS) protein adducts in the liver. Notably, when naringenin (50 mg/kg p.o.) was administered every day during the last 30 d of alcohol intoxication, the flavanone decreased the mRNA levels of all inflammatory markers^[98], indicating the potent anti-inflammatory properties of naringenin (Figure 5).

One of the main effects of alcohol abuse on the liver is lipid accumulation in hepatocytes. Even though fatty liver is a reversible condition, it can progress to inflammation and fibrosis. During alcohol consumption, there is a deregulation of pathways that regulate lipid synthesis, oxidation and very-low density lipoprotein (VLDL) exportation that leads to the accumulation of triglycerides and fatty acids in the liver^[93]. In a study performed to investigate the effect of naringenin supplements on lipid metabolism in ethanol-treated rats, the results showed that the concentrations of plasma/liver total cholesterol and plasma/liver total

triglyceride were significantly higher in the ethanol-treated rats and, conversely, decreased the high-density lipoprotein (HDL)-cholesterol level and HDL-cholesterol/total-cholesterol ratio, while naringenin reestablished normal levels of all measured lipid parameters. Another interesting effect of the glycoside was a decreased number of hepatic cells containing lipid droplets compared to the alcohol-group, where many of these cells were observed. It was concluded, therefore, that naringenin is able to prevent lipid accumulation in liver caused by alcohol^[94].

In another study, serum insulin was diminished, glucose/insulin ratio and liver triglycerides were increased in ethanol-drinking rats; however, naringenin co-administration partially protected rats from these effects produced by alcohol intoxication. Unfortunately, naringenin was not able to protect from alterations in serum glucose, triglycerides, total, free and esterified cholesterol or HDL cholesterol, or from liver and muscle triglycerides or glycogen^[99].

Naringenin has effects on several steps of ethanol

metabolism, as well as on liver damage by this xenobiotic, suggesting that it can be used in the prevention and reversion of alcohol-induced liver damage. However, more studies are necessary to further investigate naringenin's mechanism of action in alcohol-induced hepatic injury and whether it is able to protect from fibrosis induced by alcohol abuse.

EFFECT OF NARINGENIN ON CCl₄-INDUCED LIVER DAMAGE

CCl₄ is a haloalkane widely used to induce liver damage^[100]. To induce liver damage, CCl₄ must be activated by CYP2E1, CYP2B1 or CYP2B2, and CYP3A, to form the trichloromethyl radical (CCl₃[•]). This radical reacts with oxygen to form the trichloromethylperoxy radical (CCl₃OO[•]), a highly reactive species. These two species are highly reactive; they can bind to cellular molecules, for example, nucleic acids, proteins or lipids. CCl₃OO[•] initiates the chain reaction of LP, which attacks and destroys PUFAs, those associated with phospholipids in cell membranes as the mitochondrial or the reticulum membranes. This membrane damage leads to hepatocyte damage, which in turn activates Kupffer cells and HSC, regulating fibrosis and cirrhosis^[31,101] (Figure 6).

Facino *et al.*^[102] were pioneers to study the effectiveness of naringenin against CCl₄ damage. In this study, a glycosidic fraction (containing naringenin-glycoside) and naringenin-glycoside extracted from the flowering tops of *Helichrysum italicum* G. Don were utilized to investigate the effect of these flavonoids on CCl₄-induced rat microsomes, finding that microsomal LP was reduced by the glycosidic fraction and by naringenin-glycoside^[102]. Another study showed that CCl₄-induced liver damage was decreased by concomitant administration of an aqueous extract of the rhizomes of *Sansevieria liberica*, containing 5.99% naringenin, since AP, AST and ALT activities and fatty degeneration of hepatocytes were prevented^[103]. Finally, another report investigated the effect of an aqueous extract of *Trifolium pratense L.* (Leguminosae) leaves on CCl₄-induced liver damage; it was observed that naringenin in the extract was able to reduce LP levels and xanthine oxidase (XOD) activity^[104].

On the basis that natural extracts containing naringenin had positive effects against injury induced by CCl₄, different protocols have been carried out to evaluate naringenin hepatoprotective capacity. In 2009, Yen *et al.*^[105] evaluated the ability of naringenin to prevent acute liver failure induced by CCl₄ in rats. Naringenin (100 mg/kg) was administered during three consecutive days, and then on the fourth day, CCl₄ was intraperitoneally (i.p.) administered with a single dose (3 mL/kg, olive oil: CCl₄, 1:1). The flavonoid was able to prevent AST, ALT and LP elevations and the reduction of SOD, CAT and GPx levels, and it significantly suppressed the activation of caspase (Cas)3 and Cas9 induced by

CCl₄ administration^[16].

Later, Hermenean *et al.*^[105] published an experiment in which acute liver damage was induced in mice with CCl₄ (1.0 mL/kg, olive oil: CCl₄, 1:1, i.p.), and naringenin (50 mg/kg) pretreatment for seven days was evaluated. The elevation of serum AST, ALT and LP levels as well as the reduction of CAT, SOD and GPx activities and GSH levels in livers from rats intoxicated with CCl₄ were all significantly prevented by naringenin. Moreover, naringenin prevented necrotic changes of hepatocytes, fatty degeneration, sinusoidal dilatation, mild fibrosis, and inflammatory cell infiltration and retained the normal ultrastructure of the hepatocytes, including mild restoration of normal bile canalicular configuration filled with microvilli^[105].

The action mechanism of naringenin on acute liver damage induced by CCl₄ can be explained by different mechanisms. CCl₄ is activated in hepatocytes by CYP2E1; therefore, the R[•] formed attacks membranes of these cells, generating LP. During CCl₄ administration, the expression of CYP2E1 is elevated; however, it has been reported that naringenin strongly inhibited this cytochrome; therefore, one possible mechanism of hepatoprotection is the inhibition of CYP2E1 by the flavanone, preventing bioactivation of CCl₄^[59] (Figure 6). Another mechanism is associated with the ability of naringenin to induce the endogenous antioxidant system by upregulating Nrf2. It was reported that the administration of 50 mg/kg of naringenin to rats significantly increased Nrf2 protein levels in the cytoplasm and nucleus, elevating mRNA levels of its target genes, such as HO-1, NQO1 and GST^[63]; in addition, naringenin can prevent the decrease in Nrf2, HO-1 and SOD protein levels exerted by CCl₄ treatment in mice^[59] (Figure 6).

In addition to oxidative stress, inflammation plays a crucial role in the development of liver damage. During fibrosis produced by CCl₄ chronic administration, there is a proinflammatory environment generated by Kupffer cells and HSCs. In these cells, inflammatory signaling pathways, mainly NF-κB-related signaling pathways, are activated. This pathway starts when TLRs are activated; then, intermediaries lead to inhibitor κB (IKB) phosphorylation by IκB kinase (IKK) and NF-κB release into the cytoplasm. NF-κB then translocates into nucleus to induce the transcription of target genes. NF-κB regulates proinflammatory protein expression of TNF-α, IL-1β and IL-6^[59,31,106]. In addition, NF-κB binds to iNOS and COX-2 gene promoters, activating the transcription of these genes; iNOS catalyzes the production of nitric oxide (NO), which is a highly oxidizing product^[107,108]. On the other hand, during the NF-κB pathway, the intermediate TGF-β-activated kinase 1(TAK1) is activated. Additionally, through MAPKs, NF-κB activates activator protein 1 (AP-1), a factor that promotes the transcription of genes related to inflammation^[106,109]. Moreover, high mobility group box 1 (HMGB1) is widely involved in proinflammatory processes through its

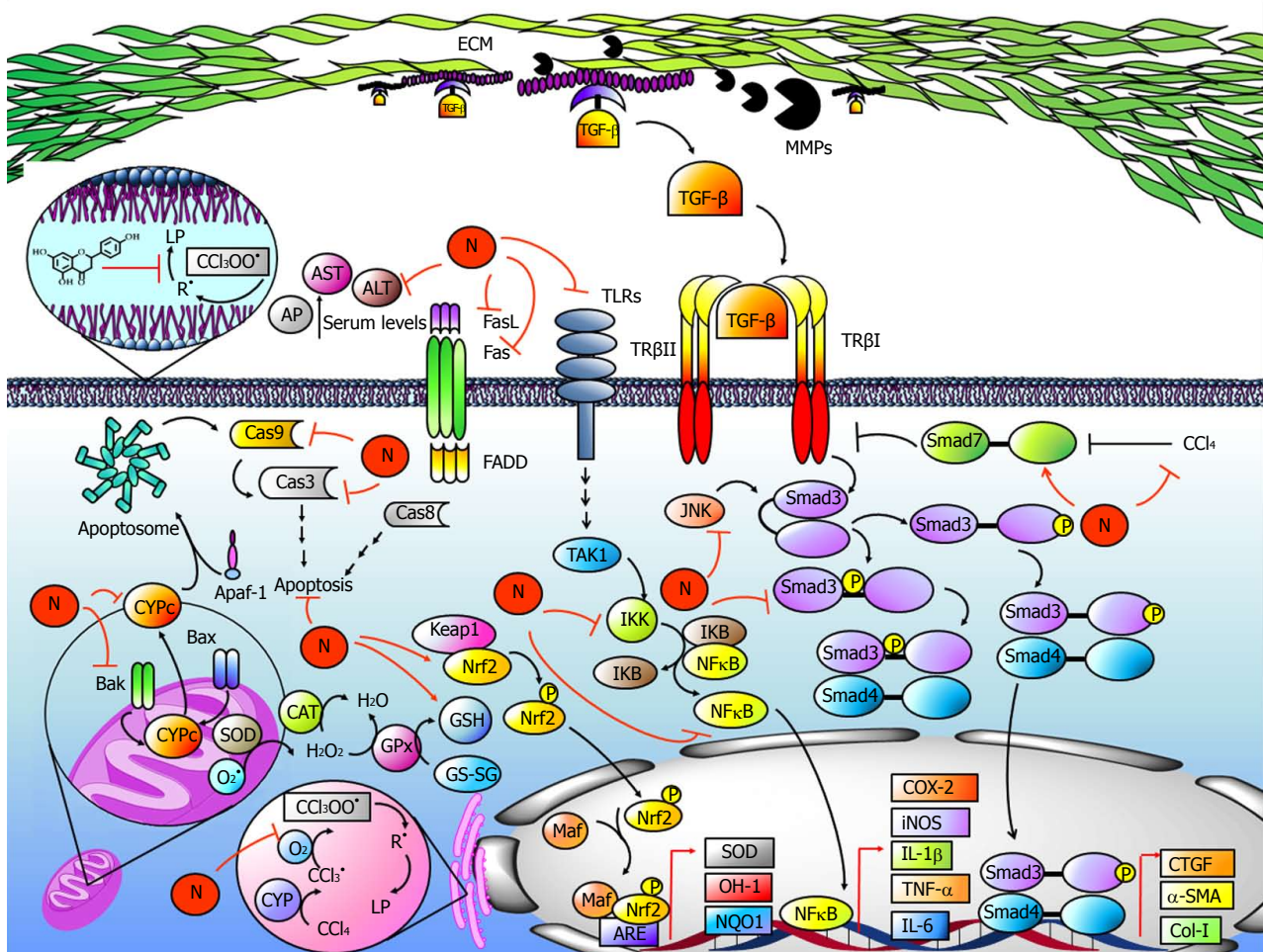


Figure 6 Naringenin prevents acute and chronic CCl_4 -induced liver damage. Carbon tetrachloride (CCl_4) is activated by CYP2E1, CYP2B1, CYP2B2, and CYP3A (CYP) to form the trichloromethyl radical ($\text{CCl}_3\cdot$); then, it reacts with the oxygen-forming trichloromethylperoxy radical ($\text{CCl}_3\text{OO}^\cdot$). The $\text{CCl}_3\text{OO}^\cdot$ initiates lipid peroxidation (LP), free radical (R') generation, and imbalance of the endogenous antioxidant system formed by superoxide dismutase (SOD), catalase (CAT), glutathione peroxidase (GPx), glutathione (GSH), heme oxygenase (OH-1), NADPH quinone oxidoreductase (NQO1) and nuclear factor-erythroid 2 related factor 2 (Nrf2). Naringenin prevents CCl_4 metabolism, LP and imbalance of the antioxidant system. Naringenin also prevents increased levels of alkaline phosphatase (AP), aspartate aminotransferase (AST), alanine aminotransaminase (ALT), and γ -glutamyl transferase (GGT). On the other hand, CCl_4 increases intrinsic and extrinsic apoptosis pathways in hepatocytes; however, naringenin prevents CYPc release, as well as BCL2-associated X protein (Bax), BCL2-antagonist/killer 1 (Bak), Caspase 3 (Cas3) and Caspase 9 (Cas9) elevation, a protein related with the intrinsic pathway. For the extrinsic apoptosis pathway, naringenin prevents Fas and Fas ligand (FasL) increases produced by CCl_4 administration. During CCl_4 -induced fibrosis, there is a proinflammatory environment generated by Kupffer cells and HSCs. The NF- κ B pathway starts when TLRs are activated; then, intermediates are activated leading to inhibitor κ B (I κ B) phosphorylation by I κ B kinase (IKK) and NF- κ B release. NF- κ B regulates inflammatory protein expression, including tumor necrosis factor-alpha (TNF- α), interleukin-6 (IL-6), cyclooxygenase-2 (COX-2), interleukin-1 (IL-1) and inducible nitric oxide synthase (iNOS), while naringenin maintains normal levels of these proteins during CCl_4 -induced liver damage. Transforming growth factor- β (TGF- β) activates receptor-activated Smad3 (Smad3), leading to transcriptional induction of α -smooth muscle actin (α -SMA), connective tissue growth factor (CTGF), and collagen-1 (Col-1). Moreover, Smad3 is also activated by JNK via linker domain phosphorylation. Naringenin prevents Smad3 activation and α -SMA, CTGF, and Col-1 elevation because it inhibits TGF- β elevation and JNK activation. Metalloproteases (MMPs) cleave extra cellular matrix (ECM) proteins, favoring TGF- β release as well as HSC migration to other sites, increasing fibrosis development; naringenin prevents MMPs elevation. On the other hand, CCl_4 decreases Smad7 protein levels; this protein inhibits the TGF- β signaling pathway by TGF- β receptor I (T β RI) ubiquitination, but nevertheless, naringenin maintains normal levels of Smad7 during CCl_4 treatment.

receptor for advanced glycation end product (RAGE) and TLRs; HMGB1 is released by necrotic cells and by monocytes or macrophage^[10].

Because inflammation plays a pivotal role in the establishment and perpetuation of liver diseases, naringenin has been evaluated as an anti-inflammatory therapeutic agent. In this context, a recent paper reported that naringenin (30, 60 and 120 mg/kg) administration to mice treated with CCl_4 (0.3% CCl_4 , 10 mL/kg, dissolved in olive oil) showed that at a dose of 120 mg/kg, the flavonoid dramatically downregulated

the expressions of TLR4, TNF- α , IL-1 β , IL-6, iNOS, AP-1, COX-2, HMGB-1 and NF- κ B^[59]. Another report of a study carried out in rats that were acutely intoxicated with CCl_4 indicates that naringenin (50 mg/kg) prevents the CCl_4 -induced increases in TNF- α and elevations in iNOS, COX-2 protein and mRNA^[63]. Figure 6 shows that naringenin and naringenin possess important anti-inflammatory properties by blocking the NF- κ B signaling pathway.

During hepatic damage, hepatocytes may undergo apoptosis mediated by intrinsic or extrinsic pathways.

In the intrinsic pathway, BCL2-associated X protein (Bax) and BCL2-antagonist/killer 1 (Bak) are activated by proapoptotic stimuli, resulting in the release of electron transport protein CYPc from the mitochondria to the cytoplasm; then, this protein binds to Apaf-1, forming the apoptosome. In turn, the apoptosome activates Cas9, which cleaves procaspase 3 zymogens, amplifying the cell death cascade^[11].

The administration of CCl₄ induces apoptosis in hepatocytes as well as DNA fragmentation, increases the mRNA levels of Bax, Bak, Cas3 and Cas9 and increases CYPc release^[59,31,101]. It has been reported that glycosylated naringenin (naringin) effectively prevented CCl₄-induced DNA fragmentation, apoptosis and mitochondrial injury by attenuating the release of CYPc, therefore inhibiting apoptosis initiation. Another explanation is that naringin significantly increased the expression of antiapoptotic proteins B-cell CLL/lymphoma 2 (Bcl-2) and BCL2-like 1 (Bcl-xL) but decreased Bax, Bak, Cas3 and Cas9 mRNA levels^[59] (Figure 6).

Through the extrinsic pathway, Fas is activated by Fas ligand (FasL), which then binds to Fas-associated protein with a death domain (FADD). The Fas-FADD complex activates procaspase 8, which in turn activates other Cas, leading to apoptosis^[111]. After CCl₄-induced acute liver damage, the mRNA levels of Fas, FasL, and proapoptotic protein p53 are increased, but preventive administration of naringin inhibited this increase and reduced apoptosis in liver^[59] (Figure 6).

While there are some reports indicating evidence of the beneficial effects of naringenin on acute liver damage induced by CCl₄, there is little information on the effect of this flavanone on chronic treatment. Recently, we have demonstrated that naringenin effectively prevents liver cirrhosis induced by chronic administration of CCl₄ in the rat^[112]. Moreover, we studied the molecular mechanisms involved in the hepatoprotective effects of naringenin on CCl₄-induced liver fibrosis. Our results indicate that naringenin prevented necrosis and cholestasis and improved liver biosynthetic capacity in CCl₄-treated rats since the flavonoid completely prevented the increase in ALT, AP and GGT serum activity and hepatic glycogen depletion. In addition, naringenin inhibited oxidative stress caused by chronic liver damage, maintaining normal levels of MDA, GSH and GPx activity. Moreover, inflammation was prevented by naringenin since the levels of NF-κB, IL-1β and IL-6 were preserved within normal values despite CCl₄ administration^[112].

Perhaps the most important feature of chronic liver damage is the deposition of scar tissue in the hepatic parenchyma, leading to fibrosis and cirrhosis. In general, livers of rats treated with CCl₄ presented macro nodular fibrosis; the tissue showed liver parenchymal disruption, steatosis, hyperchromatic nuclear hepatocytes, and atypical pleiomorphic nuclei. In addition, cirrhotic rats presented large amounts of collagen around fibrotic nodules. In contrast, rats treated with naringenin

had livers without macro nodular fibrosis; collagen accumulation as well as regenerative nodules were prevented, and it was found that total collagen and collagen-I (Col-I) accumulation was prevented by naringenin. One of the main profibrogenic signaling molecules is TGF-β, which exerts its effects by activating receptor-activated Smads (R-Smads), leading to transcriptional induction of α-smooth muscle actin (α-SMA), the main marker of transdifferentiation of HSCs, and connective tissue growth factor (CTGF), a TGF-β downstream signal amplifier^[113,114]. Notably, naringenin was able to maintain basal levels of TGF-β, as well as α-SMA, CTGF and Col-I, in rats treated with CCl₄. In addition to being activated by TGF-β, MAPKs also activate R-Smads in an alternative pathway (non-canonical), where the linker domain is phosphorylated instead of the carboxyl domain in R-Smads molecules^[115,116]. After the administration of CCl₄ for 8 wk, activated JNK levels increased significantly, as well as total and phosphorylated Smad3 in the linker domain (pSmad3L); however, naringenin was able to prevent these effects, providing another explanation for the antifibrotic effect of the flavonoid (Figure 6). Moreover, metalloproteases (MMPs), produced by the activated HSCs, cleave TGF-β, leading to further activation and proliferation of HSCs and collagen fiber formation; consequently, fibrosis ensues. In agreement with these findings, we noticed that chronic CCl₄ administration produced increased MMP2, MMP9 and MMP13; notably, we found for the first time that naringenin treatment preserved normal levels of these MMPs^[117] (Figure 6).

Furthermore, CCl₄ decreased Smad7 protein levels; Smad7 inhibits the TGF-β profibrogenic signaling pathway by TGF-β receptor I (TβRI) ubiquitination^[118]. Nevertheless, naringenin was able to maintain normal levels of Smad7 during CCl₄ treatment, therefore preserving the normal/physiological antifibrotic pathway and, thus, blocking ECM deposition in the hepatic parenchyma (Figure 6).

Our working group recently showed that naringenin also has effects on the reversion of a previously established fibrosis (unpublished data). CCl₄ was given for 12 weeks to male Wistar rats (400 mg/kg, 3 times/wk); however, naringenin (100 mg/kg/two times a day, p.o.) was administered at the beginning of week 9 of CCl₄ treatment to determine its ability to reverse established experimental cirrhosis. Different techniques demonstrated that naringenin had the ability to reverse elevated liver damage biochemical markers and to restore GSH and glycogen levels. Additionally, the high levels of TGF-β and α-SMA (protein and mRNA) observed during CCl₄ treatment were diminished by naringenin administration. The protein levels of CTGF, Col-1 and MMP13, as well as the activity of MMP2 and MMP9, proteins involved in MEC remodeling, were restored by the flavonoid. The protein levels of NF-κB, IL-1β and IL-10 were elevated during CCl₄ intoxication; however, naringenin reversed this effect. Naringenin also reversed

JNK activation and Smad3 phosphorylation in the linker domain, as well as total protein and total Smad3 mRNA. The results demonstrate that naringenin blocks TGF- β -Smad3 and JNK-Smad3 pathways, and thereby, it has antifibrotic effects, making it a good candidate for properly performed clinical studies. In summary, these results show that naringenin not only reduces CCl₄-induced acute liver damage but also reduces fibrosis. The action mechanism of naringenin to protect the liver from chronic liver damage covers several fronts. This flavonoid displays important effects on the endogenous antioxidant system, blocks the main proinflammatory factor, NF- κ B, and inhibits many profibrogenic pathways. These actions make this flavonoid an effective compound to not only to prevent but also to reverse chronic hepatic damage induced by CCl₄.

ANTICANCER ACTIVITY OF NARINGENIN IN THE LIVER

HCC is one of the most frequent tumor types worldwide. It is the fifth most common cancer in men and the ninth in women, with approximately 500000 and 200000 new cases per year, respectively^[119].

HCC is a genetically heterogeneous tumor. Hepatocarcinogenesis is complex and, therefore, requires several genetic and epigenetic alterations. Several etiological factors of HCC have been defined, including HBV, HCV, excessive alcohol consumption, obesity, and aflatoxins, and the prevalence/contribution of these risk factors vary by region^[120]. In Western countries, the increasing prevalence of nonalcoholic steatohepatitis (NASH), known as the manifestation of the metabolic syndrome, is becoming the most prevalent risk cause for liver failure and HCC^[3].

HCC is strongly associated with oxidative stress^[121], hepatic virus infection, the deposition of heavy metals, and fatty liver disease are closely associated with chronic inflammation, which in turn can induce oxidative stress in hepatocytes^[122]. Alterations in cell structure and mitochondria can generate electron leakage from the mitochondria, resulting in the activation of pro-oncogenic pathways^[123]. In addition, Kupffer cell activation during inflammation produces ROS that are liberated in the liver tissue, inducing damage to the hepatocyte membrane^[124].

Elevated levels of intracellular ROS induce the accumulation of many genetic and epigenetic modifications that may play a pivotal role in the induction of many proinflammatory, onco-suppressor- and onco-promoter-related genes that participate in HCC development^[125]. When ROS are increased for prolonged periods of time, the antioxidant defense capacity and the repair systems of the cells can be insufficient and lead to lipid, protein and DNA damage, altering different cellular pathways and influencing gene expression, cell adhesion, cell metabolism, the cell cycle, and cell death^[126]. In general, ROS have negative effects; they are potential

carcinogens because of their role in mutagenesis and the consequential chromosomal aberrations^[127], as well as in the regulation of tumor promotion and progression^[128]. It is worth noting that ROS have been linked to the hepatocarcinogenic process because they are implicated in the activation of cellular signaling pathways, such as those mediated by MAPKs, NF- κ B, PI3K, p53, and b-catenin/Wnt, which are associated with mutagenesis, angiogenesis, tumor promotion, and progression^[129,130] (Figure 7).

Abundant evidence from humans and experimental animals has shown that a high intake of natural products rich in antioxidants is associated with a decreased risk of many cancers^[131-135]. Flavonoids have diverse biological activities because of their antiallergic, anti-inflammatory, antioxidant, and anticancer properties without significant systemic toxicity^[134,135]. Naringenin has been found to exhibit antioxidant, antimutagenic and anticarcinogenic effects^[65,136,137] and acts as chemopreventive agent against colon carcinogenesis *in vitro* and *in vivo*^[138,139]. It is worth noting that naringenin inhibits cell proliferation *via* the downregulation of NF- κ B, VEGF, and MMPs and induces apoptosis *via* Bcl-2, Bax and Cas in a rat model of hepatocarcinogenesis by N-nitrosodiethylamine (NDEA)^[140]. Arul and Subramanian demonstrated that naringenin attenuates NDEA-induced hepatocarcinogenesis; they postulated that the flavanone aids in liver cell regeneration, leading to the protection of hepatic cells and membrane integrity by scavenging R \cdot and enhancing the antioxidant status, thus hindering the process of carcinogenesis^[141]. A growing body of evidence indicates that naringenin prevents liver damage in chemically induced hepatotoxicity by inhibiting R \cdot and LP and by enhancing the antioxidant system of the cell^[65,112,142-144]. Accordingly, the administration of naringenin effectively suppressed NDEA-hepatocarcinogenesis and preneoplastic lesions by modulating antioxidant enzymes and attenuating LP through the scavenging of free radicals, thus enhancing the antioxidant status^[141]. Taken together, naringenin can markedly modulate oxidative stress by its activation of the antioxidant defense system. Thus, naringenin appears to be an attractive candidate as an antioxidant supplement for HCC prevention (Figure 7).

In another study, naringenin was found to inhibit the growth of Hep G2 cells in a concentration-dependent manner^[145]. The activation of p53 has been implicated in triggering cell cycle arrest, including both G1 and G2 phases of the cell cycle. Notably, naringenin induced a rapid accumulation of p53 in a dose-dependent manner, which might account for the naringenin-induced G0/G1 and G2/M phase arrests in Hep G2 cells^[145] (Figure 7).

In addition, evidence has shown that the anti-proliferative effect of natural products is associated with the induction of apoptosis^[146,147]. In agreement, naringenin was found to exert antiproliferative effects by inducing apoptosis, as evidenced by the nuclei damage of Hep G2 cells^[148,149]. The dysregulation of the cell cycle

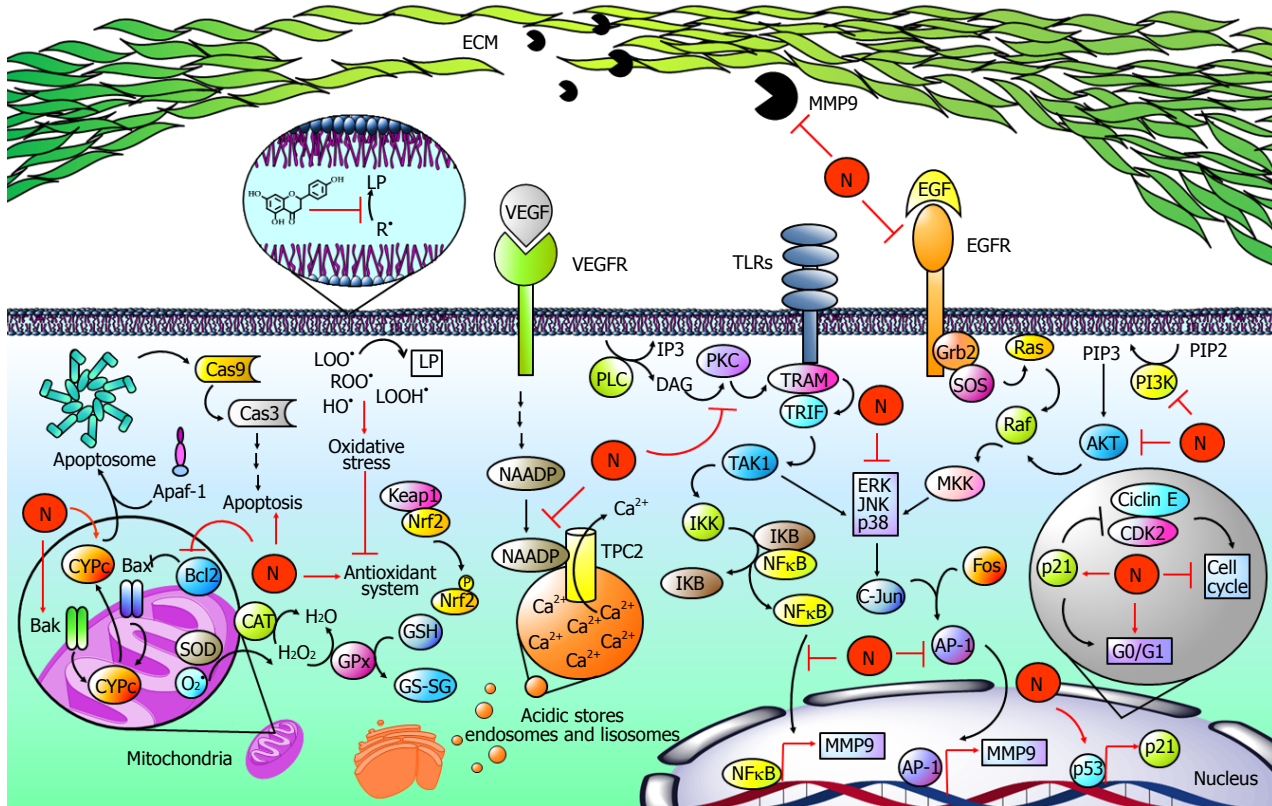


Figure 7 Naringenin in cancer development. Hepatocellular carcinoma is strongly associated with elevated levels of free radicals such as lipid hydroperoxides (LOOH), peroxyl radicals (ROO'), and hydroxyl radicals (OH'), leading to the development of lipid peroxidation (LP), oxidative stress and finally to an imbalance of the endogenous antioxidant system. Naringenin (N) inhibits oxidative stress by its intrinsic antioxidant properties and by improving the endogenous antioxidant system. Notably, oxidative stress has been linked to the hepatocarcinogenic process because it is implicated in the activation of mitogen activated protein kinases (MAPKs), nuclear factor-kappa B (NF- κ B), or phosphatidylinositol-3-kinase (PI3K/AKT) pathways, increasing the production and activity of metalloprotease 9 (MMP9), which is involved in migration and invasion processes. When toll-like receptors (TLRs) are activated, TRAMP is recruited to activate TRIF; in turn, it promotes transforming growth factor beta-activated kinase 1 (TAK1) activation, which phosphorylates I κ B kinase (IKK). Then, IKK promotes NF- κ B release via inhibitor κ B (I κ B) phosphorylation. On the other hand, phospholipase C (PLC) catalyzes phospholipid hydrolysis, generating inositol triphosphate (IP3) and diacylglycerol (DAG); the latter is an activator of protein kinase C (PKC), which can induce the NF- κ B pathway in a TRAMP-dependent manner. Then, NF- κ B induces the expression of MMP9. Epidermal growth factor (EGF) is highly involved in carcinogenic pathways; it binds to epidermal growth factor receptor (EGFR) promoting Grb2, SOS, Ras, Raf and mitogen-activated protein kinase kinase (MKK) activation, which participates in extracellular signal-regulated protein kinase (ERK), c-Jun N-terminal kinase (JNK) and p38 (MAPK) phosphorylation and activation. Then, MAPKs promote activator protein 1 (AP-1) activation by c-Jun and Fos dimerization. After that, AP-1 induces the expression of MMP9. Alternatively, MAPKs are activated via PI3K/AKT. PI3K produces phosphatidylinositol (3, 4, 5)-trisphosphate (PIP3) from phosphatidylinositol 4,5-bisphosphate (PIP2); PIP3 activates AKT, which promotes MAPK activation in a Ras-dependent pathway. It has been reported that naringenin inhibits MM9 expression and secretion through diminution of p38, JNK, ERK, IKB, and PI3K/AKT phosphorylation as well as NF- κ B and AP-1-DNA binding. In addition, naringenin inhibits PKC cytoplasm-to-membrane translocation. Notably, naringenin induces p53 accumulation, leading to p21 expression. Then, p21 inhibits cyclin E/cyclin-dependent kinase 2 (CDK2) complex, which participates in proliferation. p53 accumulation results in naringenin-induced G0/G1 phase arrests. An important mechanism for the elimination of cancer cells is apoptosis. Naringenin induces apoptosis by increased cytochrome c (CYPc) release, as well as BCL2-associated X protein (Bax), BCL2-antagonist/killer 1 (Bak) and Caspase 3 (Cas3) elevation. Additionally, naringenin inhibited B-cell CLL/lymphoma 2 (Bcl-2) an antiapoptotic protein. Two-pore channels (TPCs) are members of the voltage-gated ion channel superfamily localized in acidic calcium (Ca^{2+}) stores and have been implicated in angiogenic processes. Vascular endothelial growth factor (VEGF) and its receptor vascular endothelial growth factor receptor (VEGFR) promotes TPC activation via nicotinic acid adenine dinucleotide phosphate (NAADP); then, Ca^{2+} is transported to the cytoplasm through TPCs, activating angiogenic signals. Naringenin inhibits VEGF angiogenesis induction blocking NAADP activation and NAADP/TPC association.

mechanism and the induction of cancer cell apoptosis are recognized as important targets in cancer therapy. In this sense, naringenin is known to induce apoptosis through the modification of Bcl-2 family of proteins involved in the apoptotic mitochondrial pathway, and the results from HepG2 cells showed that naringenin increases the activity of Cas3^[145]. Additionally, flow cytometry with Annexin V-FITC/PI staining demonstrated that the flavonoid increased apoptotic cells, confirming that naringenin induced apoptosis in HepG2 cells^[145]. The accumulated data suggest that naringenin, as well

as other compounds derived from plants, may induce apoptosis through the mitochondria-initiated death pathway^[148,150,151] (Figure 7).

On the other hand, two-pore channels (TPCs), are members of the voltage-gated ion channel superfamily and localize in acidic Ca^{2+} stores and have been implicated in different pathophysiological processes^[152,153]; TPC2 is expressed predominantly in late endosomes and lysosomes^[154]. It has been found that naringenin impairs TPC2-dependent biological activities, leading to antiangiogenic effects mediated by VEGF. Overall, these

data suggest that naringenin inhibition of TPC2 activity and the observed inhibition of the angiogenic response to VEGF are linked by impaired intracellular calcium signaling^[155]. Therefore, TPC2 inhibition is emerging as a key therapeutic step in the progression and metastatic potential of malignant cells. The identification of naringenin as an inhibitor of TPC2-mediated signaling provides a novel and potentially relevant tool for the advancement of anticancer research (Figure 7).

12-O-tetradecanoylphorbol-13-acetate (TPA) is widely utilized for studying the mechanisms of carcinogenesis^[156]. TPA upregulated MMP9 expression *via* PKC-dependent activation of the Ras/ERK signaling pathway, increasing invasiveness in cell lines^[157] and tumor metastasis^[158]. Importantly, Yen *et al*^[159] demonstrated that naringenin possesses a strong antiinvasive and antimigratory effect in TPA-activated hepatoma cells *via* the downregulation of PKC, epidermal growth factor (EGF), MAPK and PI3K/Akt signaling pathways, and NF-κB, AP-1 and MMP9 activities (Figure 6).

In conclusion, naringenin is highly effective in inhibiting cell proliferation and inducing apoptotic cell death in HepG2 cells and reducing invasion and metastasis. Therefore, it may be a promising candidate for hepatocarcinogenesis treatment.

NARINGENIN PROTECTS FROM LIVER DAMAGE INDUCED BY HEAVY METALS

Heavy metals can be classified according to their mechanism of action in redox-active metals or redox-inactive metals. Redox-active metals such as iron (Fe), copper (Cu), chromium (Cr), cobalt (Co), among others, develop redox cycling reactions, and they produce R[•] in biological systems, producing oxidative stress, LP, DNA damage and other deleterious effects. Meanwhile, redox inactive metals such as cadmium (Cd), arsenic (As) and lead (Pb) bind to proteins and sulfhydryl groups and induce GSH depletion^[160].

In this section, liver damage caused by redox-active and -inactive metals will be discussed.

Iron

Iron is an indispensable micronutrient for living organisms; it participates in oxygen transport, DNA synthesis and host defense, among others. Total body iron content ranges from 3 to 5 g, but its level increases due to diseases or intoxication^[161]. The liver is the main iron depot; thus, it is highly susceptible to damage induced by iron overload^[161,162].

Iron is captured by hepatocytes through transferrin receptor 1 (TfR1); during iron overload, its transcript is degraded and its synthesis is inhibited; however, iron uptake can be mediated by TfR2 even with high iron levels^[161,162]. When iron binding capacity or transferrin saturation is exceeded, non-transferrin bound iron (NTBI) is elevated, and then it is transported into hepatocytes through divalent metal transporter 1

(DMT1). In hepatocytes, iron is incorporated into the ferritin molecule that preserves iron bioavailability^[162] (Figure 8).

One of the most reactive R[•] is O₂[•]; under normal conditions, it is produced in the respiratory chain by NADP oxidase, and then, it is neutralized by SOD, generating H₂O₂. Intracellular iron is released from ferritin by O₂[•]; next, free iron reacts with H₂O₂ in the Fenton reaction, generating high amounts of OH[•], and in turn, OH[•] attracts the double bonds of DNA bases. In the case of lipids, free iron produced LP forming ROO[•]^[160]. These processes produce hepatocyte damage, such as mitochondrial dysfunction and apoptosis, which results in the recruitment of Kupffer cells that phagocytose damaged hepatocytes, leading to the release of proinflammatory and profibrogenic cytokines that activate HSCs; as a result, hepatic fibrosis ensues^[161-163].

The Fenton reaction is inhibited by flavonoids with 3',4'-catechol, 4-oxo, and 5-OH arrangements. Chelating complexes with cations may form between the 5-OH and 4-oxo group or between the 3' - and 4'-OH^[29]. Using an electrospray mass spectrometry study, it was observed that naringenin can form complexes with Fe(III) through its 4-oxo and 5-OH groups; in addition, this flavonoid is oxidized in the presence of metal ions, which are consequently reduced^[164]. Furthermore, naringenin was investigated for its ability to suppress the Fenton reaction characteristic of the iron-ATP complex; the flavanone interfered with the voltammetry catalytic wave associated with the iron-ATP complex in the presence of H₂O₂ because it has the arrangement of 4-oxo and 5-OH that is indispensable for this inhibition^[165] (Figure 8).

In an experiment where the modulation of DNA integrity in Fenton's system by naringenin was studied, it was shown that the glycoside protected DNA from damage caused by OH[•] generated during the Fenton reaction; naringenin blocks the Fenton reaction by iron chelation rather than by antioxidant mechanisms or reduction of Fe(III) to Fe(II), and as a result, damage is prevented^[166]. In another study, the isolated mouse liver mitochondrial fraction was incubated with naringenin before Fe(III) loading, generating elevations in LP, protein carbonyl content and DNA oxidation, while iron overload decreased GSH levels and GST, GPx, CAT and SOD activities; however, pretreatment with naringenin inhibited these iron effects^[167]. Iron exposure in HepG2 cells caused a decline in cell survival, a time-dependent increase in DNA oxidation, an elevation in DNA strand breaks, a high level of LP, and a depletion of GSH as well as decreases in GPx, CAT and SOD levels. Notably, the pretreatment of HepG2 cells with naringenin resulted in cell survival induction, DNA damage prevention, improvement in the antioxidant system and the inhibition of iron-mediated cellular damage^[168] (Figure 8).

Regarding naringenin's effects on iron-induced damage *in vivo*, it has been reported that the flavanone protected against iron-induced neurotoxicity in the

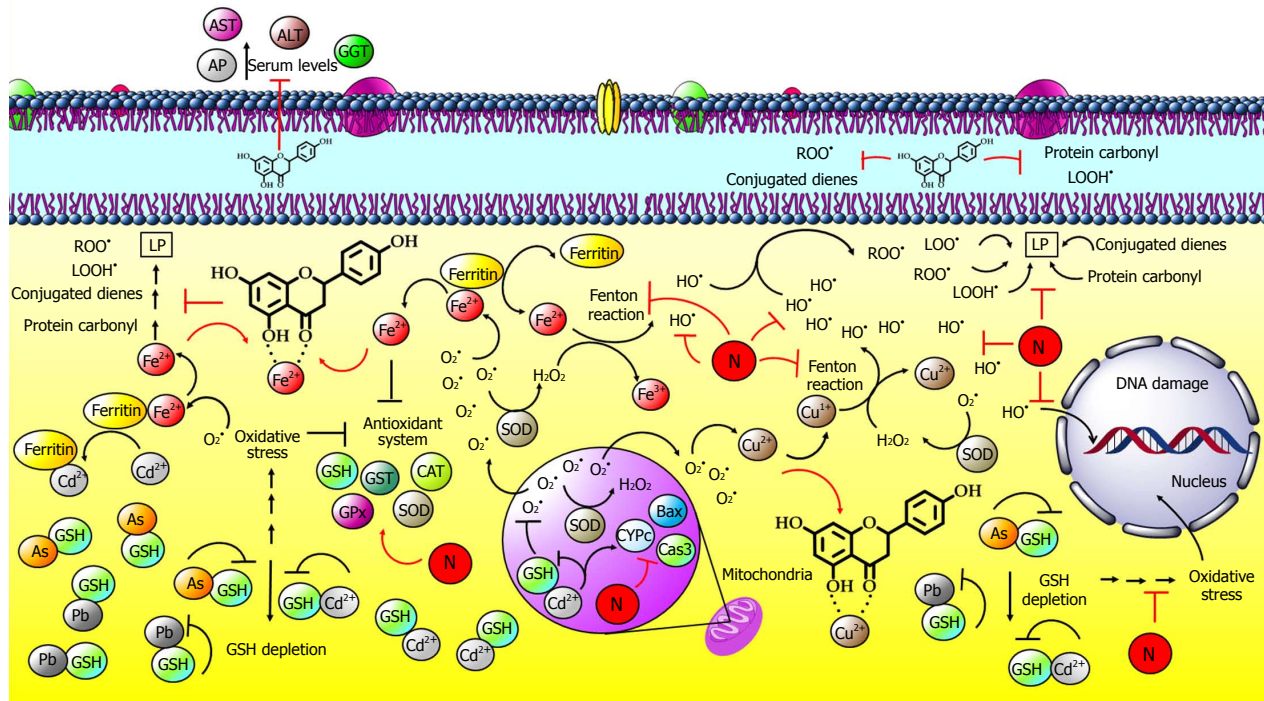


Figure 8 Naringenin inhibits hepatic damage induced by heavy metals. Heavy metals can be classified according to the mechanism of action in redox-active metals such as iron (Fe) and copper (Cu) or redox-inactive metals such as cadmium (Cd), arsenic (As) and lead (Pb). One of the main free radicals is superoxide radical (O_2^-); normally, it is produced by NADP oxidase, and then, it is neutralized by superoxide dismutase (SOD), generating hydrogen peroxide (H_2O_2). Intracellular Fe is released from ferritin by O_2^- ; next, free Fe reacts with H_2O_2 in the Fenton reaction, generating high amounts of hydroxyl radicals (OH^-). After that, OH^- attacks double bonds of DNA bases. In the case of lipids, free Fe produces lipid peroxidation (LP) through peroxy radicals (ROO'), producing lipid hydroperoxides ($LOOH'$), conjugated dienes and protein carbonyl. Regarding Cu, once inside the hepatocyte, Cu ion (Cu^{2+}), can be reduced to cuprous ion (Cu^{1+}) when reacting with O_2^- ; then, it mediates H_2O_2 decomposition in OH^- via the Fenton reaction. These processes result in hepatocyte and liver damage. Naringenin can chelate these metals, preventing their participation in the Fenton reaction; naringenin also inhibits oxidative stress by its antioxidant capacity and by promoting the endogenous antioxidant system. On the other hand, redox-inactive metals such as Cd, arsenic (As) and lead (Pb) form complexes with thiol groups, such as glutathione (GSH), in the cytoplasm and mitochondria. GSH level reduction, GSH inactivation, and GSH system deregulation increase metal toxicity. In addition, Cd can replace Fe and Cu in ferritin or apoferritin; thus, free Fe and Cu ions cause oxidative stress via the Fenton reactions and elevation of BCL2-associated X protein (Bax), Caspase 3 (Cas3) and cytochrome (CYPc) proapoptotic proteins. Naringenin improves the antioxidant system by increasing SOD, catalase (CAT), glutathione peroxidase (GPx), glutathione transferase (GST) enzymes and GSH levels.

cerebral cortex of Wistar rats. After four weeks of iron administration, LP and protein oxidation were increased, but SOD, CAT, total thiols and ascorbic acid were decreased. Significant decreases in acetylcholinesterase and Na^+/K^+ -ATPase activities were also shown, along with a substantial rise in NO levels. Co-administration with naringenin blocked the development of oxidative stress and improved antioxidant enzyme activities in the cerebral cortex^[169]. In another work, the effect of naringenin on iron-induced hippocampus damage was investigated: iron administration for 28 d induced an impairment of the anxiogenic-like behavior and induced purinergic and cholinergic dysfunctions with oxidative stress-related disorders on mitochondrial function in the rat hippocampus, but naringenin was able to restore those parameters^[170] (Figure 8).

As seen, naringenin and naringin have the ability to block iron-induced oxidative stress; these natural compounds are able to chelate metal ions such as iron; thus, free iron is not available for the Fenton reaction, and therefore, OH^- generation is blocked, as is oxidative stress. The chelation capacity is given in the naringenin molecule by the 4-oxo and 5-OH groups, which probably

represent the place where an iron ion is conjugated. In the absence of this arrangement, some flavonoids do not have chelating capacity or are less effective^[164-166]. This structure-activity relationship indicates that naringenin and naringin can act as antioxidants or as chelators, depending on the hepatotoxic agent employed.

Copper

Copper is a redox active metal, and an imbalance in its metabolism produces disorders such as Wilson's disease, Indian childhood cirrhosis or endemic Tyrolean infantile cirrhosis, which share the common end of cirrhosis due to excessive copper accumulation; another problem is copper toxicity caused by copper poisoning or dietary copper toxicity^[160,171,172]. Like iron, copper exerts its hepatotoxic effects by oxidative stress generation; this is a consequence of its redox reactivity, triggering events that end in liver damage.

Like iron, copper is stored in the liver; it is introduced into the hepatocyte through the high-affinity human copper transporter (hCtr1)^[173]. Once inside the hepatocyte, cupric ion (Cu(II)), can be reduced to cuprous ion (Cu(I)) when reacting with O_2^- , ascorbic

acid or GSH; meanwhile, Cu(I) mediates H₂O₂ decomposition in OH[•] *via* the Fenton reaction^[160]. The formed OH[•] reacts with lipids, proteins and DNA, as well as with practically any biological molecule, generating lipid radicals, protein carbonyls or DNA strand breaks and oxidation of bases; in fact, copper is more powerful than iron in enhancing DNA breakage^[160,174]. Furthermore, copper binds directly to free thiols of cysteines, which can result in oxidation and subsequent crosslinks between proteins, leading to impaired activity of target enzymes^[171]. In addition, copper induces LP and 4-hydroxy-2-nonenal (HNE) formation. Importantly, HNE may increase the phosphorylation of JNK and p38, AP-1 activity and the expression of Col-I and TGF-β^[160], resulting in the exacerbation of fibrosis (Figure 8).

As previously mentioned, naringenin may act as a metal chelator. In this regard, two studies have reported the chelating capacity of the flavonoid on copper. Fernández *et al.*^[164] showed that naringenin, at various stoichiometries (metal: flavonoid) with copper, 1:1, 1:2, 2:2 and 2:3, produces several complexes, preferably with Cu(II). Additionally, comparing the 4-oxo and 5-OH arrangement with the 4-oxo and 3-OH arrangement, the first one seems to favor copper chelation^[164]. Meanwhile, Mira *et al.*^[175] reported that naringenin has higher reducing capacity for copper ions than for iron ions. Additionally, the copper reducing activity seems to depend largely on the number of OH groups. In addition, naringenin chelates Cu²⁺ at pH 7.4 and pH 5.5 between the 5-OH and the 4-oxo groups, producing 7.1 ± 1.1 mmol Cu⁺/mmol naringenin, indicating that a large number of copper ions per molecule of flavonoid were chelated^[175] (Figure 8).

It has been shown that copper induces the oxidation of low-density lipoproteins (LDL); as a consequence, PUFAs in the lipoprotein are rapidly converted to LOOH and aldehydic breakdown products^[160,176,177]. It has been reported that when freshly isolated human LDL (50 µg protein/mL) was incubated with 2 µmol/L Cu²⁺ at 37 °C, naringenin (25 µmol/L) slightly inhibited LDL oxidation, but prenylflavanones (25 µmol/L) such as 8-geranyl naringenin, 6-prenyl naringenin, 8-prenyl naringenin and 6,8-diprenyl naringenin effectively inhibit LDL oxidation dienes formation. Then, Cu²⁺-mediated LDL oxidation was evaluated by measuring TBARS levels; the results showed that prenylflavanones significantly inhibited TBARS formation and were ranked as follows: 8-geranyl naringenin > 6,8-diprenyl naringenin, 6-geranyl naringenin, 8-prenyl naringenin > 6-prenyl naringenin^[177] (Figure 8).

As seen, naringenin and its derivatives can inhibit the first steps of copper-induced damage by preventing the Fenton reaction and by preventing lipid and protein oxidation.

Cadmium

Unlike iron and copper, cadmium is a redox inactive metal; although it does not directly form R[•], it can

induce oxidative stress in other ways. In addition, there is no mechanism for cadmium excretion in humans; thus, cadmium accumulates in tissues indefinitely^[160,178].

Cadmium is absorbed through the intestines, and in the liver, DMT1, ZIP8 and ZIP14 are responsible for Cd uptake into hepatocytes^[178]. Once inside hepatic cells, cadmium follows two pathways to exert liver damage: (1) Cadmium forms complexes with thiol groups of proteins or small peptides, such as GSH, in the cytoplasm and mitochondria. GSH is the first line of defense against cadmium-induced damage; thus, GSH level reduction, inactivation, and GSH system deregulation increase cadmium toxicity. In mitochondria, thiol group inactivation causes oxidative stress, mitochondrial permeability transition, and mitochondrial dysfunction^[178,179]. And (2) Cadmium can replace iron and copper in ferritin or apoferritin; thus, free iron and copper ions readily cause oxidative stress *via* the Fenton reaction^[160,178]. Thereby, although cadmium is unable to generate R[•] directly, indirect formation of ROS, O₂[•], OH[•] and NO has been reported. In addition, increased LP levels and antioxidant system deregulation has been observed during cadmium liver damage^[160,178,179]. Because of oxidative stress induced from cadmium intoxication, Kupffer and HSCs cells can be activated, and thus, a large number of inflammatory and cytotoxic mediators can be produced^[178,179] (Figure 8).

One of the first reports on the beneficial effect of naringenin on damage induced by cadmium was performed in kidney, and after 4 wk of CdCl₂ administration (5 mg/kg/d), TBARS, LOOH and protein carbonyl levels were elevated. Conversely, total sulphydryl groups, GSH, vitamin C and vitamin E levels, as well as SOD, CAT, GPx, GST and GR, and glutathione-6-phosphate dehydrogenase (G6PD) activities were decreased. Co-administration of naringenin (25 and 50 mg/kg daily) resulted in the prevention of Cd-induced LP and in the restoration of the endogenous antioxidant system. Histopathological analysis showed that naringenin markedly reduced CdCl₂ toxicity and preserved the normal histological architecture of renal tissue^[180].

Later, Renugadevi *et al.*^[65] reported that cadmium (5 mg/kg) administered orally for 4 wk induced liver damage. Increased activities of serum AST, ALT, AP, LDH, GGT and bilirubin were found. Furthermore, LP and protein carbonyl contents were elevated. Antioxidant enzymes such as SOD, CAT, GPx, and GST as well as GSH, vitamin C and vitamin E concentrations were diminished. Naringenin (50 mg/kg) significantly prevented the elevation of serum hepatic marker enzymes. Additionally, the flavonoid significantly reduced LP and restored antioxidant defense levels. The histopathological studies showed that naringenin preserved normal histological architecture of the tissue^[65]. The same working group reported that naringenina plus vitamins C and E improved the altered biochemical and histopathological changes in the liver of Cd-intoxicated

rats to a greater extent than naringenin or vitamins alone^[72] (Figure 8).

In another work, naringenin (4 and 8 mg/kg) was orally administered to mice 30 min before oral administration of CdCl₂ (12 mg/kg) for 11 consecutive days. Cotreatment with naringenin significantly prevented disarrangement in body and organ weights, hematological profiles, serum and hepatic altered biochemical parameters in Cd-intoxicated mice^[181].

Naringin also displays protective effects in cadmium-induced damage to HepG2 cells, where the glycoside maintained redox homeostasis, mitochondrial membrane potential, reduced Cas3 and CYPc and reduced apoptosis by regulating the Bax/Bcl2 ratio. Moreover, naringin prevented diminution of protein thiol levels, SOD, GST and CAT activities, and LP development through increasing Nrf2 and metallothionein (MT)^[182] (Figure 8).

Most evidence concurs that naringenin prevents cadmium-induced liver damage by protecting enzymatic and non-enzymatic antioxidant systems and by safeguarding GSH thiol groups. The antioxidant actions of naringenin may also be associated with its ability to chelate heavy metals, thus preventing the formation of ROS and with its ability to increase Nrf2. These data show that naringenin is effective in preventing damage induced by cadmium.

Arsenic

Arsenic is a highly distributed metal that is found in organic and inorganic forms; both forms are toxic, although inorganic arsenic is more toxic than organic arsenic^[160]. This metal is metabolized by reduction and methylation reactions, which are catalyzed by glutathione-S-transferase omega-1(GSTO1) and arsenic (III) methyltransferase (AS3MT); it has been reported that during arsenic metabolism, high amounts of reactive species are generated^[160,183].

Like cadmium, arsenic induces cellular damage through binding to sulphydryl groups and inducing mitochondrial dysfunction. Cadmium produces oxidative stress-generating species such as O₂[•], singlet oxygen (¹O₂), ROO[•], NO, H₂O₂, dimethylarsinic peroxy radical [(CH₃)₂AsOO[•]] and dimethylarsinic radical [(CH₃)₂As[•]]^[160,184]. In general, an oxidative environment results in GSH depletion, LP elevation, protein oxidation, DNA damage, morphologic changes in mitochondrial integrity and a rapid decline of mitochondrial membrane potential^[160,184,185]. Oxidative stress induces hepatocyte apoptosis as well as total bilirubin, ALT, and AST elevation and liver damage^[183] (Figure 8).

Since arsenic induces damage *via* oxidative stress, naringenin has been studied in arsenic-induced liver damage. Arsenic administration (2 mg/kg) for 28 d to rats or 14 d (3 mg/kg) to mice produced elevations in AST, ALT and AP activities, high LP markers, hepatic GSH depletion and reductions in SOD, CAT, GPx, GST and GR activities. In addition, arsenic exposure produced DNA fragmentation. However, the

simultaneous administration of naringenin prevented hepatic injury by arsenic^[68,74].

Jain *et al*^[73] reported that NaAsO₂ administration (8 mo) to male Wistar rats induced high levels of ROS in blood and liver and increased levels of hepatic LP; simultaneously, the endogenous antioxidant system was attenuated, leading to a reduction of GSH levels and to the inhibition of GPx, GST, SOD and CAT activities in liver. Once liver damage was established, naringenin was administered for two weeks; the flavanone was able to reverse oxidative stress, since ROS and TBARS levels were diminished. Moreover, the enzymatic antioxidant system was restored by naringenin^[73].

Naringin also has been shown to prevent liver and kidney damage induced by NaAsO₂ (5 mg/kg); the glycoside inhibited increased serum levels of ALT and AST as well as prevented SOD and GSH depletion. In addition, naringin downregulated the expression of TGF-β, Cas3 and TNF-α in kidney^[186] (Figure 8).

In summary, naringenin and naringin display hepatoprotective effects in arsenic-induced liver injury mainly by improving the endogenous antioxidant system and probably by their chelating effect.

Lead

The mechanism of action of lead toxicity is similar to those of cadmium and arsenic. This heavy metal does not generate free radicals directly; instead, lead deactivates antioxidant pools by binding to sulphydryl groups of protein or peptides. For instance, lead-GSH interaction inactivates GSH antioxidant activity; moreover, lead reduces GSH levels by blocking GR, GSG and δ-aminolevulinic acid dehydratase (ALAD), an enzyme in charge of preserving the GSH/GSSG balance^[160,187-189]. The inhibition of the antioxidant GSH system produces R[•] such as O₂[•], ¹O₂ and ROO[•], which destabilize cellular membranes through LP processes, resulting in mitochondria and DNA damage leading to p53 upregulation, an imbalance of Bax/Bcl-2 and apoptosis. After oxidative damage caused by lead, proinflammatory pathways are activated, exacerbating preexisting liver damage^[187,188] (Figure 8).

Two reports have been published dealing with naringenin's effects on lead-induced liver injury. Wang *et al*^[58] and Ozkaya *et al*^[144] reported that rats treated with lead acetate in drinking water showed significant increases in MDA and depletion of GSH levels and GPx activity. Elevated levels of ALT and AST in serum and decreased SOD activity in liver were also shown^[58]. Furthermore, histopathological results showed that the livers of lead-intoxicated rats had periportal cell infiltration, sinusoidal congestion, hepatic steatosis, and capsular fibrosis^[144]. Naringenin administration (50 mg/kg) prevented the disarrangement of most parameters studied, and histopathological abnormalities such as necrosis, hydropic degeneration, and hepatic cord disorganization were attenuated by naringenin treatment^[58,144] (Figure 8).

These studies show that naringenin has hepatoprotective effects against lead-induced liver damage; however, more studies are needed to further understand the naringenin mechanism of action.

ANTIVIRAL PROPERTIES OF NARINGENIN

The study of hepatovirus has been an important issue in hepatology research in the last four decades. HBV and HCV are most studied, as they produce chronic liver damage, leading to cirrhosis and HCC^[190]. As global causes of liver cirrhosis, HBV accounts for 30%, HCV for 28%, alcohol for 27% and others for 14% of cirrhosis cases. The etiology of liver cancer is HBV (45%), HCV (26%), alcohol (20%), and others (39%)^[3]. Therefore, research on treatment for these infections is important for the prevention/reversion of chronic liver diseases.

HCV is a virus belonging to the Flaviviridae family; its genome consists of a positive-sense single-stranded RNA. Hepatocytes are the major site of HCV replication, but peripheral blood mononuclear cells and lymph nodes are also natural HCV targets^[3,191,192].

HSC machinery processes three structural HCV proteins (core, E1 and E2), an ion channel protein (p7) and six non-structural proteins (NS) (NS2, NS3A, NS4A, NS4B, NS5A and NS5B)^[191]. HCV adopts an icosahedral structure with a lipid envelope and glycoproteins E1 and E2 immersed in the envelope. Underneath the envelope is the nucleocapsid, composed of multiple copies of core forming the internal viral coat that encapsulates the genomic RNA^[192] (Figure 9).

E1 and E2 are responsible for receptor binding and HCV entry into hepatocytes. Among the receptors for HCV, CD81 is probably the best characterized; low-density lipoprotein receptor (LDLR), scavenger receptor class B type I (SR-B1), human scavenger receptor, and glycosaminoglycans may also act as receptors for HCV^[191,192]. After binding to its receptor, HCV endocytosis is activated, leading to the uptake of HCV particles across the cell plasma membrane^[191]. After endocytosis, nucleocapsids are deposited into the cytoplasm *via* a low pH dependent mechanism; then, the nucleocapsids are uncoated, and their RNA is released^[191,192] (Figure 9).

Genomic RNA translation is mediated by an internal ribosome entry site (IRES) binding to the ribosome; then, the HCV polyprotein is produced in the rough endoplasmic reticulum (RER) membrane, and after that, viral proteins remain associated with intracellular membranes and gave rise to a seemingly ER-derived membranous web where NS proteins form the replication complex (RC)^[191,192]. Within the RC, the positive-stranded RNA genome is used as a template for synthesis of negative-stranded RNA, which in turn serves as a template for new positive-stranded synthesis. New viral RNA is encapsulated within multiple copies of the core to form the nucleocapsid, and then, it acquires envelope; HCV virions are exported out the cell ready to infect

healthy hepatocytes^[192] (Figure 9).

An interesting phenomenon is that HCV circulates in the blood in the form of a lipoprotein complex called lipoviroparticle (LVP); it has been reported that HCV may be associated with lipoproteins such as VLDL and low-density lipoprotein (LDL). Notably, the binding of lipoviroparticle to receptors as LDLR or SR-B1 enables the infectivity of HCV and its escape from the humoral immune response^[190-193]. A relationship between the virion production process and lipoproteins, cholesterol, triglycerides and fatty acids has been suggested. HCV assembly appears to occur on lipid droplets, and the core protein clearly coats the surface of this organelle, but the lipid droplet not only serves as a site for viral assembly but also supplies lipoproteins that complex with HCV particles^[191] (Figure 9).

It has been reported that HCV core protein is bound to apolipoprotein (Apo) B-100 and, therefore, to VLDL in HCV secreted by infected cells in the JFH1/Huh7.5.1 full viral life-cycle model. In addition, the HCV-VLDL complex is actively secreted by the cells; moreover, the colocalization of HCV's core and ApoB100 was found in the cytoplasm of infected cells. Interestingly, silencing ApoB production by a SureSilencing shRNA in the cell downregulates HCV core protein secretion and HCV-positive strand RNA secretion^[193] (Figure 9).

Naringenin was used as an ApoB100 inhibitor because the flavonoid reduces microsomal triglyceride transfer protein (MTP) and enzyme acyl-coenzyme A (CoA): cholesterol acyltransferase (ACAT) activity, whose expression is indispensable for ApoB synthesis^[11,193]. The results showed that naringenin inhibits the secretion of HCV core and HCV-positive stranded RNA, as well as HCV secretion, more than ApoB10 silencing by the SureSilencing shRNA. Nevertheless, intracellular levels of HCV-positive strand RNA and intracellular HCV core protein expression remained unchanged; despite this, the ability of the secreted virus to infect cells was strongly inhibited following naringenin treatment. This inhibition by naringenin was mediated by a reduction in MTP activity and by the transcriptional inhibition of 3-hydroxy-3-methylglutaryl CoA reductase (HMGCR) and acyl-coenzyme A: Cholesterol acyltransferase (ACAT)^[193] (Figure 9).

Inhibition of HCV secretion by naringenin is mediated by a reduction in ApoB100 synthesis because naringenin regulates proteins related with ApoB. Normally, cholesterol is synthesized in an HMGCR-dependent pathway which is the rate-limiting enzyme for cholesterol synthesis; then, cholesterol is converted to cholesteryl esters (CEs) by ACAT. CEs are very important to VLDL and LDL assembly. Another important element to VLDL and LDL assembly is MTP, which plays a key role in ApoB100 secretion by catalyzing the transfer of lipids to the nascent ApoB100; if ApoB-MTP binding is inhibited, ApoB is predicted to undergo degradation^[11].

Naringenin improves metabolic imbalance by reducing the activity and mRNA levels of HMGCR, which explains

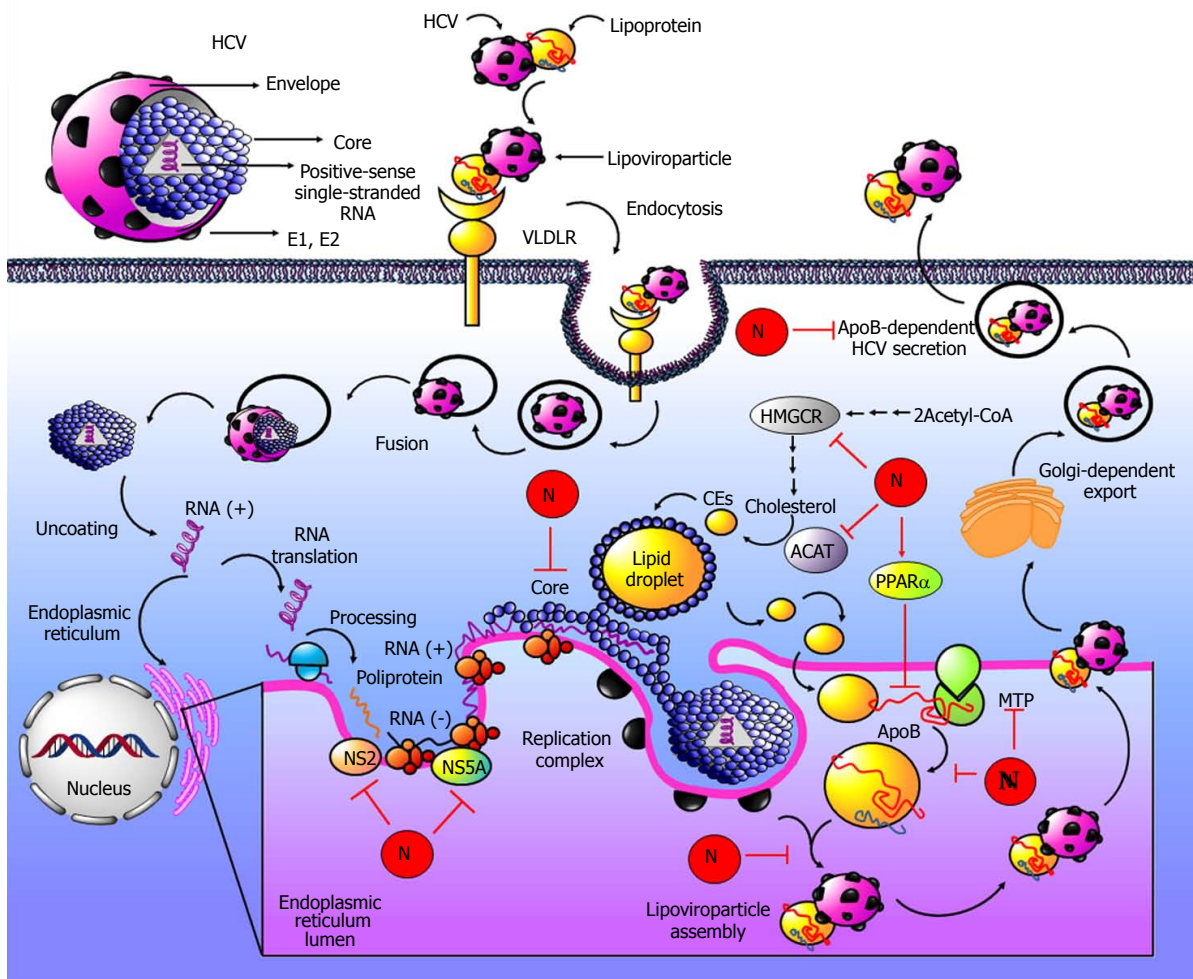


Figure 9 Antiviral properties of naringenin. The Hepatitis C virus (HCV) genome consists of a positive-sense single-stranded RNA. HCV adopts an icosahedral structure with a lipid envelope and glycoproteins E1 and E2 immersed in the envelope. Underneath the envelope is the nucleocapsid, which is composed of multiple copies of core forming the internal viral coat that encapsulates the genomic RNA. HCV may be associated with lipoproteins such as very-low density lipoprotein (VLDL), forming a lipoprotein complex called lipoviroparticle. Binding of lipoviroparticle to very-low density lipoprotein receptor (VLDLR) results in virus endocytosis; after that, nucleocapsids are deposited into the cytoplasm. Then, nucleocapsids are uncoated, and the RNA is released. The genomic RNA is translated to the endoplasmic reticulum when HCV polyprotein is produced. The positive-stranded RNA genome is used as a template for synthesis of negative-stranded RNA; this new viral RNA is encapsulated within multiple copies of the core to form the nucleocapsid, and then, it acquires envelope and HCV virions, which are exported out of the cell in a Golgi-dependent manner. Naringenin inhibits the secretion and assembly of HCV through regulating lipid metabolism via 3-hydroxy-3-methylglutaryl CoA reductase (HMGCR), and acyl-coenzyme A: cholesterol acyltransferase (ACAT) inhibition. Cholesterol is synthesized in an HMGCR-dependent pathway; it is the rate limiting enzyme for cholesterol synthesis, and then, cholesterol is converted to cholestryl esters (CEs) by ACAT. CEs are very important to VLDL assembly. In addition, microsomal triglyceride transfer protein (MTP) catalyzes the transfer of lipids to the apolipoprotein (Apo) B-100 ApoB100; if the ApoB-MTP binding is inhibited, VLDL assembly is inhibited. Reduction in the bioavailability of CEs, triglycerides and cholesterol by naringenin reduces MTP activity and apoB-MTP binding. In addition, naringenin decreased intracellular triglycerides through peroxisome proliferator activated receptor alpha (PPAR α), a regulator of lipid metabolism. Through these mechanisms, naringenin leads to a reduction in VLDL assembly and to the inhibition of ApoB-dependent HCV secretion. Additionally, naringenin inhibits viral NS5A protein, a multifunctional HCV nonstructural protein. Furthermore, naringenin could be an NS2 protease and core protein inhibitor.

the finding that the flavanone can decrease hepatic cholesterol. In addition, naringenin possesses the ability to reduce the CE mass and cholesterol esterification by decreasing ACAT1 and ACAT2 activity^[11,194-196]. The mRNA levels of MTP are significantly reduced by naringenin; therefore, ApoB-MTP binding is inhibited, and consequently, ApoB is degraded. In addition, although ApoB mRNA levels are not affected by naringenin, the protein does not accumulate in hepatocytes, suggesting that naringenin promotes the degradation of ApoB. Thereby, the reduction in the bioavailability of CEs, triglycerides and cholesterol by naringenin reduces

MTP activity and ApoB-MTP binding, leading to ApoB degradation^[11,197-203] (Figure 9). This seems to be the primary mechanism by which naringenin blocks ApoB secretion and VLDL and LDL assembly and, therefore, the inhibition of ApoB-dependent HCV secretion.

In addition, the same group^[204] reported that naringenin treatment did not lead to the intracellular accumulation of infectious HCV particles compared with brefeldin A (BFA), a toxin known to disrupt HCV mature Golgi-dependent export; hence, naringenin blocks the assembly of HCV prior to viral egress. The inhibition of MTP and BFA treatment in JFH1-infected Huh7.5.1 cells

blocks the accumulation of intracellular infectious HCV particles, indicating that MTP activity is essential for HCV assembly. Treatment of JFH1-infected Huh7.5.1 cells with naringenin (MTP inhibitor) and BFA decreased the accumulation of infectious particles, suggesting that the flavonoid inhibits the assembly of HCV LVP^[204] (Figure 9).

MTP inhibition can lead to lipid accumulation and steatosis; however, treatment with naringenin decreased intracellular triglycerides, and this was mediated by activation of peroxisome proliferator-activated receptor alpha (PPAR α), a regulator of lipid metabolism. Naringenin and WY14643 (a classical PPAR α agonist) were compared to reduce ApoB and virus production in the HCV model. The results showed that both the flavonoid and the PPAR α agonist caused a significant inhibition of MTP activity and ApoB secretion, as well as a significant inhibition of HCV RNA secretion without affecting the intracellular levels of the HCV core protein. In addition, the treatment with naringenin led to a rapid 1.4 log reduction in secreted HCV in cell culture, but this effect was reversible by PPAR α inhibitor treatment^[204]. In summary, naringenin inhibits the assembly and long-term production of infectious HCV particles through a PPAR α -mediated mechanism that includes the inhibition of MTP and the inhibition of lipid accumulation (Figure 9).

Interestingly, Khachatoorian *et al*^[205] compared the antiviral effects of naringenin, quercetin and catechin. The evidence demonstrated that in an HCV system, naringenin significantly reduced intracellular viral protein translation as well as viral protein production during one viral life cycle; however, quercetin showed better results, but the infectious virion secretion was not inhibited by any flavonoid. Naringenin significantly blocked infectious virion assembly; in this case, naringenin was more effective than quercetin^[205].

NS5A is a multifunctional NS protein and viral RC component; it participates in HCV genome replication, viral protein translation, virion assembly, and viral secretion^[191,192,205]. NS5A mRNA and protein levels were measured, finding that naringenin reduced both parameters. Then, in a cell culture-based bicistronic reporter system, catechin, naringenin, and quercetin were tested to measure levels of viral IRES-mediated translation; all bioflavonoids significantly decreased IRES-mediated translation, but quercetin completely blocked NS5A-augmented IRES activity in contrast to catechin and naringenin, which demonstrated only mild inhibition. According to these results, quercetin demonstrated a marked decrease in HSP70 expression in treated cells. A slight decrease in HSP70 was seen with naringenin and catechin treatments. The complex of HSP70 with NS5A, NS5A-HSP70, is important for viral protein production; therefore, the disruption of this complex results in a marked decrease of viral protein synthesis^[206,207] (Figure 9).

On the other hand, *in silico* studies have been carried out to evaluate naringenin activity on the HCV particle. Mathew *et al*^[208] in 2014 reported a docking

interaction study between the 3D structure of capsid core protein of HCV-genotype 3 (G3) (Q68867) and its subtypes 3b (Q68861) and 3g (Q68865) from north India and naringenin. The results indicated that the flavonoid exhibited five, seven and nine H-bond interactions within the core protein of HCV-G3, subtypes 3b and 3g, respectively. In HCV-G3, naringenin formed H-bonds individually with GLU69 and ASN115 and three H-bonds, with SER103 exhibiting the highest interaction energy (-129.636 kcal/mole). In the case of HCV-3b, naringenin formed three H-bonds with TRP90, two with GLN86, and one with GLY84 and TRP93, with an interaction energy of -145.682 kcal/mole. Finally, the flavanone binds to HCV-3g through two H-bonds with TRP73 and GLY77 and individually with ASN85, TYR78 and TRP73 with an interaction energy of -159.483 kcal/mole^[208]. These results suggest that naringenin binds to the core protein of three important HCV genotypes in India, especially to HCV-3 based on their interaction energies; this ability of naringenin to bind core protein could be involved in the inhibition of viral particle assembly that was previously reported. Naturally, *in vivo* studies are needed to confirm predictions suggested by this docking study (Figure 9).

NS2 is a transmembrane protein of 21-23 kDa that is not required for RNA replication but that is vital to produce infectious viruses *in vitro*, and it acts as an apoptosis inhibitor^[191,209]. Using a docking analysis, it has been identified that naringenin could be an NS2 protease inhibitor. Molecular rigid docking of the modeled NS2 protease was performed with the naringenin molecule. The flavanone had a binding energy of -7.97 kcal/mol when interacting with amino acids such as LEU9, VAL27, LEU54, ASP6, ALA5, ILE31, ALA30, LEU2, PHE33, ILE34, VAL44, ALA47, ALA43, and LEU46. In addition, naringenin possesses lower binding energy than the commercially available drugs such as eltrombopag (-5.07 kcal/mol), ribavirin (-5.89), and telbivudine (-6.39 kcal/mol)^[209] (Figure 9). Therefore, naringenin appears to be a strong NS2 protein inhibitor and, thus, prevents efficient HCV infection.

More *in vivo* and *in vitro* studies are needed to further investigate the effectiveness of naringenin to fight virus infection in the liver and to elucidate the action(s) mechanism(s) involved in such protection.

ANTIDIABETIC EFFECT OF NARINGENIN

In addition to its antioxidant, scavenger, anti-inflammatory, antiviral and antifibrotic properties, naringenin possesses antidiabetic effects. It has been reported that, in diabetic rats, the flavonoid reduced diabetic markers through PPAR γ and glucose transporter type 4 (GLUT4) and increased their gene and protein expression levels in pancreas^[210]. In the liver, naringenin increased glycogen content, decrease activities of glycogen phosphorylase and glucose-6-phosphatase^[211] and ameliorated diabetes-induced hepatotoxicity^[212,213]. For more information see

Nyane *et al*^[214].

NARINGENIN SAFETY AND TOXICITY

The first study about the toxicity of naringenin was carried out in 1996, and it was found that in a model system of isolated rat liver nuclei, the flavonoid induced a concentration-dependent peroxidation of nuclear membrane lipids concurrent with DNA strand breaks^[215]. It has been reported that the flavonoid can be oxidized to form naringenin phenoxy radicals^[216] and that the medium lethal dose (LD50) is > 5000 mg/kg^[217]. Interestingly, embryos exposed to naringenin with hydroxyurea were significantly protected from growth and developmental retardation, and abnormalities induced by hydroxyurea^[218]. Only a few studies on the safety, teratogenicity and toxicity of naringenin have been published, therefore use of this flavonoid in the clinical setting should be cautious.

CONCLUSION

Naringenin displays poor direct antioxidant properties as a free radical scavenger; however, due to its ability to induce the endogenous antioxidant system by upregulating Nrf2, this flavanone exerts important effects to maintain the normal redox of the cell, even in disease conditions where free radicals are generated as a mechanism of damage. In this scenario, throughout this review, we have described the benefits of this flavonoid in many types of liver damage in which oxidative stress plays a crucial role as causative agent. Of note, the anti-inflammatory activity of naringenin by blocking NF- κ B, affords protection or relief to liver pathologies as inflammation is a common cause of damage. Moreover, naringenin displays a multitarget effect to fight fibrosis through both canonical and non-canonical TGF- β pathways and by regulating metalloproteinase activity. Additionally, this abundant citrus flavonoid has shown anticancer and antiviral activities. Even though NAR has disadvantages such as its low bioavailability, there are pharmaceutical formulations that can solve this problem. Given the evidence provided in this review, it is concluded that naringenin is a useful natural product for the treatment of many liver diseases by its antioxidant capacity, anti-inflammatory abilities, antifibrogenic properties, fibrolytic actions and anticancer and antiviral properties. However, more basic and clinical studies are needed to further support the use of this flavonoid in humans.

REFERENCES

- 1 Bataller R, Brenner DA. Liver fibrosis. *J Clin Invest* 2005; **115**: 209-218 [PMID: 15690074 DOI: 10.1172/JCI24282]
- 2 Pellicoro A, Ramachandran P, Iredale JP. Reversibility of liver fibrosis. *Fibrogenesis Tissue Repair* 2012; **5**: S26 [PMID: 23259590 DOI: 10.1186/1755-1536-5-S1-S26]
- 3 Muriel P. The liver: General aspects and epidemiology. In Muriel P. Liver pathophysiology: therapies & antioxidants. Waltham, MA: Elsevier, 2017: 3-22
- 4 Lozano R, Naghavi M, Foreman K, Lim S, Shibuya K, Aboyans V, Abraham J, Adair T, Aggarwal R, Ahn SY, Alvarado M, Anderson HR, Anderson LM, Andrews KG, Atkinson C, Baddour LM, Barker-Collo S, Bartels DH, Bell ML, Benjamin EJ, Bennett D, Bhalla K, Bikbov B, Bin Abdulhak A, Birbeck G, Blyth F, Bolliger I, Boufous S, Bucello C, Burch M, Burney P, Carapetis J, Chen H, Chou D, Chugh SS, Coffeng LE, Colan SD, Colquhoun S, Colson KE, Condon J, Connor MD, Cooper LT, Corriere M, Cortinovis M, de Vaccaro KC, Couser W, Cowie BC, Criqui MH, Cross M, Dabhadkar KC, Dahodwala N, De Leo D, Degenhardt L, Delossantos A, Denenberg J, Des Jarlais DC, Dharmaratne SD, Dorsey ER, Driscoll T, Duber H, Ebel B, Erwin PJ, Espindola P, Ezati M, Feigin V, Flaxman AD, Forouzanfar MH, Fowkes FG, Franklin R, Fransen M, Freeman MK, Gabriel SE, Gakidou E, Gaspari F, Gillum RF, Gonzalez-Medina D, Halasa YA, Haring D, Harrison JE, Havmoeller R, Hay RJ, Hoen B, Hotez PJ, Hoy D, Jacobsen KH, James SL, Jasrasaria R, Jayaraman S, Johns N, Karthikeyan G, Kassebaum N, Keren A, Khoo JP, Knowlton LM, Kobusingye O, Koranteng A, Krishnamurthi R, Lipnick M, Lipschultz SE, Ohno SL, Mabwejano J, MacIntyre MF, Mallinger L, March L, Marks GB, Marks R, Matsumori A, Matzopoulos R, Mayosi BM, McAnulty JH, McDermott MM, McGrath J, Mensah GA, Merriman TR, Michaud C, Miller M, Miller TR, Mock C, Mocumbi AO, Mokdad AA, Moran A, Mulholland K, Nair MN, Naldi L, Narayan KM, Nasseri K, Norman P, O'Donnell M, Omer SB, Ortblad K, Osborne R, Ozgediz D, Pahari B, Pandian JD, Rivero AP, Padilla RP, Perez-Ruiz F, Perico N, Phillips D, Pierce K, Pope CA 3rd, Porrini E, Pourmalek F, Raju M, Ranganathan D, Rehm JT, Rein DB, Remuzzi G, Rivara FP, Roberts T, De León FR, Rosenfeld LC, Rushton L, Sacco RL, Salomon JA, Sampson U, Sanman E, Schwelbel DC, Segui-Gomez M, Shepard DS, Singh D, Singleton J, Sliwa K, Smith E, Steer A, Taylor JA, Thomas B, Tleyjeh IM, Towbin JA, Truelsen T, Undurraga EA, Venketasubramanian N, Vijayakumar L, Vos T, Wagner GR, Wang M, Wang W, Watt K, Weinstock MA, Weintraub R, Wilkinson JD, Woolf AD, Wulf S, Yeh PH, Yip P, Zabetian A, Zheng ZJ, Lopez AD, Murray CJ, AlMazroa MA, Memish ZA. Global and regional mortality from 235 causes of death for 20 age groups in 1990 and 2010: a systematic analysis for the Global Burden of Disease Study 2010. *Lancet* 2012; **380**: 2095-2128 [PMID: 23245604 DOI: 10.1016/S0140-6736(12)61728-0s]
- 5 Mehal WZ, Schuppan D. Antifibrotic therapies in the liver. *Semin Liver Dis* 2015; **35**: 184-198 [PMID: 25974903 DOI: 10.1055/s-0035-1550055]
- 6 Schuppan D. Liver fibrosis: Common mechanisms and antifibrotic therapies. *Clin Res Hepatol Gastroenterol* 2015; **39** Suppl 1: S51-S59 [PMID: 26189980 DOI: 10.1016/j.clinre.2015.05.005]
- 7 Huebert RC, Rakela J. Cellular therapy for liver disease. *Mayo Clin Proc* 2014; **89**: 414-424 [PMID: 24582199 DOI: 10.1016/j.mayocp.2013.10.023]
- 8 Poilil Surendran S, George Thomas R, Moon MJ, Jeong YY. Nanoparticles for the treatment of liver fibrosis. *Int J Nanomedicine* 2017; **12**: 6997-7006 [PMID: 29033567 DOI: 10.2147/IJN.S145951]
- 9 Girish C, Pradhan SC. Herbal drugs on the liver. In: Muriel P. Liver pathophysiology: therapies & antioxidants. Waltham, MA: Elsevier, 2017: 605-620
- 10 Abenavoli L, Milic N. Silymarin for liver disease. In: Muriel P. Liver pathophysiology: therapies & antioxidants. Waltham, MA: Elsevier, 2017: 621-631
- 11 Hernández-Aquino E, Muriel P. Naringenin and the liver. In: Muriel P. Liver pathophysiology: therapies & antioxidants. Waltham, MA: Elsevier, 2017: 633-651
- 12 Vázquez-Flores LF, Casas-Grajales S, Hernández-Aquino E, Vargas-Pozada EE, Muriel P. Antioxidant antiinflammatory and antifibrotic properties of quercetin in the liver. In: Muriel P. Liver pathophysiology: therapies & and antioxidants. Waltham, MA: Elsevier, 2017: 653-674

- 13 **Arauz J**, Ramos-Tovar E, Muriel P. Coffee and the liver. In: Muriel P. Liver pathophysiology: therapies & antioxidants. Waltham, MA: Elsevier, 2017: 675-685
- 14 **Reyes-Gordillo K**, Shah R, Lakshman, Flores-Beltrán RE, Muriel P. Hepatoprotective properties of curcumin. In: Muriel P. Liver pathophysiology: therapies & antioxidants. Waltham, MA: Elsevier, 2017: 687-704
- 15 **Ramos-Tovar E**, Muriel P. Stevia as a putative hepatoprotector. In: Muriel P. Liver pathophysiology: therapies & antioxidants. Waltham, MA: Elsevier, 2017: 715-727
- 16 **Yen FL**, Wu TH, Lin LT, Cham TM, Lin CC. Naringenin-loaded nanoparticles improve the physicochemical properties and the hepatoprotective effects of naringenin in orally-administered rats with CCl₄-induced acute liver failure. *Pharm Res* 2009; **26**: 893-902 [PMID: 19034626 DOI: 10.1007/s11095-008-9791-0]
- 17 **Nait Chabane M**, Al Ahmad A, Peluso J, Muller CD, Ubeaud G. Quercetin and naringenin transport across human intestinal Caco-2 cells. *J Pharm Pharmacol* 2009; **61**: 1473-1483 [PMID: 19903372 DOI: 10.1211/jpp/61.11.0006]
- 18 **Bredsdorff L**, Nielsen IL, Rasmussen SE, Cornett C, Barron D, Bouisset F, Offord E, Williamson G. Absorption, conjugation and excretion of the flavanones, naringenin and hesperetin from alpha-rhamnosidase-treated orange juice in human subjects. *Br J Nutr* 2010; **103**: 1602-1609 [PMID: 20100371 DOI: 10.1017/S0007114509993679]
- 19 **Scalbert A**, Morand C, Manach C, Rémesy C. Absorption and metabolism of polyphenols in the gut and impact on health. *Biomed Pharmacother* 2002; **56**: 276-282 [PMID: 12224598 DOI: 10.1016/S0753-3322(02)00205-6]
- 20 **Simons AL**, Renouf M, Murphy PA, Hendrich S. Greater apparent absorption of flavonoids is associated with lesser human fecal flavonoid disappearance rates. *J Agric Food Chem* 2010; **58**: 141-147 [PMID: 19921837 DOI: 10.1021/jf902284u]
- 21 **Xu H**, Kulkarni KH, Singh R, Yang Z, Wang SW, Tam VH, Hu M. Disposition of naringenin via glucuronidation pathway is affected by compensating efflux transporters of hydrophilic glucuronides. *Mol Pharm* 2009; **6**: 1703-1715 [PMID: 19736994 DOI: 10.1021/mp900013d]
- 22 **Mata-Bilbao Mde L**, Andrés-Lacueva C, Roura E, Jáuregui O, Escribano E, Torre C, Lamuela-Raventós RM. Absorption and pharmacokinetics of grapefruit flavanones in beagles. *Br J Nutr* 2007; **98**: 86-92 [PMID: 17391560 DOI: 10.1017/S0007114507070262]
- 23 **Zou W**, Yang C, Liu M, Su W. Tissue distribution study of naringin in rats by liquid chromatography-tandem mass spectrometry. *Arzneimittelforschung* 2012; **62**: 181-186 [PMID: 22270844 DOI: 10.1055/s-0031-1299746]
- 24 **Choudhury R**, Chowrimootoo G, Sriai K, Debnam E, Rice-Evans CA. Interactions of the flavonoid naringenin in the gastrointestinal tract and the influence of glycosylation. *Biochem Biophys Res Commun* 1999; **265**: 410-415 [PMID: 10558881 DOI: 10.1006/bbrc.1999.1695]
- 25 **Ei Mohsen MA**, Marks J, Kuhnle G, Rice-Evans C, Moore K, Gibson G, Debnam E, Sriai SK. The differential tissue distribution of the citrus flavanone naringenin following gastric instillation. *Free Radic Res* 2004; **38**: 1329-1340 [PMID: 15763957 DOI: 10.1080/10715760400017293]
- 26 **Bolli A**, Marino M, Rimbach G, Fanali G, Fasano M, Ascenzi P. Flavonoid binding to human serum albumin. *Biochem Biophys Res Commun* 2010; **398**: 444-449 [PMID: 20599706 DOI: 10.1016/j.bbrc.2010.06.096]
- 27 **Hu YJ**, Wang Y, Ou-Yang Y, Zhou J, Liu Y. Characterize the interaction between naringenin and bovine serum albumin using spectroscopic approach. *J Lumin* 2010; **130**: 1394-1399 [DOI: 10.1016/j.jlumin.2010.02.053]
- 28 **Khan MK**, Rakotomanana N, Dufour C, Dangles O. Binding of citrus flavanones and their glucuronides and chalcones to human serum albumin. *Food Funct* 2011; **2**: 617-626 [PMID: 21952533 DOI: 10.1039/c1fo10077g]
- 29 **Heim KE**, Tagliaferro AR, Bobilya DJ. Flavonoid antioxidants: chemistry, metabolism and structure-activity relationships. *J Nutr Biochem* 2002; **13**: 572-584 [PMID: 12550068 DOI: 10.1016/S0955-2863(02)00208-5]
- 30 **Rice-Evans CA**, Miller NJ, Paganga G. Structure-antioxidant activity relationships of flavonoids and phenolic acids. *Free Radic Biol Med* 1996; **20**: 933-956 [PMID: 8743980 DOI: 10.1016/0891-5849(95)02227-9]
- 31 **Weber LW**, Boll M, Stampfl A. Hepatotoxicity and mechanism of action of haloalkanes: carbon tetrachloride as a toxicological model. *Crit Rev Toxicol* 2003; **33**: 105-136 [PMID: 12708612 DOI: 10.1080/713611034]
- 32 **Ratty AK**, Das NP. Effects of flavonoids on nonenzymatic lipid peroxidation: structure-activity relationship. *Biochem Med Metab Biol* 1988; **39**: 69-79 [PMID: 3355718 DOI: 10.1016/0885-4505(88)90060-6]
- 33 **Khanduja KL**, Bhardwaj A. Stable free radical scavenging and antiperoxidative properties of resveratrol compared in vitro with some other bioflavonoids. *Indian J Biochem Biophys* 2003; **40**: 416-422 [PMID: 22900369]
- 34 **Rodriguez RJ**, Miranda CL, Stevens JF, Deinzer ML, Buhler DR. Influence of prenylated and non-prenylated flavonoids on liver microsomal lipid peroxidation and oxidative injury in rat hepatocytes. *Food Chem Toxicol* 2001; **39**: 437-445 [PMID: 11313109 DOI: 10.1016/S0278-6915(00)00159-9]
- 35 **Cavia-Saiz M**, Bustos MD, Pilar-Izquierdo MC, Ortega N, Perez-Mateos M, Muñiz P. Antioxidant properties, radical scavenging activity and biomolecule protection capacity of flavonoid naringenin and its glycoside naringin: a comparative study. *J Sci Food Agric* 2010; **90**: 1238-1244 [PMID: 20394007 DOI: 10.1002/jsfa.3959]
- 36 **van Acker FA**, Schouten O, Haenen GR, van der Vlijgh WJ, Bast A. Flavonoids can replace alpha-tocopherol as an antioxidant. *FEBS Lett* 2000; **473**: 145-148 [PMID: 10812062 DOI: 10.1016/S0014-5793(00)01517-9]
- 37 **Saija A**, Scalese M, Lanza M, Marzullo D, Bonina F, Castelli F. Flavonoids as antioxidant agents: importance of their interaction with biomembranes. *Free Radic Biol Med* 1995; **19**: 481-486 [PMID: 7590397 DOI: 10.1016/0891-5849(94)00240-K]
- 38 **Arora A**, Byram TM, Nair MG, Strasburg GM. Modulation of liposomal membrane fluidity by flavonoids and isoflavonoids. *Arch Biochem Biophys* 2000; **373**: 102-109 [PMID: 10620328 DOI: 10.1006/abbi.1999.1525]
- 39 **Bombardelli E**, Spetta M. Phospholipid-polyphenol complexes: a new concept in skin care ingredients. *Cosm Toil* 1991; **106**: 69-76
- 40 **Kaneko T**, Kaji K, Matsuo M. Protection of linoleic acid hydroperoxide-induced cytotoxicity by phenolic antioxidants. *Free Radic Biol Med* 1994; **16**: 405-409 [PMID: 8063204]
- 41 **Wang K**, Chen Z, Huang L, Meng B, Zhou X, Wen X, Ren D. Naringenin reduces oxidative stress and improves mitochondrial dysfunction via activation of the Nrf2/ARE signaling pathway in neurons. *Int J Mol Med* 2017; **40**: 1582-1590 [PMID: 28949376 DOI: 10.3892/ijmm.2017.3134]
- 42 **Manchope MF**, Calixto-Campos C, Coelho-Silva L, Zarpelon AC, Pinho-Ribeiro FA, Georgetti SR, Baracat MM, Casagrande R, Verri WA Jr. Naringenin inhibits superoxide anion-induced inflammatory pain: role of oxidative stress, cytokines, Nrf-2 and the NO-cGMP-PKG-KATP channel signaling pathway. *PLoS One* 2016; **11**: e0153015 [PMID: 27045367 DOI: 10.1371/journal.pone.0153015]
- 43 **Podder B**, Song HY, Kim YS. Naringenin exerts cytoprotective effect against paraquat-induced toxicity in human bronchial epithelial BEAS-2B cells through NRF2 activation. *J Microbiol Biotechnol* 2014; **24**: 605-613 [PMID: 24561720 DOI: 10.4014/jmb.1402.02001]
- 44 **Miler M**, Živanović J, Ajdžanović V, Oreščanin-Dušić Z, Milenković D, Konić-Ristić A, Blagojević D, Milošević V, Šošić-Jurjević B. Citrus flavanones naringenin and hesperetin improve antioxidant status and membrane lipid compositions in the liver of old-aged Wistar rats. *Exp Gerontol* 2016; **84**: 49-60 [PMID: 27587005 DOI: 10.1016/j.exger.2016.08.014]
- 45 **Ali R**, Shahid A, Ali N, Hasan SK, Majed F, Sultana S.

- Amelioration of benzo[a]pyrene-induced oxidative stress and pulmonary toxicity by naringenin in Wistar rats: a plausible role of COX-2 and NF-κB. *Hum Exp Toxicol* 2017; **36**: 349-364 [PMID: 27206700 DOI: 10.1177/0960327116650009]
- 46 **Fan R**, Pan T, Zhu AL, Zhang MH. Anti-inflammatory and anti-arthritic properties of naringenin via attenuation of NF-κB and activation of the heme oxygenase (HO)-1/related factor 2 pathway. *Pharmacol Rep* 2017; **69**: 1021-1029 [PMID: 28943290 DOI: 10.1016/j.pharep.2017.03.020]
- 47 **Al-Dosari DI**, Ahmed MM, Al-Rejaie SS, Alhomida AS, Ola MS. Flavonoid naringenin attenuates oxidative stress, apoptosis and improves neurotrophic effects in the diabetic rat retina. *Nutrients* 2017; **9**: [PMID: 29064407 DOI: 10.3390/nu9101161]
- 48 **de Oliveira MR**, Brasil FB, Andrade CMB. Naringenin attenuates H₂O₂-induced mitochondrial dysfunction by an Nrf2-dependent mechanism in SH-SY5Y Cells. *Neurochem Res* 2017; **42**: 3341-3350 [PMID: 28786049 DOI: 10.1007/s11064-017-2376-8]
- 49 **Ramprasath T**, Senthamilzharasi M, Vasudevan V, Sasikumar S, Yuvaraj S, Selvam GS. Naringenin confers protection against oxidative stress through upregulation of Nrf2 target genes in cardiomyoblast cells. *J Physiol Biochem* 2014; **70**: 407-415 [PMID: 24526395 DOI: 10.1007/s13105-014-0318-3]
- 50 **Al-Roujayed AS**. Naringenin improves the healing process of thermally-induced skin damage in rats. *J Int Med Res* 2017; **45**: 570-582 [PMID: 28415935 DOI: 10.1177/0300060517692483]
- 51 **Sahin Z**, Ozkaya A, Cuce G, Uckun M, Yologlu E. Investigation of the effect of naringenin on oxidative stress-related alterations in testis of hydrogen peroxide-administered rats. *J Biochem Mol Toxicol* 2017; **31**: [PMID: 28467669 DOI: 10.1002/jbt.21928]
- 52 **Pari L**, Gnanasoundari M. Influence of naringenin on oxytetracycline mediated oxidative damage in rat liver. *Basic Clin Pharmacol Toxicol* 2006; **98**: 456-461 [PMID: 16635103 DOI: 10.1111/j.1742-7843.2006.pto_351.x]
- 53 **Bodas R**, Prieto N, Jordán MJ, López-Campos O, Giráldez FJ, Morán L, Andrés S. The liver antioxidant status of fattening lambs is improved by naringin dietary supplementation at 0.15% rates but not meat quality. *Animal* 2012; **6**: 863-870 [PMID: 22558934 DOI: 10.1017/S17517311100214X]
- 54 **Casas-Grajales S**, Muriel P. The liver, oxidative stress and antioxidants. In: Muriel P. Liver pathophysiology: therapies & antioxidants. Waltham, MA: Elsevier, 2017: 583-604
- 55 **DeLeve LD**, Kaplanowitz N. Glutathione metabolism and its role in hepatotoxicity. *Pharmacol Ther* 1991; **52**: 287-305 [PMID: 1820580 DOI: 10.1016/0163-7258(91)90029-L]
- 56 **Kretzschmar M**. Regulation of hepatic glutathione metabolism and its role in hepatotoxicity. *Exp Toxicol Pathol* 1996; **48**: 439-446 [PMID: 8765689 DOI: 10.1016/S0940-2993(96)80054-6]
- 57 **Yuan L**, Kaplanowitz N. Glutathione in liver diseases and hepatotoxicity. *Mol Aspects Med* 2009; **30**: 29-41 [PMID: 18786561 DOI: 10.1016/j.mam.2008.08.003]
- 58 **Wang J**, Yang Z, Lin L, Zhao Z, Liu Z, Liu X. Protective effect of naringenin against lead-induced oxidative stress in rats. *Biol Trace Elem Res* 2012; **146**: 354-359 [PMID: 22109809 DOI: 10.1007/s12011-011-9268-6]
- 59 **Dong D**, Xu L, Yin L, Qi Y, Peng J. Naringenin prevents carbon tetrachloride-induced acute liver injury in mice. *J Funct Foods* 2015; **12**: 179-191 [DOI: 10.1016/j.jff.2014.11.020]
- 60 **Lou H**, Jing X, Wei X, Shi H, Ren D, Zhang X. Naringenin protects against 6-OHDA-induced neurotoxicity via activation of the Nrf2/ARE signaling pathway. *Neuropharmacology* 2014; **79**: 380-388 [PMID: 24333330 DOI: 10.1016/j.neuropharm.2013.11.026]
- 61 **Gopinath K**, Sudhandiran G. Naringin modulates oxidative stress and inflammation in 3-nitropropionic acid-induced neurodegeneration through the activation of nuclear factor-erythroid 2-related factor-2 signalling pathway. *Neuroscience* 2012; **227**: 134-143 [PMID: 22871521 DOI: 10.1016/j.neuroscience.2012.07.060]
- 62 **Han X**, Pan J, Ren D, Cheng Y, Fan P, Lou H. Naringenin-7-O-glucoside protects against doxorubicin-induced toxicity in H9c2 cardiomyocytes by induction of endogenous antioxidant enzymes. *Food Chem Toxicol* 2008; **46**: 3140-3146 [PMID: 18652870 DOI: 10.1016/j.fct.2008.06.086]
- 63 **Esmaili MA**, Alilou M. Naringenin attenuates CCl₄ -induced hepatic inflammation by the activation of an Nrf2-mediated pathway in rats. *Clin Exp Pharmacol Physiol* 2014; **41**: 416-422 [PMID: 24684352 DOI: 10.1111/1440-1681.12230]
- 64 **Jayaraman J**, Veerappan M, Namasivayam N. Potential beneficial effect of naringenin on lipid peroxidation and antioxidant status in rats with ethanol-induced hepatotoxicity. *J Pharm Pharmacol* 2009; **61**: 1383-1390 [PMID: 19814872 DOI: 10.1211/jpp/61.10.0016]
- 65 **Renugadevi J**, Prabu SM. Cadmium-induced hepatotoxicity in rats and the protective effect of naringenin. *Exp Toxicol Pathol* 2010; **62**: 171-181 [PMID: 19409769 DOI: 10.1016/j.etp.2009.03.010]
- 66 **Martinez RM**, Pinho-Ribeiro FA, Steffen VS, Silva TC, Caviglione CV, Bottura C, Fonseca MJ, Vicentini FT, Vignoli JA, Baracat MM, Georgetti SR, Verri WA Jr, Casagrande R. Topical formulation containing naringenin: efficacy against ultraviolet B irradiation-induced skin inflammation and oxidative stress in mice. *PLoS One* 2016; **11**: e0146296 [PMID: 26741806 DOI: 10.1371/journal.pone.0146296]
- 67 **Shakeel S**, Rehman MU, Tabassum N, Amin U, Mir MUR. Effect of naringenin (a naturally occurring flavanone) against pilocarpine-induced status epilepticus and oxidative stress in mice. *Pharmacogn Mag* 2017; **13**: S154-S160 [PMID: 28479741 DOI: 10.4103/0973-1296.20397]
- 68 **Roy A**, Das A, Das R, Haldar S, Bhattacharya S, Haldar PK. Naringenin, a citrus flavonoid, ameliorates arsenic-induced toxicity in Swiss albino mice. *J Environ Pathol Toxicol Oncol* 2014; **33**: 195-204 [PMID: 25272058 DOI: 10.1615/JEnvironPatholToxicolOncol.2014010317]
- 69 **Davies KJ**. Oxidative stress, antioxidant defenses, and damage removal, repair, and replacement systems. *IUBMB Life* 2000; **50**: 279-289 [PMID: 11327322 DOI: 10.1080/713803728]
- 70 **Jayaraman J**, Namasivayam N. Naringenin modulates circulatory lipid peroxidation, anti-oxidant status and hepatic alcohol metabolizing enzymes in rats with ethanol induced liver injury. *Fundam Clin Pharmacol* 2011; **25**: 682-689 [PMID: 21105911 DOI: 10.1111/j.1472-8206.2010.00899]
- 71 **Hermenean A**, Ardelean A, Stan M, Herman H, Mihali CV, Costache M, Dinischiotu A. Protective effects of naringenin on carbon tetrachloride-induced acute nephrotoxicity in mouse kidney. *Chem Biol Interact* 2013; **205**: 138-147 [PMID: 23845967 DOI: 10.1016/j.cbi.2013.06.016]
- 72 **Prabu SM**, Shagirtha K, Renugadevi J. Naringenin in combination with vitamins C and E potentially protects oxidative stress-mediated hepatic injury in cadmium-intoxicated rats. *J Nutr Sci Vitaminol (Tokyo)* 2011; **57**: 177-185 [PMID: 21697638 DOI: 10.3177/jnsv.57.177]
- 73 **Jain A**, Yadav A, Bozhkov AI, Padalko VI, Flora SJ. Therapeutic efficacy of silymarin and naringenin in reducing arsenic-induced hepatic damage in young rats. *Ecotoxicol Environ Saf* 2011; **74**: 607-614 [PMID: 20719385 DOI: 10.1016/j.ecoenv.2010.08.002]
- 74 **Mershiba SD**, Dassprakash MV, Saraswathy SD. Protective effect of naringenin on hepatic and renal dysfunction and oxidative stress in arsenic intoxicated rats. *Mol Biol Rep* 2013; **40**: 3681-3691 [PMID: 23283742 DOI: 10.1007/s11033-012-2444-8]
- 75 **Ambros V**. The functions of animal microRNAs. *Nature* 2004; **431**: 350-355 [PMID: 15372042 DOI: 10.1038/nature02871]
- 76 **Xu Y**, Fang F, Zhang J, Jossom S, St Clair WH, St Clair DK. miR-17* suppresses tumorigenicity of prostate cancer by inhibiting mitochondrial antioxidant enzymes. *PLoS One* 2010; **5**: e14356 [PMID: 21203553 DOI: 10.1371/journal.pone.0014356]
- 77 **Curti V**, Di Lorenzo A, Rossi D, Martino E, Capelli E, Collina S, Daglia M. Enantioselective modulatory effects of naringenin enantiomers on the expression levels of miR-17-3p involved in endogenous antioxidant defenses. *Nutrients* 2017; **9**: pii: E215 [PMID: 28264488 DOI: 10.3390/nu9030215]
- 78 **Tebay LE**, Robertson H, Durant ST, Vitale SR, Penning TM, Dinkova-Kostova AT, Hayes JD. Mechanisms of activation of

- the transcription factor Nrf2 by redox stressors, nutrient cues, and energy status and the pathways through which it attenuates degenerative disease. *Free Radic Biol Med* 2015; **88**: 108-146 [PMID: 26122708 DOI: 10.1016/j.freeradbiomed.2015.06.021]
- 79 **Ooi BK**, Goh BH, Yap WH. Oxidative stress in cardiovascular diseases: involvement of Nrf2 antioxidant redox signaling in macrophage foam cells formation. *Int J Mol Sci* 2017; **18**: pii: E2336 [PMID: 29113088 DOI: 10.3390/ijms18112336.]
- 80 **Tang W**, Jiang YF, Ponnusamy M, Diallo M. Role of Nrf2 in chronic liver disease. *World J Gastroenterol* 2014; **20**: 13079-13087 [PMID: 25278702 DOI: 10.3748/wjg.v20.i36.13079]
- 81 **Wang H**, Xu YS, Wang ML, Cheng C, Bian R, Yuan H, Wang Y, Guo T, Zhu LL, Zhou H. Protective effect of naringenin against the LPS-induced apoptosis of PC12 cells: implications for the treatment of neurodegenerative disorders. *Int J Mol Med* 2017; **39**: 819-830 [PMID: 28260042 DOI: 10.3892/ijmm.2017.2904]
- 82 **Chen RC**, Sun GB, Wang J, Zhang HJ, Sun XB. Naringenin protects against anoxia/reoxygenation-induced apoptosis in H9c2 cells via the Nrf2 signaling pathway. *Food Funct* 2015; **6**: 1331-1344 [PMID: 25773745 DOI: 10.1039/c4fo01164c]
- 83 **Cullinan SB**, Zhang D, Hannink M, Arvisais E, Kaufman RJ, Diehl JA. Nrf2 is a direct PERK substrate and effector of PERK-dependent cell survival. *Mol Cell Biol* 2003; **23**: 7198-7209 [PMID: 14517290 DOI: 10.1128/MCB.23.20.7198-7209.2003]
- 84 **Zipper LM**, Mulcahy RT. Erk activation is required for Nrf2 nuclear localization during pyrrolidine dithiocarbamate induction of glutamate cysteine ligase modulatory gene expression in HepG2 cells. *Toxicol Sci* 2003; **73**: 124-134 [PMID: 12657749 DOI: 10.1093/toxsci/kfg083]
- 85 **Liu XM**, Peyton KJ, Shebib AR, Wang H, Korthuis RJ, Durante W. Activation of AMPK stimulates heme oxygenase-1 gene expression and human endothelial cell survival. *Am J Physiol Heart Circ Physiol* 2011; **300**: H84-H93 [PMID: 21037234 DOI: 10.1152/ajpheart.00749]
- 86 **Lee SE**, Yang H, Jeong SI, Jin YH, Park CS, Park YS. Induction of heme oxygenase-1 inhibits cell death in crotonaldehyde-stimulated HepG2 cells via the PKC-δ-p38-Nrf2 pathway. *PLoS One* 2012; **7**: e41676 [PMID: 22848562 DOI: 10.1371/journal.pone.0041676]
- 87 **Wang K**, Chen Z, Huang J, Huang L, Luo N, Liang X, Liang M, Xie W. Naringenin prevents ischaemic stroke damage via anti-apoptotic and anti-oxidant effects. *Clin Exp Pharmacol Physiol* 2017; **44**: 862-871 [PMID: 28453191 DOI: 10.1111/1440-1681.12775]
- 88 **Liu JD**, Leung KW, Wang CK, Liao LY, Wang CS, Chen PH, Chen CC, Yeh EK. Alcohol-related problems in Taiwan with particular emphasis on alcoholic liver diseases. *Alcohol Clin Exp Res* 1998; **22**: 164S-169S [PMID: 9622397 DOI: 10.1097/00000374-199803001-00019]
- 89 **Mandayam S**, Jamal MM, Morgan TR. Epidemiology of alcoholic liver disease. *Semin Liver Dis* 2004; **24**: 217-232 [PMID: 15349801 DOI: 10.1055/s-2004-832936]
- 90 **Teli MR**, Day CP, Burt AD, Bennett MK, James OF. Determinants of progression to cirrhosis or fibrosis in pure alcoholic fatty liver. *Lancet* 1995; **346**: 987-990 [PMID: 7475591]
- 91 **Boye A**, Zou YH, Yang Y. Metabolic derivatives of alcohol and the molecular culprits of fibro-hepatocarcinogenesis: Allies or enemies? *World J Gastroenterol* 2016; **22**: 50-71 [PMID: 26755860 DOI: 10.3748/wjg.v22.i1.50]
- 92 **Rocco A**, Compare D, Angrisani D, Sanduzzi Zamparelli M, Nardone G. Alcoholic disease: liver and beyond. *World J Gastroenterol* 2014; **20**: 14652-14659 [PMID: 25356028 DOI: 10.3748/wjg.v20.i40.14652]
- 93 **Ceni E**, Mello T, Galli A. Pathogenesis of alcoholic liver disease: role of oxidative metabolism. *World J Gastroenterol* 2014; **20**: 17756-17772 [PMID: 25548474 DOI: 10.3748/wjg.v20.i47.17756]
- 94 **Seo HJ**, Jeong KS, Lee MK, Park YB, Jung UJ, Kim HJ, Choi MS. Role of naringenin supplement in regulation of lipid and ethanol metabolism in rats. *Life Sci* 2003; **73**: 933-946 [PMID: 12798418 DOI: 10.1016/S0024-3205(03)00358-8]
- 95 **Deenen MJ**, Cats A, Beijnen JH, Schellens JH. Part 2: pharmacogenetic variability in drug transport and phase I anticancer drug metabolism. *Oncologist* 2011; **16**: 820-834 [PMID: 21632461 DOI: 10.1634/theoncologist.2010-0259]
- 96 **Porta EA**. Dietary modulation of oxidative stress in alcoholic liver disease in rats. *J Nutr* 1997; **127**: 912S-915S [PMID: 9164262]
- 97 **French SW**. The pathophysiology of alcoholic liver disease. In: Muriel P. Liver pathophysiology: therapies & antioxidants. Waltham, MA: Elsevier, 2017: 141-157
- 98 **Jayaraman J**, Jesudoss VA, Menon VP, Namasivayam N. Anti-inflammatory role of naringenin in rats with ethanol induced liver injury. *Toxicol Mech Methods* 2012; **22**: 568-576 [PMID: 22900548 DOI: 10.3109/15376516.2012.707255]
- 99 **Szkudelska K**, Nogowski L, Nowicka E, Szkudelski T. In vivo metabolic effects of naringenin in the ethanol consuming rat and the effect of naringenin on adipocytes in vitro. *J Anim Physiol Anim Nutr (Berl)* 2007; **91**: 91-99 [PMID: 17355338 DOI: 10.1111/j.1439-0396.2006.00647.x]
- 100 **Muriel P**, Ramos-Tovar E, Montes-Páez G, Buendía-Montaña LD. Experimental models of liver damage mediated by oxidative stress. In: Muriel P. Liver pathophysiology: therapies & antioxidants. Waltham, MA: Elsevier, 2017: 529-546
- 101 **Ingawale DK**, Mandlik SK, Naik SR. Models of hepatotoxicity and the underlying cellular, biochemical and immunological mechanism(s): a critical discussion. *Environ Toxicol Pharmacol* 2014; **37**: 118-133 [PMID: 24322620 DOI: 10.1016/j.etap.2013.08.015]
- 102 **Facino RM**, Carini M, Franzoi L, Pirola O, Bosisio E. Phytochemical characterization and radical scavenger activity of flavonoids from Helichrysum italicum G. Don (Compositae). *Pharmacol Res* 1990; **22**: 709-721 [PMID: 2075159]
- 103 **Ikewuchi JC**, Ikewuchi CC, Igboh NM, Mark-Balm T. Protective effect of aqueous extract of the rhizomes of Sansevieria liberica Gérôme and Labroy on carbon tetrachloride induced hepatotoxicity in rats. *EXCLI J* 2011; **10**: 312-321 [PMID: 29033712]
- 104 **Kaurinovic B**, Popovic M, Vlaisavljevic S, Schwartzova H, Vojinovic-Miloradov M. Antioxidant profile of Trifolium pratense L. *Molecules* 2012; **17**: 11156-11172 [PMID: 22990457 DOI: 10.3390/molecules170911156]
- 105 **Hermenean A**, Ardelean A, Stan M, Hadaruga N, Mihali CV, Costache M, Dinischiotu A. Antioxidant and hepatoprotective effects of naringenin and its β-cyclodextrin formulation in mice intoxicated with carbon tetrachloride: a comparative study. *J Med Food* 2014; **17**: 670-677 [PMID: 24611872 DOI: 10.1089/jmf.2013.0007]
- 106 **Kawai T**, Akira S. TLR signaling. *Cell Death Differ* 2006; **13**: 816-825 [PMID: 16410796 DOI: 10.1038/sj.cdd.4401850]
- 107 **Yamanishi R**, Yoshigai E, Okuyama T, Mori M, Murase H, Machida T, Okumura T, Nishizawa M. The anti-inflammatory effects of flavanol-rich lychee fruit extract in rat hepatocytes. *PLoS One* 2014; **9**: e93818 [PMID: 24705335 DOI: 10.1371/journal.pone.0093818]
- 108 **O'Neill LA**, Kaltschmidt C. NF-κB: a crucial transcription factor for glial and neuronal cell function. *Trends Neurosci* 1997; **20**: 252-258 [PMID: 9185306]
- 109 **Czaja MJ**. The future of GI and liver research: editorial perspectives. III. JNK/AP-1 regulation of hepatocyte death. *Am J Physiol Gastrointest Liver Physiol* 2003; **284**: G875-G879 [PMID: 12736142 DOI: 10.1152/ajpgi.00549.2002]
- 110 **Wang X**, Xiang L, Li H, Chen P, Feng Y, Zhang J, Yang N, Li F, Wang Y, Zhang Q, Li F, Cao F. The role of HMGB1 signaling pathway in the development and progression of hepatocellular carcinoma: a review. *Int J Mol Sci* 2015; **16**: 22527-22540 [PMID: 26393575 DOI: 10.3390/ijms160922527]
- 111 **Pollard TD**, Earnshaw WC, Lippincott-Schwartz J. Cell Biology. 2th edition. Philadelphia: Elsevier, 2008: 433-435
- 112 **Hernández-Aquino E**, Zarco N, Casas-Grajales S, Ramos-Tovar E, Flores-Beltrán RE, Arauz J, Shibayama M, Favari L, Tsutsumi V, Segovia J, Muriel P. Naringenin prevents experimental liver fibrosis by blocking TGFβ-Smad3 and JNK-Smad3 pathways. *World J Gastroenterol* 2017; **23**: 4354-4368 [PMID: 28706418]

DOI: 10.3748/wjg.v23.i24.4354]

- 113 **Kisseleva T**, Brenner DA. Role of hepatic stellate cells in fibrogenesis and the reversal of fibrosis. *J Gastroenterol Hepatol* 2007; **22** Suppl 1: S73-S78 [PMID: 17567473 DOI: 10.1111/j.1440-1746.2006.04658.x]
- 114 **Arauz J**, Moreno MG, Cortés-Reynosa P, Salazar EP, Muriel P. Coffee attenuates fibrosis by decreasing the expression of TGF- β and CTGF in a murine model of liver damage. *J Appl Toxicol* 2013; **33**: 970-979 [PMID: 22899499 DOI: 10.1002/jat.2788]
- 115 **Matsuzaki K**. Smad phospho-isoforms direct context-dependent TGF- β signaling. *Cytokine Growth Factor Rev* 2013; **24**: 385-399 [PMID: 23871609 DOI: 10.1016/j.cytogfr.2013.06.002]
- 116 **Yoshida K**, Murata M, Yamaguchi T, Matsuzaki K, Okazaki K. Reversible human TGF- β signal shifting between tumor suppression and fibro-carcinogenesis: implications of smad phospho-isoforms for hepatic epithelial-mesenchymal transitions. *J Clin Med* 2016; **5**: [PMID: 26771649 DOI: 10.3390/jcm5010007]
- 117 **Hemann S**, Graf J, Roderfeld M, Roeb E. Expression of MMPs and TIMPs in liver fibrosis - a systematic review with special emphasis on anti-fibrotic strategies. *J Hepatol* 2007; **46**: 955-975 [PMID: 17383048 DOI: 10.1016/j.jhep.2007.02.003]
- 118 **Imamura T**, Oshima Y, Hikita A. Regulation of TGF- β family signalling by ubiquitination and deubiquitination. *J Biochem* 2013; **154**: 481-489 [PMID: 24165200 DOI: 10.1093/jb/mvt097]
- 119 **Bray F**, Ren JS, Masuyer E, Ferlay J. Global estimates of cancer prevalence for 27 sites in the adult population in 2008. *Int J Cancer* 2013; **132**: 1133-1145 [PMID: 22752881 DOI: 10.1002/ijc.27711]
- 120 **Tarocchi M**, Polvani S, Marroncini G, Galli A. Molecular mechanism of hepatitis B virus-induced hepatocarcinogenesis. *World J Gastroenterol* 2014; **20**: 11630-11640 [PMID: 25206269 DOI: 10.3748/wjg.v20.i33.11630]
- 121 **Tarocchi M**, Galli A. Oxidative stress as a mechanism for hepatocellular carcinoma. In: Muriel P. Liver pathophysiology: therapies & antioxidants. Waltham, MA: Elsevier, 2017: 279-287
- 122 **Beasley RP**, Hwang LY, Lin CC, Chien CS. Hepatocellular carcinoma and hepatitis B virus. A prospective study of 22 707 men in Taiwan. *Lancet* 1981; **2**: 1129-1133 [PMID: 6118576]
- 123 **Higgs MR**, Chouteau P, Lerat H. 'Liver let die': oxidative DNA damage and hepatotropic viruses. *J Gen Virol* 2014; **95**: 991-1004 [PMID: 24496828 DOI: 10.1099/vir.0.059485-0]
- 124 **Fisher AB**. Redox signaling across cell membranes. *Antioxid Redox Signal* 2009; **11**: 1349-1356 [PMID: 19061438 DOI: 10.1089/ars.2008.2378]
- 125 **Ei-Serag HB**, Rudolph KL. Hepatocellular carcinoma: epidemiology and molecular carcinogenesis. *Gastroenterology* 2007; **132**: 2557-2576 [PMID: 17570226 DOI: 10.1053/j.gastro.2007.04.061]
- 126 **Perry G**, Raina AK, Nunomura A, Wataya T, Sayre LM, Smith MA. How important is oxidative damage? Lessons from Alzheimer's disease. *Free Radic Biol Med* 2000; **28**: 831-834 [PMID: 10754280]
- 127 **Niu D**, Zhang J, Ren Y, Feng H, Chen WN. HBx genotype D represses GSTP1 expression and increases the oxidative level and apoptosis in HepG2 cells. *Mol Oncol* 2009; **3**: 67-76 [PMID: 19383368 DOI: 10.1016/j.molonc.2008.10.002]
- 128 **Dröge W**. Oxidative stress and aging. *Adv Exp Med Biol* 2003; **543**: 191-200 [PMID: 14713123]
- 129 **Ha HL**, Shin HJ, Feitelson MA, Yu DY. Oxidative stress and antioxidants in hepatic pathogenesis. *World J Gastroenterol* 2010; **16**: 6035-6043 [PMID: 21182217 DOI: 10.3748/wjg.v16.i48.6035]
- 130 **Scott TL**, Rangaswamy S, Wicker CA, Izumi T. Repair of oxidative DNA damage and cancer: recent progress in DNA base excision repair. *Antioxid Redox Signal* 2014; **20**: 708-726 [PMID: 23901781 DOI: 10.1089/ars.2013.5529]
- 131 **Khan N**, Afaf F, Mukhtar H. Cancer chemoprevention through dietary antioxidants: progress and promise. *Antioxid Redox Signal* 2008; **10**: 475-510 [PMID: 18154485 DOI: 10.1089/ars.2007.1740]
- 132 **Valko M**, Leibfritz D, Moncol J, Cronin MT, Mazur M, Telser J. Free radicals and antioxidants in normal physiological functions and human disease. *Int J Biochem Cell Biol* 2007; **39**: 44-84 [PMID: 16978905 DOI: 10.1016/j.biocel.2006.07.001]
- 133 **Valko M**, Rhodes CJ, Moncol J, Izakovic M, Mazur M. Free radicals, metals and antioxidants in oxidative stress-induced cancer. *Chem Biol Interact* 2006; **160**: 1-40 [PMID: 16430879 DOI: 10.1016/j.cbi.2005.12.009]
- 134 **Kandaswami C**, Middleton E Jr. Free radical scavenging and antioxidant activity of plant flavonoids. *Adv Exp Med Biol* 1994; **366**: 351-376 [PMID: 7771265]
- 135 **Russo M**, Spagnuolo C, Tedesco I, Russo GL. Phytochemicals in cancer prevention and therapy: truth or dare? *Toxins (Basel)* 2010; **2**: 517-551 [PMID: 22069598 DOI: 10.3390/toxins2040517]
- 136 **Francis AR**, Shetty TK, Bhattacharya RK. Modulating effect of plant flavonoids on the mutagenicity of N-methyl-N'-nitro-N-nitrosoguanidine. *Carcinogenesis* 1989; **10**: 1953-1955 [PMID: 2676226]
- 137 **Ekambaram G**, Rajendran P, Magesh V, Sakthisekaran D. Naringenin reduces tumor size and weight lost in N-methyl-N'-nitro-N-nitrosoguanidine-induced gastric carcinogenesis in rats. *Nutr Res* 2008; **28**: 106-112 [PMID: 19083396 DOI: 10.1016/j.nutres.2007.12.002]
- 138 **Leonardi T**, Vanamala J, Taddeo SS, Davidson LA, Murphy ME, Patil BS, Wang N, Carroll RJ, Chapkin RS, Lupton JR, Turner ND. Apigenin and naringenin suppress colon carcinogenesis through the aberrant crypt stage in azoxymethane-treated rats. *Exp Biol Med (Maywood)* 2010; **235**: 710-717 [PMID: 20511675 DOI: 10.1258/ebm.2010.009359]
- 139 **Yoon H**, Kim TW, Shin SY, Park MJ, Yong Y, Kim DW, Islam T, Lee YH, Jung KY, Lim Y. Design, synthesis and inhibitory activities of naringenin derivatives on human colon cancer cells. *Bioorg Med Chem Lett* 2013; **23**: 232-238 [PMID: 23177257 DOI: 10.1016/j.bmcl.2012.10.130]
- 140 **Subramanian P**, Arul D. Attenuation of NDEA-induced hepatocarcinogenesis by naringenin in rats. *Cell Biochem Funct* 2013; **31**: 511-517 [PMID: 23172681 DOI: 10.1002/cbf.2929]
- 141 **Arul D**, Subramanian P. Inhibitory effect of naringenin (citrus flavonone) on N-nitrosodiethylamine induced hepatocarcinogenesis in rats. *Biochem Biophys Res Commun* 2013; **434**: 203-209 [PMID: 23523793 DOI: 10.1016/j.bbrc.2013.03.039]
- 142 **Taha MM**, Abdul AB, Abdulla R, Ibrahim TA, Abdelwahab SI, Mohan S. Potential chemoprevention of diethylnitrosamine-initiated and 2-acetylaminofluorene-promoted hepatocarcinogenesis by zerumbone from the rhizomes of the subtropical ginger (*Zingiber zerumbet*). *Chem Biol Interact* 2010; **186**: 295-305 [PMID: 20452335 DOI: 10.1016/j.cbi.2010.04.029]
- 143 **Lee MH**, Yoon S, Moon JO. The flavonoid naringenin inhibits dimethylnitrosamine-induced liver damage in rats. *Biol Pharm Bull* 2004; **27**: 72-76 [PMID: 14709902]
- 144 **Ozkaya A**, Sahin Z, Dag U, Ozkaraca M. Effects of naringenin on oxidative stress and histopathological changes in the liver of lead acetate administered Rats. *J Biochem Mol Toxicol* 2016; **30**: 243-248 [PMID: 26929248 DOI: 10.1002/jbt.21785]
- 145 **Arul D**, Subramanian P. Naringenin (citrus flavonone) induces growth inhibition, cell cycle arrest and apoptosis in human hepatocellular carcinoma cells. *Pathol Oncol Res* 2013; **19**: 763-770 [PMID: 23661153 DOI: 10.1007/s12253-013-9641-1]
- 146 **Zhong Z**, Chen X, Tan W, Xu Z, Zhou K, Wu T, Cui L, Wang Y. Germacrone inhibits the proliferation of breast cancer cell lines by inducing cell cycle arrest and promoting apoptosis. *Eur J Pharmacol* 2011; **667**: 50-55 [PMID: 21497161 DOI: 10.1016/j.ejphar.2011.03.041]
- 147 **Giono LE**, Manfredi JJ. The p53 tumor suppressor participates in multiple cell cycle checkpoints. *J Cell Physiol* 2006; **209**: 13-20 [PMID: 16741928 DOI: 10.1002/jcp.20689]
- 148 **Alshatwi AA**, Shafi G, Hasan TN, Al-Hazzani AA, Alsaif MA, Alfawaz MA, Lei KY, Munshi A. Apoptosis-mediated inhibition of human breast cancer cell proliferation by lemon citrus extract. *Asian Pac J Cancer Prev* 2011; **12**: 1555-1559 [PMID: 22126498]
- 149 **Park HS**, Kim GY, Nam TJ, Deuk Kim N, Hyun Choi Y. Antiproliferative activity of fucoidan was associated with the induction of apoptosis and autophagy in AGS human gastric cancer cells. *J Food Sci* 2011; **76**: T77-T83 [PMID: 21535865 DOI: 10.1002/jfs.21785]

- 10.1111/j.1750-3841.2011.02099.x]
- 150 **Tan AC**, Konczak I, Ramzan I, Sze DM. Native Australian fruit polyphenols inhibit cell viability and induce apoptosis in human cancer cell lines. *Nutr Cancer* 2011; **63**: 444-455 [PMID: 21391128 DOI: 10.1080/01635581.2011.535953]
- 151 **Chidambara Murthy KN**, Jayaprakasha GK, Kumar V, Rathore KS, Patil BS. Citrus limonin and its glucoside inhibit colon adenocarcinoma cell proliferation through apoptosis. *J Agric Food Chem* 2011; **59**: 2314-2323 [PMID: 21338095 DOI: 10.1021/jf104498p]
- 152 **Patel S**. Function and dysfunction of two-pore channels. *Sci Signal* 2015; **8**: re7 [PMID: 26152696 DOI: 10.1126/scisignal.aab3314]
- 153 **Scholz-Starke J**, Carpaneto A, Gambale F. On the interaction of neomycin with the slow vacuolar channel of *Arabidopsis thaliana*. *J Gen Physiol* 2006; **127**: 329-340 [PMID: 16505151 DOI: 10.1085/jgp.200509402]
- 154 **Calcraft PJ**, Ruas M, Pan Z, Cheng X, Arredouani A, Hao X, Tang J, Rieddorf K, Teboul L, Chuang KT, Lin P, Xiao R, Wang C, Zhu Y, Lin Y, Wyatt CN, Parrington J, Ma J, Evans AM, Galione A, Zhu MX. NAADP mobilizes calcium from acidic organelles through two-pore channels. *Nature* 2009; **459**: 596-600 [PMID: 19387438 DOI: 10.1038/nature08030]
- 155 **Pafumi I**, Festa M, Papacci F, Lagostena L, Giunta C, Gutla V, Cornara L, Favia A, Palombi F, Gambale F, Filippini A, Carpaneto A. Naringenin impairs two-pore channel 2 activity and inhibits VEGF-induced angiogenesis. *Sci Rep* 2017; **7**: 5121 [PMID: 28698624 DOI: 10.1038/s41598-017-04974-1]
- 156 **Fürstenberger G**, Berry DL, Sorg B, Marks F. Skin tumor promotion by phorbol esters is a two-stage process. *Proc Natl Acad Sci U S A* 1981; **78**: 7722-7726 [PMID: 6801661]
- 157 **Liu JF**, Crépin M, Liu JM, Barritault D, Ledoux D. FGF-2 and TPA induce matrix metalloproteinase-9 secretion in MCF-7 cells through PKC activation of the Ras/ERK pathway. *Biochem Biophys Res Commun* 2002; **293**: 1174-1182 [PMID: 12054499 DOI: 10.1016/S0006-291X(02)00350-9]
- 158 **Lee KH**, Yeh MH, Kao ST, Hung CM, Liu CJ, Huang YY, Yeh CC. The inhibitory effect of hesperidin on tumor cell invasiveness occurs via suppression of activator protein 1 and nuclear factor-kappaB in human hepatocellular carcinoma cells. *Toxicol Lett* 2010; **194**: 42-49 [PMID: 20138977 DOI: 10.1016/j.toxlet.2010.01.021]
- 159 **Yen HR**, Liu CJ, Yeh CC. Naringenin suppresses TPA-induced tumor invasion by suppressing multiple signal transduction pathways in human hepatocellular carcinoma cells. *Chem Biol Interact* 2015; **235**: 1-9 [PMID: 25866363 DOI: 10.1016/j.cbi.2015.04.003]
- 160 **Jomova K**, Valko M. Advances in metal-induced oxidative stress and human disease. *Toxicology* 2011; **283**: 65-87 [PMID: 21414382 DOI: 10.1016/j.tox.2011.03.001]
- 161 **Pietrangelo A**. Iron and the liver. *Liver Int* 2016; **36** Suppl 1: 116-123 [PMID: 26725908 DOI: 10.1111/liv.13020]
- 162 **Sikorska K**, Bernat A, Wroblewska A. Molecular pathogenesis and clinical consequences of iron overload in liver cirrhosis. *Hepatobiliary Pancreat Dis Int* 2016; **15**: 461-479 [PMID: 27733315]
- 163 **Arthur MJ**. Iron overload and liver fibrosis. *J Gastroenterol Hepatol* 1996; **11**: 1124-1129 [PMID: 9034931]
- 164 **Fernandez MT**, Mira ML, Florêncio MH, Jennings KR. Iron and copper chelation by flavonoids: an electrospray mass spectrometry study. *J Inorg Biochem* 2002; **92**: 105-111 [PMID: 12459155]
- 165 **Cheng IF**, Breen K. On the ability of four flavonoids, baicilein, luteolin, naringenin, and quercetin, to suppress the Fenton reaction of the iron-ATP complex. *Biometals* 2000; **13**: 77-83 [PMID: 10831228]
- 166 **Benherhal PS**, Arumughan C. Studies on modulation of DNA integrity in Fenton's system by phytochemicals. *Mutat Res* 2008; **648**: 1-8 [PMID: 18824181 DOI: 10.1016/j.mrfmmm.2008.09.001]
- 167 **Jagetia GC**, Reddy TK. Alleviation of iron induced oxidative stress by the grape fruit flavanone naringenin in vitro. *Chem Biol Interact* 2011; **190**: 121-128 [PMID: 21345335 DOI: 10.1016/j.cbi.2011.02.009]
- 168 **Jagetia GC**, Reddy TK, Venkatesha VA, Kedlaya R. Influence of naringin on ferric iron induced oxidative damage in vitro. *Clin Chim Acta* 2004; **347**: 189-197 [PMID: 15313158 DOI: 10.1016/j.cccn.2004.04.022]
- 169 **Chtourou Y**, Fetoui H, Gdoura R. Protective effects of naringenin on iron-overload-induced cerebral cortex neurotoxicity correlated with oxidative stress. *Biol Trace Elem Res* 2014; **158**: 376-383 [PMID: 24682942 DOI: 10.1007/s12011-014-9948-0]
- 170 **Chtourou Y**, Slima AB, Gdoura R, Fetoui H. Naringenin mitigates iron-induced anxiety-like behavioral impairment, mitochondrial dysfunctions, ectonucleotidases and acetylcholinesterase alteration activities in rat hippocampus. *Neurochem Res* 2015; **40**: 1563-1575 [PMID: 26050208 DOI: 10.1007/s11064-015-1627-9]
- 171 **Uriu-Adams JY**, Keen CL. Copper, oxidative stress, and human health. *Mol Aspects Med* 2005; **26**: 268-298 [PMID: 16112185 DOI: 10.1016/j.mam.2005.07.015]
- 172 **Johncilla M**, Mitchell KA. Pathology of the liver in copper overload. *Semin Liver Dis* 2011; **31**: 239-244 [PMID: 21901654 DOI: 10.1055/s-0031-1286055]
- 173 **Zhou B**, Gitschier J. hCTR1: a human gene for copper uptake identified by complementation in yeast. *Proc Natl Acad Sci U S A* 1997; **94**: 7481-7486 [PMID: 9207117]
- 174 **Moriwaki H**, Osborne MR, Phillips DH. Effects of mixing metal ions on oxidative DNA damage mediated by a Fenton-type reduction. *Toxicol In Vitro* 2008; **22**: 36-44 [PMID: 17869055 DOI: 10.1016/j.tiv.2007.07.011]
- 175 **Mira L**, Fernandez MT, Santos M, Rocha R, Florêncio MH, Jennings KR. Interactions of flavonoids with iron and copper ions: a mechanism for their antioxidant activity. *Free Radic Res* 2002; **36**: 1199-1208 [PMID: 12592672]
- 176 **Esterbauer H**, Gebicki J, Puhl H, Jürgens G. The role of lipid peroxidation and antioxidants in oxidative modification of LDL. *Free Radic Biol Med* 1992; **13**: 341-390 [PMID: 1398217]
- 177 **Miranda CL**, Stevens JF, Ivanov V, McCall M, Frei B, Deinzer ML, Buhler DR. Antioxidant and prooxidant actions of prenylated and nonprenylated chalcones and flavanones in vitro. *J Agric Food Chem* 2000; **48**: 3876-3884 [PMID: 10995285]
- 178 **Rani A**, Kumar A, Lal A, Pant M. Cellular mechanisms of cadmium-induced toxicity: a review. *Int J Environ Health Res* 2014; **24**: 378-399 [PMID: 24117228 DOI: 10.1080/09603123.2013.835032]
- 179 **Rikans LE**, Yamano T. Mechanisms of cadmium-mediated acute hepatotoxicity. *J Biochem Mol Toxicol* 2000; **14**: 110-117 [PMID: 10630425]
- 180 **Renugadevi J**, Prabu SM. Naringenin protects against cadmium-induced oxidative renal dysfunction in rats. *Toxicology* 2009; **256**: 128-134 [PMID: 19063931 DOI: 10.1016/j.tox.2008.11.012]
- 181 **Das A**, Roy A, Das R, Bhattacharya S, Haldar PK. Naringenin alleviates cadmium-induced toxicity through the abrogation of oxidative stress in swiss albino mice. *J Environ Pathol Toxicol Oncol* 2016; **35**: 161-169 [PMID: 27481493 DOI: 10.1615/JEnvironPatholToxicolOncol.2016015892]
- 182 **Rathi VK**, Das S, Parampalli Raghavendra A, Rao BSS. Naringenin abates adverse effects of cadmium-mediated hepatotoxicity: An experimental study using HepG2 cells. *J Biochem Mol Toxicol* 2017; **31**: [PMID: 28422390 DOI: 10.1002/jbt.21915]
- 183 **Singh AP**, Goel RK, Kaur T. Mechanisms pertaining to arsenic toxicity. *Toxicol Int* 2011; **18**: 87-93 [PMID: 21976811 DOI: 10.4103/0971-6580.84258]
- 184 **Jomova K**, Jenisova Z, Fesztrova M, Baros S, Liska J, Hudcová D, Rhodes CJ, Valko M. Arsenic: toxicity, oxidative stress and human disease. *J Appl Toxicol* 2011; **31**: 95-107 [PMID: 21321970 DOI: 10.1002/jat.1649]
- 185 **Liu J**, Waalkes MP. Liver is a target of arsenic carcinogenesis. *Toxicol Sci* 2008; **105**: 24-32 [PMID: 18566022 DOI: 10.1093/toxsci/kfn120]
- 186 **Adil M**, Kandhare AD, Visnagri A, Bodhankar SL. Naringenin ameliorates sodium arsenite-induced renal and hepatic toxicity in rats: decisive role of KIM-1, Caspase-3, TGF- β , and TNF- α . *Ren Fail* 2015; **37**: 1396-1407 [PMID: 26337322 DOI: 10.3109/08860

- 22X.2015.1074462]
- 187 **Kim HC**, Jang TW, Chae HJ, Choi WJ, Ha MN, Ye BJ, Kim BG, Jeon MJ, Kim SY, Hong YS. Evaluation and management of lead exposure. *Ann Occup Environ Med* 2015; **27**: 30 [PMID: 26677413 DOI: 10.1186/s40557-015-0085-9]
- 188 **Matović V**, Buha A, Đukić-Ćosić D, Bulat Z. Insight into the oxidative stress induced by lead and/or cadmium in blood, liver and kidneys. *Food Chem Toxicol* 2015; **78**: 130-140 [PMID: 25681546 DOI: 10.1016/j.fct.2015.02.011]
- 189 **Pal M**, Sachdeva M, Gupta N, Mishra P, Yadav M, Tiwari A. Lead exposure in different organs of mammals and prevention by curcumin-nanocurcumin: a review. *Biol Trace Elem Res* 2015; **168**: 380-391 [PMID: 26005056 DOI: 10.1007/s12011-015-0366-8]
- 190 **Fierro NA**, Gonzalez-Aldaco K, Roman S, Panduro A. The immune system and viral hepatitis. In Muriel P. Liver pathophysiology: therapies & antioxidants. Waltham, MA: Elsevier, 2017: 129-139
- 191 **Tang H**, Grisé H. Cellular and molecular biology of HCV infection and hepatitis. *Clin Sci (Lond)* 2009; **117**: 49-65 [PMID: 19515018 DOI: 10.1042/CS20080631]
- 192 **Penin F**, Dubuisson J, Rey FA, Moradpour D, Pawlotsky JM. Structural biology of hepatitis C virus. *Hepatology* 2004; **39**: 5-19 [PMID: 14752815 DOI: 10.1002/hep.20032]
- 193 **Nahmias Y**, Goldwasser J, Casali M, van Poll D, Wakita T, Chung RT, Yarmush ML. Apolipoprotein B-dependent hepatitis C virus secretion is inhibited by the grapefruit flavonoid naringenin. *Hepatology* 2008; **47**: 1437-1445 [PMID: 18393287 DOI: 10.1002/hep.22197]
- 194 **Bok SH**, Shin YW, Bae KH, Jeong TS, Kwon YK, Park YB, Choi MS. Effects of naringin and lovastatin on plasma and hepatic lipids in high-fat and high-cholesterol fed rats. *Nutr Res* 2000; **20**: 1007-1015 [DOI: 10.1016/S0271-5317(00)00191-3]
- 195 **Kim SY**, Kim HJ, Lee MK, Jeon SM, Do GM, Kwon EY, Cho YY, Kim DJ, Jeong KS, Park YB, Ha TY, Choi MS. Naringin time-dependently lowers hepatic cholesterol biosynthesis and plasma cholesterol in rats fed high-fat and high-cholesterol diet. *J Med Food* 2006; **9**: 582-586 [PMID: 17201649 DOI: 10.1089/jmf.2006.9.582]
- 196 **Lee CH**, Jeong TS, Choi YK, Hyun BH, Oh GT, Kim EH, Kim JR, Han JI, Bok SH. Anti-atherogenic effect of citrus flavonoids, naringin and naringenin, associated with hepatic ACAT and aortic VCAM-1 and MCP-1 in high cholesterol-fed rabbits. *Biochem Biophys Res Commun* 2001; **284**: 681-688 [PMID: 11396955 DOI: 10.1006/bbrc.2001.5001]
- 197 **Mulvihill EE**, Allister EM, Sutherland BG, Telford DE, Sawyez CG, Edwards JY, Markle JM, Hegele RA, Huff MW. Naringenin prevents dyslipidemia, apolipoprotein B overproduction, and hyperinsulinemia in LDL receptor-null mice with diet-induced insulin resistance. *Diabetes* 2009; **58**: 2198-2210 [PMID: 19592617 DOI: 10.2337/db09-0634]
- 198 **Wilcox LJ**, Borradaile NM, de Dreu LE, Huff MW. Secretion of hepatocyte apoB is inhibited by the flavonoids, naringenin and hesperetin, via reduced activity and expression of ACAT2 and MTP. *J Lipid Res* 2001; **42**: 725-734 [PMID: 11352979]
- 199 **Borradaile NM**, de Dreu LE, Barrett PH, Behrsin CD, Huff MW. Hepatocyte apoB-containing lipoprotein secretion is decreased by the grapefruit flavonoid, naringenin, via inhibition of MTP-mediated microsomal triglyceride accumulation. *Biochemistry* 2003; **42**: 1283-1291 [PMID: 12564931 DOI: 10.1021/bi026731o]
- 200 **Borradaile NM**, de Dreu LE, Barrett PH, Huff MW. Inhibition of hepatocyte apoB secretion by naringenin: enhanced rapid intracellular degradation independent of reduced microsomal cholesterol esters. *J Lipid Res* 2002; **43**: 1544-1554 [PMID: 12235187]
- 201 **Borradaile NM**, de Dreu LE, Huff MW. Inhibition of net HepG2 cell apolipoprotein B secretion by the citrus flavonoid naringenin involves activation of phosphatidylinositol 3-kinase, independent of insulin receptor substrate-1 phosphorylation. *Diabetes* 2003; **52**: 2554-2561 [PMID: 14514640]
- 202 **Allister EM**, Borradaile NM, Edwards JY, Huff MW. Inhibition of microsomal triglyceride transfer protein expression and apolipoprotein B100 secretion by the citrus flavonoid naringenin and by insulin involves activation of the mitogen-activated protein kinase pathway in hepatocytes. *Diabetes* 2005; **54**: 1676-1683 [PMID: 15919788]
- 203 **Allister EM**, Mulvihill EE, Barrett PH, Edwards JY, Carter LP, Huff MW. Inhibition of apoB secretion from HepG2 cells by insulin is amplified by naringenin, independent of the insulin receptor. *J Lipid Res* 2008; **49**: 2218-2229 [PMID: 18587069 DOI: 10.1194/jlr.M800297-JLR200]
- 204 **Goldwasser J**, Cohen PY, Lin W, Kitsberg D, Balaguer P, Polyak SJ, Chung RT, Yarmush ML, Nahmias Y. Naringenin inhibits the assembly and long-term production of infectious hepatitis C virus particles through a PPAR-mediated mechanism. *J Hepatol* 2011; **55**: 963-971 [PMID: 21354229 DOI: 10.1016/j.jhep.2011.02.011]
- 205 **Khachatoorian R**, Arumugaswami V, Raychaudhuri S, Yeh GK, Maloney EM, Wang J, Dasgupta A, French SW. Divergent antiviral effects of bioflavonoids on the hepatitis C virus life cycle. *Virology* 2012; **433**: 346-355 [PMID: 22975673 DOI: 10.1016/j.virol.2012.08.029]
- 206 **Gonzalez O**, Fontanes V, Raychaudhuri S, Loo R, Loo J, Arumugaswami V, Sun R, Dasgupta A, French SW. The heat shock protein inhibitor quercetin attenuates hepatitis C virus production. *Hepatology* 2009; **50**: 1756-1764 [PMID: 19839005 DOI: 10.1002/hep.23232]
- 207 **Khachatoorian R**, Arumugaswami V, Ruchala P, Raychaudhuri S, Maloney EM, Miao E, Dasgupta A, French SW. A cell-permeable hairpin peptide inhibits hepatitis C viral nonstructural protein 5A-mediated translation and virus production. *Hepatology* 2012; **55**: 1662-1672 [PMID: 22183951 DOI: 10.1002/hep.25533]
- 208 **Mathew S**, Faheem M, Archunan G, Ilyas M, Begum N, Jahangir S, Qadri I, Qahani MA, Mathew S. In silico studies of medicinal compounds against hepatitis C capsid protein from north India. *Bioinform Biol Insights* 2014; **8**: 159-168 [PMID: 25002815 DOI: 10.4137/BBL.S15211]
- 209 **Lulu SS**, Thabitah A, Vino S, Priya AM, Rout M. Naringenin and quercetin--potential anti-HCV agents for NS2 protease targets. *Nat Prod Res* 2016; **30**: 464-468 [PMID: 25774442 DOI: 10.1080/14786419.2015.1020490]
- 210 **Singh AK**, Raj V, Keshari AK, Rai A, Kumar P, Rawat A, Maity B, Kumar D, Prakash A, De A, Samanta A, Bhattacharya B, Saha S. Isolated mangiferin and naringenin exert antidiabetic effect via PPAR γ /GLUT4 dual agonistic action with strong metabolic regulation. *Chem Biol Interact* 2018; **280**: 33-44 [PMID: 29223569 DOI: 10.1016/j.cbi.2017.12.007]
- 211 **Ahmed OM**, Hassan MA, Abdel-Twab SM, Abdel Azeem MN. Navel orange peel hydroethanolic extract, naringin and naringenin have anti-diabetic potentials in type 2 diabetic rats. *Biomed Pharmacother* 2017; **94**: 197-205 [PMID: 28759757 DOI: 10.1016/j.bioph.2017.07.094]
- 212 **Sirovina D**, Oršolić N, Gregorović G, Končić MZ. Naringenin ameliorates pathological changes in liver and kidney of diabetic mice: a preliminary study. *Arh Hig Rada Toksikol* 2016; **67**: 19-24 [PMID: 27092635 DOI: 10.1515/aiht-2016-67-2708]
- 213 **Kapoor R**, Kakkar P. Naringenin accords hepatoprotection from streptozotocin induced diabetes in vivo by modulating mitochondrial dysfunction and apoptotic signaling cascade. *Toxicol Rep* 2014; **1**: 569-581 [PMID: 28962270 DOI: 10.1016/j.toxrep.2014.08.002]
- 214 **Nyane NA**, Tlaila TB, Malefane TG, Ndwandwe DE, Owira PMO. Metformin-like antidiabetic, cardio-protective and non-glycemic effects of naringenin: Molecular and pharmacological insights. *Eur J Pharmacol* 2017; **803**: 103-111 [PMID: 28322845 DOI: 10.1016/j.ejphar.2017.03.042]
- 215 **Sahu SC**, Gray GC. Lipid peroxidation and DNA damage induced by morin and naringenin in isolated rat liver nuclei. *Food Chem Toxicol* 1997; **35**: 443-447 [PMID: 9216742]
- 216 **Galati G**, Moridani MY, Chan TS, O'Brien PJ. Peroxidative metabolism of apigenin and naringenin versus luteolin and quercetin: glutathione oxidation and conjugation. *Free Radic Biol*

- Med 2001; **30**: 370-382 [PMID: 11182292]
- 217 **Ortiz-Andrade RR**, Sánchez-Salgado JC, Navarrete-Vázquez G, Webster SP, Binnie M, García-Jiménez S, León-Rivera I, Cigarroa-Vázquez P, Villalobos-Molina R, Estrada-Soto S. Antidiabetic and toxicological evaluations of naringenin in normoglycaemic and NIDDM rat models and its implications on extra-pancreatic glucose regulation. *Diabetes Obes Metab* 2008; **10**: 1097-1104 [PMID: 18355329 DOI: 10.1111/j.1463-1326.2008.00869.x]
- 218 **Pérez-Pastén R**, Martínez-Galero E, Chamorro-Cevallos G. Quercetin and naringenin reduce abnormal development of mouse embryos produced by hydroxyurea. *J Pharm Pharmacol* 2010; **62**: 1003-1009 [PMID: 20663034 DOI: 10.1111/j.2042-7158.2010.01118.x]

P- Reviewer: Abenavoli L, Chiu KW, Shimizu Y, Tarantino G
S- Editor: Gong ZM **L- Editor:** A **E- Editor:** Huang Y



Naturally occurring hepatitis B virus reverse transcriptase mutations related to potential antiviral drug resistance and liver disease progression

Yu-Min Choi, So-Young Lee, Bum-Joon Kim

Yu-Min Choi, So-Young Lee, Bum-Joon Kim, Department of Microbiology and Immunology, Biomedical Sciences, Liver Research Institute and Cancer Research Institute, Seoul National University, College of Medicine, Seoul 110799, South Korea

ORCID number: Yu-Min Choi (0000-0003-4709-3155); So-Young Lee (0000-0002-9638-893X); Bum-Joon Kim (0000-0003-0085-6709).

Author contributions: Kim BJ conceived participated in its design and coordination; Choi YM and Lee SY analyzed and interpreted the data.

Supported by the Korea Health Technology R&D Project through the Korea Health Industry Development Institute and the Ministry of Health and Welfare, South Korea, No. HI14C0955.

Conflict-of-interest statement: There was no conflict of interest.

Open-Access: This article is an open-access article which was selected by an in-house editor and fully peer-reviewed by external reviewers. It is distributed in accordance with the Creative Commons Attribution Non Commercial (CC BY-NC 4.0) license, which permits others to distribute, remix, adapt, build upon this work non-commercially, and license their derivative works on different terms, provided the original work is properly cited and the use is non-commercial. See: <http://creativecommons.org/licenses/by-nc/4.0/>

Manuscript source: Invited manuscript

Correspondence to: Bum-Joon Kim, PhD, Professor, Department of Biomedical Sciences, Microbiology and Immunology, and Liver Research Institute, Seoul National University College of Medicine, 103, Daehak-ro, Jongno-gu, Seoul 110799, South Korea. kbmjoon@snu.ac.kr

Telephone: +82-2-7408316

Fax: +82-2-7430881

Received: March 27, 2018

Peer-review started: March 27, 2018

First decision: April 3, 2018

Revised: April 10, 2018

Accepted: April 16, 2018

Article in press: April 16, 2018

Published online: April 28, 2018

Abstract

The annual number of deaths caused by hepatitis B virus (HBV)-related disease, including cirrhosis and hepatocellular carcinoma (HCC), is estimated as 887000. The reported prevalence of HBV reverse transcriptase (RT) mutation prior to treatment is varied and the impact of preexisting mutations on the treatment of naïve patients remains controversial, and primarily depends on geographic factors, HBV genotypes, HBeAg serostatus, HBV viral loads, disease progression, intergenotypic recombination and co-infection with HIV. Different sensitivity of detection methodology used could also affect their prevalence results. Several genotype-dependent HBV RT positions that can affect the emergence of drug resistance have also been reported. Eight mutations in RT (rtL80I, rtD134N, rtN139K/T/H, rtY141F, rtM204I/V, rtF221Y, rtI224V, and rtM309K) are significantly associated with HCC progression. HBeAg-negative status, low viral load, and genotype C infection are significantly related to a higher frequency and prevalence of preexisting RT mutations. Preexisting mutations are most frequently found in the A-B interdomain of RT which overlaps with the HBsAg "a" determinant region, mutations of which can lead to simultaneous viral immune escape. In conclusion, the presence of baseline RT mutations can affect drug treatment outcomes and disease progression in HBV-infected populations via modulation of viral fitness and host-immune responses.

Key words: Polymerase; Hepatocellular carcinoma; Reverse transcriptase; Preexisting mutations; Hepatitis B virus

© The Author(s) 2018. Published by Baishideng Publishing Group Inc. All rights reserved.

Core tip: The prevalence of preexisting reverse transcriptase (RT) mutations in treatment-naïve patients largely depends on geographic factors, HBV genotypes, HBeAg serostatus, hepatitis B virus (HBV) viral loads, disease progression, intergenotypic recombination, co-infection with HIV and the method used for detecting the mutation. Genotype-dependent polymorphic amino acid substitutions in RT may affect the emergence of drug resistance, and genotype C exhibits relatively elevated spontaneous RT mutation rates. HBeAg-negative status and low viral loads are significantly associated with a higher frequency and prevalence of HBV preexisting RT mutations. Preexisting mutations are most frequently found in the A-B interdomain of RT, mutations of which can lead to simultaneous viral immune escape.

Choi YM, Lee SY, Kim BJ. Naturally occurring hepatitis B virus reverse transcriptase mutations related to potential antiviral drug resistance and liver disease progression. *World J Gastroenterol* 2018; 24(16): 1708-1724 Available from: URL: <http://www.wjgnet.com/1007-9327/full/v24/i16/1708.htm> DOI: <http://dx.doi.org/10.3748/wjg.v24.i16.1708>

INTRODUCTION

Although an effective and safe vaccine against hepatitis B virus (HBV) has been available since 1982^[1], approximately 257 million people are chronic carriers of the virus. The annual number of deaths caused by HBV related diseases, including cirrhosis and hepatocellular carcinoma (HCC), was estimated as 887000 in 2015 (WHO, 2017)^[2].

Reverse transcriptase (RT) conducts the major enzymatic activity required for viral replication. Nucleos(t)ide analogs (NAs) such as lamivudine^[3], adefovir dipivoxil^[4], entecavir^[5], telbivudine^[6], and tenofovir^[7], for treatment of HBV infection, mainly target RT and function as reverse transcriptase inhibitors by mimicking natural nucleosides and integrating within the DNA molecules to interfere with viral replication^[8,9]. However, due to the lack of proof reading ability of RT, the error rate for viral genome replication is as high as 10^{-7} per nucleotide, which is 10-fold greater than that of other DNA viruses^[10], resulting in the emergence of antiviral-drug resistance mutations^[11-15]. These NA-resistant (NAr) mutants are the greatest challenge for treatment of HBV because they change the conformational structure of RT and lower the effectiveness of NAs by impeding their binding^[16]. In addition, RT partially overlaps with HBV surface antigen (HBsAg) and RT mutation may simultaneously generate HBsAg mutations, which can alter the antigenicity, immune recognition, replication capacity, and virulence of HBV^[17-19].

The reported prevalence of preexisting HBV polymerase RT mutations is varied and the impact of

preexisting RT mutations on treatment-naïve patients remains controversial. In addition, the relationship between preexisting RT mutations and advanced liver diseases, such as cirrhosis and HCC, has not been fully investigated^[20]. Therefore, this review focuses primarily on factors affecting the prevalence and types of preexisting RT mutations in treatment-naïve patients and the relationship between these mutations and disease progression.

DISTRIBUTION OF PREEXISTING HBV NAR MUTATIONS IN SAMPLES FROM TREATMENT-NAÏVE PATIENTS

Liu et al^[21] identified pre-existing HBV RT mutations in 42 potential NAr RT positions from 192 treatment-naïve Chinese patients and arranged them into following four mutation categories: primary drug resistance (Category 1); secondary/compensatory mutation (Category 2); putative NAr (Category 3); and pretreatment (Category 4) (Table 1). To understand the global prevalence of these 42 naturally occurring NAr resistance mutations of RT, we reviewed a total of 50 previous studies^[12,20-68] and collated their results (Figure 1). These include 32 articles published from institutions based in Asia (12 published from China, four from Iran, four from Turkey, four from India, three from Japan, two from Taiwan, and one each from Korea, Jordan, and Indonesia), 11 articles published from institutions based in Europe (six from Italy, two from Germany, and one each from Austria, Ireland, and Spain), four articles published from institutions based in North America (three from United States and one from Canada), two articles published from institutions based in South America (both from Brazil), and one article published from an institution in South Africa (Supplementary Table 1). Among the 50 studies, 36^[12,20,21,32-58,60-65] used direct PCR sequencing methods, 11^[22-28,59,66-68] used the INNO-LiPA line assay, and 3^[29-31] detected RT mutations by ultra-deep pyrosequencing (UDPS). Seventeen articles^[21,26,27,30,31,34,35,37-39,42,43,46-48,53,58] included treatment-naïve patients infected with genotypes B and C, one study^[32] with genotypes A and D, eleven studies^[22,28,29,36,50,51,55,56,60,63,68] with genotype D, one study^[33] with genotype C, and fifteen studies^[20,23-25,40,41,44,45,52,54,57,61,64,65,67] with more than three genotypes (e.g., A, C, and D or A, B, C, and D). In five studies, genotypes of patients were not mentioned. Our literature-based study demonstrated that preexisting RT mutations were also found in treatment-naïve patients at 40 of 42 previously identified NAr RT positions, the two exceptions were rtF242A, a pretreatment mutation and rtF166L, a lamivudine (LMV)-associated putative mutation. The distribution and overall incidence of RT mutations is presented in Figures 1 and 2.

Primary drug resistance mutations are amino acid changes that cause direct NA resistance by decreasing viral susceptibility to NAs^[69-71]. Mutated RT positions known to induce primary drug resistance are rt169,

Table 1 Distribution of preexisting RT mutation in 42 potential NAr regions in treatment naïve patients

[Well known NA resistance mutations (primary and secondary) with phenotypic data;² Putative and pretreatment mutations relevant to NA resistance but not experimentally confirmed;³ Changes in HBsAg, reported in Sheldon et al^[47], Liu et al^[21], Locarnini et al^[72], and Yang et al^[77]. R139 is shared in both Categories 3 (N139D/E/Q) and 4 (N139K/H). Overall, 42 positions in the RT region were studied. ADV: Adenosine triphosphate-activated dipivoxil; ETV: Entecavir; Ldt: Telbivudine; LMV: Lamivudine; TNF: Tenofovir.

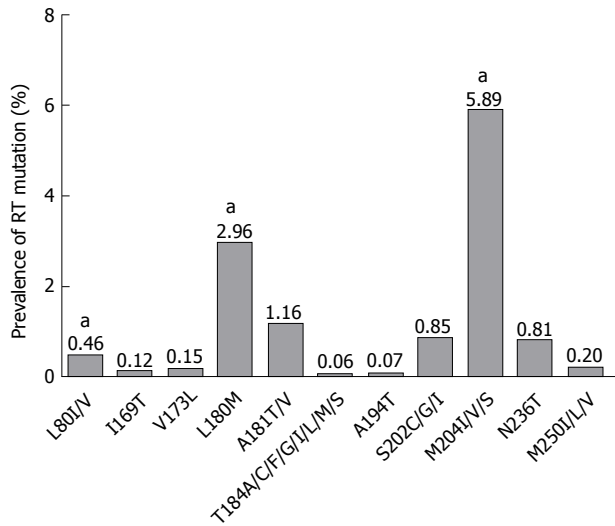


Figure 1 Pooled incidence and distribution of preexisting primary and secondary reverse transcriptase mutations compiled using data from 50 previous studies. The distribution and overall incidence of RT region is presented; numbers indicate the pooled incidence rate of the RT mutation in a total of 8,435 treatment-naïve patients. ^aPre-existing RT mutation associated with the progression of HCC in treatment-naïve patients.

rt181, rt184, rt194, rt202, rt204, rt236, and rt250. The mutations rtA181T/V, rtM204I, and rtM204V also cause the simultaneous HBsAg mutations, sW172 stop, sW196S/L/Stop, and sI195M, respectively^[17,72] (Table 1). Our literature based pooled incidence data showed that of primary drug resistance mutations, M204I/V is the most frequently encountered in treatment-naïve patients^[14,28,33] (5.89%), which was far more than the pooled mutation rate of rta181T/V, rtS202C/G/I and rtN236T (incidence: 1.16%, 0.85% and 0.81%, respectively). Mutation of rtI169T (0.12%), rtT184G (0.06%), rtA194T (0.07%), and rtM250V/L (0.20%) had a very low pooled incidence (Figure 1). A systematic review by Zhang *et al*^[73] revealed that the global incidence of rtM204I/V/S is 4.85%. Several other studies^[24,28,34-37] have also reported the frequent incidence of rtM204I/V/S in treatment-naïve patients. For examples, Kobayashi *et al*^[34], Lee *et al*^[35], Tuncbilek *et al*^[36], Fung *et al*^[24], and Huang *et al*^[37] reported rtM204I/V/S mutation frequencies in Japanese, Taiwanese, Turkish, Canadian, and Chinese treatment-naïve patients reached of 27.8%, 57%, 7.8%, 12%, and 26.9%, respectively.

Secondary, or compensatory, mutations refer to amino acid substitutions that compensate for replication defects caused by primary drug resistance mutations and may reduce drug susceptibility by restoring viral replication fitness^[38,69,74]. The mutations rtL80I/V, rtV173L, rtL180M are known for secondary resistance mutations. Our literature based incidence data showed that rtL180M had the highest natural incidence (2.96%), which was higher than the pooled mutation rate of rtL80I/V and V173L (incidence: 0.46% and 0.15%, respectively) (Figure 1). Similarly, Zhang *et al*^[73] reported that the overall frequency of rtL180M mutation

is 2.67%. Other studies, including Fung *et al*^[24], Yamani *et al*^[38], and Mirandola *et al*^[25] reported that the prevalence rates of rtL180M were 10.0%, 2.08%, and 1.18% in Chinese, Indonesian, and Italian HBV carriers, respectively. The rtL80I/V mutation also occurs frequently in treatment-naïve patients. Yamani *et al*^[38], Kim *et al*^[33], and Mirandola *et al*^[25] found pre-existing rtL80I/V mutation frequencies of 1.07%, 3.82%, and 0.78%, respectively. Notably, Kim *et al*^[33] reported that rtL80I/V was the most frequently encountered preexisting mutation of secondary drug resistance mutations in South Korea (3.8%, 5/131 patients), even higher than rtL180M frequency (2.3%, 3/131 patients). Another compensatory RT mutation, rtV173L, was also detected in several studies of treatment-naïve patients, where Zheng *et al*^[20], Wang *et al*^[39], and Mirandola *et al*^[25] reported that it occurred in 0.6%, 0.56%, and 0.39% of their patients, respectively.

RT mutations which have been identified as associated with drug resistance, but have not been confirmed experimentally *in vitro*, are defined as putative NA resistant mutations^[75-77]. A total of 26 types of RT mutations, including rtS53N, rtT54N, rtL82M, rtV84M, rtS85A, rtI91L, rtY126C, rtT128I/N, rtN139D, rtW153Q, rtF166L, rtV191I, rtA200V, rtV207I, rtS213T, rtV214A, rtQ215P/S, rtL217R, rtE218D, rtF221Y, rtL229G/V/W, rtI233V, rtP237H, rtN238D/S/T, rtY245H, and rtS/C256G, are considered putative drug resistance mutations (Category 3) (Table 1)^[21]. Other amino acid substitutions, which were detected before treatment, but for which the association between their occurrence and drug resistance has not been evaluated, are defined as pretreatment mutations, these include rtT38A, rtY124H, rtD134E/N, rtN139K/H, rtI224V, and rtR242A (Category 4) (Table 1)^[21,38].

Recently, it has been proven through *in vitro* and *in vivo* experiments that several putative or pretreatment mutations, including rtL229F, rtS13T, and rtI233V, can also contribute to the development of drug resistance^[40,78,79]. In addition, several studies have reported that treatment-naïve patients with only putative RT mutations, and without primary or secondary changes, developed drug resistance since treatment initiation^[41]. Our literature based pooled incidence data showed that several putative or pretreatment mutations, including rtI91L, mutations in 6 positions of A-B interdomain (rtY124H, rtY126C/R/H, rtT128I/N, rtD134E/N, rtN139D/E/H/K/Q and rtW153Q/R/E), rtF221Y and rtI224V, were encountered with high frequency from the treatment naïve patients^[20,21,33,38,39,42]. Of these, a RT mutation in the A-B interdomain, rtD134E/N, which also cause a simultaneous sI126N/S mutation of the HBsAg "a" determinant, was found to have the highest frequency in treatment-naïve patients (1.70%) (Figure 2). Of note, the following four putative or pretreatment mutations found in treatment naïve patients, rtD134E/N, rtN139D/E/H/K/Q, rtF221Y, and rtI224V, are also reported as associated with progression of severe liver diseases, such as HCC and cirrhosis (described below).

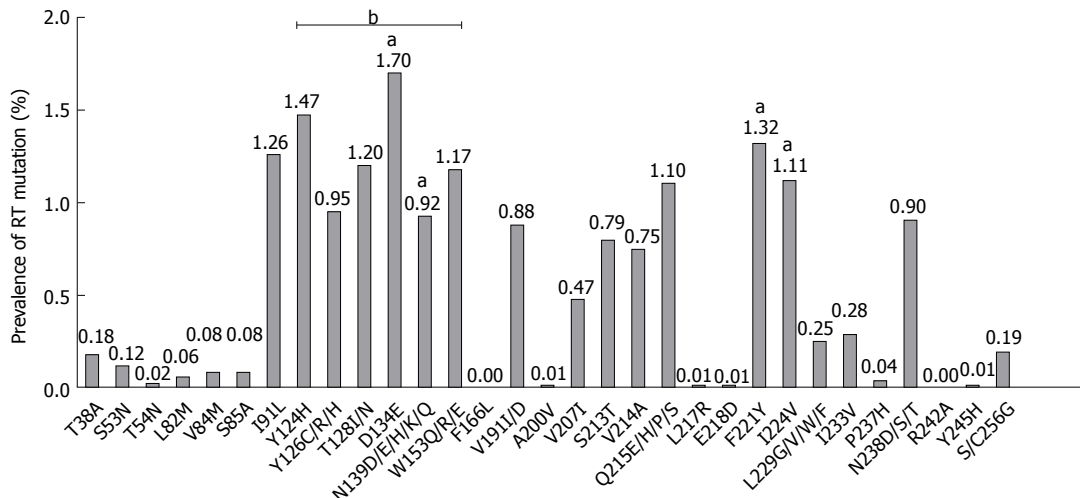


Figure 2 Pooled incidence and distribution of preexisting putative and pretreatment reverse transcriptase mutations compiled using data from 50 previous studies. The distribution and overall incidence of RT region is presented; numbers indicate the pooled incidence rate of the RT mutation in a total of 8435 treatment-naïve patients. ^aPre-existing RT mutation associated with the progression of HCC in treatment-naïve patients; ^bA-B interdomain region.

Moreover, some of these mutations also overlapped with genotype-dependent polymorphic sites, as described in the next section.

DISTRIBUTION OF GENOTYPE-DEPENDENT AMINO ACID POLYMORPHIC SITES IN TREATMENT-NAÏVE PATIENTS

To date, a total of 10 HBV genotypes (A-J) and several sub-genotypes have been identified; genotypes are separated from each other by sequence differences of more than 8% by phylogenetic analysis, based on whole genome sequences^[80,81]. HBV genotypes, including genotypes A-J and the various sub-genotypes, are associated with several distinct traits, including geographical distribution, host ethnicity, and pathogenicity^[82]. Since specific mutational patterns of mutation can be restricted by structural/functional constraints to particular genotypes, HBV genotype can influence the evolution frequency, or types, of mutations associated with NAr in treatment-naïve patients, as described by Liu et al^[21]. Moreover, HBV genotypes can affect LAM-resistant mutations in the YMDD motif of viral RT in patients with chronic infections after long term drug treatment^[42,43,83]. Two recent studies^[83,84] reported that genotype A favors the rtM204V mutation, while HBV-B, C, and D select for rtM204I at higher rates, compared with rtM204V. Moreover, Liu et al^[21] identified eight genotype-dependent AA polymorphic positions, (*i.e.*, rt53, rt91, rt124, rt134, rt221, rt224, rt238, and rt256) useful as signature for B- and C-genotypes with mutations at the 42 positions associated with NAr, and which are important for the distinction between mutations and mere polymorphisms during genotypic mutation analysis of samples from infected patients. These specific, genotype-dependent AA polymorphic positions in RT functional domains, (*i.e.*, rt91 in domain

A, rt238 in domain D and rt256 in domain E) affect drug treatment outcomes^[21,85]. Liu et al^[21] also showed that rtL91 and rtI91 were generally favored by genotypes B and C, respectively, and that rtS256 was prevalent in both genotypes, with rtC256 more common in genotype C than in genotype B. rtL91 and rtC256 were also more closely correlated with failure of extended LMV therapy, compared with other polymorphisms (rtI91 and rtS256) leading to the suggestion that they may represent potential pretreatment markers^[86].

Mirandola et al^[83] further extended the eight genotype dependent polymorphic-sites suggested by Liu et al^[21] into a total of 27 polymorphic-sites potentially affecting treatment, *via* sequence analysis of 200 treatment-naïve chronically infected patients from north-east Italy, infected with the six HBV genotypes; A, B, C, D, E, and F. In this study, substitutions at residues rt53, rt54, and rt91 of the 27 genotype-dependent polymorphic sites were the most frequent single AA substitutions, and HBV-DNA levels of patients with these mutations were significantly lower than those of patients with no mutations, suggesting that these changes contributed to reducing viral fitness during infections. The authors also found that patients with multiple mutations were mainly infected with genotype D, rather than other genotypes (A, B, C, E, or F), strongly supporting previous results indicating that HBV-D may have the highest genetic variability among all HBV-genotypes^[87].

Yamani et al^[38] demonstrated that the distribution of primary and secondary drug resistance mutations was not significantly different between genotypes B and C; however, significant differences were identified in some genotype-dependent polymorphic sites. For example, rtL91I and rtY221F were more common in genotype C, compared to genotype B ($P < 0.001$) (Table 2). Moreover, some genotype dependent mutations, such as rtM129L, rtD134N, rtM145L, and rtE263H/D/Q,

Table 2 Genotype-dependent amino acid polymorphic sites and reverse transcriptase mutations in treatment-naïve patients

| RT position | Drug resistance | Mutations in RT region of four genotypes ¹ | | | | Polymorphism | Ref. |
|-------------|-----------------|---|---|---|---|--------------|---------|
| | | A | B | C | D | | |
| 38 | | T (4.4) ⁴ | | | T (14.0) ⁴ | A/T/T/A | [83] |
| 53 | LMV | | D/T (1.8) ⁴ | | | I/N/S/N | [21] |
| 54 | ADV | N (2.2) ² | | | | T/T/T/H | [83] |
| 84 | | | | I (0.5) ² | V | [127] | |
| | | | | I (1.5) ² | | [21] | |
| 85 | | | | T (0.6) ² | S | [127] | |
| 91 | LMV | | I (20.0) ⁴ | L (23.5) ² | I (16.7) ⁴ | I/L/I/L | [83] |
| | | | | | I (14.3) ² | | [44] |
| 103 | | I (100) ³ | | | I (1.67) ³ | V | [40] |
| 122 | | H (47.0) ² | | | H (6.66) ² | F | [40] |
| | | | | | L/V/I(25.0) ² | | [44] |
| 124 | | H (2.2) ³ | H (20.0) ³ | H (11.8) ³ | | N/N/Y/H | [83] |
| | | | H (3.6) ³ | H (6.6) ³ | | | [21] |
| | | | D (5.5) ³ | | | | |
| 126 | | H (6.7) ⁴ | | | R (23.7) ⁴ | Y/H/H/H | [83] |
| | | | | | R (17.9) ⁴ | | [44] |
| | | | | | Y (1.4) ⁴ Q (0.5) ⁴ | | [83] |
| 128 | LMV | N (2.2) ² | I (1.9) ² | | N (1.4) ² I (1.4) ² | T | [83] |
| | | | | | | | [38] |
| 129 | | | | L (60.0) ² | L (21.4) ² | M | [44] |
| | | | L (1.9) ² | L (26.2) ² | | | [38] |
| | | | L (100.0) ² | L (9.0) ² | L (3.3) ² | | [40] |
| 134 | | | | N (40.5) ² | | D/N/D/D | [38,54] |
| | | | | E (23.1) ³ | E (5.0) ³ | | [21,54] |
| | | | | E (5.8) ³ | | | [21] |
| 139 | LMV | | I/S (1.8) ³ | K (3.7) ² | K (11.9) ² | Q/N/N/N | [38] |
| | | | | | K (2.3) ³ | | [83] |
| | | | | | K (1.5) ³ | | [21] |
| 145 | | | L (3.7) ² | L (40.5) ² | | M | [83] |
| 153 | LMV | Q (100) ² | | | | W/R/R/R | [40] |
| 191 | LMV | | | V (8.3) ² | | V/I/I/V | [39] |
| | | | I (4.6) ² | F (7.7) ² | | | [54] |
| 200 | LMV | V (2.2) ² | | | | A | [83] |
| 207 | LMV | | M (6.0) ² L (2.3) ² | | | V | [26] |
| | | | | I (5.9) ² | | | [83] |
| | | | | I/L/G (2.1) ² | | | [39] |
| 214 | LMV/ADV | | A (0.5) ² I (0.5) ² | A (5.9) ² | A (2.3) ² | V | [83] |
| | | | | I (0.6) ² | A (0.8) ² E (0.7) ² | | [127] |
| 215 | ADV | | H (0.9) ² | E (7.7) ² | H (5.0) ² S (5.0) ² | Q | [54] |
| | | | | | H (3.0) ² S (4.3) ² | | [127] |
| | | | | | P (2.8) ² S (4.2) ² | | [83] |
| 217 | | L (6.7) ⁴ | | | R (0.9) ² | R/L/L/L | [83] |
| 221 | ADV | | | F (40.5) ² | Y (5.1) ² | Y/Y//F/F | [38] |
| | | | | | | | [83] |
| 226 | | | H/T (33.3) ² | H/T (2.4) ² | | N | [38] |
| 237 | | | | | T (6.4) ² | P | [127] |
| 238 | LMV, ETV | H(1.0) ² W(1.0) ² | Q (3.9) ² | T (8.7) ² | H (2.3) ² | N/H/N/N | [127] |
| | | | Q (1.82) ² | S (2.19) ² T (0.73) ² | | | [21] |
| | | | | T (3.87) ² | | | [39] |
| | | | D (2.2) ² T (2.2) ² | | D (1.4) ² | | [83] |
| 245 | | | | | H (1.4) ² | Y | [83] |
| 248 | ADV | | H (7.4) ³ | H (4.8) ³ | | N | [38] |
| 256 | LMV | | G (20.0) ² | G (40.0) ² | G (10.7) ² | S/S/S/C | [44] |
| | | | G (5.45) ² | | G (3.7) ² | | [83] |
| | | | | | G (3.7) ² | | [21] |
| | | | | | | | [26] |

A total of 29 reported genotype-dependent amino acid polymorphic sites in the RT region in treatment-naïve patients are shown. The first column contains the RT positions and the second column details the relationship between mutations and drug resistance. Column three to six indicate the prevalence of each mutation as percentages, according genotype. Consensus amino acids are presented in column seven. ¹Incidence (%) of mutations in the RT region; ²Putative mutation; ³Pretreatment mutation; ⁴Novel mutation. ADV: Adefovir dipivoxil; ETV: Entecavir; Ldt: Telbivudine; LMV: Lamivudine; TNF: Tenofovir.

were more frequent in genotype C than genotype B viruses ($P < 0.001$). Notably, rtN226H/T was the

only pretreatment mutation, which is more common in genotype B than genotype C ($P < 0.001$). Singla *et al*^[44]

Table 3 Positive relationships between HBeAg negative serostatus and preexisting reverse transcriptase mutation frequency in the treatment-naïve patients

| HBeAg-positive | HBeAg-negative | HBV genotype (%) | Location | Ref. |
|------------------------|----------------------|------------------------|----------------------|---------------|
| Mutations ¹ | HBV-DNA ² | Mutations ¹ | HBV-DNA ² | |
| 3/14 (21.4) | 7.8 | 11/14 (78.6) | 5.7 | B, C, E |
| 6/24 (25.0) | 5.5 | 18/24 (75.0) | 3.9 | B, C, B-C |
| 0/4 (0.0) | 7.2 | 4/4 (100.0) | 4.7 | A, B, C, D, F |
| 3/6 (50.0) | 8.0 | 3/6 (50.0) | 3.2 | D |
| 8/12 (67.0) | 7.9 | 4/12 (33.0) | 6.9 | NA |
| 27/43 (62.8) | 5.7 | 16/43 (37.2) | 4.7 | B, C |
| 8/13 (61.5) | 6.3 | 5/13 (38.5) | 5.4 | B, C |
| 0/5 (0.0) | NA | 5/5 (100.0) | NA | NA |
| 0/4 (0.0) | NA | 4/4 (100.0) | NA | Japan |

¹Number of patients with RT mutation (%); ²HBV-DNA level (\log_{10} IU/mL).

also showed that rtL91I and rtM129L are more common in samples from genotype C, than genotype D, infected patients. Overall, these findings indicate that distribution of genotype dependent polymorphic sites in treatment-naïve patients could affect drug treatment outcomes via modulation of viral fitness or replication. The distribution of the 29 genotype-dependent polymorphic-sites in the HBV RT region among treatment naïve patients identified in other reports is summarized in Table 2.

GENOTYPE DISTRIBUTION OF PRIMARY RT MUTATIONS IN TREATMENT-NAÏVE PATIENTS

Mirandola *et al*^[25] identified the different genotype different distributions of antiviral drug resistant RT mutations using INNO LiPA line probe analysis of samples from treatment-naïve patients; RT mutations were detected in 13 (5%) of 255 HBV infected patients. Of these, 10 patients had mutations associated with primary resistance or reduced sensitivity, including three cases with a YMDD mutation (rtM204V), three with the mutation, rtM250L/V, which is associated with ETV resistance, and four with the mutation rtI233V, which is associated with reduced sensitivity to ADV. Notably all the three patients with the rtM204V mutation also had coexisting L180M compensatory mutations, and all were infected with HBV-C genotype viruses, suggesting that naturally occurring LMV-resistant HBV may be more frequent in patients infected with genotype C virus. This hypothesis is strongly supported by the recent report of Kim *et al*^[33] of the high frequency of the YMDD mutation, (rtM204V/I) (6.87%, 9/131 patients), in Korean treatment-naïve patients with HBV genotype C2 infections. Wang *et al*^[39] also reported that RT mutations were only found in genotype C treatment-naïve patients; however, no primary or secondary RT mutations were found in genotype B patients. In addition, a systemic meta-analysis review by Zhang *et al*^[73] showed that rtM204V/I had the highest incidence of 4.89% (95%CI: 4.13%-5.65%) among primary and secondary RT mutations. These authors also found, via

the subgroup analysis by genotype, that HBV genotype C had a tendency of toward a higher spontaneous YMDD mutation frequency (19.32%) than genotype B (15.01%) or D (14.79%). The increased spontaneous mutations in the viral genome of HBV genotype C could translate to a higher risk of primary NA resistance in HBV endemic areas, where genotype C infections are prevalent, including China and South Korea.

CLINICAL FACTORS (HBEAG SEROSTATUS AND HBV VIRAL LOADS) AFFECTING INCIDENCE OF PREEXISTING RT MUTATIONS IN TREATMENT-NATIVE PATIENTS

The majority of studies have consistently reported a significant association between the prevalence of preexisting RT mutations and lower HBV DNA loads, or HBeAg-negative status, in treatment-naïve patients^[26,27,34-36,45-47,88] (Table 3). Vutien *et al*^[26] reported that treatment-naïve patients with HBeAg-negative status had higher RT mutation frequencies (78.57%), compared with HBeAg-positive patients (21.42%). These authors also showed that HBeAg-negative patients had significantly lower HBV DNA viral loads compared with HBeAg-positive patients (5.65 \log_{10} IU/mL vs 7.82 \log_{10} IU/mL, respectively). Zhao *et al*^[27] also reported similar results showing that 75% of patients with RT mutations were HBeAg-negative and had lower HBV DNA levels (3.92 \log_{10} IU/mL) whereas 25% of patients with RT mutations were HBeAg-positive with higher HBV DNA loads (5.54 \log_{10} IU/mL). Similarly, Zhu *et al*^[89] found that Chinese patients with chronic HBV carrying preexisting RT mutations had significantly decreased serum baseline HBV DNA loads ($P = 0.0363$) and blood platelet counts ($P = 0.0181$) compared with those without RT mutations.

Several other studies^[34,45,88] also found RT mutations only in HBeAg-negative patients, and the patients were also more likely to have decreased HBV DNA levels compared with those who were HBeAg-positive^[45].

Kobayashi *et al*^[34] reported that all asymptomatic HBV carriers with YMDD mutation were HBeAg-negative and eAb-positive, suggesting that sustained host immune pressure may be a major force driving potential NAr mutations. Zhang *et al*^[73] also reported a systemic meta-analysis finding that patients with chronic hepatitis B (CHB) and genotype C infections, who were male and HBeAg-negative tended to have higher spontaneous mutation rates in subgroup analysis. Xu *et al*^[46] reported no significant correlation between pre-existing mutations and the majority of clinical factors including gender, age, HBV genotype, ALT, HBeAg, and HBV DNA loads, in a Chinese population; however, subgroup analysis indicated that pre-existing mutations were strongly associated with lower HBV DNA levels in HBeAg sero-negative, but not HBeAg sero-positive, patients (HBeAg+ vs HBeAg-: 5.74 log₁₀ IU/mL vs 4.72 log₁₀ IU/mL, $P = 0.0112$). These findings suggest that preexisting RT mutations might lead to lower HBV viral loads in treatment-naïve patients with HBeAg-negative serostatus. Several other studies have reported similar positive associations between the frequency of pre-existing RT mutations and decreased HBV viral loads^[33,42,83].

Taken together, there appears to be a clear causal link between preexisting RT mutations and HBeAg-negative status, decreased HBV DNA load, or liver disease progression. This may be because mutations in the RT active domain, could impair enzyme activity, particularly at the HBeAg negative immune clearance stage, thus decreasing the efficacy of virus replication and, resulting in liver disease progression and poor treatment outcomes^[17,42,90,91].

GENOTYPE DISTRIBUTION AND GEOGRAPHICAL FACTOR AFFECTING THE INCIDENCE OF PREEXISTING RT MUTATIONS

Reports of the incidence of preexisting RT mutations in treatment-naïve patients are highly variable, ranging from 0% to 57%^[25,26,28,32-35,48,92,93]. This huge discrepancy among studies may be due to differences in factors such as the geographical or ethnic backgrounds of studied patients, sample size, and viral genotype^[27]. A number of studies have reported prevalence rate of preexisting RT mutations (primary and secondary RT mutations) of more than 5% in treatment-naïve patients (Table 4). Fung *et al*^[24] found a higher rate of baseline RT mutations (12% M204I/V, 10% L180M) by using the INNO-LIPA v.3 assay. In this study, many patients, most of whom were infected with genotype D, carried rtL180M, rtM204V/I, and rtL80V/I mutations. In addition, Nishijima *et al*^[94] identified a high mutation rate (35.7%) in 14 treatment-naïve patients in Japan, using UDPS. Also, a recent study using direct sequencing^[33] of samples from

131 treatment-naïve patients infected with genotype C2 reported an overall rate of 12.98% for primary (rtT184A/C/F and rtM204I/V) or compensatory (rtL80I and rtL180M) mutations. According to a systemic meta-analysis review conducted by Zhang *et al*^[73], the overall prevalence of spontaneous mutations among treatment-naïve patients worldwide was 5.73%. The highest pooled prevalence (8.00%) was identified in samples from China, followed by Japan, Turkey, Korea, South America, and Europe at 6.62%, 6.43%, 5.72%, 3.89%, and 2.53%, respectively. Another study of 325 genotype D infected treatment-naïve patients using direct PCR sequencing^[50] reported overall incidence of 15.69% for primary and secondary drug resistance mutations, including L80V/I, L180M, M204I/V, and S213T/N.

In contrast, several studies have reported prevalence rates of less than 5 % for pre-existing RT mutations (primary and secondary RT mutations) in treatment-naïve patients (Table 4). For example, using direct sequencing of samples from treatment-naïve patients from the United States, Nguyen *et al*^[45] demonstrated that only four (0.9%) of 472 patients were infected with viruses with primary and secondary mutations (rtA181A/S, rtA194S, and rtM250I). Similarly, Zollner *et al*^[32] screened a total of 96 patients infected with HBV genotypes A and D (52.08% and 47.92%, respectively) using a direct sequencing assay, but found no primary or secondary resistance mutations. Another study by Salpini *et al*^[51] using the direct sequencing method reported that, of 140 treatment-naïve patients infected with genotype D, only 1.4% had primary drug resistance mutations, while 2.1% carried secondary mutations.

Overall, preexisting RT mutation prevalence clearly reflects the geographical distribution of HBV infection. For example, China is an area with high levels of endemic area of HBV infection (8%, according to a national survey in 2006) and also has higher prevalence of pre-existing RT mutations^[73]. Meanwhile, in Europe, which has low levels of endemic HBV infection (approximately 2%), there is a low incidence of spontaneous mutations (2.53%)^[73]. Since the HBV geographic distribution has also a close relationship with the genotype distribution, the majority of countries in Asia with prevalent genotype B and C infections have high rates of spontaneous RT mutation ($\geq 5\%$)^[27,33-35,39,47,73], whereas countries in Europe, where genotype A and D infections are dominant, tended to have low incidences ($\leq 5\%$)^[32,49,51].

HBV INTERGENOTYPIC RECOMBINATION AND COINFECTION WITH HIV AFFECTING THE INCIDENCE OF PREEXISTING RT MUTATIONS

HBV intergenotypic recombination between different

Table 4 Variation in the prevalence of preexisting reverse transcriptase mutations according to mutation detection methods, genotype, and geographic distribution

| Prevalence | Location | No. of cases | Genotype | HBV DNA loads (\log_{10} IU/ml) | RT mutations prevalence | Mutation detecting methods | Ref. |
|---------------------------------|-----------------------|--------------|---------------|------------------------------------|---|----------------------------|------|
| HBV DNA RT mutations $\geq 5\%$ | | | | | | | |
| | Italy | 255 | A, C, D | 5.0 | 5.0% mutations overall | INNO-Lipa HBV DR v.3 | [25] |
| | China | 269 | B, C, B-C | 4.9 | 8.9% mutations overall | INNO-Lipa HBV DR v.3 | [27] |
| | Canada | 209 | A, B, C, D | 7.0 | 12% M204I/V, 10% L180M, 9% L80V/I, 3% V173L | INNO-Lipa HBV DR v.3 | [24] |
| | Turkey | 71 | NA | | 18.3% YMDD mutations | INNO-Lipa HBV DR v.1 | [28] |
| | South Korea | 131 | C2 | 6.5 | 12.98% mutations overall | Direct Sequencing | [33] |
| | Turkey | 77 | D | 7.3 | 7.8% YMDD mutations | Direct Sequencing | [36] |
| | China | 213 | B, C | 6.2 | 6.1% mutations overall | Direct Sequencing | [47] |
| | China | 104 | B, C, B-C | 4.5 | 26.9% YMDD mutations | Direct Sequencing | [93] |
| | Japan | 18 | NA | NA | 27.8% YMDD mutations | Direct Sequencing | [34] |
| | Iran | 325 | D | NA | 15.69% mutations overall | Direct Sequencing | [50] |
| | Taiwan, China | 28 | NA | 7.5 | 57% YMDD mutations | Direct Sequencing | [35] |
| | China | 357 | B, C | 6.3 | 16.8% mutations overall | Direct Sequencing | [39] |
| | Meta-analysis (China) | 8156 | B, C, D | NA | 8.00% mutations overall | Record screening | [73] |
| | Japan | 14 | B, C | 4.9 | 35.7% YMDD mutations | Ultra-deep sequencing | [94] |
| | Iran | 147 | D | NA | None | Direct sequencing | [56] |
| | China | 328 | B, C | 6.9 | 3.6% mutations overall | Direct sequencing | [53] |
| | Japan | 20 | NA | NA | None | Direct sequencing | [48] |
| | California | 472 | A, B, C, D, F | 5.3 | < 1% mutations overall | Direct sequencing | [45] |
| | Italy | 100 | NA | NA | None | Direct sequencing | [49] |
| | Italy | 140 | D | 4.0 | 3.5% mutations overall | Direct sequencing | [51] |
| | Germany | 96 | A, D | NA | None | Direct sequencing | [32] |
| | Brazil | 189 | A, C, D, F | 3.2 | overall 6.0% in Northeast / 0% in North | Direct sequencing | [41] |
| | California | 198 | B, C | 4.2 | 1% mutations in polymerase | INNO-Lipa HBV DR v.3 | [26] |
| HBV DNA RT mutations < 5% | | | | | | | |

genotypes is regarded as an important strategy for HBV genetic diversity and may impose challenges on vaccine designation and antiviral therapy strategies^[95,96]. In particular, the high prevalence of vertical infections in HBV endemic areas, such as Asia or Africa, could lead to a life-long chronic infection^[97], resultantly leading to a high probability of co-infection and a high risk for virus recombination^[96,98-101]. Previous studies on HBV recombination have identified different types of intergenotypic recombinants in HBV RT, most of which have recombination in RT/S overlapping region^[96,98-103]. Of note, a recent study conducted by Liu et al^[100] demonstrated that, through full-length HBV RT sequences analysis from 201 Chinese chronic hepatitis B (CHB) patients, 38.10% (24/63) infected with genotype B had recombination with genotype C in the 3'-terminal RT sequences. These authors also showed that these intergenotypic recombinants were associated with enhanced viral DNA load and higher RT point mutation rates, compared with their parental genotype B or C, highlighting the importance of monitoring intergenotypic RT recombinants in HBV endemic areas to ensure optimal management.

Approximately, 10% of HIV-infected persons worldwide are chronically infected with HBV, and co-infection of two viruses is most frequently identified (up to 25%) in sub-Saharan Africa and Asia^[104]. HBV and HIV co-infection is a major cause of morbidity and mortality because it could contribute to an increased risk of liver cirrhosis and HCC^[105]. In general, previous studies showed a predominance of HBV genotype A in HIV infected individuals, compared with other genotypes^[106,107]. In particular, Makondo et al^[108] reported that the ratio of genotype A to non-A (97% to 3%) was higher in the HBV/HIV co-infected Southern Africa patients compared with mono-infected individuals. These authors also showed that 10 percent, 3 out of 29 patients prior to the initiation of antiretroviral therapy (ART), had drug resistance mutations rT173L, rT180M+rTM204V, and rT214A. In South Africa, rTM204I has been mainly detected in treatment-naïve HBV/HIV co-infected individuals^[12] with rTM204V in treated HBV mono-infected participants^[109], suggesting HIV co-infection could affect HBV preexisting RT mutation pattern. A study of South African patients conducted by Selabe et al^[12] demonstrated that HBV lamivudine - resistant strains were detected in three out of 15 treatment-naïve mono - infected chronic hepatitis B patients,

Table 5 Relationship of preexisting reverse transcriptase mutations with disease severity

| Type of mutation in RT | Change in HBsAg | Genotype | Location | Disease progression | P value | Ref. |
|--------------------------|-----------------|----------|-------------|-------------------------|-------------|----------|
| rtL80I ² | NC | C | South Korea | HCC | 0.036 | [33] |
| rtD134N ⁴ | sI126S/N | B, C | China | HCC | 0.007 | [114] |
| rtN139K/T/H ⁴ | sT131N/P | C | South Korea | HCC | 0.008 | [33] |
| rtY141F ⁵ | sM307T | Ce | Taiwan | HCC | 0.029 | [37] |
| rtM204I/V ¹ | sW196L/S/W | C | South Korea | HCC | 0.021 | [33] |
| rtF221Y ³ | NA | B,C,D | China | HCC, poor survival rate | 0.028/0.004 | [20,115] |
| rtI224V ⁴ | NC | C | China | HCC | 0.005 | [116] |
| rtM309K ⁵ | NA | C | China | HCC | 0.007 | [116] |

HBV polymerase RT mutation; ¹Primary; ²Secondary; ³Putative; ⁴Pretreatment; ⁵Novel RT mutation. HCC: Hepatocellular carcinoma; NA: Not available; NC: Not changed; RT: Reverse transcriptase.

whereas detected in 10 out of 20 treatment-naïve HBV/HIV-coinfected patients. In contrast, a multi-national study of HIV/HBV-coinfected individuals carried out by Thio *et al*^[110] demonstrated that no subject had preexisting RT mutations in the majority population of the quasispecies, suggesting no need for HBV drug-resistance testing prior to starting anti-HBV therapy in HIV-HBV co-infected individuals. It is also supported by a recent study of Ghana patients conducted by Archampong *et al*^[111]. Taken together, geographical factors and HBV genotypes could have effects on the preexisting HBV RT mutation in treatment-naïve HBV/HIV-coinfected patients.

DIFFERENT SENSITIVITY OF DETECTION METHODOLOGY USED CAN AFFECT THE REPORTED PREVALENCE OF PREEXISTING RT MUTATIONS: LIMITATION OF THE STUDIES IN PREEXISTING RT MUTATIONS

The detection methods used can also have a profound effect on the reported incidence results of preexisting RT mutations. The majority of studies have used direct sequencing methods, which can lead to the underestimation of preexisting RT mutations, due to the relative low sensitivity of these assays. Wang *et al*^[39] reported that the sensitivity of direct sequencing-based protocols declined when circulating viral subspecies (AA substitutions) levels were at ratio below 20%-25%. Similarly, there were several studies have reported discordance in the incidence of pre-existing RT mutations detected by direct sequencing and other screening methods, such as the INNO-LiPA assay, or UDPS. For example, Margeridon-Thermet *et al*^[52] reported that direct sequencing found an average of 5.9 mutations per sample, while UDPS identified an additional 4.6 mutations per sample, which could not be detected by direct sequencing. In that study, two of 17 treatment-naïve patients had mutations which were detected only by UDPS, but not by direct sequencing; one rtM204I mutation with (1.3% mutant ratio) and the other an

rtA181T mutation (1.0% ratio). Similarly, Aberle *et al*^[66] also compared the detection efficacies for preexisting RT mutations between the INNO-LiPA assay and direct sequencing. The former identified additional mutations in 8 (14%) of 56 patient samples, which could not be detected using the latter method, indicating the superiority of the former over the latter for RT mutation detection. Overall, these data demonstrate that the method used for detecting the mutations can affect the prevalence estimates of preexisting RT mutations in treatment-naïve patients, which may cause discrepancies among the results of different studies.

PREEEXISTING RT MUTATIONS ARE RELATED TO THE PROGRESSION OF LIVER DISEASES

Although the clear association between preexisting RT mutations and advanced liver disease has not been fully investigated, several types of HBV mutations in RT have previously been reported as related to the progression of liver diseases, such as cirrhosis and HCC (Table 5). Kim *et al*^[33] compared types and frequencies of pre-existing RT mutations between CHB and HCC treatment-naïve patients. These authors found a significantly higher rate of RT mutations in HCC patients than in those with chronic hepatitis (3.17% vs 2.09%, $P = 0.003$) and also identified a total of three NAr mutations (rtL80I, rtN139K/T/H, and rtM204I/V) significantly associated with HCC progression. RT mutations rtN139K/T/H and rtM204I/V also cause simultaneous mutations in the overlapped HBsAg coding sequence (sT131N/P and sI195M, or sW196S/L/Stop)^[17,21,72]. Of these, the YMDD-motif mutation (rtM204I/V) was found in 9 patients of 131 patients (8 HCC and 1 CHB) with the other two types of mutation, rt204I and rt204V, in 8 and 1 patients, respectively. The other HCC-related mutation (rtL80I) was first identified as a compensatory mutation associated with LMV resistance^[69,112]. Its relationship with clinical deterioration is also corroborated by other reports that it was associated with increased viral loads, accompanied by an elevation in serum aminotransferase activity, and exacerbation of liver disease in every

Table 6 Distribution of preexisting reverse transcriptase mutations among reverse transcriptase domains

| Domains ² | Mutation frequency (%) ¹ | | P value ⁵ | Ref. |
|----------------------|-------------------------------------|-----------------------------------|----------------------|------|
| | A-B interdomain ³ | Non-A-B interdomains ⁴ | | |
| 1.45 | 3.51 | 2.58 | < 0.001 | [38] |
| 1.37 | 4.4 | 3.77 | < 0.001 | [20] |
| 1.07 | 7.5 | 3.16 | 0.008 | [33] |
| 0.43 | 3.82 | 0.52 | 0.0014 | [21] |

¹Mutation frequency was calculated as the number of mutations found in a specific RT domain divided by the total number of sites in the domain;

²Domain including RT mutation sites; rt38, rt84, rt207, rt233, rt238, and rt256; ³A-B interdomain including RT mutations sites: rt53, rt191, rt213, rt218, rt229, and rt242; ⁴Non-A-B interdomains including RT mutation sites: rt124, rt126, rt128, rt134, rt139, and rt153; ⁵P-values of comparisons of mutation frequencies between A-B interdomain and other functional domains.

case^[113]. Interestingly, Kim *et al*^[33] also showed that rtL80I was combined with the rtM204I/V mutation in five of nine rtM204I/V cases, and that patients with L80I had increased HBV replication compared with those without this mutation, suggesting that, together with rtM204I/V, it may contribute to HCC generation in treatment-naïve patients by compensating for the defective replication caused by rtM204I/V.

In another study, Yin *et al*^[114] analyzed the association of the mutations of HBV polymerase with postoperative survival in 92 patients with HBV-related HCC using direct sequencing. They discovered three nucleotide sites, one (31st nucleotide) in a spacer region and two [529th ($P = 0.007$) and 1078th ($P = 0.038$)] in the RT region, which could be considered independent predictors of postoperative survival in HBV-related HCC. Of the two sites in RT related to HCC outcomes, rtD134N (mutation G529A) was associated with lamivudine resistance, further supporting previous findings of potential correlation between resistance to the anti-HBV nucleoside analog, lamivudine, and HCC prognosis^[114]. Since rtD134N also causes an amino acid change in HBsAg (sI126N/V), it can induce changes in the antigenic properties of HBsAg. Further functional studies are necessary to determine whether the rtD134N mutation can induce HCC via modulation of RT activity or through its effects on HBV replication.

Huang *et al*^[37] found seven viral single nucleotide polymorphisms (SNPs) in HBV polymerase, which enhance viral replication and liver disease progression in HBeAg negative subjects. Of these SNPs, rtY141F (Y487F), which is located in the RT region of HBV polymerase was associated with increased viral load and HCC ($P = 0.0291$). Moreover, rtY141F, a genotype C-related SNP, also led to a simultaneous amino acid change in the overlapping 'a' determinant region of HBsAg (sM307T). In addition, Li *et al*^[115] and Zheng *et al*^[20] reported that the rtF221Y mutation was strongly related to HCC prognosis after liver resection (hazard ratio, 2.345; $P = 0.001$). Moreover, the

rtF221Y mutation was also associated with poor overall survival (hazard ratio, 2.557; $P = 0.004$), suggesting that it is a potential independent risk factor and viral marker for HCC. Those results were consistent with the report of Li *et al*^[115], which identified the rtF221Y mutant as an independent risk factor for recurrence of HCC and poor overall survival ($P = 0.001$ and $P = 0.004$, respectively). Wu *et al*^[116] also investigated preexisting RT mutations potentially related to HCC in Chinese patients and identified rtI224V and rtM309K as significant risk factors for HCC ($P = 0.005$ and $P = 0.007$, respectively).

In addition, the number of RT mutations is associated with the liver disease progression. Zhu *et al*^[89] revealed that patients with multiple RT mutant sites showed a significantly higher rate of liver fibrosis ($P = 0.0128$), suggesting a link between viral mutation and clinical progression of chronic hepatitis, and also highlighting that the natural accumulation of RT mutations is a process involved in viral survival during chronic liver fibrosis.

Overall, eight mutations in the RT region, namely rtL80I, rtD134N, rtN139K/T/H, rtY141F, rtM204I/V, rtF221Y, rtI224V, and rtM309K, are significantly related to liver disease progression. The majority of HCC-related RT mutations were reported from studies of treatment-naïve patients infected with genotype C HBV. This supports previous reports that HBV genotype C is more likely to lead to severe and aggressive liver disease than other HBV genotypes^[112,117-122]. Of note, association of the following three mutations, rtM204V, rtL80I, and rtD134N, with disease progression provides a likely explanation for the positive relationship between lamivudine resistance and liver disease progression.

DISTRIBUTION AND FREQUENCY OF PREEEXISTING RT MUTATIONS IN DIFFERENT RT REGIONS

HBV RT consists of seven functional domains (G, F, A, B, C, D, and E) and five inter-domains (F-A, A-B, B-C, C-D, and D-E) which link the functional domains^[18,31,123]. Previous studies^[20,21,33,38] reported a higher frequency of preexisting RT mutations in the A-B inter-domain, compared with other regions.

Liu *et al*^[21] revealed that all six sites in the A-B interdomain, rt124, rt126, rt128, rt134, rt139, and rt153, exhibit mutations (6/6, prevalence 100%), indicating high genetic variability of this region compared with other sites within RT domains (sites with mutations: 6/22, 27.27%; $P = 0.0014$). In this study, the mutation frequency of the A-B inter-domain (44/1152, 3.82%) was also significantly higher than those in other RT domains (Table 6). This result is in line with that reported by Zheng *et al*^[20], who demonstrated that A-B interdomain exhibits higher mutation frequencies (4.3%, 5.3%, 3.6%) than those of other RT domains (1.4%, 1.4%, 1.3%) in Chinese

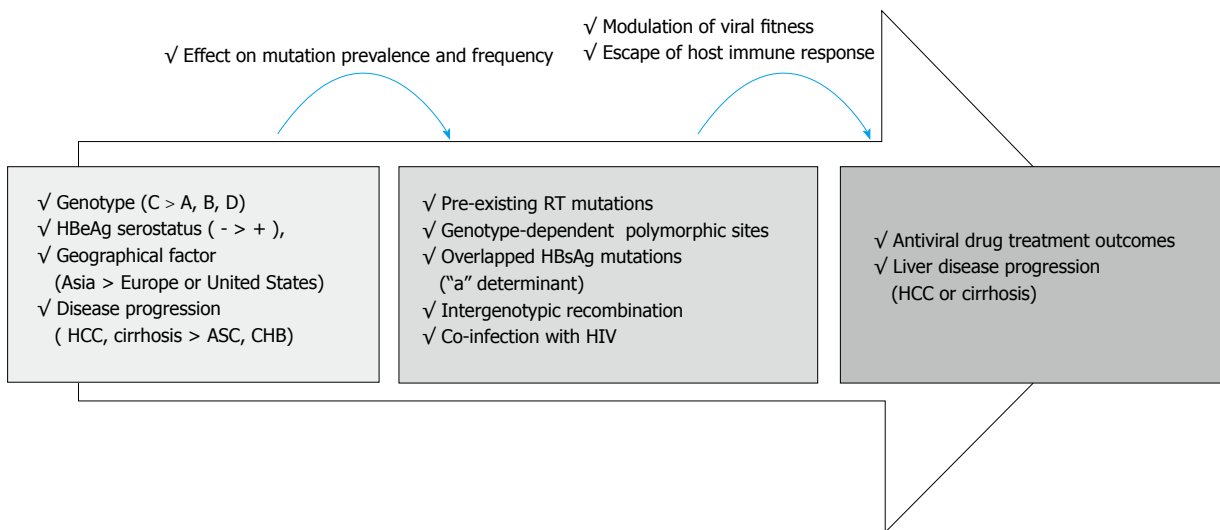


Figure 3 Schematic representation indicating the role of preexisting hepatitis B virus reverse transcriptase mutations in liver disease progression and treatment outcomes. HBV: Hepatitis B virus; HCC: Hepatocellular carcinoma; ASC: Asymptomatic carriers; CHB: Chronic hepatitis B; HIV: Human immunodeficiency virus.

treatment-naïve patients with CHB, cirrhosis, and HCC. Specifically, they found that there was a clear tendency toward frequent mutations of the A-B interdomain in patients with cirrhosis suggesting a relationship between mutations in the A-B inter-domain and the development of this condition.

Similarly, Yamani *et al*^[38] also reported that the A-B interdomain had the highest mutation prevalence and frequency ($3.51\% \pm 2.53\%$) compared with functional domains and non-A-B interdomains ($1.45\% \pm 1.05\%$ and $2.58\% \pm 0.51\%$, respectively) in Indonesian treatment-naïve patients (Table 6). Moreover, they found that genotype C had substantially higher mutations rates in the A-B interdomain than genotype B ($P < 0.001$). Kim *et al*^[33] also revealed that mutations within the A-B interdomain were most frequent in treatment-naïve Korean patients infected with genotype C2, compared with other domains, with 46 of 79 patients (58.22%) with preexisting RT mutations having changes in the A-B inter-domain. In this study, rtD134E/N/C was the most frequently encountered hot spot site among the six A-B interdomain sites and was mutated in 12/79 patients (15.2%). The authors also showed that the mutation frequency of A-B interdomain (59/786, 7.50%) was higher than that of non A-B interdomain (3.16%) (Table 6). Our pooled incidence also supported the previous notion of higher frequency of persisting RT mutations in A-B interdomain compared with other region in RT (Figure 2).

RT and HBsAg mutations can occur simultaneously, due to the overlap of RT region and HBsAg gene sequences^[19,124]. Liu *et al*^[21] reported that 14 of 18 mutated positions in RT overlapped with HBsAg, and that RT mutations at 12 out of 14 RT positions (except those at rt124 and rt126) also led to simultaneous HBsAg mutations of 19 types in 16.67% (32/192) of isolates (Figure 1). Notably, these authors also

found that RT mutations in the A-B interdomain could lead to simultaneous AA substitutions sI126A/N/S/, sG130N, sT131N/P, and sG145R of the overlapped 'a' determinant of HBsAg, including the most frequently described immune-escape mutation sG145R (1/192, 0.52%)^[125,126]. Similarly, Kim *et al*^[33] demonstrated that RT mutations at 10 of 42 NAr positions could lead to 15 types of simultaneous overlapped HBsAg mutations in 32.06% (42/131) patients. Of interest, they also found that the RT mutations at 3 NAr positions (rt134, rt139, and rt153) located in the overlapped HBsAg "a" determinant region from 22 treatment-naïve patients also had simultaneous "a" determinant mutations in two positions, S126 and S131, in 15 patients (15/22, 68.2%) (12 patients with mutations at rt134, leading to 10 changes of AA S126, and 8 patients with mutations at rt139, leading to 5 alterations of AA S131).

Overall, preexisting RT mutations are distributed in a non-random manner, and most frequently found in the A-B interdomain, overlapped with the HBsAg "a" determinant region, than in other domains. Moreover, the A-B interdomain also contains the most abundant mutations, indicating that these positions might be preexisting mutation hotspots in treatment-naïve patients. Of six positions' mutation in the A-B interdomain, three RT mutations, rtD134E/N, rtN139D/E/H/K/Q, and rtW153E/Q/R, that overlap with HBsAg "a" determinant region are hotspots found most frequently in treatment-naïve patients, which could contribute to HBV viral persistence via generation of immune escape "a" determinant mutants proteins. In general, A-B interdomain mutations are prevalent in patients with genotype C2 infections and could contribute to HBV-associated disease, such as HCC and cirrhosis.

CONCLUSION

Preexisting HBV RT mutations in treatment-naïve

patients are related to potential drug resistance and progression of liver disease, such as HCC or cirrhosis. In addition, genotype-dependent polymorphic amino acid substitution in RT can also affect the emergence of drug resistance and treatment outcomes. The reported prevalence of spontaneous RT mutations in treatment-naïve patients is varied, and largely depends on geographic factors, HBV genotypes, HBeAg serostatus, HBV viral loads, disease progression, intergenotypic recombination, and co-infection with HIV. Different sensitivity of detection methodology used could also affect their prevalence results. The INNO-LiPA assay and UDPS method detect higher prevalence rates of preexisting RT mutations compared with direct PCR sequencing in treatment-naïve patients. Genotype C infection, HBeAg-negative status, and low viral loads are significantly associated with higher frequencies and prevalence rate of pre-existing HBV RT mutations. Higher frequencies of preexisting RT mutations were also generally associated with liver disease progression, including of HCC and cirrhosis. Eight mutations in RT region, rtL80I, rtD134N, rtN139K/T/H, rtY141F, rtM204I/V, rtF221Y, rtI224V, and rtM309K were significantly associated with progression of HCC in treatment-naïve patients. Of RT domains, preexisting RT mutations occur most frequently in the A-B interdomain which overlaps with the HBsAg "a" determinant region, in which mutations can lead to simultaneous viral immune escape (Figure 3). In conclusion, the presence of baseline preexisting RT mutations can affect drug treatment outcomes and disease progression in populations by modulation of viral fitness and host-immune responses.

REFERENCES

- 1 Beasley RP, Hwang LY, Lee GC, Lan CC, Roan CH, Huang FY, Chen CL. Prevention of perinatally transmitted hepatitis B virus infections with hepatitis B immune globulin and hepatitis B vaccine. *Lancet* 1983; **2**: 1099-1102 [PMID: 6138642 DOI: 10.1016/S0140-6736(83)90624-4]
- 2 GBD 2013 Mortality and Causes of Death Collaborators. Global, regional, and national age-sex specific all-cause and cause-specific mortality for 240 causes of death, 1990-2013: a systematic analysis for the Global Burden of Disease Study 2013. *Lancet* 2015; **385**: 117-171 [PMID: 25530442 DOI: 10.1016/S0140-6736(14)61682-2]
- 3 Nevens F, Main J, Honkoop P, Tyrrell DL, Barber J, Sullivan MT, Fevery J, De Man RA, Thomas HC. Lamivudine therapy for chronic hepatitis B: a six-month randomized dose-ranging study. *Gastroenterology* 1997; **113**: 1258-1263 [PMID: 9322520 DOI: 10.1053/gast.1997.v113.pm9322520]
- 4 Marcellin P, Chang TT, Lim SG, Tong MJ, Sievert W, Schiffman ML, Jeffers L, Goodman Z, Wulfsohn MS, Xiong S, Fry J, Brosgart CL; Adefovir Dipivoxil 437 Study Group. Adefovir dipivoxil for the treatment of hepatitis B e antigen-positive chronic hepatitis B. *N Engl J Med* 2003; **348**: 808-816 [PMID: 12606735 DOI: 10.1056/NEJMoa020681]
- 5 Rivkin A. Entecavir: a new nucleoside analogue for the treatment of chronic hepatitis B. *Drugs Today (Barc)* 2007; **43**: 201-220 [PMID: 17460784 DOI: 10.1358/dot.2007.43.4.1037479]
- 6 Matthews SJ. Telbivudine for the management of chronic hepatitis B virus infection. *Clin Ther* 2007; **29**: 2635-2653 [PMID: 18201580 DOI: 10.1016/j.clinthera.2007.12.032]
- 7 Jenh AM, Thio CL, Pham PA. Tenofovir for the treatment of hepatitis B virus. *Pharmacotherapy* 2009; **29**: 1212-1227 [PMID: 19792994 DOI: 10.1592/phco.29.10.1212]
- 8 Song ZL, Cui YJ, Zheng WP, Teng DH, Zheng H. Diagnostic and therapeutic progress of multi-drug resistance with anti-HBV nucleos(t)ide analogues. *World J Gastroenterol* 2012; **18**: 7149-7157 [PMID: 23326119 DOI: 10.3748/wjg.v18.i48.7149]
- 9 Shi H, Han Z, Liu J, Xue J, Zhang S, Zhu Z, Xia J, Huang M. Comparing Efficacy of Lamivudine, Adefovir Dipivoxil, Telbivudine, and Entecavir in Treating Nucleoside Analogues Naïve for HBeAg-Negative Hepatitis B with Medium Hepatitis B Virus (HBV) DNA Levels. *Med Sci Monit* 2017; **23**: 5230-5236 [PMID: 29095799 DOI: 10.12659/MSM.903382]
- 10 Nowak MA, Bonhoeffer S, Hill AM, Boehme R, Thomas HC, McDade H. Viral dynamics in hepatitis B virus infection. *Proc Natl Acad Sci U S A* 1996; **93**: 4398-4402 [PMID: 8633078 DOI: 10.1073/pnas.93.9.4398]
- 11 Caliguri P, Cerruti R, Icardi G, Bruzzone B. Overview of hepatitis B virus mutations and their implications in the management of infection. *World J Gastroenterol* 2016; **22**: 145-154 [PMID: 26755866 DOI: 10.3748/wjg.v22.i1.145]
- 12 Selabe SG, Lukhwareni A, Song E, Leeuw YG, Burnett RJ, Mphahlele MJ. Mutations associated with lamivudine-resistance in therapy-naïve hepatitis B virus (HBV) infected patients with and without HIV co-infection: implications for antiretroviral therapy in HBV and HIV co-infected South African patients. *J Med Virol* 2007; **79**: 1650-1654 [PMID: 17854040 DOI: 10.1002/jmv.20974]
- 13 Rodriguez C, Chevaliez S, Bensadoun P, Pawlotsky JM. Characterization of the dynamics of hepatitis B virus resistance to adefovir by ultra-deep pyrosequencing. *Hepatology* 2013; **58**: 890-901 [PMID: 23505208 DOI: 10.1002/hep.26383]
- 14 Tenney DJ, Rose RE, Baldick CJ, Pokornowski KA, Eggers BJ, Fang J, Wichroski MJ, Xu D, Yang J, Wilber RB, Colombo RJ. Long-term monitoring shows hepatitis B virus resistance to entecavir in nucleoside-naïve patients is rare through 5 years of therapy. *Hepatology* 2009; **49**: 1503-1514 [PMID: 19280622 DOI: 10.1002/hep.22841]
- 15 Zhang Y, Lian JQ, Li Y, Wang JP, Huang CX, Bai XF, Wang JP. Telbivudine plus adefovir therapy for chronic hepatitis B patients with virological breakthrough or genotypic resistance to telbivudine. *Eur J Gastroenterol Hepatol* 2013; **25**: 814-819 [PMID: 23406845 DOI: 10.1097/MEG.0b013e32835ee516]
- 16 Strasfeld L, Chou S. Antiviral drug resistance: mechanisms and clinical implications. *Infect Dis Clin North Am* 2010; **24**: 809-833 [PMID: 20674805 DOI: 10.1016/j.idc.2010.07.001]
- 17 Sheldon J, Rodés B, Zoulim F, Bartholomeusz A, Soriano V. Mutations affecting the replication capacity of the hepatitis B virus. *J Viral Hepat* 2006; **13**: 427-434 [PMID: 16792535 DOI: 10.1111/j.1365-2893.2005.00713.x]
- 18 Stuyver LJ, Locarnini SA, Lok A, Richman DD, Carman WF, Dienstag JL, Schinazi RF. Nomenclature for antiviral-resistant human hepatitis B virus mutations in the polymerase region. *Hepatology* 2001; **33**: 751-757 [PMID: 11230757 DOI: 10.1053/jhep.2001.22166]
- 19 Sheldon J, Soriano V. Hepatitis B virus escape mutants induced by antiviral therapy. *J Antimicrob Chemother* 2008; **61**: 766-768 [PMID: 18218641 DOI: 10.1093/jac/dkn014]
- 20 Zheng J, Zeng Z, Zhang D, Yu Y, Wang F, Pan CQ. Prevalence and significance of Hepatitis B reverse transcriptase mutants in different disease stages of untreated patients. *Liver Int* 2012; **32**: 1535-1542 [PMID: 22882650 DOI: 10.1111/j.1478-3231.2012.02859.x]
- 21 Liu BM, Li T, Xu J, Li XG, Dong JP, Yan P, Yang JX, Yan L, Gao ZY, Li WP, Sun XW, Wang YH, Jiao XJ, Hou CS, Zhuang H. Characterization of potential antiviral resistance mutations in hepatitis B virus reverse transcriptase sequences in treatment-naïve Chinese patients. *Antiviral Res* 2010; **85**: 512-519 [PMID: 20034521 DOI: 10.1016/j.antiviral.2009.12.006]
- 22 Solmone M, Vincenti D, Prosperi MC, Bruselles A, Ippolito G, Capobianchi MR. Use of massively parallel ultradeep pyrosequencing to characterize the genetic diversity of hepatitis B virus in drug-resistant and drug-naïve patients and to detect

- minor variants in reverse transcriptase and hepatitis B S antigen. *J Virol* 2009; **83**: 1718-1726 [PMID: 19073746 DOI: 10.1128/JVI.02011-08]
- 23 **Tan YW**, Ge GH, Zhao W, Gan JH, Zhao Y, Niu ZL, Zhang DJ, Chen L, Yu XJ, Yang LJ. YMDD motif mutations in chronic hepatitis B antiviral treatment naïve patients: a multi-center study. *Braz J Infect Dis* 2012; **16**: 250-255 [PMID: 22729192 DOI: 10.1016/S1413-8670(12)70319-7]
- 24 **Fung SK**, Mazzulli T, El-Kashab M, Sherman M, Popovic V, Sablon E. Lamivudine-Resistant Mutation among Treatment-Naïve Hepatitis B Patients Is Common and May Be Associated with Treatment Failure. *Hepatology* 2008; **48**: 703a-703a
- 25 **Mirandola S**, Campagnolo D, Bortolotto G, Franceschini L, Marcolongo M, Alberti A. Large-scale survey of naturally occurring HBV polymerase mutations associated with anti-HBV drug resistance in untreated patients with chronic hepatitis B. *J Viral Hepat* 2011; **18**: e212-e216 [PMID: 21692935 DOI: 10.1111/j.1365-2893.2011.01435.x]
- 26 **Vutien P**, Trinh HN, Garcia RT, Nguyen HA, Levitt BS, Nguyen K, da Silveira E, Daugherty T, Ahmed A, Garcia G, Lutchman GA, Nguyen MH. Mutations in HBV DNA polymerase associated with nucleos(t)ide resistance are rare in treatment-naïve patients. *Clin Gastroenterol Hepatol* 2014; **12**: 1363-1370 [PMID: 24342744 DOI: 10.1016/j.cgh.2013.11.036]
- 27 **Zhao Y**, Wu J, Sun L, Liu G, Li B, Zheng Y, Li X, Tao J. Prevalence of mutations in HBV DNA polymerase gene associated with nucleos(t)ide resistance in treatment-naïve patients with Chronic Hepatitis B in Central China. *Braz J Infect Dis* 2016; **20**: 173-178 [PMID: 26876337 DOI: 10.1016/j.bjid.2015.12.006]
- 28 **Akarsu M**, Sengonul A, Tankurt E, Sayiner AA, Topalak O, Akpinar H, Abacioglu YH. YMDD motif variants in inactive hepatitis B carriers detected by Inno-Lipa HBV DR assay. *J Gastroenterol Hepatol* 2006; **21**: 1783-1788 [PMID: 17074014 DOI: 10.1111/j.1440-1746.2006.04567.x]
- 29 **Ciftci S**, Keskin F, Cakiris A, Akyuz F, Pinarbasi B, Abaci N, Dincer E, Badur S, Kaymakoglu S, Ustek D. Analysis of potential antiviral resistance mutation profiles within the HBV reverse transcriptase in untreated chronic hepatitis B patients using an ultra-deep pyrosequencing method. *Diagn Microbiol Infect Dis* 2014; **79**: 25-30 [PMID: 24630522 DOI: 10.1016/j.diagmicrobio.2014.01.005]
- 30 **Zhang X**, Li M, Xi H, Zhang R, Chen J, Zhang Y, Xu X. Pre-existing mutations related to tenofovir in chronic hepatitis B patients with long-term nucleos(t)ide analogue drugs treatment by ultra-deep pyrosequencing. *Oncotarget* 2016; **7**: 70264-70275 [PMID: 27602500 DOI: 10.18632/oncotarget.11840]
- 31 **Wasityastuti W**, Yano Y, Widasari DI, Yamani LN, Ratnasari N, Heriyanto DS, Okada R, Tanahashi T, Murakami Y, Azuma T, Hayashi Y. Different Variants in Reverse Transcriptase Domain Determined by Ultra-deep Sequencing in Treatment-naïve and Treated Indonesian Patients Infected with Hepatitis B Virus. *Kobe J Med Sci* 2016; **62**: E1-E8 [PMID: 27492206]
- 32 **Zöllner B**, Sterneck M, Wurstthorn K, Petersen J, Schröter M, Laufs R, Feucht HH. Prevalence, incidence, and clinical relevance of the reverse transcriptase V207I mutation outside the YMDD motif of the hepatitis B virus polymerase during lamivudine therapy. *J Clin Microbiol* 2005; **43**: 2503-2505 [PMID: 15872296 DOI: 10.1128/JCM.43.5.2503-2505.2005]
- 33 **Kim JE**, Lee SY, Kim H, Kim KJ, Choe WH, Kim BJ. Naturally occurring mutations in the reverse transcriptase region of hepatitis B virus polymerase from treatment-naïve Korean patients infected with genotype C2. *World J Gastroenterol* 2017; **23**: 4222-4232 [PMID: 28694662 DOI: 10.3748/wjg.v23.i23.4222]
- 34 **Kobayashi S**, Ide T, Sata M. Detection of YMDD motif mutations in some lamivudine-untreated asymptomatic hepatitis B virus carriers. *J Hepatol* 2001; **34**: 584-586 [PMID: 11394659 DOI: 10.1016/S0168-8278(00)00023-4]
- 35 **Lee CZ**, Lee HS, Huang GT, Yang PM, Sheu JC. Detection of YMDD mutation using mutant-specific primers in chronic hepatitis B patients before and after lamivudine treatment. *World J Gastroenterol* 2006; **12**: 5301-5305 [PMID: 16981258 DOI: 10.3748/wjg.v12.i33.5301]
- 36 **Tunçbilek S**, Köse S, Elaldi A, Akman S. Lamivudine resistance in untreated chronic hepatitis B patients in Turkey. *Turk J Gastroenterol* 2008; **19**: 99-103 [PMID: 19110664]
- 37 **Huang CJ**, Wu CF, Lan CY, Sung FY, Lin CL, Liu CJ, Liu HF, Yu MW. Impact of genetic heterogeneity in polymerase of hepatitis B virus on dynamics of viral load and hepatitis B progression. *PLoS One* 2013; **8**: e70169 [PMID: 23936156 DOI: 10.1371/journal.pone.0070169]
- 38 **Yamani LN**, Yano Y, Utsumi T, Wasityastuti W, Rinonce HT, Widasari DI, Juniaستuti, Lusida MI, Soetjipto, Hayashi Y. Profile of Mutations in the Reverse Transcriptase and Overlapping Surface Genes of Hepatitis B Virus (HBV) in Treatment-Naïve Indonesian HBV Carriers. *Jpn J Infect Dis* 2017; **70**: 647-655 [PMID: 29093313 DOI: 10.7883/yoken.JJID.2017.078]
- 39 **Wang LP**, Han FZ, Duan HL, Ji F, Yan XB, Fan YC, Wang K. Hepatitis B virus pre-existing drug resistant mutation is related to the genotype and disease progression. *J Infect Dev Countr* 2017; **11**: 727-732 [DOI: 10.3855/jidc.9021]
- 40 **Ismail AM**, Samuel P, Eapen CE, Kannangai R, Abraham P. Antiviral resistance mutations and genotype-associated amino acid substitutions in treatment-naïve hepatitis B virus-infected individuals from the Indian subcontinent. *Intervirology* 2012; **55**: 36-44 [PMID: 21311172 DOI: 10.1159/000323521]
- 41 **Pacheco SR**, Dos Santos MIMA, Stocker A, Zarife MAS, Schinoni MI, Paraná R, Dos Reis MG, Silva LK. Genotyping of HBV and tracking of resistance mutations in treatment-naïve patients with chronic hepatitis B. *Infect Drug Resist* 2017; **10**: 201-207 [PMID: 28740410 DOI: 10.2147/IDR.S135420]
- 42 **Fan J**, Zhang Y, Xiong H, Wang Y, Guo X. Nucleotide analogue-resistant mutations in hepatitis B viral genomes found in hepatitis B patients. *J Gen Virol* 2015; **96**: 663-670 [PMID: 25481755 DOI: 10.1099/jgv.0.000010]
- 43 **Li X**, Liu Y, Zhao P, Wang Y, Chen L, Xin S, Zhang XX, Xu D. Investigation into drug-resistant mutations of HBV from 845 nucleoside/nucleotide analogue-naïve Chinese patients with chronic HBV infection. *Antivir Ther* 2015; **20**: 141-147 [PMID: 24992206 DOI: 10.3851/IMP2813]
- 44 **Singla B**, Chakraborti A, Sharma BK, Kapil S, Chawla YK, Arora SK, Das A, Dhiman RK, Duseja A. Hepatitis B virus reverse transcriptase mutations in treatment Naïve chronic hepatitis B patients. *J Med Virol* 2013; **85**: 1155-1162 [PMID: 23918533 DOI: 10.1002/jmv.23608]
- 45 **Nguyen MH**, Garcia RT, Trinh HN, Nguyen HA, Nguyen KK, Nguyen LH, Levitt B. Prevalence of hepatitis B virus DNA polymerase mutations in treatment-naïve patients with chronic hepatitis B. *Aliment Pharmacol Ther* 2009; **30**: 1150-1158 [PMID: 19785624 DOI: 10.1111/j.1365-2036.2009.04151.x]
- 46 **Xu J**, Wu B, Wang JH, Huang L, Wang DY, Zhao L, Zhao GP, Wang Y. Pre-existing mutations in reverse transcriptase of hepatitis B virus in treatment-naïve Chinese patients with chronic hepatitis B. *PLoS One* 2015; **10**: e0117429 [PMID: 25821965 DOI: 10.1371/journal.pone.0117429]
- 47 **Qian F**, Zou W, Qin J, Li D. Naturally occurring genotypic drug-resistant mutations of HBV in Huzhou, China: a single-center study. *Infect Drug Resist* 2017; **10**: 507-509 [PMID: 29276396 DOI: 10.2147/IDR.S149992]
- 48 **Matsuda M**, Suzuki F, Suzuki Y, Tsubota A, Akuta N, Hosaka T, Someya T, Kobayashi M, Saitoh S, Arase Y, Satoh J, Takagi K, Kobayashi M, Ikeda K, Kumada H. Low rate of YMDD motif mutations in polymerase gene of hepatitis B virus in chronically infected patients not treated with lamivudine. *J Gastroenterol* 2004; **39**: 34-40 [PMID: 14767732 DOI: 10.1007/s00535-003-1242-4]
- 49 **Pollicino T**, Isgrò G, Di Stefano R, Ferraro D, Maimone S, Brancatelli S, Squadrito G, Di Marco V, Craxi A, Raimondo G. Variability of reverse transcriptase and overlapping S gene in hepatitis B virus isolates from untreated and lamivudine-resistant chronic hepatitis B patients. *Antivir Ther* 2009; **14**: 649-654 [PMID: 19704167]

- 50 **Mahabadi M**, Norouzi M, Alavian SM, Samimrad K, Azad TM, Saberfar E, Mahmoodi M, Ramezani F, Karimzadeh H, Malekzadeh R, Montazeri G, Nejatizadeh A, Ziae M, Abedi F, Ateai B, Yaran M, Sayad B, Hossein Somi M, Sarizadeh G, Sanei-Moghaddam I, Mansour-Ghanaei F, Rafatpanah H, Pourhosseingholi MA, Keyvani H, Kalantari E, Saberifirooz M, Ali Judaki M, Ghamari S, Daram M, Fazeli Z, Goodarzi Z, Khedive A, Moradi A, Jazayeri SM. Drug-related mutational patterns in hepatitis B virus (HBV) reverse transcriptase proteins from Iranian treatment-naïve chronic HBV patients. *Hepat Mon* 2013; **13**: e6712 [PMID: 23596461 DOI: 10.5812/hepatmon.6712]
- 51 **Salpini R**, Svicher V, Cento V, Gori C, Bertoli A, Scopelliti F, Micheli V, Cappiello T, Spanò A, Rizzardini G, De Sanctis GM, Sarrecchia C, Angelico M, Perno CF. Characterization of drug-resistance mutations in HBV D-genotype chronically infected patients, naïve to antiviral drugs. *Antiviral Res* 2011; **92**: 382-385 [PMID: 21920388 DOI: 10.1016/j.antiviral.2011.08.013]
- 52 **Margeridon-Thermet S**, Shulman NS, Ahmed A, Shahriar R, Liu T, Wang C, Holmes SP, Babrzadeh F, Gharizadeh B, Hanczaruk B, Simen BB, Egholm M, Shafer RW. Ultra-deep pyrosequencing of hepatitis B virus quasispecies from nucleoside and nucleotide reverse-transcriptase inhibitor (NRTI)-treated patients and NRTI-naïve patients. *J Infect Dis* 2009; **199**: 1275-1285 [PMID: 19301976 DOI: 10.1086/597808]
- 53 **Han Y**, Huang LH, Liu CM, Yang S, Li J, Lin ZM, Kong XF, Yu DM, Zhang DH, Jin GD, Lu ZM, Gong QM, Zhang XX. Characterization of hepatitis B virus reverse transcriptase sequences in Chinese treatment naïve patients. *J Gastroenterol Hepatol* 2009; **24**: 1417-1423 [PMID: 19486254 DOI: 10.1111/j.1440-1746.2009.05864.x]
- 54 **Panigrahi R**, Biswas A, De BK, Chakrabarti S, Chakravarty R. Characterization of antiviral resistance mutations among the Eastern Indian Hepatitis B virus infected population. *Virol J* 2013; **10**: 56 [PMID: 23409946 DOI: 10.1186/1743-422X-10-56]
- 55 **Altindis M**, Aslan FG, Koroglu M, Eren A, Demir L, Uslan MI, Aslan S, Ozdemir M, Baykan M. Hepatitis B Virus Carrying Drug-resistance Compensatory Mutations in Chronically Infected Treatment-naïve Patients. *Viral Hepat J* 2016; **22**: 103-107 [DOI: 10.4274/vhd.07830]
- 56 **Amini-Bavil-Olyae S**, Hosseini SY, Sabahi F, Alavian SM. Hepatitis B virus (HBV) genotype and YMDD motif mutation profile among patients infected with HBV and untreated with lamivudine. *Int J Infect Dis* 2008; **12**: 83-87 [PMID: 17698384 DOI: 10.1016/j.ijid.2007.05.001]
- 57 **Jardi R**, Rodriguez-Frias F, Schaper M, Ruiz G, Elefsoniotis I, Esteban R, Buti M. Hepatitis B virus polymerase variants associated with entecavir drug resistance in treatment-naïve patients. *J Viral Hepat* 2007; **14**: 835-840 [PMID: 18070286 DOI: 10.1111/j.1365-2893.2007.00877.x]
- 58 **Li XG**, Liu BM, Xu J, Liu XE, Ding H, Li T. Discrepancy of potential antiviral resistance mutation profiles within the HBV reverse transcriptase between nucleos(t)ide analogue-untreated and -treated patients with chronic hepatitis B in a hospital in China. *J Med Virol* 2012; **84**: 207-216 [PMID: 22170539 DOI: 10.1002/jmv.23182]
- 59 **Lampertico P**, Vigano M, Facchetti F, Puoti M, Minola E, Suter F, Brunetto M, Coco B, Fargion S, Fotta E, Del Poggio P, Pozzi M, Milanese M, Colloredo G, Fagioli S, Colombi M, Pasulo L. Effectiveness of entecavir for the treatment of NUC-naïve chronic hepatitis B patients: A large multicenter cohort study in clinical practice. *Hepatology* 2008; **48**: 707A-708A
- 60 **Ramezani A**, Velayati AA, Roshan MR, Gachkar L, Banifazl M, Keyvani H, Aghakhani A. Rate of YMDD motif mutants in lamivudine-untreated Iranian patients with chronic hepatitis B virus infection. *Int J Infect Dis* 2008; **12**: 252-255 [PMID: 17954033 DOI: 10.1016/j.ijid.2007.08.003]
- 61 **Ghosh S**, Mondal RK, Banerjee P, Nandi M, Sarkar S, Das K, Santra A, Banerjee S, Chowdhury A, Datta S. Tracking the naturally occurring mutations across the full-length genome of hepatitis B virus of genotype D in different phases of chronic e-antigen negative infection. *Clin Microbiol Infect* 2012; **18**: E412-E418 [PMID: 22827722 DOI: 10.1111/j.1469-0691.2012.03975.x]
- 62 **Ludwig AD**, Goebel T, Adams O, Baumann N, Hauck K, Fey H, Hengel H, Haussinger D, Erhardt A. Primary Resistance Mutations against Nucleos(t)ide Analogue in Treatment Name Patients with HBV-Infection. *Hepatology* 2008; **48**: 701A-701A
- 63 **Hamidi-Fard M**, Makvandi M, Samaraf-Zadeh A, Hajiani E, Shayesteh A, Masjedizadeh A. Mutation analysis of hepatitis B virus reverse transcriptase region among untreated chronically infected patients in Ahvaz city (South-West of Iran). *Indian J Med Microbiol* 2013; **31**: 360-365 [PMID: 24064642 DOI: 10.4103/025-5085.118882]
- 64 **Villa E**, Lei B, Taliani G, Graziosi A, Critelli R, Luongo M, Gennari W, Bianchini M, Ferretti I. Pretreatment with pegylated interferon prevents emergence of lamivudine mutants in lamivudine-naïve patients: a pilot study. *Antivir Ther* 2009; **14**: 1081-1087 [PMID: 20032538 DOI: 10.3851/IMP1465]
- 65 **Mantovani N**, Cicero M, Santana LC, Silveira C, do Carmo EP, Abrão PR, Diaz RS, Caseiro MM, Kominakis SV. Detection of lamivudine-resistant variants and mutations related to reduced antigenicity of HBsAg in individuals from the cities of Santos and São Paulo, Brazil. *Virol J* 2013; **10**: 320 [PMID: 24165277 DOI: 10.1186/1743-422X-10-320]
- 66 **Aberle SW**, Kletzmayr J, Watschinger B, Schmied B, Vetter N, Puchhammer-Stöckl E. Comparison of sequence analysis and the INNO-LiPA HBV DR line probe assay for detection of lamivudine-resistant hepatitis B virus strains in patients under various clinical conditions. *J Clin Microbiol* 2001; **39**: 1972-1974 [PMID: 11326026 DOI: 10.1128/JCM.39.5.1972-1974.2001]
- 67 **Feehey F**, Fanning LJ, Horgan M. Baseline genotypic resistance in untreated hepatitis B virus infection. *Gastroenterology* 2007; **132**: 35A
- 68 **Masaadeh HA**, Hayajneh WA, Alqudah EA. Hepatitis B virus genotypes and lamivudine resistance mutations in Jordan. *World J Gastroenterol* 2008; **14**: 7231-7234 [PMID: 19084939 DOI: 10.3748/wjg.14.7231]
- 69 **Lok AS**, Zoulim F, Locarnini S, Bartholomeusz A, Ghany MG, Pawlotsky JM, Liaw YF, Mizokami M, Kuiken C; Hepatitis B Virus Drug Resistance Working Group. Antiviral drug-resistant HBV: standardization of nomenclature and assays and recommendations for management. *Hepatology* 2007; **46**: 254-265 [PMID: 17596850 DOI: 10.1002/hep.21698]
- 70 **Shaw T**, Bartholomeusz A, Locarnini S. HBV drug resistance: mechanisms, detection and interpretation. *J Hepatol* 2006; **44**: 593-606 [PMID: 16455151 DOI: 10.1016/j.jhep.2006.01.001]
- 71 **Langley DR**, Walsh AW, Baldick CJ, Eggers BJ, Rose RE, Levine SM, Kapur AJ, Colombo RJ, Tenney DJ. Inhibition of hepatitis B virus polymerase by entecavir. *J Virol* 2007; **81**: 3992-4001 [PMID: 17267485 DOI: 10.1128/JVI.02395-06]
- 72 **Locarnini S**. Primary resistance, multidrug resistance, and cross-resistance pathways in HBV as a consequence of treatment failure. *Hepatol Int* 2008; **2**: 147-151 [PMID: 19669299 DOI: 10.1007/s12072-008-9048-3]
- 73 **Zhang Q**, Liao Y, Cai B, Li Y, Li L, Zhang J, An Y, Wang L. Incidence of natural resistance mutations in naïve chronic hepatitis B patients: a systematic review and meta-analysis. *J Gastroenterol Hepatol* 2015; **30**: 252-261 [PMID: 25318660 DOI: 10.1111/jgh.12831]
- 74 **Lai CL**, Leung N, Teo EK, Tong M, Wong F, Hann HW, Han S, Poynard T, Myers M, Chao G, Lloyd D, Brown NA; Telbivudine Phase II Investigator Group. A 1-year trial of telbivudine, lamivudine, and the combination in patients with hepatitis B e antigen-positive chronic hepatitis B. *Gastroenterology* 2005; **129**: 528-536 [PMID: 16083710 DOI: 10.1016/j.gastro.2005.05.053]
- 75 **Fu L**, Cheng YC. Role of additional mutations outside the YMDD motif of hepatitis B virus polymerase in L(-)SddC (3TC) resistance. *Biochem Pharmacol* 1998; **55**: 1567-1572 [PMID: 9633992 DOI: 10.1016/S0006-2952(98)00050-1]
- 76 **Wakil SM**, Kazim SN, Khan LA, Raisuddin S, Parvez MK, Gupta RC, Thakur V, Hasnain SE, Sarin SK. Prevalence and

- profile of mutations associated with lamivudine therapy in Indian patients with chronic hepatitis B in the surface and polymerase genes of hepatitis B virus. *J Med Virol* 2002; **68**: 311-318 [PMID: 12226816 DOI: 10.1002/jmv.10205]
- 77 **Yang H**, Westland CE, Delaney WE 4th, Heathcote EJ, Ho V, Fry J, Brosgart C, Gibbs CS, Miller MD, Xiong S. Resistance surveillance in chronic hepatitis B patients treated with adefovir dipivoxil for up to 60 weeks. *Hepatology* 2002; **36**: 464-473 [PMID: 12143057 DOI: 10.1053/jhep.2002.34740]
- 78 **Ahn SH**, Park YK, Park ES, Kim JH, Kim DH, Lim KH, Jang MS, Choe WH, Ko SY, Sung IK, Kwon SY, Kim KH. The impact of the hepatitis B virus polymerase rtA181T mutation on replication and drug resistance is potentially affected by overlapping changes in surface gene. *J Virol* 2014; **88**: 6805-6818 [PMID: 24696492 DOI: 10.1128/JVI.00635-14]
- 79 **Schildgen O**, Sirma H, Funk A, Olotu C, Wend UC, Hartmann H, Helm M, Rockstroh JK, Willems WR, Will H, Gerlich WH. Variant of hepatitis B virus with primary resistance to adefovir. *N Engl J Med* 2006; **354**: 1807-1812 [PMID: 16641397 DOI: 10.1056/NEJMoa051214]
- 80 **Kramvis A**, Kew M, François G. Hepatitis B virus genotypes. *Vaccine* 2005; **23**: 2409-2423 [PMID: 15752827 DOI: 10.1016/j.vaccine.2004.10.045]
- 81 **Schaefer S**. Hepatitis B virus taxonomy and hepatitis B virus genotypes. *World J Gastroenterol* 2007; **13**: 14-21 [PMID: 17206751 DOI: 10.3748/wjg.v13.i1.14]
- 82 **Sunbul M**. Hepatitis B virus genotypes: global distribution and clinical importance. *World J Gastroenterol* 2014; **20**: 5427-5434 [PMID: 24833873 DOI: 10.3748/wjg.v20.i18.5427]
- 83 **Mirandola S**, Sebastiani G, Rossi C, Velo E, Erne EM, Vario A, Tempesta D, Romualdi C, Campagnolo D, Alberti A. Genotype-specific mutations in the polymerase gene of hepatitis B virus potentially associated with resistance to oral antiviral therapy. *Antiviral Res* 2012; **96**: 422-429 [PMID: 23026293 DOI: 10.1016/j.antiviral.2012.09.014]
- 84 **Damerow H**, Yuen L, Wiegand J, Walker C, Bock CT, Locarnini S, Tillmann HL. Mutation pattern of lamivudine resistance in relation to hepatitis B genotypes: hepatitis B genotypes differ in their lamivudine resistance associated mutation pattern. *J Med Virol* 2010; **82**: 1850-1858 [PMID: 20872711 DOI: 10.1002/jmv.21902]
- 85 **Colombo RJ**, Rose R, Baldick CJ, Levine S, Pokornowski K, Yu CF, Walsh A, Fang J, Hsu M, Mazzucco C, Eggers B, Zhang S, Plym M, Kleczewski K, Tenney DJ. Entecavir resistance is rare in nucleoside naïve patients with hepatitis B. *Hepatology* 2006; **44**: 1656-1665 [PMID: 17133475 DOI: 10.1002/hep.21422]
- 86 **Ciancio A**, Smedile A, Rizzetto M, Lagget M, Gerin J, Korba B. Identification of HBV DNA sequences that are predictive of response to lamivudine therapy. *Hepatology* 2004; **39**: 64-73 [PMID: 14752824 DOI: 10.1002/hep.20019]
- 87 **Chu CJ**, Keeffe EB, Han SH, Perrillo RP, Min AD, Soldevila-Pico C, Carey W, Brown RS Jr, Luketic VA, Terrault N, Lok AS; U.S. HBV Epidemiology Study Group. Prevalence of HBV precore/core promoter variants in the United States. *Hepatology* 2003; **38**: 619-628 [PMID: 12939588 DOI: 10.1053/jhep.2003.50352]
- 88 **Kirishima T**, Okanoue T, Daimon Y, Itoh Y, Nakamura H, Morita A, Toyama T, Minami M. Detection of YMDD mutant using a novel sensitive method in chronic liver disease type B patients before and during lamivudine treatment. *J Hepatol* 2002; **37**: 259-265 [PMID: 12127432 DOI: 10.1016/S0168-8278(02)00145-9]
- 89 **Zhu B**, Wang T, Wei X, Zhuo Y, Liu A, Zhang G. Accumulation of mutations in reverse transcriptase of hepatitis B virus is associated with liver disease severity in treatment-naïve Chinese patients with chronic hepatitis B. *Adv Clin Exp Med* 2017; **26**: 1123-1129 [PMID: 29211361 DOI: 10.17219/acem/63998]
- 90 **Fukai K**, Zhang KY, Imazeki F, Kurihara T, Mikata R, Yokosuka O. Association between lamivudine sensitivity and the number of substitutions in the reverse transcriptase region of the hepatitis B virus polymerase. *J Viral Hepat* 2007; **14**: 661-666 [PMID: 17697019 DOI: 10.1111/j.1365-2893.2007.00852.x]
- 91 **Wang YX**, Xu X, Luo C, Ma ZM, Jiang HL, Ding JP, Wen YM. A putative new domain target for anti-hepatitis B virus: residues flanking hepatitis B virus reverse transcriptase residue 306 (rtP306). *J Med Virol* 2007; **79**: 676-682 [PMID: 17457904 DOI: 10.1002/jmv.20835]
- 92 **Pollincino T**, Cacciola I, Saffiotti F, Raimondo G. Hepatitis B virus PreS/S gene variants: pathobiology and clinical implications. *J Hepatol* 2014; **61**: 408-417 [PMID: 24801416 DOI: 10.1016/j.jhep.2014.04.041]
- 93 **Huang ZM**, Huang QW, Qin YQ, He YZ, Qin HJ, Zhou YN, Xu X, Huang MJ. YMDD mutations in patients with chronic hepatitis B untreated with antiviral medicines. *World J Gastroenterol* 2005; **11**: 867-870 [PMID: 15682483 DOI: 10.3748/wjg.v11.i6.867]
- 94 **Nishijima N**, Marusawa H, Ueda Y, Takahashi K, Nasu A, Osaki Y, Kou T, Yazumi S, Fujiwara T, Tsuchiya S, Shimizu K, Uemoto S, Chiba T. Dynamics of hepatitis B virus quasispecies in association with nucleos(t)ide analogue treatment determined by ultra-deep sequencing. *PLoS One* 2012; **7**: e35052 [PMID: 22523569 DOI: 10.1371/journal.pone.0035052]
- 95 **Sugauchi F**, Orito E, Ichida T, Kato H, Sakugawa H, Kakumu S, Ishida T, Chutaputti A, Lai CL, Ueda R, Miyakawa Y, Mizokami M. Hepatitis B virus of genotype B with or without recombination with genotype C over the precore region plus the core gene. *J Virol* 2002; **76**: 5985-5992 [PMID: 12021331 DOI: 10.1128/JVI.76.12.5985-5992.2002]
- 96 **Yang J**, Xing K, Deng R, Wang J, Wang X. Identification of Hepatitis B virus putative intergenotype recombinants by using fragment typing. *J Gen Virol* 2006; **87**: 2203-2215 [PMID: 16847116 DOI: 10.1099/vir.0.81752-0]
- 97 **Rehermann B**, Nascimbeni M. Immunology of hepatitis B virus and hepatitis C virus infection. *Nat Rev Immunol* 2005; **5**: 215-229 [PMID: 15738952 DOI: 10.1038/nri1573]
- 98 **Shi W**, Carr MJ, Dunford L, Zhu C, Hall WW, Higgins DG. Identification of novel inter-genotypic recombinants of human hepatitis B viruses by large-scale phylogenetic analysis. *Virology* 2012; **427**: 51-59 [PMID: 22374235 DOI: 10.1016/j.virol.2012.01.030]
- 99 **Shi W**, Zhu C, Zheng W, Carr MJ, Higgins DG, Zhang Z. Subgenotype reclassification of genotype B hepatitis B virus. *BMC Gastroenterol* 2012; **12**: 116 [PMID: 22925657 DOI: 10.1186/1471-230X-12-116]
- 100 **Liu B**, Yang JX, Yan L, Zhuang H, Li T. Novel HBV recombinants between genotypes B and C in 3'-terminal reverse transcriptase (RT) sequences are associated with enhanced viral DNA load, higher RT point mutation rates and place of birth among Chinese patients. *Infect Genet Evol* 2018; **57**: 26-35 [PMID: 29111272 DOI: 10.1016/j.meegid.2017.10.023]
- 101 **Lee SY**, Lee SH, Kim JE, Kim H, Kim K, Kook YH, Kim BJ. Identification of Novel A2/C2 Inter-Genotype Recombinants of Hepatitis B Virus from a Korean Chronic Patient Co-Infected with Both Genotype A2 and C2. *Int J Mol Sci* 2017; **18**: pii: E737 [PMID: 28358313 DOI: 10.3390/ijms18040737]
- 102 **Pan D**, Zhou B, Yang J, Hou J. [Identification of hepatitis B virus intergenotype recombination in Chinese patients]. *Nan Fang Yi Ke Da Xue Xue Bao* 2014; **34**: 1436-1442 [PMID: 25345938]
- 103 **Simmonds P**, Midgley S. Recombination in the genesis and evolution of hepatitis B virus genotypes. *J Virol* 2005; **79**: 15467-15476 [PMID: 16306618 DOI: 10.1128/JVI.79.24.15467-15476.2005]
- 104 **Burnett RJ**, François G, Kew MC, Leroux-Roels G, Meheus A, Hoosen AA, Mphahlele MJ. Hepatitis B virus and human immunodeficiency virus co-infection in sub-Saharan Africa: a call for further investigation. *Liver Int* 2005; **25**: 201-213 [PMID: 15780040 DOI: 10.1111/j.1478-3231.2005.01054.x]
- 105 **Thio CL**, Seaberg EC, Skolasky R Jr, Phair J, Visscher B, Muñoz A, Thomas DL; Multicenter AIDS Cohort Study. HIV-1, hepatitis B virus, and risk of liver-related mortality in the Multicenter Cohort Study (MACS). *Lancet* 2002; **360**: 1921-1926 [PMID: 12493258 DOI: 10.1016/S0140-6736(02)11913-1]
- 106 **Audsley J**, Arrifin N, Yuen LK, Ayres A, Crowe SM, Bartholomeusz A, Locarnini SA, Mijch A, Lewin SR, Sasadeusz J. Prolonged use

- of tenofovir in HIV/hepatitis B virus (HBV)-coinfected individuals does not lead to HBV polymerase mutations and is associated with persistence of lamivudine HBV polymerase mutations. *HIV Med* 2009; **10**: 229-235 [PMID: 19178592 DOI: 10.1111/j.1468-1293.2008.00675.x]
- 107 **Quarleri J**, Moretti F, Bouzas MB, Laufer N, Carrillo MG, Giuliano SF, Pérez H, Cahn P, Salomon H. Hepatitis B virus genotype distribution and its lamivudine-resistant mutants in HIV-coinfected patients with chronic and occult hepatitis B. *AIDS Res Hum Retroviruses* 2007; **23**: 525-531 [PMID: 17506609 DOI: 10.1089/aid.2006.0172]
- 108 **Makondo E**, Bell TG, Kramvis A. Genotyping and molecular characterization of hepatitis B virus from human immunodeficiency virus-infected individuals in southern Africa. *PLoS One* 2012; **7**: e46345 [PMID: 23029487 DOI: 10.1371/journal.pone.0046345]
- 109 **Selabe SG**, Song E, Burnett RJ, Mphahlele MJ. Frequent detection of hepatitis B virus variants associated with lamivudine resistance in treated South African patients infected chronically with different HBV genotypes. *J Med Virol* 2009; **81**: 996-1001 [PMID: 19382250 DOI: 10.1002/jmv.21479]
- 110 **Thio CL**, Smeaton L, Saulynas M, Hwang H, Saravanan S, Kulkarni S, Hakim J, Nyirenda M, Iqbal HS, Laloo UG, Mehta AS, Hollabaugh K, Campbell TB, Lockman S, Currier JS. Characterization of HIV-HBV coinfection in a multinational HIV-infected cohort. *AIDS* 2013; **27**: 191-201 [PMID: 23032418 DOI: 10.1097/QAD.0b013e32835a9984]
- 111 **Archampong TN**, Boyce CL, Lartey M, Sagoe KW, Obo-Akwa A, Kenu E, Blackard JT, Kwara A. HBV genotypes and drug resistance mutations in antiretroviral treatment-naïve and treatment-experienced HBV-HIV-coinfected patients. *Antivir Ther* 2017; **22**: 13-20 [PMID: 27167598 DOI: 10.3851/IMP3055]
- 112 **Warner N**, Locarnini S, Kuiper M, Bartholomeusz A, Ayres A, Yuen L, Shaw T. The L80I substitution in the reverse transcriptase domain of the hepatitis B virus polymerase is associated with lamivudine resistance and enhanced viral replication in vitro. *Antimicrob Agents Chemother* 2007; **51**: 2285-2292 [PMID: 17438047 DOI: 10.1128/AAC.01499-06]
- 113 **Shi YH**, Shi CH. Molecular characteristics and stages of chronic hepatitis B virus infection. *World J Gastroenterol* 2009; **15**: 3099-3105 [PMID: 19575488 DOI: 10.3748/wjg.15.3099]
- 114 **Yin F**, Xie Y, Fan H, Zhang J, Guo Z. Mutations in hepatitis B virus polymerase are associated with the postoperative survival of hepatocellular carcinoma patients. *PLoS One* 2017; **12**: e0189730 [PMID: 29287068 DOI: 10.1371/journal.pone.0189730]
- 115 **Li H**, Jia J, Wang M, Wang H, Gu X, Fang M, Gao C. F221Y mutation in hepatitis B virus reverse transcriptase is associated with hepatocellular carcinoma prognosis following liver resection. *Mol Med Rep* 2017; **15**: 3292-3300 [PMID: 28339094 DOI: 10.3892/mmr.2017.6362]
- 116 **Wu Y**, Gan Y, Gao F, Zhao Z, Jin Y, Zhu Y, Sun Z, Wu H, Chen T, Wang J, Sun Y, Fan C, Xiang Y, Qian G, Groopman JD, Gu J, Tu H. Novel natural mutations in the hepatitis B virus reverse transcriptase domain associated with hepatocellular carcinoma. *PLoS One* 2014; **9**: e94864 [PMID: 24788140 DOI: 10.1371/journal.pone.0094864]
- 117 **Kao JH**, Chen PJ, Lai MY, Chen DS. Hepatitis B genotypes correlate with clinical outcomes in patients with chronic hepatitis B. *Gastroenterology* 2000; **118**: 554-559 [PMID: 10702206 DOI: 10.1016/S0016-5085(00)70261-7]
- 118 **Lee CM**, Chen CH, Lu SN, Tung HD, Wang JH, Chen TM, Huang CC. Hepatitis B virus genotypes and the progression of chronic liver disease. *J Hepatol* 2002; **36**: 238 [DOI: 10.1016/S0168-8278(02)80854-6]
- 119 **Fujie H**, Moriya K, Shintani Y, Yotsuyanagi H, Iino S, Koike K. Hepatitis B virus genotypes and hepatocellular carcinoma in Japan. *Gastroenterology* 2001; **120**: 1564-1565 [PMID: 11339239 DOI: 10.1053/gast.2001.24501]
- 120 **Tsubota A**, Arase Y, Ren F, Tanaka H, Ikeda K, Kumada H. Genotype may correlate with liver carcinogenesis and tumor characteristics in cirrhotic patients infected with hepatitis B virus subtype adw. *J Med Virol* 2001; **65**: 257-265 [PMID: 11536231 DOI: 10.1002/jmv.20028]
- 121 **Zhong YW**, Li J, Song HB, Duan ZP, Dong Y, Xing XY, Li XD, Gu ML, Han YK, Zhu SS, Zhang HF. Virologic and clinical characteristics of HBV genotypes/subgenotypes in 487 Chinese pediatric patients with CHB. *BMC Infect Dis* 2011; **11**: 262 [PMID: 21961963 DOI: 10.1186/1471-2334-11-262]
- 122 **Chan HL**, Hui AY, Wong ML, Tse AM, Hung LC, Wong VW, Sung JJ. Genotype C hepatitis B virus infection is associated with an increased risk of hepatocellular carcinoma. *Gut* 2004; **53**: 1494-1498 [PMID: 15361502 DOI: 10.1136/gut.2003.033324]
- 123 **Kwon H**, Lok AS. Hepatitis B therapy. *Nat Rev Gastroenterol Hepatol* 2011; **8**: 275-284 [PMID: 21423260 DOI: 10.1038/nrgastro.2011.33]
- 124 **Datta S**, Chatterjee S, Veer V, Chakravarty R. Molecular biology of the hepatitis B virus for clinicians. *J Clin Exp Hepatol* 2012; **2**: 353-365 [PMID: 25755457 DOI: 10.1016/j.jceh.2012.10.003]
- 125 **Avellón A**, Echevarría JM. Frequency of hepatitis B virus 'a' determinant variants in unselected Spanish chronic carriers. *J Med Virol* 2006; **78**: 24-36 [PMID: 16299725 DOI: 10.1002/jmv.20516]
- 126 **Svicher V**, Gori C, Trignetti M, Visca M, Micheli V, Bernassola M, Salpini R, Gubertini G, Longo R, Niero F, Ceccherini-Silberstein F, De Sanctis GM, Spanò A, Cappiello G, Perno CF. The profile of mutational clusters associated with lamivudine resistance can be constrained by HBV genotypes. *J Hepatol* 2009; **50**: 461-470 [PMID: 19041149 DOI: 10.1016/j.jhep.2008.07.038]
- 127 **Rhee SY**, Margeridon-Thermet S, Nguyen MH, Liu TF, Kagan RM, Beggel B, Verheyen J, Kaiser R, Shafer RW. Hepatitis B virus reverse transcriptase sequence variant database for sequence analysis and mutation discovery. *Antiviral Res* 2010; **88**: 269-275 [PMID: 20875460 DOI: 10.1016/j.antiviral.2010.09.012]
- 128 **Ji D**, Liu Y, Li L, Xu Z, Si LL, Dai JZ, Li X, Wang L, Yao Z, Xin SJ, Chen GF, Xu D. The rtL229 substitutions in the reverse transcriptase region of hepatitis B virus (HBV) polymerase are potentially associated with lamivudine resistance as a compensatory mutation. *J Clin Virol* 2012; **54**: 66-72 [PMID: 22398037 DOI: 10.1016/j.jcv.2012.02.003]

P- Reviewer: Quarleri J, Tamori A **S- Editor:** Gong ZM
L- Editor: A **E- Editor:** Huang Y



Nucleotide-binding oligomerization domain 1 and *Helicobacter pylori* infection: A review

Kosuke Minaga, Tomohiro Watanabe, Ken Kamata, Naoki Asano, Masatoshi Kudo

Kosuke Minaga, Tomohiro Watanabe, Ken Kamata, Masatoshi Kudo, Department of Gastroenterology and Hepatology, Kindai University Faculty of Medicine, Osaka 589-8511, Japan

Naoki Asano, Division of Gastroenterology, Tohoku University Graduate School of Medicine, Miyagi 980-8574, Japan

ORCID number: Kosuke Minaga (0000-0001-5407-7925); Tomohiro Watanabe (0000-0001-7781-6305); Ken Kamata (0000-0003-1568-0769); Naoki Asano (0000-0003-4452-8459); Masatoshi Kudo (0000-0002-4102-3474).

Author contributions: Minaga K and Watanabe T wrote the manuscript draft and prepared the figures; Kamata K, Asano N and Kudo M assisted in writing the manuscript and reviewed the final version.

Conflict-of-interest statement: None of the authors has any conflict of interests related to this manuscript.

Open-Access: This article is an open-access article which was selected by an in-house editor and fully peer-reviewed by external reviewers. It is distributed in accordance with the Creative Commons Attribution Non Commercial (CC BY-NC 4.0) license, which permits others to distribute, remix, adapt, build upon this work non-commercially, and license their derivative works on different terms, provided the original work is properly cited and the use is non-commercial. See: <http://creativecommons.org/licenses/by-nc/4.0/>

Manuscript source: Invited manuscript

Correspondence to: Tomohiro Watanabe, MD, PhD, Associate Professor, Department of Gastroenterology and Hepatology, Kindai University Faculty of Medicine, 377-2 Ohno-Higashi, Osaka-Sayama, Osaka 589-8511, Japan. tomohiro@med.kindai.ac.jp
Telephone: +81-72-366-0221
Fax: +81-72-367-2880

Received: March 6, 2018

Peer-review started: March 6, 2018

First decision: March 29, 2018

Revised: April 3, 2018

Accepted: April 9, 2018

Article in press: April 9, 2018

Published online: April 28, 2018

Abstract

Nucleotide-binding oligomerization domain 1 (NOD1) is an intracellular innate immune sensor for small molecules derived from bacterial cell components. NOD1 activation by its ligands leads to robust production of pro-inflammatory cytokines and chemokines by innate immune cells, thereby mediating mucosal host defense systems against microbes. Chronic gastric infection due to *Helicobacter pylori* (*H. pylori*) causes various upper gastrointestinal diseases, including atrophic gastritis, peptic ulcers, and gastric cancer. It is now generally accepted that detection of *H. pylori* by NOD1 expressed in gastric epithelial cells plays an indispensable role in mucosal host defense systems against this organism. Recent studies have revealed the molecular mechanism by which NOD1 activation caused by *H. pylori* infection is involved in the development of chronic gastritis and gastric cancer. In this review, we have discussed and summarized how sensing of *H. pylori* by NOD1 mediates the prevention of chronic gastritis and gastric cancer.

Key words: Nucleotide-binding oligomerization domain 1; *Helicobacter pylori*; Gastritis; Gastric cancer

© The Author(s) 2018. Published by Baishideng Publishing Group Inc. All rights reserved.

Core tip: Nucleotide-binding oligomerization domain 1 (NOD1), an intracellular innate immune sensor, plays a role in mucosal host defense systems against *Helicobacter pylori* (*H. pylori*) infection. NOD1 activation is involved in the generation of T helper type 1 responses against *H. pylori* through activation of type I IFN signaling pathways. NOD1 activation prevents gastric carcinogenesis through negative regulation of caudal-related homeobox 2 expression.

Minaga K, Watanabe T, Kamata K, Asano N, Kudo M. Nucleotide-binding oligomerization domain 1 and *Helicobacter pylori* infection: A review. *World J Gastroenterol* 2018; 24(16): 1725-1733 Available from: URL: <http://www.wjgnet.com/1007-9327/full/v24/i16/1725.htm> DOI: <http://dx.doi.org/10.3748/wjg.v24.i16.1725>

INTRODUCTION

Helicobacter pylori (*H. pylori*) is a Gram negative bacterium that preferentially colonizes the human gastric mucosa^[1,2]. Infection due to this organism is usually established during childhood^[1,2], which then causes various upper gastrointestinal (GI) disorders, including atrophic gastritis, peptic ulcers, gastric mucosa-associated lymphoid tissue lymphoma, and gastric cancer. Thus, it is now generally accepted that persistent *H. pylori* infection in the gastric mucosa is the highest risk factor for the development of the aforementioned diseases^[3]. This notion is supported by recent studies indicating that successful eradication of *H. pylori* prevents the development of gastric cancer^[4,5].

Colonization of the human stomach by *H. pylori* triggers innate and adaptive immune responses. As in the cases of other microbial infections, sensing of *H. pylori* by pattern recognition receptors (PRRs) expressed in innate immune cells, such as epithelial cells (ECs) and antigen-presenting cells (APCs), is an initial step for eradicating this organism. Toll-like receptors (TLRs) and nucleotide-binding oligomerization domain (NOD)-like receptors (NLRs) are the prototypical PRRs and represent the first line of defense against *H. pylori*^[6,7]. Indeed, gastric epithelial cells and APCs express functional TLRs and lipopolysaccharide (LPS)-mediated TLR4 activation is involved in the development of gastric mucosal inflammatory responses^[8]. However, the ability to stimulate TLRs by *H. pylori*-derived antigens is much lower than that by other pathogenic bacteria. For example, *H. pylori*-derived LPS and flagellin exhibit low stimulatory activity toward TLR4 and TLR5^[9,10]. Thus, *H. pylori* might evade the major innate immune system molecules, TLRs, to establish persistent gastric infection. Therefore, it is possible that PRRs other than TLRs might play a major role in mucosal host defense systems against *H. pylori* although roles played by TLRs need to be determined in future studies.

NOD1 is a prototypical innate immune receptor belonging to the NLR protein family, which detects small molecules derived from Gram-negative bacteria^[7,11]. NOD1 activation induced by intestinal microflora is associated with lymphoid tissue genesis^[12] and development of pancreatitis^[13-15]. In 2004, Viala et al^[16] demonstrated that gastric mucosal host defense against *H. pylori* depends on the activation of NOD1 in gastric ECs. Many efforts have been made by gastroenterologists, microbiologists, and immunologists to elucidate the molecular mechanisms by which colonization of the human stomach by *H. pylori*

induces the activation of NOD1 and such NOD1 activation mediates antimicrobial immune responses^[11]. In this review, we have summarized and discussed how sensing of *H. pylori* by NOD1 mediates the prevention of chronic gastritis and gastric cancer.

CYTOKINE AND CHEMOKINE RESPONSES IN THE GASTRIC MUCOSA HARBORING *H. PYLORI* INFECTION

Gastric inflammation caused by chronic *H. pylori* infection is mediated by gastric mucosal T helper type 1 (Th1) and Th17 cells producing IFN- γ and IL-17, respectively^[17]. Initial studies addressing the role of IFN- γ in *H. pylori*-induced gastritis revealed that lack of chronic gastritis in IFN- γ -deficient mice is associated with higher colonization of the gastric mucosa by this organism than in IFN- γ -intact mice^[18]. In addition, gastric mucosal CD4 $^{+}$ T cells isolated from *H. pylori*-infected patients have been reported to produce a high level of IFN- γ ^[19]. Thus, gastric mucosa harboring chronic *H. pylori* infection is characterized by Th1 responses that are involved in both eradication and inflammation^[20]. In addition to a well-established role played by Th1 cells, recent studies have highlighted the importance of another type of Th cells, Th17 cells, producing IL-17^[20]. The development of chronic gastritis is significantly attenuated in IL-17-deficient mice in long-term *H. pylori* infection^[20]. Moreover, treatment of mice with a neutralizing anti-IL-17 antibody reduced the *H. pylori* burden and inflammation in the stomach^[21]. In line with these experimental studies, Serrano et al^[22] provided evidence that downregulation of Th17 responses is associated with reduced gastritis in *H. pylori*-infected patients. Therefore, both Th1 and Th17 cells are involved in the development of chronic gastritis caused by persistent *H. pylori* infection in the gastric mucosa.

Differentiation of Th1 and Th17 cells requires cytokines produced by APCs such as dendritic cells and macrophages^[23]. Differentiation of Th1 cells depends on IL-12, whereas that of Th17 cells depends on IL-1 β , IL-6, and IL-23. Expression of IFN- γ and IL-17 in the gastric mucosa of mice challenged with *H. pylori* was accompanied by IL-12 and IL-23 expression, derived from APCs^[21]. Furthermore, the levels of APC-derived pro-inflammatory cytokines in the gastric mucosa, including IL-1 β , IL-6 and TNF- α were significantly higher in *H. pylori*-positive patients than in *H. pylori*-negative patients^[24]. Thus, it is likely that pro-inflammatory cytokines produced by APCs contribute to *H. pylori*-induced gastric pathology through differentiation of Th1 and Th17 cells. Consistent with this idea, the exposure of human APCs to *H. pylori* results in robust production of IL-6, IL-12, and TNF- α ^[25,26].

ECs are an important source of chemokines that attract immune cells to the lesions^[27,28]. Yamaoka et al^[28] assessed chemokine responses in the gastric mucosa

of patients with *H. pylori* infection and found that *H. pylori* infection is associated with increased expression of C-X-C motif chemokine ligand 8 (CXCL8) and chemokine (C-C motif) ligand 5 (CCL5). In addition to CXCL8 and CCL5, the gastric mucosa of *H. pylori*-positive patients exhibited enhanced expression of CXCL9 and CXCL10^[29]. Given the fact that CXCL8 is a strong attractant for neutrophils and that CXCL9 and CXCL10 are strong attractants for Th1 cells^[28,29], these results suggest that EC-derived chemokines are also involved in the development of chronic gastritis caused by persistent *H. pylori* infection. Taken together, these findings suggest that cytokines and chemokines produced by immune cells and ECs play a substantial role in the development of *H. pylori*-induced gastric pathology.

TYPE IV SECRETION SYSTEM OF *H. PYLORI* AND NOD1 ACTIVATION

NOD1 is expressed in the cytosolic regions of innate immune cells, such as APCs and ECs^[7,11]. Peptidoglycan (PGN) is a polymer consisting of sugars and amino acids that constitute the cell wall of both Gram-positive and Gram-negative bacteria^[7]. Small peptides derived from the PGN layer of Gram-negative bacteria activate intracellular NOD1^[7,11]. γ -D-glutamyl-meso-diaminopimelic acid (iE-DAP) is considered as the minimal motif of the NOD1 ligand, and NOD1-deficient mice exhibit impaired responses to iE-DAP^[30]. Two models have been proposed by which *H. pylori* activates intracellular NOD1.

H. pylori is classified into two types according to the expression of cag pathogenicity island (cagPAI)^[1]. cagPAI is a gene locus necessary to assemble type IV secretion system (T4SS), a syringe and needle-like structure^[1,31]. The primary function of T4SS, encoded by cagPAI, is the injection of pathogenic factors, such as cytotoxin-associated gene A (CagA) into the host gastric ECs upon attachment to the epithelium^[1,31]. Thus, cagPAI-positive *H. pylori* can cause gastric mucosal injury through injection of CagA mediated by T4SS. Hence, T4SS may enable *H. pylori* to deliver its cell wall components, such as PGN, into the host ECs. Viala *et al*^[16] addressed this possibility and demonstrated that intracellular NOD1 expressed in gastric ECs sense *H. pylori*-derived PGN delivered to the cytosolic region through T4SS. NOD1 activation is not observed in gastric ECs upon exposure to *H. pylori* harboring non-functional cagPAI, which supports the idea that NOD1 functions as an intracellular innate immune sensor for cagPAI-positive *H. pylori*. Interestingly, *H. pylori* burden in the stomach was much higher in NOD1-deficient mice than in the NOD1-intact ones, when they were orally challenged with cagPAI-positive *H. pylori*^[16]. In contrast, *H. pylori* burden in the stomach was comparable between NOD1-intact and NOD1-deficient mice when mice were orally challenged with cagPAI-mutated *H. pylori*. Thus, these studies showed that NOD1 is an

intracellular receptor for cagPAI-positive *H. pylori* and that NOD1 activation is necessary for eradication of this organism.

OUTER MEMBRANE VESICLE OF *H. PYLORI* AND NOD1 ACTIVATION

Outer membrane vesicles (OMVs), which are released by Gram-negative bacteria during normal growth, contain bacterial cell components, including PGN^[32]. Kaparakis *et al*^[33] addressed the possibility that OMVs released from *H. pylori* activate cytosolic NOD1 through intracellular delivery of PGN. OMVs isolated from *H. pylori* activate nuclear factor kappa B (NF- κ B) in AGS cells, a gastric cancer cell line, in a cagPAI-independent manner. Importantly, knockdown of NOD1 expression by siRNA abrogated CXCL8 production in AGS cells upon exposure to *H. pylori*-derived OMVs. Furthermore, intragastrically delivered OMVs efficiently induced gastric mucosal expression of CXCL2, a murine chemoattractant for neutrophils, and antibody responses against OMVs. These innate and adaptive responses to OMVs depend on NOD1 activation because NOD1-deficient mice exhibit defective CXCL2 expression and OMV-specific antibody responses. Thus, these data suggest that intracellular delivery of PGN as a form of OMVs activates NOD1 in gastric ECs in a cagPAI-independent manner.

A study has highlighted the role of autophagy to address the molecular mechanisms accounting for OMV-mediated NOD1 activation^[34]. Irving *et al*^[34] first found that *H. pylori*-derived OMVs induce autophagy in ECs. Consistent with autophagy induction, mouse embryonic fibroblasts (MEFs) deficient in ATG5, a critical molecule for autophagy, exhibited diminished production of CXCL2 compared with ATG5-intact MEFs upon exposure to *H. pylori*-derived OMVs. Autophagosome formation was diminished in NOD1-knockdown AGS cells stimulated with *H. pylori*-derived OMVs, suggesting the involvement of NOD1 activation in autophagy induction. Fluorescent labeling studies clearly demonstrated that EEA1 (early endosome antigen 1)-positive early endosomes containing both OMVs and PGN recruit NOD1 and its downstream kinase, receptor interacting protein 2 (RIP2). Such endosomal interactions between *H. pylori*-derived OMVs, NOD1, and RIP2 are necessary for chemokine production and autophagy induction, as RIP2 inhibitor efficiently blocks these responses. Collectively, these studies provide the evidence that NOD1 recognizes *H. pylori*-derived PGN within EEA1⁺ early endosomes and subsequently activates RIP2 to induce autophagy and pro-inflammatory chemokine responses^[34]. However, it should be noted that involvement of RIP2 in the induction of NOD1-mediated autophagy requires future studies, as it has been previously observed that NOD1 activation induces RIP2-independent autophagy in case of *Shigella flexneri* infection^[35].

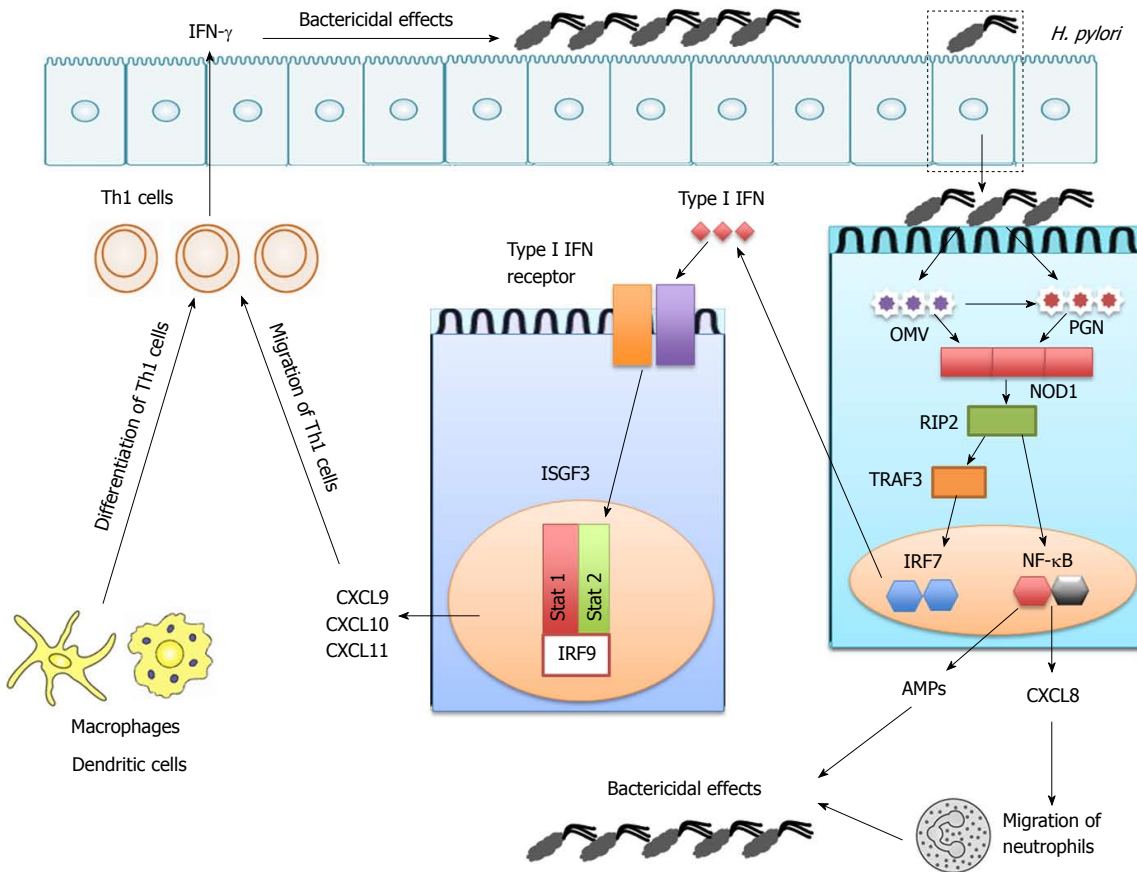


Figure 1 Nucleotide-binding oligomerization domain 1-mediated mucosal host defense against *Helicobacter pylori* infection. Nucleotide-binding oligomerization domain 1 (NOD1) recognizes *Helicobacter pylori* (*H. pylori*)-derived peptidoglycan (PGN) or outer membrane vesicles (OMVs). Sensing of *H. pylori*-derived PGN or OMVs by intracellular NOD1 in the gastric epithelial cells induces production of type I IFN and C-X-C motif chemokine ligand 10 (CXCL10) through the receptor interacting protein 2 (RIP2)-TNF receptor-associated factor 3 (TRAF3)-interferon regulatory factor 7 (IRF7)-IFN-stimulated gene factor 3 (ISGF3) pathway, thereby promoting T helper type 1 (Th1) responses. ISGF3 is a heterotrimeric complex composed of signal transduction and activator of transcription 1 (Stat1), Stat2, and IRF9. NOD1 activation also induces production of anti-microbial peptides (AMPs) through nuclear translocation of nuclear factor-kappa B (NF-κB) subunits. IFN-γ and AMPs exert bactericidal effects.

CYTOKINE AND CHEMOKINE RESPONSES AGAINST *H. PYLORI* BY NOD1 ACTIVATION

NOD1 senses *H. pylori*-derived PGN that is delivered to the cytosolic region of gastric ECs via T4SS and/or OMV transport. The next question is how NOD1 activation leads to the induction of Th1 and Th17 responses, both of which are characteristics of chronic *H. pylori* infection (Figure 1).

NOD1 activation leads to the physical interaction between NOD1 and RIP2, its downstream effector molecule^[7,11]. NOD1-induced RIP2 activation triggers the pro-inflammatory signaling cascade through nuclear translocation of NF-κB subunits^[7,11]. In addition to NF-κB, the interaction between NOD1 and RIP2 leads to the activation of mitogen-activated kinases (MAPKs), including extracellular signal-regulated kinase, c-JUN N-terminal kinase, and p38^[7,11]. Thus, one major outcome of NOD1-mediated signaling pathways is the activation of NF-κB and MAPKs^[7,11]. Activation of NF-κB and MAPKs as well as production of CXCL8 is induced

in gastric ECs, such as AGS cells, upon exposure to *H. pylori*^[36-38]. However, it remains controversial whether activation of NF-κB/MAPKs and production of CXCL8 are dependent upon the recognition of *H. pylori* by NOD1. Grubman et al^[36] established a stable AGS cell line with diminished expression of NOD1 (NOD1 knockdown, NOD1 KD cells), and found that NF-κB activation and CXCL8 production are markedly reduced in NOD1 KD cells than in AGS cells with intact NOD1 expression. Moreover, *H. pylori*-induced CXCL8 production by gastric ECs is partially mediated by MAPK activation following the recognition of this organism by NOD1, as knockdown of NOD1 expression by siRNA results in reduced activation of MAPKs and MAPKs inhibitors efficiently blocks CXCL8 production^[39]. These reports support the idea that activation of NF-κB/MAPK and production of CXCL8 induced by exposure to *H. pylori* are dependent on NOD1. On the other hand, Hirata et al^[38] reported that knockdown of NOD1 or RIP2 expression by specific siRNAs did not affect *H. pylori*-induced NF-κB/MAPK activation or CXCL8 production in AGS cells. Future *in vitro* studies are required to determine the contribution of NOD1 in NF-κB activation

in response to *H. pylori* infection.

Human gastric mucosa with persistent *H. pylori* infection is characterized by Th1 responses. CXCL9, CXCL10, and CXCL11 are EC-derived chemokines that play a pivotal role in the generation of Th1 responses through the attraction of Th1 cells expressing C-X-C chemokine receptor type 3 (CXCR3)^[40]. High expression of CXCL9 and CXCL10 in the human gastric mucosa with chronic *H. pylori* infection strongly suggests that CXCL9 and CXCL10 contribute to the generation of Th1 responses^[29,41]. We discerned from previous studies that stimulation of colon and gastric cancer cell lines (HT-29 and AGS cells) with NOD1 ligands lead to the robust production of CXCL9, CXCL10, and CXCL11^[11,27,42]. Surprisingly, NOD1-induced CXCL10 production by colonic and gastric ECs is not dependent on NF-κB or MAPK activation, because blockade of these pathways by specific pharmacological inhibitors or siRNA transfection did not alter the production of CXCL10^[11,27,42]. Instead, NOD1-induced CXCL10 production is markedly decreased by the addition of type I IFN receptor antibody, suggesting that type I IFN production is one of the major outcomes following NOD1 activation. Indeed, HT-29 cells produce a large amount of type I IFN upon stimulation with NOD1 ligand.

Next, we focused on identifying the signaling pathways involved in type I IFN production through NOD1 activation. Detailed knockdown and over-expression studies revealed the involvement of TNF receptor-associated factor 3 (TRAF3) in the induction of type I IFN^[11,27,42]. The interaction between NOD1 and RIP2 initiates recruitment of TRAF3 to this complex and leads to the activation of downstream signaling molecules, TANK-binding kinase 1 (TBK1) and IκB kinase ε (IKKε), both of which play an indispensable role in the induction of type I IFN responses through nuclear translocation of interferon regulatory factor 3 (IRF3) and IRF7^[43,44]. Indeed, the RIP2-TRAF3-TBK1-IKKε-IRF7 axis plays a key role in inducing the production of type I IFN by ECs^[27,42]. Furthermore, NOD1-mediated type I IFN production promotes the transcription of CXCL10 through nuclear translocation of the heterotrimeric complex, IFN-stimulated gene factor 3 (ISGF3), composed of signal transduction and activator of transcription 1 (Stat1), Stat2, and IRF9, because gene silencing of Stat1 or Stat2 by siRNA leads to a marked reduction in CXCL10 production. Thus, these data suggest that NOD1 activation induces the production of type I IFN and CXCL10 through activation of the RIP2-TRAF3-TBK1-IKKε-IRF7-ISGF3 pathway^[11,27,42].

The relevance of NOD1-mediated type I IFN responses was examined in animal studies in which NOD1-intact and NOD1-deficient mice were challenged with *H. pylori*. As expected, NOD1-deficient mice exhibited a higher bacterial burden in the stomach two weeks after the infection, and the effects were

accompanied by reduced expression of type I IFN-related factors, such as IFN-β, IFN-γ and CXCL10, rather than NF-κB-related factors, such as TNF-α and CXCL2^[11,27,42]. Reduced expression of phospho-Stat1 (p-Stat1) and p-Stat2 is observed in the gastric mucosa of NOD1-deficient mice, when compared with that in NOD1-intact mice. However, comparable levels of NF-κB activation are observed in both mice. Finally, the blockade of type I IFN signaling pathways by Stat1 siRNA increased bacterial burden in the stomach upon oral infection with *H. pylori* in NOD1-intact mice. Its effects were accompanied by reduced expression of IFN-γ and CXCL10 in the stomach. In contrast, blockade of NF-κB signaling pathways by NF-κB decoy oligonucleotide did not alter the bacterial burden or expression of IFN-γ or CXCL10 in the stomach, although these treatments reduced the gastric expression of TNF-α and CXCL2. Collectively, these data suggest that sensing of *H. pylori*-derived PGN by intracellular NOD1 in gastric ECs induces production of type I IFN and CXCL10 through the RIP2-TRAF3-TBK1-IKKε-IRF7-ISGF3 pathway and thereby promotes Th1 responses. Because IFN-γ produced by Th1 cells enhances the expression of NOD1^[27,42,45], we propose that the type I IFN-CXCL10-IFN-γ axis induced by NOD1 activation forms a positive feedback loop for the generation of Th1 responses in the gastric mucosa with persistent *H. pylori* infection.

Little is known about the molecular mechanisms accounting for NOD1-mediated Th17 responses in *H. pylori* infection. In this regard, a recent study has highlighted the importance of NOD1 activation in non-hematopoietic cells, i.e. ECs, in the generation of Th17 responses^[46]. Therefore, it is possible that the sensing of *H. pylori*-derived PGN or OMVs by intracellular NOD1 in gastric ECs is involved in Th17 responses.

RESPONSE OF ANTI-MICROBIAL PEPTIDES AGAINST *H. PYLORI* BY NOD1 ACTIVATION

Antimicrobial peptides (AMPs) constitute a part of the innate host defense system^[47]. AMPs released by APCs and ECs rapidly act to eradicate invading microorganisms^[47]. Grubman et al^[36] reported that AGS cells release β-defensins upon exposure to *cagPAI*-positive *H. pylori*. Production of β-defensins by AGS cells is dependent on NOD1 activation, because stable NOD1-knockdown AGS cells exhibit reduced production of AMPs. Moreover, AMPs induced by exposure to *H. pylori* exhibit potent *H. pylori* eradicating activity. Consistent with this, the expression of β-defensin 4 in the stomach is markedly decreased in NOD1-deficient mice than in NOD1-intact mice following *H. pylori* infection^[48]. Collectively, these *in vitro* and *in vivo* studies suggest the possible involvement of NOD1-dependent production of AMPs in the mucosal host

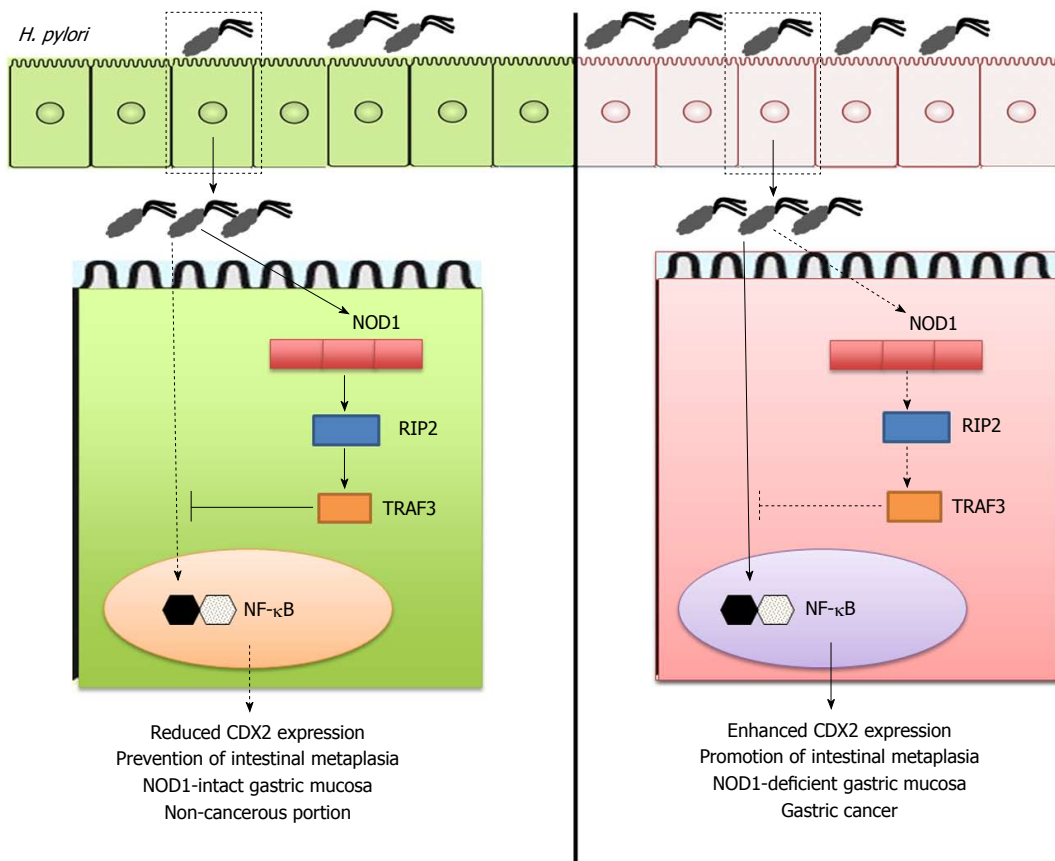


Figure 2 Prevention of gastric cancer development by nucleotide-binding oligomerization domain 1. Sensing of *Helicobacter pylori* (*H. pylori*)-derived peptidoglycan (PGN) by intracellular nucleotide-binding oligomerization domain 1 (NOD1) in gastric epithelial cells induces activation of TNF receptor associated factor 3 (TRAF3) as mentioned in Figure 1. TRAF3 activation by NOD1 negatively regulates expression of caudal-related homeobox 2 (Cdx2) via the inhibition of nuclear factor- κ B (NF- κ B) activation to prevent intestinal metaplasia and gastric cancer (left panel). On the other hand, lack of NOD1-mediated negative regulation on Cdx2 expression promotes the development of gastric cancer (right panel).

defenses against *H. pylori* infection (Figure 1).

NOD1 POLYMORPHISMS AND UPPER GASTROINTESTINAL DISEASES

Several reports have suggested an association between NOD1 gene polymorphisms and upper GI diseases^[49-51]. Wang *et al*^[51] identified the NOD1 rs7789045 TT genotype as an increased risk for gastric cancer in a Chinese population. Another Chinese cohort study reported that the risk of gastric cancer is high in *H. pylori*-infected subjects carrying the NOD1 rs 2709800 TT genotype^[52]. Moreover, Hofner *et al*^[53] reported that the G796A NOD1 polymorphism is associated with peptic ulcers in *H. pylori*-infected patients. Although these studies support the correlation between NOD1 polymorphisms and upper GI disorders caused by *H. pylori*, the mechanisms by which NOD1 polymorphisms lead to the development of *H. pylori*-associated diseases remain unknown. Because NOD1 deficiency increases gastric *H. pylori* burden in animals and its expression is lower in the cancerous tissues of the stomach than in the non-cancerous tissues^[54], it would be interesting to study whether NOD1 function is impaired or enhanced

in the presence of such polymorphisms associated with gastric cancer.

PREVENTION OF GASTRIC CANCER BY NOD1 ACTIVATION

NOD1 activation is required for mucosal host defense against *H. pylori* infection. This protective effect is partially mediated by the activation of type I IFN signaling pathways following the molecular interaction between NOD1 and TRAF3^[11,27]. Suarez *et al*^[54] have addressed the clinical relevance of NOD1-TRAF3 interaction in human *H. pylori*-associated diseases. They reported that expression levels of NOD1 and TRAF3 are much weaker in gastric cancer tissues than in non-cancerous tissues. Thus, these studies utilizing human gastric cancer samples strongly suggest that impaired activation of NOD1 and TRAF3 is involved in the pathogenesis of gastric cancer and that NOD1-TRAF3 interaction may play a protective role in the development of gastric cancer (Figure 2).

Thus, after confirming the possible involvement of NOD1 activation in the development of human gastric cancer, the next question is how NOD1 serves

as a protective factor for gastric cancer development. Intestinal metaplasia, wherein the gastric mucosa exhibits an intestinal phenotype, is a pre-neoplastic lesion of gastric cancer^[55]. Aberrant expression of caudal-related homeobox 2 (Cdx2)^[55], a transdifferentiation factor, in the gastric tissue induces intestinal metaplasia and gastric carcinogenesis. We hypothesized that NOD1 activation inhibits the development of gastric cancer through negative regulation of Cdx2^[37]. To address this question, we performed a long-term infection study in which NOD1-intact and NOD1-deficient mice were challenged with *cagPAI*-positive *H. pylori*. Interestingly, formation of gastric intestinal metaplasia was observed in NOD1-deficient mice, eight months after initial challenge with *H. pylori*, but not in NOD1-intact mice. This effect was accompanied with higher expression of Cdx2 in the gastric mucosa of NOD1-deficient mice than in the NOD1-intact mice. On the contrary, expression of TRAF3 was lower in the gastric mucosa of NOD1-deficient mice than in NOD1-intact mice. Furthermore, development of gastric intestinal metaplasia in the absence of intact NOD1 signaling pathways is associated with enhanced activation of NF-κB, because most gastric ECs are positive for nuclear p65 staining. Detection of *H. pylori* in gastric mucosa exhibiting intestinal metaplasia is difficult in human samples^[56]. Consistent with this, *H. pylori* burden in the gastric mucosa was much lower in NOD1-deficient mice than in the NOD1-intact mice^[37]. Thus, the results of our long-term *H. pylori* infection study support the data^[54] obtained from human gastric cancer samples, demonstrating that impaired activation of NOD1-TRAF3 signaling pathways is involved in the development of intestinal metaplasia^[37].

Regarding the molecular mechanisms by which NOD1 activation prevents the development of intestinal metaplasia and gastric cancer, we provided evidence that NOD1 activation upon exposure to *H. pylori* negatively regulates Cdx2 expression through activation of TRAF3^[37]. Exposure to *H. pylori* upregulates Cdx2 expression in gastric cancer cell lines, and the effects are enhanced or diminished by gene silencing of NOD1 by siRNA or over-expression of TRAF3, respectively^[37]. Furthermore, promoter gene and gel shift assays revealed that interaction between NOD1 and TRAF3 inhibits the expression of Cdx2 through negative regulation of NF-κB activation. Thus, these *in vitro* studies have elucidated a part of the molecular mechanisms accounting for the prevention of intestinal metaplasia followed by gastric cancer via *H. pylori*-induced NOD1 activation. Collectively, these two recent studies strongly suggest that NOD1 activation by *H. pylori* infection plays a protective role in the development of gastric cancer.

CONCLUSION

NOD1 contributes to mucosal host defense against *H. pylori* infection through the activation of type I IFN signaling pathways and production of AMPs. In

addition, NOD1 activation negatively regulates Cdx2 expression, and thereby inhibits the development of gastric cancer. Molecules involved in NOD1-mediated signaling pathways might be new therapeutic targets for treating chronic gastric diseases and gastric cancer.

REFERENCES

- 1 Hatakeyama M. Helicobacter pylori CagA and gastric cancer: a paradigm for hit-and-run carcinogenesis. *Cell Host Microbe* 2014; **15**: 306-316 [PMID: 24629337 DOI: 10.1016/j.chom.2014.02.008]
- 2 Amieva M, Peek RM Jr. Pathobiology of Helicobacter pylori-Induced Gastric Cancer. *Gastroenterology* 2016; **150**: 64-78 [PMID: 26385073 DOI: 10.1053/j.gastro.2015.09.004]
- 3 Chiba T, Marusawa H, Ushijima T. Inflammation-associated cancer development in digestive organs: mechanisms and roles for genetic and epigenetic modulation. *Gastroenterology* 2012; **143**: 550-563 [PMID: 22796521 DOI: 10.1053/j.gastro.2012.07.009]
- 4 Fukase K, Kato M, Kikuchi S, Inoue K, Uemura N, Okamoto S, Terao S, Amagai K, Hayashi S, Asaka M; Japan Gast Study Group. Effect of eradication of Helicobacter pylori on incidence of metachronous gastric carcinoma after endoscopic resection of early gastric cancer: an open-label, randomised controlled trial. *Lancet* 2008; **372**: 392-397 [PMID: 18675689 DOI: 10.1016/S0140-6736(08)61159-9]
- 5 Uemura N, Okamoto S, Yamamoto S, Matsumura N, Yamaguchi S, Yamakido M, Taniyama K, Sasaki N, Schlemper RJ. Helicobacter pylori infection and the development of gastric cancer. *N Engl J Med* 2001; **345**: 784-789 [PMID: 11556297 DOI: 10.1056/NEJMoa001999]
- 6 Akira S, Takeda K. Toll-like receptor signalling. *Nat Rev Immunol* 2004; **4**: 499-511 [PMID: 15229469 DOI: 10.1038/nri1391]
- 7 Strober W, Murray PJ, Kitani A, Watanabe T. Signalling pathways and molecular interactions of NOD1 and NOD2. *Nat Rev Immunol* 2006; **6**: 9-20 [PMID: 16493424 DOI: 10.1038/nri1747]
- 8 Slomiany BL, Slomiany A. Role of LPS-elicited signaling in triggering gastric mucosal inflammatory responses to *H. pylori*: modulatory effect of ghrelin. *Inflammopharmacology* 2017; **25**: 415-429 [PMID: 28516374 DOI: 10.1007/s10787-017-0360-1]
- 9 Andersen-Nissen E, Smith KD, Strober KL, Barrett SL, Cookson BT, Logan SM, Aderem A. Evasion of Toll-like receptor 5 by flagellated bacteria. *Proc Natl Acad Sci USA* 2005; **102**: 9247-9252 [PMID: 15956202 DOI: 10.1073/pnas.0502040102]
- 10 Ferrero RL. Innate immune recognition of the extracellular mucosal pathogen, Helicobacter pylori. *Mol Immunol* 2005; **42**: 879-885 [PMID: 15829277 DOI: 10.1016/j.molimm.2004.12.001]
- 11 Watanabe T, Asano N, Kudo M, Strober W. Nucleotide-binding oligomerization domain 1 and gastrointestinal disorders. *Proc Jpn Acad Ser B Phys Biol Sci* 2017; **93**: 578-599 [PMID: 29021509 DOI: 10.2183/pjab.93.037]
- 12 Bouskra D, Brézillon C, Bérard M, Werts C, Varona R, Boneca IG, Eberl G. Lymphoid tissue genesis induced by commensals through NOD1 regulates intestinal homeostasis. *Nature* 2008; **456**: 507-510 [PMID: 18987631 DOI: 10.1038/nature07450]
- 13 Tsuji Y, Watanabe T, Kudo M, Arai H, Strober W, Chiba T. Sensing of commensal organisms by the intracellular sensor NOD1 mediates experimental pancreatitis. *Immunity* 2012; **37**: 326-338 [PMID: 22902233 DOI: 10.1016/j.immuni.2012.05.024]
- 14 Watanabe T, Kudo M, Strober W. Immunopathogenesis of pancreatitis. *Mucosal Immunol* 2017; **10**: 283-298 [PMID: 27848953 DOI: 10.1038/mi.2016.101]
- 15 Watanabe T, Sadakane Y, Yagama N, Sakurai T, Ezoe H, Kudo M, Chiba T, Strober W. Nucleotide-binding oligomerization domain 1 acts in concert with the cholecystokinin receptor agonist, cerulein, to induce IL-33-dependent chronic pancreatitis. *Mucosal Immunol* 2016; **9**: 1234-1249 [PMID: 26813347 DOI: 10.1038/mi.2015.144]
- 16 Viala J, Chaput C, Boneca IG, Cardona A, Girardin SE, Moran AP, Athman R, Mémet S, Huerre MR, Coyle AJ, DiStefano PS, Sansonetti PJ, Labigne A, Bertin J, Philpott DJ, Ferrero RL. Nod1

- responds to peptidoglycan delivered by the Helicobacter pylori cag pathogenicity island. *Nat Immunol* 2004; **5**: 1166-1174 [PMID: 15489856 DOI: 10.1038/ni1131]
- 17 **Moyat M**, Velin D. Immune responses to Helicobacter pylori infection. *World J Gastroenterol* 2014; **20**: 5583-5593 [PMID: 24914318 DOI: 10.3748/wjg.v20.i19.5583]
- 18 **Sawai N**, Kita M, Kodama T, Tanahashi T, Yamaoka Y, Tagawa Y, Iwakura Y, Imanishi J. Role of gamma interferon in Helicobacter pylori-induced gastric inflammatory responses in a mouse model. *Infect Immun* 1999; **67**: 279-285 [PMID: 9864227]
- 19 **Itoh T**, Wakatsuki Y, Yoshida M, Usui T, Matsunaga Y, Kaneko S, Chiba T, Kita T. The vast majority of gastric T cells are polarized to produce T helper 1 type cytokines upon antigenic stimulation despite the absence of Helicobacter pylori infection. *J Gastroenterol* 1999; **34**: 560-570 [PMID: 10535482]
- 20 **Gray BM**, Fontaine CA, Poe SA, Eaton KA. Complex T cell interactions contribute to Helicobacter pylori gastritis in mice. *Infect Immun* 2013; **81**: 740-752 [PMID: 23264048 DOI: 10.1128/IAI.01269-12]
- 21 **Shi Y**, Liu XF, Zhuang Y, Zhang JY, Liu T, Yin Z, Wu C, Mao XH, Jia KR, Wang FJ, Guo H, Flavell RA, Zhao Z, Liu KY, Xiao B, Guo Y, Zhang WJ, Zhou WY, Guo G, Zou QM. Helicobacter pylori-induced Th17 responses modulate Th1 cell responses, benefit bacterial growth, and contribute to pathology in mice. *J Immunol* 2010; **184**: 5121-5129 [PMID: 20351183 DOI: 10.4049/jimmunol.0901115]
- 22 **Serrano C**, Wright SW, Bimeczok D, Shaffer CL, Cover TL, Venegas A, Salazar MG, Smythies LE, Harris PR, Smith PD. Downregulated Th17 responses are associated with reduced gastritis in Helicobacter pylori-infected children. *Mucosal Immunol* 2013; **6**: 950-959 [PMID: 23299619 DOI: 10.1038/mi.2012.133]
- 23 **Strober W**, Fuss IJ. Proinflammatory cytokines in the pathogenesis of inflammatory bowel diseases. *Gastroenterology* 2011; **140**: 1756-1767 [PMID: 21530742 DOI: 10.1053/j.gastro.2011.02.016]
- 24 **Yamaoka Y**, Kita M, Kodama T, Sawai N, Kashima K, Imanishi J. Induction of various cytokines and development of severe mucosal inflammation by cagA gene positive Helicobacter pylori strains. *Gut* 1997; **41**: 442-451 [PMID: 9391240]
- 25 **Amedei A**, Cappon A, Codolo G, Cabrelle A, Polenghi A, Benagiano M, Tasca E, Azzurri A, D'Elios MM, Del Prete G, de Bernard M. The neutrophil-activating protein of Helicobacter pylori promotes Th1 immune responses. *J Clin Invest* 2006; **116**: 1092-1101 [PMID: 16543949 DOI: 10.1172/JCI27177]
- 26 **Kranzer K**, Eckhardt A, Aigner M, Knoll G, Deml L, Speth C, Lehn N, Rehli M, Schneider-Brachert W. Induction of maturation and cytokine release of human dendritic cells by Helicobacter pylori. *Infect Immun* 2004; **72**: 4416-4423 [PMID: 15271898 DOI: 10.1128/IAI.72.8.4416-4423.2004]
- 27 **Watanabe T**, Asano N, Fichtner-Feigl S, Gorelick PL, Tsuji Y, Matsumoto Y, Chiba T, Fuss IJ, Kitani A, Strober W. NOD1 contributes to mouse host defense against Helicobacter pylori via induction of type I IFN and activation of the ISGF3 signaling pathway. *J Clin Invest* 2010; **120**: 1645-1662 [PMID: 20389019 DOI: 10.1172/JCI39481]
- 28 **Yamaoka Y**, Kita M, Kodama T, Sawai N, Tanahashi T, Kashima K, Imanishi J. Chemokines in the gastric mucosa in Helicobacter pylori infection. *Gut* 1998; **42**: 609-617 [PMID: 9659152]
- 29 **Eck M**, Schmausser B, Scheller K, Toksoy A, Kraus M, Menzel T, Müller-Hermelink HK, Gillitzer R. CXC chemokines Gro(alpha)/IL-8 and IP-10/MIG in Helicobacter pylori gastritis. *Clin Exp Immunol* 2000; **122**: 192-199 [PMID: 11091274]
- 30 **Chamaillard M**, Hashimoto M, Horie Y, Masumoto J, Qiu S, Saab L, Ogura Y, Kawasaki A, Fukase K, Kusumoto S, Valvano MA, Foster SJ, Mak TW, Nuñez G, Inohara N. An essential role for NOD1 in host recognition of bacterial peptidoglycan containing diaminopimelic acid. *Nat Immunol* 2003; **4**: 702-707 [PMID: 12796777 DOI: 10.1038/ni945]
- 31 **Varga MG**, Peek RM. DNA Transfer and Toll-like Receptor Modulation by Helicobacter pylori. *Curr Top Microbiol Immunol* 2017; **400**: 169-193 [PMID: 28124154 DOI: 10.1007/978-3-319-50520-6_8]
- 32 **Kuehn MJ**, Kesty NC. Bacterial outer membrane vesicles and the host-pathogen interaction. *Genes Dev* 2005; **19**: 2645-2655 [PMID: 16291643 DOI: 10.1101/gad.129905]
- 33 **Kaparakis M**, Turnbull L, Carneiro L, Firth S, Coleman HA, Parkington HC, Le Bourhis L, Karrar A, Viala J, Mak J, Hutton ML, Davies JK, Crack PJ, Hertzog PJ, Philpott DJ, Girardin SE, Whitchurch CB, Ferrero RL. Bacterial membrane vesicles deliver peptidoglycan to NOD1 in epithelial cells. *Cell Microbiol* 2010; **12**: 372-385 [PMID: 19888998 DOI: 10.1111/j.1462-5822.2009.01404.x]
- 34 **Irving AT**, Mimuro H, Kufer TA, Lo C, Wheeler R, Turner LJ, Thomas BJ, Malosse C, Gantier MP, Casillas LN, Votta BJ, Bertin J, Boneca IG, Sasakawa C, Philpott DJ, Ferrero RL, Kaparakis-Liaskos M. The immune receptor NOD1 and kinase RIP2 interact with bacterial peptidoglycan on early endosomes to promote autophagy and inflammatory signaling. *Cell Host Microbe* 2014; **15**: 623-635 [PMID: 24746552 DOI: 10.1016/j.chom.2014.04.001]
- 35 **Travassos LH**, Carneiro LA, Ramjeet M, Hussey S, Kim YG, Magalhães JG, Yuan L, Soares F, Chea E, Le Bourhis L, Boneca IG, Allaoui A, Jones NL, Nuñez G, Girardin SE, Philpott DJ. Nod1 and Nod2 direct autophagy by recruiting ATG16L1 to the plasma membrane at the site of bacterial entry. *Nat Immunol* 2010; **11**: 55-62 [PMID: 19898471 DOI: 10.1038/ni.1823]
- 36 **Grubman A**, Kaparakis M, Viala J, Allison C, Badea L, Karrar A, Boneca IG, Le Bourhis L, Reeve S, Smith IA, Hartland EL, Philpott DJ, Ferrero RL. The innate immune molecule, NOD1, regulates direct killing of Helicobacter pylori by antimicrobial peptides. *Cell Microbiol* 2010; **12**: 626-639 [PMID: 20039881 DOI: 10.1111/j.1462-5822.2009.01421.x]
- 37 **Asano N**, Imatani A, Watanabe T, Fushiya J, Kondo Y, Jin X, Ara N, Uno K, Iijima K, Koike T, Strober W, Shimosegawa T. Cdx2 Expression and Intestinal Metaplasia Induced by *H. pylori* Infection of Gastric Cells Is Regulated by NOD1-Mediated Innate Immune Responses. *Cancer Res* 2016; **76**: 1135-1145 [PMID: 26759244 DOI: 10.1158/0008-5472.CAN-15-2272]
- 38 **Hirata Y**, Ohmae T, Shibata W, Maeda S, Ogura K, Yoshida H, Kawabe T, Omata M. MyD88 and TNF receptor-associated factor 6 are critical signal transducers in Helicobacter pylori-infected human epithelial cells. *J Immunol* 2006; **176**: 3796-3803 [PMID: 16517750]
- 39 **Allison CC**, Kufer TA, Kremmer E, Kaparakis M, Ferrero RL. Helicobacter pylori induces MAPK phosphorylation and AP-1 activation via a NOD1-dependent mechanism. *J Immunol* 2009; **183**: 8099-8109 [PMID: 20007577 DOI: 10.4049/jimmunol.0900664]
- 40 **Antonelli A**, Ferrari SM, Giuggioli D, Ferrannini E, Ferri C, Fallahi P. Chemokine (C-X-C motif) ligand (CXCL)10 in autoimmune diseases. *Autoimmun Rev* 2014; **13**: 272-280 [PMID: 24189283 DOI: 10.1016/j.autrev.2013.10.010]
- 41 **Allison CC**, Ferrand J, McLeod L, Hassan M, Kaparakis-Liaskos M, Grubman A, Bhathal PS, Dev A, Sievert W, Jenkins BJ, Ferrero RL. Nucleotide oligomerization domain 1 enhances IFN- γ signaling in gastric epithelial cells during Helicobacter pylori infection and exacerbates disease severity. *J Immunol* 2013; **190**: 3706-3715 [PMID: 23460743 DOI: 10.4049/jimmunol.1200591]
- 42 **Watanabe T**, Asano N, Kitani A, Fuss IJ, Chiba T, Strober W. Activation of type I IFN signaling by NOD1 mediates mucosal host defense against Helicobacter pylori infection. *Gut Microbes* 2011; **2**: 61-65 [PMID: 21637021 DOI: 10.4161/gmic.2.1.15162]
- 43 **Kawai T**, Akira S. Signaling to NF-kappaB by Toll-like receptors. *Trends Mol Med* 2007; **13**: 460-469 [PMID: 18029230 DOI: 10.1016/j.molmed.2007.09.002]
- 44 **Honda K**, Yanai H, Takaoka A, Taniguchi T. Regulation of the type I IFN induction: a current view. *Int Immunopharmacol* 2005; **17**: 1367-1378 [PMID: 16214811 DOI: 10.1093/intimm/dxh318]
- 45 **Hisamatsu T**, Suzuki M, Podolsky DK. Interferon-gamma augments CARD4/NOD1 gene and protein expression through interferon regulatory factor-1 in intestinal epithelial cells. *J Biol Chem* 2003; **278**: 32962-32968 [PMID: 12813035 DOI: 10.1074/jbc.M212004200]

- jbc.M304355200]
- 46 **Fritz JH**, Le Bourhis L, Sellge G, Magalhaes JG, Fsihi H, Kufer TA, Collins C, Viala J, Ferrero RL, Girardin SE, Philpott DJ. Nod1-mediated innate immune recognition of peptidoglycan contributes to the onset of adaptive immunity. *Immunity* 2007; **26**: 445-459 [PMID: 17433730 DOI: 10.1016/j.immuni.2007.03.009]
- 47 **Roudi R**, Syn NL, Roudbary M. Antimicrobial Peptides As Biologic and Immunotherapeutic Agents against Cancer: A Comprehensive Overview. *Front Immunol* 2017; **8**: 1320 [PMID: 29081781 DOI: 10.3389/fimmu.2017.01320]
- 48 **Boughan PK**, Argent RH, Body-Malapel M, Park JH, Ewings KE, Bowie AG, Ong SJ, Cook SJ, Sorensen OE, Manzo BA, Inohara N, Klein NJ, Nuñez G, Atherton JC, Bajaj-Elliott M. Nucleotide-binding oligomerization domain-1 and epidermal growth factor receptor: critical regulators of beta-defensins during Helicobacter pylori infection. *J Biol Chem* 2006; **281**: 11637-11648 [PMID: 16513653 DOI: 10.1074/jbc.M510275200]
- 49 **Castaño-Rodríguez N**, Kaakoush NO, Mitchell HM. Pattern-recognition receptors and gastric cancer. *Front Immunol* 2014; **5**: 336 [PMID: 25101079 DOI: 10.3389/fimmu.2014.00336]
- 50 **Rosenstiel P**, Hellwig S, Hampe J, Ott S, Till A, Fischbach W, Sahly H, Lucius R, Fölsch UR, Philpott D, Schreiber S. Influence of polymorphisms in the NOD1/CARD4 and NOD2/CARD15 genes on the clinical outcome of Helicobacter pylori infection. *Cell Microbiol* 2006; **8**: 1188-1198 [PMID: 16819970 DOI: 10.1111/j.1462-5822.2006.00701.x]
- 51 **Wang P**, Zhang L, Jiang JM, Ma D, Tao HX, Yuan SL, Wang YC, Wang LC, Liang H, Zhang ZS, Liu CJ. Association of NOD1 and NOD2 genes polymorphisms with Helicobacter pylori related gastric cancer in a Chinese population. *World J Gastroenterol* 2012; **18**: 2112-2120 [PMID: 22563200 DOI: 10.3748/wjg.v18.i7.2112]
- 52 **Li ZX**, Wang YM, Tang FB, Zhang L, Zhang Y, Ma JL, Zhou T, You WC, Pan KF. NOD1 and NOD2 Genetic Variants in Association with Risk of Gastric Cancer and Its Precursors in a Chinese Population. *PLoS One* 2015; **10**: e0124949 [PMID: 25933107 DOI: 10.1371/journal.pone.0124949]
- 53 **Hofner P**, Gyulai Z, Kiss ZF, Tiszai A, Tiszlavicz L, Tóth G, Szőke D, Molnár B, Lonovics J, Tulassay Z, Mádi Y. Genetic polymorphisms of NOD1 and IL-8, but not polymorphisms of TLR4 genes, are associated with Helicobacter pylori-induced duodenal ulcer and gastritis. *Helicobacter* 2007; **12**: 124-131 [PMID: 17309748 DOI: 10.1111/j.1523-5378.2007.00481.x]
- 54 **Suarez G**, Romero-Gallo J, Piazuelo MB, Wang G, Maier RJ, Forsberg LS, Azadi P, Gomez MA, Correa P, Peek RM Jr. Modification of Helicobacter pylori Peptidoglycan Enhances NOD1 Activation and Promotes Cancer of the Stomach. *Cancer Res* 2015; **75**: 1749-1759 [PMID: 25732381 DOI: 10.1158/0008-5472.CAN-14-2291]
- 55 **Camilo V**, Barros R, Sousa S, Magalhães AM, Lopes T, Mário Santos A, Pereira T, Figueiredo C, David L, Almeida R. Helicobacter pylori and the BMP pathway regulate CDX2 and SOX2 expression in gastric cells. *Carcinogenesis* 2012; **33**: 1985-1992 [PMID: 22791809 DOI: 10.1093/carcin/bgs233]
- 56 **Yabuki N**, Sasano H, Tobita M, Imatani A, Hoshi T, Kato K, Ohara S, Asaki S, Toyota T, Nagura H. Analysis of cell damage and proliferation in Helicobacter pylori-infected human gastric mucosa from patients with gastric adenocarcinoma. *Am J Pathol* 1997; **151**: 821-829 [PMID: 9284831]

P- Reviewer: Day AS, Ozen H, Slomiany BL **S- Editor:** Gong ZM
L- Editor: A **E- Editor:** Huang Y



Diversion colitis and pouchitis: A mini-review

Kentaro Tominaga, Kenya Kamimura, Kazuya Takahashi, Junji Yokoyama, Satoshi Yamagiwa, Shuji Terai

Kentaro Tominaga, Kenya Kamimura, Kazuya Takahashi, Junji Yokoyama, Satoshi Yamagiwa, Shuji Terai, Division of Gastroenterology and Hepatology, Graduate School of Medical and Dental Sciences, Niigata University, Niigata 951-8510, Japan

ORCID number: Kentaro Tominaga (0000-0001-6792-1005); Kenya Kamimura (0000-0001-7182-4400); Kazuya Takahashi (0000-0002-3097-9841); Junji Yokoyama (0000-0002-1810-7709); Satoshi Yamagiwa (0000-0003-4791-6107); Shuji Terai (0000-0002-5439-635X).

Author contributions: Tominaga K and Kamimura K wrote the manuscript; Takahashi K, Yokoyama J, Yamagiwa S and Terai S collected information; all authors read and approved the final version of the manuscript.

Conflict-of-interest statement: The authors declare that they have no current financial arrangement or affiliation with any organization that may have a direct influence on their work.

Open-Access: This article is an open-access article which was selected by an in-house editor and fully peer-reviewed by external reviewers. It is distributed in accordance with the Creative Commons Attribution Non Commercial (CC BY-NC 4.0) license, which permits others to distribute, remix, adapt, build upon this work non-commercially, and license their derivative works on different terms, provided the original work is properly cited and the use is non-commercial. See: <http://creativecommons.org/licenses/by-nc/4.0/>

Manuscript source: Invited manuscript

Correspondence to: Kenya Kamimura, MD, PhD, Lecturer, Division of Gastroenterology and Hepatology, Graduate School of Medical and Dental Sciences, Niigata University, 1-757 Asahimachi-dori, Chuo-ku, Niigata 951-8510, Japan. kenya-k@med.niigata-u.ac.jp
Telephone: +81-25-2272207
Fax: +81-25-2270776

Received: March 12, 2018

Peer-review started: March 13, 2018

First decision: March 30, 2018

Revised: April 1, 2018

Accepted: April 16, 2018

Article in press: April 16, 2018

Published online: April 28, 2018

Abstract

Diversion colitis is characterized by inflammation of the mucosa in the defunctioned segment of the colon after colostomy or ileostomy. Similar to diversion colitis, diversion pouchitis is an inflammatory disorder occurring in the ileal pouch, resulting from the exclusion of the fecal stream and a subsequent lack of nutrients from luminal bacteria. Although the vast majority of patients with surgically-diverted gastrointestinal tracts remain asymptomatic, it has been reported that diversion colitis and pouchitis might occur in almost all patients with diversion. Surgical closure of the stoma, with reestablishment of gut continuity, is the only curative intervention available for patients with diversion disease. Pharmacologic treatments using short-chain fatty acids, mesalamine, or corticosteroids are reportedly effective for those who are not candidates for surgical reestablishment; however, there are no established assessment criteria for determining the severity of diversion colitis, and no management strategies to date. Therefore, in this mini-review, we summarize and review various recently-reported treatments for diversion disease. We are hopeful that the information summarized here will assist physicians who treat patients with diversion colitis and pouchitis, leading to better case management.

Key words: Diversion colitis; Diversion pouchitis; Ileitis; Inflammatory bowel disease

© The Author(s) 2018. Published by Baishideng Publishing Group Inc. All rights reserved.

Core tip: Diversion colitis is characterized by inflammation of the mucosa in the defunctioned segment of the colon after colostomy or ileostomy. The vast majority of diverted patients remain asymptomatic,

however diversion colitis occurs in almost all diverted patients. Pharmacologic treatment using short-chain fatty acids, mesalamine, or corticosteroids are reportedly effective for those who are not candidates for surgical reestablishment; however, there are no established assessment criteria for determining the severity of diversion colitis, and no management strategies to date. In this mini-review, we summarize and review various recently-reported diversion disease treatments. We hope this review will be useful for future treatment.

Tominaga K, Kamimura K, Takahashi K, Yokoyama J, Yamagiwa S, Terai S. Diversion colitis and pouchitis: A mini-review. *World J Gastroenterol* 2018; 24(16): 1734-1747 Available from: URL: <http://www.wjgnet.com/1007-9327/full/v24/i16/1734.htm> DOI: <http://dx.doi.org/10.3748/wjg.v24.i16.1734>

INTRODUCTION

Diversion colitis was first described by Morson *et al*^[1] in 1974 as a non-specific inflammation in the diverted colon. Glotzer *et al*^[2] labeled this inflammation “diversion colitis” in 1981. Since then, the disease has been reported in both retrospective^[3-20] and prospective studies^[21-27] which have described the characteristic clinical, endoscopic, and pathological findings. Surprisingly, the prospective study reported that almost all cases exhibit colitis, evidenced by endoscopic analyses, 3 to 36 mo after the colostomy^[21]. Symptomatic cases make up only around 30% of all cases diagnosed via endoscopic studies, and the precise pathogenesis of this condition remains unclarified. Although a wide range of symptoms are reportedly associated with the disease, including abdominal discomfort, tenesmus, anorectal pain, mucous discharge, and rectal bleeding^[3,4], there are no established diagnostic criteria for assessing disease severity. Diversion pouchitis is similar to diversion colitis, featuring inflammation of the ileal pouch that results from fecal stream exclusion and the subsequent lack of nutrients from luminal bacteria. Therefore, the difference between the pouchitis and diversion puchitis is whether the lesion is exposed to the fecal stream or not. Patients generally present with varying symptoms such as tenesmus, bloody or mucus-like discharge, and abdominal pain^[28]. The incidence of diversion pouchitis is unknown; however, it appears more commonly in patients with underlying inflammatory bowel disease (IBD). Nonsurgical approaches for the treatment of diversion pouchitis include the use of short chain fatty acids (SCFA), topical 5-aminosalicylic acids, and topical glucocorticoids. Unfortunately, efficacy study outcomes are conflicting, and the only curative approach is surgical re-anastomosis with the reestablishment of gut continuity^[28-30].

In their 1989 examination of non-surgical treatment options procedure, Harig *et al*^[5] reported the efficacy of short-chain fatty acids. The usefulness of the 5-ASA enema in patients with diversion colitis was reported for

the first time by Triantafillidis *et al*^[31] in 1991; Glotzer *et al*^[2] reported the efficacy of steroid enemas in patients with diversion colitis in 1984, and similar results were subsequently reported by Lim *et al*^[32] and Jowett *et al*^[33]. Nonsurgical treatments include short-chain fatty acids, 5-aminosalicylic acids, glucocorticoids, antibiotics, and so on. However, due to the lack established assessment methods, the efficacy of these treatments has not been clearly confirmed. Consequently, surgical re-anastomosis remains the most reliable and effective treatment option. There is an unmet need for a summary of these therapeutic options and information regarding the disease assessment, and this need informed the present literature review. We believe that the information summarized in this mini-review will help physicians treat cases and, by increasing the number of treated cases, we will support the establishment of novel criteria for disease assessments and therapeutic decision trees.

LITERATURE ANALYSIS

A literature search was conducted using PubMed and Ovid, with the terms “diversion colitis” or “diversion proctitis” and “diversion pouchitis” used to extract studies published over the preceding 45 years. All appropriate English-language publications from relevant journals were selected. We summarized the available information on demographics, clinical symptoms, endoscopic and histological findings, treatment, and the clinical course.

CLINICAL CHARACTERS

Epidemiology

A total of 69 articles, including 25 case reports, were matched to our definition of diversion colitis and pouchitis assessment; this information is summarized in Tables 1 and 2. Based on our review, the prevalence estimates of these conditions appear extremely high, reaching almost the entire population of interest if the phenomenon is followed prospectively, beginning at 3 to 36 mo after colostomy^[21]. In a recent study, Szczebkowski *et al*^[3] described more than 90% incidence of diversion colitis on endoscopy in a series of 145 patients. The study further reported that there were no significant associations between diversion colitis and age, sex, type of stoma, or mode of surgery performed. The frequency of disease occurrence ranged from 70%-74% in patients without pre-existing IBD^[22] and 91% in patients with pre-existing IBD^[6,21]. In patients with histories of Crohn’s disease chronic severe inflammation, often with transmural disease, has been described after defunctioning colostomies^[34]. It has also been hypothesized that diversion colitis may be a risk factor for ulcerative colitis in predisposed individuals, and that ulcerative colitis can be triggered by anatomically discontinuous inflammation in the large bowel^[35]. Among the 46 reported cases of diversion colitis and

Table 1 Clinical characteristics of case report

| Case (No) | Reference | Reporting yr | Country | Age (yr) | Gender (male/female) | Primary illness (reason for diversion) | Type of diversion (surgical procedure) | Period of up to diagnosis from operation | Symptoms | Endoscopy findings | Pathological findings | Diagnosis |
|--------------|---------------------------|-----------------|---------------|-------------|-------------------------|---|---|--|------------------|--|--|-------------------|
| 1 | Glotzer <i>et al</i> [2] | 1981 | United States | 49 | M | Free perforation sigmoid diverticulum | Loop sigmoid colostomy | 2.5 mo | No symptoms | Erythema, friability, petechiae, atrophy | Crypt abscess, surface epithelial cell degeneration, acute inflammation, chronic inflammation, regeneration | Diversion colitis |
| | | | | 56 | F | Adenocarcinoma. Protect low anastomosis | Loop transverse colostomy | 3 mo | No symptoms | Erythema, friability, petechiae | Normal | Diversion colitis |
| | | | | 78 | M | Sigmoid diverticulitis with perforation | Loop sigmoid colostomy | 6 mo | No symptoms | Erythema, friability, granularity | No biopsy | Diversion colitis |
| | | | | 70 | F | Sigmoid diverticulitis found at pelvic operation | Loop sigmoid colostomy | 3 mo | No symptoms | Erythema, friability, nodularity | Regeneration | Diversion colitis |
| | | | | 43 | F | Sigmoid diverticulitis with perforation | Loop sigmoid colostomy | 8 mo | No symptoms | Erythema, friability | Crypt abscess, acute inflammation. | Diversion colitis |
| | | | | 41 | F | Fecal incontinence secondary to cordotomy for pain | Loop sigmoid colostomy | 18 mo | No symptoms | Erythema, friability, petechiae | No biopsy | Diversion colitis |
| | | | | 65 | M | Sigmoid diverticulitis with perforation | Loop transverse colostomy | 3 yr | No symptoms | Erythema, friability, granularity, petechiae, inflammatory polyp | Crypt abscess, surface epithelial cell degeneration, chronic inflammation, regeneration. | Diversion colitis |
| | | | | 83 | M | Sigmoid diverticulitis with perforation | Loop transverse colostomy | 6 mo | No symptoms | Erythema, friability, granularity | Crypt abscess | Diversion colitis |
| | | | | 26 | M | Fecal incontinence after T9-10 cord transection | Loop transverse colostomy | 7 yr | Rectal discharge | Erythema, friability, petechiae | Surface epithelial cell degeneration, chronic inflammation. | Diversion colitis |
| | | | | 70 | M | Colonic ileus secondary to anticholinergics for Parkinson's disease | Loop transverse colostomy | 4 mo | No symptoms | Erythema, friability, petechiae, inflammatory polyp | Crypt abscess | Diversion colitis |
| 2 | Iusk <i>et al</i> [3] | 1984 | United States | 28 | M | Perforated sigmoid colon for gunshot | Loop sigmoid colostomy | 6 wk | No symptoms | Red granular rectum with aphthous ulcers | Moderate loss of goblet cells with focal edema and lymphocytosis of the lamina propria. | Diversion colitis |
| | | | | 68 | M | Sigmoid carcinoma | Loop transverse colostomy | 6 wk | No symptoms | Multiple aphthae | Not obtained | Diversion colitis |
| 3 | Scott <i>et al</i> [4] | 1984 | United States | 21 | M | Gunshot | Loop transverse colostomy | 2 mo | No symptoms | Multiple, small, polyoid lesions in the rectum and sigmoid colon up to the cutaneous part of the mucous fistula. | Mucosal biopsies of the rectal lesions were interpreted as "chronic nonspecific colitis with pseudopolyps, probably from diversion colitis". | Diversion colitis |
| 4 | Korelitz <i>et al</i> [5] | 1984 | United States | 22 | F | Crohn's Disease | Ileostomy and subtotal colectomy | 2 yr | No symptoms | Friable, nodular | Not obtained | Diversion colitis |

| | | | | | | | | | |
|----|-----------------------------------|-----------------------|--|--|--|------------------------|--|---|-------------------|
| 34 | F | Crohn's ileitis | Ileocolic anastomosis and Loop ileostomy | 2 yr | No symptoms | Exudate | Focal chronic inflammation, edema, erosions, and an increased number of lymphoid follicles. | Diversion colitis | |
| 31 | M | Crohn's ileitis | Ileocolic anastomosis and Loop ileostomy | 1 yr | No symptoms | Aphthous lesions | Chronic inflammation | Diversion colitis | |
| 32 | M | Crohn's ileitis | Ileocolic anastomosis and Loop ileostomy | 1 yr | No symptoms | Friable, exudate | Not obtained | Perforation due to complication of barium enema and diversion colitis | |
| 5 | Fernand <i>et al</i> [40] | 1985 | United States | Perforated sigmoid diverticulum | 22 yr | Rectal bleeding | N/A | Diffuse multiple superficial ulcerations and intense inflammatory infiltrates composed mainly of plasma cells, lymphocytes, and some eosinophils. | |
| 6 | Frank <i>et al</i> [3] | 1987 | United States | Perineal laceration as result of a motor vehicle accident | End sigmoid colostomy | 1 yr | Rectal bleeding | Moderate to severe nonspecific inflammation. | |
| 7 | Hariog <i>et al</i> [5] | 1989 | United States | Neurogenic fecal incontinence | Mucus fistula | 13 mo | Bloody discharge | Diffuse nodularity and ulceration | |
| 63 | F | Irradiation of rectum | Mucus fistula | 2 wk | Bloody discharge | Endoscopic index of 10 | Inflammatory infiltrate of both acute and chronic cells in the lamina propria and the crypt abscess. Lining epithelial cells show decreased mucus secretion. | Diversion colitis | |
| 54 | M | Perianal fistulas | Rectosigmoid pouch | 35 mo | Bloody discharge | Endoscopic index of 9 | Erosions, surface exudate, crypt abscesses, edema. | Diversion colitis | |
| 56 | M | Diverticulitis | Mucus fistula | N/A | N/A | Endoscopic index of 8 | Lymph follicles | Diversion colitis | |
| 8 | Triantafyllidis <i>et al</i> [31] | 1991 | Greece | Diverticula with perforation | Hartman's type of operation laparotomy | 16 mo | Bloody rectal discharge | Severe inflammatory infiltration, formation of lymph follicles, surface erosions, edema, and crypt abnormalities. | Diversion colitis |
| 9 | Tripodi <i>et al</i> [43] | 1992 | United States | Small bowel perforation with a ruptured chronic pelvic abscess secondary to diverticular disease | End transverse colostomy | 10 wk | Erythematous and friable, with diffuse exudation, petechiae, and ulceration | Acute and chronic inflammation with cryptitis. | Diversion colitis |
| 10 | Lu <i>et al</i> [38] | 1995 | United States | Chronic constipation | Loop transverse colostomy | 25 yr | Sepsis(no symptoms such as rectal bleeding) | Large ulcers with overlying pseudomembrane | Diversion colitis |

| | | | | | | | | | | | | |
|----|-------------------------------------|------|----------------|----|---|---|--------------------------------------|-----------------------------------|-------------------------------------|--|--|--------------------------|
| 11 | Lai <i>et al</i> ^[47] | 1997 | United States | 49 | M | Intractable ileus, C6 ASIA B tetraplegic | Colostomy | 10 yr | Rectal pain and bleeding. | Partial stricture 70 cm proximally to the rectum. The colonic mucosa appeared granular and friable with evidence of linear ulceration. | Extravasation of erythrocytes, lymphocytic and neutrophilic cells infiltrates, and edema were present within the lamina propria. No evidence of malignancy and glandular dysplasia was found. Pathologic report was consistent with chronic colitis. | Diversion colitis |
| 12 | Lim <i>et al</i> ^[23] | 1999 | United Kingdom | 60 | F | Faecal incontinence for DM | End sigmoid colostomy | 6 mo | Blood and mucus per rectum | Edematous mucosa with bloodstained muco-purulent exudate | Active chronic colitis with focal cryptitis and crypt abscesses. | Diversion colitis → UC |
| 13 | Jowett <i>et al</i> ^[33] | 2000 | United Kingdom | 75 | F | Faecal incontinence | Ileostomy and colostomy | 6 mo | Blood and mucus per rectum | Granular, erythematous mucosa with contact bleeding | Active inflammation with polymorphs infiltrating crypts and a diffuse increase in lymphocytes and plasma cells in the lamina propria. | Diversion colitis → UC |
| 14 | Lim <i>et al</i> ^[33] | 2000 | United Kingdom | 66 | M | Sigmoid carcinoma | End colostomy | 8 mo | Blood and mucus per rectum | Granular, congested, and oedematous mucosa with contact bleeding | Mixed inflammatory cell infiltrate with distortion of the crypt architecture and cryptitis. | Diversion colitis (→ UC) |
| 15 | Kiely <i>et al</i> ^[38] | 2001 | United Kingdom | 6 | M | Ulcerative colitis | Hartmann's procedure with colostomy. | 18 mo | No symptoms | Mildly inflamed | Active colitis | Diversion colitis (→ UC) |
| | | | | | | Total colectomy and ileostomy | | 9 mo | Rectal bleeding | Endoscopic index of 8 | Lymphoid hyperplasia, lymphoplasmacytosis, crypt abscesses and moderate mucosal architectural disruption. | Diversion proctocolitis |
| | | | | | | | | 5 mo | Rectal bleeding and abdominal pains | Endoscopic index of 8 | Lymphoplasmacytic infiltration of lamina propria, and architectural disruption. | Diversion proctocolitis |
| | | | | | | | | 4 mo | Rectal discharge | Endoscopic index of 9 | Lymphoplasmacytic and neutrophilic infiltrate in the lamina propria, mucin depletion, and Paneth cell metaplasia. | Diversion proctocolitis |
| | | | | | | | | N/A | Rectal bleeding | Florid colitis | Lymphoid hyperplasia, depletion, lymphoplasmacytosis and mucin depletion. | Diversion proctocolitis |
| | | | | | | | | N/A | Rectal discharge | Florid colitis | Lymphoid hyperplasia, lymphoplasmacytosis. | Diversion proctocolitis |
| | | | | | | | | N/A (On surveillance colonoscopy) | No symptoms | Mild colitis with a decreased vascular pattern, oedema and mucosal tear | N/A | Diversion colitis |
| 16 | Komuro <i>et al</i> ^[41] | 2003 | Japan | 46 | M | Rectovesical fistula | Loop sigmoid colostomy | 10 yr | Rectal discharge | Florid colitis | Lymphoid hyperplasia, lymphoplasmacytosis. | Diversion proctocolitis |
| | | | | | | Ascending colon diverticular perforation (systemic lupus erythematosus and chronic renal failure) | Loop transverse colostomy | | | | | |

| | | | | | | | | | | | | |
|----|--|------|----------------|----|---|--|---|-------|------------------------------------|--|---|--|
| 17 | Tsironi <i>et al</i> ^[48] | 2006 | United Kingdom | 40 | M | UC pancolitis-type | Rectal stump and ileostomy, subtotal colectomy and ileostomy | 5 mo | Blood and mucus per rectum | Severe chronic inflammation with ulceration and numerous inflammatory polyps | Diffuse chronic inflammation with patchy cryptitis caused by clostridium difficile infection. | Diversion colitis with pouchitis |
| 18 | Boyce <i>et al</i> ^[37] | 2008 | United Kingdom | 29 | M | Life-long constipation | Subtotal colectomy | 15 yr | Rectal bleeding and anal pain | The mucosa of the rectal stump was found to be chronically inflamed and ulcerated. | Inflammatory change | Diversion pouchitis |
| 19 | Haugen <i>et al</i> ^[49] | 2008 | United States | 36 | F | Faecal incontinence due to spina bifida | Laparoscopic sigmoid colostomy and creation of a Hartmann's pouch | N/A | Rectal discharge | N/A | N/A | Diversion colitis |
| 20 | Talisetti <i>et al</i> ^[50] | 2009 | United States | 19 | F | Megacystis-microcolon-intestinal hypoperistalsis syndrome (MMHS) | Gastrostomy and ileostomy | 4 yr | Abdominal pain and rectal bleeding | Friable mucose with areas of pinpoint hemorrhage from the anal verge to 30 cm proximally | Acute cryptitis and scattered crypt abscesses, consistent with diversion colitis. | Diversion colitis |
| 21 | Kominami <i>et al</i> ^[51] | 2013 | Japan | 84 | M | Angiodysplasia S/O | Subtotal colectomy and ileostomy | 5 yr | Blood in the stool | Granular, edematous mucosa with contact bleeding | Lymphoplasmacytic and neutrophilic infiltrate in the lamina propria. | Diversion colitis |
| 22 | Watanabe <i>et al</i> ^[44] | 2014 | Japan | 76 | F | UC | 3-stage pancolectomy with construction of an IPAA | 13 yr | Bloody purulent rectal discharge | Pouchitis with large erosions | N/A | Diversion pouchitis |
| 23 | Gundling <i>et al</i> ^[45] | 2015 | Germany | 75 | F | Chronic constipation | Permanent end-colostomy | N/A | Tenesmus and severe rectal pain | Severe DC was seen on colonoscopy | Confirmed histologically | Diversion colitis |
| 24 | Matsumoto <i>et al</i> ^[52] | 2016 | Japan | 65 | M | UC pancolitis-type | Subtotal colectomy and ileostomy | 4 mo | Rectal bleeding | Moderate mucosal inflammation | Ulcer, granulation tissue and epithelial defect | Diversion colitis or exacerbation of UC was suspected. |
| 25 | Custon <i>et al</i> ^[29] | 2017 | United States | 44 | M | UC complicated by colitis-associated low-grade dysplasia | Total proctocolectomy with 2-stage IPAA | 7 yr | Blood in the stool | Edematous and coated with old and fresh blood | N/A | Severe diversion pouchitis |

pouchitis, there was a slight male predominance (28 males, 18 females), and the age of the patients ranged from 3 to 85 years old^[2,5,13,29,31-33,35-52]. The period from diagnosis to surgical treatment was a median of 8 mo, ranging from 2 wk to 25 years (Table 1). The types of diversions included: 9 cases of loop sigmoid colostomy; 3 cases of end sigmoid colostomy; 9 cases of loop transverse colostomy; 4 cases of loop ileostomy; 7 cases of ileostomy and colostomy; 3 cases of proctocolectomy; 2 cases of Hartmann's type with colostomy; and only one case of other operations (Table 1).

Pathogenesis

The basic mechanisms underlying diversion colitis are still unclear. Götzer hypothesized that it might be the result of bacterial overgrowth, the presence of harmful bacteria,

Table 2 Clinical course of case reports

| Case (No) | Ref. | Age (yr) | Gender (male/female) | Ineffective treatment | Effective treatment | Prognosis |
|-----------|-----------------------------------|----------|----------------------|--|---|---|
| 1 | Glotzer <i>et al</i> [2] | 49 | M | N/A | Closure 4 mo post-diversion | Asymptomatic. Proctoscopy and biopsy normal 2.5 and 30 mo postclosure. |
| | | 56 | F | N/A | Closure 3 mo post-diversion | Recurrent Ca. Mucosa not inflamed grossly or microscopically 18 mo post closure. |
| | | 78 | M | N/A | Closure 6 mo post-diversion | Asymptomatic 1 yr postclosure. |
| | | 70 | F | N/A | Closure 5 mo post-diversion | Asymptomatic. Normal sigmoidoscopy 2 mo postclosure. |
| | | 43 | F | N/A | Closure 2 yr post-diversion | Asymptomatic. Normal sigmoidoscopy 3 yr postclosure. |
| | | 41 | F | N/A | None | Asymptomatic 2 yr after ileostomy. |
| | | 65 | M | N/A | None | Abdominal cramps purulent rectal discharge. Continued inflammation 8 yr after colostomy. |
| | | 83 | M | N/A | None | Asymptomatic. Continued mild inflammation 4.5 yr after colostomy. |
| | | 26 | M | N/A | Steroid enemas | Improved. Continued 8 yr after colostomy. |
| | | 70 | M | N/A | Steroid enemas | Tenesmus, discharge and fever 4 yr after colostomy. Resolved with steroid enemas. |
| | | | | | | Continued inflammation at 8 yr. |
| 2 | Lusk <i>et al</i> [39] | 28 | M | - | Colostomy closure | Normal at 16 mo follow-up. |
| | | 68 | M | - | Colostomy closure | Normal at 7 wk after closure. |
| 3 | Scott <i>et al</i> [46] | 21 | M | - | Colostomy closure | One month later, the patient was examined by flexible sigmoidoscopy, which demonstrated normal mucosa throughout with no sign of pseudopolyps. |
| 4 | Korelitz <i>et al</i> [42] | 22 | F | Steroid enemas | Ileocolic reanastomosis (ileostomy closure) | 3 mo (interval from reanastomosis to normal sigmoidoscopy), 7 yr (duration normal). |
| | | 34 | F | - | Ileostomy closure | 1 mo (interval from reanastomosis to normal sigmoidoscopy), 2 yr (duration normal). |
| | | 31 | M | - | Ileostomy closure | 3 mo (interval from reanastomosis to normal sigmoidoscopy), 18 mo (duration normal). |
| | | 32 | M | - | Ileostomy closure | 2 mo (interval from reanastomosis to normal sigmoidoscopy), 14 mo (duration normal). |
| 5 | Fernand <i>et al</i> [40] | 67 | F | - | Left hemicolectomy and left salpingo-oophorectomy | She recovered well and discharged 9 d later. |
| 6 | Frank <i>et al</i> [13] | 38 | M | Oral and topical steroids | Abdominoperineal resection of the diverted loop and permanent colostomy | No evidence of inflammatory bowel disease has developed. Barium study of the small bowel was normal 1 yr after surgery. |
| 7 | Harig <i>et al</i> [9] | 63 | M | N/A | Short-chain-fatty acid irrigation | N/A |
| | | 63 | F | N/A | Short-chain-fatty acid irrigation | N/A |
| | | 54 | M | N/A | Short-chain-fatty acid irrigation | N/A |
| | | 56 | M | N/A | Short-chain-fatty acid irrigation | N/A |
| 8 | Triantafyllidis <i>et al</i> [31] | 64 | F | - | 5 aminosalicylic acid enemas comparison with Betamethasone enemas | There were no differences in the degree of clinical improvement, or in the endoscopic and histologic scores seen at the end of the trials, between betamethasone and 5-ASA. |
| 9 | Tripodi <i>et al</i> [43] | 85 | F | - | 5 aminosalicylic acid enemas | Clinically asymptomatic at a 6-mo follow-up. |
| 10 | Lu <i>et al</i> [38] | 45 | F | Intravenous metronidazole | Colectomy of the diverted segment | Without complications and has been doing well postoperatively. |
| 11 | Lai <i>et al</i> [47] | 49 | M | - | Daily 5-ASA suppository and total parenteral nutrition | 6 wk of treatment with 5-ASA, the patient had decreased rectal pain and bleeding. |
| 12 | Lim <i>et al</i> [32] | 60 | F | - | Oral prednisolone, oral mesalazine, and mesalazine enemas | PSL was tapered off over four months and she remained well. |
| | | 0 | M | Closure of the loop ileostomy → oral prednisolone, oral olsalazine and oral metronidazole → sigmoid loop colostomy | The defunctioned rectosigmoid was partially removed, leaving the lower rectum and anal canal; the loop colostomy was refashioned into an end colostomy → colectomy and removal of residual rectal stump and anal canal was performed and an end ileostomy fashioned | He subsequently made a good recovery and steroid therapy was discontinued. |
| 13 | Jowett <i>et al</i> [33] | 75 | F | - | Topical steroid enemas. | UC |
| 14 | Lim <i>et al</i> [35] | 66 | M | - | Steroid enemas | 6 mo later he developed ulcerative colitis. |

| | | | | | | |
|----|---------------------------------|----|---|--|---|---|
| 15 | Kiely et al ^[36] | 6 | M | PSL and AZA | SCFA | Oral PSL was continued at the reduced rate of 5mg on alternate days until he underwent an uneventful rectal excision and J-pouch anal anastomosis 1 mo later. Two months after this, his ileostomy was closed. |
| | | 3 | M | Salazopyrine | SCFA | His ileostomy was closed 3 mo later, and he was remained symptom free. |
| | | 8 | F | - | SCFA | Her ulceration was virtually healed and showed a reduction in endoscopic index from 9 to 3. Treatment was maintained until her colostomy was reversed a month later. After stoma closure, SCFAs were discontinued with no further recurrence of symptoms. |
| | | 3 | M | N/A | SCFA | For redo pull-through Rectal excision |
| | | 10 | M | N/A | SCFA | The post endoscopic course was uneventful without any treatment. |
| 16 | Komuro et al ^[41] | 46 | M | - | - | |
| 17 | Tsironi et al ^[48] | 40 | M | Mesalazine suppository and steroid enemas | Metronidazole suppository | Improved quickly and remains well and asymptomatic 12 wk after treatment. |
| 18 | Boyce et al ^[37] | 29 | M | - | Completion proctectomy | Completion proctectomy was uneventful and from which the patient made an unremarkable recovery. |
| 19 | Haugen et al ^[49] | 36 | F | The water and vinegar solution enema, steroid enema, bismuth subsalicylate (standard treatment SCFA enemas was not option due to insurance and spina bifida) | Antegrade irrigations of her distal bowel with tap water | Weekly to twice weekly irrigations completely stopped the malodorous and troublesome discharge. |
| 20 | Talisetti et al ^[50] | 19 | F | SCFA enema, steroids, metronidazole | Colectomy(entire colon was ultimately resected, Since only 15 cm of jejunum appeared healthy, her mid and distal small bowel was also resected up to 15 cm from the ligament of Treitz) | N/A |
| 21 | Kominami et al ^[51] | 84 | M | Short-chain fatty acid enema Oral mesalazine, corticosteroid, metronidazole, and ciprofloxacin | 5-aminosalicylic acid enemas | Undergoing 5-aminosalicylic acid enemas maintenance therapy. |
| 22 | Watanabe et al ^[44] | 76 | F | Enemas containing 5-aminosalicylic acid and steroids and antibiotic therapy Corticosteroid and mesalazine enemas, prednisolone injections. | Leukocytapheresis, following low dose of metronidazole and ciprofloxacin | After 18 mo, her condition remains stable without the need for medication. |
| 23 | Gundling et al ^[45] | 75 | F | | Autologous fecal transplantation | All symptoms improved dramatically within 5 d after the first treatment. Colonoscopy 28 d after the first treatment showed no major signs of inflammation in the colonic stump. |
| 24 | Matsumoto et al ^[52] | 65 | M | | A combined mesalazine plus corticosteroid enema | Finally proctectomy and ileal pouch-anal anastomosis were successfully performed. |
| 25 | Custon et al ^[29] | 44 | M | - | Dextrose(hypertonic glucose) spray endoscopically | The patient did not experience further episodes of recurrent bleeding during the 6-mo follow-up. No prescribed medicines were given after the endoscopic therapy. |

nutritional deficiencies, toxins, or disturbance in the symbiotic relationship between luminal bacteria and the mucosal layer^[2]. Reportedly, concentrations of carbohydrate-fermenting anaerobic bacteria and pathogenic bacteria are reduced in de-functioned colons^[5,23,53] and these reports indicate that the overgrowth of anaerobic bacteria or a pathogenic bacterium is unlikely to be an important etiological factor. On the

other hand, there is an increase of nitrate-reducing bacteria in patients with diversion colitis^[7] and nitrate-reducing bacteria produce nitric oxide (NO) which plays a protective role in low concentrations, but at higher levels it becomes toxic to the colonic tissue^[54]. Thus, it has been suggested that increases in nitrate-reducing bacteria may result in toxic levels of NO, leading to the diversion colitis.

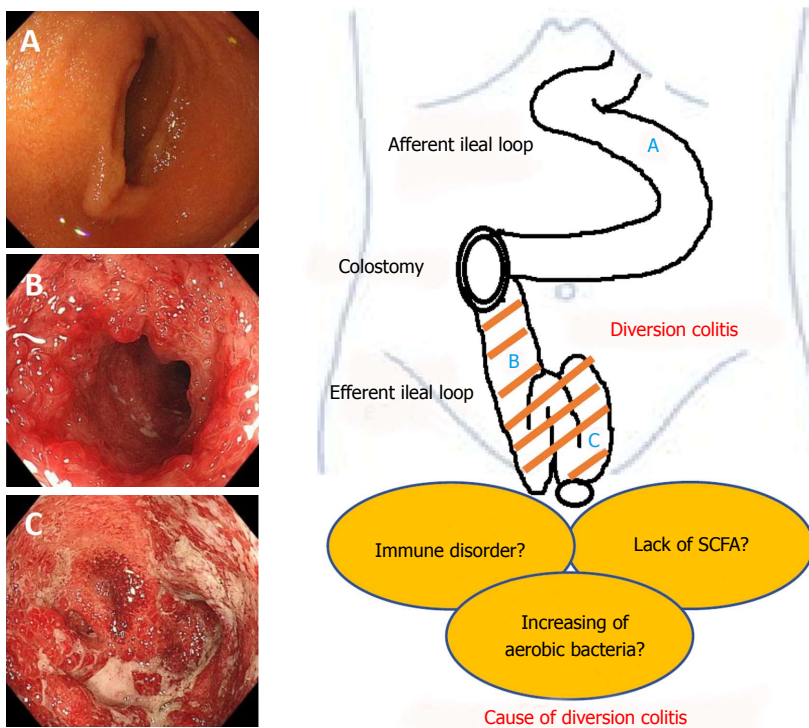


Figure 1 Schematic presentation of diversion colitis and pouchitis.

Recently, ischemia has been proposed as a cause of diversion colitis^[8]. The explanation surely lies in changes to the luminal flora consequent to fecal stream interruption. Normal luminal bacteria produce SCFA, such as butyric acid. Butyrate is the principal oxidative substrate for colonocytes^[55] and patients with diversion colitis may improve following topical treatment with SCFA, especially with butyrate enemas^[5,36]. This hypothesis is based on evidence that suggests SCFA relax vascular smooth muscle and that butyrate deficiencies may induce increased tone in the pelvic arteries, therefore leading to relative ischemia of the colorectal mucosa and intestinal wall^[5]. It is obvious that additional, basic research is necessary in order to discern disease mechanisms. We have summarized the pathogenesis of this disease entity in Figure 1.

Symptoms

Most patients are asymptomatic^[22], however about one third of patients may exhibit symptoms of diversion colitis^[2,3,6,9]. Patients generally present with varying symptoms such as abdominal discomfort, tenesmus, anorectal pain, mucous discharge, and rectal bleeding. The most common symptoms include bloody, serous, or mucous discharge in 40% of the population, and abdominal pain and tenesmus in 15% of the population^[3]. There have been several reports of severe rectal bleeding^[24,29,56]. There is a report of massive rectal distension causing bilateral ureteric obstruction^[37] and a case report of diversion colitis causing severe sepsis requiring a colectomy^[38]. These symptoms can start within 1 mo to 3 years after surgery^[22,24]. Our

review also showed that clinical symptoms of rectal bleeding were seen in 25 cases, abdominal pain in 3 cases, anal pain in 3 cases, and sepsis in 1 case^[38]. On the other hand, 21 of 46 cases had no symptoms (Table 1), as previously reported^[24]. Additionally, in the presence of Crohn's disease and ulcerative colitis, the number of symptomatic patients rises to 33% and 87% respectively^[53]. Our review showed cases with primary illness of diverticula with perforation ($n = 11$), fecal incontinence ($n = 6$), chronic constipation or ileus ($n = 5$), ulcerative colitis ($n = 5$), Crohn's disease ($n = 4$), carcinoma ($n = 3$), and various other diseases (Table 1).

Macroscopic findings

Macroscopically, diversion colitis may involve the whole de-functioned colon or isolated segments. These findings include erythema, diffuse granularity, and blurring of vascular pattern in about 90% of the population. It is also associated with mucosal friability (80%) edema (60%), aphous ulceration, and bleeding, to varying degrees^[2,3,8-12,39,40]. There is a case report of diversion colitis causing mucosal tears within the defunctioned colon^[41]. Recently, Hundorfean et al^[57] reported a first description and *in vivo* diagnosis of diversion colitis after surgery, by virtual chromoendoscopy and fluorescein-guided confocal laser endomicroscopy. Our literature review showed that endoscopic findings were evidenced in 44 out of 46 cases, and severe inflammation with ulceration (endoscopic index ≥ 8) in 17 cases.

Microscopic findings

The pathological finding of diversion colitis and pouchitis

usually vary with degree of severity, therefore, no specific microscopic findings have been noted. The histological features of diversion colitis can mimic those of IBD, even when a pre-existing IBD has not been documented^[10,11,13-15]. The most notable feature often seen in diversion colitis is lymphoid follicular hyperplasia^[9,14,58]. Atrophy, crypt branching, mucin depletion, crypt distortion, regenerative hyperplasia, paneth cell metaplasia, thickening of muscularis mucosa, diffuse active mucosal inflammation with crypt abscesses, ulceration, and vacuolar and epithelial degeneration along with features of chronic inflammation (usually confined to the mucosa) are seen with varying degrees of severity^[9-12,14,16,17,59]. More recently, features of ischemia, such as superficial coagulative necrosis and fibrosis, have been described^[8]. Our review showed that 37 out of 46 cases exhibited pathological findings including 15 cases of crypt abscess or cryptitis^[2], and 14 cases of lymphoid follicular hyperplasia (which was not previously identified as a feature of diversion colitis). These features are non-specific and, to date, no characteristic feature or features of diversion colitis have been identified.

Treatment

Because of the small number of patients and the unknown etiology, there is no established standard therapy for diversion colitis and pouchitis. Szczepkowski *et al*^[4] proposed a management strategy for patients with de-functioned distal stomas. He divided patients with diversion colitis into three groups based on a study of 145 patients. These groups consisted of Group 1 (no clinical, morphological or endoscopic evidence of diversion colitis), Group 2, (mild or moderate signs of diversion colitis), and Group 3 (severe diversion colitis). Group 1 can be treated conservatively, Group 2 can be treated using conservative management prior to restoration of colonic continuity and Group 3 should ideally undergo restoration of colonic continuity. If a surgical option is not feasible, pharmacologic treatment options should be tried to resolve the inflammation. A summary of the clinical courses of case reports is shown in Table 2.

Surgery

Treatment of diversion colitis should be primarily directed at restoring bowel continuity to restore the luminal flow. This will resolve the symptoms and assist the bowel to return to normal. Re-anastomosis has proven to be consistently effective in halting the symptoms of diversion colitis in a number of studies^[2,10,25,39,42]. Re-anastomosis of diverted segments in patients with preexisting inflammatory bowel disease is a more difficult decision because inflammation in the diverted segment could represent inflammatory bowel disease or diversion colitis, each of which dictate different courses of action^[3,21,42]. Resection is not typically required. Indications for resection include uncontrolled perianal

sepsis, perianal fistulous disease, anal incontinence, and uncontrolled symptoms related to diversion colitis.

Diet and lifestyle

Nutritional imbalance in the excluded colon is likely responsible for the pathologic changes and symptoms of diversion colitis. However, current evidence does not support the effectiveness of lifestyle modifications or nutritional imbalance^[60].

Pharmacologic treatment is generally indicated for the temporary control of symptoms in preparation for surgery. It is used occasionally for patients who are not considered surgical candidates because of severe medical comorbidities, poor sphincter function, or reasons of technical difficulty.

Short-chain-fatty acid

Short-chain fatty acids, mainly butyrate, are the major fuel source for the epithelium. Their absence in the diverted tract may produce mucosal atrophy and inflammation. Bacteria produce SCFAs as byproducts of carbohydrate fermentation in the colonic lumen, and SCFAs provide the primary energy source for colonic mucosal cells^[13]. In human neutrophils, SCFAs reduce the production of reactive oxygen species, which are the agents of oxidative tissue damage^[61]. Treatment of diversion colitis with SCFA or butyrate has shown inconsistent results. Harig successfully improved symptoms and endoscopic inflammatory change by SCFA^[5]. Komorowski *et al*^[10] reported similar results in four patients with diversion colitis with SCFA irrigation. However, Guillmot *et al*^[16,28] failed to demonstrate either histological or endoscopic improvement. The differences in response may be partially accounted for by disease groupings. In recent years, several studies on the usefulness of SCFA, including of butyrate, are reported^[19,62]. Cristina *et al*^[27] proposed that butyrate enemas may prevent the atrophy of the diverted colon/rectum, thus improving the recovery of tissue integrity.

5-aminosalicylic acid

Usefulness of 5-aminosalicylic acid (5-ASA) enemas in diversion colitis was reported for the first time by Triantafillidis *et al*^[31] in 1991. Tripodi *et al*^[43] has also reported similar results in 1992. Caltabiano *et al*^[63] reported that 5-ASA enema reduces oxidative DNA damage in colonic mucosa and reduces mucosal damage using rats in a diversion colitis model. It is considered that the mucosal disorder may be improved by protective action against oxidative DNA damage and the anti-inflammatory action of 5ASA^[64].

Corticosteroids

Glotzer reported on several patients with diversion colitis treated by steroid enemas in 1984^[2]. Lim and Jowett also reported the efficacy of the steroid enemas in 2000^[32,33]. Corticosteroids are first-line agents for symptomatic diversion colitis, with varying effectiveness.

Table 3 Summary of pharmacologic treatments

| Treatment | Ref. | Procedure/standard dosage | Efficacy | Complications/main side effects |
|--------------------------------------|-----------------------------|---|--|--|
| Surgical anastomosis | [2,3,10,21,25,39,42] | Mobilization of both ends of the bowel with either sutured or stapled anastomosis. | The most effective method of eliminating the signs and symptoms | Bleeding, infection, anastomotic leak, anastomotic stricture, anesthetic risks |
| Corticosteroids | [2,32,33] | Hydrocortisone (100 mg per 60 mL bottle) enema is administered once daily for up to 3 wk. Occasional treatment may be given for 2 to 3 mo depending on clinical response. | Response to treatment is generally seen in 3 to 5 d. | Local pain and burning, occasionally rectal bleeding. |
| 5-aminosalicylic acid (5-ASA) enemas | [31,43,63,64] | 4 g of mesalazine in 60 mL suspensions, administered rectally once-daily dose for 4 to 5 wk. | Varying effect | Prolonged treatment may result in systemic absorption, causing systemic side effects. Occasionally produces acute intolerance manifested by cramping, acute abdominal pain, bloody diarrhea, fever, headache, and rash. |
| Short-chain-fatty acid (SCFA) | [5,10,13,18,19,26,27,61,62] | SCFA enema rectally twice a day for 2 wk, and then tapered according to response over 2 to 4 wk. | Varying effect | None |
| Irrigation with Fibers | [65,66] | Solution containing 5% fibers (10 g/d) for 7 d. | The endoscopic score which is used to quantify the intensity of the inflammation at the mucosa at the diverted colon diminished after treatment. | Probably none |
| Leukocytapheresis | [44] | Leukocytapheresis, at flow rate of 40 mL/min for 60 min, once weekly for 5 wk, following low dose of metronidazole and ciprofloxacin, another set of weekly leukocytapheresis was added. | Significant improvement in her pouchitis disease activity index (PDAI) from 14 to 1. | The common side effects were nausea, vomiting, fever, chills, and nasal obstruction. |
| Autologous fecal transplantation | [45] | Feces were collected from the colostomy bag, diluted with 600 mL of sterile saline (0.9 %), stirred and filtered three times using an ordinary coffee filter, irrigation endoscopically. This procedure was repeated 3 times within 4 wk (on day 0, day 10 and day 28). | All symptoms improved dramatically within 5 d after the first treatment. Colonoscopy 28 d after the first treatment showed no major signs of inflammation in the colonic stump | None, patient's tolerance required. |
| Dextrose spray (hypertonic glucose) | [29] | Endoscopically sprayed with 150 mL 50% dextrose via a catheter. | Follow-up pouchoscopy 2 wk after the dextrose spray showed normal pouch mucosa with no evidence of bleeding or mucosal friability. | It has a very low chance of causing transient hyperglycemia because there is no direct injection of the hypertonic solution into blood vessels. |

SCFA: Short chain fatty acids; 5-ASA: 5-aminosalicylic acid.

Irrigation with fibers

Resolution of diversion colitis, based on endoscopic and histologic examination, has been reported following irrigation of the diverted segment of the colon with fibers^[65,66]. Joaquim *et al*^[66] investigated the effect of irrigating the colorectal mucosa of patients with a colostomy using a solution of fibers. In 11 patients with loop colostomies, the diverted colorectal segment was irrigated with a solution containing 5% fibers (10 g/d) for 7 d. Irrigation with fibers improves inflammation within the defunctionalized colon, so this therapy may play a role in the preoperative management of colostomies, potentially decreasing the high incidence of diarrhea after reestablishment of the intestinal transit.

Leukocytapheresis

Watanabe *et al*^[44] reported successful treatment of

leukocytapheresis in a patient with chronic antibiotic-refractory diversion pouchitis following IPAA for UC with diverting ileostomy. The mucosa of the diverted pouch is less exposed to the fecal stream and pathogens. Therefore, altered immunity likely plays a major role in the maintenance of diversion pouchitis. Leukocytapheresis to address the altered immunity would seem a reasonable approach for antibiotic-refractory pouchitis following IPAA for UC with diverting ileostomy, and its effectiveness in the case suggests that altered immunity may be a key contributing factor compared with dysbiosis, bacterial pathogens, and ischemia.

Autologous fecal microbiota transplantation

Fecal microbiota transplantation (FMT), which consists of transferring stool from a healthy donor to the patient's colon, is an effective treatment for some diseases of the

colon such as Crohn's disease and recurrent Clostridium difficile infections^[67]. Gundling *et al*^[45] presented that autologous FMT might be an effective and safe option for relapsing DC after standard therapies have failed. Since the interruption of the fecal stream is central to the development of DC, FMT seems to be a hopeful treatment.

Dextrose spray

Custon *et al*^[29] presented a patient with ulcerative colitis with severe hematochezia and diffuse mucosal bleeding in a diverted ileal pouch, which was successfully treated with endoscopic spray of hypertonic glucose (50% dextrose). Hypertonic glucose may work thorough osmotic dehydration and sclerosant effects, inducing long-term mural necrosis and fibrotic obliteration of mucosal vessels^[68,69]. Glucose spray is safe and inexpensive, and it carries a very low risk of complications. The approach has the potential to reduce recurrent bleeding and need for surgical interventions.

SUMMARY OF PHARMACOLOGIC TREATMENTS

The goal of treatment is the reduction or elimination of symptoms. Patients who desire stoma closure and have acceptable risks should undergo surgery to re-establish intestinal continuity. In their prospective study, Son *et al*^[20] reported that the severity of DC is related to diarrhea after an ileostomy reversal and may adversely affect quality of life. Pharmacologic treatments are needed for symptomatic patients with permanent stomas and patients who are unable to undergo stoma closure for reasons of technical difficulty, poor anal sphincter function, or persistent perianal sepsis. In our review, SCFA^[5,10,18,19,26,27,36,62], 5-ASA enemas^[31,43,47,51], steroid enemas^[21,32,33], and irrigation with fibers^[65,66] have been tried with various efficacies for mucosal inflammation. Only case reports of therapy involving leukocytapheresis^[44], autologous fecal microbiota transplantation (FMT)^[45] and dextrose (hypertonic glucose) spray^[29] have been tried with some effect. We have summarized the method, advantages and disadvantages of each pharmacologic treatment in Table 3.

CONCLUSION

The vast majority of diverted patients remain asymptomatic, however diversion colitis occurs in almost all diverted patients. It generally resolves following colostomy closure. However, those patients with significant symptoms or histories of colitis or diarrhea should undergo a complete proximal and distal colonic evaluation prior to stoma closure, and some treatments need not be delayed in these patients. Patients with permanent diversions should undergo periodic pharmacologic treatment. This review of various treatments for diversion colitis will hopefully be useful for determining future treatments.

REFERENCES

- 1 Morson BC, Dawson IMP. *Gastrointestinal Pathology*, first ed., Blackwellflic Publications, London, 1972
- 2 Glotzer DJ, Glick ME, Goldman H. Proctitis and colitis following diversion of the fecal stream. *Gastroenterology* 1981; **80**: 438-441 [PMID: 7450438]
- 3 Mudretsova-Viss KA, Gabriél'iants GM. [Enterococcal survival in forcemeat preserved in polymer films and in cutlets made from it]. *Vopr Pitan* 1975; **1**: 68-72 [PMID: 1906]
- 4 Ma CK, Gottlieb C, Haas PA. Diversion colitis: a clinicopathologic study of 21 cases. *Hum Pathol* 1990; **21**: 429-436 [PMID: 2318485]
- 5 Harig JM, Soergel KH, Komorowski RA, Wood CM. Treatment of diversion colitis with short-chain-fatty acid irrigation. *N Engl J Med* 1989; **320**: 23-28 [PMID: 2909876 DOI: 10.1056/NEJM198901053200105]
- 6 Frisbie JH, Ahmed N, Hirano I, Klein MA, Soybel DI. Diversion colitis in patients with myelopathy: clinical, endoscopic, and histopathological findings. *J Spinal Cord Med* 2000; **23**: 142-149 [PMID: 10914356]
- 7 Neut C, Guillemot F, Colombel JF. Nitrate-reducing bacteria in diversion colitis: a clue to inflammation? *Dig Dis Sci* 1997; **42**: 2577-2580 [PMID: 9440640]
- 8 Villanacci V, Talbot IC, Rossi E, Bassotti G. Ischaemia: a pathogenetic clue in diversion colitis? *Colorectal Dis* 2007; **9**: 601-605 [PMID: 17824976 DOI: 10.1111/j.1463-1318.2006.01182.x]
- 9 Roe AM, Warren BF, Brodribb AJ, Brown C. Diversion colitis and involution of the defunctioned anorectum. *Gut* 1993; **34**: 382-385 [PMID: 8472988]
- 10 Komorowski RA. Histologic spectrum of diversion colitis. *Am J Surg Pathol* 1990; **14**: 548-554 [PMID: 2337203]
- 11 Geraghty JM, Talbot IC. Diversion colitis: histological features in the colon and rectum after defunctioning colostomy. *Gut* 1991; **32**: 1020-1023 [PMID: 1916483]
- 12 Winslet MC, Poxon V, Youngs DJ, Thompson H, Keighley MR. A pathophysiologic study of diversion proctitis. *Surg Gynecol Obstet* 1993; **177**: 57-61 [PMID: 8322151]
- 13 Murray FE, O'Brien MJ, Birkett DH, Kennedy SM, LaMont JT. Diversion colitis. Pathologic findings in a resected sigmoid colon and rectum. *Gastroenterology* 1987; **93**: 1404-1408 [PMID: 3678755]
- 14 Yeom ML, Bethwaite PB, Prasad J, Isbister WH. Lymphoid follicular hyperplasia--a distinctive feature of diversion colitis. *Histopathology* 1991; **19**: 55-61 [PMID: 1916687]
- 15 Asplund S, Gramlich T, Fazio V, Petras R. Histologic changes in defunctioned rectums in patients with inflammatory bowel disease: a clinicopathologic study of 82 patients with long-term follow-up. *Dis Colon Rectum* 2002; **45**: 1206-1213 [PMID: 12352238 DOI: 10.1097/01.DCR.0000027037.66166.F3]
- 16 Haque S, West AB. Diversion colitis--20 years a-growing. *J Clin Gastroenterol* 1992; **15**: 281-283 [PMID: 1294631]
- 17 Vujićić GM, Dojcinov SD. Diversion colitis in children: an iatrogenic appendix vermiciformis? *Histopathology* 2000; **36**: 41-46 [PMID: 10632750]
- 18 Neut C, Guillemot F, Gower-Rousseau C, Biron N, Cortot A, Colombel JF. [Treatment of diversion colitis with short-chain fatty acids. Bacteriological study]. *Gastroenterol Clin Biol* 1995; **19**: 871-875 [PMID: 8746044]
- 19 Pal K, Tinalal S, Al Buainain H, Singh VP. Diversion proctocolitis and response to treatment with short-chain fatty acids--a clinicopathological study in children. *Indian J Gastroenterol* 2015; **34**: 292-299 [PMID: 26243588 DOI: 10.1007/s12664-015-0577-0]
- 20 Son DN, Choi DJ, Woo SU, Kim J, Keom BR, Kim CH, Baek SJ, Kim SH. Relationship between diversion colitis and quality of life in rectal cancer. *World J Gastroenterol* 2013; **19**: 542-549 [PMID: 23382634 DOI: 10.3748/wjg.v19.i4.542]
- 21 Korelitz BI, Cheskin LJ, Sohn N, Sommers SC. The fate of the rectal segment after diversion of the fecal stream in Crohn's disease: its implications for surgical management. *J Clin*

- Gastroenterol* 1985; **7**: 37-43 [PMID: 3980962]
- 22 **Ferguson CM**, Siegel RJ. A prospective evaluation of diversion colitis. *Am Surg* 1991; **57**: 46-49 [PMID: 1796797]
- 23 **Baek SJ**, Kim SH, Lee CK, Roh KH, Keum B, Kim CH, Kim J. Relationship between the severity of diversion colitis and the composition of colonic bacteria: a prospective study. *Gut Liver* 2014; **8**: 170-176 [PMID: 24672659 DOI: 10.5009/gnl.2014.8.2.170]
- 24 **Whelan RL**, Abramson D, Kim DS, Hashmi HF. Diversion colitis. A prospective study. *Surg Endosc* 1994; **8**: 19-24 [PMID: 8153859]
- 25 **Orsay CP**, Kim DO, Pearl RK, Abcarian H. Diversion colitis in patients scheduled for colostomy closure. *Dis Colon Rectum* 1993; **36**: 366-367 [PMID: 8458263]
- 26 **Guillemot F**, Colombel JF, Neut C, Verplanck N, Lecomte M, Romond C, Paris JC, Cortot A. Treatment of diversion colitis by short-chain fatty acids. Prospective and double-blind study. *Dis Colon Rectum* 1991; **34**: 861-864 [PMID: 1914718]
- 27 **Luceri C**, Femia AP, Fazi M, Di Martino C, Zolfanelli F, Dolara P, Tonelli F. Effect of butyrate enemas on gene expression profiles and endoscopic/histopathological scores of diverted colorectal mucosa: A randomized trial. *Dig Liver Dis* 2016; **48**: 27-33 [PMID: 26607831 DOI: 10.1016/j.dld.2015.09.005]
- 28 **Fazio VW**, Ziv Y, Church JM, Oakley JR, Lavery IC, Milsom JW, Schroeder TK. Ileal pouch-anal anastomoses complications and function in 1005 patients. *Ann Surg* 1995; **222**: 120-127 [PMID: 7639579]
- 29 **Nyabanga CT**, Shen B. Endoscopic Treatment of Bleeding Diversion Pouchitis with High-Concentration Dextrose Spray. *ACG Case Rep J* 2017; **4**: e51 [PMID: 28377939 DOI: 10.14309/crj.2017.51]
- 30 **Gorgun E**, Remzi FH. Complications of ileoanal pouches. *Clin Colon Rectal Surg* 2004; **17**: 43-55 [PMID: 20011284 DOI: 10.1055/s-2004-823070]
- 31 **Triantafillidis JK**, Nicolakis D, Mountaneas G, Pomonis E. Treatment of diversion colitis with 5-aminosalicylic acid enemas: comparison with betamethasone enemas. *Am J Gastroenterol* 1991; **86**: 1552-1553 [PMID: 1928058]
- 32 **Lim AG**, Langmead FL, Feakins RM, Rampton DS. Diversion colitis: a trigger for ulcerative colitis in the in-stream colon? *Gut* 1999; **44**: 279-282 [PMID: 9895391]
- 33 **Jowett SL**, Cobden I. Diversion colitis as a trigger for ulcerative colitis. *Gut* 2000; **46**: 294 [PMID: 10712080]
- 34 **Burman JH**, Thompson H, Cooke WT, Williams JA. The effects of diversion of intestinal contents on the progress of Crohn's disease of the large bowel. *Gut* 1971; **12**: 11-15 [PMID: 5543369]
- 35 **Lim AG**, Lim W. Diversion colitis: a trigger for ulcerative colitis in the instream colon. *Gut* 2000; **46**: 441 [PMID: 10733317]
- 36 **Kiely EM**, Ajayi NA, Wheeler RA, Malone M. Diversion proctocolitis: response to treatment with short-chain fatty acids. *J Pediatr Surg* 2001; **36**: 1514-1517 [PMID: 11584399 DOI: 10.1053/jpsu.2001.27034]
- 37 **Boyce SA**, Hendry WS. Diversion colitis presenting with massive rectal distension and bilateral ureteric obstruction. *Int J Colorectal Dis* 2008; **23**: 1143-1144 [PMID: 18443804 DOI: 10.1007/s00384-008-0491-3]
- 38 **Lu ES**, Lin T, Harms BL, Gaumnitz EA, Singaram C. A severe case of diversion colitis with large ulcerations. *Am J Gastroenterol* 1995; **90**: 1508-1510 [PMID: 7661179]
- 39 **Lusk LB**, Reichen J, Levine JS. Aphthous ulceration in diversion colitis. Clinical implications. *Gastroenterology* 1984; **87**: 1171-1173 [PMID: 6479539]
- 40 **Ona FV**, Boger JN. Rectal bleeding due to diversion colitis. *Am J Gastroenterol* 1985; **80**: 40-41 [PMID: 3871305]
- 41 **Komuro Y**, Watanabe T, Hata K, Nagawa H. Diversion colitis with a mucosal tear on endoscopic insufflation. *Gut* 2003; **52**: 1388-1389 [PMID: 12912883]
- 42 **Korelitz BI**, Cheskin LJ, Sohn N, Sommers SC. Proctitis after fecal diversion in Crohn's disease and its elimination with reanastomosis: implications for surgical management. Report of four cases. *Gastroenterology* 1984; **87**: 710-713 [PMID: 6745620]
- 43 **Tripodi J**, Gorcey S, Burakoff R. A case of diversion colitis treated with 5-aminosalicylic acid enemas. *Am J Gastroenterol* 1992; **87**: 645-647 [PMID: 1595655]
- 44 **Watanabe C**, Hokari R, Miura S. Chronic antibiotic-refractory diversion pouchitis successfully treated with leukocyteapheresis. *Ther Apher Dial* 2014; **18**: 644-645 [PMID: 24571541 DOI: 10.1111/1744-9987.12175]
- 45 **Gundling F**, Tiller M, Agha A, Schepp W, Iesalnieks I. Successful autologous fecal transplantation for chronic diversion colitis. *Tech Coloproctol* 2015; **19**: 51-52 [PMID: 25300242 DOI: 10.1007/s10151-014-1220-2]
- 46 **Scott RL**, Pinstein ML. Diversion colitis demonstrated by double-contrast barium enema. *AJR Am J Roentgenol* 1984; **143**: 767-768 [PMID: 6332481 DOI: 10.2214/ajr.143.4.767]
- 47 **Lai JM**, Chuang TY, Francisco GE, Strayer JR. Diversion colitis: a cause of abdominal discomfort in spinal cord injury patients with colostomy. *Arch Phys Med Rehabil* 1997; **78**: 670-671 [PMID: 9196478]
- 48 **Tsironi E**, Irving PM, Feakins RM, Rampton DS. "Diversion" colitis caused by Clostridium difficile infection: report of a case. *Dis Colon Rectum* 2006; **49**: 1074-1077 [PMID: 16729217 DOI: 10.1007/s10350-006-0577-3]
- 49 **Haugen V**, Rothenberger DA, Powell J. Antegrade irrigations of a surgically reconstructed Hartmann's pouch to treat intractable diversion colitis. *J Wound Ostomy Continence Nurs* 2008; **35**: 231-232 [PMID: 18344801 DOI: 10.1097/01.WON.0000313649.90612.a1]
- 50 **Talisetti A**, Longacre T, Pai RK, Kerner J. Diversion colitis in a 19-year-old female with megacystis-microcolon-intestinal hypoperistalsis syndrome. *Dig Dis Sci* 2009; **54**: 2338-2340 [PMID: 19582576 DOI: 10.1007/s10620-009-0882-5]
- 51 **Kominami Y**, Ohe H, Kobayashi S, Higashi R, Uchida D, Morimoto Y, Nakarai A, Numata N, Hirao K, Ogawa T, Ueki T, Nakagawa M, Araki Y, Mizuno M, Chayama K. [Classification of the bleeding pattern in colonic diverticulum is useful to predict the risk of bleeding or re-bleeding after endoscopic treatment]. *Nihon Shokakibyo Gakkai Zasshi* 2012; **109**: 393-399 [PMID: 22398904]
- 52 **Matsumoto S**, Mashima H. Efficacy of Combined Mesalazine Plus Corticosteroid Enemas for Diversion Colitis after Subtotal Colectomy for Ulcerative Colitis. *Case Rep Gastroenterol* 2016; **10**: 157-160 [PMID: 27403119 DOI: 10.1159/000445868]
- 53 **Neut C**, Colombel JF, Guillemot F, Cortot A, Gower P, Quandalle P, Ribet M, Romond C, Paris JC. Impaired bacterial flora in human excluded colon. *Gut* 1989; **30**: 1094-1098 [PMID: 2767506]
- 54 **McCafferty DM**, Mudgett JS, Swain MG, Kubes P. Inducible nitric oxide synthase plays a critical role in resolving intestinal inflammation. *Gastroenterology* 1997; **112**: 1022-1027 [PMID: 9041266]
- 55 **Velázquez OC**, Lederer HM, Rombeau JL. Butyrate and the colonocyte. Production, absorption, metabolism, and therapeutic implications. *Adv Exp Med Biol* 1997; **427**: 123-134 [PMID: 9361838]
- 56 **Bosshardt RT**, Abel ME. Proctitis following fecal diversion. *Dis Colon Rectum* 1984; **27**: 605-607 [PMID: 6468202]
- 57 **Hundorfean G**, Chiriac MT, Siebler J, Neurath MF, Mudter J. Confocal laser endomicroscopy for the diagnosis of diversion colitis. *Endoscopy* 2012; **44** Suppl 2 UCTN: E358-E359 [PMID: 23012020 DOI: 10.1055/s-0032-1310019]
- 58 **Lechner GL**, Frank W, Jantsch H, Pichler W, Hall DA, Wanek R, Wunderlich M. Lymphoid follicular hyperplasia in excluded colonic segments: a radiologic sign of diversion colitis. *Radiology* 1990; **176**: 135-136 [PMID: 2353081 DOI: 10.1148/radiology.176.1.2353081]
- 59 **Edwards CM**, George B, Warren B. Diversion colitis--new light through old windows. *Histopathology* 1999; **34**: 1-5 [PMID: 9934577]
- 60 **Eggenberger JC**, Farid A. Diversion Colitis. *Curr Treat Options Gastroenterol* 2001; **4**: 255-259 [PMID: 11469982]
- 61 **Liu Q**, Shimoyama T, Suzuki K, Umeda T, Nakaji S, Sugawara K. Effect of sodium butyrate on reactive oxygen species generation

- by human neutrophils. *Scand J Gastroenterol* 2001; **36**: 744-750 [PMID: 11444474]
- 62 **Schauber J**, Bark T, Jaramillo E, Katouli M, Sandstedt B, Svenberg T. Local short-chain fatty acids supplementation without beneficial effect on inflammation in excluded rectum. *Scand J Gastroenterol* 2000; **35**: 184-189 [PMID: 10720118]
- 63 **Caltabiano C**, Máximo FR, Spadari AP, da Conceição Miranda DD, Serra MM, Ribeiro ML, Martinez CA. 5-aminosalicylic acid (5-ASA) can reduce levels of oxidative DNA damage in cells of colonic mucosa with and without fecal stream. *Dig Dis Sci* 2011; **56**: 1037-1046 [PMID: 21042854 DOI: 10.1007/s10620-010-1378-z]
- 64 **Grisham MB**, Granger DN. Neutrophil-mediated mucosal injury. Role of reactive oxygen metabolites. *Dig Dis Sci* 1988; **33**: 6S-15S [PMID: 2831016]
- 65 **Agarwal VP**, Schimmel EM. Diversion colitis: a nutritional deficiency syndrome? *Nutr Rev* 1989; **47**: 257-261 [PMID: 2689929]
- 66 **de Oliveira-Neto JP**, de Aguilar-Nascimento JE. Intraluminal irrigation with fibers improves mucosal inflammation and atrophy in diversion colitis. *Nutrition* 2004; **20**: 197-199 [PMID: 14962686 DOI: 10.1016/j.nut.2003.10.006]
- 67 **van Nood E**, Vrieze A, Nieuwdorp M, Fuentes S, Zoetendal EG, de Vos WM, Visser CE, Kuijper EJ, Bartelsman JF, Tijssen JG, Speelman P, Dijkgraaf MG, Keller JJ. Duodenal infusion of donor feces for recurrent Clostridium difficile. *N Engl J Med* 2013; **368**: 407-415 [PMID: 23323867 DOI: 10.1056/NEJMoa1205037]
- 68 **Chang KY**, Wu CS, Chen PC. Prospective, randomized trial of hypertonic glucose water and sodium tetradecyl sulfate for gastric variceal bleeding in patients with advanced liver cirrhosis. *Endoscopy* 1996; **28**: 481-486 [PMID: 8886633 DOI: 10.1055/s-2007-1005527]
- 69 **Tian C**, Mehta P, Shen B. Endoscopic Therapy of Bleeding from Radiation Enteritis with Hypertonic Glucose Spray. *ACG Case Rep J* 2014; **1**: 181-183 [PMID: 26157869 DOI: 10.14309/crj.2014.45]

P- Reviewer: De Silva AP, Triantafillidis JK, Tandon RK
S- Editor: Wang XJ **L- Editor:** A **E- Editor:** Huang Y



Basic Study

Nonalcoholic steatohepatitis severity is defined by a failure in compensatory antioxidant capacity in the setting of mitochondrial dysfunction

Michelle L Boland, Stephanie Oldham, Brandon B Boland, Sarah Will, Jean-Martin Lapointe, Silvia Guionaud, Christopher J Rhodes, James L Trevaskis

Michelle L Boland, Stephanie Oldham, Brandon B Boland, Sarah Will, Christopher J Rhodes, James L Trevaskis, Cardiovascular and Metabolic Diseases, MedImmune LLC, Gaithersburg, MD 20878, United States

Jean-Martin Lapointe, Pathology, MedImmune Ltd., Cambridge CB21 6GH, United Kingdom

Silvia Guionaud, Pathology, Drug Safety and Metabolism, IMED Biotech Unit, AstraZeneca, Cambridge CB22 3AT, United Kingdom

ORCID number: Michelle L Boland (0000-0002-9920-2088); Stephanie Oldham (0000-0002-0295-1921); Brandon B Boland (0000-0003-1280-9547); Sarah Will (0000-0001-9408-9234); Jean-Martin Lapointe (0000-0003-0141-4603); Silvia Guionaud (0000-0003-1929-6094); Christopher J Rhodes (0000-0002-4852-516X); James L Trevaskis (0000-0002-5356-6118).

Author contributions: Boland ML and Trevaskis JL conceived of the project; Boland ML, Rhodes CJ and Trevaskis JL designed and interpreted experiments; Boland ML, Oldham S, Boland BB, Will S, Lapointe JM and Guionaud S acquired and analyzed data; Boland ML, Boland BB, Rhodes CJ and Trevaskis JL wrote and edited the manuscript.

Supported by MedImmune.

Institutional animal care and use committee statement: All animal experiments were conducted in accordance with policies of the NIH Guide for the Care and Use of Laboratory Animals and the Institutional Animal Care and Use Committee (IACUC) of MedImmune, LLC. Specific protocols used in this study were approved by the MedImmune IACUC, protocol number MI-16-0034.

Conflict-of-interest statement: All authors are current employees and/or stockholders of MedImmune/AstraZeneca.

ARRIVE guidelines statement: The authors have read the ARRIVE guidelines, and the manuscript was prepared and

revised according to the ARRIVE guidelines

Open-Access: This article is an open-access article which was selected by an in-house editor and fully peer-reviewed by external reviewers. It is distributed in accordance with the Creative Commons Attribution Non Commercial (CC BY-NC 4.0) license, which permits others to distribute, remix, adapt, build upon this work non-commercially, and license their derivative works on different terms, provided the original work is properly cited and the use is non-commercial. See: <http://creativecommons.org/licenses/by-nc/4.0/>

Manuscript source: Unsolicited manuscript

Correspondence to: James L Trevaskis, PhD, Principal Scientist, Cardiovascular and Metabolic Diseases, MedImmune, LLC, Gaithersburg, MD 20878, United States. trevaskisj@medimmune.com

Telephone: +1-301-3986695

Received: January 17, 2018

Peer-review started: January 17, 2018

First decision: February 11, 2018

Revised: February 22, 2018

Accepted: February 26, 2018

Article in press: February 25, 2018

Published online: April 28, 2018

Abstract

AIM

To comprehensively evaluate mitochondrial (dys) function in preclinical models of nonalcoholic steatohepatitis (NASH).

METHODS

We utilized two readily available mouse models of nonalcoholic fatty liver disease (NAFLD) with or without

progressive fibrosis: *Lep^{ob}/Lep^{ob}* (*ob/ob*) and FATZO mice on high *trans*-fat, high fructose and high cholesterol (AMLN) diet. Presence of NASH was assessed using immunohistochemical and pathological techniques, and gene expression profiling. Morphological features of mitochondria were assessed *via* transmission electron microscopy and immunofluorescence, and function was assessed by measuring oxidative capacity in primary hepatocytes, and respiratory control and proton leak in isolated mitochondria. Oxidative stress was measured by assessing activity and/or expression levels of *Nrf1*, *Sod1*, *Sod2*, catalase and 8-OHdG.

RESULTS

When challenged with AMLN diet for 12 wk, *ob/ob* and FATZO mice developed steatohepatitis in the presence of obesity and hyperinsulinemia. NASH development was associated with hepatic mitochondrial abnormalities, similar to those previously observed in humans, including mitochondrial accumulation and increased proton leak. AMLN diet also resulted in increased numbers of fragmented mitochondria in both strains of mice. Despite similar mitochondrial phenotypes, we found that *ob/ob* mice developed more advanced hepatic fibrosis. Activity of superoxide dismutase (SOD) was increased in *ob/ob* AMLN mice, whereas FATZO mice displayed increased catalase activity, irrespective of diet. Furthermore, 8-OHdG, a marker of oxidative DNA damage, was significantly increased in *ob/ob* AMLN mice compared to FATZO AMLN mice. Therefore, antioxidant capacity reflected as the ratio of catalase:SOD activity was similar between FATZO and C57BL6J control mice, but significantly perturbed in *ob/ob* mice.

CONCLUSION

Oxidative stress, and/or the capacity to compensate for increased oxidative stress, in the setting of mitochondrial dysfunction, is a key factor for development of hepatic injury and fibrosis in these mouse models.

Key words: Nonalcoholic steatohepatitis; Steatosis; Fibrosis; Mitochondrial function; Oxidative stress

© The Author(s) 2018. Published by Baishideng Publishing Group Inc. All rights reserved.

Core tip: *ob/ob* and FATZO mice developed nonalcoholic fatty liver disease/nonalcoholic steatohepatitis (NASH) when fed a high *trans*-fat, high fructose and high cholesterol diet, in the context of obesity and insulin resistance, but showed differences in liver disease severity including collagen deposition and monocyte/macrophage infiltration. Mitochondrial dysfunction and increased numbers of mitochondria were observed in both models, similar to that reported in human NASH. Oxidative damage and antioxidant capacity were associated with disease severity. FATZO mice displayed increased catalase activity and reduced oxidative DNA damage compared to *ob/ob* mice, which may explain their lower disease burden.

Boland ML, Oldham S, Boland BB, Will S, Lapointe JM, Guionaud S, Rhodes CJ, Trevaskis JL. Nonalcoholic steatohepatitis severity is defined by a failure in compensatory antioxidant capacity in the setting of mitochondrial dysfunction. *World J Gastroenterol* 2018; 24(16): 1748-1765 Available from: URL: <http://www.wjgnet.com/1007-9327/full/v24/i16/1748.htm> DOI: <http://dx.doi.org/10.3748/wjg.v24.i16.1748>

INTRODUCTION

Non-alcoholic fatty liver disease (NAFLD), now the most common liver disease, encompasses a spectrum of disorders from benign simple fatty liver to the more severe non-alcoholic steatohepatitis (NASH) that can progress to liver cirrhosis and hepatocellular carcinoma. Given the strong association of NAFLD with obesity, type II diabetes and other aspects of the metabolic syndrome, the current estimated NAFLD prevalence of 20%-40% worldwide is expected to increase^[1-3]. While no FDA-approved pharmacotherapies for NAFLD/NASH currently exist, more than 100 clinical trials are now targeting this highly significant unmet medical need.

Insulin resistance is a major pathophysiological factor that underlies the strong association between obesity/type II diabetes and NAFLD. Increased circulating free fatty acids and *de novo* lipogenesis lead to excess lipid storage in the hepatocyte, and accumulation of intrahepatic lipid is linked to pathogenic insulin resistance and subsequent onset of type 2 diabetes. This lipid overload also places a unique burden on the mitochondria and promotes mitochondrial dysfunction *in vitro* and in animal models. Data from multiple studies suggest that while TCA cycle activity is increased in NAFLD, mitochondrial respiratory chain inefficiencies lead to increased generation of reactive oxygen species (ROS) and lipotoxic intermediates that further promote oxidative damage and inflammation^[4-7]. Importantly, while increased hepatic mitochondrial respiration was observed in obese patients with and without fatty liver, this increase was lost in obese patients with NASH and was associated with increased mitochondrial content, proton leakage and oxidative stress^[8].

While dysregulated mitochondrial metabolism has been implicated in NALFD pathogenesis and progression, the specific contribution to disease etiology remains an active area of investigation^[9,10]. Multiple lines of evidence suggest that therapeutically targeting the mechanisms leading to mitochondrial dysfunction may improve liver disease^[10,11]. The use of pre-clinical models that mimic human pathology in the context of known risk factors, including obesity and insulin resistance, are necessary to understand the clinical translatability of pharmacological interventions given the difficulty of studying humans with a slow progressing disease that cannot be confirmed non-invasively^[12].

Hepatic mitochondrial function and oxidative stress in metabolically-relevant, pre-clinical models of simple fatty liver vs NASH have not been fully assessed. Here,

two pre-clinical mouse models of simple steatosis and NASH were investigated: *ob/ob* mice on NASH-inducing AMLN diet^[13], and the recently described polygenic FATZO mouse which develops high-fat diet-induced obesity and impaired glucose tolerance and which retains an intact leptin axis^[14,15]. Importantly, these models are readily available and rapidly and consistently develop clinically relevant disease. We characterized the contribution of mitochondria and oxidative stress to disease phenotype and demonstrate that a reduced ability to combat oxidative stress in the setting of mitochondrial dysfunction is associated with the progression to NASH with advanced fibrosis. These data highlight the utility of these models to dissect the underlying pathobiology of NAFLD disease progression and to predict pharmacological efficacy.

MATERIALS AND METHODS

Animals

Animal studies were conducted in accordance with protocols approved by the Institutional Animal Care and Use Committee (IACUC) at MedImmune and in compliance with the applicable national laws and regulations concerning use of laboratory animals and the AstraZeneca Animal Welfare and Bioethics policies. Eight-week old male C57BL6J or *Lep^{ob}/Lep^{ob}* (*ob/ob*) mice (Jackson labs, Bar Harbor, ME, United States) and 8-week-old male FATZO mice (Crown Bioscience, Indianapolis, IN, United States) were housed in standard caging at 22 °C in a 12-h light: 12-h dark cycle at standard temperature and humidity conditions with *ad libitum* access to water and food. Mice were maintained on test diets for 12 wk. The following test diets were used: 2018 Tekland rodent diet (Envigo, United States), low-fat diet (LFD; 10% kcal/fat; D09100304, Research Diets, New Brunswick, NJ, United States) and the Amylin Liver NASH (AMLN) diet high in fat (40% kcal), fructose (22% by weight), and cholesterol (2% by weight) (D09100301 Research Diets). Study groups comprised C57BL6J chow fed (lean) mice ($n = 6$), *ob/ob* mice on LFD ($n = 8$) and *ob/ob* mice on AMLN diet ($n = 10$), or C57BL6J lean mice, FATZO mice on LFD, or FATZO mice on AMLN diet (all $n = 5$ per group).

Measurement of plasma ALT

Terminal blood was collected in EDTA-coated tubes and centrifuged at 10000 $\times g$ for 10 min. The plasma was collected and analyzed for ALT levels using a biochemistry analyzer (Cobas c-111, Roche Diagnostics, Indianapolis, IN, United States).

Liver lipid quantification

Total lipids were measured in liver samples using a Bruker LF-90 minispec system (Bruker Biospin Corporation, Billerica, MA, United States). The data are expressed as the percent lipid relative to the total tissue mass.

Plasma insulin and pancreatic insulin content

To isolate pancreatic insulin, the tissue was incubated in a 1.5% HCl/70% EtOH solution overnight at -20 °C. The tissue was homogenized and frozen again overnight at -20 °C. Following centrifugation at 2000 rpm for 15 min, the aqueous layer was transferred to a new tube and neutralized upon the addition of 1 mol/L Tris, pH 7.5 at a 1:1 ratio. Plasma and pancreatic insulin levels were measured via immunoassay (K152BZC, MesoScale Diagnostics, Rockville, MD, United States).

Histological analysis and quantification of liver tissue

Livers were fixed in 10% neutral buffered formalin for 24 h. Paraffin-embedded tissue sections were stained with hematoxylin and eosin using standard procedures. Histological assessments were conducted by a pathologist under blinded conditions. A modified scoring system, based on the Brunt and Kleiner NAFLD activity score, previously developed and validated to enable a more reproducible and semi-quantitative assessment of murine liver was used to quantify various parameters of liver phenotype^[16]. The following parameters were graded to generate the overall NASH score: macrovesicular steatosis (0: < 5%, 1: 5%-33%, 2: 34%-66%, 3: > 66%); ballooning degeneration (0 = absent, 1 = present); lobular inflammation (0 = no foci, 1 = rare foci, 2 = occasional foci, 3 = frequent foci); biliary hyperplasia (0 = none, 1 = mild, 2 = prominent); CD68 immunoreactivity (0 = normal, 1 = minimal increased, 2 = more than minimal increase).

Customized algorithms (Definiens, Munich, Germany) were applied to the liver sections to quantify macrosteatosis per liver area, total collagen area and number of CD68-positive cells. White spaces, non-native liver tissues, large blood vessels and bile ducts were excluded from the analyses.

Immunohistochemistry

Immunohistochemistry was performed using a Ventana Discovery ULTRA Staining Module (Ventana Medical Systems, Tucson, AZ, United States). Formalin-fixed, paraffin embedded liver sections were stained with anti-CD68 (ab125212 Abcam, Cambridge, MA, United States), anti-collagen type 1 A1 (1310-01 Southern Biotech, Birmingham, AL, United States), or anti-catalase (PA5-29183, ThermoFisher).

Transmission electron microscopy

Freshly isolated liver was chemically fixed in 0.1 mol/L cacodylate buffer containing 4% paraformaldehyde and 2% glutaraldehyde. Samples were resin-embedded, sectioned, and stained as previously described^[17]. Samples were imaged using the FEI Tecnai G2 SPIRIT electron microscope equipped with a CCD camera (Pleasanton, CA, United States) at 120000 V. Images were acquired using GATAN digital micrograph software (Warrendale, PA, United States). Electron micrographs

were viewed in a blinded fashion using 3Dmod software^[18] on a Wacom Cintiq 22HD art tablet (Vancouver, WA, United States). Mitochondrial area and number were quantified per total cytoplasmic area from ≥ 10 electron micrographs per group *via* manual tracing using the art tablet as previously described (N ≥ 3 biological replicates, $\geq 1.5 \text{ mm}^2$ total cytoplasmic area)^[19].

Immunofluorescence

FFPE liver sections were deparaffinized followed by blocking of endogenous peroxidases. Antigen retrieval was carried out by heating samples at 119 °C for 6.5 min in citrate buffer solution (Dako Target Retrieval Solution, Agilent Technologies, Santa Clara, CA, United States). After blocking with 1.5% horse serum, slides were incubated overnight in anti-HSP60 (D6F1, Cell Signaling Technology, Danvers, MA, United States) in Dako antibody diluent (S3022, Agilent Technologies). Secondary antibody incubation with goat anti-rabbit Alexa 488 (ThermoFisher) was carried out at room temperature for 1 h. Slides were mounted using Prolong Gold plus DAPI (ThermoFisher). Slides were imaged using a Leica TCS SP5 X confocal microscope. Confocal images were viewed in a blinded fashion using 3Dmod software on a Wacom Cintiq 22HD art tablet (Vancouver, WA, United States). Mitochondrial length and number per total cytoplasmic area were quantified from ≥ 15 images per group ($n \geq 3$ biological replicates) *via* manual tracing of cell boundaries, nuclei, lipid droplets and mitochondria. Total cytoplasmic area was calculated as area within the cell boundary minus the nuclei and lipid droplet areas.

Primary hepatocyte isolation

Murine primary hepatocytes were isolated using a modified two-step non-recirculating perfusion method as previously described^[20]. All assays were carried out within 18-24 h post-plating.

Mitochondrial oxygen consumption

Mitochondrial oxygen consumption was measured using the Seahorse Xfe96 analyzer (Agilent Technologies). Primary hepatocytes were plated at a density of 7500 cells per well and allowed to recover overnight. The medium was exchanged (DMEM containing 5 mmol/L glucose, 4 mmol/L L-glutamine, 2 mmol/L sodium pyruvate, pH 7.4) and the plate was placed in a CO₂-free incubator for 30 min prior to being placed in the analyzer. The following compounds were used in the mitochondrial stress test: 1 μmol/L oligomycin (Sigma, St Louis, MO, United States), 0.5 μmol/L FCCP (Sigma), and 5 μmol/L antimycin A (Sigma). The data represent the average of three independent experiments each with a minimum of 8 replicates per group.

Mitochondrial coupling and proton leak

The respiratory control ratio (RCR) and leak control ratio (LCR) were quantified using freshly isolated hepatic mitochondria as an index of mitochondrial coupling and

proton leak, respectively^[8]. Briefly, 5 μg of mitochondria were loaded per well of the seahorse plate in assay medium (70 mmol/L sucrose, 220 mmol/L mannitol, 10 mmol/L KH₂PO₄, 5 mmol/L MgCl₂, 2 mmol/L HEPES, 1 mmol/L EGTA, 0.2% (w/v) fatty acid-free BSA, pH 7.2 supplemented with complex II substrate succinate at 10 mmol/L). The following injections were performed: 4 mmol/L ADP (state 3), 1 μmol/L oligomycin (state 3_o), 1 μmol/L FCCP (state 3_u) and 4 μmol/L antimycin A/ 2 μmol/L rotenone. RCR is represented by the ratio of ADP-stimulated respiration (state 3) to respiration in the presence of oligomycin (state 3_o), and LCR is represented by the ratio of respiration in the presence of oligomycin (State 3_o) to FCCP-stimulated respiration (state 3_u).

Citrate synthase activity

Mitochondrial content was quantified by citrate synthase activity (CSA) of freshly isolated primary hepatocytes or liver mitochondria using the Citrate Synthase Activity Colorimetric Assay Kit (BioVision, Milpitas, CA, United States) according to the manufacturer's instructions and normalized to total protein assessed by the Pierce BCA protein assay kit (ThermoFisher).

Isolation of liver mitochondria

Excised liver was rinsed in several changes of PBS and homogenized in ice cold isolation buffer (70 mmol/L sucrose, 210 mmol/L mannitol, 5 mmol/L HEPES, 1 mmol/L EGTA, 0.5% w/v fatty acid-free BSA, pH 7.2) using a Wheaton™ Dounce Tissue Grinder (Fisher Scientific). After centrifugation at 800 $\times g$ for 10 min at 4 °C, the supernatants were collected and centrifuged at 8000 $\times g$ for 10 min at 4 °C. The resulting mitochondrial pellet was washed two times and resuspended in a minimal volume of isolation buffer. The isolated mitochondria were kept on ice until use. Protein concentration was determined using the Pierce BCA Protein Assay Kit (ThermoFisher).

RNA isolation and real-Time PCR

Total liver RNA and genomic DNA were isolated using standard procedures. Qiagen RNeasy® columns (Qiagen, United States) were used for RNA purification according to the manufacturer's protocol, including an on-column DNA digestion using DNaseI. Equal amounts of RNA were reverse transcribed to cDNA using SuperScript III First Strand cDNA synthesis kit (Invitrogen, Carlsbad, CA, United States) according to the manufacturer's instructions. Real-Time PCR was performed on a QuantStudio-7 Flex System (Applied Biosystems, Foster City, CA, United States) using Applied Biosystems TaqMan Fast Universal PCR Master Mix and TaqMan probes. Each sample was assayed in triplicate and quantified using the ΔΔCT method normalized to endogenous control *Ppia* (mRNA) or nuclear encoded gene β-globin (gDNA). The following Taqman probes were used in qPCR assays: collagen type 1 alpha 1 (Col1a1, Mm00801666_g1), collagen type 1 alpha 2

(Col1a2, Mm00483888_m1), TIMP metallopeptidase inhibitor 1 (Timp1, Mm01341361_m1), interleukin 1 beta (Il1b, Mm00434228_m1), cluster of differentiation 68 (Cd68, Mm03047343_m1), tumor necrosis factor alpha (Tnf, Mm00443258_m1), PPARG coactivator 1 alpha (Ppargc1a, Mm01208835_m1), nuclear respiratory factor 1 (Nrf1, Mm01135606_m1), transcription factor A, mitochondrial (Tfam, Mm00447485_m1), superoxide dismutase 1, soluble (Sod1, Mm1344233_g1), superoxide dismutase 2, mitochondrial (Sod2, Mm01313000_m1), catalase (Cat, Mm00437992_m1), glutathione peroxidase (Gpx1, Mm00656767_g1), and peptidylprolyl isomerase A (Ppia, Mm02342430_g1).

Oxidative stress assays

Superoxide dismutase activity (7501-500-K, Trevigen, Gaithersburg, MD, United States) and catalase activity (707002, Cayman Chemical, Ann Arbor, MI, United States) were measured in freshly prepared liver homogenates according to the manufacturer's protocols. The levels of 8-hydroxydeoxyguanosine (8-OHdG) were measured via ELISA using approximately 20 µg of total hepatic genomic DNA (4380-096-K, Trevigen).

Statistical analysis

All statistical analyses were carried out using GraphPad Prism 7 (GraphPad Software, San Diego, CA, United States). The data were analyzed via one-way or two-way ANOVA and Tukey's post-test. Data are shown as the mean ± SE. Values of $P \leq 0.05$ were considered significant.

RESULTS

Ob/ob mice develop NASH with fibrosis in the setting of obesity and insulin resistance

NASH induction was assessed in *ob/ob* mice, a proposed NASH model when challenged with AMLN diet. C57BL6J mice served as healthy age-matched controls (lean) and were compared to *ob/ob* mice maintained on LFD (*ob/ob* LFD) or AMLN diet (*ob/ob* AMLN) for 12 wk. After the 12-wk disease induction period, *ob/ob* LFD and *ob/ob* AMLN mice weighed significantly more than lean controls ($P < 0.0001$), but did not significantly differ from one another (Figure 1A). While non-fasting blood glucose was slightly reduced in *ob/ob* AMLN animals compared to lean controls (132 mg/dL vs 186 mg/dL, $P < 0.05$; Figure 1B), plasma insulin levels ($P < 0.05$; Figure 1C) and pancreatic insulin content ($P < 0.01$; Figure 1D) were concomitantly increased.

We measured markers associated with NAFLD including liver weight, liver lipid, and plasma alanine aminotransferase (ALT). Liver weight was significantly greater in *ob/ob* LFD vs lean animals (8.6% vs 4.5%, $P < 0.0001$), and was further increased in *ob/ob* AMLN animals (12.7%, $P < 0.0001$; Figure 2A). Similarly, *ob/ob* AMLN livers contained approximately 34% intrahepatic lipid, which was significantly greater than livers from *ob/ob* LFD (25% lipid, $P < 0.0001$) and lean animals

(5% lipid, $P < 0.0001$; Figure 2B). Plasma ALT was also significantly increased in *ob/ob* LFD vs lean animals (771 U/L vs 160 U/L, $P < 0.0001$) and was further elevated in *ob/ob* AMLN animals (1160 U/L, $P < 0.001$ vs *ob/ob* LFD; Figure 2C).

Macrovesicular steatosis was prominent in both *ob/ob* LFD (60%) and *ob/ob* AMLN animals (67%, $P < 0.001$ vs *ob/ob* LFD; Figure 2D). Hepatic fibrosis assessed by quantification of type 1 collagen stained area was significantly greater in *ob/ob* LFD vs lean livers ($P < 0.01$) and even greater in *ob/ob* AMLN liver ($P < 0.0001$ vs *ob/ob* LFD) (Figure 2E). Immunolabeling with the monocyte/macrophage marker CD68 was also markedly elevated in *ob/ob* AMLN livers compared to *ob/ob* LFD and lean controls ($P < 0.0001$ vs *ob/ob* LFD; Figure 2F).

We analyzed hepatic transcript levels of genes involved in fibrosis and inflammation that differentiate the more benign disease observed in *ob/ob* LFD liver histopathology from the steatohepatitis observed in *ob/ob* AMLN livers. Transcripts encoding the most abundant form of liver collagen, type 1 (*Col1a1* and *Col1a2*), in addition to type 3 collagen (*Col3a1*) were significantly elevated in *ob/ob* AMLN livers vs lean and *ob/ob* LFD livers ($P < 0.001$, $P < 0.01$, $P < 0.0001$, respectively, vs *ob/ob* LFD; Figure 2G). *Timp1*, another gene associated with increased extracellular matrix turnover, was significantly elevated in *ob/ob* AMLN compared to *ob/ob* LFD and lean livers ($P < 0.001$ vs *ob/ob* LFD; Figure 2G). The expression of cytokines including *Tgfb*, *Tnf*, *Il1b*, and *Il10*, and chemokines including *Ccl2*, *Ccl3*, and *Ccl11* were similarly upregulated in *ob/ob* AMLN livers compared to *ob/ob* LFD and lean controls ($P < 0.01$, $P < 0.05$, $P = 0.2$; $P < 0.01$, $P < 0.001$, $P < 0.01$, respectively, vs *ob/ob* LFD; Figure 2H). Additionally, *Lgals3*, a marker associated with multiple inflammatory cell types and thought to contribute to fibrogenesis, was highly expressed in the livers of *ob/ob* AMLN but not lean or *ob/ob* LFD mice (30-fold induction vs lean controls, $P < 0.001$ vs *ob/ob* LFD; Figure 2H).

The steatosis grade was significantly higher in *ob/ob* LFD (grade 2.5, $P < 0.0001$) and *ob/ob* AMLN (grade 3, $P < 0.0001$) compared to lean livers (grade 0; Figure 3A). A significant increase in the number of inflammatory foci (Figure 3B), biliary hyperplasia (Figure 3C) and CD68-positive cells (Figure 3D) was observed in *ob/ob* AMLN vs lean ($P < 0.0001$) and *ob/ob* LFD livers ($P < 0.0001$). Ballooned hepatocytes were only observed in *ob/ob* AMLN livers (Figure 3E). An integrated NASH score was generated by combining the grades of steatosis, inflammation, biliary hyperplasia, CD68 positive cells, and ballooning degeneration (Figure 3F), which reflected the clear distinction between *ob/ob* LFD and *ob/ob* AMLN liver histopathology.

Fragmented mitochondria in *ob/ob* AMLN hepatocytes

We examined mitochondrial ultrastructure in livers from lean, *ob/ob* LFD and *ob/ob* AMLN mice by transmission

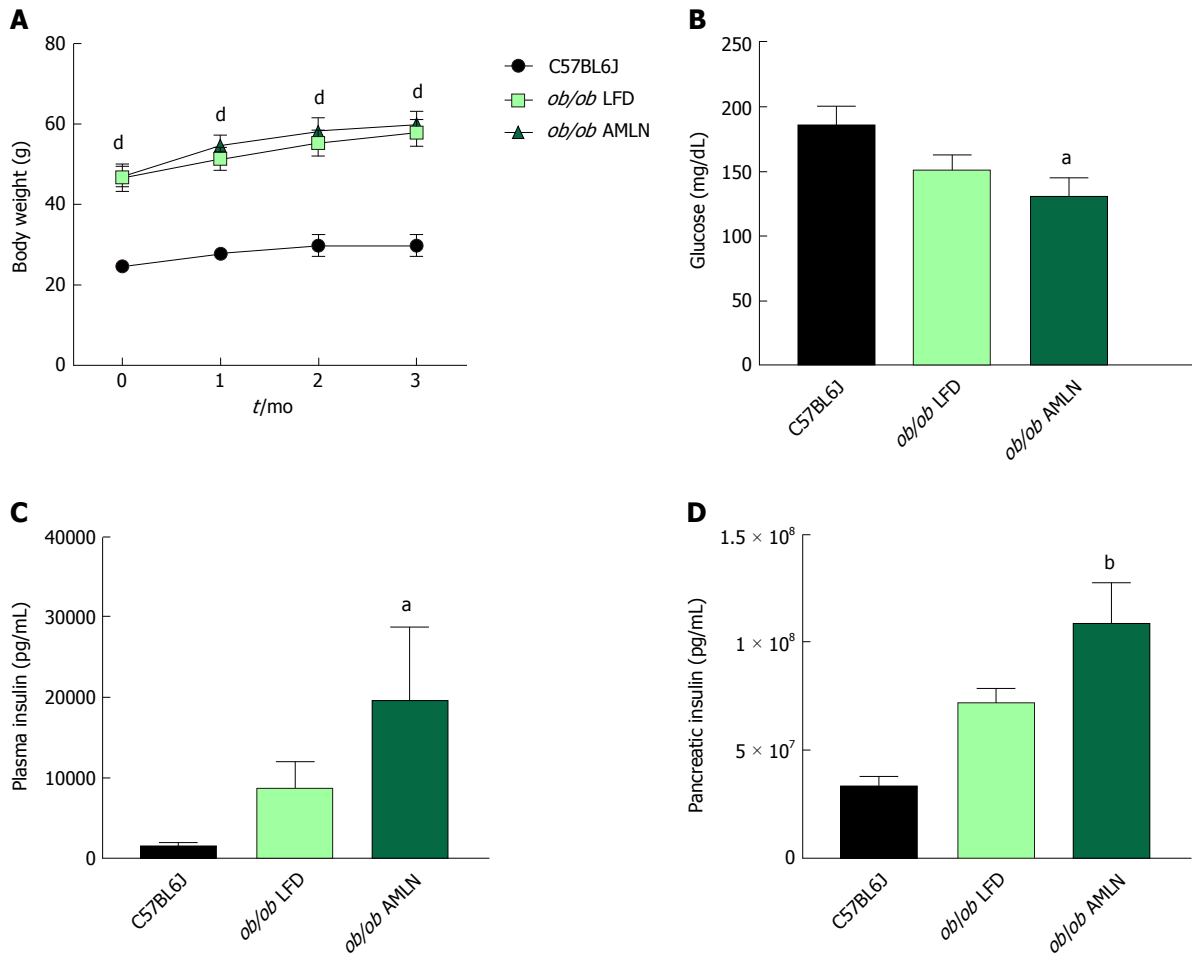


Figure 1 Obese *ob/ob* mice display increased hyperinsulinemia on AMLN diet. (A): Average body weight over 12-wk disease induction period; (B): Terminal non-fasting blood glucose levels; (C): Terminal non-fasting plasma insulin levels; (D): Pancreatic insulin content. ^a*P* ≤ 0.05, ^b*P* ≤ 0.01, ^d*P* ≤ 0.0001 vs C57BL6J. LFD: Low-fat diet.

electron microscopy (TEM; Figure 4A). Quantitative assessment of TEM images showed *ob/ob* AMLN hepatocytes had increased numbers of mitochondria (approximately 1.5-fold, *P* < 0.001 vs *ob/ob* LFD; Figure 4B). While lean and *ob/ob* LFD hepatocytes contained a mixture of elongated and fragmented mitochondria, *ob/ob* AMLN hepatocytes contained smaller, more fragmented mitochondria (average area = 70 μm^2 for lean controls vs 45 μm^2 for *ob/ob* AMLN, *P* < 0.01; Figure 4C); however, no overt defects in outer membrane integrity or cristae formation were observed. Similarly, quantification of mitochondrial length and number from HSP60 immunostained liver sections revealed increased numbers of mitochondria overall in *ob/ob* AMLN livers (*P* < 0.005 vs lean controls; Figure 4D) and a significant increase in shorter, more fragmented mitochondria (Figure 4E). Citrate synthase activity (CSA), another measure of mitochondrial content, was increased over 2-fold in primary hepatocytes isolated from *ob/ob* AMLN mice vs lean controls (*P* < 0.05; Figure 4F). In line with smaller mitochondria in *ob/ob* AMLN hepatocytes, the expression of proteins required for mitochondrial fusion, mitofusin 1 (*Mfn1*) and dynamin-like 120 kDa protein, mitochondrial (*Opa1*), was significantly decreased in *ob/ob* AMLN livers compared to lean controls (*P* < 0.01 and *P* < 0.05, respectively; Supplementary Figure 4G).

To assess whether this increase in mitochondrial number was due to increased biogenesis, we quantified the expression of transcription factors required for mitochondrial biogenesis and components of the electron transport chain (ETC). While the expression of PPARy-coactivator 1a (*Ppargc1a*) was slightly increased in *ob/ob* LFD livers (1.4-fold, *P* = 0.06 vs lean controls), it was unchanged in *ob/ob* AMLN vs lean livers (data not shown). Similarly, nuclear respiratory factor 1 (*Nrf1*) and mitochondrial transcription factor A (*Tfam*) mRNA levels were unchanged in *ob/ob* AMLN vs lean and *ob/ob* LFD livers (data not shown). Additionally, expression of mitochondrial autophagy genes *Bnip3*, *Park2* and *Pink1* was not different between groups (Figure 4G). Although *ob/ob* AMLN hepatocytes displayed increased mitochondrial number, they contained significantly less mitochondrial DNA (mtDNA) as assessed by the expression of mitochondrial-encoded genes *Cytb* and *Nd-1* relative to the expression of nuclear encoded β -globin (approximately 30% reduction, *P* < 0.05 vs lean controls; Supplementary Figure 4H).

Hepatic *ob/ob* AMLN mitochondria have reduced respiratory capacity and increased proton leak

To assess mitochondrial function, oxygen consumption of intact primary hepatocytes from lean, *ob/ob* LFD

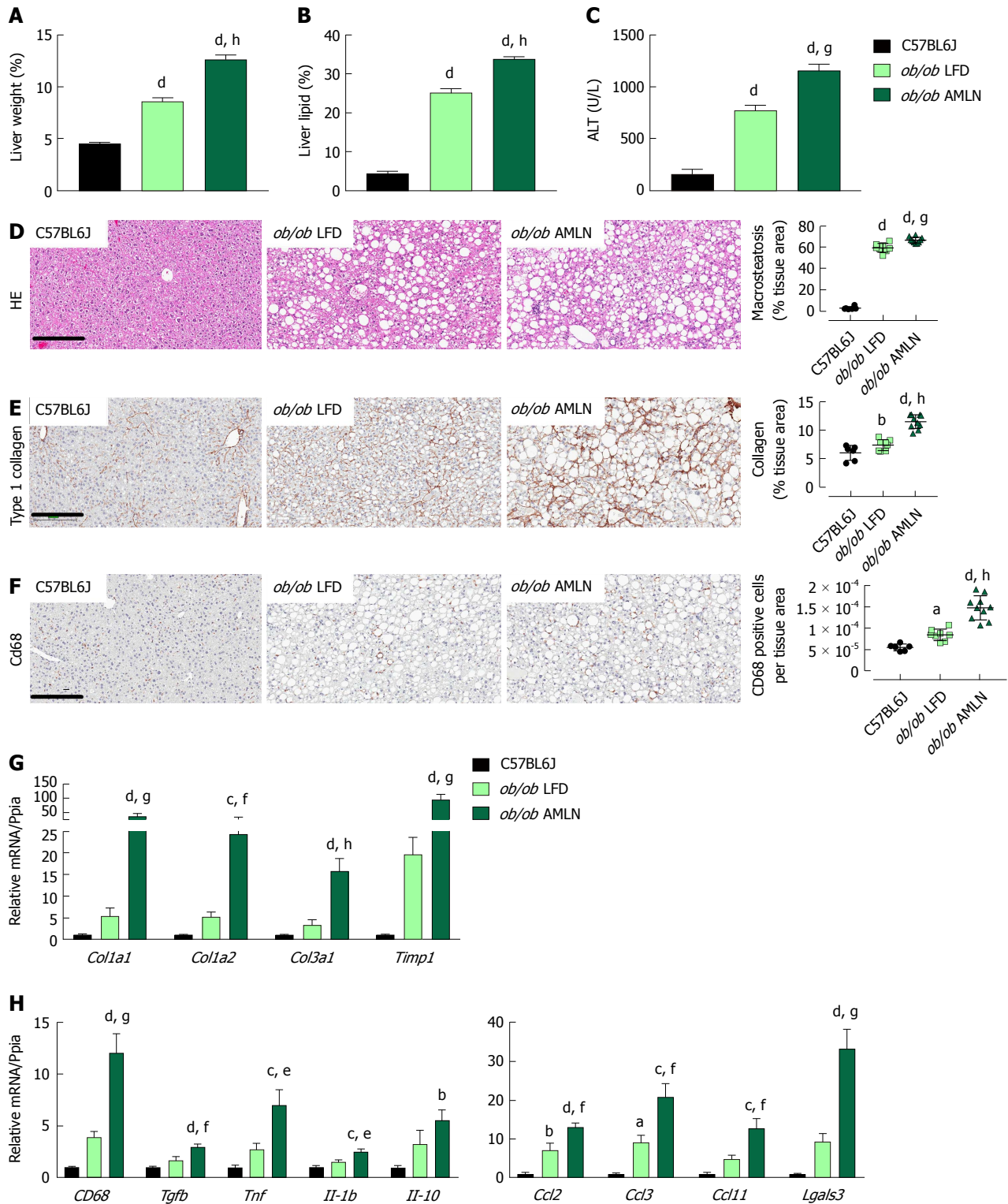


Figure 2 Comparison of metabolic and hepatic abnormalities associated with diet-induced nonalcoholic fatty liver disease/nonalcoholic steatohepatitis in ob/ob mice. Liver weight (A), liver lipid (B), and plasma alanine aminotransferase (ALT) levels (C) of lean (C57BL6J) and ob/ob mice maintained on control low-fat diet (ob/ob LFD) or AMLN diet (ob/ob AMLN) for 12 wk; (D): Representative hematoxylin and eosin stained liver sections and quantification of percentage of liver area containing macrosteatosis; (E): Representative collagen type 1 alpha 1 stained liver sections and quantification of collagen area. Scale bar = 200 μ m; (F): Representative CD68-stained liver sections and quantification of CD68-positive cells; G, H: Relative expression of genes associated with fibrosis and inflammation. $^aP \leq 0.05$, $^bP \leq 0.01$, $^cP \leq 0.001$, $^dP \leq 0.0001$ vs C57BL6J; $^eP \leq 0.05$, $^fP \leq 0.01$, $^gP \leq 0.001$, $^hP \leq 0.0001$ vs LFD. LFD: Low-fat diet.

and ob/ob AMLN animals was measured (Figure 5A). ob/ob AMLN hepatocytes displayed significantly reduced basal respiration that was approximately

50% lower compared to lean ($P < 0.01$) and ob/ob LFD hepatocytes ($P < 0.05$) (Figure 5B). Maximal mitochondrial respiratory capacity was significantly

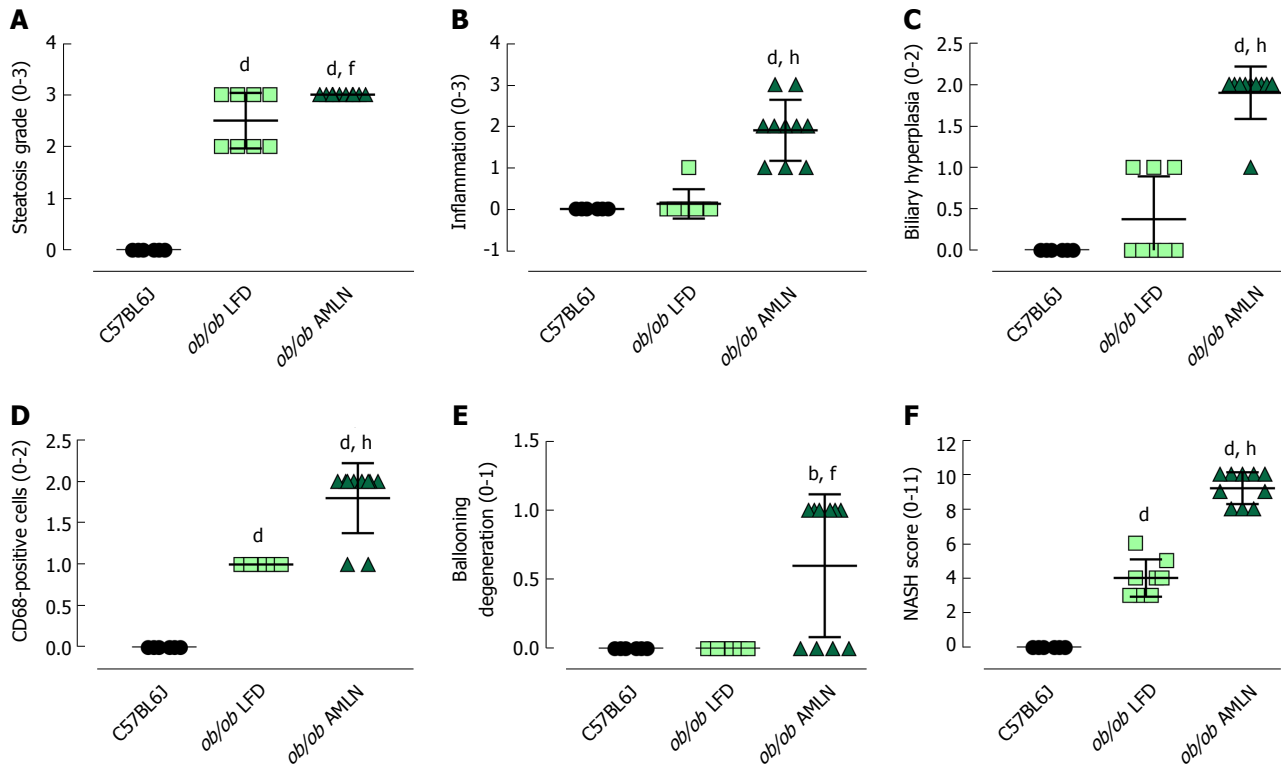


Figure 3 Histopathological grading of C57BL6J, ob/ob low-fat diet and ob/ob AMLN liver. Individual grades of steatosis (A), inflammation (B), biliary hyperplasia (C), CD68-positive cells (D) and ballooning degeneration (E) are shown; (F): Comparison of the total NASH scores representing the sum of all histologic parameters. ^a $P \leq 0.01$, ^b $P \leq 0.0001$ vs C57BL6J; ^c $P \leq 0.01$, ^d $P \leq 0.0001$ vs LFD. LFD: Low-fat diet.

increased in ob/ob LFD compared to lean hepatocytes (+45%, $P < 0.05$; Figure 5B). In contrast, ob/ob AMLN hepatocytes displayed significantly reduced maximal respiration compared to lean (-45%, $P < 0.05$) and ob/ob LFD hepatocytes (-60%, $P < 0.001$; Figure 5B).

We also assessed mitochondrial coupling and proton leak. The mitochondrial respiratory control ratio (RCR) and leak control ratio (LCR) were quantified using isolated mitochondria from lean, ob/ob LFD and ob/ob AMLN livers. Mitochondria from ob/ob mouse liver displayed slightly increased proton leak without a significant decrease in respiratory control^[21], and AMLN diet further increased proton leak and reduced RCR. Mitochondrial coupling was decreased in ob/ob AMLN mice compared to mitochondria from lean mice (4.2 vs 5.6; Figure 5C), although this difference did not reach statistical significance. ob/ob AMLN mitochondria also displayed a higher LCR compared to lean controls (0.35 vs 0.23, $P = 0.06$; Figure 5D), indicating increased proton leak.

FATZO mice fed AMLN diet display enhanced microvesicular steatosis and lobular inflammation but minimal fibrosis

While the ob/ob mouse exhibits key aspects of human metabolic disease and, importantly, develops diet-induced NASH with consistent grade 2-3 fibrosis, most humans with NAFLD/NASH are likely hyperleptinemic as opposed to leptin-deficient. We therefore investigated the FATZO mouse, an inbred polygenic cross of AKR/J

and C57BL6J strains with a predisposition to obesity and insulin resistance, but intact leptin axis^[14,15].

After 12 wk on diet, FATZO mice fed LFD (FATZO LFD) weighed significantly more than lean (C57BL6J) controls (43 g vs 35 g, $P < 0.0001$), while FATZO mice fed AMLN diet (FATZO AMLN) weighed significantly more than both FATZO LFD and lean controls (50 g, $P < 0.001$ vs FATZO LFD; Figure 6A). Plasma glucose was slightly elevated in FATZO LFD (271 mg/dL) and FATZO AMLN mice (236 mg/dL) compared to lean controls (186 mg/dL; Figure 6B). FATZO AMLN mice displayed severe hyperinsulinemia with average plasma insulin levels that were significantly greater compared to FATZO LFD and lean controls ($P < 0.01$ for ob/ob AMLN vs lean controls; Figure 6C). Both FATZO LFD and FATZO AMLN mice had increased pancreatic insulin content, which was significantly greater in FATZO AMLN mice compared to lean controls (+50%, $P < 0.05$; Figure 6D).

Markers of liver disease including hepatomegaly, hepatic steatosis and elevated plasma ALT levels were present in both FATZO LFD and FATZO AMLN mice. Relative liver weight was significantly increased in FATZO LFD vs lean animals (7.3% vs 4.4%, $P < 0.0001$), and was further increased in FATZO AMLN animals (10.6%, $P < 0.001$ vs FATZO LFD) (Figure 7A). Similarly, hepatic lipid content was significantly greater in FATZO LFD compared to lean controls (20% vs 6%) and was greatest in FATZO AMLN mice (30%, $P < 0.0001$ vs FATZO LFD; Figure 7B). Plasma ALT was also significantly increased in FATZO LFD vs lean animals

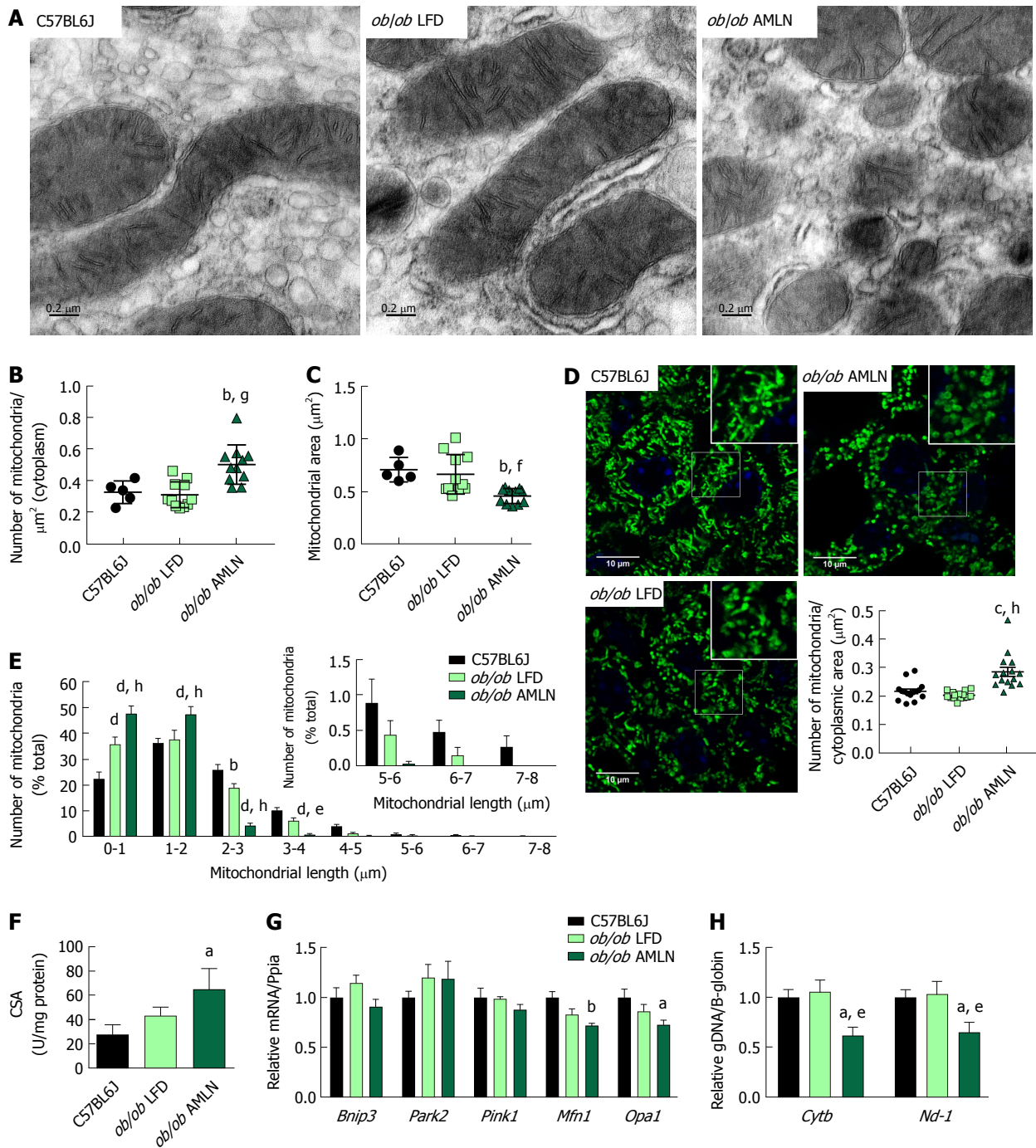


Figure 4 *ob/ob* AMLN hepatocytes display increased numbers of fragmented mitochondria. (A) Transmission electron micrographs (TEM) showing mitochondrial morphology and ultrastructure in the liver. Scale bar = 0.2 μm. Quantification of the number of mitochondria (B) and mitochondrial area (C) from TEM images; (D): Confocal images of HSP60 stained liver sections and quantification of mitochondrial number per cytoplasmic area. Scale bar = 10 μm; (E): Histogram depicting the number of mitochondria per binned mitochondrial length as a percentage of total mitochondria per cell; (F): Mitochondrial content measured by citrate synthase activity in isolated primary hepatocytes; (G): Relative hepatic expression of genes associated with mitophagy; (H): Quantification of mitochondrial genome-encoded *Cytb* or *Nd1* relative to nuclear-encoded β-globin from total genomic DNA extracted from the liver. ^a*P* ≤ 0.05, ^b*P* ≤ 0.01, vs C57BL6J; ^c*P* ≤ 0.05, ^d*P* ≤ 0.01, ^e*P* ≤ 0.001, ^f*P* ≤ 0.0001 vs LFD. LFD: Low-fat diet.

(260 U/L vs 50 U/L, $P < 0.0001$) and was further elevated in FATZO AMLN animals (370 U/L, $P < 0.01$ vs FATZO LFD; Figure 7C), but was nonetheless still much lower than levels observed in *ob/ob* AMLN mice (>1100 U/L, Figure 1C).

Assessment of HE-stained liver samples revealed the presence of prominent steatosis, both micro- and

macrovesicular, in both FATZO LFD and FATZO AMLN animals (Figure 7D). Increased macrophage/monocyte infiltration was also observed in FATZO LFD and FATZO AMLN mice (Figure 7E), paralleled by increased expression of hepatic *Cd68* (3.5-fold in FATZO LFD and 5.2-fold in FATZO AMLN; $P < 0.05$ FATZO LFD vs FATZO AMLN; Figure 7H). Mild collagen deposition was also

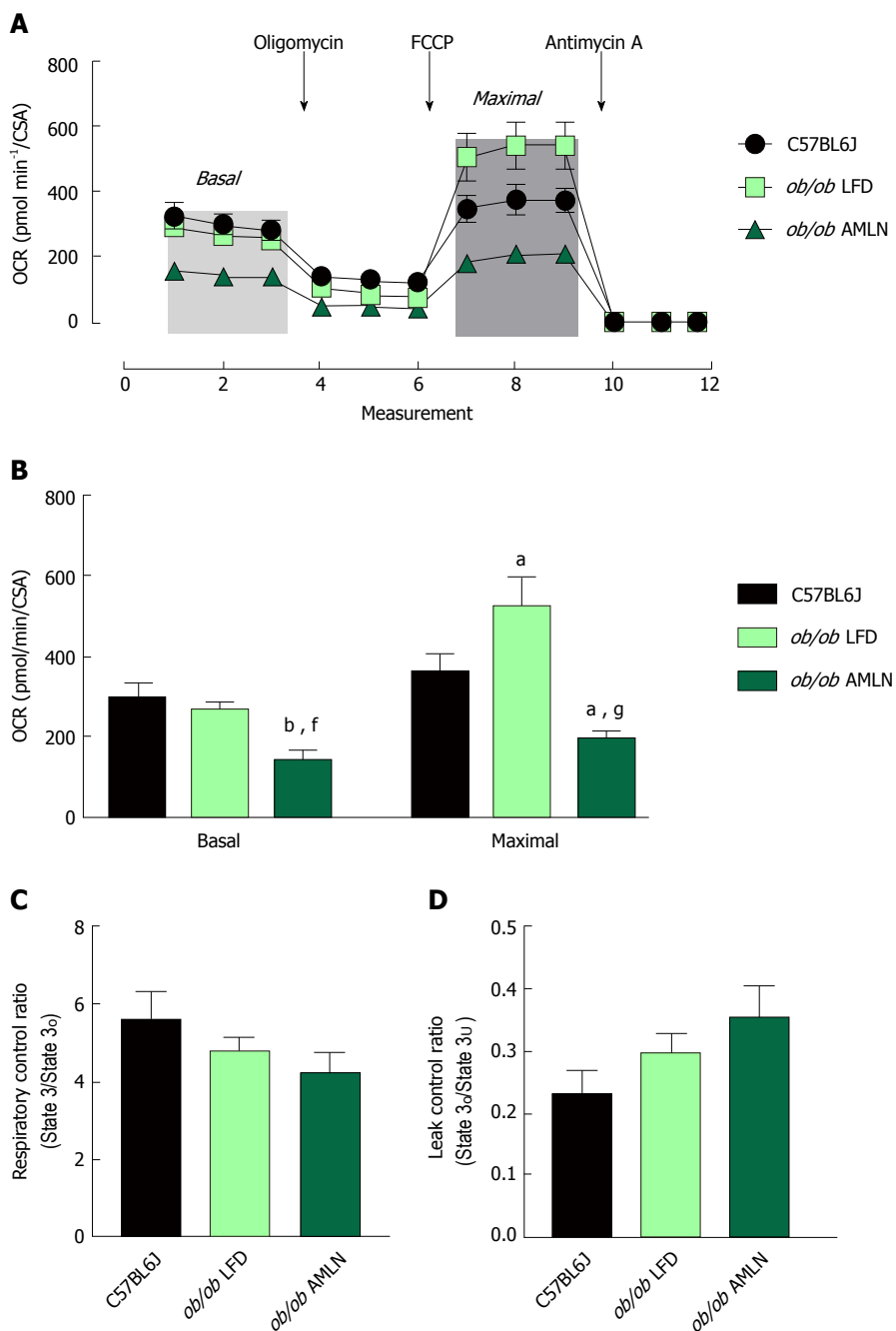


Figure 5 Mitochondria from *ob/ob* AMLN livers display reduced respiratory capacity and increased proton leak. (A) Oxygen consumption of primary hepatocytes isolated from C57BL6J, *ob/ob* LFD and *ob/ob* AMLN livers normalized to mitochondrial content (citrate synthase activity, CSA). Changes in mitochondrial respiration in response to oligomycin, FCCP and antimycin A are shown. Light grey box = basal respiration, dark grey box = maximal uncoupled respiration; (B) Quantification of baseline oxygen consumption (basal respiration) and FCCP-stimulated oxygen consumption (maximal respiration) normalized to CSA; (C) Mitochondrial respiratory control ratio, a measure of mitochondrial coupling, defined as state 3/ state 0 respiration of mitochondria isolated from the livers of C57BL6J, *ob/ob* LFD and *ob/ob* AMLN mice; (D) Mitochondrial leaking control ratio, a measure of proton leak, defined as state 0/ state 3_U respiration. ^aP ≤ 0.05, ^bP ≤ 0.01, vs C57BL6J; ^cP ≤ 0.01, ^dP ≤ 0.001, vs LFD. LFD: Low-fat diet.

apparent in FATZO animals but did not worsen upon AMLN diet feeding (Figure 7F).

Transcriptional profiling of genes involved in hepatic fibrosis and inflammation revealed additional evidence of active liver disease in FATZO mice. Collagens including *Col1a1*, *Col1a2* and *Col3a1* were increased in FATZO LFD livers compared to lean controls (approximately 6-8-fold for each), and were further induced in FATZO AMLN livers (Figure 7G). All

cytokines assayed including *Tgfb*, *Tnf*, *Il1b*, and *Il10*, and chemokines including *Ccl2*, *Ccl3*, and *Ccl11* were similarly upregulated in FATZO LFD livers compared to lean controls and even further induced in FATZO AMLN livers (Figure 7H). Additional fibrosis related genes *Timp1* and *Lgals3* were significantly elevated in FATZO LFD livers compared to lean controls, with even further induction observed in FATZO AMLN livers (Figure 7G, H). Integrated NASH scores generated from combining

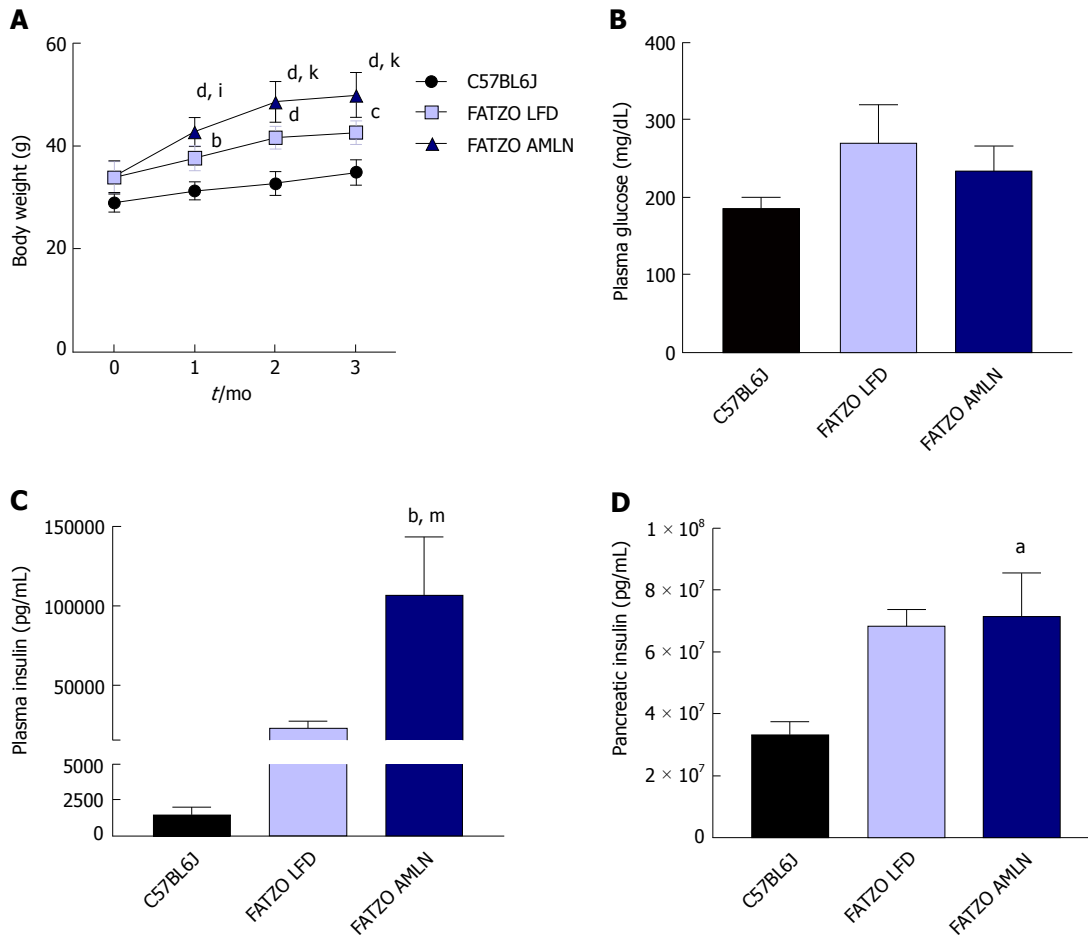


Figure 6 AMLN diet exacerbates obesity and hyperinsulinemia in FATZO mice. (A): Average body weight over 12-wk disease induction period; (B): Terminal non-fasting blood glucose levels; (C): Terminal non-fasting plasma insulin levels; (D): Pancreatic insulin content. ^a $P \leq 0.05$, ^b $P \leq 0.01$, ^c $P \leq 0.001$, ^d $P \leq 0.0001$ vs C57BL6J; ⁱ $P \leq 0.05$, ^k $P \leq 0.001$, FATZO LFD; ^m $P \leq 0.05$, FATZO AMLN unless noted otherwise. LFD: Low-fat diet.

grades of steatosis (Figure 8A), inflammation (Figure 8B), biliary hyperplasia (Figure 8C), CD68-positive cells (Figure 8D) and hepatocyte ballooning (Figure 8E) were significantly greater for FATZO LFD and FATZO AMLN mice compared to lean controls, but did not significantly differ from one another (Figure 8F).

Increased mitochondrial fragmentation in FATZO mice is associated with mild mitochondrial dysfunction

Similar to *ob/ob* mice, FATZO AMLN mice displayed significantly increased numbers of fragmented mitochondria (Figure 9A, B) and hepatic CSA (Figure 9C) compared to FATZO LFD and lean controls. In contrast, this increase was associated with a significant induction of mitochondrial biogenesis genes in FATZO mice. *Nrf1* was consistently induced in both FATZO LFD and FATZO AMLN livers compared to lean controls ($P < 0.01$ for FATZO LFD, $P < 0.0001$ for FATZO AMLN vs lean), *Ppargc1a* was significantly induced in FATZO LFD livers compared to lean controls (1.75-fold, $P < 0.001$) and *Tifam* was significantly induced in FATZO AMLN livers vs lean controls 1.4-fold, $P < 0.01$; Figure 9D). Additionally, decreased mitophagy may contribute to increased mitochondrial content, although only *Bnip3* expression was significantly reduced in FATZO LFD and

FATZO AMLN livers compared to lean controls (-40%, $P < 0.05$ for FATZO LFD, -25%, $P = 0.08$ for FATZO AMLN vs lean) with no changes observed in *Park2* or *Pink1* expression (Supplementary Figure 9E). No differences in the mitochondrial:nuclear DNA ratio were observed (Figure 9F), suggesting that mtDNA replication is occurring normally in contrast to that observed in the *ob/ob* AMLN model.

To assess hepatic mitochondrial function in the FATZO mice we measured mitochondrial coupling and proton leak in isolated mitochondria. While there was a trend for reduced RCR in FATZO AMLN mitochondria compared to lean controls, this reduction was small and did not reach statistical significance (4.1 vs 4.9, $P = 0.5$; Figure 9G). Similar to the *ob/ob* models, both FATZO LFD and FATZO AMLN mitochondria displayed a trend for increased proton leak compared to lean controls (0.43 for both FATZO LFD and AMLN vs 0.32 for lean controls; $P = 0.08$ and $P = 0.07$, respectively; Figure 9H).

Ob/ob mice display a reduced ability to manage oxidative stress compared to FATZO mice

The oxidative stress responsive transcription factor *Nrf2* was significantly induced in both *ob/ob* and

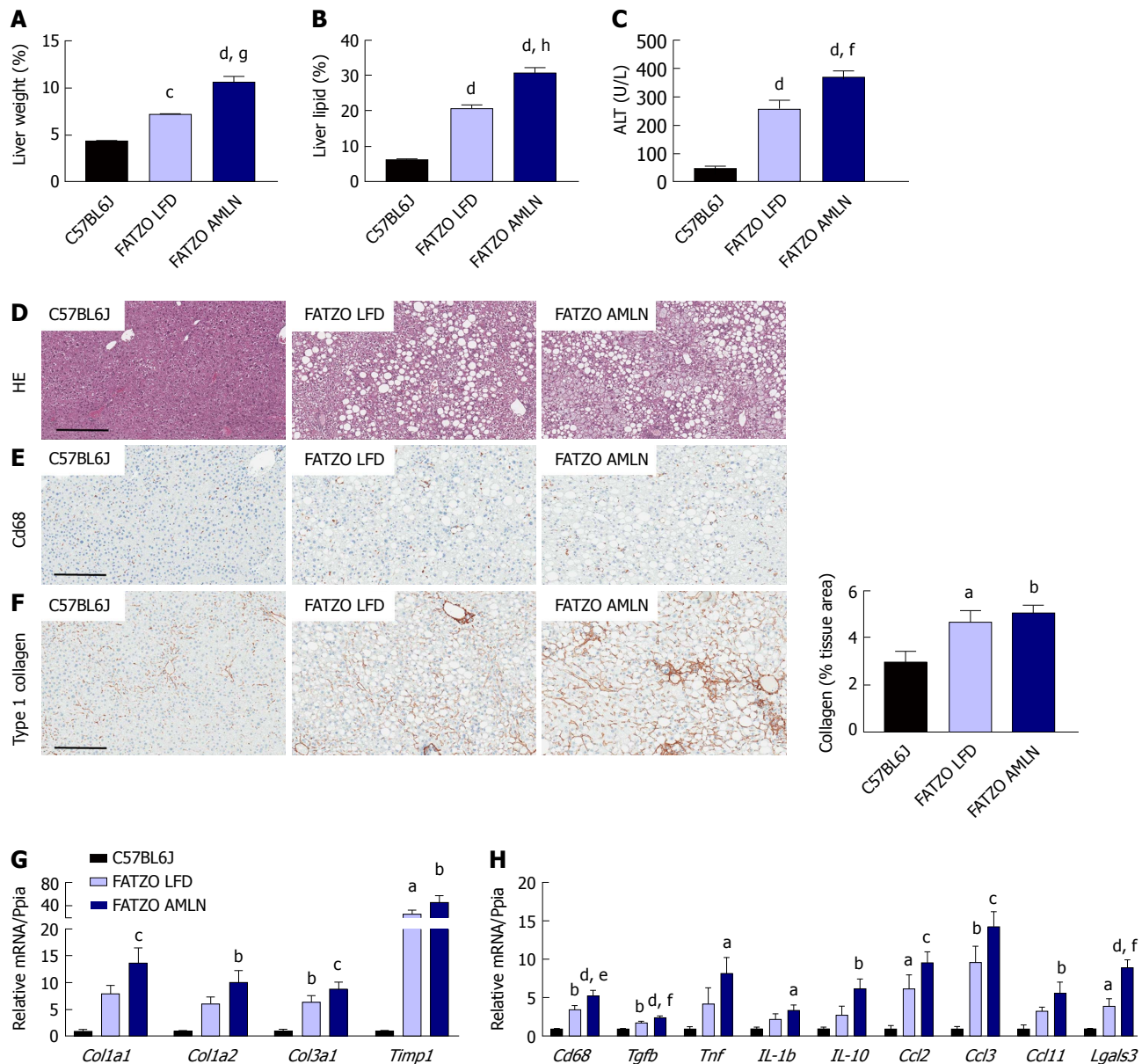


Figure 7 Comparison of metabolic and hepatic abnormalities associated with diet-induced nonalcoholic fatty liver disease/nonalcoholic steatohepatitis in FATZO mice. Liver weight (A), liver lipid (B), and plasma alanine aminotransferase (ALT) levels (C) of lean (C57BL6J) and FATZO mice maintained on control LFD (FATZO LFD) or AMLN diet (FATZO AMLN) for 12 wk; (D): Representative hematoxylin and eosin stained liver sections and quantification of percentage of liver area containing macrosteatosis; (E): Representative CD68-stained liver sections; (F): Representative collagen type 1 alpha 1 stained liver sections and quantification of collagen area; (G, H): Hepatic expression of genes associated with fibrosis and inflammation. ^aP ≤ 0.05, ^bP ≤ 0.01, ^cP ≤ 0.001, ^dP ≤ 0.0001 vs C57BL6J; ^eP ≤ 0.05, ^fP ≤ 0.01, ^gP ≤ 0.001, ^hP ≤ 0.0001 vs LFD. LFD: Low-fat diet.

FATZO mice on LFD and further induced by AMLN diet, indicating that the antioxidant response system was induced. Interestingly, when we quantified the expression levels of antioxidant enzymes that are collectively required for ROS detoxification, including superoxide dismutase 1 (*Sod1*), superoxide dismutase 2 (*Sod2*) and catalase (*Cat*), we detected unchanged or reduced hepatic expression in all diseased livers. *Sod1* mRNA was significantly reduced in both *ob/ob* LFD and *ob/ob* AMLN livers compared to lean controls (-25%, *P* < 0.001 for both; Figure 6A), while *Sod2* expression was significantly reduced in *ob/ob* AMLN livers compared to lean controls (-25%, *P* < 0.05; Figure 10A). All diseased livers displayed significantly reduced *Cat* expression

compared to lean controls (-50%, *P* < 0.0001 for *ob/ob* LFD and AMLN vs lean controls; -20%, *P* < 0.05 for FATZO LFD and AMLN vs lean controls; Figure 10A). FATZO AMLN livers, however, did display significantly increased glutathione peroxidase (*Gpx1*) mRNA levels (+50%, *P* < 0.01 vs C57BL6J, Figure 10A).

Despite reduced (*ob/ob* mice) or unchanged (FATZO mice) *Sod1* and *Sod2* mRNA, there was a trend for increased hepatic superoxide dismutase activity for *ob/ob* and FATZO mice compared to lean controls (*P* < 0.05 *ob/ob* AMLN vs lean; Figure 10B). Catalase activity was increased approximately 2-fold in both FATZO LFD (*P* < 0.001) and FATZO AMLN livers (*P* < 0.01), but unchanged in *ob/ob* LFD and *ob/ob* AMLN

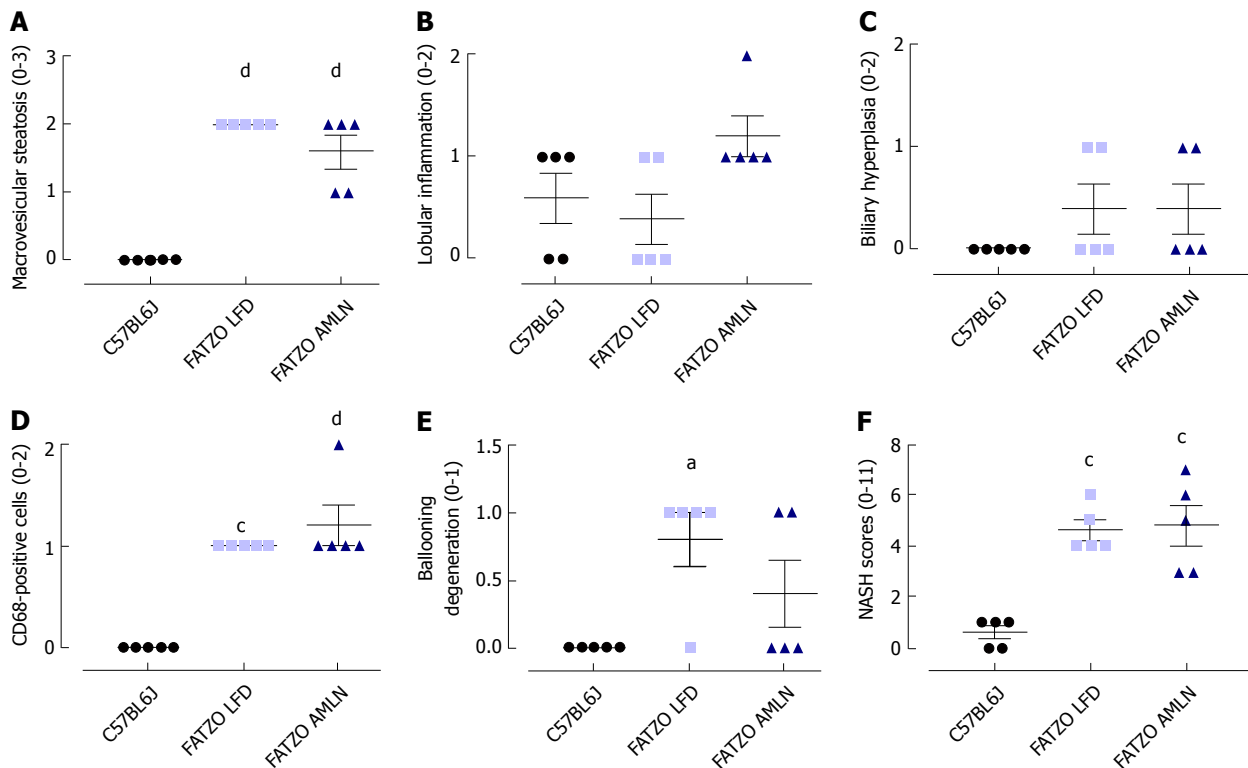


Figure 8 Histopathological scoring of FATZO mice. Individual grades of macrovesicular steatosis (A), lobular inflammation (B), biliary hyperplasia (C), CD68-positive cells (D) and ballooning degeneration. (E) Composite NASH scores. ^aP ≤ 0.05, ^bP ≤ 0.001, ^cP ≤ 0.0001 vs C57BL6J.

livers compared to lean controls (Figure 10C). We also detected increased catalase expression in liver sections from FATZO LFD and FATZO AMLN mice compared to lean controls (Figure 10D). Further, the ratio of hepatic catalase:SOD activity was reduced in *ob/ob* LFD mice and worsened by AMLN diet, but unchanged in FATZO animals compared to lean controls (Figure 10E). Hepatic 8-hydroxydeoxyguanosine (8-OHdG), a marker of oxidative DNA damage, tended to be higher in *ob/ob* LFD animals compared to both lean controls and FATZO LFD mice (Figure 10F). In *ob/ob* AMLN mice, hepatic 8-OHdG levels were significantly higher than both FATZO mice and lean controls (2.5-fold, P < 0.01 vs lean; Figure 10E). Additionally, we observed a negative correlation between catalase activity and hepatic 8-OHdG levels (Figure 10G). Taken together these data suggest that a reduced ability to manage ROS may be a key mechanism underlying the more severe liver phenotype observed in *ob/ob* AMLN mice.

DISCUSSION

The increasing health and economic burden and lack of FDA-approved therapies underscore the importance of appropriate pre-clinical models for NAFLD/NASH^[22]. Surprisingly, only a handful of animal models are available that reflect human disease with respect to metabolic status and liver pathology^[23,24]. These models are similar in that their genetic background predisposes to diet-induced NASH, and include the DIAMOND model^[25], the *ob/ob* mouse^[13,26], and the LDLR knockout

mouse^[27]. To a lesser extent, C57BL6J mice fed a high-fat (AMLN) diet will also develop NASH when given enough time (> 24 wk), but this model does not develop as advanced fibrosis^[28,29]. Other reported models of liver disease do not develop liver inflammation, such as the APOE2 knock-in mouse^[27], or lack metabolic context, such as the CCl₄ and MCDD models.

We report herein that both the leptin-deficient *ob/ob* mouse and hyperleptinemic FATZO mouse develop steatohepatitis within 12 wk of AMLN diet feeding. Despite similar levels of liver lipid and less severe hyperinsulinemia, *ob/ob* AMLN mice displayed a worse liver phenotype with increased inflammation and more advanced fibrosis relative to FATZO mice. Notably, hepatic expression of macrophage markers and related inflammatory chemokines were more prominently upregulated in *ob/ob* AMLN compared to FATZO AMLN mice, but were similar in *ob/ob* LFD and FATZO LFD animals, suggesting that the baseline inflammatory status and matrix deposition of the livers is similar in these models and that leptin deficiency *per se* does not predispose the liver to inflammation and fibrosis, but nonetheless may contribute to a proinflammatory, profibrotic phenotype upon dietary challenge.

While the precise pathophysiology of NASH remains to be fully determined, one aspect that has emerged in recent years is the role of mitochondrial (dys)function in hepatocytes associated with NAFLD/NASH. Evidence from human studies has recently emerged^[8,30], however similar analyses in mouse models of NASH has not

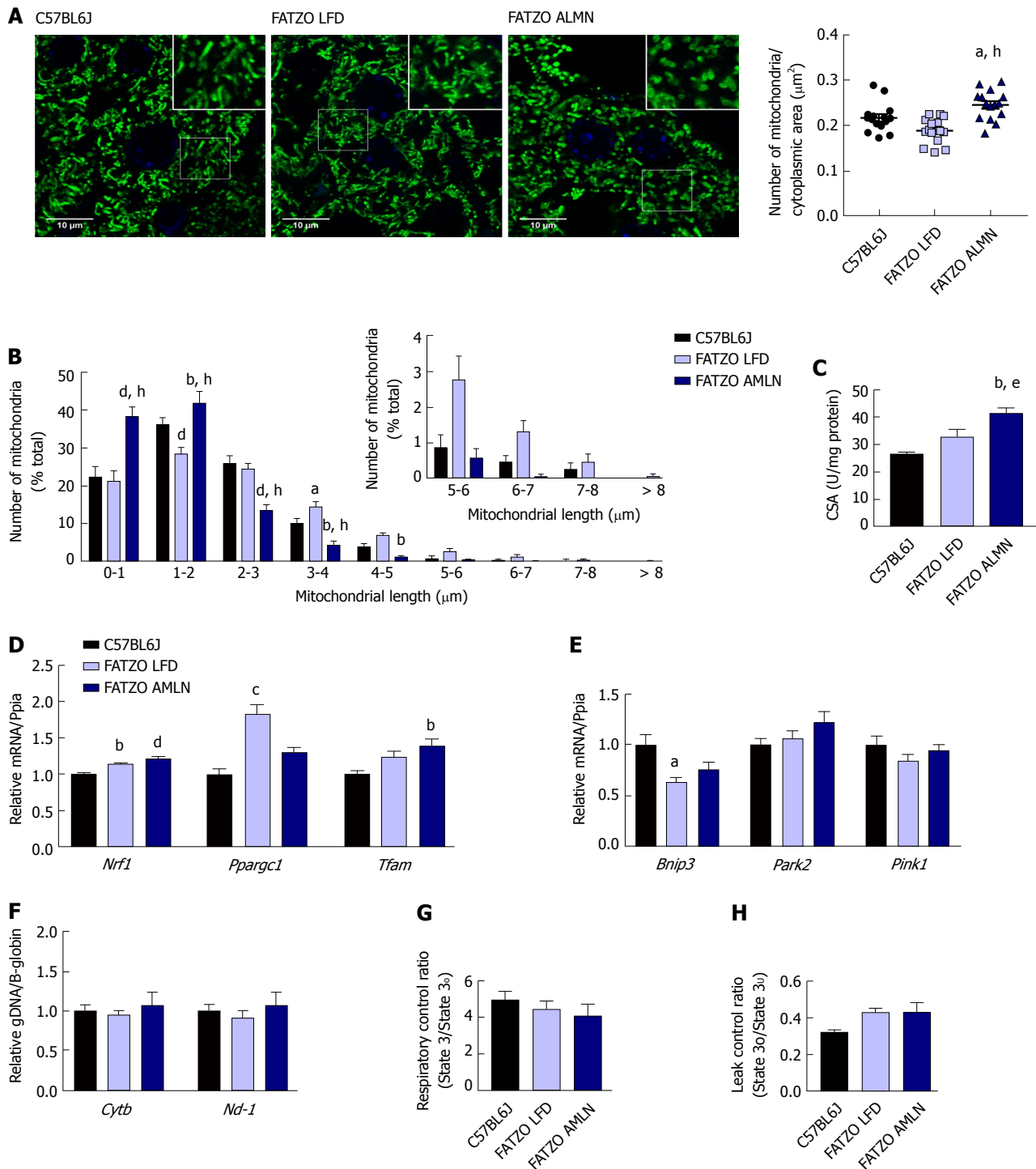


Figure 9 Mitochondrial content alterations in FATZO mice are associated with increased biogenesis and elevated proton leak. (A): Confocal images of HSP60 stained liver sections with quantification of mitochondrial number per cytoplasmic area. Scale bar = 10 μm ; (B): Histogram depicting the number of mitochondria per binned mitochondrial length as a percentage of total mitochondria per cell; (C): Mitochondrial content measured by citrate synthase activity of isolated hepatic mitochondria; (D): Expression of hepatic mitochondrial biogenesis genes; (E): Relative hepatic expression of mitophagy-associated genes; (F): Quantification of mitochondrial genome-encoded *Cytb* or *Nd1* relative to nuclear-encoded β -globin from total genomic DNA extracted from the liver; (G): Mitochondrial respiratory control ratio; (H): Mitochondrial leak control ratio. $^aP \leq 0.05$, $^bP \leq 0.01$, $^cP \leq 0.001$, $^dP \leq 0.0001$ vs C57BL6J; $^eP \leq 0.05$, $^fP \leq 0.0001$ vs LFD. LFD: Low-fat diet.

been reported. Multiple interconnected facets of mitochondrial biology including morphology, overall content (numbers and size), and respiratory capacity influence mitochondrial function. Our data show that *ob/ob* AMLN mice developed NASH associated with increased numbers of fragmented mitochondria with

reduced respiratory capacity but without overt defects in mitochondrial membrane integrity or cristae structure. Similarly, FATZO AMLN mice displayed fragmented mitochondria with a trend for reduced respiratory control, but nonetheless better responded to oxidative damage and presented less overall fibrosis.

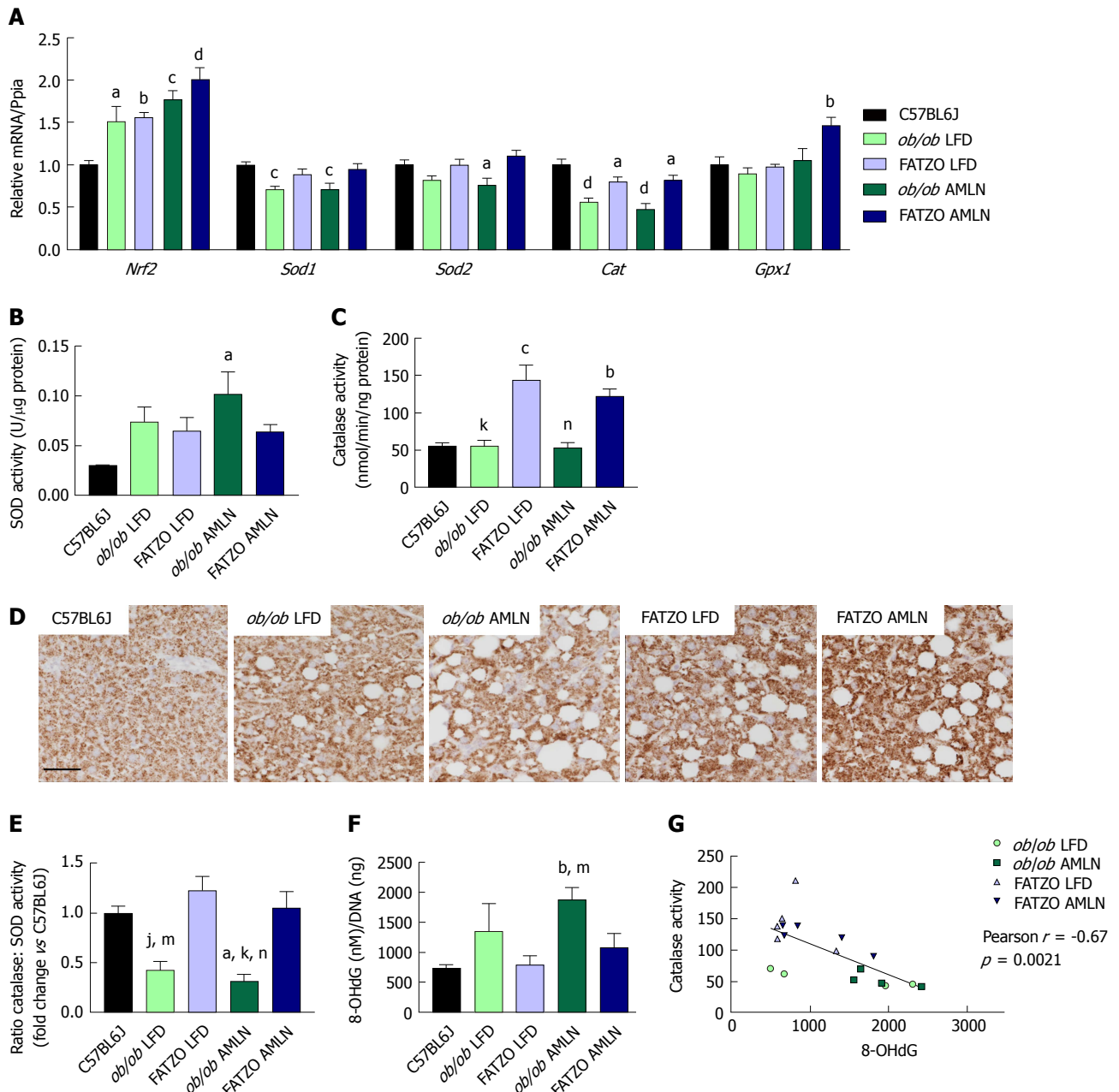


Figure 10 Hepatic oxidative stress is mitigated by increased catalase activity in FATZO but not ob/ob mice. (A): Expression of antioxidant genes *Nrf2*, *Sod1*, *Cat* and *Gpx1* in ob/ob LFD, FATZO LFD, ob/ob AMLN and FATZO AMLN livers relative to lean controls. Superoxide dismutase activity (B) and catalase activity (C) in hepatic lysates from C57BL6J, ob/ob LFD, FATZO LFD, ob/ob AMLN and FATZO AMLN animals; (D): Representative images of catalase stained liver sections. Scale bar represents 100 μ m; (E): Ratio of catalase: SOD activities; (F): Levels of 8-hydroxydeoxyguanosine (8-OHdG) in genomic DNA isolated from C57BL6J, ob/ob LFD, FATZO LFD, ob/ob AMLN and FATZO AMLN livers; (G): Pearson's correlation of catalase activity and 8-OHdG levels in ob/ob and FATZO livers. ^aP ≤ 0.05, ^bP ≤ 0.01, ^cP ≤ 0.001, ^dP ≤ 0.0001 vs C57BL6J, ^jP ≤ 0.01, ^mP ≤ 0.001, ⁿP ≤ 0.0001, FATZO LFD; ^eP ≤ 0.05, ^fP ≤ 0.01, FATZO AMLN unless noted otherwise. LFD: Low-fat diet.

Mitochondrial morphology is appreciated to play an active role in regulating energy metabolism and cell death and can therefore influence NASH development at numerous stages^[31,32]. Leptin has previously been shown to alter mitochondrial morphology and function. In primary mouse hepatocytes, leptin treatment induced mitochondrial fusion through induction of *Ppargc1a* and *Mfn1* and was associated with protection from high-glucose induced fatty acid accumulation^[33]. Complementary work demonstrated that inhibition of mitochondrial fission reduced steatosis and development of

NAFLD^[34]. *Mfn1* and *Opa1* expression were significantly reduced in ob/ob mice when fed AMLN diet. Consistent with transcript levels, we observed smaller but more numerous mitochondria in both ob/ob AMLN and FATZO AMLN hepatocytes. Increased mitochondrial fragmentation and uncoupling have been proposed as adaptive mechanisms to reduce ROS levels and maintain energy balance by limiting ATP production in states of excess substrate supply which may explain the more fragmented, leaky mitochondria in ob/ob AMLN and FATZO AMLN livers.

Reduced mitochondrial function assessed by coupling efficiency and proton leak was also observed in both models; however, only *ob/ob* AMLN livers displayed significantly reduced mtDNA levels, similar to patients with NAFLD^[35,36], which may affect other aspects of mitochondrial function including ATP generation and ROS production. Moreover, ROS itself may promote mtDNA mutation and degradation^[37], leading to a feed-forward loop of continuous oxidative damage that leads to hepatocyte cell death, inflammation and fibrosis development. As such, targeting hepatic oxidative stress driven by chronic overnutrition could be an important therapeutic target for NASH prevention.

The capacity to manage oxidative stress was dissimilar between *ob/ob* and FATZO mice. Multiple antioxidant molecules within the cell are regulated by the transcription factor NRF2. While hepatic *Nrf2* expression was significantly upregulated in both *ob/ob* and FATZO livers, indicative of increased oxidative stress, oxidative DNA damage was only detected in *ob/ob* livers. Increased hepatic superoxide dismutase activity was detected in both *ob/ob* and FATZO animals, suggestive of elevated hydrogen peroxide in these livers, but concomitantly increased catalase activity and *Gpx1* expression was detected only in FATZO liver. Increased hepatic hydrogen peroxide levels have been reported for humans with NASH and correlated with catalase activity and oxidative DNA damage^[8]. In line with these human studies, hepatic catalase activity was indeed negatively correlated with 8-OHdG levels.

In the clinic, single antioxidant therapy has shown mixed efficacy. Among these agents, vitamin E (despite its limited antioxidant efficacy) is the most investigated^[38,39]. While the majority of studies showed improvements in select features, including steatosis, serum ALT and histopathology, none have demonstrated improvement in fibrosis, the key feature linked to disease progression^[40]. Strategies to enhance antioxidant defenses are also being actively explored. One such target is NRF2, which can be activated by numerous natural products, including resveratrol and synthetic compounds^[41]. Combination strategies that include the oxidant scavenging effects with an anti-fibrotic molecule such as the anti-galectin 3 drug GR-MD-02, currently in Phase 2 trials^[42] may be informative.

In summary, we have described convenient mouse models of NAFLD/NASH that accurately reflect human disease context (obesity and insulin resistance) and liver pathology (steatosis, ballooning degeneration, inflammation and fibrosis). Additionally, both models appear to mimic reported aspects of mitochondrial phenotype in human NASH, including elevated mitochondrial numbers and increased proton leak. The unanticipated differences in disease severity may in part be due to an increased ability to manage oxidative stress in the FATZO mouse. These models may better predict therapeutic efficacy of putative NASH treatments in the clinic, particularly for agents targeting mitochondrial/

oxidative pathways.

ARTICLE HIGHLIGHTS

Research background

Non-alcoholic steatohepatitis (NASH) is an unmet medical need with no approved therapies. Studies here characterize the hepatic phenotype of two different diet-induced mouse models of NASH with a focus on mitochondrial function and ability to regulate oxidative damage.

Research motivation

Emerging evidence from cross-sectional human studies suggests a role for mitochondrial function in the development of NASH. As the pathogenesis of NASH remains largely unknown it is imperative to characterize potential therapeutic agents in a relevant preclinical model.

Research objectives

The primary objective was to characterize NASH histopathology (e.g., NASH activity score for steatosis, inflammation, ballooning and fibrosis) and function with a focus on mitochondrial biology and capacity to respond to oxidative stress. We contrast these endpoints in two distinct mouse strains (genetically obese *Lep^{ob}/Lep^{ob}* (*ob/ob*) and polygenic obesity-prone FATZO mice) on a previously validated NASH-inducing diet that is high in *trans*-fat, fructose and cholesterol (AMLN diet).

Research methods

Development of NASH was assessed using blinded qualitative (HE stained sections) and quantitative (% collagen-stained area) methods. Mitochondria were assessed via transmission electron micrography and immunofluorescent detection of HSP60. Mitochondrial function was assessed in primary hepatocytes using Seahorse. Activity of superoxide dismutase and catalase were measured from whole liver tissue homogenates. Candidate genes from total liver RNA were measured using quantitative PCR.

Research results

Both *ob/ob* and FATZO mice developed NASH with concomitant obesity and hyperinsulinemia when challenged with AMLN diet for 12 wk, and was associated with mitochondrial accumulation and reduced function. The degree of hepatic fibrosis, however, was markedly greater in *ob/ob* mice and was associated with increased activity of superoxide dismutase (SOD), whereas FATZO mice displayed increased catalase activity. Antioxidant capacity, reflected as the ratio of catalase: SOD activity, was significantly perturbed in *ob/ob* mice with diet-induced NASH.

Research conclusions

Both of these commonly available mouse models develop AMLN diet-induced NASH after 12 wk, associated with reduced mitochondrial function and perturbed morphology. The intrinsic capacity of the FATZO mice to increase antioxidant capacity in the face of impaired mitochondrial function/increased oxidative damage due to diet may be contributory towards the reduced level of fibrosis in that model.

Research perspectives

The AMLN mouse model of NASH is gaining widespread academic and industry acceptance as a translatable model of NASH. These studies extend previous observations in the model to highlight mitochondrial dysfunction thus confirming the model as relevant for prosecution of therapeutic agents targeting improvement in mitochondrial function for NASH. Furthermore, the contrasting fibrosis between *ob/ob* and FATZO mice implicates the capacity to adapt to oxidative damage as a key regulator of liver fibrosis in diet-induced NASH.

ACKNOWLEDGMENTS

We gratefully acknowledge the assistance of Sally Lee, Holly Koelkebeck, Wanda King, Kenesha Riley and Charles Brown (MedImmune, Gaithersburg, MD, United

States) for expert technical assistance with tissue processing and immunohistochemistry. We thank Lorenz Rognoni and Farzad Sekhavati (Definiens, Germany) for tissue image analysis. We also thank Donna Goldsteen, Krystal Nacel and the Laboratory Animal Resource staff (MedImmune, Gaithersburg, MD) for their assistance with animal husbandry and care.

REFERENCES

- 1 Younossi ZM, Blissett D, Blissett R, Henry L, Stepanova M, Younossi Y, Racila A, Hunt S, Beckerman R. The economic and clinical burden of nonalcoholic fatty liver disease in the United States and Europe. *Hepatology* 2016; **64**: 1577-1586 [PMID: 27543837 DOI: 10.1002/hep.28785]
- 2 Younossi ZM, Koenig AB, Abdelatif D, Fazel Y, Henry L, Wymer M. Global epidemiology of nonalcoholic fatty liver disease-Meta-analytic assessment of prevalence, incidence, and outcomes. *Hepatology* 2016; **64**: 73-84 [PMID: 26707365 DOI: 10.1002/hep.28431]
- 3 Kabbany MN, Conjeevaram Selvakumar PK, Watt K, Lopez R, Akras Z, Zein N, Carey W, Alkhouri N. Prevalence of Nonalcoholic Steatohepatitis-Associated Cirrhosis in the United States: An Analysis of National Health and Nutrition Examination Survey Data. *Am J Gastroenterol* 2017; **112**: 581-587 [PMID: 28195177 DOI: 10.1038/ajg.2017.5]
- 4 Patterson RE, Kalavalapalli S, Williams CM, Nautiyal M, Mathew JT, Martinez J, Reinhard MK, McDougall DJ, Rocca JR, Yost RA, Cusi K, Garrett TJ, Sunny NE. Lipotoxicity in steatohepatitis occurs despite an increase in tricarboxylic acid cycle activity. *Am J Physiol Endocrinol Metab* 2016; **310**: E484-E494 [PMID: 26814015 DOI: 10.1152/ajpendo.00492.2015]
- 5 Satapati S, Kucejova B, Duarte JA, Fletcher JA, Reynolds L, Sunny NE, He T, Nair LA, Livingston KA, Fu X, Merritt ME, Sherry AD, Malloy CR, Shelton JM, Lambert J, Parks EJ, Corbin I, Magnuson MA, Browning JD, Burgess SC. Mitochondrial metabolism mediates oxidative stress and inflammation in fatty liver. *J Clin Invest* 2016; **126**: 1605 [PMID: 27035816 DOI: 10.1172/JCI86695]
- 6 Begriche K, Massart J, Robin MA, Bonnet F, Fromenty B. Mitochondrial adaptations and dysfunctions in nonalcoholic fatty liver disease. *Hepatology* 2013; **58**: 1497-1507 [PMID: 23299992 DOI: 10.1002/hep.26226]
- 7 Satapati S, Sunny NE, Kucejova B, Fu X, He TT, Méndez-Lucas A, Shelton JM, Perales JC, Browning JD, Burgess SC. Elevated TCA cycle function in the pathology of diet-induced hepatic insulin resistance and fatty liver. *J Lipid Res* 2012; **53**: 1080-1092 [PMID: 22493093 DOI: 10.1194/jlr.M023382]
- 8 Koliaki C, Szendroedi J, Kaul K, Jelenik T, Nowotny P, Jankowiak F, Herder C, Carstensen M, Krausch M, Knoefel WT, Schlessak M, Roden M. Adaptation of hepatic mitochondrial function in humans with non-alcoholic fatty liver is lost in steatohepatitis. *Cell Metab* 2015; **21**: 739-746 [PMID: 25955209 DOI: 10.1016/j.cmet.2015.04.004]
- 9 Auger C, Alhasawi A, Contavado M, Appanna VD. Dysfunctional mitochondrial bioenergetics and the pathogenesis of hepatic disorders. *Front Cell Dev Biol* 2015; **3**: 40 [PMID: 26161384 DOI: 10.3389/fcell.2015.00040]
- 10 Sunny NE, Bril F, Cusi K. Mitochondrial Adaptation in Nonalcoholic Fatty Liver Disease: Novel Mechanisms and Treatment Strategies. *Trends Endocrinol Metab* 2017; **28**: 250-260 [PMID: 27986466 DOI: 10.1016/j.tem.2016.11.006]
- 11 Gusdon AM, Song KX, Qu S. Nonalcoholic Fatty liver disease: pathogenesis and therapeutics from a mitochondria-centric perspective. *Oxid Med Cell Longev* 2014; **2014**: 637027 [PMID: 25371775 DOI: 10.1155/2014/637027]
- 12 Machado MV, Michelotti GA, Xie G, Almeida Pereira T, Boursier J, Bohnic B, Guy CD, Diehl AM. Mouse models of diet-induced nonalcoholic steatohepatitis reproduce the heterogeneity of the human disease. *PLoS One* 2015; **10**: e0127991 [PMID: 26017539 DOI: 10.1371/journal.pone.0127991]
- 13 Trevaskis JL, Griffin PS, Wittmer C, Neuschwander-Tetri BA, Brunt EM, Dolman CS, Erickson MR, Napora J, Parkes DG, Roth JD. Glucagon-like peptide-1 receptor agonism improves metabolic, biochemical, and histopathological indices of nonalcoholic steatohepatitis in mice. *Am J Physiol Gastrointest Liver Physiol* 2012; **302**: G762-G772 [PMID: 22268099 DOI: 10.1152/ajpgi.00476.2011]
- 14 Droz BA, Snead BL, Jackson CV, Zimmerman KM, Michael MD, Emmerson PJ, Coskun T, Peterson RG. Correlation of disease severity with body weight and high fat diet in the FATZO/Pco mouse. *PLoS One* 2017; **12**: e0179808 [PMID: 28640904 DOI: 10.1371/journal.pone.0179808]
- 15 Peterson RG, Jackson CV, Zimmerman KM, Alsina-Fernandez J, Michael MD, Emmerson PJ, Coskun T. Glucose dysregulation and response to common anti-diabetic agents in the FATZO/Pco mouse. *PLoS One* 2017; **12**: e0179856 [PMID: 28640857 DOI: 10.1371/journal.pone.0179856]
- 16 Kleiner DE, Brunt EM, Van Natta M, Behling C, Contos MJ, Cummings OW, Ferrell LD, Liu YC, Torbenson MS, Unalp-Arida A, Yeh M, McCullough AJ, Sanyal AJ; Nonalcoholic Steatohepatitis Clinical Research Network. Design and validation of a histological scoring system for nonalcoholic fatty liver disease. *Hepatology* 2005; **41**: 1313-1321 [PMID: 15915461 DOI: 10.1002/hep.20701]
- 17 Alarcon C, Boland BB, Uchizono Y, Moore PC, Peterson B, Rajan S, Rhodes OS, Noske AB, Haataja L, Arvan P, Marsh BJ, Austin J, Rhodes CJ. Pancreatic β -Cell Adaptive Plasticity in Obesity Increases Insulin Production but Adversely Affects Secretory Function. *Diabetes* 2016; **65**: 438-450 [PMID: 26307586 DOI: 10.2337/db15-0792]
- 18 Kremer JR, Mastronarde DN, McIntosh JR. Computer visualization of three-dimensional image data using IMOD. *Journal of Structural Biology* 1996; **116**: 71-76 [PMID: 8742726 DOI: 10.1006/jsb.1996.0013]
- 19 Boland BB, Brown C Jr, Alarcon C, Demozay D, Grimsby JS, Rhodes CJ. β -Cell Control of Insulin Production During Starvation-Refeeding in Male Rats. *Endocrinology* 2018; **159**: 895-906 [PMID: 29244064 DOI: 10.1210/en.2017-03120]
- 20 Glick D, Zhang W, Beaton M, Marsboom G, Gruber M, Simon MC, Hart J, Dorn GW 2nd, Brady MJ, Macleod KF. BNip3 regulates mitochondrial function and lipid metabolism in the liver. *Mol Cell Biol* 2012; **32**: 2570-2584 [PMID: 22547685 DOI: 10.1128/MCB.00167-12]
- 21 Chavin KD, Yang S, Lin HZ, Chatham J, Chacko VP, Hoek JB, Walajtys-Rode E, Rashid A, Chen CH, Huang CC, Wu TC, Lane MD, Diehl AM. Obesity induces expression of uncoupling protein-2 in hepatocytes and promotes liver ATP depletion. *J Biol Chem* 1999; **274**: 5692-5700 [PMID: 10026188]
- 22 Abdelmalek MF. NAFLD: The clinical and economic burden of NAFLD: time to turn the tide. *Nat Rev Gastroenterol Hepatol* 2016; **13**: 685-686 [PMID: 27826139 DOI: 10.1038/nrgastro.2016.178]
- 23 Hansen HH, Feigh M, Veidal SS, Rigbolt KT, Vrang N, Fosgerau K. Mouse models of nonalcoholic steatohepatitis in preclinical drug development. *Drug Discov Today* 2017; **22**: 1707-1718 [PMID: 28687459 DOI: 10.1016/j.drudis.2017.06.007]
- 24 Larter CZ, Yeh MM. Animal models of NASH: getting both pathology and metabolic context right. *J Gastroenterol Hepatol* 2008; **23**: 1635-1648 [PMID: 18752564 DOI: 10.1111/j.1440-1746.2008.05543.x]
- 25 Asgharpour A, Cazanave SC, Pacana T, Seneshaw M, Vincent R, Banini BA, Kumar DP, Daita K, Min HK, Mirshahi F, Bedossa P, Sun X, Hoshida Y, Koduru SV, Contaifer D Jr, Warncke UO, Wijesinghe DS, Sanyal AJ. A diet-induced animal model of non-alcoholic fatty liver disease and hepatocellular cancer. *J Hepatol* 2016; **65**: 579-588 [PMID: 27261415 DOI: 10.1016/j.jhep.2016.05.005]
- 26 Clapper JR, Hendricks MD, Gu G, Wittmer C, Dolman CS, Herich J, Athanacio J, Villegas C, Ghosh SS, Heilig JS, Lowe C, Roth JD.

- Diet-induced mouse model of fatty liver disease and nonalcoholic steatohepatitis reflecting clinical disease progression and methods of assessment. *Am J Physiol Gastrointest Liver Physiol* 2013; **305**: G483-G495 [PMID: 23886860 DOI: 10.1152/ajpgi.00079.2013]
- 27 **Bieghs V**, Van Gorp PJ, Wouters K, Hendrikx T, Gijbels MJ, van Bilzen M, Bakker J, Binder CJ, Lütjohann D, Staels B, Hofker MH, Shiri-Sverdlov R. LDL receptor knock-out mice are a physiological model particularly vulnerable to study the onset of inflammation in non-alcoholic fatty liver disease. *PLoS One* 2012; **7**: e30668 [PMID: 22295101 DOI: 10.1371/journal.pone.0030668]
- 28 **Liedtke C**, Luedde T, Sauerbruch T, Scholten D, Streetz K, Tacke F, Tolba R, Trautwein C, Trebicka J, Weiskirchen R. Experimental liver fibrosis research: update on animal models, legal issues and translational aspects. *Fibrogenesis Tissue Repair* 2013; **6**: 19 [PMID: 24274743 DOI: 10.1186/1755-1536-6-19]
- 29 **Kristiansen MN**, Veidal SS, Rigbolt KT, Tølbøl KS, Roth JD, Jelsing J, Vrang N, Feigh M. Obese diet-induced mouse models of nonalcoholic steatohepatitis-tracking disease by liver biopsy. *World J Hepatol* 2016; **8**: 673-684 [PMID: 27326314 DOI: 10.4254/wjh.v8.i16.673]
- 30 **Hyötyläinen T**, Jerby L, Petäjä EM, Mattila I, Jäntti S, Auvinen P, Gastaldelli A, Yki-Järvinen H, Ruppin E, Orešić M. Genome-scale study reveals reduced metabolic adaptability in patients with non-alcoholic fatty liver disease. *Nat Commun* 2016; **7**: 8994 [PMID: 26839171 DOI: 10.1038/ncomms9994]
- 31 **Westermann B**. Mitochondrial fusion and fission in cell life and death. *Nat Rev Mol Cell Biol* 2010; **11**: 872-884 [PMID: 21102612 DOI: 10.1038/nrm3013]
- 32 **Wai T**, Langer T. Mitochondrial Dynamics and Metabolic Regulation. *Trends Endocrinol Metab* 2016; **27**: 105-117 [PMID: 26754340 DOI: 10.1016/j.tem.2015.12.001]
- 33 **Hsu WH**, Lee BH, Pan TM. Leptin-induced mitochondrial fusion mediates hepatic lipid accumulation. *Int J Obes (Lond)* 2015; **39**: 1750-1756 [PMID: 26119995 DOI: 10.1038/ijo.2015.120]
- 34 **Galloway CA**, Lee H, Brookes PS, Yoon Y. Decreasing mitochondrial fission alleviates hepatic steatosis in a murine model of nonalcoholic fatty liver disease. *Am J Physiol Gastrointest Liver Physiol* 2014; **307**: G632-G641 [PMID: 25080922 DOI: 10.1152/ajpgi.00182.2014]
- 35 **Sookoian S**, Rosselli MS, Gemma C, Burgueño AL, Fernández Gianotti T, Castaño GO, Pirola CJ. Epigenetic regulation of insulin resistance in nonalcoholic fatty liver disease: impact of liver methylation of the peroxisome proliferator-activated receptor γ coactivator 1 α promoter. *Hepatology* 2010; **52**: 1992-2000 [PMID: 20890895 DOI: 10.1002/hep.23927]
- 36 **Sookoian S**, Fliehman D, Scian R, Rohr C, Dopazo H, Gianotti TF, Martino JS, Castaño GO, Pirola CJ. Mitochondrial genome architecture in non-alcoholic fatty liver disease. *J Pathol* 2016; **240**: 437-449 [PMID: 27577682 DOI: 10.1002/path.4803]
- 37 **Shokolenko I**, Venediktova N, Bochkareva A, Wilson GL, Alexeyev MF. Oxidative stress induces degradation of mitochondrial DNA. *Nucleic Acids Res* 2009; **37**: 2539-2548 [PMID: 19264794 DOI: 10.1093/nar/gkp100]
- 38 **Al-Busafi SA**, Bhat M, Wong P, Ghali P, Deschenes M. Antioxidant therapy in nonalcoholic steatohepatitis. *Hepat Res Treat* 2012; **2012**: 947575 [PMID: 23227320 DOI: 10.1155/2012/947575]
- 39 **Sanyal AJ**, Chalasani N, Kowdley KV, McCullough A, Diehl AM, Bass NM, Neuschwander-Tetri BA, Lavine JE, Tonascia J, Unalp A, Van Natta M, Clark J, Brunt EM, Kleiner DE, Hoofnagle JH, Robuck PR; NASH CRN. Pioglitazone, vitamin E, or placebo for nonalcoholic steatohepatitis. *N Engl J Med* 2010; **362**: 1675-1685 [PMID: 20427778 DOI: 10.1056/NEJMoa0907929]
- 40 **Hagström H**, Nasr P, Ekstedt M, Hammar U, Stål P, Hultcrantz R, Kechagias S. Fibrosis stage but not NASH predicts mortality and time to development of severe liver disease in biopsy-proven NAFLD. *J Hepatol* 2017; **67**: 1265-1273 [PMID: 28803953 DOI: 10.1016/j.jhep.2017.07.027]
- 41 **Musso G**, Cassader M, Gambino R. Non-alcoholic steatohepatitis: emerging molecular targets and therapeutic strategies. *Nat Rev Drug Discov* 2016; **15**: 249-274 [PMID: 26794269 DOI: 10.1038/nrd.2015.3]
- 42 **Harrison SA**, Marri SR, Chalasani N, Kohli R, Aronstein W, Thompson GA, Irish W, Miles MV, Xanthakos SA, Lawitz E, Noureddin M, Schiano TD, Siddiqui M, Sanyal A, Neuschwander-Tetri BA, Traber PG. Randomised clinical study: GR-MD-02, a galectin-3 inhibitor, vs. placebo in patients having non-alcoholic steatohepatitis with advanced fibrosis. *Aliment Pharmacol Ther* 2016; **44**: 1183-1198 [PMID: 27778367 DOI: 10.1111/apt.13816]

P- Reviewer: Garcia-Fernandez MI, Novo E, Streba LAM
 S- Editor: Ma YJ L- Editor: A E- Editor: Huang Y



Basic Study

Mucosa repair mechanisms of Tong-Xie-Yao-Fang mediated by CRH-R2 in murine, dextran sulfate sodium-induced colitis

Shan-Shan Gong, Yi-Hong Fan, Shi-Yi Wang, Qing-Qing Han, Bin Lv, Yi Xu, Xi Chen, Yao-Er He

Shan-Shan Gong, Shi-Yi Wang, Qing-Qing Han, Xi Chen, Yao-Er He, The First Clinical Medical College of Zhejiang Chinese Medical University, Hangzhou 310053, Zhejiang Province, China

Yi-Hong Fan, Bin Lv, Yi Xu, Department of Gastroenterology, The First Affiliated Hospital of Zhejiang Chinese Medical University, Hangzhou 310006, Zhejiang Province, China

ORCID number: Shan-Shan Gong (0000-0001-5483-720X); Yi-Hong Fan (0000-0001-8217-9793); Shi-Yi Wang (0000-0002-2134-3892); Qing-Qing Han (0000-0002-3155-3746); Bin Lv (0000-0002-6247-571X); Yi Xu (0000-0002-3265-9534); Xi Chen (0000-0002-6236-6345); Yao-Er He (0000-0003-3511-8554).

Author contributions: Gong SS and Wang SY performed the experiments, analyzed the data and wrote the paper; Fan YH and Han QQ designed the research, revised the paper and contributed equally to this study; Xu Y and Lv B performed parts of the experiments and provided valuable suggestions for this study; Chen X and He YE contributed new analytic tools; All authors have read and approved the final manuscript.

Supported by National Natural Science Foundation of China, No. 81473506; Natural Science Foundation of Zhejiang Province, No. LY13H030011 and No. LY17H290009; State Administration of Traditional Chinese Medicine of Zhejiang Province, No. 2013ZB050; Department of Zhejiang Province to Build Funded Project, No. WKJ-ZJ-1531; Zhejiang TCM Science and Technology Project, No. 2016ZB047, No. 2017ZA056 and No. 2018ZB046.

Institutional review board statement: The study was reviewed and approved by the Institutional Review Board of Zhejiang Chinese Medical University.

Institutional animal care and use committee statement: All procedures involving animals were reviewed and approved by the Institutional Animal Care and Use Committee of Zhejiang Chinese Medical University.

Conflict-of-interest statement: No potential conflicts of interest exist.

Data sharing statement: No additional data are available.

Open-Access: This article is an open-access article which was selected by an in-house editor and fully peer-reviewed by external reviewers. It is distributed in accordance with the Creative Commons Attribution Non Commercial (CC BY-NC 4.0) license, which permits others to distribute, remix, adapt, build upon this work non-commercially, and license their derivative works on different terms, provided the original work is properly cited and the use is non-commercial. See: <http://creativecommons.org/licenses/by-nc/4.0/>

Manuscript source: Unsolicited manuscript

Correspondence to: Yi-Hong Fan, PhD, Associate Professor, Department of Gastroenterology, The First Affiliated Hospital of Zhejiang Chinese Medical University, No. 54, Youdian Road, Shangcheng District, Hangzhou 310006, Zhejiang Province, China. yhfansjr@163.com

Telephone: +86-571-87608001
Fax: +86-571-87608001

Received: February 12, 2018

Peer-review started: February 13, 2018

First decision: March 9, 2018

Revised: March 14, 2018

Accepted: March 31, 2018

Article in press: March 31, 2018

Published online: April 28, 2018

Abstract**AIM**

To explore the significance of corticotropin-releasing hormone (CRH)-receptor (R)2 in mucosal healing of dextran sulfate sodium (DSS)-induced colitis and the effect of Tong-Xie-Yao-Fang (TXYF) on CRH-R2 expression and regulation.

METHODS

Ulcerative colitis was induced in mice by administration of 3% (w/v) DSS for 7 d. Once the model was established,

mice were administered urocortin-2 (30 µg/kg), a peptide which binds exclusively to CRH-R2, or various doses of aqueous TXYF extracts (2.8–11.2 g/kg), a CRH-R2 antagonist Astressin (Ast)2B (20 µg/kg), Ast2B + Ucn2, or Ast2B with various doses of aqueous TXYF extracts for 9 d. Colonic mucosal permeability was then evaluated by measuring the fluorescence intensity in serum. The colitis disease activity index (DAI), histology, body weight loss and colon length were assessed to evaluate the condition of colitis. Terminal deoxynucleotidyl transferase dUTP nick-end labeling was used to detect apoptosis of the intestinal epithelial cells. The expression level of Ki-67 represented the proliferation of colonic epithelial cells and was detected by immunohistochemistry. The expression levels of inflammation cytokines IL-6, TNF-α and CXCL-1 were examined in colon tissues using real-time PCR and ELISA kits.

RESULTS

Compared with the DSS group, mice treated with the CRH-R2 antagonist Ast2B showed greater loss of body weight, shorter colon lengths (4.90 ± 0.32 vs 6.21 ± 0.34 cm, $P < 0.05$), and higher DAI (3.61 ± 0.53 vs 2.42 ± 0.32 , $P < 0.05$) and histological scores (11.50 ± 1.05 vs 8.33 ± 1.03 , $P < 0.05$). Additionally, the Ast2B group showed increased intestinal permeability (2.76 ± 0.11 µg/mL vs 1.47 ± 0.11 µg/mL, $P < 0.001$), improved secretion of inflammatory cytokines in colon tissue, and reduced colonic epithelial cell proliferation (4.97 ± 4.25 vs 22.51 ± 8.22 , $P < 0.05$). Increased apoptosis (1422.39 ± 90.71 vs 983.01 ± 98.17 , $P < 0.001$) was also demonstrated. The Ucn2 group demonstrated lower DAI (0.87 ± 0.55 vs 2.42 ± 0.32 , $P < 0.001$) and histological scores (4.33 ± 1.50 vs 8.33 ± 1.03 , $P < 0.05$). Diminished weight loss, longer colon length (9.58 ± 0.62 vs 6.21 ± 0.34 cm, $P < 0.001$), reduced intestinal permeability (0.75 ± 0.07 vs 1.47 ± 0.11 µg/mL, $P < 0.001$), inhibited secretion of inflammatory cytokines in colon tissue and increased colonic epithelial cell proliferation (90.04 ± 15.50 vs 22.51 ± 8.22 , $P < 0.01$) were all observed. Reduced apoptosis (149.55 ± 21.68 vs 983.01 ± 98.17 , $P < 0.05$) was also observed. However, significant statistical differences in the results of the Ast2B group and Ast2B + Ucn2 group were observed. TXYF was also found to ameliorate symptoms of DSS-induced colitis in mice and to promote mucosal repair like Ucn2. There were significant differences between the Ast2B + TXYF groups and the TXYF groups.

CONCLUSION

CRH-R2 activates the intestinal mucosal antiinflammatory response by regulating migration, proliferation and apoptosis of intestinal epithelial cells in colitis-induced mice, and plays an important antiinflammatory role. TXYF promotes mucosal repair in colitis mice by regulating CRH-R2.

Key words: Tong-Xie-Yao-Fang; Aqueous extracts; Corticotropin-releasing hormone receptor 2; Urocortin 2;

Astressin 2B; Mucosal healing; Ulcerative colitis

© The Author(s) 2018. Published by Baishideng Publishing Group Inc. All rights reserved.

Core tip: Mucosal healing is a desired therapeutic endpoint in the treatment of inflammatory bowel disease. However, it is difficult to treat inflammatory bowel disease thoroughly, and there are some adverse reactions. Studies have shown that corticotropin-releasing hormone (CRH)-receptor (R)2 can activate the inflammatory response of intestinal mucosa and exert an antiinflammatory effect. Our preliminary study found that Tong-Xie-Yao-Fang could reduce the expression of CRH-R1, increase CRH-R2, and participate in reconstruction of the intestinal barrier. The aim of this study was to explore the significance of CRH-R2 in the mucosal healing of dextran sulfate sodium-induced colitis and study the effect of Tong-Xie-Yao-Fang on CRH-R2 expression and regulation.

Gong SS, Fan YH, Wang SY, Han QQ, Lv B, Xu Y, Chen X, He YE. Mucosa repair mechanisms of Tong-Xie-Yao-Fang mediated by CRH-R2 in murine, dextran sulfate sodium-induced colitis. *World J Gastroenterol* 2018; 24(16): 1766-1778 Available from: URL: <http://www.wjgnet.com/1007-9327/full/v24/i16/1766.htm> DOI: <http://dx.doi.org/10.3748/wjg.v24.i16.1766>

INTRODUCTION

Inflammatory bowel diseases (IBD), including Crohn's disease and ulcerative colitis (UC), are a group of chronic inflammatory disorders of the gastrointestinal tract, characterized by intestinal inflammation and mucosal damage^[1]. In traditional Chinese medicine theory, UC is known as the "changpi" and chronic dysentery^[2]. Characterized by chronic mucosal inflammation and damage of the colon, UC presents with bloody diarrhea, tenesmus, abdominal pain, weight loss, anemia, and even toxic megacolon. Intestinal perforation, intestinal obstruction, intestinal bleeding and cancer are also observed, thus affecting an individual's quality of life^[3].

Treatment targets for IBD have changed over the recent years. Previous therapeutic strategies focusing on induction and maintenance of clinical remission have shown no effect on the natural course of the disease^[4,5]. However, in the late 1990s, the advent of biologic agents for the treatment of IBD showed that while patients may be in clinical remission, ongoing mucosal inflammation may still be present, resulting in structural damage^[6-11].

This finding has led to the concept of mucosal healing as a more meaningful therapeutic target in clinical practice. Indeed, emerging data suggests that mucosal healing is strongly associated with a reduction in steroid use, complications, hospitalizations, and surgeries^[12].

Mucosal repair of the intestinal barrier is a tightly coordinated response to injury that preserves homeostasis and limits the adverse effects of inflammation. After damage to the epithelial tissue, intestinal epithelial cells migrate to the site of injury in a critical process known as epithelial restitution^[13-15]. Restitution is followed by epithelial cell proliferation and differentiation which is regulated by factors that promote cell viability and limit apoptosis^[14,16]. IBD is a chronic relapsing inflammatory disorder that involves a defective epithelial barrier^[17].

Corticotropin-releasing hormone (CRH), the primary mediator of the stress response, is expressed in both the central nervous system and the periphery, including the intestine^[18]. The CRH family of peptides interacts with a variety of cell types in the intestinal mucosa, including epithelial cells, enteric neurons, and immune cells^[19]. In addition to CRH, three distinct peptides known as urocortins (Ucn1, Ucn2, and Ucn3) bind to two types of G protein-coupled receptors to exert their effects, CRH receptor (R)1 and CRH-R2. Yet, Ucn1 has greater affinity for CRH-R2 than CRH-R1, and Ucn2 and Ucn3 bind exclusively to CRH-R2^[20]. Interactions between CRH-Rs and their ligands modulate several functional and pathophysiologic responses within the gut, including stress-induced alterations in motility, ion secretion, and visceral pain, and the development and maintenance of intestinal inflammation^[21].

Studies from others have found that CRH may be involved in the maintenance of intestinal barrier integrity by regulating autophagy in the intestinal epithelial cells^[18]. Our previous studies have also found that CRH could cause an increase in intercellular permeability in the intestinal epithelium^[22]. Some studies have found that CRH-R2 can activate the antiinflammatory response of intestinal mucosa and exert an antiinflammatory effect^[23]. In addition, activation of CRH-R2 can promote the migration and proliferation of colon cancer cells and gastric mucosa cells^[24,25]. Furthermore, the expression of CRH-R2 was found to be down-regulated in the biopsy specimens of UC patients^[26] and CRH-deficient mice are unable to initiate healing responses after acute experimental colitis^[27], suggesting a role for the CRH peptide family, especially CRH-R2, in mucosal repair mechanisms.

Tong-Xie-Yao-Fang (TXYF) is a prescription in traditional Chinese medicine, used for relieving abdominal pain and diarrhea. TXYF has also been shown to be involved in the reconstruction of the intestinal epithelial barrier and to promote the healing of mucosa in UC^[28,29]. While the mechanism is not understood, it is thought to target and intervene with CRH-R2. This regulates the migration, proliferation and apoptosis of epithelial cells, like the role of Ucn2^[30,31].

The overall aim of the present investigation was to determine whether CRH-R2 regulates mucosal repair on dextran sulfate sodium (DSS)-induced colitis in mice and to examine the relationship between TXYF and

Table 1 Criteria for disease activity index

| Score | Weight loss, % | Stool consistency | Bloodstain or gross bleeding |
|-------|----------------|-------------------|------------------------------|
| 0 | None | Normal | Negative |
| 1 | 1-5 | - | - |
| 2 | 5-10 | Loose stool | Positive |
| 3 | 10-15 | - | - |
| 4 | > 15 | Diarrhea | Gross bleeding |

CRH-R2 signaling.

MATERIALS AND METHODS

TXYF composition and dosage preparation

TXYF was prepared with large head atractylodes rhizome (*Rhizoma Atractylodis Macrocephalae*), white peony root (*Radix Paeoniae Alba*), dried tangerine peel (*Pericarpium Citri Reticulatae*) and divaricate saponnikovia root (*Radix Saposhnikoviae*)^[32], which were used in a 15:12:6:10 proportion. Raw components were soaked in an 8-fold volume of distilled water for 1 h and boiled twice for 0.5 h each time. Two of the boiled ingredients were filtered, mixed together, concentrated at a 1:1 ratio (100% concentration), and stored at 4 °C for later use.

Animal modeling and drug treatment

Male CD-1(ICR) mice (8-10 wk old) were purchased from Shanghai Xipuer-bikai Experimental Animal Co., Ltd., (Shanghai, China) and housed 1 wk under a 12 h light/dark cycle at 22-24 °C with 50%-60% humidity and a noise level < 50 d. Prior to experimentation, mice were allowed free access to food and tap water. All the procedures involving animals were conducted in accordance with the ethical principles adopted by the Animal Experimental Center of Zhejiang Chinese Medical University and were approved by the Ethics Committee on Animal Experiments at Zhejiang Chinese Medical University.

Mice ($n = 110$) were randomized into 11 assigned groups as follows: control group ($n = 10$), DSS group ($n = 10$), DSS + Astressin (Ast)2B group (Ast2B group; $n = 10$), DSS + Ucn2 group (Ucn2 group; $n = 10$), DSS + Ast2B + Ucn2 group (Ast2B + Ucn2 group; $n = 10$), DSS + Ast2B + low-dose (2.8 g/kg·d) aqueous TXYF extract group (Ast2B + TXYF-L group; $n = 10$), DSS + Ast2B + medium-dose (5.6 g/kg·d) aqueous TXYF extract group (Ast2B + TXYF-M group; $n = 10$), DSS + Ast2B + high-dose (11.2 g/kg·d) aqueous TXYF extract group (Ast2B + TXYF-H group; $n = 10$), DSS + low-dose (2.8 g/kg·d) aqueous TXYF extract group (TXYF-L group; $n = 10$), DSS + medium-dose (5.6 g/kg·d) aqueous TXYF extract group (TXYF-M group; $n = 10$), and DSS + high-dose (11.2 g/kg·d) aqueous TXYF extract group (TXYF-H group; $n = 10$). Colitis was induced in mice by administering 3% (w/v) DSS (MP Biomedicals, Inc., Aurora, OH, United States) in

Table 2 Histological score to quantify the degree of colitis

| Score | Inflammation | Depth of lesions | Destruction of crypt | Width of lesions, % |
|-------|--------------|----------------------|----------------------------|---------------------|
| 0 | None | None | None | |
| 1 | Slight | Mucosa | Basal 1/3 damaged | 1-25 |
| 2 | Moderate | Mucosa and submucosa | Basal 2/3 damaged | 26-50 |
| 3 | Severe | Transmural | Intact epithelium only | 51-75 |
| 4 | - | - | Total crypt and epithelium | 76-100 |

their drinking water for 7 d. On days 8 to 16, mice were switched to normal water. Additionally, the mice treated with Ast2B were injected daily with the CRH-R2 antagonist Ast2B (Sigma-Aldrich, St. Louis, MO, United States) administered intraperitoneally (20 µg/kg). The mice treated with Ucn2 received an intraperitoneal injection of Ucn2 (Peptide Institute Inc., Osaka, Japan) (30 µg/kg). The mice treated with TXYF were administered the aqueous TXYF extract. The doses of 2.8 g/kg·d, 5.6 g/kg·d, and 11.2 g/kg·d aqueous TXYF extract represented an equivalent of 0.5 ×, 1.0 × and 2.0 × for the human adult dosage.

Disease activity index

Intestinal disease activity was assessed based on weight loss, the presence of diarrhea accompanied by blood and mucus, and colonic shortening^[33]. DAI was calculated by scoring weight loss, diarrhea and rectal bleeding, based on a previous scoring system (Table 1) described by Murthy *et al*^[34] with little modification. Weight loss was defined as the difference between the initial and final weights. Diarrhea was defined by the absence of fecal pellet formation and the presence of continuous fluid fecal material in the colon. Rectal bleeding was assessed based on the presence of diarrhea containing visible blood and on the presence of gross rectal bleeding, and was scored as diarrhea. Disease activity index (DAI) values were calculated using the following formula: DAI = [(weight loss score) + (diarrhea score) + (rectal bleeding score)]/3. The clinical parameters used in the present study were chosen to represent the subjective clinical symptoms observed in human UC.

Histological process

Sections of colon fixed in 10% formalin, paraffin-embedded and stained with hematoxylin and eosin were used for histological scoring. The sections were graded by two blinded investigators, using a range from 0 to 3 as to amount of inflammation (acute and chronic) and depth of inflammation and with a range from 0 to 4 as to the amount of crypt damage or regeneration, as indicated in Table 2^[35]. These changes were also quantified as to the percent involvement by the disease process: (1) 1%-25%; (2) 26%-50%; (3) 51%-75%; (4) 76%-100%. Histological score was calculated using the following formula: histological colitis score = inflammation + depth of lesions + destruction of crypt + width of lesions.

Immunohistochemistry and imaging

Formalin-fixed, paraffin-embedded colons were sectioned (1 µm) and stained with a Ki-67 antigen (dilution 1:100; AF0198; Affinity Biosciences, Cincinnati, OH, United States) or terminal deoxynucleotidyl transferase dUTP nick-end labeling (TUNEL) with the Apop-Tag Plus Peroxidase *in situ* cell death detection kit, POD (11684817910; Roche, Basel, Switzerland) according to the manufacturer's instructions. To quantify Ki-67 immunoreactivity and TUNEL, pixel-based quantification of staining intensity was performed with Image-ProPlus 6.0 software. Stained sections were observed under a 40 × objective lens.

In vivo intestinal permeability

The intestinal permeability was measured by determination of the amount of FITC-dextran (molecular weight 4.0 kDa; Sigma-Aldrich) in blood after oral administration, as described previously^[36]. Briefly, mice were fasted overnight and FITC-dextran solution (4 kDa, 600 mg/kg) was administered. Blood samples were obtained after 3 h, centrifuged at 10000× rpm for 5 min, and serum was collected. Serum levels of FITC were read at 483 nm and 525 nm on a full wavelength multifunctional enzyme spectrometer (Varioskan Flash, Thermo Fisher Scientific, Waltham, MA, United States).

Real-time quantitative PCR

RNAiso Plus (9108; Takara Bio, Inc., Shiga, Japan) was used to extract RNA from frozen tissue samples, and the concentration of RNA was measured using a trace nucleic acid analyzer (Thermo Fisher Scientific). RNA was reverse-transcribed to cDNA using a PrimeScript RT reverse transcription kit (RR036A; Takara Bio, Inc.). Quantitative real-time PCR was carried out by ABI 7500 real-time PCR system (7500; Applied Biosystems of Thermo Fisher Scientific). Primers were designed and synthesized by Shenggong Biology and Engineering Co., Ltd. (Shanghai, China) (Table 3). β-actin was used as the normalization control, and the 2^{-ΔΔCT} method was used to calculate the relative expression of target genes.

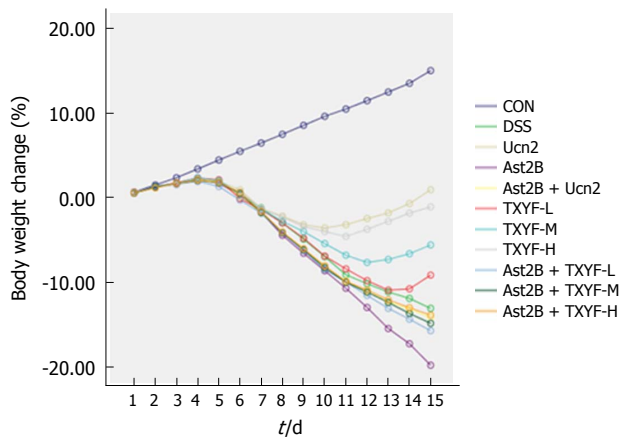
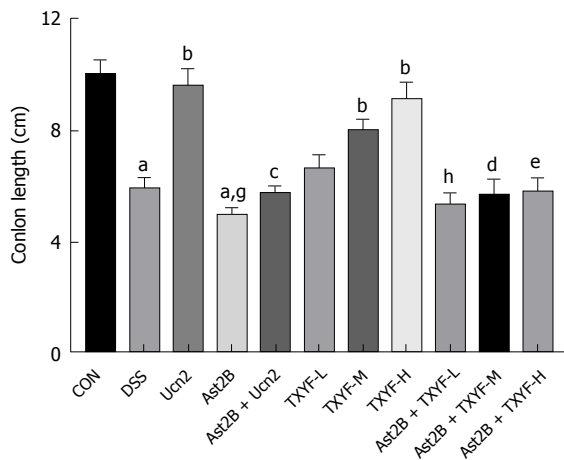
TNF-α, CXCL-1 and IL-6 measurement

CXCL-1 level and IL-6 level were measured by mouse TNF-α enzyme-linked immunosorbent assay (ELISA) kit, mouse CXCL-1 ELISA kit and Mouse IL-6 ELISA kit (Shanghai WesTang Bio-Tech Co., Ltd., Shanghai,

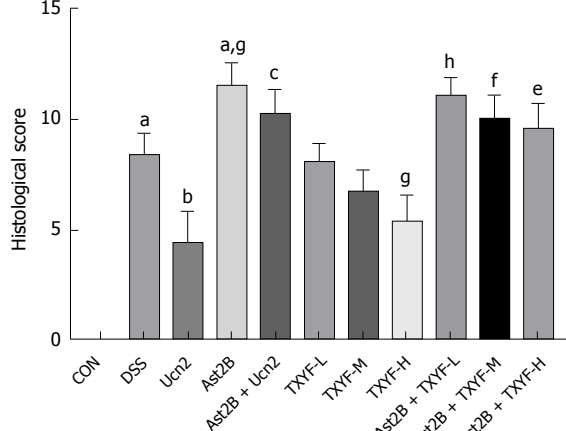
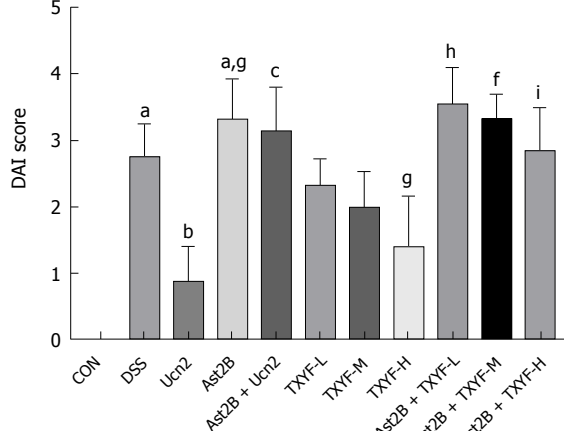
Table 3 Primer sequences and amplification length

| Gene | Primer sequences | Amplification length |
|----------------|---|----------------------|
| TNF- α | Forward: 5'-GCCTATGTCTCAGCCTCTTC-3' Reverse: 5'-TGGTGGTTTGCTACGACGTG-3' | 22 20 |
| CXCL-1 | Forward: 5'-TCACCTAAGAACATCCAGAGC-3' Reverse: 5'-ACTTGGGGACACCTTTAGCAT-3' | 22 22 |
| IL-6 | Forward: 5'-TCTCTGCAAGAGACTTCCATCC-3' Reverse: 5'-TTCCACGATTCCCAGAGAAC-3' | 22 22 |
| β -actin | Forward: 5'-AGATCAAGATCATTGCTCCTCC-3' Reverse: 5'-GGTGAAAACGCAGCTCAGTAA-3' | 22 22 |

TNF- α : Tumor necrosis factor-alpha; CXCL-1: Chemokine (C-X-C motif) ligand-1; IL-6: Interleukin-6; β -actin: Beta-actin.

A**B****C**

| | | | | | | | | | | |
|--------|---|---|---|---|---|---|---|---|---|---|
| DSS | - | + | + | + | + | + | + | + | + | + |
| Ast2B | - | - | - | + | + | + | + | - | - | - |
| Ucn2 | - | + | - | + | - | - | - | - | - | - |
| TXYF-L | - | - | - | - | + | - | - | - | - | + |
| TXYF-M | - | - | - | - | - | + | - | - | + | - |
| TXYF-H | - | - | + | - | - | - | + | - | - | - |

**D****E**

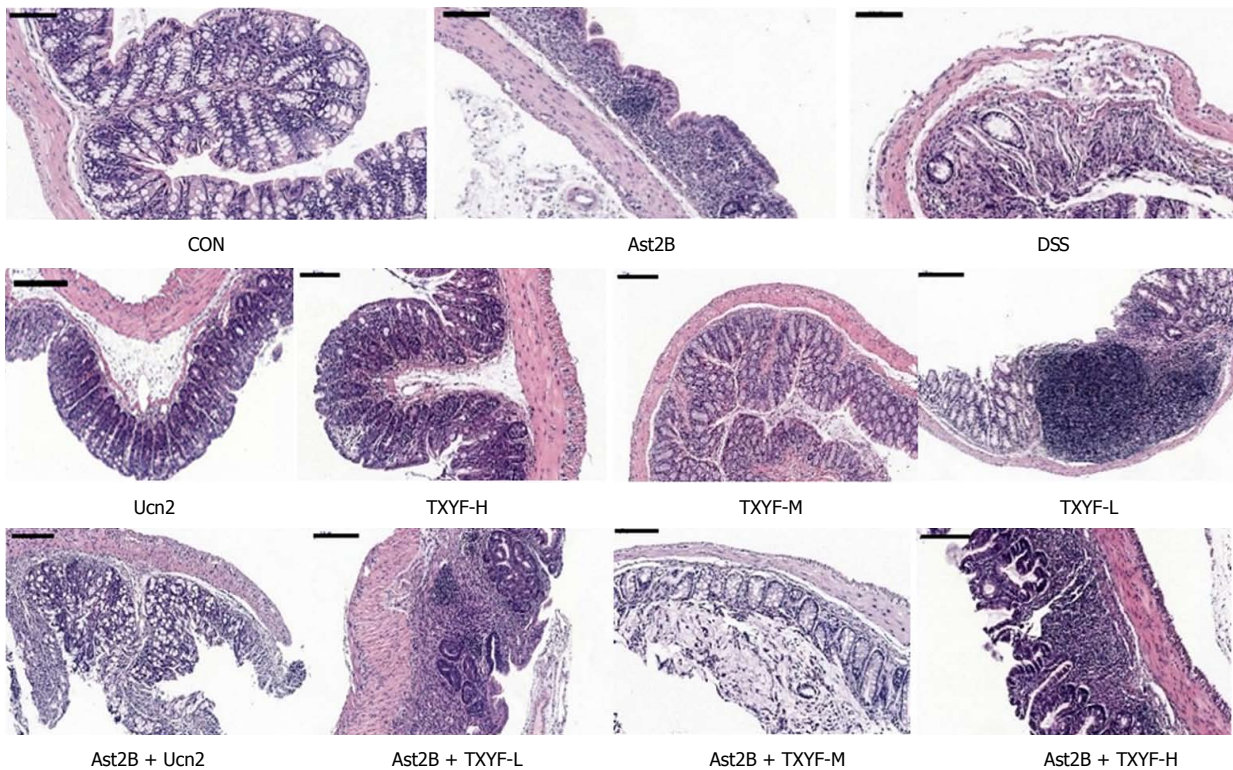


Figure 1 Inhibition of CRH-R2 signaling aggravates symptoms of DSS-induced colitis in mice. A: Mice body weights measured for 16 d, and shown as percentage of weight change; B: Colon length; C: Representative photographs of colon lengths; D: DAI; E: Histological scores were evaluated on the 16th day; F: Representative images of hematoxylin-eosin staining histology. Data are presented as mean \pm standard deviation, $n = 6\text{--}10$ per group, scale bar = 200 μm . $^{\text{a}}P < 0.001$ vs control group; $^{\text{b}}P < 0.05$, $^{\text{c}}P < 0.001$ vs DSS group; $^{\text{d}}P < 0.001$ vs Ucn2 group; $^{\text{e}}P < 0.05$ vs TXYF-L group; $^{\text{f}}P < 0.01$, $^{\text{g}}P < 0.001$ vs TXYF-M group; $^{\text{h}}P < 0.05$, $^{\text{i}}P < 0.001$ vs TXYF-H group. CRH-R2: Corticotropin-releasing hormone-receptor 2; DAI: Disease activity index; DSS: Dextran sulfate sodium; TXYF: Tong-Xie-Yao-Fang.

China), respectively. All assays were conducted by following the manufacturer's instruction.

Statistical analysis

All analyses were performed using SPSS 24.0 statistical software (IBM Corp., Armonk, NY, United States). Comparisons between groups were performed using one-way analysis of variance (ANOVA), followed by Scheffe post hoc test for multiple comparisons, otherwise a Dunnett's T3 method was used. All data are expressed as the mean \pm SD. $P < 0.05$ was considered statistically significant.

RESULTS

Inhibition of CRH-R2 signaling aggravates the symptoms of DSS-induced colitis in mice

We first assessed the involvement of CRH-R2 signaling in mucosal repair after colitis by administering the CRH-R2 antagonist Ast2B to mice after induction of DSS colitis. Mice received an intraperitoneal injection of Ast2B daily for 9 d after withdrawal of DSS, and body weight loss, DAI, colon length and histological score were monitored.

Compared with the DSS group, mice treated with the CRH-R2 antagonist Ast2B showed more body weight loss ($P < 0.05$) (Figure 1A) and shorter colon lengths (4.90 ± 0.32 cm vs 6.21 ± 0.34 cm, $P < 0.05$)

(Figure 1B). DAI score and histological score were used to evaluate the severity of UC in mice. The mice in the Ast2B group exhibited significantly higher DAI scores (3.61 ± 0.53 vs 2.42 ± 0.32 , $P < 0.05$) (Figure 1D) and histological scores (11.50 ± 1.05 vs 8.33 ± 1.03 , $P < 0.05$) (Figure 1E) compared to the mice in the DSS group.

Interestingly, mice treated with Ucn2 after DSS-induced colitis showed a smaller degree of body weight loss ($P < 0.001$) (Figure 1A), longer colon length (9.58 ± 0.62 cm vs 6.21 ± 0.34 cm, $P < 0.001$) (Figure 1B), lower DAI (0.87 ± 0.55 vs 2.42 ± 0.32 , $P < 0.001$) (Figure 1D) and improved histological scores (4.33 ± 1.50 vs 8.33 ± 1.03 , $P < 0.05$) (Figure 1E) compared to the mice in the DSS group. However, a significant statistical difference was found between the Ast2B + Ucn2 group and the Ucn2 group (Figure 1A-F).

Inhibition of CRH-R2 signaling increases secretion of inflammatory cytokines in colon tissues of DSS-induced UC mice

The levels of proinflammatory factors such as TNF- α , CXCL-1 and IL-6 in mouse colon tissues were detected by real time-PCR and ELISA. Compared with the DSS group, the Ast2B group showed significantly up-regulated mRNA expression of TNF- α (6.19 ± 0.51 vs 3.87 ± 0.98 , $P < 0.05$) (Figure 2A), CXCL-1 (10.77 ± 2.55 vs 5.08 ± 0.76 , $P < 0.05$) (Figure 2B), and IL-6

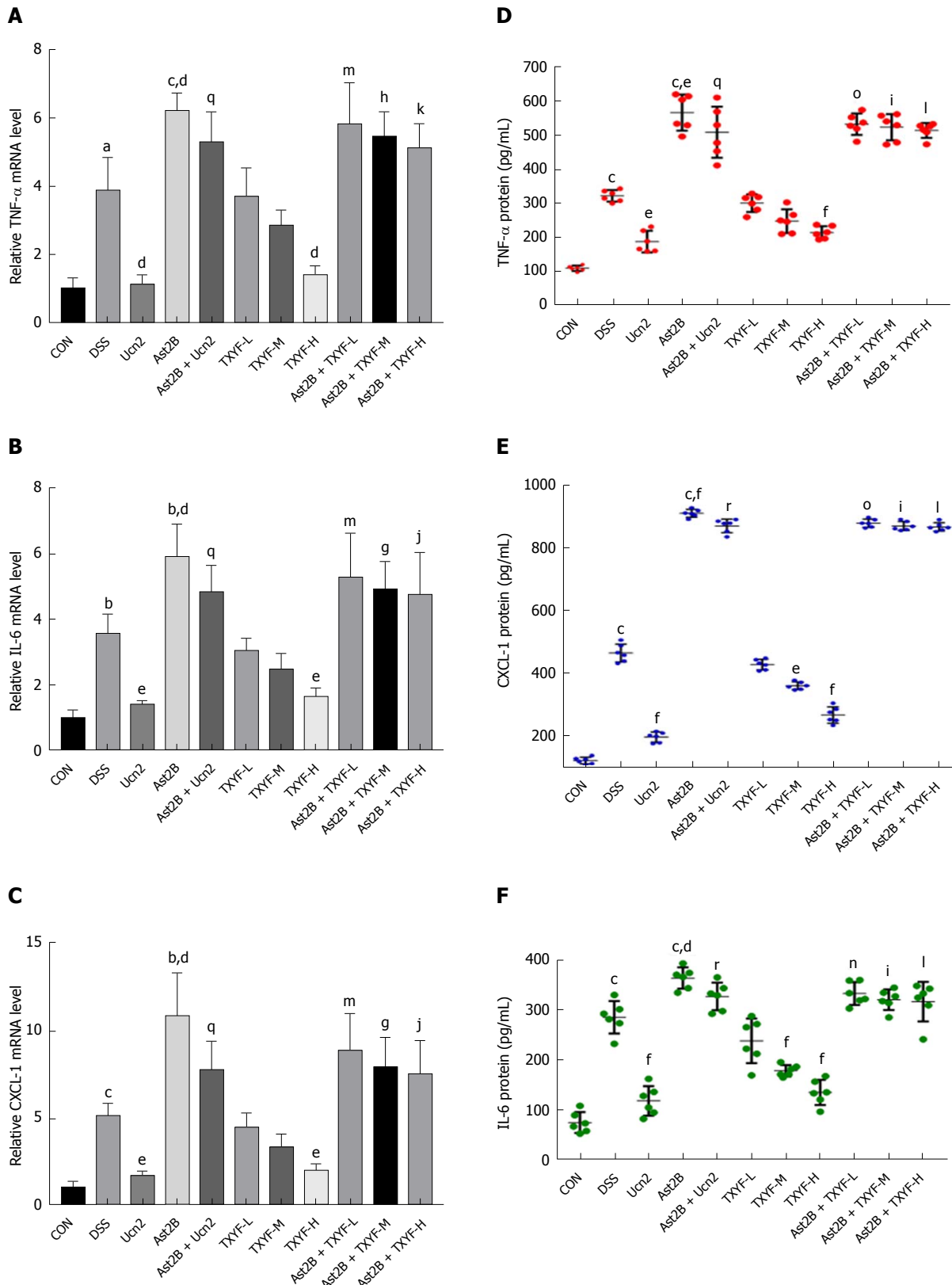


Figure 2 Inhibition of CRH-R2 signaling increases secretion of inflammatory cytokines in colon tissues of DSS-induced ulcerative colitis mice. A-C: Real time-PCR-assessed mRNA level of TNF α (A), CXCL-1 (B) and IL 6 (C) in colon tissues. The mRNA level in each group was determined relative to the level in the control group (defined as 100%); E-F: Enzyme-linked immunosorbent assay-detected protein levels of TNF α (D), CXCL-1 (E) and IL 6 (F) in colon tissues. Data are presented as mean \pm standard deviation, $n = 6$ per group. $^bP < 0.01$, $^cP < 0.001$ vs control group; $^dP < 0.05$, $^eP < 0.01$, $^fP < 0.001$ vs DSS group; $^gP < 0.01$, $^hP < 0.001$ vs Ucn2 group; $^iP < 0.05$, $^jP < 0.01$, $^kP < 0.001$ vs TXYF-L group; $^lP < 0.05$, $^mP < 0.01$, $^nP < 0.001$ vs TXYF-M group; $^oP < 0.05$, $^pP < 0.01$, $^qP < 0.001$ vs TXYF-H group. CRH-R2: Corticotropin-releasing hormone-receptor 2; DSS: Dextran sulfate sodium; TXYF: Tong-Xie-Yao-Fang.

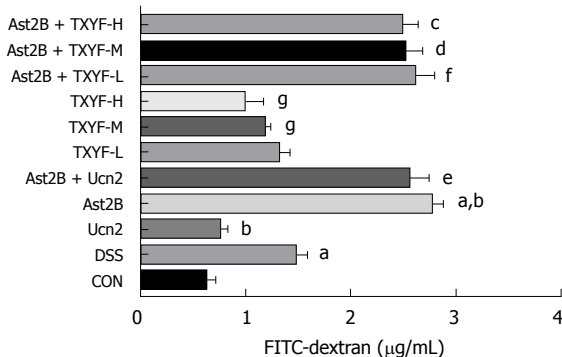


Figure 3 Inhibition of CRH-R2 signaling promotes intestinal permeability in DSS-induced colitis. The FITC-dextran levels in serum were determined. Data are presented as mean \pm standard deviation, $n = 6$ per group. ^a $P < 0.001$ vs control group; ^b $P < 0.05$, ^c $P < 0.001$ vs DSS group; ^d $P < 0.001$ vs Ucn2 group; ^e $P < 0.001$ vs TXYF-L group; ^f $P < 0.001$ vs TXYF-M group; ^g $P < 0.001$ vs TXYF-H group. CRH-R2: Corticotropin-releasing hormone-receptor 2; DSS: Dextran sulfate sodium; TXYF: Tong-Xie-Yao-Fang.

(5.93 ± 0.99 vs 3.55 ± 0.62 , $P < 0.05$) (Figure 2C). Meanwhile, the protein expression levels of TNF- α (Figure 2D), CXCL-1 (Figure 2E) and IL-6 (Figure 2F) were increased markedly in the Ast2B group.

However, compared with the DSS group, the Ucn2 group showed significantly decreased mRNA expression of TNF- α (Figure 2A), CXCL-1 (Figure 2B) and IL-6 (Figure 2C). Simultaneously, the Ucn2 group demonstrated reduced protein expression of TNF- α (Figure 2D), CXCL-1 (Figure 2E) and IL-6 (Figure 2F). Interestingly, the Ast2B + Ucn2 group showed drastically increased mRNA and protein expression of TNF- α , CXCL-1 and IL-6 compared with the Ucn2 group ($P < 0.05$ for all).

Inhibition of CRH-R2 signaling promotes intestinal permeability in DSS induced colitis

To determine the effect of CRH-R2 signaling on epithelial permeability, we analyzed intestinal permeability in DSS-induced colitis model by measuring the concentration of the serum FITC. The concentration of serum FITC-dextran was higher in the Ast2B group than DSS group ($2.76 \pm 0.11 \mu\text{g/mL}$ vs $1.47 \pm 0.11 \mu\text{g/mL}$, $P < 0.05$) (Figure 3). However, the concentration of serum FITC-dextran in the Ucn2 group was lower than DSS group ($0.75 \pm 0.07 \mu\text{g/mL}$ vs $1.47 \pm 0.11 \mu\text{g/mL}$, $P < 0.05$) (Figure 3). An obvious difference was observed between the Ast2B+Ucn2 group and the Ucn2 group.

Inhibition of CRH-R2 signaling promotes colonic epithelial cell apoptosis and reduces epithelial cell proliferation

The effect of Ast2B on cell proliferation and cell death was then determined. TUNEL staining was significantly increased in the Ast2B group compared with the DSS group (1422.39 ± 90.71 vs 983.01 ± 98.17 , $P < 0.001$) (Figure 4L). At the same time, the Ast2B group showed significantly decreased cell proliferation (4.97 ± 4.25

vs 22.51 ± 8.22 , $P < 0.05$) (Figure 5L). Interestingly, the Ucn2 group showed promoted colonic epithelial cell proliferation (Figure 5L) and reduced epithelial cell apoptosis (Figure 4L). However, significant statistical differences were found between the Ucn2 group and the Ast2B + Ucn2 group with regards to colonic epithelial cell apoptosis and proliferation ($P < 0.01$ for both).

TXYF promotes mucosal repair in colitis mice by regulating CRH-R2 signaling

To obtain insight into the underlying mechanism responsible for promoting mucosal repair of TXYF, DSS-induced colitis mice were pretreated with the CRH-R2 antagonist Ast2B, and later treated with various doses of aqueous TXYF extracts.

Compared with the DSS group, the TXYF-H groups had lower DAI scores (Figure 1D) and histological scores (Figure 1E), and decreased body weight loss (Figure 1A). TXYF-M,H groups, on the other hand, had longer colon length (Figure 1B) and improved intestinal permeability (Figure 3). Furthermore, TXYF inhibited secretion of inflammatory cytokines in colon tissues (Figure 2A-F) and promoted colonic epithelial cell proliferation (Figure 5L), along with reducing apoptosis (Figure 4L). However, the Ast2B + TXYF groups showed significant statistical difference in DAI, body weight loss, colon length and histological scores, when compared with the TXYF groups. As for inhibiting secretion of inflammatory cytokines, the Ast2B + TXYF groups demonstrated significant differences within the TXYF groups. Additionally, the Ast2B + TXYF groups showed markedly improved intestinal permeability in DSS-induced colitis compared with the TXYF groups, respectively. In addition, the Ast2B + TXYF groups demonstrated significant differences with the TXYF groups in promoting colonic epithelial cell proliferation and reducing epithelial cell apoptosis.

These results further confirm the idea that CRH-R2 signaling is the main mechanism of TXYF-mediated mucosal repair in DSS-induced colitis in mice.

DISCUSSION

Mucosal healing is a desired therapeutic end-point in the treatment of IBD; interventions that promote restoration of the epithelial barrier are needed to limit inflammation and to prevent future injury. Mucosal healing consists of two processes^[15]. Firstly, intact cells in the adjacent region migrate to the injured area; then, the cells compensate for damaged cells by proliferation and help to maintain normal thickness of the intestinal epithelium. Therefore, the migration and proliferation of intestinal epithelial cells are the key mechanisms for the healing of epithelial defects after mucosal injury. In addition, inhibiting apoptosis of intestinal epithelial cells can promote the healing process of mucosa^[37]. It is well known that intestinal epithelial barrier defects are

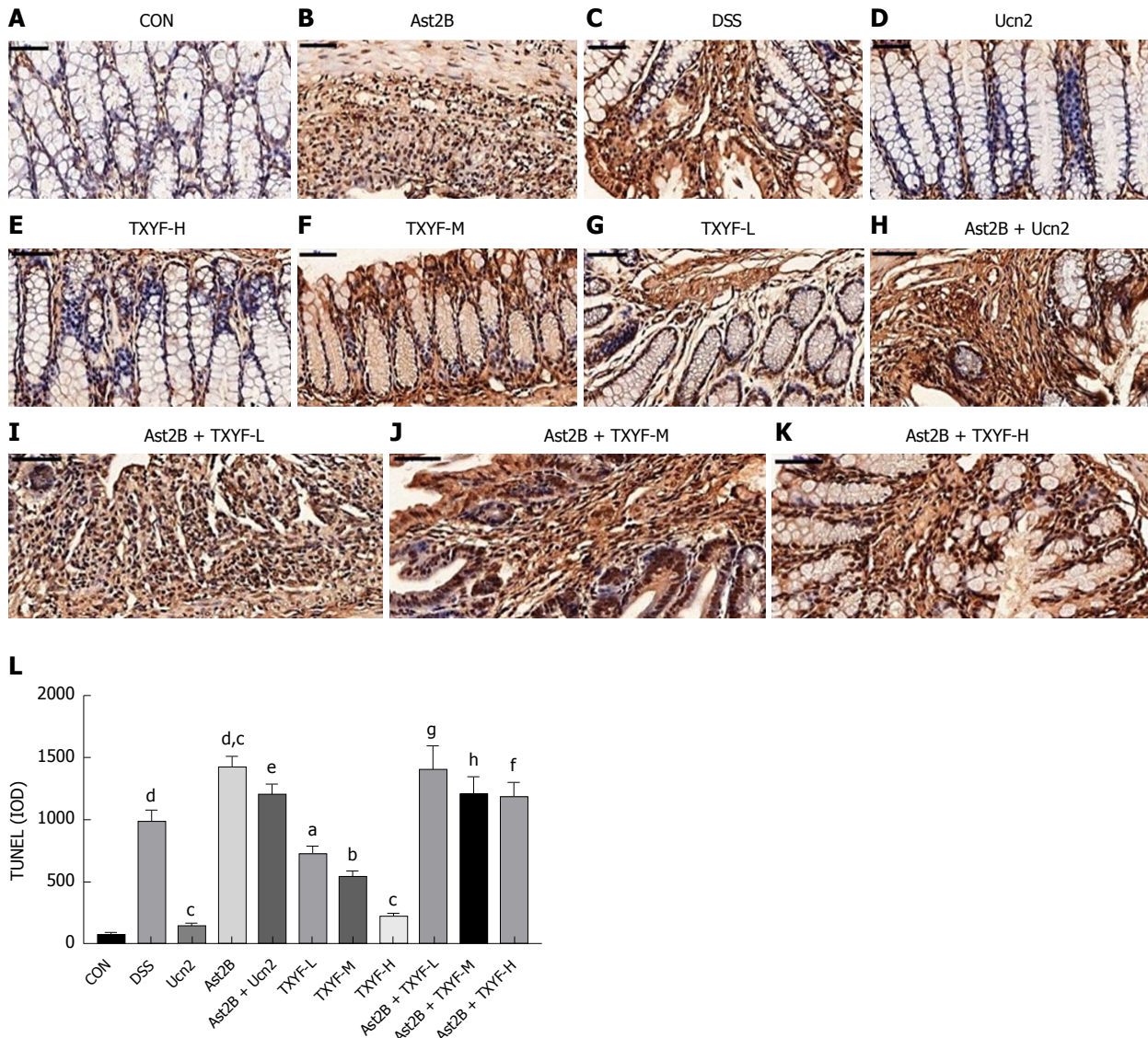


Figure 4 Inhibition of CRH-R2 signaling promotes colonic epithelial cell apoptosis in DSS-induced colitis. A-K: Representative images from TUNEL sections; L: Quantification of TUNEL data. Data are presented as mean \pm standard deviation, $n = 6$ per group, scale bar = 50 μ m. ^a $P < 0.001$ vs control group; ^b $P < 0.05$, ^c $P < 0.01$, ^d $P < 0.001$ vs DSS group; ^e $P < 0.001$ vs Ucn2 group; ^f $P < 0.01$ vs TXYF-L group; ^g $P < 0.01$ vs TXYF-M group; ^h $P < 0.001$ vs TXYF-H group. CRH-R2: Corticotropin-releasing hormone-receptor 2; DSS: Dextran sulfate sodium; TUNEL: Terminal deoxynucleotidyl transferase dUTP nick-end labeling; TXYF: Tong-Xie-Yao-Fang.

characterized by increased intestinal permeability.

In the present study, it was found that selective inhibition of CRH-R2 signaling can aggravate symptoms of DSS-induced colitis, destroy the impaired intestinal barrier function, promote colonic epithelial cell apoptosis and reduce epithelial cell proliferation. After treatment with Ucn2 and TXYF, DSS-induced mice demonstrated ameliorated symptoms of DSS-induced colitis, improved impaired intestinal barrier function, promoted colonic epithelial cell proliferation and reduced epithelial cell apoptosis. Moreover, Ucn2 and TXYF reduced the expression of the proinflammatory factors TNF- α , CXCL-1, and IL-6 in colon tissues.

Cytokines play a central role in the regulation of both intestinal inflammation and mucosal repair mechanisms^[38]. Treatments that neutralize the proinflammatory actions of TNF- α promote mucosal healing and are a standard

of current IBD treatment paradigms^[7,38]. In addition, production of the key proinflammatory cytokine IL-6 correlates with the degree of active intestinal inflammation in IBD patients^[39], further supporting the concept that therapeutic interventions that modulate cytokine production and/or release may promote mucosal repair after inflammation. Taken together, these results indicate that Ucn2 and TXYF promote mucosal repair.

Studies from others have found that CRH may be involved in the maintenance of intestinal barrier integrity by regulating autophagy in the intestinal epithelial cells^[18]. Our previous studies also found that CRH could induce an increase in intercellular permeability in the intestinal epithelium^[22]. Some studies have also found that CRH-R2 can activate the antiinflammatory response of intestinal mucosa and exert an antiinflammatory effect^[23]. In addition, activation of CRH-R2 can promote

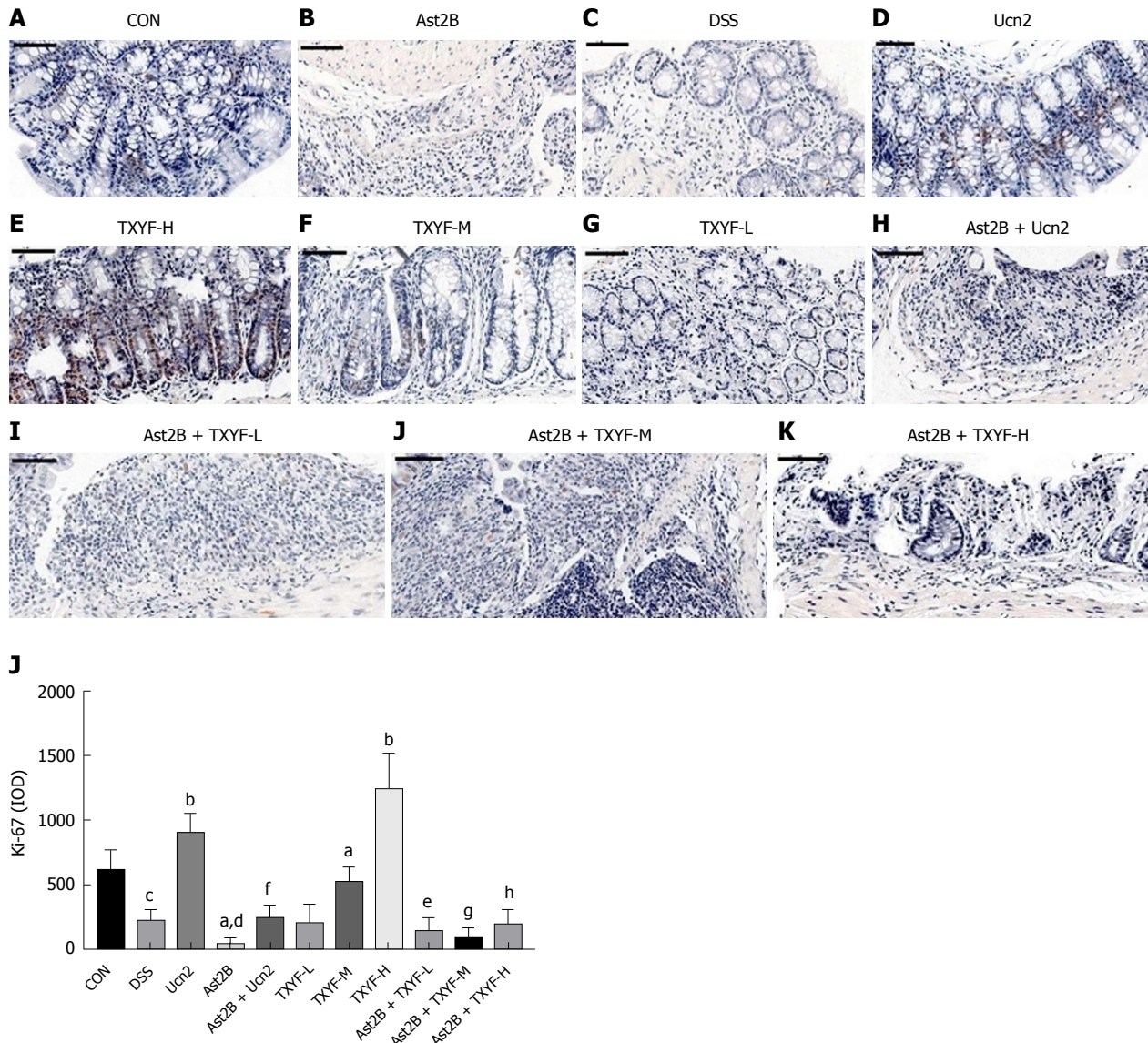


Figure 5 Inhibition of CRH-R2 signaling reduces epithelial cell proliferation in DSS-induced colitis. A-K: Representative images from Ki-67 immunoreactive sections; L: Quantification of Ki-67 immunohistochemistry data. Data presented as mean \pm standard deviation, $n = 6$ per group, scale bar = 50 μ m. $^aP < 0.05$, $^bP < 0.01$ vs control group; $^cP < 0.05$, $^dP < 0.01$ vs DSS group. $^eP < 0.01$ vs Ucn2 group; $^fP < 0.05$ vs TXYF-L group; $^gP < 0.01$ vs TXYF-M group; $^hP < 0.01$ vs TXYF-H group. CRH-R2: Corticotropin-releasing hormone-receptor 2; DSS: Dextran sulfate sodium; TXYF: Tong-Xie-Yao-Fang.

the migration and proliferation of colon cancer cells and gastric mucosa cells^[24,25]. Furthermore, the expression of CRH-R2 has been reported as down-regulated in biopsy specimens of UC patients^[26] and CRH-deficient mice have been reported as unable to initiate healing responses after acute experimental colitis^[27].

These results suggest a role for the CRH peptide family, especially CRH-R2, in mucosal repair mechanisms. It is known that Ucn2 is a peptide which binds exclusively to CRH-R2. Significant statistical differences were found between the Ast2B group and the Ast2B + Ucn2 group. Thus, a conclusion can be made that CRH-R2 activated the intestinal mucosal antiinflammatory response by regulating the migration, proliferation and apoptosis of intestinal epithelial cells in colitis mice.

Subsequently, the efficacy of TXYF was assessed.

According to the theory of traditional Chinese medicine, IBD belongs to "diarrhea, dysentery". The principle of treatment is focused on relieving pain and eliminating dampness and diarrhea. TXYF is a classic formula in the Jing yue quan shu (Jingyue's Complete Book), which consists of atractylodes rhizome (*Rhizoma Atractylodis Macrocephalae*) head groups, white peony root (*Radix Paeoniae Alba*), dried tangerine peel (*Pericarpium Citri Reticulatae*), and divaricate saponnikovia root (*Radix Saponnikoviae*). TXYF has been believed to be effective in improving disorders of the digestive system and alleviating abdominal pain, diarrhea, and has been used widely as a medication to treat inflammatory bowel syndrome and UC clinically, without inducing hepatomegaly or splenomegaly^[40-42].

TXYF has also been shown to improve reconstruction

of the intestinal epithelial barrier and promote the healing of mucosa in UC^[28,29]. Our previous study found that TXYF down-regulated CRH-R1 and up-regulated CRH-R2. While the mechanism underlying TXYF promotion of mucosal repair is not well understood, it is thought to intervene using CRH-R2 and to regulate the migration, proliferation and apoptosis of epithelial cells, like the role of Ucn2^[30,31].

Herein, we describe the selective inhibition of CRH-R2 signaling in the intestinal mucosa of mice after experimental colitis, along with TXYF treatment, leading to exacerbated symptoms of DSS-induced colitis, delayed healing, increased expression of proinflammatory factors TNF- α , CXCL-1 and IL-6 in colon tissues, decreased epithelial cell proliferation and promoted cell apoptosis. These results suggest that TXYF promoted the mucosal repair process of colitis mice by regulating CRH-R2.

In conclusion, CRH-R2 activates the intestinal mucosal antiinflammatory response by regulating the migration, proliferation and apoptosis of intestinal epithelial cells in colitis mice, and exerts an antiinflammatory effect. The effects of TXYF on the mucosal repair process are focused on regulating CRH-R2 in colitis mice.

ARTICLE HIGHLIGHTS

Research background

Mucosal healing is a desired therapeutic end-point in the treatment of inflammatory bowel disease (IBD). However, thorough treatment of IBD is difficult and there are some adverse reactions. According to studies, corticotropin-releasing hormone (CRH)-receptor (R)2 can activate the inflammatory response of intestinal mucosa. Our preliminary study found that Tong-Xie-Yao-Fang could lower CRH-R1, increase the expression of CRH-R2, and participates in reconstruction of the intestinal barrier.

Research motivation

Mucosal healing is a desired therapeutic end-point in the treatment of IBD. However, the mechanism of mucosal healing is still unclear.

Research objectives

To explore the significance of CRH-R2 in the mucosal healing of dextran sulfate sodium (DSS)-induced colitis and study the effect of Tong-Xie-Yao-Fang (TXYF) on CRH-R2.

Research methods

Ulcerative colitis (UC) was induced in mice by administration of 3% (w/v) DSS for 7 d. Then, mice were administered urocortin (Ucn)-2 or various doses of aqueous TXYF extracts, the CRH-R2 antagonist Astressin (Ast)2B, Ast2B + Ucn2, or Ast2B with various doses of aqueous TXYF extracts for 9 d. The colitis disease activity index (DAI) was assessed to evaluate the condition of colitis. The expression level of Ki-67 represented the proliferation of colonic epithelial cells. The expression levels of inflammation cytokines IL-6, TNF- α and CXCL-1 were examined by PCR and enzyme-linked immunosorbent assay.

Research results

Compared with the DSS group, mice treated with the CRH-R2 antagonist Ast2B showed greater loss of body weight, shorter colon lengths, and higher DAI and histological scores. Additionally, the Ast2B group showed increased intestinal permeability, improved secretion of inflammatory cytokines in colon tissue and reduced colonic epithelial cell proliferation. Increased apoptosis was also demonstrated. The Ucn2 group demonstrated lower DAI and histological

scores. Diminished weight loss, longer colon length, reduced intestinal permeability, inhibited secretion of inflammatory cytokines in colon tissue and increased colonic epithelial cell proliferation were all observed. Reduced apoptosis was also observed.

Research conclusions

CRH-R2 activates the intestinal mucosal antiinflammatory response and plays an important antiinflammatory role. TXYF promotes the mucosal repair process in colitis mice.

Research perspectives

The CRH-R2 signaling pathway plays a pivotal role in mucosal healing in experimental UC in mice. Mucosal healing is a desired therapeutic end-point in the treatment of IBD. Thus, the findings of this study indicate a new potential mechanism by which CRH-R2 treats UC. TXYF, which has fewer side effects than other medicines, promotes the mucosal repair process of colitis mice by regulating CRH-R2. Therefore, TXYF can be used in patients with UC to promote their mucosal repair.

ACKNOWLEDGMENTS

We would like to thank our colleagues in the Institute of Digestive Disease affiliated the First Clinical Medical College of Zhejiang Chinese Medical University for their help and support in this research.

REFERENCES

- Norouzinia M, Chaleshi V, Alizadeh AHM, Zali MR. Biomarkers in inflammatory bowel diseases: insight into diagnosis, prognosis and treatment. *Gastroenterol Hepatol Bed Bench* 2017; **10**: 155-167 [PMID: 29118930]
- Jin F L, Yi-Ping L I. Progress in the traditional Chinese medicine treatment of ulcerative colitis. *China Modern Medicine* 2016
- Ouyang Q, Xue LY. Inflammatory bowel disease in the 21(st) century in China: turning challenges into opportunities. *J Dig Dis* 2012; **13**: 195-199 [PMID: 22435503 DOI: 10.1111/j.1751-2980.2012.00579.x]
- Bernstein CN, Loftus EV Jr, Ng SC, Lakatos PL, Moum B; Epidemiology and Natural History Task Force of the International Organization for the Study of Inflammatory Bowel Disease (IOIBD). Hospitalisations and surgery in Crohn's disease. *Gut* 2012; **61**: 622-629 [PMID: 22267595 DOI: 10.1136/gutjnl-2011-301397]
- Magro F, Rodrigues A, Vieira AI, Portela F, Cremers I, Cotter J, Correia L, Duarte MA, Tavares ML, Lago P, Ministro P, Peixe P, Lopes S, Garcia EB. Review of the disease course among adult ulcerative colitis population-based longitudinal cohorts. *Inflamm Bowel Dis* 2012; **18**: 573-583 [PMID: 21793126 DOI: 10.1002/ibd.21815]
- Baars JE, Nuij VJ, Oldenburg B, Kuipers EJ, van der Woude CJ. Majority of patients with inflammatory bowel disease in clinical remission have mucosal inflammation. *Inflamm Bowel Dis* 2012; **18**: 1634-1640 [PMID: 22069022 DOI: 10.1002/ibd.21925]
- van Dullemen HM, van Deventer SJ, Hommes DW, Bijl HA, Jansen J, Tytgat GN, Woody J. Treatment of Crohn's disease with anti-tumor necrosis factor chimeric monoclonal antibody (cA2). *Gastroenterology* 1995; **109**: 129-135 [PMID: 7797011 DOI: 10.1016/0016-5085(95)90277-5]
- Rutgeerts P, D'Haens G, Targan S, Vasiliauskas E, Hanauer SB, Present DH, Mayer L, Van Hogezand RA, Braakman T, DeWoody KL, Schaible TF, Van Deventer SJ. Efficacy and safety of retreatment with anti-tumor necrosis factor antibody (infliximab) to maintain remission in Crohn's disease. *Gastroenterology* 1999; **117**: 761-769 [PMID: 10500056 DOI: 10.1016/S0016-5085(99)70332-X]

- 9 **Rutgeerts P**, Diamond RH, Bala M, Olson A, Lichtenstein GR, Bao W, Patel K, Wolf DC, Safdi M, Colombel JF, Lashner B, Hanauer SB. Scheduled maintenance treatment with infliximab is superior to episodic treatment for the healing of mucosal ulceration associated with Crohn's disease. *Gastrointest Endosc* 2006; **63**: 433-442; quiz 464 [PMID: 16500392 DOI: 10.1016/j.gie.2005.08.011]
- 10 **Hanauer SB**, Feagan BG, Lichtenstein GR, Mayer LF, Schreiber S, Colombel JF, Rachmilewitz D, Wolf DC, Olson A, Bao W, Rutgeerts P; ACCENT I Study Group. Maintenance infliximab for Crohn's disease: the ACCENT I randomised trial. *Lancet* 2002; **359**: 1541-1549 [PMID: 12047962 DOI: 10.1016/S0140-6736(02)08512-4]
- 11 **Sands BE**, Anderson FH, Bernstein CN, Chey WY, Feagan BG, Fedorak RN, Kamm MA, Korzenik JR, Lashner BA, Onken JE, Rachmilewitz D, Rutgeerts P, Wild G, Wolf DC, Marsters PA, Travers SB, Blank MA, van Deventer SJ. Infliximab maintenance therapy for fistulizing Crohn's disease. *N Engl J Med* 2004; **350**: 876-885 [PMID: 14985485 DOI: 10.1056/NEJMoa030815]
- 12 **Römkens TE**, Gijsbers K, Kievit W, Hoentjen F, Drent JP. Treatment Targets in Inflammatory Bowel Disease: Current Status in Daily Practice. *J Gastrointest Liver Dis* 2016; **25**: 465-471 [PMID: 27981302 DOI: 10.15403/jgld.2014.1121.254.ken]
- 13 **Taupin D**, Podolsky DK. Trefoil factors: initiators of mucosal healing. *Nat Rev Mol Cell Biol* 2003; **4**: 721-732 [PMID: 14506475 DOI: 10.1038/nrm1203]
- 14 **Sturm A**, Dignass AU. Epithelial restitution and wound healing in inflammatory bowel disease. *World J Gastroenterol* 2008; **14**: 348-353 [PMID: 18200658 DOI: 10.3748/wjg.14.348]
- 15 **Neurath MF**. New targets for mucosal healing and therapy in inflammatory bowel diseases. *Mucosal Immunol* 2014; **7**: 6-19 [PMID: 24084775 DOI: 10.1038/mi.2013.73]
- 16 **Neurath MF**, Travis SP. Mucosal healing in inflammatory bowel diseases: a systematic review. *Gut* 2012; **61**: 1619-1635 [PMID: 22842618 DOI: 10.1136/gutjnl-2012-302830]
- 17 **Laukoetter MG**, Nava P, Nusrat A. Role of the intestinal barrier in inflammatory bowel disease. *World J Gastroenterol* 2008; **14**: 401-407 [PMID: 18200662]
- 18 **Giannogonas P**, Apostolou A, Manousopoulou A, Theocharis S, Macari SA, Psarras S, Garbis SD, Pothoulakis C, Karalis KP. Identification of a novel interaction between corticotropin releasing hormone (Crh) and macroautophagy. *Sci Rep* 2016; **6**: 23342 [PMID: 26987580 DOI: 10.1038/srep23342]
- 19 **Bonaz BL**, Bernstein CN. Brain-gut interactions in inflammatory bowel disease. *Gastroenterology* 2013; **144**: 36-49 [PMID: 23063970 DOI: 10.1053/j.gastro.2012.10.003]
- 20 **Hillhouse EW**, Grammatopoulos DK. The molecular mechanisms underlying the regulation of the biological activity of corticotropin-releasing hormone receptors: implications for physiology and pathophysiology. *Endocr Rev* 2006; **27**: 260-286 [PMID: 16484629 DOI: 10.1210/er.2005-0034]
- 21 **Hoffman JM**, Baritaki S, Ruiz JJ, Sideri A, Pothoulakis C. Corticotropin-Releasing Hormone Receptor 2 Signaling Promotes Mucosal Repair Responses after Colitis. *Am J Pathol* 2016; **186**: 134-144 [PMID: 26597886 DOI: 10.1016/j.ajpath.2015.09.013]
- 22 **Wang X T**, Hu Y, Li M, Lv B. Study on the role of stress through CRF up regulation of CK8 mediated change of close connexin in the pathogenesis of irritable bowel syndrome. The national association of Chinese and western medicine on digestive system disease academic conference, 2015
- 23 **Im E**, Rhee SH, Park YS, Fiocchi C, Taché Y, Pothoulakis C. Corticotropin-releasing hormone family of peptides regulates intestinal angiogenesis. *Gastroenterology* 2010; **138**: 2457-2467, 2467.e1-2467.e5 [PMID: 20206175 DOI: 10.1053/j.gastro.2010.02.055]
- 24 **Ducarouge B**, Pelissier-Rota M, Lainé M, Cristina N, Vachez Y, Scoazec JY, Bonaz B, Jacquier-Sarlin M. CRF2 signaling is a novel regulator of cellular adhesion and migration in colorectal cancer cells. *PLoS One* 2013; **8**: e79335 [PMID: 24260200 DOI: 10.1371/journal.pone.0079335]
- 25 **Chatzaki E**, Lambropoulou M, Constantinidis TC, Papadopoulos N, Taché Y, Minopoulos G, Grigoriadis DE. Corticotropin-releasing factor (CRF) receptor type 2 in the human stomach: protective biological role by inhibition of apoptosis. *J Cell Physiol* 2006; **209**: 905-911 [PMID: 16972272 DOI: 10.1002/jcp.20792]
- 26 **Chatzaki E**, Anton PA, Million M, Lambropoulou M, Constantinidis T, Kolios G, Taché Y, Grigoriadis DE. Corticotropin-releasing factor receptor subtype 2 in human colonic mucosa: down-regulation in ulcerative colitis. *World J Gastroenterol* 2013; **19**: 1416-1423 [PMID: 23539366 DOI: 10.3748/wjg.v19.i9.1416]
- 27 **Chaniotou Z**, Giannogonas P, Theocharis S, Teli T, Gay J, Savidge T, Koutmani Y, Brugni J, Kokkotou E, Pothoulakis C, Karalis KP. Corticotropin-releasing factor regulates TLR4 expression in the colon and protects mice from colitis. *Gastroenterology* 2010; **139**: 2083-2092 [PMID: 20732324 DOI: 10.1053/j.gastro.2010.08.024]
- 28 **Stanisic V**, Quigley EM. The overlap between IBS and IBD: what is it and what does it mean? *Expert Rev Gastroenterol Hepatol* 2014; **8**: 139-145 [PMID: 24417262 DOI: 10.1586/17474124.2014.876361]
- 29 **Quigley EM**. Overlapping irritable bowel syndrome and inflammatory bowel disease: less to this than meets the eye? *Therap Adv Gastroenterol* 2016; **9**: 199-212 [PMID: 26929782 DOI: 10.1177/1756283X15621230]
- 30 **Chao G**, Lv B, Meng L, Zhang S, Zahng L, Guo Y. [Influence of tongxie prescription on CRF expression in spinal cord and brain of hypersensitive viscera rats]. *Zhongguo Zhong Yao Za Zhi* 2010; **35**: 2012-2016 [PMID: 20931858]
- 31 **Ding Y**, Lv B, Meng L N, Fan Y H, Shen Y. Effect of Tongxieyaofang on Colonic Mucosal Protein Expression Profile in Rats with Visceral Hypersensitivity. *Chinese Journal of Gastroenterology* 2012; **17**: 660-664 [DOI: 10.3969/j.issn.1008-7125.2012.11.005]
- 32 **Yang C**, Xiong Y, Zhang SS, An FM, Sun J, Zhang QL, Zhan Q. Regulating effect of TongXie-YaoFang on colonic epithelial secretion via Cl⁻ and HCO₃⁻ channel. *World J Gastroenterol* 2016; **22**: 10584-10591 [PMID: 28082810 DOI: 10.3748/wjg.v22.i48.10584]
- 33 **Hendrickson BA**, Gokhale R, Cho JH. Clinical aspects and pathophysiology of inflammatory bowel disease. *Clin Microbiol Rev* 2002; **15**: 79-94 [PMID: 11781268]
- 34 **Murthy SN**, Cooper HS, Shim H, Shah RS, Ibrahim SA, Sedergran DJ. Treatment of dextran sulfate sodium-induced murine colitis by intracolonic cyclosporin. *Dig Dis Sci* 1993; **38**: 1722-1734 [PMID: 8359087]
- 35 **Dieleman LA**, Palmen MJ, Akol H, Bloemena E, Peña AS, Meuwissen SG, Van Rees EP. Chronic experimental colitis induced by dextran sulphate sodium (DSS) is characterized by Th1 and Th2 cytokines. *Clin Exp Immunol* 1998; **114**: 385-391 [PMID: 9844047]
- 36 **Nguyen HT**, Dalmasso G, Torkvist L, Halfvarson J, Yan Y, Laroui H, Shmerling D, Tallone T, D'Amato M, Sitaraman SV, Merlin D. CD98 expression modulates intestinal homeostasis, inflammation, and colitis-associated cancer in mice. *J Clin Invest* 2011; **121**: 1733-1747 [PMID: 21490400 DOI: 10.1172/JCI44631]
- 37 **Seidelin JB**, Larsen S, Linnemann D, Vainer B, Coskun M, Troelsen JT, Nielsen OH. Cellular inhibitor of apoptosis protein 2 controls human colonic epithelial restitution, migration, and Rac1 activation. *Am J Physiol Gastrointest Liver Physiol* 2015; **308**: G92-G99 [PMID: 25394657 DOI: 10.1152/ajpgi.00089.2014]
- 38 **Neurath MF**. Cytokines in inflammatory bowel disease. *Nat Rev Immunol* 2014; **14**: 329-342 [PMID: 24751956 DOI: 10.1038/nri3661]
- 39 **Suzuki Y**, Saito H, Kasanuki J, Kishimoto T, Tamura Y, Yoshida S. Significant increase of interleukin 6 production in blood mononuclear leukocytes obtained from patients with active inflammatory bowel disease. *Life Sci* 1990; **47**: 2193-2197 [PMID: 2266787]
- 40 **Fan H**, Qiu MY, Mei JJ, Shen GX, Liu SL, Chen R. Effects of four regulating-intestine prescriptions on pathology and ultrastructure

- of colon tissue in rats with ulcerative colitis. *World J Gastroenterol* 2005; **11**: 4800-4806 [PMID: 16097047]
- 41 **Hu X**, Zhang X, Han B, Bei W. The inhibitory effect of tongxieyaofang on rats with post infectious irritable bowel syndrome through regulating colonic par-2 receptor. *BMC Complement Altern Med* 2013; **13**: 246 [PMID: 24088410 DOI: 10.1186/1472-6882-13-246]
- 42 **Lu X**, Zhang S, Yang C, Wang Z, Zhao L, Wu Z, Xie J. Effect of TongXie-YaoFang on Cl(-) and HCO₃ (-) Transport in Diarrhea-Predominant Irritable Bowel Syndrome Rats. *Evid Based Complement Alternat Med* 2016; **2016**: 7954982 [PMID: 27403199 DOI: 10.1155/2016/7954982]

P- Reviewer: Gassler N, Ozen H, Tarnawski AS **S- Editor:** Wang XJ
L- Editor: Filopodia **E- Editor:** Huang Y



Basic Study

Sodium chloride exacerbates dextran sulfate sodium-induced colitis by tuning proinflammatory and antiinflammatory lamina propria mononuclear cells through p38/MAPK pathway in mice

Hong-Xia Guo, Nan Ye, Ping Yan, Min-Yue Qiu, Ji Zhang, Zi-Gang Shen, Hai-Yang He, Zhi-Qiang Tian, Hong-Li Li, Jin-Tao Li

Hong-Xia Guo, Jin-Tao Li, Department of Microbiology, Third Military Medical University (Army Medical University), District Shapingba, Chongqing 400038, China

Hong-Xia Guo, Nan Ye, Min-Yue Qiu, Jin-Tao Li, Institute of Tropical Medicine, Third Military Medical University (Army Medical University), District Shapingba, Chongqing 400038, China

Ping Yan, Department of Obstetrics and Gynecology, Southwest Hospital, Third Military Medical University (Army Medical University), Chongqing 400038, China

Ji Zhang, Zi-Gang Shen, Hai-Yang He, Zhi-Qiang Tian, Institute of Immunology, Third Military Medical University (Army Medical University), District Shapingba, Chongqing 400038, China

Hong-Li Li, Department of Histology and Embryology, College of Basic Medicine, Third Military Medical University (Army Medical University), Chongqing 400038, China

ORCID number: Hong-Xia Guo (0000-0003-4476-3141); Nan Ye (0000-0001-8929-7813); Ping Yan (0000-0001-7984-9880); Min-Yue Qiu (0000-0002-7718-3111); Ji Zhang (0000-0002-6444-3949); Zi-Gang Shen (0000-0001-5224-5315); Hai-Yang He (0000-0002-2862-3600); Zhi-Qiang Tian (0000-0003-4609-6637); Hong-Li Li (0000-0003-0851-2310); Jin-Tao Li (0000-0003-3637-2386).

Author contributions: Li JT designed the research; Guo HX, Ye N, Li HL and Qiu MY performed the research; Yan P, Zhang J, Shen ZG, He HY and Tian ZQ contributed reagents and analytic tools; Ye N contributed to the statistical analysis; Guo HX and Li JT wrote the manuscript and carried out the critical revision of the manuscript; all authors provided final approval of the article.

Supported by National Natural Science Foundation of China, No. 81271813 and No. 81570497.

Institutional review board statement: This study was reviewed and approved by the Third Military Medical University (Army Medical University) Institutional Review Board.

Institutional animal care and use committee statement: All procedures involving the care and use of animals were approved by The Institutional Animal Care and Use Committee of the Third Military Medical University (Army Medical University).

Conflict-of-interest statement: All authors declared there were no conflicts of interests.

Data sharing statement: No additional data are available.

ARRIVE guidelines statement: The authors have read the ARRIVE guidelines, and the manuscript was prepared and revised according to the ARRIVE guidelines.

Open-Access: This article is an open-access article which was selected by an in-house editor and fully peer-reviewed by external reviewers. It is distributed in accordance with the Creative Commons Attribution Non Commercial (CC BY-NC 4.0) license, which permits others to distribute, remix, adapt, build upon this work non-commercially, and license their derivative works on different terms, provided the original work is properly cited and the use is non-commercial. See: <http://creativecommons.org/licenses/by-nc/4.0/>

Manuscript source: Unsolicited manuscript

Correspondence to: Jin-Tao Li, PhD, Professor, Institute of Tropical Medicine, Third Military Medical University (Army Medical University), Gaotanyan Street 30, Chongqing 400038, China. jltqms@tmmu.edu.cn

Telephone: +86-23-68752329

Fax: +86-23-68752329

Received: January 25, 2018

Peer-review started: January 26, 2018

First decision: February 24, 2018
Revised: March 11, 2018
Accepted: March 18, 2018
Article in press: March 18, 2018
Published online: April 28, 2018

Abstract

AIM

To investigate the influence of high salt on dextran sulfate sodium (DSS)-induced colitis in mice and explore the underlying mechanisms of this effect.

METHODS

DSS and NaCl were used to establish the proinflammatory animal model. We evaluated the colitis severity. Flow cytometry was employed for detecting the frequencies of Th1, macrophages and Tregs in spleen, mesenteric lymph node and lamina propria. The important role of macrophages in the promotion of DSS-induced colitis by NaCl was evaluated by depleting macrophages with clodronate liposomes. Activated peritoneal macrophages and lamina propria mononuclear cells (LPMCs) were stimulated with NaCl, and proteins were detected by western blotting. Cytokines and inflammation genes were analyzed by enzyme-linked immunosorbent assay and RT-PCR, respectively.

RESULTS

The study findings indicate that NaCl up-regulates the frequencies of CD11b⁺ macrophages and CD4⁺IFN- γ ⁺IL-17⁺ T cells in lamina propria in DSS-treated mice. CD3⁺CD4⁺CD25⁺Foxp3⁺ T cells, which can secrete high levels of IL-10 and TGF- β , increase through feedback in NaCl- and DSS-treated mice. Furthermore, clodronate liposomes pretreatment significantly alleviated DSS-induced colitis, indicating that macrophages play a vital role in NaCl proinflammatory activity. NaCl aggravates peritoneal macrophage inflammation by promoting the expressions of interleukin (IL)-1, IL-6 and mouse inducible nitric oxide synthase. Specifically, high NaCl concentrations promote p38 phosphorylation in lipopolysaccharide- and IFN- γ -activated LPMCs mediated by SGK1.

CONCLUSION

Proinflammatory macrophages may play an essential role in the onset and development of NaCl-promoted inflammation in DSS-induced colitis. The underlining mechanism involves up-regulation of the p38/MAPK axis.

Key words: Inflammatory bowel disease; Macrophage; NaCl; CD4⁺IFN- γ ⁺IL-17⁺ T cell; p38/MAPK

© The Author(s) 2018. Published by Baishideng Publishing Group Inc. All rights reserved.

Core tip: NaCl, as an indispensable environmental factor, evokes both innate and adaptive immune proinflammation cell activation in mice affected by dextran

sulfate sodium (DSS)-induced colitis. Proinflammatory CD4⁺ cells in DSS- and NaCl-treated mice are mainly double-positive IL-17⁺IFN- γ ⁺ T cells. Macrophage depletion significantly alleviates DSS-induced colitis. M1 macrophages play an important role in the proinflammatory effect of NaCl in the mouse gut. NaCl promotes M1 proinflammatory gene expression in lipopolysaccharide-activated peritoneal macrophage. The mechanism by which NaCl promotes DSS-induced colitis involves up-regulation of the p38/MAPK axis.

Guo HX, Ye N, Yan P, Qiu MY, Zhang J, Shen ZG, He HY, Tian ZQ, Li HL, Li JT. Sodium chloride exacerbates dextran sulfate sodium-induced colitis by tuning proinflammatory and antiinflammatory lamina propria mononuclear cells through p38/MAPK pathway in mice. *World J Gastroenterol* 2018; 24(16): 1779-1794 Available from: URL: <http://www.wjgnet.com/1007-9327/full/v24/i16/1779.htm> DOI: <http://dx.doi.org/10.3748/wjg.v24.i16.1779>

INTRODUCTION

Inflammatory bowel disease (IBD) is a chronic and recurrent disease, usually manifesting as ulcerative colitis and Crohn's disease (CD)^[1]. IBD is a high-risk factor for colorectal cancer and it is a serious threat to the human health globally. Although its etiology is presently unclear, findings yielded by extant studies indicate that IBD is a complex process involving heredity, environment and immunity^[2-5].

Innate and adaptive immune cells play different roles in IBD pathogenesis. Results obtained in a large number of studies have shown that Th17, Th1, regulatory T cells (Tregs) and macrophages play important roles in IBD pathogenesis. For instance, the number of Th17 cells increases significantly in mucosa lamina propria (LP) of colitis patients, whereby interleukin (IL)-17 is produced, resulting in mucosal damage and enhancing disease activity^[6,7]. Th1 polarization is related to colonic inflammation, through its induction of IFN- γ and TNF- α production, whereas the differential propensity to develop colitis is linked to the inherent tendency of the immune system to give rise to Th1 or Th17/Treg responses^[8]. Tregs, which are very important regulatory T cells, express IL-10 highly and inhibit inflammation in IBD^[9]. Macrophages in the intestinal mucosa of colitis patients can secrete the cytokines TNF- α , IL-1 and IL-6^[10]. Intestinal macrophages are the major population of antigen presenting cells in intestinal mucosa and they shape the types of T cell response to luminal antigens^[11].

Sodium chloride mediates the inflammatory effects of immune cells that are very important to IBD. NaCl exacerbates experimental autoimmune encephalomyelitis in mice by promoting Th17 cell differentiation^[12]. High salt content strengthens the lipopolysaccharides (LPS)-induced macrophage activation by activating

signaling pathways of p38 and ERK1 to induce the production of proinflammatory factors^[13]. Extant studies have shown that the high-salt diet promotes Th17 cell activation in LP and exacerbates experimental colitis in mice^[14,15]. However, high-salt diet effect on other immune cells, such as Th1, Tregs and macrophages, which are also associated with pathogenesis in IBD, is still unclear. Macrophage activation plays a pivotal role in inflammation initiation and progression in diverse pathological conditions. Findings obtained in our previous research indicate that, in mice treated with clodronate liposomes (MDP), gut macrophages were successfully depleted. Macrophage depletion could protect mice against colitis induced by dextran sulfate sodium (DSS), suggesting that the macrophages play an important role in colitis pathogenesis.

In the present study, we hypothesized that NaCl promotes the onset and course of DSS-induced colitis, as well as sustains the disease. The promotion effect may be due to monocyte-macrophages shifting the T cell response toward Th17, Th1 and Treg cells. We tested this hypothesis in a DSS-induced colitis mouse model, which shares many characteristics with human ulcerative colitis^[16,17]. We found that NaCl promoted both macrophages and CD4⁺ proinflammatory cell immune response, whereby CD4⁺ proinflammatory cells were mainly CD4⁺IFN- γ ⁺IL-17⁺ T cells. NaCl enhanced the proinflammatory gene expression and cytokine secretion in the colons of mice affected by colitis. Depletion of gut macrophages significantly alleviated DSS-induced colitis, suggesting that macrophages play a vital role in the NaCl proinflammation process. High NaCl enhanced M1 proinflammation gene expression in LPS-activated peritoneal macrophages. Therefore, colitis promoted by high NaCl levels may be a result of M1 macrophage polarization. M1 polarization shifts T cell response toward proinflammatory CD4⁺IFN- γ ⁺IL-17⁺ T cells. High NaCl proinflammation in LPS- and IFN- γ -activated lamina propria mononuclear cells (LPMCs) relies on up-regulation of the p38 mitogen-activated protein kinase (p38/MAPK) axis.

MATERIALS AND METHODS

Animal treatment

For this study, 8- to 10-wk-old female C57BL/6J mice were purchased from the Animal Center of Third Military Medical University (Army Medical University). Mice were housed at 24 °C, under light-controlled cycle (12 h) and with free access to standard laboratory water and food. All processes were supported by the Committee on Use and Care of Laboratory Animals at Third Military Medical University (Army Medical University).

Establishment of the animal model with DSS and NaCl

Mice purchased from the Animal Center were allowed at least 7 d to adapt to the environment before being randomly divided into four groups. They received water

containing 2% NaCl (Sinopharm Chemical Reagent, China) and/or water containing 2.5% DSS (160110; MP Biomedicals, United States) for 10 d. The intestinal macrophages were depleted using MDP (van Rooijen and van Kesteren-Hendrikx, 2003, clodronate liposomes. org, Holland)^[18]. Briefly, 200 μ L MDP was injected i.p. into mice 4 d prior to the onset of inflammation and on days -1, 1, 3 and 5 during the 2.5% DSS and 2% NaCl treatment. The disease activity index (DAI), which was used for the clinical scoring of stool consistency, bleeding and weight loss, served as the measure of colitis severity. The criteria for grading the DAI were adopted from elsewhere^[19].

Cell isolation

Spleen (SP) and mesenteric lymph node (MLN) cells from each mouse in all groups were separated by grinding on filters. SP red blood cells were lysed using red blood cell lysis buffer (C3702; Beyotime, China). Single cell suspensions of SP and MLN were obtained through filters. Cells were washed twice with phosphate-buffered saline (PBS) (Zhongshanjinqiao, China) containing 2% fetal calf serum (FBS; as 2% FBS/PBS) (Gibco, Life Technologies, United States) through centrifugation.

Cell pellets were resuspended in the 2% FBS/PBS and were kept on ice for later use. Intestinal LPMCs were isolated in accordance with the Lamina Propria Dissociation Kit instructions (130-097-410; Miltenyi Biotec, Germany). Cell pellets were resuspended in 40% percoll (Ruitaibio, China) and added slowly to the upper part of centrifuge tubes, which had 5 mL of 80% percoll at the bottoms. LPMCs were obtained by washing twice with 2% FBS/PBS after density gradient centrifuging at 420 g for 20 min.

Flow analysis

The isolated cells from SP, MLN and LP from each experimental group were cultured in 96-well U plates in 0.2 mL 1640 medium containing 1% penicillin-streptomycin (C0222; Beyotime) and 10% FBS with ionomycin (I) (1 μ g/mL) (S1672; Beyotime), phorbol 12-myristate 13-acetate (PMA) (25 ng/mL) (S1819; Beyotime) and Brefeldin A (BFA) (10 μ g/mL) (51-2092KZ; BD Bioscience, United States) for 6 h. The cells were collected and preblocked by Fc receptors for 20 min. Cell-surface staining was performed using PE-, FITC-, APC- or percp-conjugated anti-CD4, CD3, CD25 or CD11b (eBioscience, United States). Intracellular staining was performed using the FITC-conjugated anti-mouse IFN- γ , PE-conjugated anti-mouse IL-17 or Foxp3 (eBioscience). The intracellular or nuclear staining for IFN- γ , IL-17 and Foxp3 analysis was performed according to the BD Bioscience protocol.

LPMC stimulation

Isolated LPMCs were cultured at a concentration of 5×10^6 cells/mL for 24 h, after which the culture

supernatants were collected and cytokine levels were analyzed by enzyme-linked immunosorbent assay (ELISA) or were stimulated using different NaCl concentrations (5, 10, 20, 40, 60 or 80 mmol/L) in the presence of 100 ng/mL LPS (Sigma, United States) and 20 ng/mL IFN- γ (Sigma) with SB20358 (p38 inhibitor) or DMSO (ST038; Beyotime) for 24 h. The cells were detected by western blot (WB) or real time-PCR (RT-PCR).

Mouse peritoneal macrophage preparation

Mice were injected intraperitoneally with 2 mL of 4% sterile thioglycollate medium (Becton Dickinson, United States)^[20]. Peritoneal macrophages were obtained by washing the peritoneal cavity with 8 mL PBS containing 1% penicillin-streptomycin per mouse. Peritoneal macrophages were centrifuged and resuspended in DMEM (Gibco, Thermo Fisher Scientific, United States) containing 10% FBS and 1% penicillin-streptomycin. Next, peritoneal macrophages were seeded in 24-well plates (Corning, United States) and nonadherent cells were removed 4 h after seeding by washing with medium^[21]. Once adhered to the culture plates, cells were stimulated with NaCl (10, 20, 40, 60 or 80 mmol/L) and 100 ng/mL LPS for 24 h. Finally, cells were collected for gene expression evaluation.

Colon culture

Colon tissues were cultured as previously described^[22,23]. Briefly, after cutting longitudinally, colon tissues were washed with PBS for removing intestinal contents and were cut into 1-cm segments. These pieces were cultured in 24-well plates in 2 mL of RPMI1640 medium (Gibco, Life Technology, Shanghai, China) containing 1% penicillin-streptomycin for 24 h. Supernatant was obtained by centrifuging at 10000 g at 4 °C for 10 min and was immediately stored at -80 °C until required for further ELISA detection.

RNA isolation and RT-PCR

RNAs of cells and tissues were extracted by Trizol (Ambion, Life Technology, United States). RNA was transcribed into cDNA using reverse transcription kits (RR047A; Takara, Japan). Quantitative RT-PCR was performed using Bio-Rad instruments (United States) in duplicates with the reagent SYBR Green (RR820A; Takara) to measure the products. Gene expression was analyzed using the comparative Ct method and was normalized to GAPDH, which served as internal control. The primer sequences are shown in Table 1.

ELISA

Cytokine content was expressed in pg/mL. Abs, including purified and biotinylated antimouse, and related reagents were purchased from eBioscience. Briefly, 2 µg/mL capture antibody diluted with coat buffering was incubated at 4 °C overnight in 96-well plates (Corning) and was blocked with 5% bovine serum albumin (BSA) (Sigma) at 37 °C for 2 h. Samples

were incubated at 37 °C for 2 h after being washed three times with PBS containing 0.05% Tween-20 (PBST). Biotinylated antibodies were incubated at 37 °C for 1 h after being washed with PBST three times. Horseradish peroxidase-conjugated antibody was incubated at 37 °C for 30 min after being washed with PBST five times. The reaction of detection reagent at 37 °C required 15 min after the unbounded antibody was removed by washing with PBST five times. The plate was analyzed at 450 nm wavelength after terminating the reaction with the stop solution.

Histology and immunohistochemistry

Colon tissues were fixed with 4% paraformaldehyde before being embedding in paraffin. To assess inflammation, colon tissue cross sections were stained with hematoxylin and eosin (HE). Sections were incubated with rabbit anti-mouse inducible nitric oxide synthase (iNOS) antibody labeled with FITC (orb14179; Biorbyt, United Kingdom) and rabbit anti-mouse F4/80 antibody labeled with PE (123109; Biolegend). All immunofluorescence images were taken by a fluorescence microscope (Leica, Germany) under the same exposure and intensity settings.

Western blotting

Proteins were extracted by RIPA lysis buffer containing protease inhibitor cocktail. The protein concentration was detected using the Protein Concentration Kits (P0012; Beyotime) and the samples were boiled for 5 min at 98 °C. Then, 30 µg of protein for each sample was separated with SDS-PAGE. Next, proteins were electrotransferred onto a nitrocellulose membrane (GE Healthcare, Sweden) and were blocked with 5% BSA in TBS-0.05% Tween-20 (TBST) at room temperature for 2 h. The membrane was subsequently incubated with GAPDH (1:1000) (Santa Cruz Biotechnologies, United States), p38 or phosphorylated p38 (1:250) (Abcam, United States) at 4 °C for 16 h. The membrane was washed with TBST before being incubated at room temperature for 1 h with antibody conjugated with horseradish peroxidase (1:2000) (Zhongshanjinqiao, China). Antibody binding was detected with the ECL substrate (170-5060; Bio-Rad) after washing with TBST. The optical density of bands was analyzed using ImageJ 1.42 software (United States).

Statistical analysis

All data were expressed as mean ± SD. GraphPad Prism 5.00 software for Windows (United States) was used for data analysis. Statistical results were evaluated using unpaired Student's *t*-test or ANOVA, and *P* < 0.05 was considered statistically significant.

RESULTS

NaCl aggravates DSS-induced colitis in mice

To determine the influence of NaCl on enteritis, mice

Table 1 Primers used in the real time-PCR

| Gene name | | Primer sequences |
|----------------|------------|---------------------------------|
| GAPDH | Sense | 5'-AGGTCGGTGTGAACGGATT-3' |
| | Anti-sense | 5'-AATCTCCACTTGCCTACTGC-3' |
| IL-1 β | Sense | 5'-TGGTGTGTGACGTTCCCATT-3' |
| | Anti-sense | 5'-CAGCACGAGGCTTTGTTG-3' |
| IL-1 α | Sense | 5'-CGCCAATGACTCAGAGGAAGA-3' |
| | Anti-sense | 5'-GGCGTCATTAGGATGAATT-3' |
| IL-6 | Sense | 5'-ACAACCACGGCCTCCCTACTT-3' |
| | Anti-sense | 5'-CACGATTCCCAGAGAACATGTG-3' |
| IFN- γ | Sense | 5'-CTGCTGATGGGAGGAGATGT-3' |
| | Anti-sense | 5'-ATTITGTCATTGGGTGAGTCA-3' |
| Arg1 | Sense | 5'-CTCCAAGCCAAAGTCCTTAGAG-3' |
| | Anti-sense | 5'-GGAGCTGTCATTAGGGACATCA-3' |
| iNOS | Sense | 5'-ACATGACCCGTCCACAGTAT-3' |
| | Anti-sense | 5'-CAGAGGGTAGGCTGTCTC-3' |
| IL-10 | Sense | 5'-GCTCTTACTGACTGGCATGAG-3' |
| | Anti-sense | 5'-CGCAGCTCTAGGAGCATGTG-3' |
| TNF- α | Sense | 5'-CTGAACCTCGGGGTGATCGG-3' |
| | Anti-sense | 5'-GGCTTGTCACTCGAATTIGAGA-3' |
| IL-17 α | Sense | 5'-TGTGAAGGTCAACCTCAAAGTCT-3' |
| | Anti-sense | 5'-GAGGGATATCTATCAGGGTCTTCAT-3' |
| SGK1 | Sense | 5'-CTGCTGAAGCACCCTTACC-3' |
| | Anti-sense | 5'-TCCTGAGGATGGGACATTTCAT-3' |

were given 2.5% DSS and/or 2% NaCl. Mice that received both NaCl and DSS started losing weight from day 5 and subsequently exhibited greater weight loss compared to the DSS group (Figure 1A). Moreover, the death rate in the DSS + NaCl group was markedly higher than in the DSS group (Figure 1B). Compared to other groups, colons of mice in the DSS + NaCl group became shorter (Figure 1C). HE staining displayed obvious inflammatory cell infiltration in both groups, but the DSS + NaCl group exhibited more inflammatory cell infiltration in colon tissues than the DSS group (Figure 1D). These findings suggest that NaCl aggravated inflammation in DSS-induced colitis.

NaCl up-regulates the frequency of CD4 $^{+}$ IFN- γ $^{+}$ IL17 $^{+}$ T cells and promotes the secretion of inflammatory cytokines in mice with DSS-induced colitis

Increasing evidence indicates that CD4 $^{+}$ T cells play a crucial role in the pathogenesis of chronic intestinal inflammation, and related cytokines (such as IFN- γ , IL-6, IL-17A and TNF) are highly expressed in the inflamed mucosa of IBD patients^[24,25]. To explore the influence of NaCl on CD4 $^{+}$ T cells in colitis-affected mice, the CD4 $^{+}$ IFN- γ $^{+}$ IL-17 $^{+}$ T cell subsets were detected. Compared to the DSS group, the flow cytometry analysis indicated that frequencies of CD4 $^{+}$ IL-17 $^{+}$ and CD4 $^{+}$ IFN- γ $^{+}$ T cell subsets were markedly up-regulated in the DSS + NaCl group (Figure 2A). NaCl promotion of the DSS-induced colitis development is associated with both CD4 $^{+}$ IL-17 $^{+}$ and CD4 $^{+}$ IFN- γ $^{+}$ T cells in LP, MLN and SP. In addition, the frequencies of inflammatory CD4 $^{+}$ T cells (IL-17 $^{+}$ and IFN- γ $^{+}$ single-positive T cells and IFN- γ $^{+}$ IL-17 $^{+}$ double-positive T cells) in the DSS + NaCl group were higher than in the DSS group. It is also noteworthy that the frequency of CD4 $^{+}$ IFN- γ $^{+}$ T cells

was up-regulated the most (Figure 2B). These findings suggest that CD4 $^{+}$ IFN- γ $^{+}$ IL-17 $^{+}$ T cells are crucial in the inflammation promotion by NaCl in DSS-treated mice.

Cytokines IFN- γ , IL-17 α , IL-1 α , IL-6 and TNF- α secreted by colon tissues were detected by ELISA, and the gene expression of colon tissues from the animal model was measured by RT-PCR. Compared to the DSS group, IFN- γ , IL-17 α , IL-1 α , IL-1 β , IL-6 and TNF- α were all higher in the DSS + NaCl group (Figure 2C and D). Therefore, high NaCl levels up-regulate inflammation gene expression and promote the secretion of multiple proinflammatory cytokines in mice affected by DSS-induced colitis.

NaCl up-regulates macrophage frequency in DSS-treated mice

Macrophages play a crucial role in the Th1 and Th17 responses, and are also important regulators of salt homeostasis^[26]. To determine the effect of NaCl on macrophages in mice affected by colitis, we detected the frequency of CD11b $^{+}$ macrophages in mice that received DSS and/or NaCl by flow cytometry. We observed that the macrophages increased significantly in the LP, MLN and SP of the DSS + NaCl group compared to those of the DSS group (Figure 3A). The increased CD11b $^{+}$ macrophages were mainly located in intestinal LP and MLN (Figure 3B). These findings indicate that the macrophages also participate in the NaCl proinflammation activities in DSS-induced colitis.

Tregs increase through feedback in the development of NaCl aggravating inflammation associated with DSS-induced colitis

Tregs play an important role in the maintenance of intestinal mucosal homeostasis by suppressing

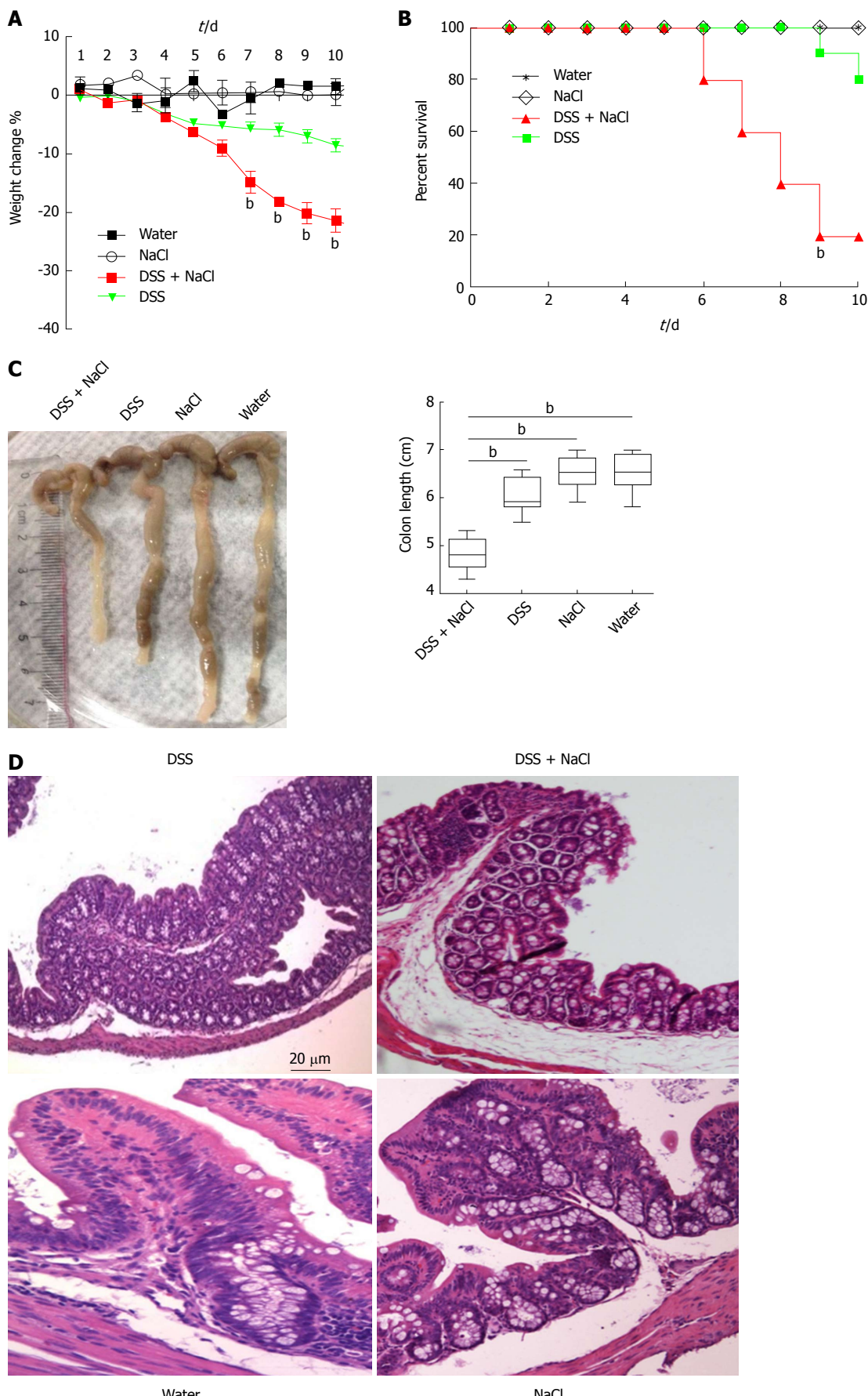


Figure 1 Mice treated with DSS and NaCl develop more severe colitis. **A:** Mice were given DSS and/or NaCl, and were weighed daily; **B:** Death status was recorded daily; **C:** Colonic tissues were collected from four groups of mice and colonic length was measured; **D:** Histological analyses show sections of the colon stained with HE for DSS- or NaCl-treated mice. In all the panels, data indicate three separate experiments, whereby 10 mice per group were used in each experiment. ^aP < 0.05; ^bP < 0.01; ^cP < 0.001. DSS: Dextran sulfate sodium.

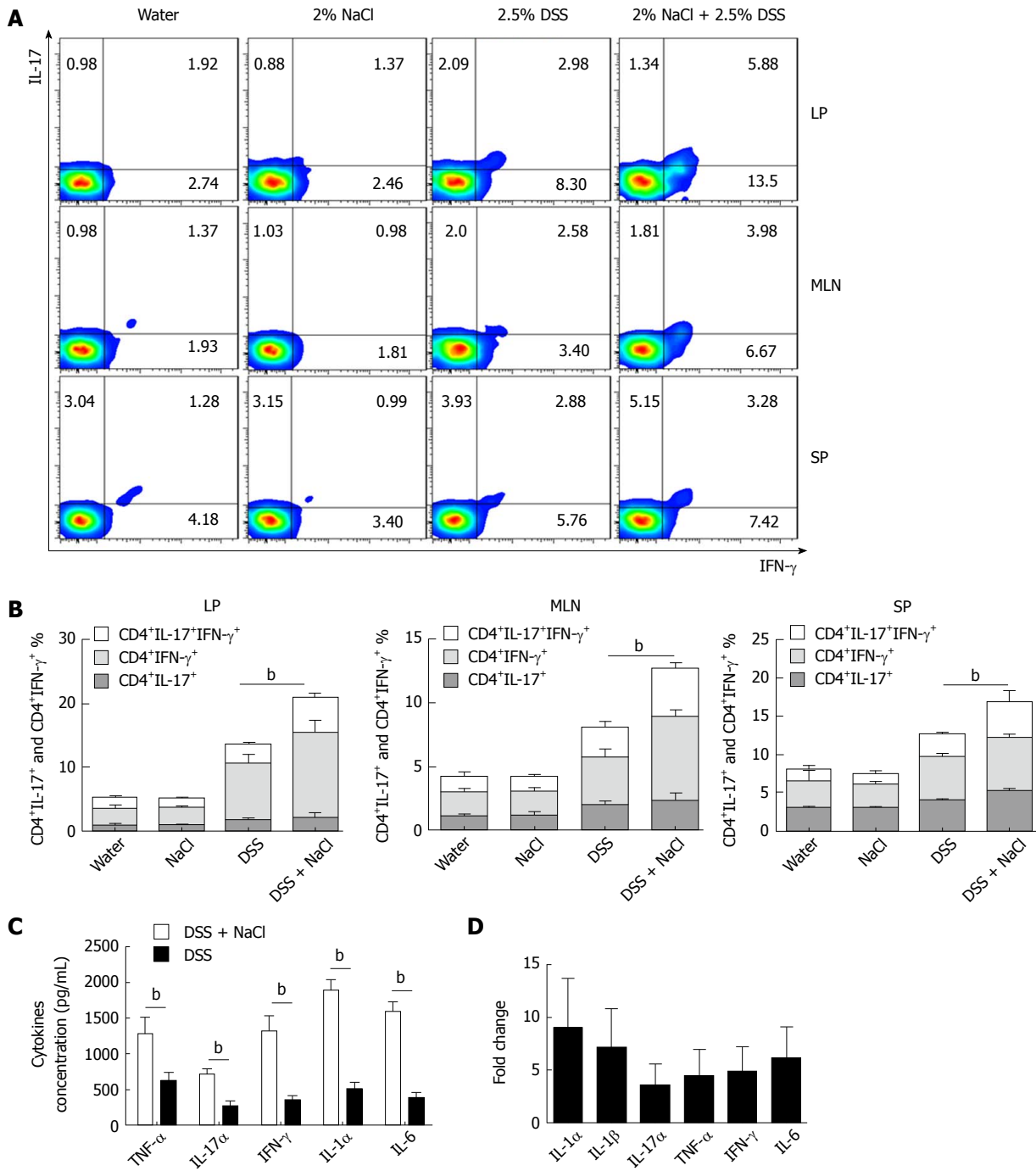


Figure 2 NaCl promotes CD4+IFN- γ +IL-17+ T cell increase and inflammatory cytokine secretion in DSS-treated mice. A: The CD4+IFN- γ +IL-17+ T cells in LP, MLN and SP from mice treated with NaCl and/or DSS were detected by flow cytometry; B: Combined flow cytometry data of CD4+IL-17+, CD4+IFN- γ + and CD4+IFN- γ +IL-17+ T cell subsets distribution in LP, MLN and SP; C: Colon tissues collected from mice treated with DSS or DSS + NaCl, which were washed with phosphate-buffered saline and cultured for 24 h, and the supernatants were collected and detected by enzyme-linked immunosorbent assay; D: Colon tissues collected from mice treated with NaCl and DSS (or only DSS) were detected by RT-PCR. The relative fold-change in DSS + NaCl-treated mice vs DSS-treated mice. In all the panels, data indicate three separate experiments, whereby 3 mice per group were used in each experiment. $^aP < 0.05$; $^bP < 0.01$; $^cP < 0.001$. DSS: Dextran sulfate sodium; LP: Lamina propria; MLN: Mesenteric lymph node; SP: Spleen.

abnormal immune response against dietary antigens or commensal flora^[8]. To explore the changes in Tregs in the mice that received DSS and NaCl, we detected CD3+CD4+CD25+Foxp3+ T cells by flow cytometry and observed that their levels were higher in the DSS + NaCl group than in the DSS group (Figure 4A). The increased Tregs were mainly distributed in the LP and MLN, while

their prevalence in SP did not change significantly (Figure 4B). To explore the influence of NaCl on Tregs in DSS-induced colitis, we evaluated cytokine levels in culture supernatants of LPMCs by ELISA. The results yielded by the analyses indicate that NaCl induces LPMCs to secrete TNF- α , IL-1 α , IL-6 and IL-17, which are critical Th17 cell-related cytokines. Moreover, NaCl promotes

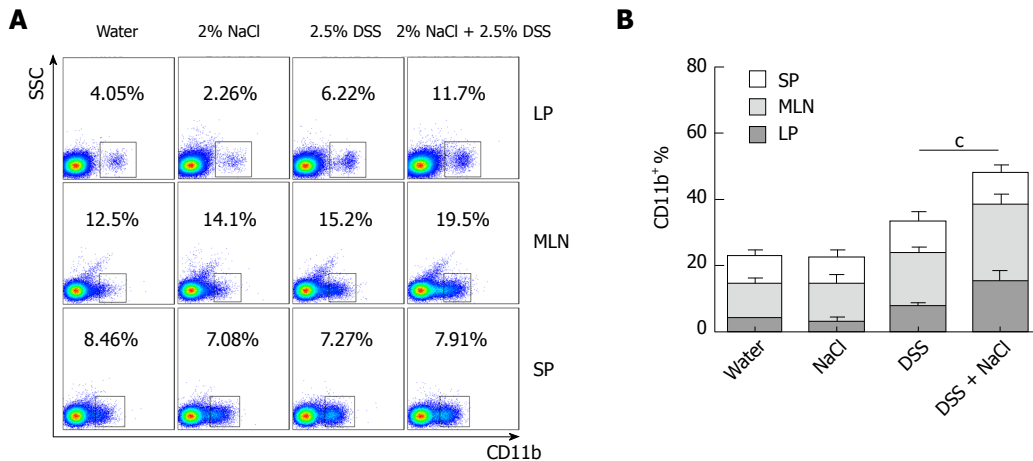


Figure 3 CD11b⁺ macrophages are increased in DSS- and NaCl-treated mice. **A:** The CD11b⁺ cells in LP, MLN and SP from the four groups were detected by flow cytometry; **B:** Quantification of the flow cytometry data indicates the CD11b⁺ cell distribution in LP, MLN and SP. In the panels, data indicate three separate experiments, whereby 3 mice per group were used in each experiment. ^aP < 0.05; ^bP < 0.01; ^cP < 0.001. DSS: Dextran sulfate sodium; LP: Lamina propria; MLN: Mesenteric lymph node; SP: Spleen.

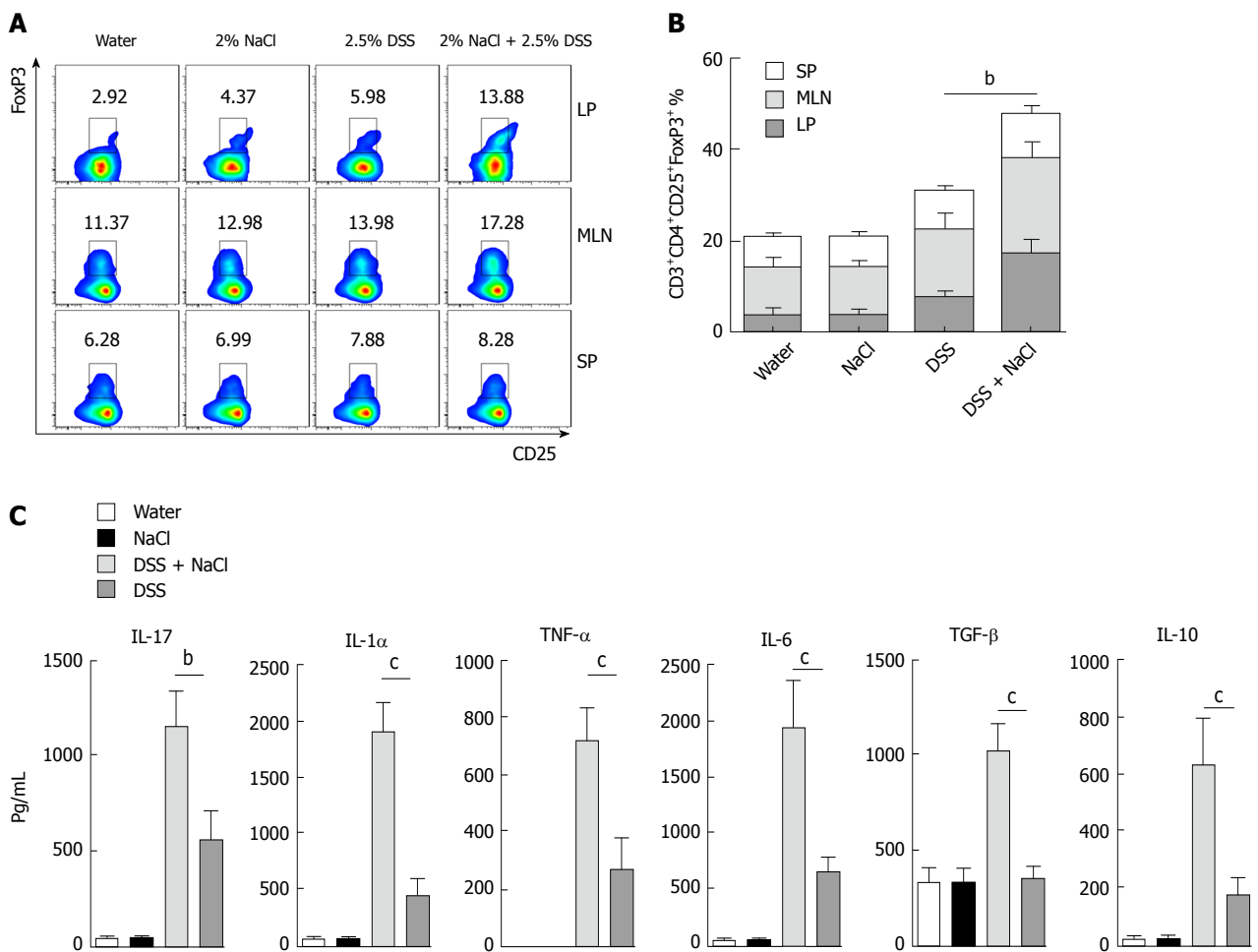


Figure 4 CD3⁺CD4⁺CD25⁺Foxp3⁺ T cells are increased in mice treated with DSS and NaCl. **A:** CD3⁺CD4⁺CD25⁺Foxp3⁺ T cells in LP, MLN and SP from animal models were detected by flow cytometry; **B:** A summary of the percentages of CD3⁺CD4⁺CD25⁺Foxp3⁺ T cell distribution in LP, MLN and SP; **C:** LPMCs from the four groups were isolated and cultured for 24 h, and the levels of cytokines in the culture supernatants were collected and analyzed by enzyme-linked immunosorbent assay. In all the panels, data indicate three separate experiments, whereby 3 mice per group were used in each experiment. ^aP < 0.05; ^bP < 0.01; ^cP < 0.001 vs the DSS group. DSS: Dextran sulfate sodium; LPMCs: Lamina propria mononuclear cells; LP: Lamina propria; MLN: Mesenteric lymph node; SP: Spleen.

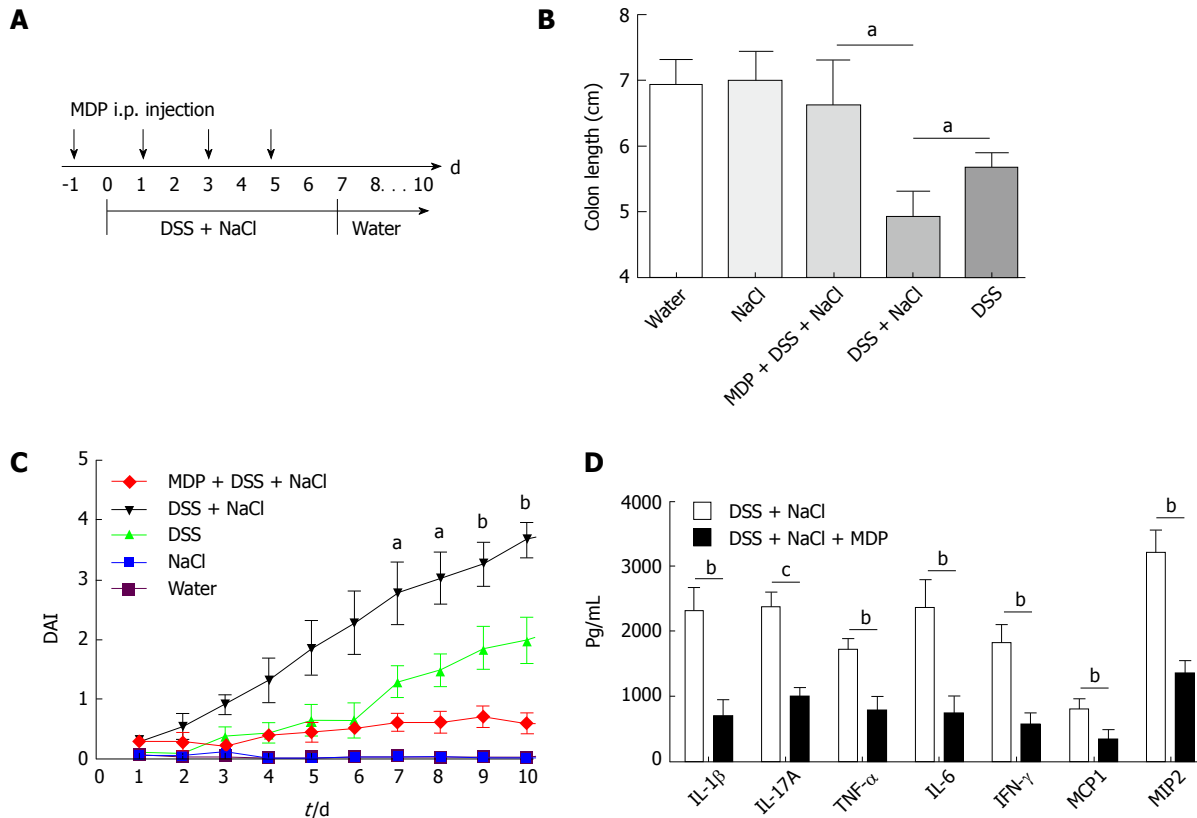


Figure 5 Depletion of macrophages reduces the severity of DSS-induced colitis promoted by NaCl. A: Clodronate liposomes (denoted as MDP) or control PBS-liposomes (denoted as PBS) were administrated intravenously to all mice, as the schematic protocol indicated during DSS and NaCl treatment; B: The disease activity index was monitored daily; C: Colon length was measured in each group of mice ($n = 10$); D: Colon explants were cultured for 24 h and the inflammatory cytokines in supernatants were detected by enzyme-linked immunosorbent assay ($n = 3$). $^aP < 0.05$; $^bP < 0.01$; $^cP < 0.001$ (clodronate liposomes + DSS + NaCl vs DSS + NaCl). DSS: Dextran sulfate sodium.

the secretion of TGF- β and IL-10, which are significant antiinflammatory cytokines secreted by Tregs (Figure 4C). These findings show that Tregs' levels also increase as a result of inflammation promotion by NaCl in mice with DSS-induced colitis.

Macrophages play a critical role in NaCl aggravating DSS-induced colitis

Extant studies have shown that MDP can deplete macrophages in mice^[27]. We used MDP to deplete the macrophages in mice during the DSS and NaCl treatments to determine their role in the promotion of DSS-induced colitis by NaCl (Figure 5A). We observed that macrophage depletion by MDP could prevent colon shortening in the mice treated with NaCl and DSS (Figure 5B). The DAI also showed that macrophage depletion alleviated inflammation in NaCl proinflammatory processes (Figure 5C). The levels of inflammatory cytokines IFN- γ , TNF- α , IL-1 β , IL-17A, IL-6, MCP1 and MIP2 secreted by colon tissues were reduced in MDP-treated mice (Figure 5D). The colon tissues from the DSS + NaCl group contained a greater number of F4/80 $^{+}$ iNOS $^{+}$ macrophages compared to the DSS group. In addition, the MDP-treated mice had fewer F4/80 $^{+}$ iNOS $^{+}$ macrophages compared to the DSS + NaCl group

(Figure 6). Thus, we posit that macrophage depletion can reduce colitis severity in mice.

High NaCl promotes M1 macrophage polarization in vitro

Macrophages in both peritoneal cavity and gastrointestinal tract are linked to IBD^[28]. Different NaCl concentrations (10, 20, 40, 60 and 80 mmol/L) were used to stimulate the macrophages from the abdominal cavity and the gene expression was detected by RT-PCR. Our findings indicate that IL-1 β , IL-6 and iNOS, which usually exhibit proinflammatory roles, gradually increased as the NaCl concentration increased (Figure 7A-C). It is worth noting that IL-10 and Arg1, which are M2 macrophage markers, increased modestly at low NaCl concentrations, whereas their expression markedly increased at 40 mmol/L and above (Figure 7D and E). These results display that high NaCl levels promote LPS-activated peritoneal macrophages toward M1 polarization.

NaCl promotes the inflammation response in LP, whereas LPS and IFN- γ activated LPMCs rely on p38/MAPK

p38/MAPK is related to both IBD and hyperosmotic

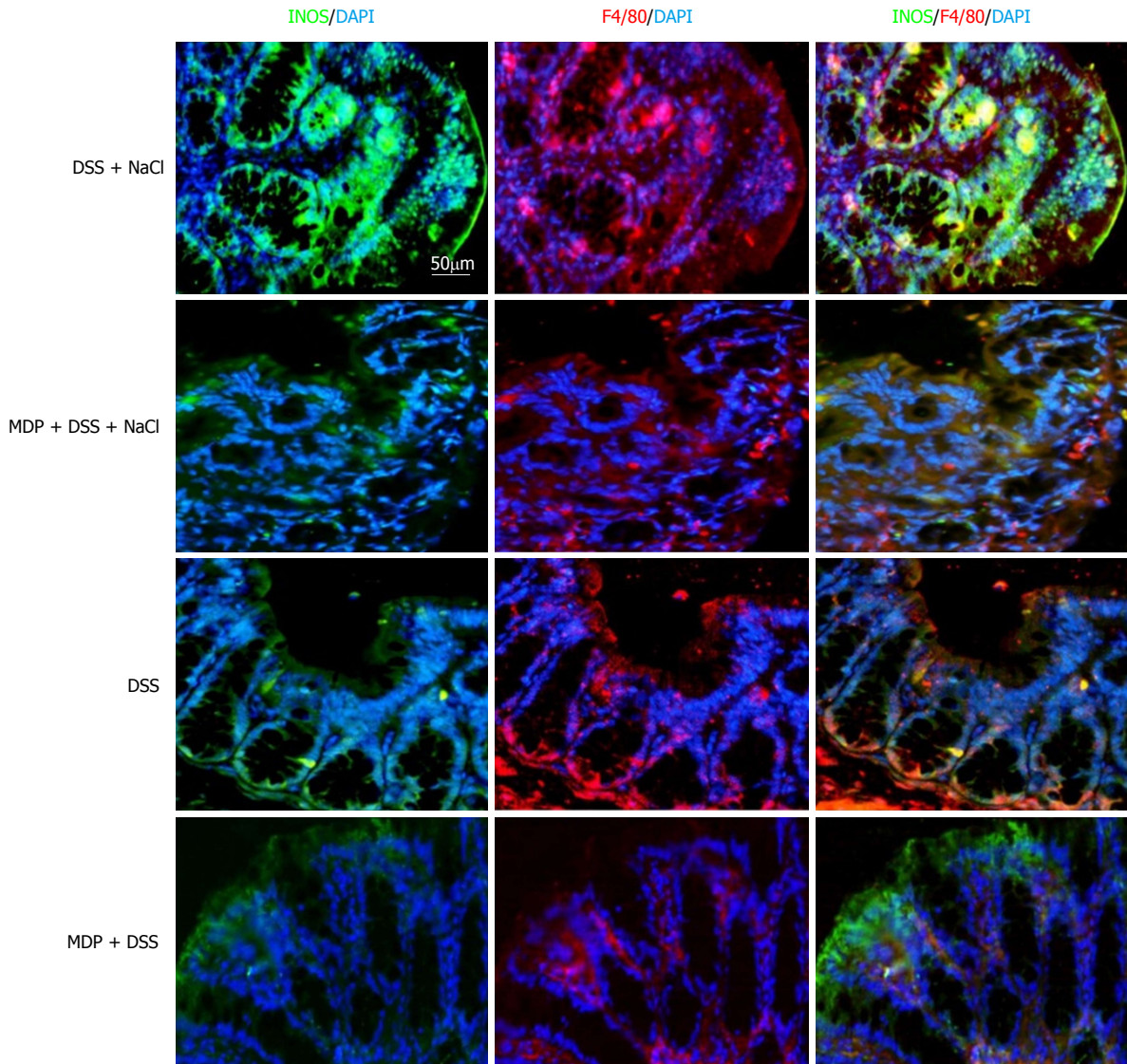


Figure 6 *iNOS⁺F4/80⁺* macrophages increase in the colon of DSS- and NaCl-treated mice. Macrophages in colon tissue obtained from mice injected intraperitoneally with PBS-containing liposomes (denoted as PBS), or clodronate liposomes (denoted as MDP) during the NaCl and DSS treatment were analyzed. The sections were stained with antibodies of anti-F4/80 (red) and anti-iNOS (green). Nuclei were stained with DAPI (blue). Laser confocal microscopy was used to detect fluorescence. (Scale bar = 50 μ m). DSS: Dextran sulfate sodium; iNOS: inducible nitric oxide synthase.

stress^[29,30]. Western blot analysis revealed that high NaCl levels significantly up-regulated phosphorylated-p38 of LPMCs stimulated with LPS and IFN- γ for different time periods (1 h, 6 h, 12 h, 24 h); however, they did not affect the total level of p38, and p38 phosphorylation reached the highest level after 12 h (Figure 8A). LPMCs were treated with NaCl at different concentrations (5, 10, 20, 40, 60 and 80 mmol/L) in the presence of LPS and IFN- γ for 24 h. The western blotting revealed that p38 phosphorylation increased in a dose-dependent manner (Figure 8B). Serum glucocorticoid regulated kinase 1 (SGK1) increased in LPMCs activated by LPS and IFN- γ due to NaCl stimulation (Figure 8C). The results further indicated that p38 inhibitor can decrease high NaCl-promoted p38 phosphorylation in LPMCs (Figure 8D). These findings confirmed that NaCl promotes inflammatory response in the LPS and IFN- γ activated

LPMCs, and the proinflammation effect depends on p38/MAPK phosphorylation mediated by SGK1.

DISCUSSION

NaCl has been shown to exert a proinflammatory effect in many diseases, including experimental colitis, experimental autoimmune encephalomyelitis and cardiovascular disease^[31-33]. In the present study, we observed that macrophages play an important role in the promotion of DSS-induced colitis by NaCl. Macrophages, as antigen-presenting cells, are important in regulating innate and adaptive immune responses and have a crucial role in resolving tissue injury and promoting tissue repair in IBD^[34,35]. Even though the cause of IBD remains unclear, mice with lymphocyte deficiency developed more severe inflammation,

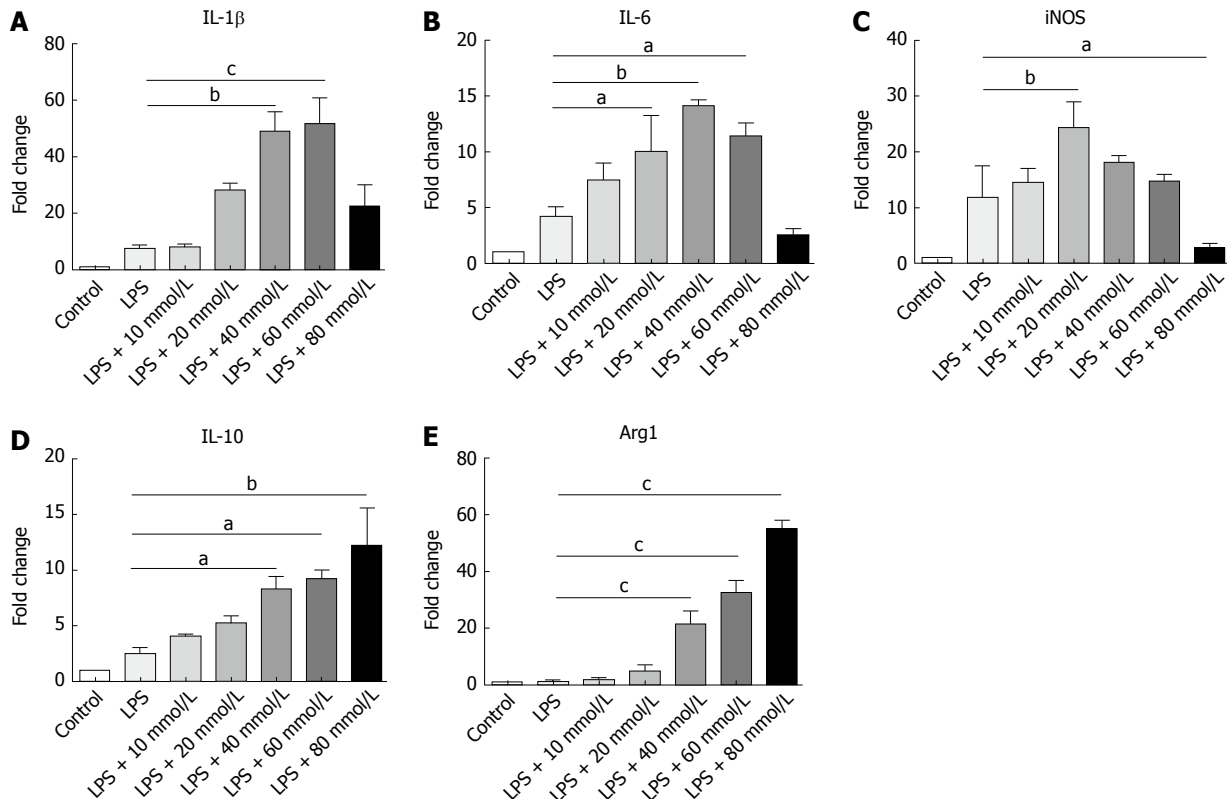


Figure 7 High NaCl levels enhance proinflammation gene expression in LPS-activated peritoneal macrophage. A-E: Peritoneal macrophages were stimulated with different NaCl concentrations (10-80 mmol/L) in the presence of LPS for 24 h. mRNA expression was measured by RT-PCR for the indicated genes. In all the panels, data indicate three separate experiments. $^aP < 0.05$; $^bP < 0.01$; $^cP < 0.001$. LPS: Lipopolysaccharide.

suggesting that innate immune cells are capable of triggering the onset and development of disease^[36]. Activation of the innate immune system is regarded as the most direct cause of IBD because it can recruit cells of the adaptive immune system to the inflammatory site, thus resulting in inflammation^[37].

Findings yielded by the present study further indicated that NaCl promoted the increase in the CD4 $^{+}$ T cell count, especially the IFN- γ $^{+}$ IL-17 $^{+}$ double-positive T cells in DSS-treated mice. Extant research indicates that high-salt diet promotes the differentiation of CD4 $^{+}$ T cells into Th17 as well as Th1^[32]. However, Wei et al^[38] showed that, in 2,4,6-trinitrobenzene sulfonic acid (TNBS)-induced colitis, NaCl promoted Th17 polarization, but not Th1 polarization^[15]. DSS and TNBS may involve different pathogenic mechanisms. Wei et al^[38] used TNBS to induce colitis, which mainly simulated CD. However, we used DSS to induce colitis, which mainly simulated ulcerative colitis. In both CD and ulcerative colitis patients, activation and mucosal infiltration of CD4 $^{+}$ T lymphocytes has been reported^[39].

Extant studies have revealed that blocking CD4 $^{+}$ T cell activation was capable of limiting the development of mucosal inflammation in experimental colitis models^[40]. CD4 $^{+}$ IFN- γ $^{+}$ IL-17 $^{+}$ T cells, as an intermediate form between Th17 and Th1, are an easily observable crossover subset promoted by IL-12 signaling beyond IL-17^[41,42]. Th17 cells play an important role in colitis pathogenesis by directly giving rise to Th1-like cell response^[43]. Empirical evidence indicates that IBD is

characterized by Th1 cell activation and subsequent over-expression of cytokines such as TNF- α , IL-6 and IL-1 β ^[44,45]. In addition, findings yielded by extant research suggest that Th1 cytokines are important promoters of continuous mucosal inflammation in DSS-induced colitis^[46,47].

The results obtained in the present work confirmed the important role of CD4 $^{+}$ IFN- γ $^{+}$ IL-17 $^{+}$ T cells in the promotion of inflammation by NaCl in DSS-treated mice. High NaCl content up-regulates inflammation gene expression and promotes the secretion of multiple proinflammatory cytokines for promoting intestinal inflammation in mice affected by DSS-induced colitis.

IL-6 and IL-17 are critical Th17 cell-related cytokines that are involved in inflammatory responses during IBD development^[7,48]. In contrast, antiinflammatory TGF- β and IL-10, are mainly produced by Tregs^[49]. Wei and colleagues^[15] demonstrated that, while high-salt diet did not change Tregs' percentage, it did inhibit the secretion of IL-10 and the suppressive function of Tregs in TNBS-induced colitis. In our study, NaCl promoted an increase in Tregs' frequency in MLN and LP, as well as enhanced IL-10 and TGF- β expression, in DSS-induced colitis. Tregs, as immune suppressing cells, are essential in maintaining intestinal homeostasis^[50].

In DSS-treated beta7-deficient mice, in which colonic Tregs were depleted, excessive macrophage infiltration in colons occurred by up-regulation of colonic epithelial intercellular ICAM1, which promoted proinflammatory cytokine expression, aggravating DSS-induced colitis^[51].

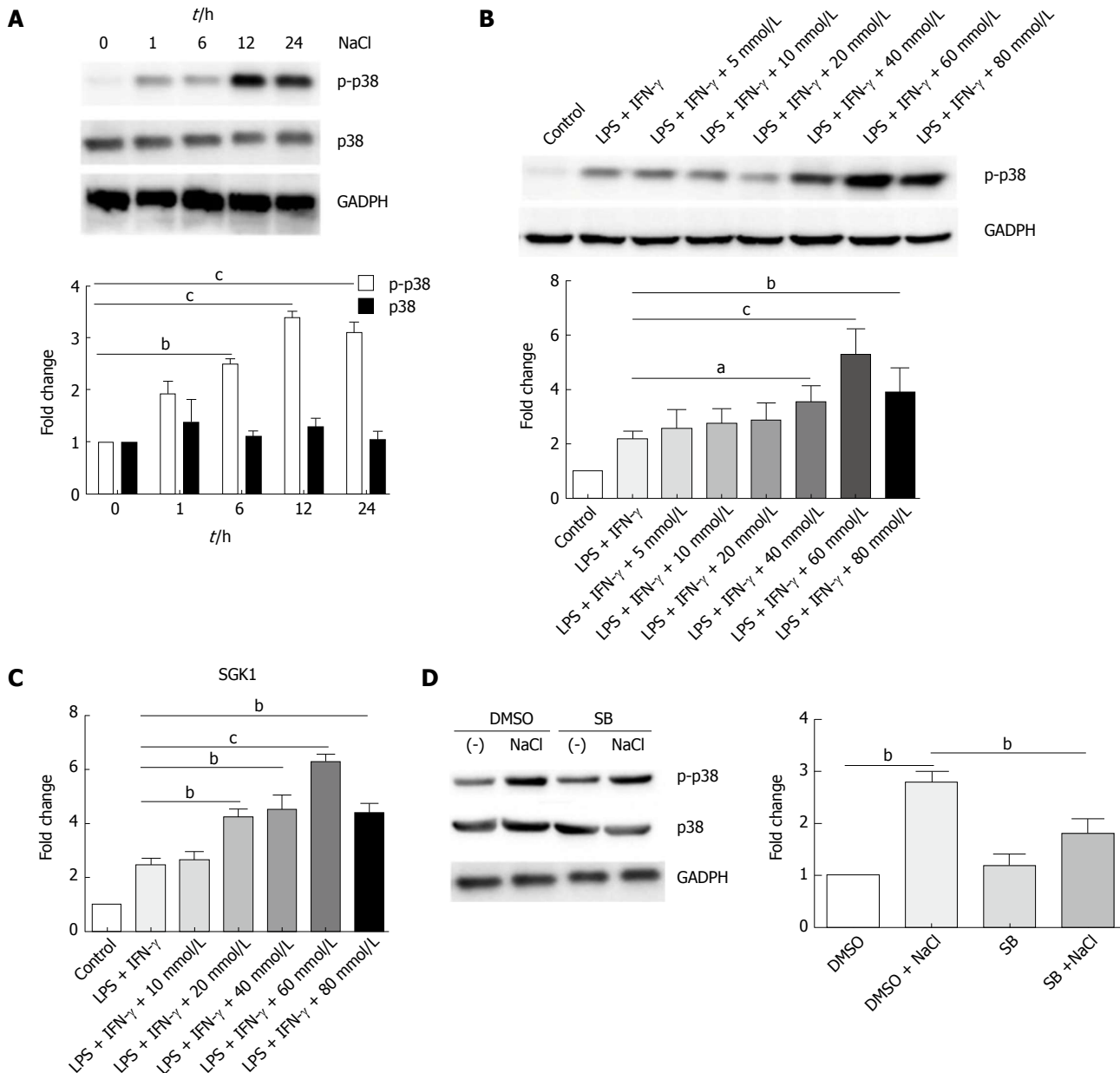


Figure 8 NaCl promotion of inflammation relies on the p38/MAPK pathway. A: LPMCs were stimulated with 60 mmol/L NaCl in the presence of 100 ng/mL LPS and 20 ng/mL IFN-γ for 1 h, 6 h, 12 h and 24 h, and the p38 and phosphorylated-p38 proteins were detected by western blot; B: LPMCs were stimulated with different NaCl concentrations in the presence of 100 ng/mL LPS and 20 ng/mL IFN-γ for 24 h and phosphorylated p38 protein was detected by western blot; C: LPMCs were stimulated with different NaCl concentrations in the presence of LPS and IFN-γ, and the mRNA expression of SGK1 was measured by RT-PCR; D: LPMCs were pretreated with 10 μmol/L SB or DMSO for 2 h and were subsequently stimulated with 60 mmol/L NaCl along with 100 ng/mL LPS and 20 ng/mL IFN-γ in the presence of DMSO or 10 μmol/L SB for 24 h and the proteins of p38 and phosphorylated-p38 were detected by western blot. In all the panels, data indicate three separate experiments. ^aP < 0.05; ^bP < 0.01; ^cP < 0.001. DSS: Dextran sulfate sodium; LPMCs: Lamina propria mononuclear cells; LP: Lamina propria; LPS: Lipopolysaccharide; MLN: Mesenteric lymph node; SB: SB20358; SP: Spleen.

Disruption in balance may allow T cells to proliferate in an increased fashion, thereby promoting chronic intestinal inflammatory development^[52]. Therefore, continuous Tregs' differentiation and trafficking in the gut is required to dampen immune responses to dietary antigens and commensal bacteria^[53].

We also found that NaCl promoted an increase in CD11b⁺ cells in the LP and MLN from mice treated with DSS. Denning *et al*^[54] have shown that CD11b⁺F4/80⁺CD11c⁻ macrophages in LP could induce Foxp3⁺ Tregs' differentiation, while CD11b⁺ dendritic cells in LP elicited responses of IL-17-producing T cells^[54]. Empirical

evidence indicates that the intake of high dietary salt could boost Th17 response through activating the caspase-1 in macrophages^[15,55]. Moreover, in reaction to NaCl, macrophages with enhanced expression of immune-stimulatory molecules promote proinflammatory cytokine production and T cell proliferation^[10,56].

Human monocyte-derived granulocyte-macrophage colony-stimulating factors exhibit potent antigen-presenting functions, produce IL-12p40 and IL-23p19, and promote development of Th1 immunity^[57,58]. In our study, inflammation was relieved when the intestinal macrophages were depleted by MDP, which indicated

that the activation of Th17 and Th1 cells required macrophage participation.

Peritoneal macrophages from mice are among the best-studied macrophage populations and their role in the regulation of inflammatory responses and mucosal immunity is well understood^[59,60]. Macrophages in peritoneal cavity, which are crucial in the regulation of inflammatory pathologies, are also related to IBD^[28,61]. In the present study, we have shown that high NaCl content enhanced the expression of proinflammation genes for IL-1 β , IL-6 and iNOS and antiinflammation genes for Arg1 and IL-10 in macrophages from the abdominal cavity of mice.

Macrophages can be polarized to either classically activated (M1) or alternatively activated (M2) macrophages^[62]. M1 macrophages are proinflammatory cells due to their high capacity for producing proinflammatory cytokines, such as IL-23, IL-12, IL-1 β , TNF- α and iNOS^[63,64]. M2 macrophages highly express IL-10 and Arg1, which are involved in antiinflammatory, antimicrobial response^[62,65]. These cytokines promote the activation of the adaptive immune and T cell response^[66].

In the present study, high NaCl content was found to boost M1 polarization and up-regulate expression of proinflammation genes to promote inflammation. Under low NaCl concentrations, IL-1, IL-6 and iNOS mainly produced by M1 macrophages were up-regulated, while the negative adjustment factor expressions were low. When the NaCl concentration rose to a certain dose, high levels of proinflammation factors IL-1, IL-6 and iNOS induced the cell protective response through feedback, and caused the up-regulation of negative adjustment factors IL-10 and Arg1. Thus, when the inflammation continues to worsen, the M2 macrophages will respond to balance inflammation with protective immunity, and inhibit the expression of proinflammation factors.

We explored the influence of NaCl on LPS- and IFN- γ -activated LPMCs and demonstrated that high NaCl enhanced phosphorylation of p38, as inflammation and salt intake are both linked to p38/MAPK. The p38/MAPK signaling pathway is important in IBD and the inhibition of p38/MAPK can effectively suppress the production of inflammatory mediators^[29]. Available evidence indicates that p38/MAPK mediates intestinal inflammation gene expression, such as TNF- α , IL-1 and IL-6, and this up-regulation occurs in multiple types of cells, especially monocytes and macrophages^[67]. In addition, p38/MAPK can regulate the SGK1 activation^[30].

High NaCl concentration promotes p38/MAPK phosphorylation and activates SGK1^[32]. SGK1 has been shown to control Na(+) transport and NaCl homeostasis in cells, and could trigger Th17 responses and promote tissue inflammation^[12]. Human LPMCs exposed to high NaCl concentrations highly express IL-17A, IL-23R and TNF- α , and pharmacological inhibition of p38/MAPK has been shown to abrogate the effect of NaCl on LPMC-derived cytokines^[14]. In the present study, high NaCl content was shown to promote inflammation in LPS-

and IFN- γ -activated LPMCs. However, this process relies on the up-regulation of p38/MAPK and SGK1.

In summary, the study findings reported here indicate that NaCl induces alterations to both the innate and acquired immune system in mice with DSS-induced colitis. NaCl promotes M1 macrophage polarization, and M1 polarization may shift T cell response toward the proinflammatory CD4 $^+$ IFN- γ $^+$ IL-17 $^+$ T cells' aggravating colitis. The mechanism by which high NaCl concentrations promote inflammation relies on the up-regulation of p38/MAPK and SGK1. Although results obtained in the present study indicate that excessive NaCl intake can promote the inflammation in mice with the DSS-induced colitis, the causality of high-salt diet and IBD still needs to be confirmed by further investigations. More clinical and experimental studies are required to fully clarify the role of salt in IBD.

ARTICLE HIGHLIGHTS

Research background

At present, most diets are characterized by high salt content. Extant studies have shown that high salt intake contributes to inflammatory bowel disease (IBD) incidence and pathogenesis. However, the mechanism underlying these effects remains unclear.

Research motivation

NaCl mediates the inflammatory effects of immune cells. Both innate and adaptive immune proinflammatory cells play important roles in IBD. Studies have shown the high salt intake promotes the activation of Th17 cells in lamina propria (LP) and exacerbates experimental colitis in mice. However, the influence of high salt content in diet on other immune cells is still unclear. The present study explored the influence of high NaCl concentration on immune cell subsets and the underlying mechanisms.

Research objectives

The aim of the present study was to determine the impact of high NaCl concentration on dextran sulfate sodium (DSS)-induced colitis in mice and explore its influence on other immune cells, such as T helper 1 cells, regulatory T cells and macrophages, while attempting to elucidate the mechanism underlying this effect.

Research methods

DSS and NaCl were used to establish a proinflammatory animal model. The immune cell subsets were detected by flow cytometry in order to determine the target cells of NaCl. Cytokines secreted by intestinal tissue were detected. In the present study, clodronate liposomes treatment was used to deplete macrophages to further delineate their vital role in the promotion of DSS-induced colitis in mice by NaCl. In cell experiments, NaCl at different concentrations acted directly on lamina propria mononuclear cells (LPMCs) and macrophages. mRNA levels of inflammation genes and p38/MAPK proteins were determined by RT-PCR and western blot, respectively.

Research results

High NaCl concentration exacerbated the DSS-induced colitis. Intestinal CD4 $^+$ IFN- γ $^+$ IL-17 $^+$ T cells and macrophages both play crucial roles in the promotion of inflammation by NaCl in mice with colitis. NaCl promotes M1 proinflammatory gene expression in lipopolysaccharide (LPS)-activated peritoneal macrophages. High NaCl concentrations promote the up-regulation of the p38/MAPK axis in the LPS and IFN- γ -activated LPMCs.

Research conclusions

NaCl evokes both innate and adaptive immune proinflammatory cell activation in mice affected by colitis. Colitis may be promoted by high NaCl levels, by

NaCl initially by acting on macrophages, pushing them towards M1 polarization. Then, M1 polarization shifts the T cell response toward proinflammatory CD4⁺IFN- γ /IL-17⁺ T cells. Inflammation promotion by NaCl in LPS- and IFN- γ -activated LPMCs relies on the up-regulation of the p38/MAPK axis.

Research perspectives

Although results in this study indicate that high NaCl intake can promote the inflammation in mice with DSS-induced colitis, the causality of high-salt diet and IBD still needs to be confirmed by further investigations. More clinical and experimental studies are inspired to fully clarify the role of salt in IBD.

REFERENCES

- 1 **Vasovic M**, Gajovic N, Brajkovic D, Jovanovic M, Zdravkovaic N, Kanjevac T. The relationship between the immune system and oral manifestations of inflammatory bowel disease: a review. *Cent Eur J Immunol* 2016; **41**: 302-310 [PMID: 27833449 DOI: 10.5114/ceji.2016.63131]
- 2 **Boedeker EC**. Gut microbes, the innate immune system and inflammatory bowel disease: location, location, location. *Curr Opin Gastroenterol* 2007; **23**: 1-3 [PMID: 17133076 DOI: 10.1097/MOG.0b013e328011b837]
- 3 **Van Limbergen J**, Russell RK, Nimmo ER, Ho GT, Arnott ID, Wilson DC, Satsangi J. Genetics of the innate immune response in inflammatory bowel disease. *Inflamm Bowel Dis* 2007; **13**: 338-355 [PMID: 17206667 DOI: 10.1002/ibd.20096]
- 4 **Reinisch W**. Fecal Microbiota Transplantation in Inflammatory Bowel Disease. *Dig Dis* 2017; **35**: 123-126 [PMID: 28147375 DOI: 10.1159/000449092]
- 5 **Dutta AK**, Chacko A. Influence of environmental factors on the onset and course of inflammatory bowel disease. *World J Gastroenterol* 2016; **22**: 1088-1100 [PMID: 26811649 DOI: 10.3748/wjg.v22.i3.1088]
- 6 **Jiang W**, Su J, Zhang X, Cheng X, Zhou J, Shi R, Zhang H. Elevated levels of Th17 cells and Th17-related cytokines are associated with disease activity in patients with inflammatory bowel disease. *Inflamm Res* 2014; **63**: 943-950 [PMID: 25129403 DOI: 10.1007/s00011-014-0768-7]
- 7 **Hundorfean G**, Neurath MF, Mudter J. Functional relevance of T helper 17 (Th17) cells and the IL-17 cytokine family in inflammatory bowel disease. *Inflamm Bowel Dis* 2012; **18**: 180-186 [PMID: 21381156 DOI: 10.1002/ibd.21677]
- 8 **Yang F**, Wang D, Li Y, Sang L, Zhu J, Wang J, Wei B, Lu C, Sun X. Th1/Th2 Balance and Th17/Treg-Mediated Immunity in relation to Murine Resistance to Dextran Sulfate-Induced Colitis. *J Immunol Res* 2017; **2017**: 7047201 [PMID: 28584821 DOI: 10.1155/2017/7047201]
- 9 **Groux H**, O'Garra A, Bigler M, Rouleau M, Antonenko S, de Vries JE, Roncarolo MG. A CD4⁺ T-cell subset inhibits antigen-specific T-cell responses and prevents colitis. *Nature* 1997; **389**: 737-742 [PMID: 9338786 DOI: 10.1038/39614]
- 10 **Kamada N**, Hisamatsu T, Okamoto S, Chinen H, Kobayashi T, Sato T, Sakuraba A, Kitazume MT, Sugita A, Koganei K, Akagawa KS, Hibi T. Unique CD14⁺ intestinal macrophages contribute to the pathogenesis of Crohn disease via IL-23/IFN-gamma axis. *J Clin Invest* 2008; **118**: 2269-2280 [PMID: 18497880 DOI: 10.1172/JCI34610]
- 11 **Mahida YR**. The key role of macrophages in the immunopathogenesis of inflammatory bowel disease. *Inflamm Bowel Dis* 2000; **6**: 21-33 [PMID: 10701146]
- 12 **Wu C**, Yosef N, Thalhamer T, Zhu C, Xiao S, Kishi Y, Regev A, Kuchroo VK. Induction of pathogenic TH17 cells by inducible salt-sensing kinase SGK1. *Nature* 2013; **496**: 513-517 [PMID: 23467085 DOI: 10.1038/nature11984]
- 13 **Zhang WC**, Zheng XJ, Du LJ, Sun JY, Shen ZX, Shi C, Sun S, Zhang Z, Chen XQ, Qin M, Liu X, Tao J, Jia L, Fan HY, Zhou B, Yu Y, Ying H, Hui L, Liu X, Yi X, Liu X, Zhang L, Duan SZ. High salt primes a specific activation state of macrophages, M(Na). *Cell Res* 2015; **25**: 893-910 [PMID: 26206316 DOI: 10.1038/cr.2015.87]
- 14 **Monteleone I**, Marafini I, Dinallo V, Di Fusco D, Troncone E, Zorzi F, Laudisi F, Monteleone G. Sodium chloride-enriched Diet Enhanced Inflammatory Cytokine Production and Exacerbated Experimental Colitis in Mice. *J Crohns Colitis* 2017; **11**: 237-245 [PMID: 27473029 DOI: 10.1093/ecco-jcc/jjw139]
- 15 **Wei Y**, Lu C, Chen J, Cui G, Wang L, Yu T, Yang Y, Wu W, Ding Y, Li L, Uede T, Chen Z, Diao H. High salt diet stimulates gut Th17 response and exacerbates TNBS-induced colitis in mice. *Oncotarget* 2017; **8**: 70-82 [PMID: 27926535 DOI: 10.18632/oncotarget.13783]
- 16 **Ko JK**, Auyeung KK. Inflammatory bowel disease: etiology, pathogenesis and current therapy. *Curr Pharm Des* 2014; **20**: 1082-1096 [PMID: 23782147]
- 17 **Li K**, Wang B, Sui H, Liu S, Yao S, Guo L, Mao D. Polymorphisms of the macrophage inflammatory protein 1 alpha and ApoE genes are associated with ulcerative colitis. *Int J Colorectal Dis* 2009; **24**: 13-17 [PMID: 18762952 DOI: 10.1007/s00384-008-0575-0]
- 18 **Weisser SB**, van Rooijen N, Sly LM. Depletion and reconstitution of macrophages in mice. *J Vis Exp* 2012; **1**: 4105 [PMID: 22871793 DOI: 10.3791/4105]
- 19 **Li YH**, Xiao HT, Hu DD, Fatima S, Lin CY, Mu HX, Lee NP, Bian ZX. Berberine ameliorates chronic relapsing dextran sulfate sodium-induced colitis in C57BL/6 mice by suppressing Th17 responses. *Pharmacol Res* 2016; **110**: 227-239 [PMID: 26969793 DOI: 10.1016/j.phrs.2016.02.010]
- 20 **Nam TG**, Lim TG, Lee BH, Lim S, Kang H, Eom SH, Yoo M, Jang HW, Kim DO. Comparison of Anti-Inflammatory Effects of Flavonoid-Rich Common and Tartary Buckwheat Sprout Extracts in Lipopolysaccharide-Stimulated RAW 264.7 and Peritoneal Macrophages. *Oxid Med Cell Longev* 2017; **2017**: 9658030 [PMID: 28928906 DOI: 10.1155/2017/9658030]
- 21 **He G**, Zhang X, Chen Y, Chen J, Li L, Xie Y. Isoalantolactone inhibits LPS-induced inflammation via NF- κ B inactivation in peritoneal macrophages and improves survival in sepsis. *Biomed Pharmacother* 2017; **90**: 598-607 [PMID: 28407580 DOI: 10.1016/j.biopha.2017.03.095]
- 22 **Rakoff-Nahoum S**, Paglino J, Eslami-Varzaneh F, Edberg S, Medzhitov R. Recognition of commensal microflora by toll-like receptors is required for intestinal homeostasis. *Cell* 2004; **118**: 229-241 [PMID: 15260992 DOI: 10.1016/j.cell.2004.07.002]
- 23 **Siegmund B**, Lehr HA, Fantuzzi G, Dinarello CA. IL-1 beta-converting enzyme (caspase-1) in intestinal inflammation. *Proc Natl Acad Sci USA* 2001; **98**: 13249-13254 [PMID: 11606779 DOI: 10.1073/pnas.231473998]
- 24 **Zhou R**, Chang Y, Liu J, Chen M, Wang H, Huang M, Liu S, Wang X, Zhao Q. JNK Pathway-Associated Phosphatase/DUSP22 Suppresses CD4⁺ T-Cell Activation and Th1/Th17-Cell Differentiation and Negatively Correlates with Clinical Activity in Inflammatory Bowel Disease. *Front Immunol* 2017; **8**: 781 [PMID: 28725226 DOI: 10.3389/fimmu.2017.00781]
- 25 **Strober W**, Fuss IJ. Proinflammatory cytokines in the pathogenesis of inflammatory bowel diseases. *Gastroenterology* 2011; **140**: 1756-1767 [PMID: 21530742 DOI: 10.1053/j.gastro.2011.02.016]
- 26 **Machnik A**, Neuhofer W, Jantsch J, Dahlmann A, Tammela T, Machura K, Park JK, Beck FX, Müller DN, Derer W, Goss J, Ziombert A, Dietsch P, Wagner H, van Rooijen N, Kurtz A, Hilgers KF, Alitalo K, Eckardt KU, Luft FC, Kerjaschki D, Titze J. Macrophages regulate salt-dependent volume and blood pressure by a vascular endothelial growth factor-C-dependent buffering mechanism. *Nat Med* 2009; **15**: 545-552 [PMID: 19412173 DOI: 10.1038/nm.1960]
- 27 **Zhao A**, Urban JF Jr, Anthony RM, Sun R, Stiltz J, van Rooijen N, Wynn TA, Gause WC, Shea-Donohue T. Th2 cytokine-induced alterations in intestinal smooth muscle function depend on alternatively activated macrophages. *Gastroenterology* 2008; **135**: 217-225.e1 [PMID: 18471439 DOI: 10.1053/j.gastro.2008.03.077]
- 28 **Gross M**, Salame TM, Jung S. Guardians of the Gut - Murine Intestinal Macrophages and Dendritic Cells. *Front Immunol* 2015; **6**: 254 [PMID: 26082775 DOI: 10.3389/fimmu.2015.00254]
- 29 **Feng YJ**, Li YY. The role of p38 mitogen-activated protein

- kinase in the pathogenesis of inflammatory bowel disease. *J Dig Dis* 2011; **12**: 327-332 [PMID: 21955425 DOI: 10.1111/j.1751-2980.2011.00525.x]
- 30 **Bell LM**, Leong ML, Kim B, Wang E, Park J, Hemmings BA, Firestone GL. Hyperosmotic stress stimulates promoter activity and regulates cellular utilization of the serum- and glucocorticoid-inducible protein kinase (Sgk) by a p38 MAPK-dependent pathway. *J Biol Chem* 2000; **275**: 25262-25272 [PMID: 10842172 DOI: 10.1074/jbc.M002076200]
- 31 **Tubbs AL**, Liu B, Rogers TD, Sartor RB, Miao EA. Dietary Salt Exacerbates Experimental Colitis. *J Immunol* 2017; **199**: 1051-1059 [PMID: 28637899 DOI: 10.4049/jimmunol.1700356]
- 32 **Kleinewietfeld M**, Manzel A, Titze J, Kvakan H, Yosef N, Linker RA, Muller DN, Hafler DA. Sodium chloride drives autoimmune disease by the induction of pathogenic TH17 cells. *Nature* 2013; **496**: 518-522 [PMID: 23467095 DOI: 10.1038/nature11868]
- 33 **Zidek W**. [High salt consumption increases cardiovascular risk in hypertonic patients]. *Dtsch Med Wochenschr* 2016; **141**: 1524 [PMID: 27750335 DOI: 10.1055/s-0042-117074]
- 34 **Gren ST**, Grip O. Role of Monocytes and Intestinal Macrophages in Crohn's Disease and Ulcerative Colitis. *Inflamm Bowel Dis* 2016; **22**: 1992-1998 [PMID: 27243595 DOI: 10.1097/MIB.0000000000000824]
- 35 **Steinbach EC**, Plevy SE. The role of macrophages and dendritic cells in the initiation of inflammation in IBD. *Inflamm Bowel Dis* 2014; **20**: 166-175 [PMID: 23974993 DOI: 10.1097/MIB.0b013e3182a69dca]
- 36 **Kim TW**, Seo JN, Suh YH, Park HJ, Kim JH, Kim JY, Oh KI. Involvement of lymphocytes in dextran sulfate sodium-induced experimental colitis. *World J Gastroenterol* 2006; **12**: 302-305 [PMID: 16482634]
- 37 **Katakura K**, Watanabe H, Ohira H. Innate immunity and inflammatory bowel disease: a review of clinical evidence and future application. *Clin J Gastroenterol* 2013; **6**: 415-419 [PMID: 26182129 DOI: 10.1007/s12328-013-0436-4]
- 38 **Alex P**, Zachos NC, Nguyen T, Gonzales L, Chen TE, Conklin LS, Centola M, Li X. Distinct cytokine patterns identified from multiplex profiles of murine DSS and TNBS-induced colitis. *Inflamm Bowel Dis* 2009; **15**: 341-352 [PMID: 18942757 DOI: 10.1002/ibd.20753]
- 39 **Fantini MC**, Monteleone G, Macdonald TT. New players in the cytokine orchestra of inflammatory bowel disease. *Inflamm Bowel Dis* 2007; **13**: 1419-1423 [PMID: 17712836 DOI: 10.1002/ibd.20212]
- 40 **Elson CO**, Cong Y, Brandwein S, Weaver CT, McCabe RP, Mähler M, Sundberg JP, Leiter EH. Experimental models to study molecular mechanisms underlying intestinal inflammation. *Ann NY Acad Sci* 1998; **859**: 85-95 [PMID: 9928372]
- 41 **Annuziato F**, Romagnani S. Do studies in humans better depict Th17 cells? *Blood* 2009; **114**: 2213-2219 [PMID: 19494349 DOI: 10.1182/blood-2009-03-209189]
- 42 **Li J**, Ueno A, Iacucci M, Fort Gasia M, Jijon HB, Panaccione R, Kaplan GG, Beck PL, Luider J, Barkema HW, Qian J, Gui X, Ghosh S. Crossover Subsets of CD⁺ T Lymphocytes in the Intestinal Lamina Propria of Patients with Crohn's Disease and Ulcerative Colitis. *Dig Dis Sci* 2017; **62**: 2357-2368 [PMID: 28573508 DOI: 10.1007/s10620-017-4596-9]
- 43 **Harbour SN**, Maynard CL, Zindl CL, Schoeb TR, Weaver CT. Th17 cells give rise to Th1 cells that are required for the pathogenesis of colitis. *Proc Natl Acad Sci U S A* 2015; **112**: 7061-7066 [PMID: 26038559 DOI: 10.1073/pnas.1415675112]
- 44 **Fuss IJ**, Neurath M, Boirivant M, Klein JS, de la Motte C, Strong SA, Fiocchi C, Strober W. Disparate CD4⁺ lamina propria (LP) lymphokine secretion profiles in inflammatory bowel disease. Crohn's disease LP cells manifest increased secretion of IFN-gamma, whereas ulcerative colitis LP cells manifest increased secretion of IL-5. *J Immunol* 1996; **157**: 1261-1270 [PMID: 8757634]
- 45 **Yamamoto M**, Yoshizaki K, Kishimoto T, Ito H. IL-6 is required for the development of Th1 cell-mediated murine colitis. *J Immunol* 2000; **164**: 4878-4882 [PMID: 10779797]
- 46 **Fichtner-Feigl S**, Fuss IJ, Preiss JC, Strober W, Kitani A. Treatment of murine Th1- and Th2-mediated inflammatory bowel disease with NF-kappa B decoy oligonucleotides. *J Clin Invest* 2005; **115**: 3057-3071 [PMID: 16239967 DOI: 10.1172/JCI24792]
- 47 **Dieleman LA**, Palmen MJ, Akol H, Bloemena E, Peña AS, Meuwissen SG, Van Rees EP. Chronic experimental colitis induced by dextran sulphate sodium (DSS) is characterized by Th1 and Th2 cytokines. *Clin Exp Immunol* 1998; **114**: 385-391 [PMID: 9844047]
- 48 **Li L**, Shi QG, Lin F, Liang YG, Sun LJ, Mu JS, Wang YG, Su HB, Xu B, Ji CC, Huang HH, Li K, Wang HF. Cytokine IL-6 is required in Citrobacter rodentium infection-induced intestinal Th17 responses and promotes IL-22 expression in inflammatory bowel disease. *Mol Med Rep* 2014; **9**: 831-836 [PMID: 24430732 DOI: 10.3892/mmr.2014.1898]
- 49 **Ma L**, Liang Y, Fang M, Guan Y, Si Y, Jiang F, Wang F. The cytokines (IFN-gamma, IL-2, IL-4, IL-10, IL-17) and Treg cytokine (TGF-beta1) levels in adults with immune thrombocytopenia. *Pharmazie* 2014; **69**: 694-697 [PMID: 25272942]
- 50 **Geng X**, Xue J. Expression of Treg/Th17 cells as well as related cytokines in patients with inflammatory bowel disease. *Pak J Med Sci* 2016; **32**: 1164-1168 [PMID: 27882014 DOI: 10.12669/pjms.325.10902]
- 51 **Zhang HL**, Zheng YJ, Pan YD, Xie C, Sun H, Zhang YH, Yuan MY, Song BL, Chen JF. Regulatory T-cell depletion in the gut caused by integrin β7 deficiency exacerbates DSS colitis by evoking aberrant innate immunity. *Mucosal Immunol* 2016; **9**: 391-400 [PMID: 26220167 DOI: 10.1038/mi.2015.68]
- 52 **Gibson DJ**, Ryan EJ, Doherty GA. Keeping the bowel regular: the emerging role of Treg as a therapeutic target in inflammatory bowel disease. *Inflamm Bowel Dis* 2013; **19**: 2716-2724 [PMID: 23899545 DOI: 10.1097/MIB.0b013e31829ed7df]
- 53 **Curotto de Lafaille MA**, Lafaille JJ. Natural and adaptive foxp3⁺ regulatory T cells: more of the same or a division of labor? *Immunity* 2009; **30**: 626-635 [PMID: 19464985 DOI: 10.1016/j.immuni.2009.05.002]
- 54 **Denning TL**, Wang YC, Patel SR, Williams IR, Pulendran B. Lamina propria macrophages and dendritic cells differentially induce regulatory and interleukin 17-producing T cell responses. *Nat Immunol* 2007; **8**: 1086-1094 [PMID: 17873879 DOI: 10.1038/ni1511]
- 55 **Ip WK**, Medzhitov R. Macrophages monitor tissue osmolarity and induce inflammatory response through NLRP3 and NLRC4 inflammasome activation. *Nat Commun* 2015; **6**: 6931 [PMID: 25959047 DOI: 10.1038/ncomms7931]
- 56 **Hausmann M**, Kiessling S, Mestermann S, Webb G, Spöttl T, Andus T, Schölmerich J, Herfarth H, Ray K, Falk W, Rogler G. Toll-like receptors 2 and 4 are up-regulated during intestinal inflammation. *Gastroenterology* 2002; **122**: 1987-2000 [PMID: 12055604]
- 57 **Akagawa KS**. Functional heterogeneity of colony-stimulating factor-induced human monocyte-derived macrophages. *Int J Hematol* 2002; **76**: 27-34 [PMID: 12138892]
- 58 **Verreck FA**, de Boer T, Langenberg DM, Hoeve MA, Kramer M, Vaisberg E, Kastelein R, Kolk A, de Waal-Malefyt R, Ottenhoff TH. Human IL-23-producing type 1 macrophages promote but IL-10-producing type 2 macrophages subvert immunity to (myco)bacteria. *Proc Natl Acad Sci USA* 2004; **101**: 4560-4565 [PMID: 15070757 DOI: 10.1073/pnas.0400983101]
- 59 **Ghosh EE**, Cassado AA, Govoni GR, Fukuhara T, Yang Y, Monack DM, Bortoluci KR, Almeida SR, Herzenberg LA, Herzenberg LA. Two physically, functionally, and developmentally distinct peritoneal macrophage subsets. *Proc Natl Acad Sci USA* 2010; **107**: 2568-2573 [PMID: 20133793 DOI: 10.1073/pnas.0915000107]
- 60 **Wynn TA**, Chawla A, Pollard JW. Macrophage biology in development, homeostasis and disease. *Nature* 2013; **496**: 445-455 [PMID: 23619691 DOI: 10.1038/nature12034]
- 61 **Asano K**, Takahashi N, Ushiki M, Monya M, Aihara F, Kuboki E,

- Moriyama S, Iida M, Kitamura H, Qiu CH, Watanabe T, Tanaka M. Intestinal CD169(+) macrophages initiate mucosal inflammation by secreting CCL8 that recruits inflammatory monocytes. *Nat Commun* 2015; **6**: 7802 [PMID: 26193821 DOI: 10.1038/ncomms8802]
- 62 **Lawrence T**, Natoli G. Transcriptional regulation of macrophage polarization: enabling diversity with identity. *Nat Rev Immunol* 2011; **11**: 750-761 [PMID: 22025054 DOI: 10.1038/nri3088]
- 63 **Mosser DM**, Edwards JP. Exploring the full spectrum of macrophage activation. *Nat Rev Immunol* 2008; **8**: 958-969 [PMID: 19029990 DOI: 10.1038/nri2448]
- 64 **Cibiček N**, Roubalová L, Vrba J, Zatloukalová M, Ehrmann J, Zapletalová J, Večeřa R, Křen V, Ulrichová J. Protective effect of isoquercitrin against acute dextran sulfate sodium-induced rat colitis depends on the severity of tissue damage. *Pharmacol Rep* 2016; **68**: 1197-1204 [PMID: 27657482 DOI: 10.1016/j.pharep.2016.07.007]
- 65 **Mills CD**, Kincaid K, Alt JM, Heilman MJ, Hill AM. M-1/M-2 macrophages and the Th1/Th2 paradigm. *J Immunol* 2000; **164**: 6166-6173 [PMID: 10843666]
- 66 **Cassado Ados A**, D'Império Lima MR, Bortoluci KR. Revisiting mouse peritoneal macrophages: heterogeneity, development, and function. *Front Immunol* 2015; **6**: 225 [PMID: 26042120 DOI: 10.3389/fimmu.2015.00225]
- 67 **Scaldaferri F**, Correale C, Gasbarrini A, Danese S. Molecular signaling blockade as a new approach to inhibit leukocyte-endothelial interactions for inflammatory bowel disease treatment. *Cell Adh Migr* 2009; **3**: 296-299 [PMID: 19571660]

P- Reviewer: Chiba T, Day AS, De Ponti F, Triantafyllidis JK
S- Editor: Gong ZM **L- Editor:** Filopodia **E- Editor:** Huang Y



Retrospective Cohort Study

High tacrolimus intra-patient variability is associated with graft rejection, and *de novo* donor-specific antibodies occurrence after liver transplantation

Arnaud Del Bello, Nicolas Congy-Jolivet, Marie Danjoux, Fabrice Muscari, Laurence Lavayssiére, Laure Esposito, Anne-Laure Hebral, Julie Bellière, Nassim Kamar

Arnaud Del Bello, Laurence Lavayssiére, Laure Esposito, Anne-Laure Hebral, Julie Bellière, Nassim Kamar, Department of Nephrology and Organ Transplantation, CHU Rangueil, Toulouse 31000, France

Arnaud Del Bello, Nicolas Congy-Jolivet, Fabrice Muscari, Julie Bellière, Nassim Kamar, Université Paul Sabatier, Toulouse 31000, France

Julie Bellière, Molecular Immunogenetics Laboratory, Faculté de Médecine Purpan, IFR150 (INSERM), Montréal H3G 1Y6, France

Nicolas Congy-Jolivet, Department of Immunology, CHU de Toulouse, Hôpital de Rangueil, CHU de Toulouse, Toulouse 31000, France

Marie Danjoux, Department of Pathology, Institut Universitaire du Cancer, CHU Toulouse 31000, France

Fabrice Muscari, Department of Surgery and Liver Transplantation, Toulouse 31000, France

Nassim Kamar, INSERM, IFR-BMT, CHU Purpan, Toulouse 31000, France

ORCID number: Arnaud Del Bello (0000-0003-3115-868X); Nicolas Congy-Jolivet (0000-0002-2441-6145); Fabrice Muscari (0000-0001-6754-1686); Julie Bellière (0000-0002-4229-8584); Nassim Kamar (0000-0003-1930-8964).

Author contributions: Del Bello A and Kamar N designed research; Del Bello A, Congy-Jolivet N, Danjoux M, Muscari F, Lavayssiére L, Esposito L, Hebral AL, Bellière J and Kamar N followed patients and performed research; Del Bello A, Bellière J, and Kamar N contributed analytic tools; Del Bello A and Kamar N analysed data; Del Bello A and Kamar N wrote the paper.

Institutional review board statement: The study was reviewed and approved for publication by our Institutional Reviewer.

Conflict-of-interest statement: All the authors have no conflict of interest related to the manuscript.

Data sharing statement: No additional data are available.

Open-Access: This article is an open-access article which was selected by an in-house editor and fully peer-reviewed by external reviewers. It is distributed in accordance with the Creative Commons Attribution Non Commercial (CC BY-NC 4.0) license, which permits others to distribute, remix, adapt, build upon this work non-commercially, and license their derivative works on different terms, provided the original work is properly cited and the use is non-commercial. See: <http://creativecommons.org/licenses/by-nc/4.0/>

Manuscript source: Unsolicited manuscript

Correspondence to: Arnaud Del Bello, MD, Doctor, Department of Nephrology and Organ Transplantation, CHU Rangueil, TSA 50032, Cedex 9, Toulouse 31059, France. delbello.a@chu-toulouse.fr
Telephone: +33-5-61323923
Fax: +33-5-61323989

Received: December 5, 2017

Peer-review started: December 5, 2017

First decision: January 18, 2018

Revised: March 6, 2018

Accepted: March 31, 2018

Article in press: March 30, 2018

Published online: April 28, 2018

Abstract

AIM

To investigate the role of tacrolimus intra-patient variability (IPV) in adult liver-transplant recipients.

METHODS

We retrospectively assessed tacrolimus variability in a cohort of liver-transplant recipients and analyzed its effect on the occurrence of graft rejection and *de novo* donor-specific antibodies (*dnDSAs*), as well as graft

survival during the first 2 years posttransplantation. Between 02/08 and 06/2015, 116 patients that received tacrolimus plus mycophenolate mofetil (with or without steroids) were included.

RESULTS

Twenty-two patients (18.5%) experienced at least one acute-rejection episode (BPAR). Predictive factors for a BPAR were a tacrolimus IPV of > 35% [OR = 3.07 95%CI (1.14-8.24), $P = 0.03$] or > 40% [OR = 4.16 (1.38-12.50), $P = 0.01$], and a tacrolimus trough level of < 5 ng/mL [OR=3.68 (1.3-10.4), $P = 0.014$]. Thirteen patients (11.2%) developed at least one *dnDSA* during the follow-up. Tacrolimus IPV [coded as a continuous variable: OR = 1.1, 95%CI (1.0-1.12), $P = 0.006$] of > 35% [OR = 4.83, 95%CI (1.39-16.72), $P = 0.01$] and > 40% [OR = 9.73, 95%CI (2.65-35.76), $P = 0.001$] were identified as predictors to detect *dnDSAs*. IPV did not impact on patient- or graft-survival rates during the follow-up.

CONCLUSION

Tacrolimus-IPV could be a useful tool to identify patients with a greater risk of graft rejection and of developing a *de novo* DSA after liver transplantation

Key words: Variability; Liver transplantation; Donor-specific antibodies; Immunosuppression

© The Author(s) 2018. Published by Baishideng Publishing Group Inc. All rights reserved.

Core tip: Tacrolimus intra-patient variability (Tac IPV) was associated with kidney-graft rejection and worse long-term outcomes, but until now, was not well studied after liver transplantation in adult recipients. We found that the coefficient of variability-IPV of tacrolimus was a predictive factor for acute rejection and the occurrence of *de novo* donor-specific antibodies (DSA) after liver transplantation in a retrospective cohort of 116 recipients treated with tacrolimus and mycophenolate mofetil. This could be a useful tool to identify patients with a greater risk of graft rejection and of developing a *de novo* DSA after liver transplantation.

Del Bello A, Congy-Jolivet N, Danjoux M, Muscari F, Lavayssiére L, Esposito L, Hebral AL, Bellière J, Kamar N. High tacrolimus intra-patient variability is associated with graft rejection, and *de novo* donor-specific antibodies occurrence after liver transplantation. *World J Gastroenterol* 2018; 24(16): 1795-1802 Available from: URL: <http://www.wjgnet.com/1007-9327/full/v24/i16/1795.htm> DOI: <http://dx.doi.org/10.3748/wjg.v24.i16.1795>

INTRODUCTION

Tacrolimus (Tac) is considered a cornerstone within immunosuppression protocols to prevent T-cell and

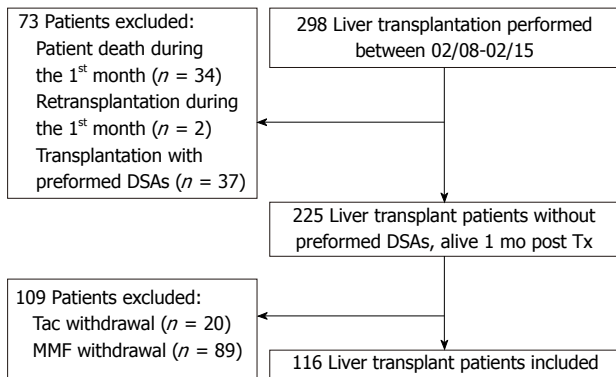
antibody-mediated rejection after liver transplantation^[1-3]. However, this treatment presents a narrow therapeutic index: overexposure can lead to clinically serious events^[4] thus necessitating regular therapeutic drug monitoring, whereas underexposure can lead to acute or chronic graft rejection^[4-6]. Inter-individual variability from Tac therapy may be explained by the polymorphism of cytochromes P450 3A4 and 5 (responsible for biotransformation of Tac)^[7] and the drug transporter ABCB1^[8], circadian rhythms^[9] and also drug-drug interactions^[10]. In addition to inter-individual variability, the pharmacokinetics of Tac can vary within individual patients. The concept of intra-patient variability (IPV) refers to the fluctuations in Tac blood concentrations (and consequently episodes of over- and under-immunosuppression) that some patients experience over time^[11].

Several non-modifiable and modifiable factors contribute to Tac IPV (e.g., polymorphism in CYP3A genes, the circadian rhythm of Tac exposure, gastrointestinal events such as diarrhea, cholestasis, changes in protein levels, anemia, but also drug-drug interactions with macrolides or azole anti-fungal treatments, foods, or changes in formulation or generic substitution)^[11], but non-adherence to Tac seems to be the main cause of IPV^[12,13]. It was previously suggested that higher degree of Tac IPV was associated with kidney-graft rejection and worse long-term outcomes after kidney transplantation^[14,15]. Similar limited data have been reported after liver transplantation^[16,17], mainly in pediatric cohorts. Moreover, little is known concerning the relationship between Tac variability and the occurrence of donor-specific antibodies (DSAs). Herein, we retrospectively assessed the variability of Tac in a cohort of liver-transplant recipients and analyzed its impact on the number of acute rejections, the occurrence of *de novo* DSAs, and patient- and graft-survival rates.

MATERIALS AND METHODS

Patients

Between February 2008 (*i.e.*, the date when the solid-phase Luminex assay was set up in our institution) and June 2015, a total of 298 adult patients received a liver transplant from deceased donors (DDLT) in our center. Patients excluded from the study were those that died within the first month posttransplantation ($n = 34$), those that needed a re-transplant during the first month ($n = 2$), and those that received a transplant with a preformed DSA (mean fluorescence intensity cut-off > 1000) directed against human leukocyte antigen (HLA) A, B, Cw, DR, DQ, or DP ($n = 37$). In order to avoid confounding factors associated with others immunosuppressive treatments, only patients that received and were maintained under Tac and mycophenolate mofetil (MMF) (with or without steroids) were included in this study (Figure 1). All patients but five received Tac given twice daily (Prograf®). The other five received Tac once daily (Advagraf®). We excluded patients that had Tac or MMF withdrawn.

**Figure 1** Flow chart.

Moreover, to calculate intra-patient variability, at least three trough levels of Tac had to be available. Hence, 116 patients with a functioning liver allograft at 1 mo posttransplantation were included in this study after having given their informed consent and after we had obtained Toulouse University IRB approval.

The target concentration of Tac trough level was 7-10 ng/mL during the first 3 mo, and 5-10 ng/mL thereafter during the follow-up. Each participant was followed for 2 years or until re-transplantation ($n = 3$) or death ($n = 6$). The median follow-up was 24 mo (range: 6-24). All rejection episodes were biopsy proven. Biopsies were only performed for cause during the study period and were analyzed according to the Banff criteria^[18-20]. Graft failure was defined as the need for re-transplantation or as death from liver failure.

Detection of cytomegalovirus was performed using real-time PCR, as previously described^[21], at month 3, 6, 12, and 24, and at any other time if clinically indicated.

Intra-patient variability

Tac trough levels were routinely assessed using high-performance liquid chromatography-linked tandem mass spectrometry (HPLC-MS) at discharge, then monthly between months 1-6, and thereafter at months 9, 12, 15, 18, and 24. To calculate the IPV of Tac, at least three Tac trough levels from each patient had to be available. The median number of available Tac measurements was 10 (range: 4-12).

Tac IPV was estimated using the coefficient of variability (CV). The CV-IPV was calculated as follows: $\text{CV-IPV} (\%) = (\text{standard deviation}/\text{mean Tac trough-level concentration}) \times 100$. Because all patients received the same drug dose between discharge and M24, the obtained levels were corrected for the corresponding daily dose of tacrolimus (CV Co/D-IPV). In addition, because some patients were converted from one formulation to another during the follow-up, we calculated CV and CV Co/D-IPV after excluding the Tac trough levels obtained during the adjustment dose period, i.e., the month following a switch.

To compare IPV with the two formulations of Tac,

the Tac twice-daily CV-IPV was calculated using Tac trough levels obtained from patients that had received Tac twice daily since transplantation until last follow-up and those obtained in patients switched for Tac once daily before the switch. The Tac once-daily CV-IPV was calculated using Tac trough levels from patients that received Tac once daily since transplantation until the last follow-up, and those obtained from patients that were later switched from twice- to a once-daily formulation after the switch (this excluded Tac trough levels obtained in the month following the switch).

Immunological analyses

All patients were screened for anti-HLA DSAs at transplantation, and at month 3 and 12, and annually thereafter. Additional screening was performed in case of graft dysfunction. Luminex® assays were used to determine the specificity of class I HLAs in A/B/Cw and class II in DR/DQ/DP IgG antibodies in the recipients' sera (centrifuged at 10000 g for 10 min) using LabScreen single Ag HLA class-I and class-II detection tests (One Lambda, Canoga Park, CA, United States), according to the manufacturer's instructions. The presence and specificity of antibodies were then detected using a LabScan 100®, and the mean fluorescence (baseline) value for each sample in each bead was evaluated. The baseline value was calculated as follows: [raw sample mean fluorescence intensity (MFI)-raw negative serum control MFI-negative-bead raw MFI sample-negative-bead raw MFI negative serum control]. A baseline value of > 1000 was considered positive.

Statistical analyses

Categorical variables are expressed as percentages and comparisons between groups were made using the chi-squared test or, if appropriate, Fisher's exact test. Continuous variables were expressed as medians and ranges, and compared using the Mann-Whitney test. Logistic regression analysis was used to determine the predictors for acute-rejection episodes and the occurrence of *de novo* anti-HLA DSAs. Variables with a $P < 0.1$ in the univariate analyses were included in the stepwise multivariable analyses. $P < 0.05$ was considered statistically significant.

RESULTS

The patients' characteristics at transplantation are presented in Table 1. All liver transplantations performed in this study were performed from DDLT. The mean DDLT age was 51 ± 17 years. To note, one DDLT was < 18 years, and 4 DDLT were > 80 years.

Tacrolimus levels and variability

During the follow-up, 44 (38%) patients were switched from Tac immediate-release given twice a day (Prograf®), to Tac once a day to improve quality of life. The switch was performed at a mean of 15 (range: 1-18) mo post-

Table 1 Characteristics of the liver-transplant recipients

| Variable | n = 116 |
|--|----------------|
| Donors' age at transplantation, yr (range) | 53 (9-85) |
| Recipients' age at transplantation, yr (range) | 57 (18-72) |
| Recipients' gender: male, n (%) | 96 (83) |
| Initial liver disease, n (%) | |
| Alcohol | 49 (43) |
| Viral (HCV, HBV) | 36 (31) |
| Autoimmune disease (AIH, PSC, PBC) | 13 (11) |
| Other ¹ | 18 (17) |
| Median MELD score at transplantation (range) (%) | 22 (6-40) |
| Positive HCV RNA at transplantation, n (%) | 21 (18) |
| Re-transplantation, yes (%) | 3 (3) |
| Induction therapy, yes: n (%) | 87 (75) |
| Polyclonal antibodies, n (%) | 9 (8) |
| Interleukin-2 receptor blocker, n (%) | 78 (67) |
| Conversion during the follow-up from twice-daily to once daily tacrolimus, n (%) | 42 (36) |
| Number of patients receiving tacrolimus once daily, n (%) | 5 (4) |
| At discharge | |
| Month 1 | 8 (7) |
| Month 3 | 9 (8) |
| Month 6 | 12 (10) |
| Month 9 | 18 (16) |
| Month 12 | 26 (31) |
| Month 18 | 39 (34) |
| Month 24 | 47 (41) |
| Tacrolimus trough level (ng/mL) | 7.6 ± 3 |
| At discharge | |
| Month 1 | 8 ± 3 |
| Month 3 | 8.4 ± 3 |
| Month 6 | 8.4 ± 3 |
| Month 9 | 7.4 ± 3 |
| Month 12 | 7.8 ± 3 |
| Month 18 | 7.5 ± 2 |
| Month 24 | 6.9 ± 3 |
| Mycophenolate mofetil dose (mg/d) | 1700 ± 600 |
| At discharge | |
| Month 3 | 1250 ± 550 |
| Month 6 | 1100 ± 450 |
| Month 12 | 1000 ± 300 |
| Month 24 | 1000 ± 300 |
| Steroids (mg/d) | |
| At discharge: Yes (%) | 116 (100) |
| Dose (mg/d) | 20 ± 12 |
| Month 3: Yes (%) | 114 (98) |
| Dose (mg/d) | 8 ± 4 |
| Month 6: Yes (%) | 110 (95) |
| Dose (mg/d) | 7 ± 5 |
| Month 12: Yes (%) | 104 (90) |
| Dose (mg/d) | 6 ± 6 |
| Month 24: Yes (%) | 97 (84) |
| Dose (mg/d) | 5 ± 2 |

¹Polycystic disease (n = 7), NASH syndrome (n = 4), Wilson disease (n = 2), bile duct atrophy (n = 1), drug intoxication (n = 2), and cryptogenic cirrhosis (n = 1). HBV: Hepatitis B virus; HCV: Hepatitis C virus; AIH: Auto-immune hepatitis; PSC: Primary sclerosing cholangitis; PBC: Primary biliary cirrhosis.

transplantation.

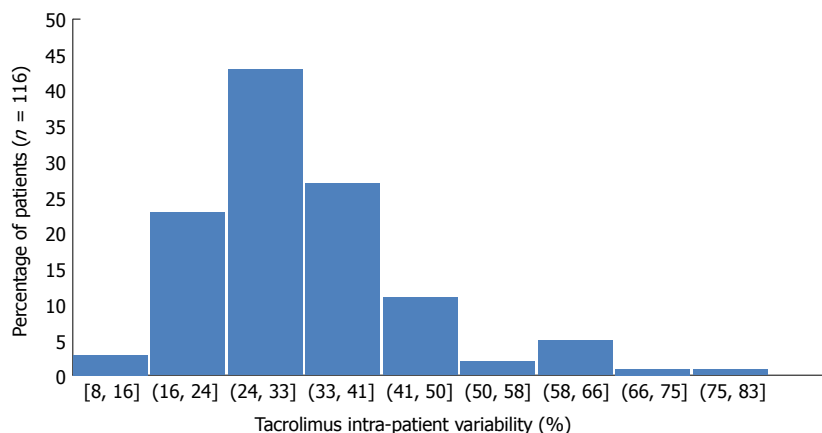
Mean tacrolimus trough level was 8 ± 3 ng/mL during the follow-up (Table 1). The mean dose of Tac was 6.8, 6.7, 6.4, 5.9, 5.4, 5.1, 4.8, and 4.6 mg/d, respectively, at discharge and at months 1, 3, 6, 9, 12, 18, and 24. Forty-five (38.8%) patients presented with a Tac trough level of < 5 ng/mL at least once during the follow-up. The overall mean Tac CV-IPV was 32 ± 12% [median CV-IPV 30.5% (7.6-80.6)]. Tac CV-IPV distribution is presented in Figure 2. The 1th, 2th, 3th, and

4th quartiles were, respectively, 25%, 30.5%, 36.5%, and 80.6%. The mean Tac CV-IPV was 30% ± 11% in patients given Tac once daily and was 32% ± 12% in patients that received Tac twice daily (P = 0.10). The mean Tac CV-IPV in the five patients that had received Tac once-daily since transplantation was 30% ± 7%. In the 44 patients that were converted from Tac twice-daily to once daily, the mean values of Tac CV-IPV were 32.3% ± 12% and 30% ± 12% before and after the switch, respectively (P = 0.21).

Table 2 Risk factors for a graft-rejection episode

| Variable | Univariate analyses | | | Multivariate analyses | | |
|---|---------------------|------------|---------|-----------------------|------------|---------|
| | OR | 95%CI | P value | OR | 95%CI | P value |
| MELD score > 30 (n = 31) | 0.55 | 0.12-1.90 | 0.42 | - | - | - |
| Initial liver disease | | | | | | |
| (1) Alcohol cirrhosis (n = 49) vs (2, 3, 4) | 0.58 | 0.18-1.68 | 0.34 | - | - | - |
| (2) Viral disease (n = 36) vs (1, 3, 4) | 1.34 | 0.44-3.90 | 0.61 | - | - | - |
| (3) Auto-immune ILD (n = 13) vs (1, 2, 4) | 3.12 | 0.71-12.47 | 0.07 | 1.00 | 0.51-1.15 | 0.210 |
| (4) Other (n = 18) vs (1, 2, 3) | 0.49 | 0.05-2.37 | 0.52 | - | - | - |
| Induction therapy, yes (n = 87) | 0.66 | 0.22-2.15 | 0.42 | - | - | - |
| Polyclonal antibodies (vs other) | 3.89 | 0.70-20.13 | 0.06 | 2.87 | 0.61-13.47 | 0.180 |
| IL2R blockers (vs other) | 0.40 | 0.14-1.70 | 0.08 | 0.52 | 0.185-1.50 | 0.230 |
| Donors' age > 50 yr (n = 69) | 0.98 | 0.35-2.88 | 1.00 | - | - | - |
| Recipients' age > 50 yr (n = 92) | 0.61 | 0.20-2.01 | 0.41 | - | - | - |
| HCV-RNA + At transplantation (n = 21) | 1.96 | 0.54-6.45 | 0.22 | - | - | - |
| Steroid withdrawal during the FU (n = 19) | 2.30 | 0.63-7.82 | 0.20 | - | - | - |
| De novo DSAs during the FU (n = 13) | 2.80 | 0.64-11.19 | 0.13 | - | - | - |
| Tacrolimus trough level < 5 ng/mL (n = 34) | 3.00 | 1.05-8.96 | 0.02 | 3.68 | 1.30-10.41 | 0.014 |
| CV-IPV tacrolimus (continuous variable) | 2.70 | 1.88-13.45 | 0.01 | 1.10 | 1.01-1.11 | 0.008 |
| CV-IPV > 35% | 3.05 | 1.05-8.96 | 0.03 | 3.07 | 1.14-8.24 | 0.030 |
| CV-IPV > 0% | 2.97 | 0.91-9.30 | 0.04 | 4.16 | 1.38-12.50 | 0.010 |
| CV-C ₀ /d-IPV | 1.89 | 0.67-5.74 | 0.24 | - | - | - |

FU: Follow-up; ILD: Initial liver disease; HCV: Hepatitis C virus; CV-IPV: Coefficient of variability-intra-patient variability; CV-C₀/d-IPV: Coefficient of variability corrected for the corresponding daily dose-intra-patient variability.

**Figure 2** Distribution of tacrolimus according to intra-patient variability.

Overall mean CV C₀/d- IPV was 73% ± 43%. It was 69% ± 29% with Tac twice-daily compared to 79% ± 50% for Tac given once daily ($P = 0.9$).

Incidence of acute rejection and de novo donor-specific antibodies

During the follow-up, 22 patients (19%) presented with at least one episode of acute rejection. The time between transplantation and a diagnosis of acute rejection (*i.e.*, the date of the biopsy) was 3.5 mo (range: 0.5-12). Fourteen patients (12%) experienced a T-cell steroid-sensitive acute rejection, and six patients (5%) presented with a T-cell steroid-resistant acute rejection, which was treated with polyclonal antibodies. One patient presented with an acute antibody-mediated rejection at 4 mo posttransplantation. The Tac CV-IPV in this patient was high: CV-IPV of 63.2% and CV C₀/d- IPV = 68.2%. The risk factors for acute rejection

after liver transplantation are presented in Table 2. The predictive factors for a biopsy-proven acute rejection were a Tac trough level of < 5 ng/mL [OR = 3.68; 95%CI (1.30-10.41), $P = 0.014$], the Tac CV-IPV (coded as a continuous variable) [OR = 1.1; 95%CI (1.01-1.11), $P = 0.008$], a CV-IPV of > 35% [OR = 3.07; 95%CI (1.14-8.24), $P = 0.03$], and a CV-IPV of > 40% [OR = 4.16; 95%CI (1.38-12.50), $P = 0.01$]. Twenty-one of the 22 patients that presented with an acute-rejection episode were receiving Tac twice daily when the rejection was diagnosed.

Thirteen patients (11.2%) presented with at least one *de novo* DSA during the posttransplantation follow-up (nine anti-HLA class II, three anti-HLA class I, one anti-HLA class I and II). Only one of these patients developed an antibody-mediated rejection. The median time between transplantation and detection of a *de novo* DSA was 3.5 mo (range: 1-12). The risk

Table 3 Risk factors for developing *de novo* donor-specific antibodies after liver transplantation.

| Variable | Univariate analyses | | | Multivariate analyses | | |
|---|---------------------|-------------|---------|-----------------------|------------|---------|
| | OR | 95%CI | P value | OR | 95%CI | P value |
| MELD score > 30 (n = 31) | 1.84 | 0.43-7.10 | 0.33 | - | - | - |
| Initial liver disease | | | | | | |
| (1) Alcohol cirrhosis (n = 49) vs (2, 3, 4) | 0.58 | 0.12-2.22 | 0.55 | - | - | - |
| (2) Viral disease (n = 36) vs (1, 3, 4) | 0.98 | 0.21-3.86 | 1.0 | - | - | - |
| (3) Autoimmune ILD (n = 13) vs (1, 2, 4) | 1.51 | 0.14-8.46 | 0.64 | - | - | - |
| (4) Other (n = 18) vs (1, 2, 3) | 2.79 | 0.55-11.83 | 0.64 | - | - | - |
| Induction therapy, yes (n = 87) | 1.61 | 0.41-7.61 | 0.55 | - | - | - |
| Polyclonal antibodies (vs other) | 0.59 | 0.70-18.00 | 0.60 | - | - | - |
| IL2R blockers (vs other) | 1.1 | 0.28-5.28 | 1.0 | - | - | - |
| Donors' age > 50 yr (n = 69) | 0.78 | 0.20-3.00 | 0.77 | - | - | - |
| Recipients' age > 50 yr (n = 92) | 0.36 | 0.09-1.58 | 0.10 | 0.2 | 0.07-0.85 | 0.3 |
| HCV RNA + at transplantation (n = 21) | 1.41 | 0.23-6.23 | 0.70 | - | - | - |
| Steroid withdrawal during the FU (n = 19) | 0.39 | 0.01-3.01 | 0.69 | - | - | - |
| Tacrolimus trough level < 5 ng/mL (n = 34) | 1.59 | 0.38-6.05 | 0.52 | - | - | - |
| CV-IPV tacrolimus (continuous variable) | 1.92 | -1.28-21.39 | 0.08 | 1.1 | 1.0-1.12 | 0.006 |
| CV-IPV > 35% | 4.66 | 1.22-19.82 | 0.02 | 4.83 | 1.39-16.72 | 0.01 |
| CV-IPV > 40% | 9.10 | 2.28-40.63 | < 0.001 | 9.73 | 2.65-35.76 | 0.001 |
| CV-C ₀ /d-IPV | 3.15 | 5.47-27.31 | 0.005 | 1.0 | 0.97-1.02 | 0.09 |

FU: Follow-up; ILD: Initial liver disease; HCV: Hepatitis C virus; CV-IPV: Coefficient of variability-intra-patient variability; CV-C₀/d-IPV: Coefficient of variability corrected for the corresponding daily dose-intra-patient variability.

factors for a *de novo* DSA are presented in Table 3. The Tac CV-IPV [coded as a continuous variable: OR = 1.1, 95%CI (1.0-1.12), P = 0.006], and a CV-IPV of > 35% [OR = 4.83, 95%CI (1.39-16.72), P = 0.01] or of > 40% [OR = 9.73, 95%CI (2.65-35.76), P = 0.001] were identified as predictors for the occurrence of *de novo* DSAs detection.

Survival of patients

During the follow-up, six patients died [at a mean of 13 mo (range: 6-23) posttransplantation]. The causes of death were infections (n = 3), cardiovascular (n = 2), and neoplastic (n = 1) complications. No difference in Tac CV-IPV was observed between patients that died during the follow-up (CV-IPV 33% ± 6%) and those that did not (CV-IPV 32% ± 12%; P = 0.70). Three patients required re-transplantation at month 5, 10, and 14, respectively, for ischemic cholangitis that occurred posttransplantation. During the follow-up, 24 patients presented with posttransplant replication of cytomegalovirus. No difference in Tac CV-IPV was observed between patients with replication of cytomegalovirus (CV-IPV 32% ± 9%) and those without replication (32% ± 12%, P = 0.90).

DISCUSSION

High IPV has been previously associated with a greater risk of graft rejection, an accelerated progression of chronic histological lesions, and worse long-term survival after kidney transplantation^[11,14,22,23]. In pediatric liver-transplants, Tac variability was associated with late acute rejection^[16]. In the present study, we investigated the impact of Tac variability in 116 adult liver-transplant recipients. In order to avoid confounding factors, we focused on patients that received a graft

without preformed DSAs and that had received Tac associated with MMF. Although the mean Tac trough level was 8 ± 3 ng/mL during the study period, nearly 40% of patients had a Tac trough level of < 5 ng/mL at least once during the follow-up. Tac CV-IPV varied from 7.6%-80.6% (median 30.5%), and median Tac CV C₀/d-IPV was 62% (18-147). Almost one-third of patients presented with a Tac CV-IPV of > 35%. This high value is similar to those reported in previous studies, mainly after kidney transplantation^[24,25]. In kidney-transplant^[13,25] and pediatric liver-transplant patients^[16], high CV-IPV was associated with an increased risk of acute rejection. In the present study, we found that a Tac trough level of < 5 ng/mL, the Tac CV-IPV (coded as a continuous variable), a CV-IPV of > 35%, and a CV-IPV > 40% were independent predictive factors for a biopsy-proven graft rejection.

Posttransplant positive DSAs were associated with decreased graft survival and increased acute or chronic graft rejections^[2,3,26]. It has been previously suggested that iterative transplantation, low levels of calcineurin inhibitors, the use of cyclosporine (compared to Tac), and non-adherence can promote the development of a *de novo* DSA after liver transplantation^[2]. Herein, we found that the Tac CV-IPV (coded as a continuous variable), a CV-IPV of > 35%, and CV-IPV > 40% were independent predictive factors for the occurrence of a *de novo* DSA. Similar data, reported after kidney transplantation^[24], from a cohort of 310 adult kidney-transplant patients given Tac twice-daily during the first year posttransplant, showed that a history of acute rejection, re-transplantation and a Tac CV greater than 30% were associated with the occurrence of a *de novo* DSA. In our study, one patient presented with an acute antibody-mediated rejection associated with an anti-class II *de novo* DSA at 3 mo after liver transplantation.

Interestingly, this patient had high tacrolimus variability (CV-IPV 63.2%, CV Co/d-IPV 68.2%). None of the other 12 patients that developed a DSA experienced an acute antibody-mediated rejection. However, it was suggested that patients with positive DSAs would present lower graft survival, consecutive to chronic antibody mediated rejection^[27] rather than to acute antibody-mediated rejection episodes.

In several studies, but not all, the use of once-daily tacrolimus compared to a twice daily formulation has been found to improve adherence and to reduce IPV^[11,28-31]. In the present study, no difference between Tac formulations was observed.

This study has several limitations. Because of its retrospective design, we could not evaluate the cause of Tac variability. It has been suggested previously that non-adherence is the main cause of Tac variability^[11]. However, in our study, adherence was not evaluated using objective methods, such as those previously reported using electronic devices^[28]. Moreover, we did not evaluate MMF variability in our study because we do not perform this analysis routinely in our center. Of note, conflicting results have been reported concerning the use of MMF variability after solid-organ transplantation^[14,25]. It was also previously suggested that pre-transplant determination of CYP3A5 and MDR1 polymorphisms^[32] allows more rapid achievement of therapeutic Tac trough level. However, no association between the pharmacogenomics parameters and Tac intra-patient variability is expected and was reported.

In conclusion, we found that the CV-IPV of Tac was a predictive factor for acute rejection and the occurrence of a *de novo* DSA after liver transplantation. This could be a useful tool to identify patients with a greater risk of graft rejection and of developing a *de novo* DSA after liver transplantation. Future studies should investigate the role of Tac IPV on long-term outcomes, on chronic graft rejection, and over-immunosuppression-related diseases (cancer, and related immunocompromised infections).

ARTICLE HIGHLIGHTS

Research background

Tacrolimus (Tac) is considered a cornerstone within immunosuppression protocols to prevent T-cell and antibody-mediated rejection after liver transplantation. However, this treatment presents a narrow therapeutic index: overexposure can lead to clinically serious events, thus necessitating regular therapeutic drug monitoring, whereas underexposure can lead to acute or chronic graft rejection. The concept of intra-patient variability (IPV) refers to the fluctuations in Tac blood concentrations (and consequently episodes of over- and under-immunosuppression) that some patients experience over time.

Research motivation

Tac-IPV is an inexpensive assay to explore fluctuations in Tac blood concentrations. We investigated the potential usefulness of Tac-IPV to predict the incidence of donor specific antibodies and graft rejection episodes.

Research objectives

Our aim was to investigate the role of tacrolimus IPV in adult liver-transplant recipients.

Research methods

We retrospectively assessed tacrolimus variability and analyzed its effect on the occurrence of graft rejection and *de novo* donor-specific antibodies.

Research results

Twenty-two patients experienced at least one acute-rejection episode (BPAR). Predictive factors for a BPAR were a tacrolimus IPV of > 35% or > 40%, and a tacrolimus trough level of < 5 ng/mL. Thirteen patients developed at least one *dnDSA* during the follow-up. Tacrolimus IPV and tacrolimus IPV of > 35%, and > 40% were identified as predictors to detect *dnDSAs*. IPV did not impact on patient- or graft-survival rates during the follow-up.

Research conclusions

In our study higher Tac-IPV was associated with graft rejection and occurrence of DSAs.

Research perspective

Tacrolimus-IPV could be a useful tool to identify patients with a greater risk of graft rejection and of developing a *de novo* DSA after liver transplantation.

REFERENCES

- Price DC. Radioisotopic evaluation of the thyroid and the parathyroids. *Radioi Clin North Am* 1993; **31**: 991-1015 [PMID: 8362060 DOI: 10.1002/14651858.CD011639.pub2]
- Kaneko H, O'Leary JG, Banuelos N, Jennings LW, Susskind BM, Klintmalm GB, Terasaki PI. *De novo* donor-specific HLA antibodies decrease patient and graft survival in liver transplant recipients. *Am J Transplant* 2013; **13**: 1541-1548 [PMID: 23721554 DOI: 10.1111/ajt.12212]
- European Association for the Study of the Liver.** EASL Clinical Practice Guidelines: Liver transplantation. *J Hepatol* 2016; **64**: 433-485 [PMID: 26597456 DOI: 10.1016/j.jhep.2015.10.006]
- de Mare-Bredemeijer EL, Metselaar HJ. Optimization of the use of Calcineurin inhibitors in liver transplantation. *Best Pract Res Clin Gastroenterol* 2012; **26**: 85-95 [PMID: 22482528 DOI: 10.1016/j.bpg.2012.01.017]
- Rodríguez-Perálvarez M, Germani G, Papastergiou V, Tsochatzis E, Thalassinos E, Luong TV, Rolando N, Dhillon AP, Patch D, O'Beirne J, Thorburn D, Burroughs AK. Early tacrolimus exposure after liver transplantation: relationship with moderate/severe acute rejection and long-term outcome. *J Hepatol* 2013; **58**: 262-270 [PMID: 23023010 DOI: 10.1016/j.jhep.2012.09.019]
- Del Bello A, Congy-Jolivet N, Muscari F, Lavayssiére L, Esposito L, Cardeau-Desangles I, Guitard J, Dörr G, Suc B, Duffas JP, Alric L, Bureau C, Danjoux M, Guilbeau-Frugier C, Blancher A, Rostaing L, Kamar N. Prevalence, incidence and risk factors for donor-specific anti-HLA antibodies in maintenance liver transplant patients. *Am J Transplant* 2014; **14**: 867-875 [PMID: 24580771 DOI: 10.1111/ajt.12651]
- Staatz CE, Tett SE. Clinical pharmacokinetics and pharmacodynamics of tacrolimus in solid organ transplantation. *Clin Pharmacokinet* 2004; **43**: 623-653 [PMID: 15244495 DOI: 10.1007/s40262-015-0282-2]
- Hesselink DA, Bouamar R, Elens L, van Schaik RH, van Gelder T. The role of pharmacogenetics in the disposition of and response to tacrolimus in solid organ transplantation. *Clin Pharmacokinet* 2014; **53**: 123-139 [PMID: 24249597 DOI: 10.1007/s40262-013-0120-3]
- Tada H, Satoh S, Inuma M, Shimoda N, Murakami M, Hayase Y, Kato T, Suzuki T. Chronopharmacokinetics of tacrolimus in kidney transplant recipients: occurrence of acute rejection. *J Clin Pharmacol* 2003; **43**: 859-865 [PMID: 12953343 DOI: 10.1177/091270003254797]
- van Gelder T. Drug interactions with tacrolimus. *Drug Saf* 2002; **25**: 707-712 [PMID: 12167066 DOI: 10.2165/00002018-200225100-00003]
- Shuker N, van Gelder T, Hesselink DA. Intra-patient variability

- in tacrolimus exposure: causes, consequences for clinical management. *Transplant Rev (Orlando)* 2015; **29**: 78-84 [PMID: 25687818 DOI: 10.1016/j.trre.2015.01.002]
- 12 **Shemesh E**, Schneider BL, Savitzky JK, Arnott L, Gondolesi GE, Krieger NR, Kerkar N, Magid MS, Stuber ML, Schmeidler J, Yehuda R, Emre S. Medication adherence in pediatric and adolescent liver transplant recipients. *Pediatrics* 2004; **113**: 825-832 [PMID: 15060234 DOI: 10.1542/peds.113.4.825]
- 13 **Pollock-Barziv SM**, Finkelstein Y, Manlhiot C, Dipchand AI, Hebert D, Ng VL, Solomon M, McCrindle BW, Grant D. Variability in tacrolimus blood levels increases the risk of late rejection and graft loss after solid organ transplantation in older children. *Pediatr Transplant* 2010; **14**: 968-975 [PMID: 21040278 DOI: 10.1111/j.1399-3046.2010.01409.x]
- 14 **Borra LC**, Roodnat JI, Kal JA, Mathot RA, Weimar W, van Gelder T. High within-patient variability in the clearance of tacrolimus is a risk factor for poor long-term outcome after kidney transplantation. *Nephrol Dial Transplant* 2010; **25**: 2757-2763 [PMID: 20190242 DOI: 10.1093/ndt/gfq096]
- 15 **Ro H**, Min SI, Yang J, Moon KC, Kim YS, Kim SJ, Ahn C, Ha J. Impact of tacrolimus intraindividual variability and CYP3A5 genetic polymorphism on acute rejection in kidney transplantation. *Ther Drug Monit* 2012; **34**: 680-685 [PMID: 23149441 DOI: 10.1097/FTD.0b013e3182731809]
- 16 **Shemesh E**, Bucuvalas JC, Anand R, Mazariegos GV, Alonso EM, Venick RS, Reyes-Mugica M, Annunziato RA, Schneider BL. The Medication Level Variability Index (MLVI) Predicts Poor Liver Transplant Outcomes: A Prospective Multi-Site Study. *Am J Transplant* 2017; **17**: 2668-2678 [PMID: 28321975 DOI: 10.1111/ajt.14276]
- 17 **Christina S**, Annunziato RA, Schiano TD, Anand R, Vaidya S, Chuang K, Zack Y, Florman S, Schneider BL, Shemesh E. Medication level variability index predicts rejection, possibly due to nonadherence, in adult liver transplant recipients. *Liver Transpl* 2014; **20**: 1168-1177 [PMID: 24931127 DOI: 10.1002/lt.23930]
- 18 Banff schema for grading liver allograft rejection: an international consensus document. *Hepatology* 1997; **25**: 658-663 [PMID: 9049215 DOI: 10.1002/hep.510250328]
- 19 **Demetris AJ**, Adams D, Bellamy C, Blakolmer K, Clouston A, Dhillon AP, Fung J, Gouw A, Gustafsson B, Haga H, Harrison D, Hart J, Hubscher S, Jaffe R, Khettry U, Lassman C, Lewin K, Martinez O, Nakazawa Y, Neil D, Pappo O, Parizhskaya M, Randhawa P, Rasoul-Rockenschaub S, Reinholt F, Reynes M, Robert M, Tsamandas A, Wanless I, Wiesner R, Wernerson A, Wrba F, Wyatt J, Yamabe H. Update of the International Banff Schema for Liver Allograft Rejection: working recommendations for the histopathologic staging and reporting of chronic rejection. An International Panel. *Hepatology* 2000; **31**: 792-799 [PMID: 10706577 DOI: 10.1002/hep.510310337]
- 20 **Demetris AJ**, Bellamy C, Hübscher SG, O'Leary J, Randhawa PS, Feng S, Neil D, Colvin RB, McCaughan G, Fung JJ, Del Bello A, Reinholt FP, Haga H, Adeyi O, Czaja AJ, Schiano T, Fiel MI, Smith ML, Sebagh M, Tanigawa RY, Yilmaz F, Alexander G, Baiocchi L, Balasubramanian M, Batal I, Bhan AK, Bucuvalas J, Cerski CTS, Charlotte F, de Vera ME, ElMonayeri M, Fontes P, Furth EE, Gouw ASH, Hafezi-Bakhtiari S, Hart J, Honsova E, Ismail W, Itoh T, Jhala NC, Khettry U, Klintmalm GB, Knechtle S, Koshiba T, Kozlowski T, Lassman CR, Lerut J, Levitsky J, Licini L, Liotta R, Mazariegos G, Minervini MI, Misraji J, Mohanakumar T, Mölne J, Nasser I, Neuberger J, O'Neil M, Pappo O, Petrovic L, Ruiz P, Sağol Ö, Sanchez Fueyo A, Sasatomi E, Shaked A, Shiller M, Shimizu T, Sis B, Sonzogni A, Stevenson HL, Thung SN, Tisone G, Tsamandas AC, Wernerson A, Wu T, Zeevi A, Zen Y. 2016 Comprehensive Update of the Banff Working Group on Liver Allograft Pathology: Introduction of Antibody-Mediated Rejection. *Am J Transplant* 2016; **16**: 2816-2835 [PMID: 27273869 DOI: 10.1111/ajt.13909]
- 21 **Mengelle C**, Sandres-Sauné K, Pasquier C, Rostaing L, Mansuy JM, Marty M, Da Silva I, Attal M, Massip P, Izopet J. Automated extraction and quantification of human cytomegalovirus DNA in whole blood by real-time PCR assay. *J Clin Microbiol* 2003; **41**: 3840-3845 [PMID: 12904398 DOI: 10.1128/JCM.41.8.3840-3845.2003]
- 22 **Taber DJ**, Su Z, Fleming JN, McGillicuddy JW, Posadas-Salas MA, Treiber FA, Dubay D, Srinivas TR, Mauldin PD, Moran WP, Baliga PK. Tacrolimus Trough Concentration Variability and Disparities in African American Kidney Transplantation. *Transplantation* 2017; **101**: 2931-2938 [PMID: 28658199 DOI: 10.1097/TP.00000000000001840]
- 23 **Vanhove T**, Vermeulen T, Annaert P, Lerut E, Kuypers DRJ. High Intrapatient Variability of Tacrolimus Concentrations Predicts Accelerated Progression of Chronic Histologic Lesions in Renal Recipients. *Am J Transplant* 2016; **16**: 2954-2963 [PMID: 27013142 DOI: 10.1111/ajt.13803]
- 24 **Rodrigo E**, Segundo DS, Fernández-Fresnedo G, López-Hoyos M, Benito A, Ruiz JC, de Cos MA, Arias M. Within-Patient Variability in Tacrolimus Blood Levels Predicts Kidney Graft Loss and Donor-Specific Antibody Development. *Transplantation* 2016; **100**: 2479-2485 [PMID: 26703349 DOI: 10.1097/TP.0000000000001040]
- 25 **Hsiau M**, Fernandez HE, Gjertson D, Ettenger RB, Tsai EW. Monitoring nonadherence and acute rejection with variation in blood immunosuppressant levels in pediatric renal transplantation. *Transplantation* 2011; **92**: 918-922 [PMID: 21857278 DOI: 10.1097/TP.0b013e31822dc34f]
- 26 **O'Leary JG**, Kaneku H, Jennings LW, Bañuelos N, Susskind BM, Terasaki PI, Klintmalm GB. Preformed class II donor-specific antibodies are associated with an increased risk of early rejection after liver transplantation. *Liver Transpl* 2013; **19**: 973-980 [PMID: 23780820 DOI: 10.1002/lt.23687]
- 27 **O'Leary JG**, Cai J, Freeman R, Banuelos N, Hart B, Johnson M, Jennings LW, Kaneku H, Terasaki PI, Klintmalm GB, Demetris AJ. Proposed Diagnostic Criteria for Chronic Antibody-Mediated Rejection in Liver Allografts. *Am J Transplant* 2016; **16**: 603-614 [PMID: 26469278 DOI: 10.1111/ajt.13476]
- 28 **Kuypers DR**, Peeters PC, Sennesael JJ, Kianda MN, Vrijens B, Kristanto P, Dobbels F, Vanrenterghem Y, Kanaan N; ADMIRAD Study Team. Improved adherence to tacrolimus once-daily formulation in renal recipients: a randomized controlled trial using electronic monitoring. *Transplantation* 2013; **95**: 333-340 [PMID: 23263559 DOI: 10.1097/TP.0b013e3182725532]
- 29 **van Hooff J**, Van der Walt I, Kallmeyer J, Miller D, Dawood S, Moosa MR, Christians M, Karpf C, Undre N. Pharmacokinetics in stable kidney transplant recipients after conversion from twice-daily to once-daily tacrolimus formulations. *Ther Drug Monit* 2012; **34**: 46-52 [PMID: 22249344 DOI: 10.1097/FTD.0b013e318244a7fd]
- 30 **Wehland M**, Bauer S, Brakemeier S, Burgwinkel P, Glander P, Kreutz R, Lorkowski C, Slowinski T, Neumayer HH, Budde K. Differential impact of the CYP3A5*1 and CYP3A5*3 alleles on pre-dose concentrations of two tacrolimus formulations. *Pharmacogenet Genomics* 2011; **21**: 179-184 [PMID: 20818295 DOI: 10.1097/FPC.0b013e32833ea085]
- 31 **Shuker N**, Cadogan M, van Gelder T, Roodnat JI, Kho MM, Weimar W, Hesselink DA. Conversion from twice-daily to once-daily tacrolimus does not reduce intrapatient variability in tacrolimus exposure. *Ther Drug Monit* 2015; **37**: 262-269 [PMID: 25265255 DOI: 10.1097/FTD.0000000000000136]
- 32 **Tang JT**, Andrews LM, van Gelder T, Shi YY, van Schaik RH, Wang LL, Hesselink DA. Pharmacogenetic aspects of the use of tacrolimus in renal transplantation: recent developments and ethnic considerations. *Expert Opin Drug Metab Toxicol* 2016; **12**: 555-565 [PMID: 27010623 DOI: 10.1517/17425255.2016.1170808]

P- Reviewer: Chiu KW, Sergi CM, Sugawara Y **S- Editor:** Wang XJ
L- Editor: A **E- Editor:** Huang Y



Randomized Clinical Trial

Papillary fistulotomy vs conventional cannulation for endoscopic biliary access: A prospective randomized trial

Carlos Kiyoshi Furuya, Paulo Sakai, Fabio Ramalho Tavares Marinho, Jose Pinhata Otoch, Spencer Cheng, Lívia Lemes Prudencio, Eduardo Guimarães Hourneaux de Moura, Everson Luiz de Almeida Artifon

Carlos Kiyoshi Furuya, Paulo Sakai, Fabio Ramalho Tavares Marinho, Spencer Cheng, Eduardo Guimarães Hourneaux de Moura, Department of Gastrointestinal Endoscopy Unit, University of São Paulo, São Paulo 05409001, Brazil

Jose Pinhata Otoch, Lívia Lemes Prudencio, Department of Surgery, University of São Paulo, São Paulo 05403000, Brazil

Everson Luiz de Almeida Artifon, Department of Gastroenterology and Radiology, University of São Paulo, São Paulo 04107-030, Brazil

ORCID number: Carlos Kiyoshi Furuya (0000-0002-6512-5029); Paulo Sakai (0000-0003-3088-9210); Fabio Ramalho Tavares Marinho (0000-0002-7509-7113); Jose Pinhata Otoch (0000-0002-8293-1508); Spencer Cheng (0000-0001-9584-203X); Lívia Lemes Prudencio (0000-0002-8256-9035); Eduardo Guimarães Hourneaux de Moura (0000-0003-1215-5731); Everson Luiz de Almeida Artifon (0000-0003-1900-8777).

Author contributions: Furuya CK designed and performed the research; Sakai P, Marinho FRT and Prudencio LL wrote the paper; Otoch JP and de Moura EGH analyzed the data; Artifon EL performed the research and analyzed the data.

Institutional review board statement: The study was reviewed and approved by Ethics Committee for Research Project Analysis of Clinics Hospital, University of São Paulo and UNILUS Ethics Subcommittee.

Informed consent statement: All study participants, or their legal guardian, provided informed written consent prior to study enrollment.

Conflict-of-interest statement: All authors declare no potential conflicting interests related to this paper.

Data sharing statement: No additional data are available.

Open-Access: This article is an open-access article which was selected by an in-house editor and fully peer-reviewed by external reviewers. It is distributed in accordance with the Creative

Commons Attribution Non Commercial (CC BY-NC 4.0) license, which permits others to distribute, remix, adapt, build upon this work non-commercially, and license their derivative works on different terms, provided the original work is properly cited and the use is non-commercial. See: <http://creativecommons.org/licenses/by-nc/4.0/>

Manuscript source: Unsolicited manuscript

Correspondence to: Carlos Kiyoshi Furuya, MD, PhD, Medical Assistant, Department of Gastrointestinal Endoscopy Unit, University of São Paulo, Av. Dr. Eneas de Carvalho Aguiar, 255 Predio dos Ambulatórios-6 andar-Bloco 3, São Paulo 5409001, Brazil. carloskfjr@gmail.com
Telephone: +55-11-30697579

Received: February 25, 2018

Peer-review started: February 26, 2018

First decision: March 9, 2018

Revised: March 12, 2018

Accepted: March 25, 2018

Article in press: March 25, 2018

Published online: April 28, 2018

Abstract

AIM

To compare the cannulation success, biochemical profile, and complications of the papillary fistulotomy technique *vs* catheter and guidewire standard access.

METHODS

From July 2010 to May 2017, patients were prospectively randomized into two groups: Cannulation with a catheter and guidewire (Group I) and papillary fistulotomy (Group II). Amylase, lipase and C-reactive protein at T0, as well as 12 h and 24 h after endoscopic retrograde cholangiopancreatography, and complications (pancreatitis, bleeding, perforation) were recorded.

RESULTS

We included 102 patients (66 females and 36 males, mean age 59.11 ± 18.7 years). Group I and Group II had 51 patients each. The successful cannulation rates were 76.5% and 100%, respectively ($P = 0.0002$). Twelve patients (23.5%) in Group I had a difficult cannulation and underwent fistulotomy, which led to successful secondary biliary access (Failure Group). The complication rate was 13.7% (2 perforations and 5 mild pancreatitis) vs 2.0% (1 patient with perforation and pancreatitis) in Groups I and II, respectively ($P = 0.0597$).

CONCLUSION

Papillary fistulotomy was more effective than guidewire cannulation, and it was associated with a lower profile of amylase and lipase. Complications were similar in both groups.

Key words: Catheterization; Complications; Endoscopic retrograde cholangiopancreatography; Therapeutic use; Common bile duct

© The Author(s) 2018. Published by Baishideng Publishing Group Inc. All rights reserved.

Core tip: Biliary cannulation is the first step of therapeutic endoscopic retrograde cholangiopancreatography and can determine several complications. There are small numbers of papers regarding comparison between conventional cannulation *vs* fistulotomy. Our study is a well-designed approach in its matter. In fact, we compare the cannulation success, biochemical profile and complications of the papillary fistulotomy technique *versus* catheter and guidewire standard access. Papillary fistulotomy was more effective than guidewire cannulation, and it was associated with a lower profile of amylase and lipase, as the routine endoscopic access to the biliary tree, including difficult cases. Complications were similar in both groups.

Furuya CK, Sakai P, Marinho FR, Otoch JP, Cheng S, Prudencio LL, de Moura EG, Artifon EL. Papillary fistulotomy vs conventional cannulation for endoscopic biliary access: A prospective randomized trial. *World J Gastroenterol* 2018; 24(16): 1803-1811 Available from: URL: <http://www.wjgnet.com/1007-9327/full/v24/i16/1803.htm> DOI: <http://dx.doi.org/10.3748/wjg.v24.i16.1803>

INTRODUCTION

Biliary tract cannulation is the critical step in diagnosis and treatment of biliopancreatic diseases during endoscopic retrograde cholangiopancreatography (ERCP). Catheter introduction through the papillary ostium fails in 5% to 20% of the patients^[1,2]. Several alternatives can be used for difficult cases, such as double-guidewire, pancreatic stent, rendezvous, precut

papillotomy, transpancreatic sphincterotomy and papillary fistulotomy (PF) techniques. Acute pancreatitis after ERCP is the most feared complication. It is also one of the most frequent, with an incidence of 1% up to 10% or more, and a mortality of 0.1%-1%^[3].

Selective cannulation of the biliary tract, thereby avoiding the pancreatic duct, can curb the mechanisms that trigger pancreatitis, and therefore prevent its occurrence. The precut sphincterotomy has been identified as an independent risk factor of postERCP pancreatitis (PEP). It is unclear whether prolonged cannulation attempts, or precut incisions are to blame. Studies suggest that an early precut is a protective factor, compared to persistent attempts at cannulation^[4,5]. However, all protocols that found a lower risk of PEP with a precut technique were performed at specialized centers, and the use of pancreatic stents was limited and inconsistent.

There are few investigations in which the precut and PF techniques were initially employed, to access the biliary tract^[6-8]. The PF technique is based on accessing the bile duct far from the pancreatic duct, by sectioning the papilla proximally, and thus avoiding the ostium (proximal half of the papilla). PF was initially described by Osnes *et al*^[9]. These authors observed a spontaneous choledochoduodenal fistula during ERCP. Contrast injection through the fistula detected bile duct stones. After enlargement of the fistula with a diathermic snare, the patients were observed for a few days with the spontaneous exit of the stones. Sakai *et al*^[10] reported a pancreatitis occurrence rate of 7.6% in 2001, particularly in the setting of previous manipulation of the papilla, and trauma to the pancreatic duct, after several frustrated attempts at biliary tract cannulation.

The main objective of this study was to evaluate the success of the PF technique, in the cannulation of the biliary tract. The secondary objective was to assess the enzyme profile and ensuing complications, in comparison with direct cannulation.

MATERIALS AND METHODS

From July 2010 to May 2017, candidates for ERCP due to choledocolithiasis were recruited at Ana Costa Santos Hospital and the Endoscopy Unit of the Clinical Hospital, Faculty of Medicine, University of São Paulo. Enrolled patients were randomized for conventional cannulation with a catheter and guidewire (Group I) and PF (Group II).

Inclusion criteria were adult (both sexes) with choledocholithiasis and diagnosis by abdominal ultrasound, computed tomography (CT), cholangio resonance, or intraoperative cholangiography. Exclusion criteria were Billroth II gastrectomy, duodenal obstruction, coagulopathy or anticoagulant use, pregnancy or lactation, acute pancreatitis, myocardial infarction in the last 6 mo, previous papillotomy, or refusal to participate in the study.

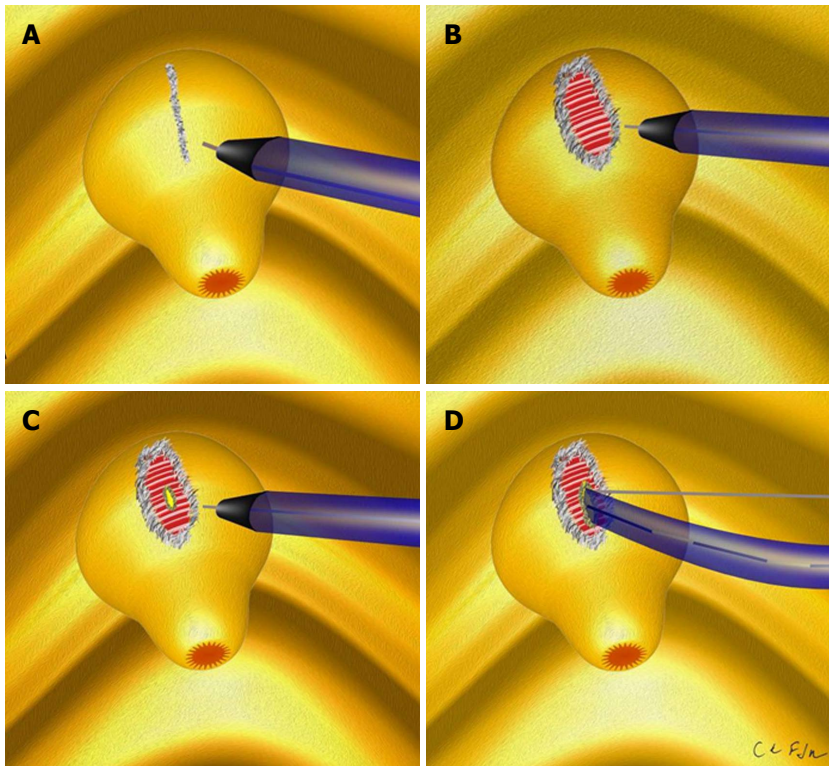


Figure 1 Schematic sequence of papillary fistulotomy. A and B: Dissection of the major papilla; C: Sphincterotome in the bile duct; D: Radiological image.

The protocol was approved by the institutional Ethical Committee, and also registered as a randomized trial at the University of São Paulo Registry-MA3: 014/2010 and 0671/09. Informed consent was signed by all participants. Side-view endoscopes (Pentax ED-3670TK, Olympus TJF-160, or Fujinon ED-250XT5) were used during the ERCP. WEM SS-200E, Erbe ICC 200 and ValleyLab Force FX electrosurgical units were employed.

Group I

Cannulation of the papillary ostium was performed using a 4.4 Fr sphincterotome (TRUEtome; Boston Scientific) with a 0.035-inch guidewire (Jagwire; Boston Scientific). A pure cut current (50 watts), applied in short-duration pulses, was adopted to perform papillotomy. A 30-watt pure cut current was indicated for intradiverticular papillae, and the complementation of fistulotomies (Figures 1 and 2).

A difficult cannulation was recognized if it took > 10 min, required > 5 cannulation attempts, or when > 2 pancreatic duct penetrations occurred. Difficult cases were referred to PF. Pancreatic plastic stents were placed in case of prolonged procedure.

Group II

Incision was made on the mucosa, using a needle-knife catheter (MicroKnife XL; Boston Scientific), in distal to proximal direction, aiming at the papillary apex. It involved the proximal two-thirds of the papillary protuberance, and above the papillary orifice (approximately 5 mm far from the ostium). A pure

cutting current (30 watts) was used to section the mucosa and the choledochal sphincter. The dissection was stopped when biliary secretion, open bile duct mucosa, or bulging of the bile duct mucosa was identified. The fistula was cannulated into the bile duct with a guidewire and sphincterotome, and it was enlarged by cutting the sphincter, to the limit of the transverse mucosal fold.

The PF procedure was stopped when there were signs of perforation, false route, major bleeding, loss of anatomy, or if cannulation of the bile duct was not achieved within 15 min. In these cases, the procedure was repeated after 5 to 7 d.

Enzymatic abnormalities (serum amylase and lipase) were documented up to 24 h before the examination (T0), as well as 12 h and 24 h after the endoscopic procedure. The diagnosis of acute pancreatitis was based on persistent or worsening abdominal pain 24 h following ERCP and abnormal laboratory data, complemented by imaging methods. An amylase or lipase concentration of more than three times the upper limit of normal was considered diagnostic^[11].

Hyperamylasemia was defined as amylase and/or lipase 3 times the upper limit of normal (> 300 U/L), without clinical features of pancreatitis. Inflammatory changes were monitored by serum C-reactive protein, collected at the same times.

A duodenal perforation was defined as gas or contrast accumulation in the retroperitoneum detected by simple X-ray of the abdomen. Endoscopic evidence, and clinical-laboratory findings consistent with bleeding were carefully monitored. These included bloody vomit or stools.

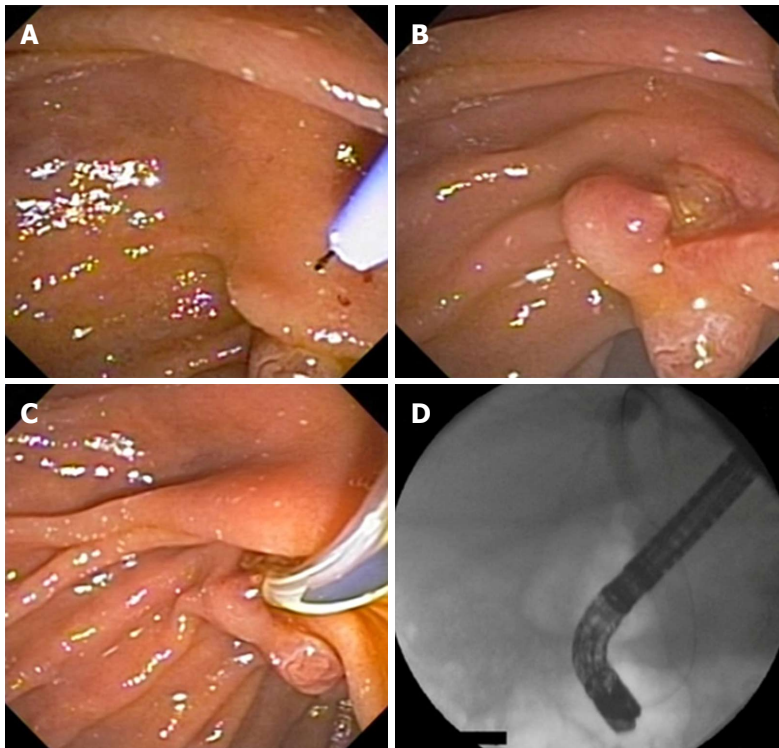


Figure 2 Sequence of papillary fistulotomy. A and B: Dissection of the major papilla; D: Sphincterotomy in the bile duct; D: Radiological image.

Whenever the problem was suspected, hemoglobin concentration was serially measured, starting at 12 h after the intervention, and compared with preprocedure values, with hemoglobin drop of 2 g/dL.

Patients were admitted for 24 h after the endoscopic procedure and under fasting condition. Asymptomatic patients without laboratorial or radiological signs of pancreatitis or other complications were discharged after 24 h and contacted by phone call 36 h and 48 h after discharge to ensure there were no symptoms. Any symptomatic patient would be referred to the hospital for clinical and laboratorial assessment. If a complication occurred, the patient remained hospitalized until complete recovery was observed. All complications were managed using a multidisciplinary approach and according to international guidelines, with consensus between the Endoscopist and Surgeon.

Sample size calculation

Calculations were based on similar studies, reporting a biliary cannulation failure rate of 5% to 20%^[1,2]. Adopting a 95% confidence interval of 3.65, a total population of 90 patients, and a minimum method failure rate of 2% (total ERCP success of 98% as maximum), 35 patients were deemed necessary per group. For safety, 51 patients were allocated to each group.

Statistical analysis

Analyses were performed with IBM SPSS for Windows version 20.0. The significance level was 5%. Randomization employed sealed envelopes, and descriptive statistics comprised mean \pm SD as well as

median, minimum and maximum, whenever appropriate. Student's *t* test and Mann-Whitney test were used for comparisons, depending on initial normality assessment. Qualitative characteristics were informed as absolute and relative frequencies, and compared by means of chi-square, Fisher's exact test, and likelihood ratio test^[12]. Pancreatic enzyme curves were compared by generalized estimating equations (GEE), with gamma marginal distribution and identity link function, within a first order autoregressive correlation matrix between the evaluation times.

RESULTS

A total of 102 patients were selected and randomized into Group I (51 patients) and Group II (51 patients). There were no post hoc exclusions. Table 1 demonstrates that the demographic and preliminary clinical findings were comparable ($P > 0.05$).

As informed in Table 2, choledocholithiasis was confirmed in 80.4% and 62.7% of Groups I and II, respectively ($P = 0.048$). The success rate for biliary duct cannulation was higher in Group II (100%) than in Group I (76.48%) ($P = 0.0002$). PF was performed in a single session. Dilated intrahepatic and extrahepatic bile ducts, and placement of biliary stents, were not different between the groups ($P > 0.05$). No difference in the risk of pancreatitis could be accounted to either intrahepatic or extrahepatic dilatation.

Intra- or peridiverticular papillae were observed in 15.7% and 3.9% of the populations, respectively ($P = 0.046$). Twelve cannulations (23.5%) were classified

Table 1 Patient characteristics and baseline laboratory tests

| Variable | Group I, n = 51 | Group II, n = 51 | Total, n = 102 | P value |
|-------------------|------------------|------------------|-----------------|----------------------|
| Age in yr | | | | 0.343 ¹ |
| Mean ± σ | 57.4 ± 19.3 | 60.9 ± 18.1 | 59.1 ± 18.7 | |
| Median (min; max) | 56 (19; 91) | 64 (22; 95) | 58 (19; 95) | |
| Sex, n (%) | | | | > 0.999 ² |
| Female | 33 (64.7) | 33 (64.7) | 66 (64.7) | |
| Male | 18 (35.3) | 18 (35.3) | 36 (35.3) | |
| AST | | | | 0.680 |
| Mean ± σ | 116.3 ± 143.4 | 124.3 ± 168.3 | 120.1 ± 155.1 | |
| Median (min; max) | 44 (8; 691) | 60 (13; 762) | 50 (8; 762) | |
| ALT | | | | 0.873 |
| Mean ± σ | 163.6 ± 191.6 | 154.1 ± 169.3 | 159 ± 180.4 | |
| Median (min; max) | 83 (9; 776) | 104 (11; 662) | 90 (9; 776) | |
| AP | | | | 0.585 |
| Mean ± σ | 267.8 ± 329.7 | 301.9 ± 320.4 | 284.3 ± 323.9 | |
| Median (min; max) | 153.5 (8; 1567) | 173 (32; 1320) | 162 (8; 1567) | |
| GGT | | | | 0.821 |
| Mean ± σ | 532 ± 454.3 | 543.4 ± 578.2 | 537.5 ± 515.1 | |
| Median (min; max) | 466.5 (39; 1684) | 284 (11; 2269) | 382 (11; 2269) | |
| Total bilirubin | | | | 0.994 |
| Mean ± σ | 4.1 ± 4.9 | 5.3 ± 7.5 | 4.7 ± 6.3 | |
| Median (min; max) | 2 (0.1; 23.4) | 2.1 (0.2; 29.2) | 2.1 (0.1; 29.2) | |
| Direct bilirubin | | | | 0.683 |
| Mean ± σ | 3.6 ± 4.4 | 4.2 ± 6.3 | 3.9 ± 5.4 | |
| Median (min; max) | 1.6 (0.1; 20.9) | 1.1 (0.1; 22.4) | 1.5 (0.1; 22.4) | |

¹Student's t-test; ²Chi-square test, Mann-Whitney test. AST: Aspartate transaminase; ALT: Alanine transaminase; AP: Alkaline phosphatase; GGT: Gamma-glutamyl transpeptidase; σ: Standard deviation.

Table 2 Endoscopic retrograde cholangiopancreatography findings and complications n (%)

| Variable | Group I, n = 51 | Group II, n = 51 | Total, n = 102 | P value |
|---|-----------------|------------------|----------------|---------------------|
| Choledocolithiasis | | | | 0.048 |
| No | 10 (19.6) | 19 (37.3) | 29 (28.4) | |
| Yes | 41 (80.4) | 32 (62.7) | 73 (71.6) | |
| Intrahepatic dilatation | | | | 0.6572 |
| No | 36 (70.6) | 38 (74.5) | 74 (72.6) | |
| Yes | 15 (29.4) | 13 (25.5) | 28 (27.4) | |
| Extrahepatic dilatation | | | | 0.5512 |
| No | 25 (49.02) | 22 (43.1) | 47 (46.1) | |
| Pancreatitis | 2 (3.9) | 1 (1.9) | 3 (2.9) | 1 ¹ |
| Yes | 26 (50.98) | 29 (56.9) | 55 (53.9) | |
| Pancreatitis | 3 | 0 | 3 (2.9) | 0.0991 ¹ |
| Intra- or peridiverticular papilla | | | | 0.046 |
| No | 43 (84.3) | 49 (96.1) | 92 (90.2) | |
| Yes | 8 (15.7) | 2 (3.9) | 10 (9.8) | |
| Prosthesis | | | | 0.236 |
| No | 42 (82.4) | 37 (72.6) | 79 (77.5) | |
| Yes | 9 (17.6) | 14 (27.4) | 23 (22.5) | |
| Biliary prosthesis | | | | 0.463 |
| No | 42 (82.4) | 39 (76.5) | 81 (79.4) | |
| Yes | 9 (17.6) | 12 (23.5) | 21 (20.6) | |
| Cholangitis | | | | 0.678 ¹ |
| No | 49 (96.1) | 47 (92.2) | 96 (94.1) | |
| Yes | 2 (3.9) | 4 (7.9) | 6 (5.9) | |
| Biliary access | | | | 0.0002 ¹ |
| No | 12 (23.5) | 0 | | |
| Yes | 39 (76.5) | 51 (100) | | |
| Complications,pancreatitis, bleeding or perforation | | | | 0.0537 ¹ |
| No | 44 (86.3) | 50 (98) | 94 (92.2) | |
| Yes | 7 (13.7) | 1 (2) | 8 (7.8) | |
| Pancreatitis | 5 | 1 | | |
| Perforation | 2 | 1 | | |
| Bleeding | 0 | 0 | | |

Data are presented as n (%). ¹Fisher's exact test; Chi-square test.

Table 3 Endoscopic retrograde cholangiopancreatography findings and complications according to group and subgroup

| Variable | Groups | | Total, n = 102 | P value | | |
|--|-----------------|-------------------------------|----------------|----------------------|--|--|
| | Group I, n = 51 | | | | | |
| | GWC, n = 39 | Difficult cannulation, n = 12 | | | | |
| Complications, pancreatitis, bleeding or perforation | | | | 0.062 | | |
| No | 34 (87.2) | 10 (83.3) | 50 (98) | 94 (92.2) | | |
| Yes | 5 (12.8) | 2 (16.7) | 1 (2) | 8 (7.8) | | |
| Number of cannulations | | | | < 0.001 ¹ | | |
| Mean ± σ | 3.3 ± 1.9 | 7.5 ± 2.8 | | 4.3 ± 2.8 | | |
| Median (min.; max.) | 3 (1; 10) | 8.5 (3; 10) | | 3 (1; 10) | | |

¹Mann-Whitney test, Likelihood ratio test. GWC: Guidewire cannulation; σ: Standard deviation.**Table 4** Lipase, amylase and C-reactive protein measurements at the different evaluation times

| Variable | Group I, n = 51 | | | Group II, n = 51 | | | P value | P value for time | P value for interaction |
|--------------------|------------------|-------------------|--------------------|------------------|-----------------|-------------------|---------|------------------|-------------------------|
| | Pre | 12 h | 24 h | Pre | 12 h | 24 h | | | |
| Lipase | | | | | | | 0.006 | < 0.001 | 0.026 |
| mean ± σ | 69.4 ± 102.1 | 439.0 ± 1064.8 | 199.5 ± 528.3 | 41.4 ± 37.2 | 100.6 ± 183.3 | 85.2 ± 189.1 | | | |
| median (min; max) | 38 (9; 611) | 52 (10; 5014) | 48 (8; 3000) | 32 (0; 239) | 42.5 (8; 968) | 40 (5; 1334) | | | |
| Amylase | | | | | | | 0.003 | < 0.001 | 0.013 |
| mean ± σ | 76.4 ± 57.8 | 453.5 ± 1287.4 | 304.0 ± 979.3 | 59.6 ± 36.2 | 98.1 ± 94.3 | 85.8 ± 102.6 | | | |
| median (min; max) | 59 (12; 310) | 80 (14; 7900) | 70 (13; 6721) | 50 (14; 236) | 69 (21; 624) | 67.5 (12; 732) | | | |
| C-reactive protein | | | | | | | 0.189 | 0.070 | 0.353 |
| mean ± σ | 126.6 ± 539.7 | 49.5 ± 89.7 | 45.4 ± 70.5 | 58.6 ± 104.8 | 41.4 ± 62.0 | 38.8 ± 52.9 | | | |
| median (min; max) | 11.1 (0.1; 3813) | 15.5 (0.3; 486.1) | 19.16 (0.5; 340.9) | 12 (0.2; 549) | 13.8 (0.3; 271) | 16.6 (0.5; 223.1) | | | |

GEE with gamma distribution and identity link function. Not all patients were evaluated at all times. GEE: Generalized estimating equations; σ: Standard deviation.

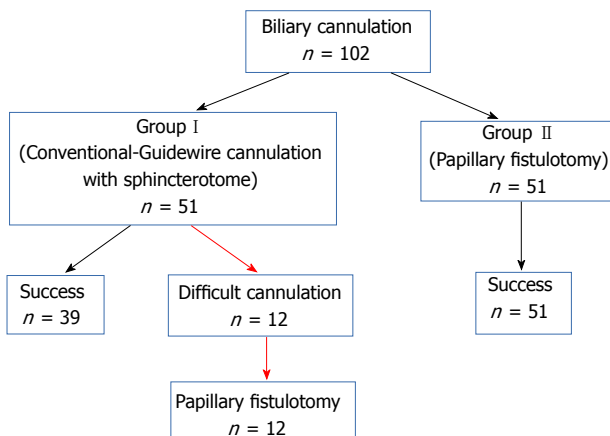


Figure 3 Flowchart showing the sequence of procedures performed in the study.

as difficult, thus migrating to the PF technique (Figure 3). Groups I and II had complication rates of 13.7% and 2.0%, respectively, which barely failed to reach significance ($P = 0.0597$). Two perforations and five cases of pancreatitis were observed in the first group, compared to a single case of retroperitoneal perforation and pancreatitis in the second one.

Table 3 reveals that the number of cannulations, as expected, was significantly different in the difficult cannulation group ($P < 0.001$), unlike ERCP findings, stent placement or complications ($P > 0.05$).

In Table 4 it can be appreciated that both lipase and

amylase differed between the groups and over time ($P = 0.026$ and $P = 0.013$, respectively). In contrast, no discrepancy for C-reactive protein was detected regarding groups ($P = 0.189$) or time ($P = 0.07$).

Figures 4–6 depict the amylase and lipase elevations in Group I patients. C-reactive protein, as alluded to, failed to exhibit discriminant patterns.

DISCUSSION

Pancreatitis is the most frequent complication of ERCP, occurring in as many as 15.1% of the patients^[6–8,13,14]. It is associated with considerable morbidity and mortality. Precut techniques have been associated with a high risk of PEP in previous studies^[7,8,15–17].

A difficult cannulation is an independent risk factor^[18,19]. The failure rate of primary biliary tract cannulation, with the use of a sphincterotome, was calculated as 2.5%–24% without a guidewire^[20–23] and 1.5%–10%^[21,23,24] adopting the wire. The American Society for Gastrointestinal Endoscopy benchmark for cannulation success during ERCP procedures of low to moderate complexity is > 90% for all indications^[25].

In this study, the primary success rate was 76.5%, with 9.8% of PEP. Difficult cannulation occurred in 12 patients, yet access was achieved via PF in all these individuals. The high failure rate (23.5%) may be explained by the participation of fellows, who are less experienced, thus making additional attempts by endoscopists with greater expertise required.

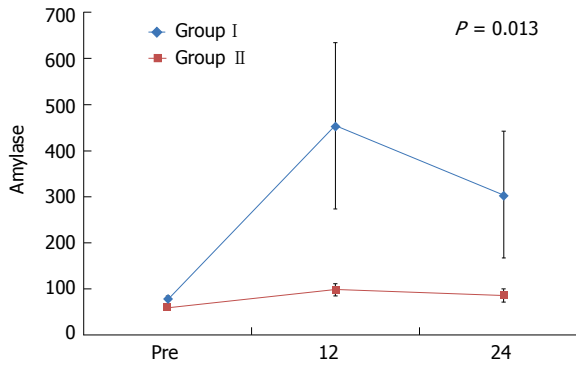


Figure 4 Amylase profile after the procedure.

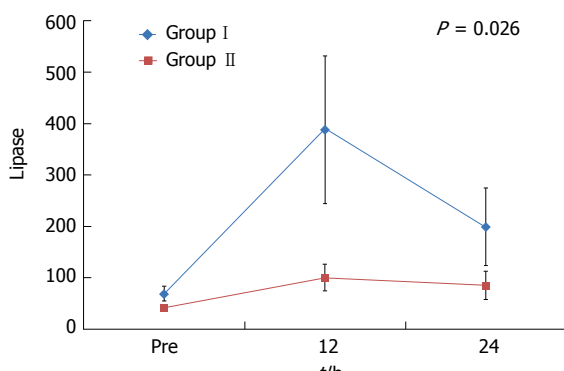


Figure 5 Lipase profile for the two groups.

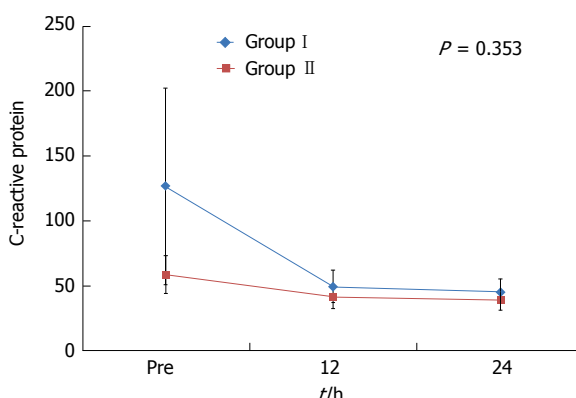


Figure 6 Evolution of C-reactive protein.

Nevertheless, papillary trauma eventually inflicted during the first intervention may hinder subsequent access, thus compromising the overall success rate.

Common bile duct stones were not found in all cases during ERCP, possibly on account of the long period that had elapsed since the original diagnosis in the primary care institution. It is important to mention that per protocol, PF was conducted directly, without prior manipulation by conventional techniques. Cannulation of the bile duct using PF was accomplished in all patients in Group II. Three previous studies with a similar design displayed 89.3%-96.5% success rates for fistulotomy^[26-28]. In the control group (conventional technique), the corresponding values were 70.6% and 88%^[26-28].

The mean diameter of the common bile duct in this experience was 8.7 mm (5-18.2 mm). Sakai *et al*^[10] in 2001, suggested that PF be reserved mainly for patients with a dilated common bile duct. Jin *et al*^[27] concluded in 2016, based on 55 interventions, that a bile duct < 9 mm was a risk factor. Yet Khatibian *et al*^[26] reported in 2008 that the diameter of the common bile duct was not relevant for need of PF.

In the current series, PF (Group II and Failures) was performed in 28 of 63 patients (44.4%; $P = 0.834$); for each, being performed through the common bile duct without dilatation. No difference in the risk of pancreatitis emerged when considering the caliber of the intra- and extrahepatic biliary tracts. Bile duct stones could not be removed in the first attempt in 20.8% of the cases, due to large size; therefore, in these cases, a biliary stent was placed.

Hyperamylasemia was observed in 2 patients in Group I ($P = 0.49$). Transient asymptomatic elevations in amylase, lipase, or both, range from 0 to 64% in the literature^[29-31]. Asymptomatic hyperamylasemia, defined as amylase levels > 5 times the upper limit at 24 h after ERCP, has been reported in approximately 27% of the cases^[32].

In our study, the number of cannulation attempts significantly correlated with increased lipase and amylase levels, at 12 h and 24 h after the procedure. In a series of 907 patients, the rates of PEP were 0.6%, 3.1%, 6.1% and 11.9% following one, two, three to four, and more than five primary cannulation attempts that led to success, respectively. PEP risk increased to 11.5% if the primary cannulation method failed^[19]. In our study, PEP occurred following the guidewire cannulation (GWC) technique in 5 patients (9.8%), of which 2 (3.9%) exhibited a difficult papillary access, which was only achieved by means of PF.

No significant increase in pancreatic enzymes was observed, and the incidence of PEP was not greater in the group that underwent PF as the initial procedure; neither did the 12 patients with PF as a rescue procedure exhibit a different pattern. This demonstrates the safety of PF, whenever performed or supervised by experienced physicians. In 2016, Zagalsky *et al*^[33] compared early precut (PCP) techniques and use of a pancreatic duct stent in 101 patients who suffered difficult cannulations. The success rates of biliary cannulation (98% and 96%), and the occurrence of PEP (4% and 3.92%) were similar between the early PCP and stent groups, respectively. Two perforations and bleeds occurred in the early PCP group, which also demonstrates the safety of the procedure compared to standard PEP prevention technique after a failed GWC.

Other recent studies have shown that precut techniques lead to an increased rate of successful deep biliary tract access and that their early use by experienced endoscopists results in a decrease in PEP^[4,27,34]. Weerth *et al*^[2] compared primary PCP and GWC for bile duct access and reported a success rate at the first attempt of 100% and 71%, respectively.

They observed mild to moderate PEP in 2.1% and 2.9% ($P > 0.05$), after primary PCP or GWC, respectively. Only 1 patient (in the GWC group) suffered from postpapillotomy bleeding. In our experience, a single patient presented a retroperitoneal perforation and pancreatitis in Group II, both of which were conservatively managed.

There were two perforations (3.9%) in Group I, and the one (1.9%) in Group II already alluded to, which were always conservatively treated. No bleeding was observed. The negligible incidence of bleeding is consistent with previous precut studies (0-3.4%)^[2,17,26,28,35]. In regards to perforation (0-1.8%), our results are also quite acceptable^[2,17,26,28,35].

In conclusion, PF was more effective than GWC, and it was associated with a lower profile of amylase and lipase, as the routine endoscopic access to the biliary tree, including difficult cases. Complications were similar in both groups.

ARTICLE HIGHLIGHTS

Research background

Successfully cannulating the biliary tract is important in the diagnosis and treatment of biliopancreatic diseases with endoscopic retrograde cholangiopancreatography (ERCP), but it can be associated with severe complications and mortality.

Research motivation

The number of papers regarding comparison between conventional cannulation versus fistulotomy is small. Our study is a well-designed approach in its matter.

Research objectives:

To compare the cannulation success, biochemical profile, and complications of the papillary fistulotomy technique versus catheter and guidewire standard access.

Research methods

Patients were prospectively randomized into two groups: cannulation with a catheter and guidewire (Group I) and papillary fistulotomy (Group II). Amylase, lipase and C-reactive protein at T0 as well as 12 h and 24 h after ERCP, and complications (pancreatitis, bleeding, perforation) were recorded. Comparison was made of the cannulation success, biochemical profile and complications of the papillary fistulotomy technique vs catheter and guidewire standard access.

Research results

We included 102 patients, and Groups I and II had 51 patients each. The successful cannulation rates were 76.5% and 100%, respectively ($P = 0.0002$). Twelve patients (23.5%) in Group I had a difficult cannulation and underwent fistulotomy, which led to successful secondary biliary access (Failure Group). The complication rate was 13.7% (2 perforations and 5 mild pancreatitis) in Group I versus 2.0% (1 patient with perforation and pancreatitis) in Group II ($P = 0.0597$).

Research conclusions

Papillary fistulotomy was more effective than guidewire cannulation, and it was associated with a lower profile of amylase and lipase. Complications were similar in both groups.

Research perspectives

The fistulotomy demonstrated safety similar to conventional cannulation and less local trauma into the ampulla, according to the levels of the amylase, lipase

and C-reactive protein.

REFERENCES

- Abu-Hamda EM, Baron TH, Simmons DT, Petersen BT. A retrospective comparison of outcomes using three different precut needle knife techniques for biliary cannulation. *J Clin Gastroenterol* 2005; **39**: 717-721 [PMID: 16082283]
- de Weerth A, Seitz U, Zhong Y, Groth S, Omar S, Papageorgiou C, Bohnacker S, Seewald S, Seifert H, Binmoeller KF, Thonke F, Soehendra N. Primary precutting versus conventional over-the-wire sphincterotomy for bile duct access: a prospective randomized study. *Endoscopy* 2006; **38**: 1235-1240 [PMID: 17163325 DOI: 10.1055/s-2006-944962]
- Freeman ML, Guda NM. ERCP cannulation: a review of reported techniques. *Gastrointest Endosc* 2005; **61**: 112-125 [PMID: 15672074]
- Sundaralingam P, Masson P, Bourke MJ. Early Precut Sphincterotomy Does Not Increase Risk During Endoscopic Retrograde Cholangiopancreatography in Patients With Difficult Biliary Access: A Meta-analysis of Randomized Controlled Trials. *Clin Gastroenterol Hepatol* 2015; **13**: 1722-1729.e2 [PMID: 26144018 DOI: 10.1016/j.cgh.2015.06.035]
- Mariani A, Di Leo M, Giardullo N, Giussani A, Marini M, Buffoli F, Cipolletta L, Radaelli F, Ravelli P, Lombardi G, D'Onofrio V, Macchiarelli R, Iiritano E, Le Grazie M, Pantaleo G, Testoni PA. Early precut sphincterotomy for difficult biliary access to reduce post-ERCP pancreatitis: a randomized trial. *Endoscopy* 2016; **48**: 530-535 [PMID: 26990509 DOI: 10.1055/s-0042-102250]
- Freeman ML, Nelson DB, Sherman S, Haber GB, Herman ME, Dorsher PJ, Moore JP, Fennerty MB, Ryan ME, Shaw MJ, Lande JD, Pheley AM. Complications of endoscopic biliary sphincterotomy. *N Engl J Med* 1996; **335**: 909-918 [PMID: 8782497 DOI: 10.1056/NEJM199609263351301]
- Mavrogiannis C, Liatsos C, Romanos A, Petoumenos C, Nakos A, Karvountzis G. Needle-knife fistulotomy versus needle-knife precut papillotomy for the treatment of common bile duct stones. *Gastrointest Endosc* 1999; **50**: 334-339 [PMID: 10462652 DOI: 10.1053/ge.1999.v50.98593]
- Zhou W, Li Y, Zhang Q, Li X, Meng W, Zhang L, Zhang H, Zhu K, Zhu X. Risk factors for postendoscopic retrograde cholangiopancreatography pancreatitis: a retrospective analysis of 7,168 cases. *Pancreatology* 2011; **11**: 399-405 [PMID: 21894057 DOI: 10.1016/S1424-3903(11)80094-3]
- Osnes M, Kahrs T. Endoscopic choledochoduodenostomy for choledocholithiasis through choledochoduodenal fistula. *Endoscopy* 1977; **9**: 162-165 [PMID: 913369 DOI: 10.1055/s-0028-1098510]
- Sakai P, Artifon ELA, Maluf Filho F. Fistulopapilotomia Endoscópica: Uma Alternativa à Papila de Difícil Cateterização. *GED* 2001; **20**: 208-212
- Lerch MM. Classifying an unpredictable disease: the revised Atlanta classification of acute pancreatitis. *Gut* 2013; **62**: 2-3 [PMID: 23220948 DOI: 10.1136/gutjnl-2012-303724]
- Kirkwood B, JAC S. Essential Medical Statistics. 2nd ed. Massachusetts, United States: Blackwell Science; 2006
- Cheng CL, Sherman S, Watkins JL, Barnett J, Freeman M, Geenen J, Ryan M, Parker H, Frakes JT, Fogel EL, Silverman WB, Dua KS, Aliperti G, Yaksh P, Uzer M, Jones W, Goff J, Lazzell-Pannell L, Rashdan A, Temkit M, Lehman GA. Risk factors for post-ERCP pancreatitis: a prospective multicenter study. *Am J Gastroenterol* 2006; **101**: 139-147 [PMID: 16405547 DOI: 10.1111/j.1572-0241.2006.00380.x]
- Bailey AA, Bourke MJ, Williams SJ, Walsh PR, Murray MA, Lee EY, Kwan V, Lynch PM. A prospective randomized trial of cannulation technique in ERCP: effects on technical success and post-ERCP pancreatitis. *Endoscopy* 2008; **40**: 296-301 [PMID: 18389448 DOI: 10.1055/s-2007-995566]
- Bailey AA, Bourke MJ, Kafes AJ, Byth K, Lee EY, Williams SJ. Needle-knife sphincterotomy: factors predicting its use and the

- relationship with post-ERCP pancreatitis (with video). *Gastrointest Endosc* 2010; **71**: 266-271 [PMID: 20003969 DOI: 10.1016/j.gie.2009.09.024]
- 16 **Halttunen J**, Keränen I, Udd M, Kylänpää L. Pancreatic sphincterotomy versus needle knife precut in difficult biliary cannulation. *Surg Endosc* 2009; **23**: 745-749 [PMID: 18649101 DOI: 10.1007/s00464-008-0056-0]
- 17 **O'Connor HJ**, Bhutta AS, Redmond PL, Carruthers DA. Suprapapillary fistulosphincterotomy at ERCP: a prospective study. *Endoscopy* 1997; **29**: 266-270 [PMID: 9255529 DOI: 10.1055/s-2007-1004187]
- 18 **Freeman ML**, DiSario JA, Nelson DB, Fennerty MB, Lee JG, Bjorkman DJ, Overby CS, Aas J, Ryan ME, Bochna GS, Shaw MJ, Snady HW, Erickson RV, Moore JP, Roel JP. Risk factors for post-ERCP pancreatitis: a prospective, multicenter study. *Gastrointest Endosc* 2001; **54**: 425-434 [PMID: 11577302 DOI: 10.1067/mge.2001.117550]
- 19 **Halttunen J**, Meissner S, Aabakken L, Arnelo U, Grönroos J, Hauge T, Kleleveland PM, Nordblad Schmidt P, Saarela A, Swahn F, Toth E, Mustonen H, Löhr JM. Difficult cannulation as defined by a prospective study of the Scandinavian Association for Digestive Endoscopy (SADE) in 907 ERCPs. *Scand J Gastroenterol* 2014; **49**: 752-758 [PMID: 24628493 DOI: 10.3109/00365521.2014.894120]
- 20 **Laasch HU**, Tringali A, Wilbraham L, Marriott A, England RE, Mutignani M, Perri V, Costamagna G, Martin DF. Comparison of standard and steerable catheters for bile duct cannulation in ERCP. *Endoscopy* 2003; **35**: 669-674 [PMID: 12929062 DOI: 10.1055/s-2003-41515]
- 21 **Lella F**, Bagnolo F, Colombo E, Bonassi U. A simple way of avoiding post-ERCP pancreatitis. *Gastrointest Endosc* 2004; **59**: 830-834 [PMID: 15173796]
- 22 **Schwacha H**, Allgaier HP, Deibert P, Olszewski M, Allgaier U, Blum HE. A sphincterotome-based technique for selective transpapillary common bile duct cannulation. *Gastrointest Endosc* 2000; **52**: 387-391 [PMID: 10968855 DOI: 10.1067/mge.2000.107909]
- 23 **Artifon EL**, Sakai P, Cunha JE, Halwan B, Ishioka S, Kumar A. Guidewire cannulation reduces risk of post-ERCP pancreatitis and facilitates bile duct cannulation. *Am J Gastroenterol* 2007; **102**: 2147-2153 [PMID: 17581267 DOI: 10.1111/j.1572-0241.2007.01378.x]
- 24 **Zhou PH**, Yao LQ, Xu MD, Zhong YS, Gao WD, He GJ, Zhang YQ, Chen WF, Qin XY. Application of needle-knife in difficult biliary cannulation for endoscopic retrograde cholangiopancreatography. *Hepatobiliary Pancreat Dis Int* 2006; **5**: 590-594 [PMID: 17085348]
- 25 **Adler DG**, Lieb JG 2nd, Cohen J, Pike IM, Park WG, Rizk MK, Sawhney MS, Scheiman JM, Shaheen NJ, Sherman S, Wani S. Quality indicators for ERCP. *Gastrointest Endosc* 2015; **81**: 54-66 [PMID: 25480099 DOI: 10.1016/j.gie.2014.07.056]
- 26 **Khatibian M**, Sotoudehmanesh R, Ali-Asgari A, Movahedi Z, Kolahdoozan S. Needle-knife fistulotomy versus standard method for cannulation of common bile duct: a randomized controlled trial. *Arch Iran Med* 2008; **11**: 16-20 [PMID: 18154417]
- 27 **Jin YJ**, Jeong S, Lee DH. Utility of needle-knife fistulotomy as an initial method of biliary cannulation to prevent post-ERCP pancreatitis in a highly selected at-risk group: a single-arm prospective feasibility study. *Gastrointest Endosc* 2016; **84**: 808-813 [PMID: 27102829 DOI: 10.1016/j.gie.2016.04.011]
- 28 **Ayoubi M**, Sansoè G, Leone N, Castellino F. Comparison between needle-knife fistulotomy and standard cannulation in ERCP. *World J Gastrointest Endosc* 2012; **4**: 398-404 [PMID: 23125897 DOI: 10.4253/wjge.v4.i9.398]
- 29 **Tanaka R**, Itoi T, Sofuni A, Itokawa F, Kurihara T, Tsuchiya T, Tsuji S, Ishii K, Ikeuchi N, Umeda J, Tonozuka R, Honjo M, Mukai S, Moriyasu F. Is the double-guidewire technique superior to the pancreatic duct guidewire technique in cases of pancreatic duct opacification? *J Gastroenterol Hepatol* 2013; **28**: 1787-1793 [PMID: 23800118 DOI: 10.1111/jgh.12303]
- 30 **Nishino T**, Toki F, Oyama H, Shiratori K. More accurate prediction of post-ercp pancreatitis by 4-h serum lipase levels than amylase levels. *Dig Endosc* 2008; **20**: 169-177
- 31 **Dumonceau JM**, Devière J, Cremer M. A new method of achieving deep cannulation of the common bile duct during endoscopic retrograde cholangiopancreatography. *Endoscopy* 1998; **30**: S80 [PMID: 9826155]
- 32 **Testoni PA**, Testoni S, Giussani A. Difficult biliary cannulation during ERCP: how to facilitate biliary access and minimize the risk of post-ERCP pancreatitis. *Dig Liver Dis* 2011; **43**: 596-603 [PMID: 21377432 DOI: 10.1016/j.dld.2011.01.019]
- 33 **Zagalsky D**, Guidi MA, Curvale C, Lasa J, de Maria J, Iannicillo H, Hwang HJ, Matano R. Early precut is as efficient as pancreatic stent in preventing post-ERCP pancreatitis in high-risk subjects - A randomized study. *Rev Esp Enferm Dig* 2016; **108**: 258-262 [PMID: 27604474 DOI: 10.17235/reed.2016.4348/2016]
- 34 **Cennamo V**, Fuccio L, Zagari RM, Eusebi LH, Ceroni L, Laterza L, Fabbri C, Bazzoli F. Can early precut implementation reduce endoscopic retrograde cholangiopancreatography-related complication risk? Meta-analysis of randomized controlled trials. *Endoscopy* 2010; **42**: 381-388 [PMID: 20306386 DOI: 10.1055/s-0029-1243992]
- 35 **Huibregtsse K**, Katon RM, Tytgat GN. Precut papillotomy via fine-needle knife papillotomy: a safe and effective technique. *Gastrointest Endosc* 1986; **32**: 403-405 [PMID: 3803839]

P- Reviewer: Kahraman A, Ker CG **S- Editor:** Wang XJ
L- Editor: Filopodia **E- Editor:** Huang Y



Compared efficacy of preservation solutions on the outcome of liver transplantation: Meta-analysis

Ágnes Lilla Szilágyi, Péter Mátrai, Péter Hegyi, Eszter Tuboly, Daniella Pécz, András Garami, Margit Solymár, Erika Pétervári, Márta Balaskó, Gábor Veres, László Czopf, Bastian Wobbe, Dorottya Szabó, Juliane Wagner, Petra Hartmann

Ágnes Lilla Szilágyi, Eszter Tuboly, Daniella Pécz, Petra Hartmann, Institute of Surgical Research, University of Szeged, Szeged H-6720, Hungary

Péter Mátrai, Institute of Bioanalysis, University of Pécs, Pécs H-7624, Hungary

Péter Hegyi, András Garami, Margit Solymár, Erika Pétervári, Márta Balaskó, Institute for Translational Medicine and First Department of Medicine, University of Pécs, Pécs H-7624, Hungary

Péter Hegyi, MTA-SZTE Translational Gastroenterology Research Group, Szeged H-6720, Hungary

Péter Hegyi, János Szentágothai Research Center, University of Pécs, Pécs H-7624, Hungary

Gábor Veres, 1st Department of Paediatrics, University of Semmelweis, Budapest H-1085, Hungary

László Czopf, Bastian Wobbe, Dorottya Szabó, Juliane Wagner, Department of Cardiology, 1st Department of Medicine, University of Pécs, Pécs H-7624, Hungary

ORCID number: Ágnes Lilla Szilágyi (0000-0003-1584-5906); Péter Mátrai (0000-0001-5144-0733); Péter Hegyi (0000-0002-4333-265X); Eszter Tuboly (0000-0003-0333-6952); Daniella Pécz (0000-0002-0214-8389); András Garami (0000-0003-2493-0571); Margit Solymár (0000-0001-6667-6263); Erika Pétervári (0000-0002-3673-8491); Márta Balaskó (0000-0003-4377-9758); Gábor Veres (0000-0002-0911-1941); László Czopf (0000-0001-9565-0732); Bastian Wobbe (0000-0002-7278-1470); Dorottya Szabó (0000-0001-7351-2929); Juliane Wagner (0000-0002-7762-0377); Petra Hartmann (0000-0002-4746-9792).

Author contributions: Szilágyi ÁL, Garami A, Solymár M, Pétervári E, Balaskó M and Hartmann P designed the study; Szilágyi ÁL, Tuboly E, Pécz D, Veres G, Szabó D and Wagner J collected and analyzed the data; Mátrai P performed the statistical

analysis; Hartmann P drafted and wrote the manuscript; Wobbe B performed language editing; Hegyi P and Czopf L revised the manuscript critically for intellectual content; and all the authors provided intellectual input for the study and approved the final version of the manuscript.

Supported by grants from the National Research Development and Innovation Office, NKFI K120232; Hungarian Science Research Fund, No. GINOP 2.3.2-15-2016-00015 and No. EFOP -3.6.2-16-2017-00006; and New National Excellence Program of the Ministry of Human Capacities, No. UNKP-17-4.

Conflict-of-interest statement: None of the authors has any conflict of interests related to this manuscript.

Data sharing statement: No additional data are available.

Open-Access: This article is an open-access article which was selected by an in-house editor and fully peer-reviewed by external reviewers. It is distributed in accordance with the Creative Commons Attribution Non Commercial (CC BY-NC 4.0) license, which permits others to distribute, remix, adapt, build upon this work non-commercially, and license their derivative works on different terms, provided the original work is properly cited and the use is non-commercial. See: <http://creativecommons.org/licenses/by-nc/4.0/>

Manuscript source: Unsolicited manuscript

Correspondence to: Petra Hartmann, MD, PhD, Assistant Professor, Institute of Surgical Research, University of Szeged, Szőkefalvi-Nagy Béla street 6, Szeged H-6720, Hungary. hartmann.petra@med.u-szeged.hu
Telephone: +36-62-545103
Fax: +36-62-545743

Received: January 31, 2018

Peer-review started: January 31, 2018

First decision: February 24, 2018

Revised: April 2, 2018

Accepted: April 9, 2018

Article in press: April 9, 2018

Published online: April 28, 2018

Abstract

AIM

To compare the effects of the four most commonly used preservation solutions on the outcome of liver transplantations.

METHODS

A systematic literature search was performed using MEDLINE, Scopus, EMBASE and the Cochrane Library databases up to January 31st, 2017. The inclusion criteria were comparative, randomized controlled trials (RCTs) for deceased donor liver (DDL) allografts with adult and pediatric donors using the gold standard University of Wisconsin (UW) solution or histidine-tryptophan-ketoglutarate (HTK), Celsior (CS) and Institut Georges Lopez (IGL-1) solutions. Fifteen RCTs (1830 livers) were included; the primary outcomes were primary non-function (PNF) and one-year post-transplant graft survival (OGS-1).

RESULTS

All trials were homogenous with respect to donor and recipient characteristics. There was no statistical difference in the incidence of PNF with the use of UW, HTK, CS and IGL-1 (RR = 0.02, 95%CI: 0.01-0.03, $P = 0.356$). Comparing OGS-1 also failed to reveal any difference between UW, HTK, CS and IGL-1 (RR = 0.80, 95%CI: 0.80-0.80, $P = 0.369$). Two trials demonstrated higher PNF levels for UW in comparison with the HTK group, and individual studies described higher rates of biliary complications where HTK and CS were used compared to the UW and IGL-1 solutions. However, the meta-analysis of the data did not prove a statistically significant difference: the UW, CS, HTK and IGL-1 solutions were associated with nearly equivalent outcomes.

CONCLUSION

Alternative solutions for UW yield the same degree of safety and effectiveness for the preservation of DDLs, but further well-designed clinical trials are warranted.

Key words: Liver transplantation; Preservation solution; Primary non-function; One-year post-transplant graft survival; Systematic review; Meta-analysis

© The Author(s) 2018. Published by Baishideng Publishing Group Inc. All rights reserved.

Core tip: The University of Wisconsin (UW) solution is the gold standard for static cold storage in liver transplantation. Numerous clinical trials have investigated the potential benefit of the most frequently used alternative solutions, histidine-tryptophan-ketoglutarate, Celsior and Institut Georges Lopez, but their results have been variable. This meta-analysis has

reviewed the current evidence and found no significant differences in risk of transplant outcomes: primary non-function (RR = 0.02, 95%CI: 0.01-0.03, $P = 0.36$) and one-year post-transplant graft survival (RR = 0.80, 95%CI: 0.80-0.80, $P = 0.37$) between UW and the other examined solutions.

Szilágyi ÁL, Mátrai P, Hegyi P, Tuboly E, Pécz D, Garami A, Solymár M, Pétervári E, Balaskó M, Veres G, Czopf L, Wobbe B, Szabó D, Wagner J, Hartmann P. Compared efficacy of preservation solutions on the outcome of liver transplantation: Meta-analysis. *World J Gastroenterol* 2018; 24(16): 1812-1824 Available from: URL: <http://www.wjgnet.com/1007-9327/full/v24/i16/1812.htm> DOI: <http://dx.doi.org/10.3748/wjg.v24.i16.1812>

INTRODUCTION

Organ transplantation is inevitably associated with ischemia-reperfusion (IR) injury; several methods have thus been formulated to reduce IR-related morbidity and to maintain the viability of tissues^[1,2]. The introduction of the University of Wisconsin (UW) solution in 1987 has led to significant clinical progress and increased cold ischemic tolerance and has become the most widely used, gold standard preservation solution for liver transplantation^[3]. Nevertheless, in spite of the clinical success, it has many potential shortcomings (Table 1). UW is an intracellular colloid solution with high potassium and low sodium concentration that inhibits activity of Na-K-adenosine triphosphatase and the resultant depletion of adenosine triphosphate stores. However, its low sodium content promotes the accumulation of calcium during ischemia, resulting in calcium-dependent endothelial dysfunction in renal glomeruli and in bile ducts during reperfusion^[4,5]. Additionally, the high potassium increases the risk for hyperkalemia-induced cardiac arrest, requiring liver flushing before reperfusion. Moreover, low temperature storage in the container bag may result in the formation of adenosine crystals^[6]. Therefore, the use of UW has been intensively challenged, and alternative solutions with potentially more benefits were developed. Among them, histidine-tryptophan-ketoglutarate (HTK), Celsior (CS) and Institut George Lopez (IGL-1) are the most commonly used preservation solutions in transplantation centers^[7].

A number of prospective trials have investigated the effects of these preservation solutions on liver transplant outcomes over many years with variable results. HTK, also known as Bretschneider's solution, is mostly used in European liver transplantation centers, especially in Germany. It has very low viscosity, which is based on a histidine buffer system with two additional substrates (tryptophan and ketoglutarate). A lower index of viscosity allows faster cooling and, theoretically, an

Table 1 Ingredients in the investigated preservation solutions

| | UW | HTK | CS | IGL-1 |
|-----------------|-----------|------------|-----------|--------------|
| HES | 0.25 | - | - | - |
| PEG-35 | - | - | - | 0.03 |
| Na ⁺ | 27 | 15 | 100 | 120 |
| K ⁺ | 125 | 10 | 15 | 25 |

Concentrations are expressed in mmol/L. HES: Hydroxyethyl starch; PEG-35: Polyethylene glycol 35 kDa.

improved washout of blood cells from the graft^[8]. UW was first compared to HTK in a randomized fashion in liver transplantation in 1994, and these solutions were found to have similar outcomes in terms of initial non-function of the graft and 30-mo patient survival^[9]. However, more recent studies with a larger liver transplant population from Europe and North America have provided different conclusions^[10,11].

CS has initially been applied in heart transplantation and then for kidney and liver transplantation as well, with the idea of providing preservation for all organs with a single solution^[12]. The use of CS is based on similar principles to those of UW and HTK, but certain aspects are different. CS and HTK are categorized as extracellular preservation fluids; however, their buffering systems and substrates, which provide high-energy phosphates, are different. With its high sodium (above 70 mmol/L) and low potassium content, CS is specifically designed to limit calcium overload (Table 1). It contains reduced glutathione concentration together with the addition of mannitol and histidine to prevent reactive oxygen species-induced oxidative injury. Like HTK, CS is devoid of colloids, therefore resulting in decreased viscosity and improved perfusability, it is thus unnecessary to the liver prior to reperfusion^[13]. Due to its characteristically low viscosity, high sodium, low potassium and antioxidant properties, CS is considered particularly suitable for preserving liver grafts.

There are promising preliminary reports on the recently introduced Institut Georges Lopez (IGL-1) solution, also known as the UW-polyethylene glycol (PEG) solution. IGL-1 combines a cationic inversion (lower concentration of potassium) and replacement of hydroxyethyl starch with PEG. These properties could improve hepatic microcirculatory changes, thereby decreasing IR- injury^[14].

The aim of our study was to provide a systematic review of this topic. The goal was to update current knowledge and compare data evidence on the effectiveness of the most frequently used preservation solutions. The primary endpoint of the study was primary non-function (PNF) of the graft after liver transplantation. PNF is the most common cause of early graft loss, and it has been shown that the organ preservation method is an independent predictive factor of PNF^[15]. The secondary endpoint was one-year post-transplant graft survival (OGS-1), this being

an appropriate period to evaluate the effect of the preservation solutions according to an expert consensus opinion^[16]. Other outcomes, such as primary dysfunction (PDF), early retransplantation rate (RT), post-transplant death within 30 d (POD) and one-year post-transplant patient survival (OPS-1) were also evaluated together with donors and recipient characteristics.

It should be added that three previous systematic reviews and two registry data analyses have explored this topic, each with limitations^[10,16-19]. In 2015, Adam et al^[10] analyzed the efficacy of the four most commonly used preservation solutions based on the European Liver Transplant Registry (ELTR) database. The largest and most comprehensive study in recent times was performed by analyzing outcomes of 42869 (first) liver transplantations, including living and deceased donors, as well as partial liver graft transplantations. Although the study population in this registry data analysis was relatively large, non-selective groups of donors were included^[10,18,20]. Two systematic reviews lacked sufficient sample sizes and therefore were underpowered to identify clinically relevant differences in important outcomes, such as PNF of the graft.^[16,17] A systematic review by O'Callaghan et al^[19] chose 16 RCTs for analysis; however, it included unpublished data and conference abstracts as well. Since then, new prospective trials have also been published, especially with the IGL-1 solution^[8,21].

Therefore, the aim of this systematic review was to evaluate, compare and update the evidence obtained in randomized controlled trials (RCTs) on the efficacy of the four most frequently used preservation solutions for static cold storage of deceased donor liver (DDL) allografts.

MATERIALS AND METHODS

This study was conducted in accordance with the PRISMA (Preferred Reporting Items in Systematic Reviews and Meta-Analysis) statement^[22]. The review protocol was registered with the National Institute for Health Research PROSPERO system on January 12th, 2017, and can be found online (Registration No. CRD42017054908)^[23].

Literature search

A systematic literature search was performed using EMBASE/MEDLINE, PubMed, Scopus and Cochrane. Database searches were conducted with MeSH keywords, combined with various terms for organ transplantation and organ preservation solutions (Figure 1). No language limitation was applied. The end date for the literature search was January 31st, 2017.

Inclusion criteria

Inclusion criteria specified any RCT comparing two or more preservation solutions for the static cold storage of DDLs, from both adult and pediatric donors. Living

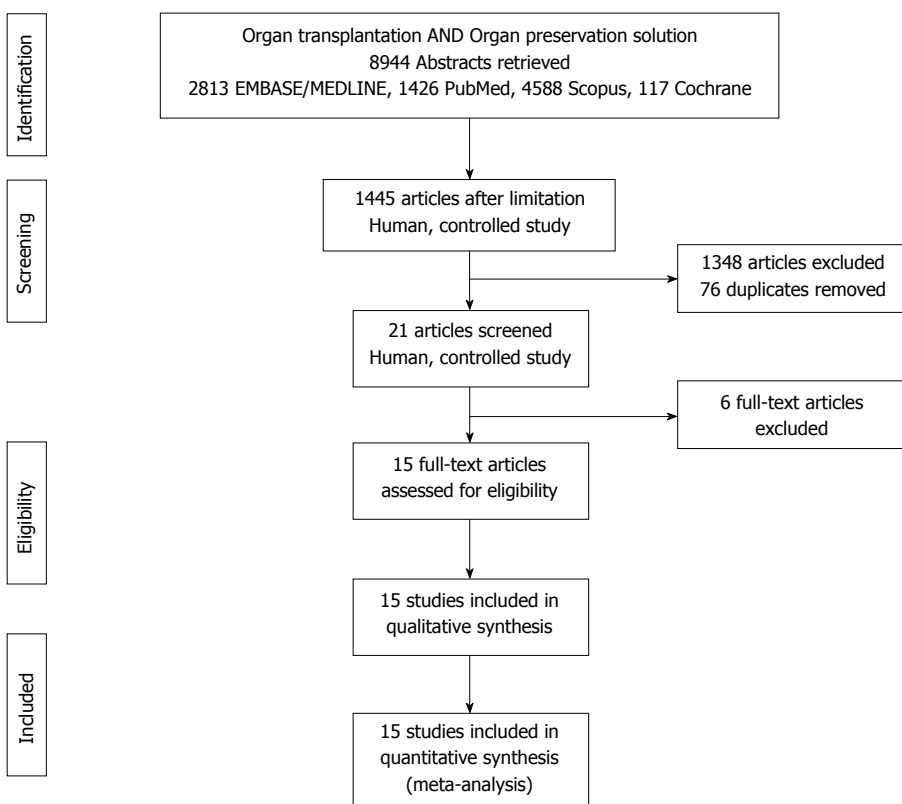


Figure 1 PRISMA flowchart of search strategy with inclusions and exclusions.

donor transplantation, multiple organ transplantation, retransplantation, nonhuman and uncontrolled studies were excluded. Abstracts for inclusion were independently reviewed by two authors, and disagreements were resolved by discussion with a third author (Figure 1).

Outcomes

The primary outcome was PNF of the liver grafts. PNF is a life-threatening condition after transplantation that leads to death or to the need for retransplantation within seven days of transplantation. It is characterized by hepatic cytolysis, elevated fasting transaminase levels, diminishing or absent bile production, coagulation deficit related to severely impaired liver function, high lactate levels, hypoglycemia, respiratory failure requiring ventilatory support, circulatory failure requiring catecholamines, and the onset of renal and multi-organ failure^[15].

The secondary outcome was OGS-1, since the one-year post-transplant time point was considered by an expert consensus opinion as most suitable to evaluate the effect of the preservation solutions^[16].

Data extraction

Demographic, quality and outcome data were extracted independently into Microsoft Excel by two authors. Data were collected from all articles describing the studies; in the case of discrepancies, the article with the largest

number of patients was used. Any questions in data extraction were settled by discussion with a third author.

Statistical analysis

The statistical analysis for this study was conducted by Péter Mátrai, Institute of Bioanalysis, University of Pécs, H-7624 Pécs, Hungary. Risk ratios (RR) from individual studies were pooled statistically by random effect model using the DerSimonian-Laird estimator and were displayed on forest plots. As RR allows for the comparison of two samples, the Celsior and HTK solutions were compared to UW. Summary RRs were calculated with 95% confidence intervals (CI) and p values to test if summary RR = 1 can be rejected. $P < 0.05$ was defined as a significant difference between solutions. In the analysis of outcomes for PNF and PDF, we used a computational correction recommended in the Cochrane Handbook and proposed by Sweeting *et al*^[24] to overcome the difficulty of dividing by 0. Statistical heterogeneity was tested using the I^2 statistic and the chi-square test to obtain probability-values; $P < 0.05$ was defined to indicate significant heterogeneity. All statistical calculations were performed using Stata 11 SE (Stata Corp) and Comprehensive Meta-analysis Software (Version 3, Biostat, Englewood). We sought signs of a small study effect with the funnel plot. To identify potential sources of heterogeneity, we defined *a priori* subgroup analyses with the model of end-stage

Table 2 Primary non-function rate in included studies

| Study | Solution 1 | | | Solution 2 | | | RR | P value | | |
|--|------------|-----|---|------------|-------|-----|----|---------|------|------|
| | N | n | % | N | n | % | | | | |
| Cavallari et al ^[13] , 2003 | UW | 90 | 1 | 1.100 | CS | 83 | 0 | 0.000 | 2.77 | 0.53 |
| Lopez-Andujar et al ^[26] , 2009 | UW | 104 | 2 | 1.900 | CS | 92 | 2 | 2.200 | 0.88 | 0.90 |
| García-Gil et al ^[33] , 2006 | UW | 40 | 0 | 0.000 | CS | 40 | 0 | 0.000 | 1.00 | 1.00 |
| Nardo et al ^[27] , 2001 | UW | 60 | 2 | 3.333 | CS | 53 | 0 | 0.000 | 4.43 | 0.33 |
| Duca et al ^[28] , 2010 | UW | 51 | 0 | 0.000 | CS | 51 | 0 | 0.000 | 1.00 | 1.00 |
| García-Gil et al ^[35] , 2011 | UW | 51 | 4 | 11.100 | CS | 51 | 4 | 11.100 | 1.00 | 1.00 |
| Lama et al ^[29] , 2002 | UW | 10 | 0 | 0.000 | CS | 10 | 0 | 0.000 | 1.00 | 1.00 |
| Rayya et al ^[30] , 2008 | UW | 68 | 1 | 1.471 | HTK | 69 | 1 | 1.449 | 1.01 | 0.99 |
| Meine et al ^[32] , 2006 | UW | 65 | 2 | 3.070 | HTK | 37 | 1 | 3.030 | 1.14 | 0.91 |
| Erhard et al ^[9] , 1994 | UW | 30 | 2 | 6.660 | HTK | 30 | 0 | 0.000 | 5.00 | 0.29 |
| Mangus et al ^[31] , 2008 | UW | 98 | 5 | 5.102 | HTK | 111 | 3 | 2.703 | 1.89 | 0.38 |
| Dondéro et al ^[37] , 2010 | UW | 92 | 4 | 4.350 | IGL-1 | 48 | 1 | 2.080 | 2.09 | 0.51 |
| Meine et al ^[8] , 2015 | HTK | 65 | 2 | 3.100 | IGL-1 | 113 | 3 | 2.700 | 1.16 | 0.87 |
| Wiederkehr et al ^[21] , 2014 | HTK | 125 | 1 | 0.700 | IGL-1 | 53 | 0 | 0.000 | 1.29 | 0.88 |
| Nardo et al ^[12] , 2005 | HTK | 20 | 1 | 5.000 | CS | 20 | 0 | 0.000 | 3.00 | 0.49 |

Studies are grouped by preservation solutions. PNF: Primary non-function; N: Indicates number in group; n: Number of PNF; RR: Relative risk; UW: University of Wisconsin solution; HTK: Histidine-tryptophan-ketoglutarate solution; CS: Celsior solution; IGL-1: Institut Georges Lopez solution.

Table 3 One-year post-transplant graft survival rate in included studies

| Study | Solution 1 | | | Solution 2 | | | RR | P value | | |
|--|------------|-----|----|------------|-------|-----|----|---------|------|------|
| | N | n | % | N | n | % | | | | |
| Cavallari et al ^[13] , 2003 | UW | 90 | 75 | 83.0 | CS | 83 | 71 | 85.0 | 0.97 | 0.69 |
| Lopez-Andujar et al ^[26] , 2009 | UW | 104 | 83 | 80.0 | CS | 92 | 75 | 81.0 | 0.98 | 0.76 |
| García-Gil et al ^[33] , 2006 | UW | 40 | 26 | 66.1 | CS | 40 | 31 | 78.0 | 0.84 | 0.22 |
| Nardo et al ^[27] , 2001 | UW | 60 | 54 | 90.0 | CS | 53 | 48 | 90.6 | 0.99 | 0.92 |
| Duca et al ^[28] , 2010 | UW | 51 | 31 | 60.6 | CS | 51 | 37 | 73.5 | 0.84 | 0.21 |
| Rayya et al ^[30] , 2008 | UW | 68 | 53 | 78.0 | HTK | 69 | 49 | 71.0 | 1.01 | 0.35 |
| Meine et al ^[32] , 2006 | UW | 65 | 61 | 94.0 | HTK | 37 | 35 | 94.0 | 0.99 | 0.88 |
| Mangus et al ^[31] , 2008 | UW | 98 | 82 | 84.0 | HTK | 111 | 95 | 86.0 | 0.98 | 0.70 |
| Dondéro et al ^[37] , 2010 | UW | 92 | 73 | 79.1 | IGL-1 | 48 | 19 | 39.8 | 2.00 | 0.00 |
| Meine et al ^[8] , 2015 | HTK | 65 | 54 | 83.0 | IGL-1 | 113 | 96 | 85.0 | 0.98 | 0.74 |
| Nardo et al ^[12] , 2005 | HTK | 20 | 15 | 75.0 | CS | 20 | 18 | 90.0 | 0.83 | 0.22 |

Studies are grouped by preservation solutions. OGS-1: One-year post-transplant graft survival; N: Number in group; n: Number of OGS-1; RR: Relative risk; UW: University of Wisconsin solution; HTK: Histidine-tryptophan-ketoglutarate solution; CS: Celsior solution; IGL-1: Institut Georges Lopez solution.

liver disease (MELD) score and cold ischemia time (CIT). All other outcomes related to the solutions were also investigated by subgroup analysis.

RESULTS

Demographic and clinical characteristics of donors and recipients were homogenous in all trials (Supplementary Tables 1-3).

MELD score

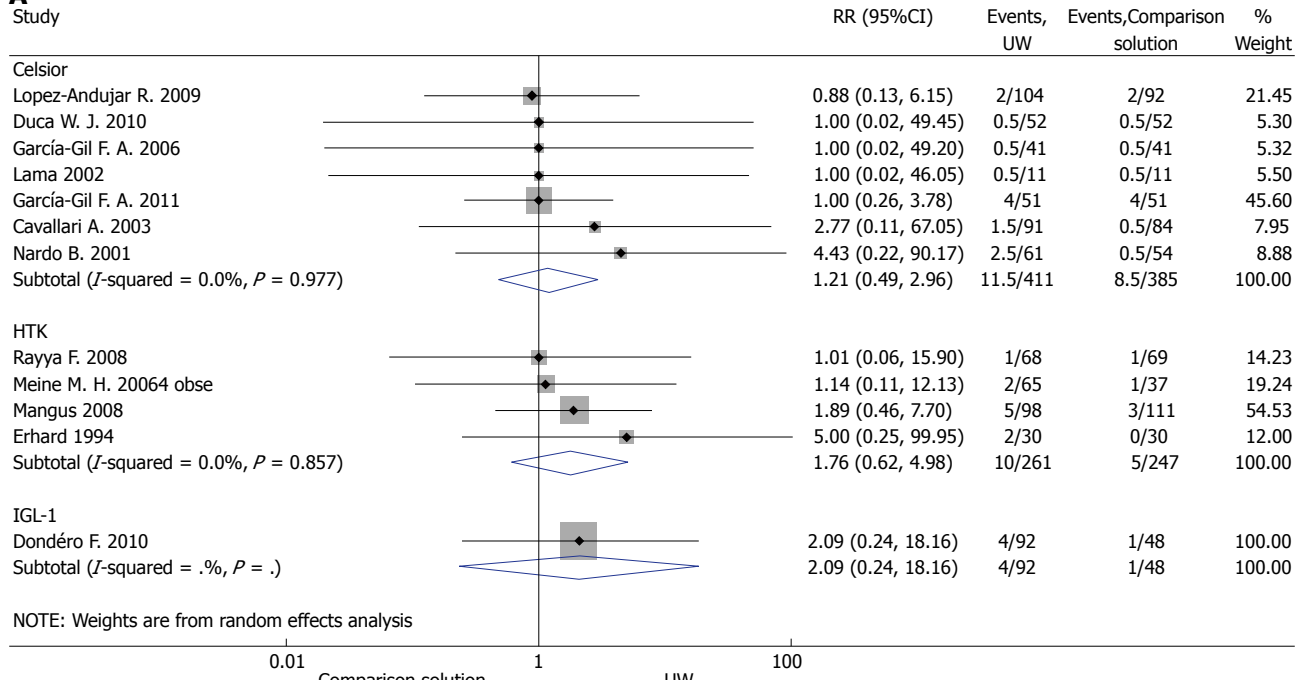
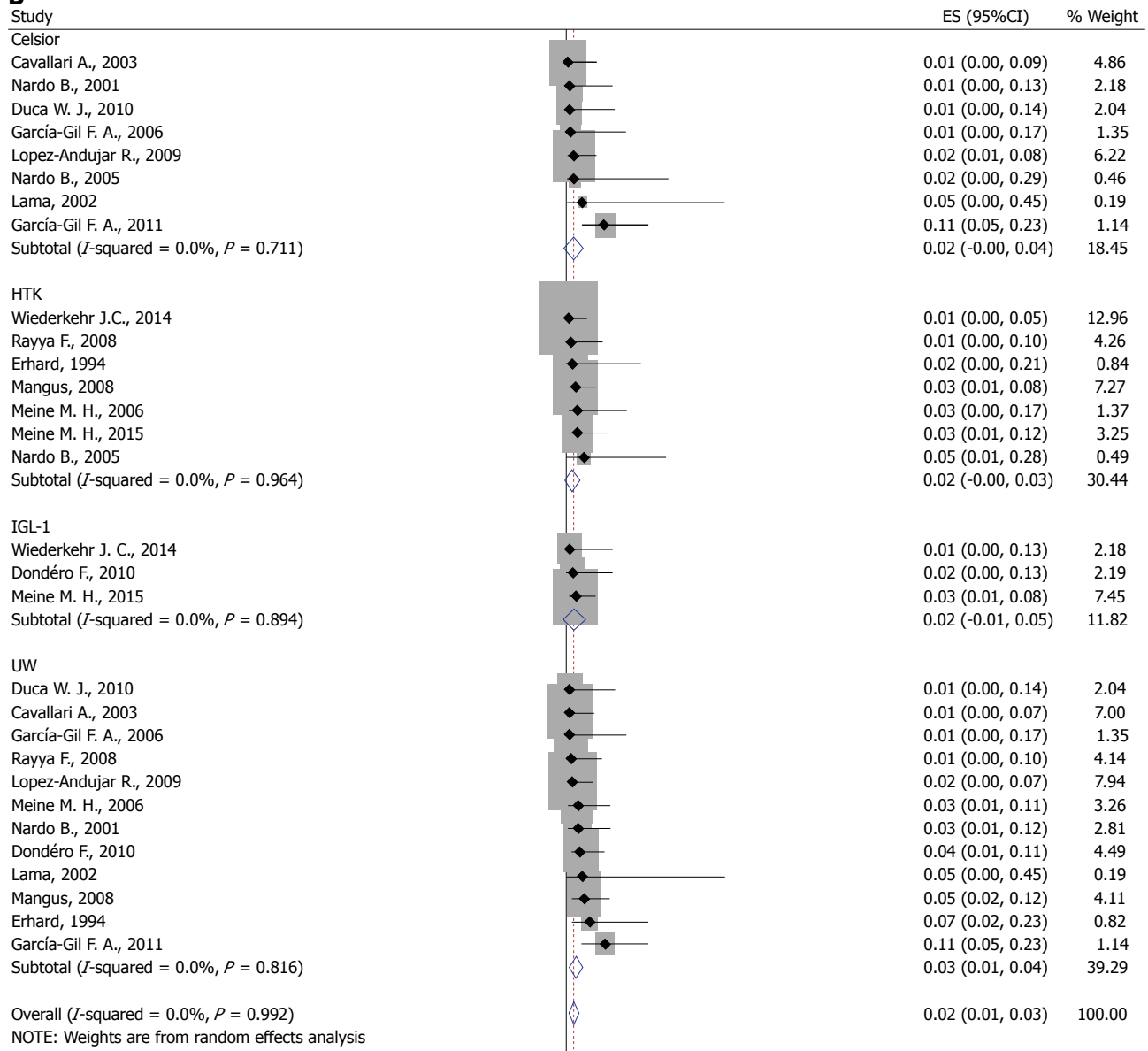
The MELD score incorporates parameters of recipients (such as abnormal coagulation, creatinine and serum bilirubin levels and the etiology of cirrhosis) and serves as a predictor of mortality after liver transplantation^[25]. MELD scores were reported in five studies (Supplementary Table 2). Subgroup analysis showed no significant difference in MELD score between the four solutions (RR = 18.6, 95%CI: 15.7-21.5, P = 0.379) (Supplementary Figure 1A).

CIT

CIT (time interval from the clamping of the donor aorta to the anastomosis of the organ to the recipient's vascular system or organs disposal) was reported in five studies (Supplementary Table 3). Subgroup analysis showed no significant difference in risk of CIT between the four solutions (RR = 484.7, 95%CI: 445.4-524.0, P = 0.1) (Supplementary Figure 1B).

PNF

PNF rates were reported in 15 studies (Table 2)^[8,9,12,13,21,26-35]. In four studies, PNF was defined as patient death or retransplantation in the first week. In eleven studies, PNF was undefined. Overall rates of PNF were very low (range 0-13.7%). Our meta-analysis showed no significant difference in risk of PNF between the UW and CS solutions (z = 0.41, P = 0.680) and between UW and HTK (z = 1.07, P = 0.284) (Figure 2A). We found only one RCT that dealt with IGL-1, which was not sufficient for a meta-analysis to compare IGL-1 with the UW

A**B**

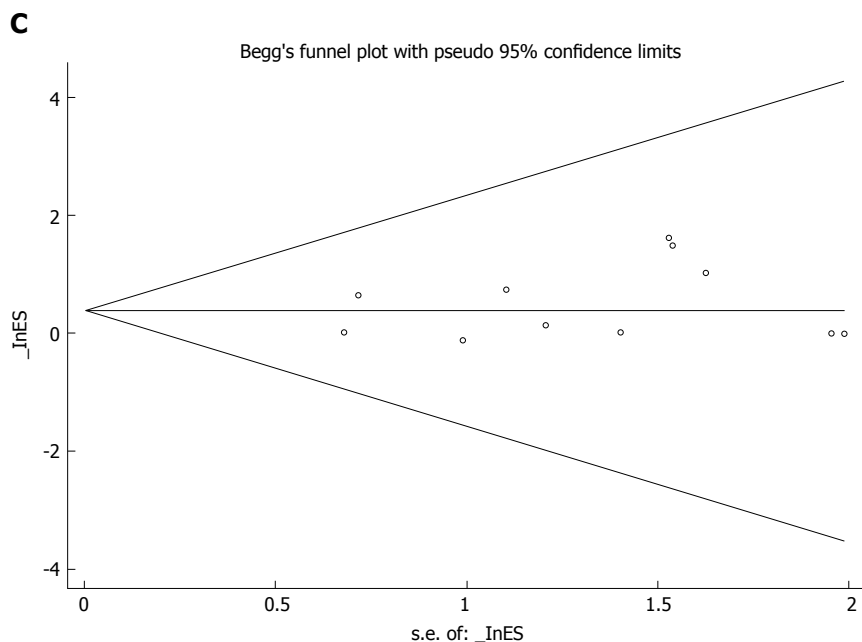


Figure 2 Effects of preservation solutions on primary non-function. A: Meta-analysis of the relative risk (-RR-) of PNF comparing studies using different preservation solutions: UW vs Celsior and UW vs HTK; B: Forest plot for subgroup analysis of PNF; and C: Funnel plot for PNF in studies. Squares represent individual study effects, with the size of the box relating to the weight of the study in the meta-analysis. Each diamond represents a summary effect from meta-analysis. Horizontal bars represent 95% CIs. There is no evidence of a small study effect in the test or the formal plot. PNF: Primary non-function; RCTs: Randomized controlled trials; ES: Effect size; UW: University of Wisconsin solution; HTK: Histidine-tryptophan-ketoglutarate solution; CS: Celsior solution; IGL-1: Institut Georges Lopez solution.

solution. We performed a subgroup analysis to compare the four solutions in the context of PNF. There was no significant difference between solutions ($RR = 0.02$, 95%CI: 0.01-0.03, $P = 0.356$) (Figure 2B). We found no evidence of a small study effect using the funnel plot analysis of the meta-analyses for the primary outcome ($P = 0.846$) (Figure 2C).

OGS-1

OGS-1 was reported in eleven studies (Table 3). No study was individually powered for small differences in graft survival, and no study reported a difference related to the preservation fluid used. Meta-analysis of the data showed no significant difference in the risk of OGS-1 between the UW and CS solutions ($z = 0.30$, $P = 0.763$) (Figure 3A) or between the UW and HTK solutions ($z = 0.01$, $P = 0.991$) (Figure 3A). We also performed a subgroup analysis to compare all four solutions, including IGL-1. There was no significant difference between the solutions ($RR = 0.80$, 95%CI: 0.80-0.80, $P = 0.369$) (Figure 3B). We found no evidence of a small study effect using the funnel plot analysis from either of the meta-analyses for the OGS-1 ($P = 0.397$) (Figure 3C).

PDF

PDF rates were reported in six studies: five of them compared UW with CS, and one compared UW with HTK (Supplementary Table 4). Overall rates of PDF were very low (range 0-15.5%). The difference in PDF

rate was found higher with the use of UW solutions in one study^[32]. However, the subgroup analysis showed no increased risk of PDF in the UW group ($RR = 0.1$, 95%CI: 0.0-0.1, $P = 0.582$) (Supplementary Figure 2).

Early RT

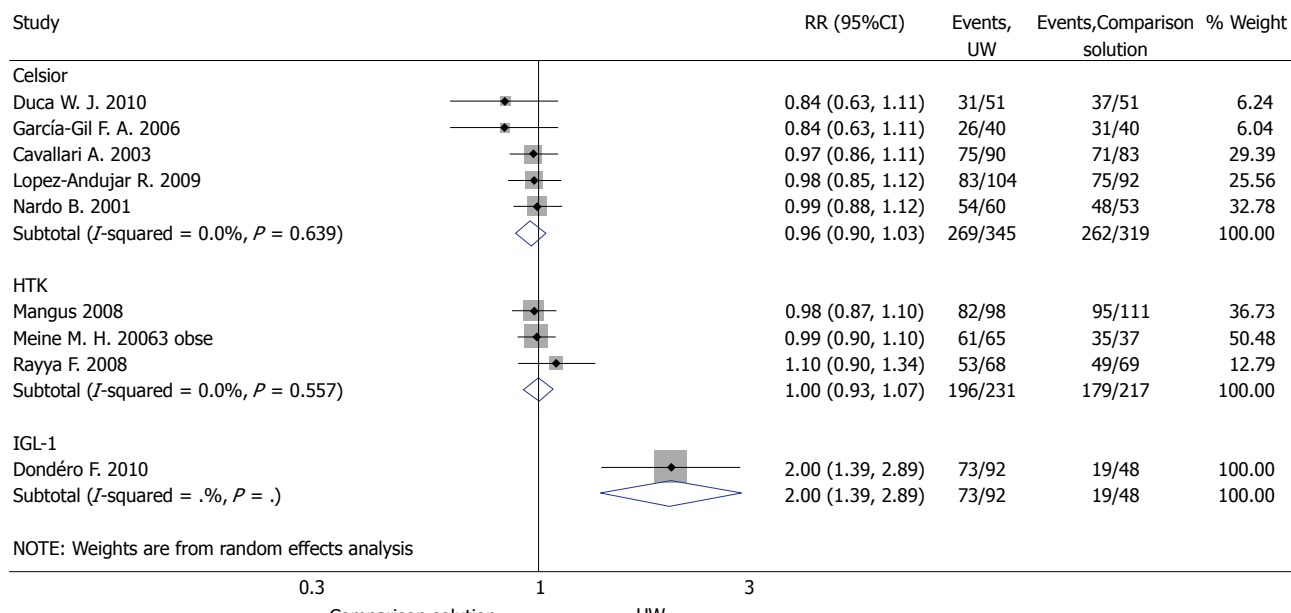
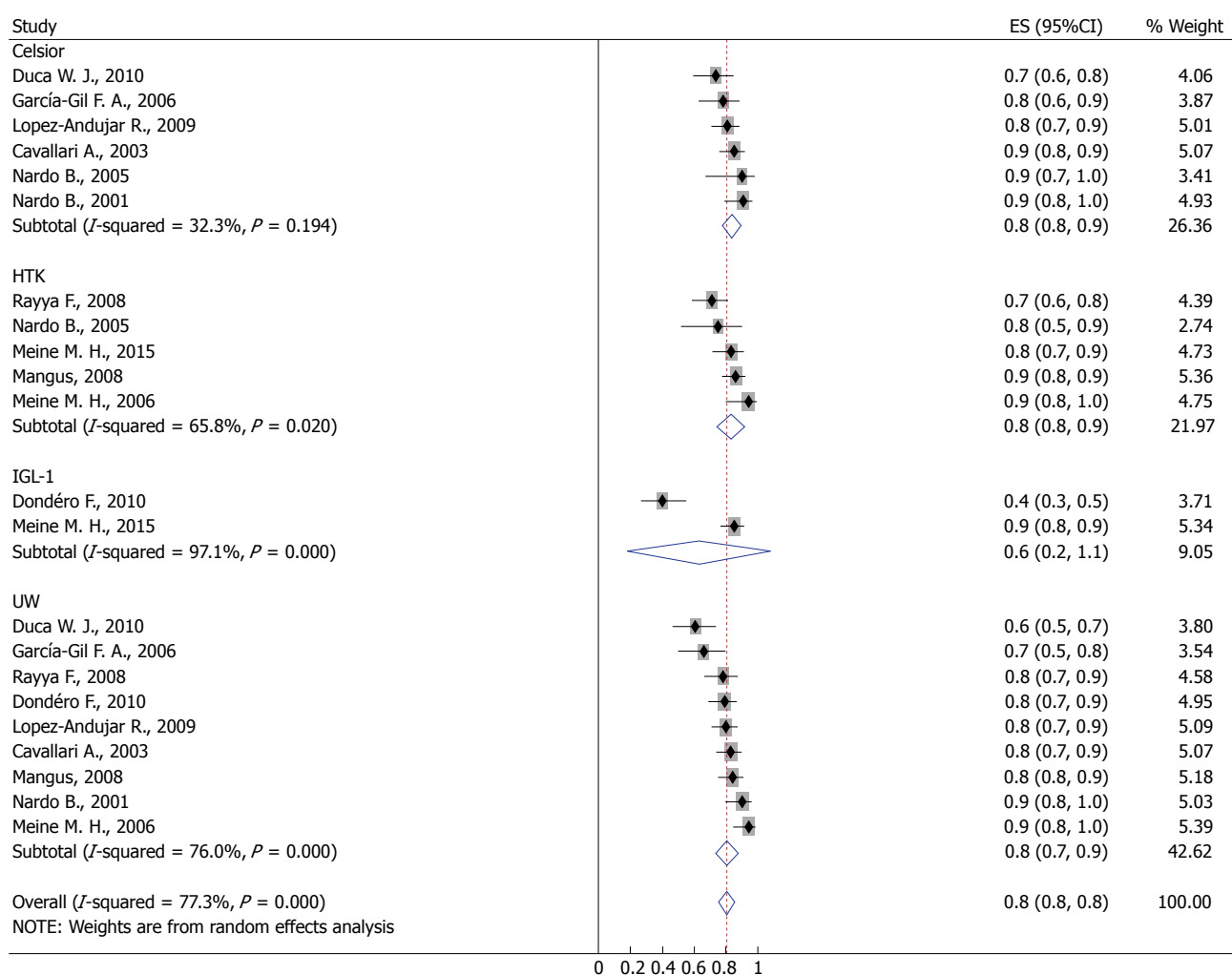
Early RT was reported in seven studies and ranged from 0.9% to 20% (Supplementary Table 4). None of the studies found a significant difference in early RT between groups; however, they were underpowered to detect such a low incidence outcome. Similarly, subgroup analysis showed no increased risk of early RT in the UW group ($RR = 0.0$, 95%CI: 0.0-0.1, $P = 0.698$) (Supplementary Figure 3).

POD

POD rates were reported in seven studies (Supplementary Table 4). Overall rates of POD were very low (range 1.7%-14.4%). The difference in POD rate was higher with the use of the CS solution compared with the UW solution in two studies^[12,33]; however, subgroup analysis showed no increased risk (Supplementary Figure 4). In contrast, there was a significant difference when UW was compared to HTK or IGL-1 ($RR = 0.07$, 95%CI: 0.04-0.09, $P < 0.01$).

OPS-1

OPS-1 rates were reported in ten studies (Supplementary Table 4). No study was individually powered for small differences in graft survival, and no study reported

A**B**

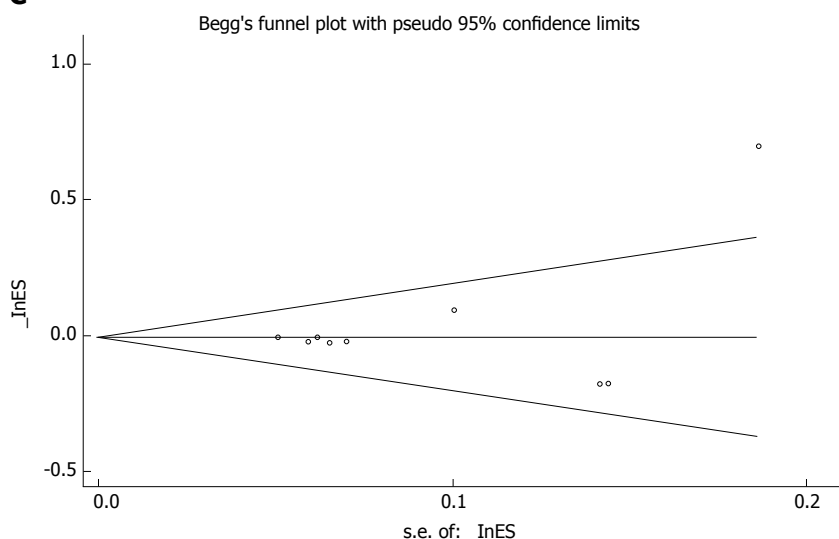
C

Figure 3 Effects of preservation solutions on one-year post-transplant graft survival. A: Meta-analysis of the relative risk (-RR-) of OGS-1 comparing studies using different preservation solutions: UW vs Celsior and UW vs HTK; B: Forest plot for subgroup analysis of OGS-1; and C: Funnel plot for OGS-1 in studies. Squares represent individual study effects, with the size of the box relating to the weight of the study in the meta-analysis. Each diamond represents a summary effect from meta-analysis. Horizontal bars represent 95% CIs. There is no evidence of a small study effect in the test or the formal plot. OGS-1: One-year post-transplant graft survival; RR: Relative risk; RCTs: Randomized controlled trials; ES: Effect size; UW: University of Wisconsin solution; HTK: Histidine-tryptophan-ketoglutarate solution; CS: Celsior solution; IGL-1: Institut Georges Lopez solution.

a difference related to the preservation fluid used. Subgroup analysis showed no significant difference in risk of OPS-1 between the four solutions (RR = 0.9, 95%CI: 0.8-0.9, $P = 0.786$) (Supplementary Figure 5).

DISCUSSION

This study reviews the current evidence and updates knowledge on four frequently used preservation solutions for static cold storage of DDLs for transplantation. The treatment groups were homogenous in terms of donor and recipient characteristics; the prediction of primary and secondary outcomes (*i.e.*, PNF and OGS-1) was thus likely independent of individual risk variables, patient selection or the overall severity of the disease at liver transplantation. More importantly, the analysis of outcome parameters (*i.e.*, PNF and OGS-1) provided good evidence that UW is not outperformed by CS, HTK and IGL-1 solutions in maintaining organ function and viability of liver grafts in cold storage.

PNF mainly depends on the organ preservation method^[15]. It occurs in 2%-6% of transplants and is unrelated to any direct surgical, immunologic or other complications^[34]. Our meta-analysis included eleven trials that evaluated the effectiveness of the UW solution as compared to either the CS or HTK solution. In accordance with the literature, the overall rates of PNF were very low, except in one trial (13%)^[35]. When analyzing the single studies, we found two trials with a higher incidence of PNF in the UW group than in the HTK group^[9,36], but the difference did not reach statistical significance upon meta-analysis. It

should be added that a recent analysis of the ELTR database demonstrated that use of HTK represented an individual risk factor for the development of PNF when compared to the UW solution^[10]. The contradictory conclusions can be explained with the selection bias of the database analysis^[20]. In either case, we found no difference between UW and the other solutions with regard to the risk of PNF. As regards IGL-1 and HTK, two prospective randomized clinical studies with 356 patients reported identical results^[8,21]. Similar outcome was detected in a single-center study with 140 patients that compared IGL-1 and UW solutions^[37]. This was confirmed in the current study, since IGL-1 showed a similar PNF risk to that of UW and HTK in our subgroup analyses.

In our study, OGS-1 was the secondary endpoint. Graft survival rates were evaluated one, three and five years after liver transplantation in single studies. The one-year term was chosen as an appropriate period to evaluate the effect of the preservation solutions because other factors could have a greater impact on this outcome parameter after this time. A retrospective analysis of the ELTR database demonstrated that HTK preservation was independently associated with higher mortality than UW, CS and IGL-1 in a multivariate analysis^[10]. Another analysis of a large national registry database (United Network for Organ Sharing, UNOS) has also demonstrated differences in graft survival rate between the HTK and UW solutions^[18]. However, important risk factors among donors were not considered in the ELTR analysis^[20], and selected groups of transplant patients were not homogenous in the

other analysis: HTK was utilized in allografts with more favorable recipient traits, as well as shorter CIT and less local and national export^[18]. In accordance with the findings from numerous clinical trials, the meta-analyses and subgroup analyses in this study did not show a significant difference in risk of OGS-1 between UW and any of the examined solutions. Similarly, there was no evidence for a difference between IGL-1 and UW solutions and between IGL-1 and HTK in the subgroup analyses.

Apart from the preservation methods used to protect the organ from IR injury, the final outcome of transplantation can also be linked to factors such as donor age, general condition and CIT^[38]. A recent UNOS study showed a more pronounced risk for graft loss with longer CIT and donors over 70 years^[18]. In our study, subgroup analysis showed that the included trials did not vary significantly and that the mean CITs were beyond the critical 12 h^[39]. Several experimental studies demonstrated that the use of the UW solution allows for longer CITs with better graft preservation; however, it remains to be determined whether any of the alternative solutions is better than UW when CIT is prolonged over 12 h.

Recipient morbidity and MELD scores are also important contributing factors to the outcome of liver transplantation. Recipient parameters are incorporated into the MELD score, which indicates the state of health of the recipient; the MELD score-based organ allocation algorithm could thus significantly influence the graft survival rate^[40]. In the present study, there was no significant difference between the preservation solutions in the context of the MELD score and other recipient characteristics.

In recent times, the crisis in organ supply has made it necessary to extend the scope of potential donors by using extended criteria donors (ECD). Although there is no precise definition of ECD, frequently cited characteristics are donor age, steatosis, donation after cardiac death (DCD), donors with increased risk of disease transmission and transplantation after prolonged CIT, as well as the use of partial grafts (split grafts and living donor liver transplantation)^[41]. Unfortunately, higher rates of graft failure were documented in this class of extended allograft; in addition, very little data is available on the influence of preservation solutions on their post-transplant outcomes^[42]. A single-center study by Mangus *et al*^[30] failed to find statistically significant differences in overall graft survival when they compared UW to HTK in ECD transplants. However, they suggested that HTK may be protective against biliary complications. In contrast, in 2009, the UNOS database analysis reported that HTK was associated with an increased risk of graft loss and early graft loss^[18]. More recently, Adam *et al*^[10] compared the four most frequently used preservation solutions and concluded that HTK is an

independent risk factor for graft loss after ECD liver transplantations. The remaining three solutions, UW, CE and IGL-1, provided similar results in post-transplant outcomes after ECD transplantations. In the special condition of using a partially deceased donor liver graft, IGL-1 offered the best graft outcome^[10]. In another study, it was suggested that IGL-1 was superior to other solutions for preserving fatty livers by protecting against PNF and early allograft dysfunction^[43]. However, a prospective randomized study could not show any significant improvement in the subgroup of patients receiving IGL-1-preserved grafts^[36]. In living donor liver transplantations, risk-adjusted analyses of single- and double-center studies consistently reported that UW and HTK were equally effective and safe for cold preservation^[44-47]. There is currently no evidence-based recommendation on the optimal preservation solution in ECD liver transplantations because the number and quality of RCTs are not sufficient. However, based on the above data, differences in the indications of various preservation solutions are expected.

This study has some limitations. There are so far only three small RCTs that compare IGL-1 with UW or IGL-1 with HTK. Therefore, we could not run a meta-analysis to compare IGL-1 with any of the solutions. In order to compare the risk of the four solutions for PNF, we had to perform a subgroup analysis. In addition, surgery time and hemoderivative transfusions due to recipient coagulation problems are often not cited in the literature as predictors of poor outcome^[36]. This factor was not considered in the selected trials. Moreover, different trials presented some differences as regards the operative procedure. Furthermore, the included RCTs were homogenous with regard to donor and recipient parameters. On the one hand, this provided the possibility to exclude selection bias, but, on the other hand, the effects of preservation solutions in the case of longer CIT and involvement of expanded criteria donors could not be evaluated.

In conclusion, elucidation of the role of preservation solutions in the outcome of liver transplantation is complicated by the intrinsic complexity of the clinical procedure, which is made up of many different, but interacting phases. This review evaluated the best available evidence from comparisons of the four most frequently used preservation fluids in DDL transplantation. A direct meta-analysis comparison was made and the sample size of included trials was large enough to estimate the risk of low-incidence outcomes such as PNF or OGS-1 correctly. Based on our results, there is good evidence that the UW, CS, HTK and IGL-1 solutions are associated with nearly equivalent outcomes. Additional studies on larger patient populations including marginal donors, longer cold ischemia time, multi-organ transplantations and economic aspects are needed to evaluate the superiority of any alternative solution over UW.

ARTICLE HIGHLIGHTS

Research background

The introduction of the University of Wisconsin (UW) solution for static cold storage of liver grafts was a breakthrough and has remained the conventional method of organ preservation. However, many alternative preservation solutions exist, and each is thought to offer an advantage over UW solution.

Research motivation

At present, 98% of liver transplants use the UW, histidine-tryptophan-ketoglutarate (HTK), Celsior (CS) or Institute Georges Lopez (IGL-1) solution for the cold preservation of grafts. Previously, prospective trials have investigated their effects on liver transplant outcomes, but with contradictory results. Furthermore, no systematic review reports the effect of IGL-1, which was first used by 2003, as compared to other solutions.

Research objectives

To provide an update and to compare the latest findings from clinical trials on the effects of the four most frequently used preservation solutions on liver transplant outcomes.

Research methods

A systematic review and meta-analysis were conducted on randomized controlled trials of deceased donor liver transplants using UW and either HTK, CS or IGL-1 for cold storage of allografts. Primary and secondary outcomes were primary non-function (PNF) and one-year post-transplant graft survival (OGS-1).

Research results

In spite of differences found in individual studies, a meta-analysis of PNF and OGS-1 showed no statistical difference between groups. Subgroup analysis showed no increased risk for other outcomes, such as primary dysfunction, early retransplantation rate, post-transplantation death and one-year post-transplant patient survival.

Research conclusions

This meta-analysis provided evidence that UW and alternative solutions are associated with almost the same transplant outcome. Further studies are needed with extended criteria donors to ascertain the superiority of any alternative solution over UW.

REFERENCES

- 1 **Jia JJ**, Li JH, Jiang L, Lin BY, Wang L, Su R, Zhou L, Zheng SS. Liver protection strategies in liver transplantation. *Hepatobiliary Pancreat Dis Int* 2015; **14**: 34-42 [PMID: 25655288 DOI: 10.1016/S1499-3872(15)60332-0]
- 2 **Brisson H**, Arbelot C, Monsel A, Parisot C, Girard M, Savier E, Vezinet C, Lu Q, Vaillant JC, Golmard JL, Gorochov G, Langeron O, Rouby JJ; Members of the Pitié-Salpêtrière Liver Transplantation Study Group. Impact of graft preservation solutions for liver transplantation on early cytokine release and postoperative organ dysfunctions. A pilot study. *Clin Res Hepatol Gastroenterol* 2017; **41**: 564-574 [PMID: 28330599 DOI: 10.1016/j.clinre.2016.12.011]
- 3 **Stewart ZA**. UW solution: still the “gold standard” for liver transplantation. *Am J Transplant* 2015; **15**: 295-296 [PMID: 25612481 DOI: 10.1111/ajt.13062]
- 4 **Sanchez-Urdazpal L**, Gores GJ, Ward EM, Maus TP, Wahlstrom HE, Moore SB, Wiesner RH, Krom RA. Ischemic-type biliary complications after orthotopic liver transplantation. *Hepatology* 1992; **16**: 49-53 [PMID: 1618482 DOI: 10.1002/hep.1840160110]
- 5 **Cutrin JC**, Cantino D, Biasi F, Chiarpotto E, Salizzoni M, Andorno E, Massano G, Lanfranco G, Rizzetto M, Boveris A, Poli G. Reperfusion damage to the bile canaliculi in transplanted human liver. *Hepatology* 1996; **24**: 1053-1057 [PMID: 8903374 DOI: 10.1002/hep.510240512]
- 6 **Tullius SG**, Filatenkow A, Horch D, Mehlitz T, Reutzel-Selke A, Pratschke J, Steinmüller T, Lun A, Al-Abadi H, Neuhaus P. Accumulation of crystal deposits in abdominal organs following perfusion with defrosted University of Wisconsin solutions. *Am J Transplant* 2002; **2**: 627-630 [PMID: 12201363 DOI: 10.1034/j.1600-6143.2002.20707.x]
- 7 **Fridell JA**, Rogers J, Stratton RJ. The pancreas allograft donor: current status, controversies, and challenges for the future. *Clin Transplant* 2010; **24**: 433-449 [PMID: 20384731 DOI: 10.1111/j.1399-0012.2010.01253.x]
- 8 **Meine MH**, Leipnitz I, Zanotelli ML, Schlindwein ES, Kiss G, Martini J, de Medeiros Fleck A Jr, Mucenig M, de Mello Brandão A, Marroni CA, Craco Cantisani GP. Comparison Between IGL-1 and HTK Preservation Solutions in Deceased Donor Liver Transplantation. *Transplant Proc* 2015; **47**: 888-893 [PMID: 26036479 DOI: 10.1016/j.transproceed.2015.03.033]
- 9 **Erhard J**, Lange R, Scherer R, Kox WJ, Bretschneider HJ, Gebhard MM, Eigler FW. Comparison of histidine-tryptophan-ketoglutarate (HTK) solution versus University of Wisconsin (UW) solution for organ preservation in human liver transplantation. A prospective, randomized study. *Transpl Int* 1994; **7**: 177-181 [PMID: 8060466]
- 10 **Adam R**, Delvart V, Karam V, Ducerf C, Navarro F, Letoublon C, Belghiti J, Pezet D, Castaing D, Le Treut YP, Gugenheim J, Bachellier P, Pirenne J, Muijsen P; ELTR contributing centres, the European Liver, Intestine Transplant Association (ELITA). Compared efficacy of preservation solutions in liver transplantation: a long-term graft outcome study from the European Liver Transplant Registry. *Am J Transplant* 2015; **15**: 395-406 [PMID: 25612492 DOI: 10.1111/ajt.13060]
- 11 **Fridell JA**, Agarwal A, Milgrom ML, Goggins WC, Murdock P, Pescovitz MD. Comparison of histidine-tryptophan-ketoglutarate solution and University of Wisconsin solution for organ preservation in clinical pancreas transplantation. *Transplantation* 2004; **77**: 1304-1306 [PMID: 15114104 DOI: 10.1097/01.TP.000012222.93740.B2]
- 12 **Nardo B**, Bertelli R, Montalti R, Beltempo P, Puviani L, Pacile V, Cavallari A. Preliminary results of a clinical randomized study comparing Celsior and HTK solutions in liver preservation for transplantation. *Transplant Proc* 2005; **37**: 320-322 [PMID: 15808630 DOI: 10.1016/j.transproceed.2004.11.028]
- 13 **Cavallari A**, Cillo U, Nardo B, Filippone F, Gringeri E, Montalti R, Vistoli F, D'amico F, Faenza A, Mosca F, Vitale A, D'amico D. A multicenter pilot prospective study comparing Celsior and University of Wisconsin preserving solutions for use in liver transplantation. *Liver Transpl* 2003; **9**: 814-821 [PMID: 12884193 DOI: 10.1053/jlts.2003.50161]
- 14 **Tabka D**, Bejaoui M, Javellaud J, Roselló-Catafau J, Achard JM, Abdennebi HB. Effects of Institut Georges Lopez-1 and Celsior preservation solutions on liver graft injury. *World J Gastroenterol* 2015; **21**: 4159-4168 [PMID: 25892865 DOI: 10.3748/wjg.v21.i14.4159]
- 15 **Ploeg RJ**, D'Alessandro AM, Knechtle SJ, Stegall MD, Pirsch JD, Hoffmann RM, Sasaki T, Sollinger HW, Belzer FO, Kalayoglu M. Risk factors for primary dysfunction after liver transplantation—a multivariate analysis. *Transplantation* 1993; **55**: 807-813 [PMID: 8475556]
- 16 **Lema Zuluaga GL**, Serna Agudelo RE, Zuleta Tobón JJ. Preservation solutions for liver transplantation in adults: celsior versus custodiol: a systematic review and meta-analysis with an indirect comparison of randomized trials. *Transplant Proc* 2013; **45**: 25-32 [PMID: 23267794 DOI: 10.1016/j.transproceed.2012.02.031]
- 17 **Feng L**, Zhao N, Yao X, Sun X, Du L, Diao X, Li S, Li Y. Histidine-tryptophan-ketoglutarate solution vs. University of Wisconsin solution for liver transplantation: a systematic review. *Liver Transpl* 2007; **13**: 1125-1136 [PMID: 17665493 DOI: 10.1002/lt.21208]
- 18 **Stewart ZA**, Cameron AM, Singer AL, Montgomery RA, Segev

- DL. Histidine-Tryptophan-Ketoglutarate (HTK) is associated with reduced graft survival in deceased donor livers, especially those donated after cardiac death. *Am J Transplant* 2009; **9**: 286-293 [PMID: 19067658 DOI: 10.1111/j.1600-6143.2008.02478.x]
- 19 **O'Callaghan JM**, Morgan RD, Knight SR, Morris PJ. The effect of preservation solutions for storage of liver allografts on transplant outcomes: a systematic review and meta-analysis. *Ann Surg* 2014; **260**: 46-55 [PMID: 24374537 DOI: 10.1097/SLA.0000000000000402]
- 20 **Nashan B**, Spetzler V, Schemmer P, Kirste G, Rahmel A. Regarding "Compared Efficacy of Preservation Solutions in Liver Transplantation: A Long-Term Graft Outcome Study From the European Liver Transplant Registry". *Am J Transplant* 2015; **15**: 3272-3273 [PMID: 26555321 DOI: 10.1111/ajt.13513]
- 21 **Wiederkehr JC**, Igrela MR, Nogara MS, Goncalves N, Montemezzo GP, Wiederkehr HA, Wassen MP, Nobrega HA, Zenatti KB, Mori LY, Tudisco MS. Use of IGL-1 preservation solution in liver transplantation. *Transplant Proc* 2014; **46**: 1809-1811 [PMID: 25131043 DOI: 10.1016/j.transproceed.2014.05.040]
- 22 **Moher D**, Liberati A, Tetzlaff J, Altman DG; PRISMA Group. Preferred reporting items for systematic reviews and meta-analyses: the PRISMA statement. *PLoS Med* 2009; **6**: e1000097 [PMID: 19621072 DOI: 10.1371/journal.pmed.1000097]
- 23 The University of York Centre for Reviews and Dissemination. PROSPERO Register of ongoing systematic reviews. Available from: https://www.crd.york.ac.uk/PROSPERO/display_record.asp?ID=CRD42017054908
- 24 **Sweeting MJ**, Sutton AJ, Lambert PC. What to add to nothing? Use and avoidance of continuity corrections in meta-analysis of sparse data. *Stat Med* 2004; **23**: 1351-1375 [PMID: 15116347 DOI: 10.1002/sim.1761]
- 25 **Huo TI**, Lee SD, Lin HC. Selecting an optimal prognostic system for liver cirrhosis: the model for end-stage liver disease and beyond. *Liver Int* 2008; **28**: 606-613 [PMID: 18433390 DOI: 10.1111/j.1478-3231.2008.01727.x]
- 26 **Lopez-Andujar R**, Deusa S, Montalvá E, San Juan F, Moya A, Pareja E, DeJuan M, Berenguer M, Prieto M, Mir J. Comparative prospective study of two liver graft preservation solutions: University of Wisconsin and Celsior. *Liver Transpl* 2009; **15**: 1709-1717 [PMID: 19938119 DOI: 10.1002/lt.21945]
- 27 **Nardo B**, Catena F, Cavallari G, Montalti R, Di Naro A, Faenza A, Cavallari A. Randomized clinical study comparing UW and Celsior solution in liver preservation for transplantation: preliminary results. *Transplant Proc* 2001; **33**: 870-872 [PMID: 11267110 DOI: 10.1016/S0041-1345(00)02357-5]
- 28 **Duea WJ**, da Silva RF, Arroyo PC Jr, Sgnolf A, Cabral CM, Ayres DC, Felício HC, da Silva RD. Liver transplantation using University of Wisconsin or Celsior preserving solutions in the portal vein and Euro-Collins in the aorta. *Transplant Proc* 2010; **42**: 429-434 [PMID: 20304157 DOI: 10.1016/j.transproceed.2010.01.035]
- 29 **Lama C**, Rafecas A, Figueras J, Torras J, Ramos E, Fabregat J, Busquets J, Garcia-Barrasa A, Jaurrieta E. Comparative study of Celsior and Belzer solutions for hepatic graft preservation: preliminary results. *Transplant Proc* 2002; **34**: 54-55 [PMID: 11959183 DOI: 10.1016/S0041-1345(01)02664-1]
- 30 **Rayya F**, Harms J, Martin AP, Bartels M, Hauss J, Fangmann J. Comparison of histidine-tryptophan-ketoglutarate solution and University of Wisconsin solution in adult liver transplantation. *Transplant Proc* 2008; **40**: 891-894 [PMID: 18555073 DOI: 10.1016/j.transproceed.2008.03.044]
- 31 **Mangus RS**, Fridell JA, Viana RM, Milgrom MA, Chestovich P, Chihara RK, Tector AJ. Comparison of histidine-tryptophan-ketoglutarate solution and University of Wisconsin solution in extended criteria liver donors. *Liver Transpl* 2008; **14**: 365-373 [PMID: 18306380 DOI: 10.1002/lt.21372]
- 32 **Meine MH**, Zanotelli ML, Neumann J, Kiss G, de Jesus Grezzana T, Leipnitz I, Schlindwein ES, Fleck A Jr, Gleisner AL, de Mello Brandão A, Marroni CA, Cantisani GP. Randomized clinical assay for hepatic grafts preservation with University of Wisconsin or histidine-tryptophan-ketoglutarate solutions in liver transplantation. *Transplant Proc* 2006; **38**: 1872-1875 [PMID: 16908310 DOI: 10.1016/j.transproceed.2006.06.071]
- 33 **Garcia-Gil FA**, Arenas J, Güemes A, Esteban E, Tomé-Zelaya E, Lamata F, Sousa R, Jiménez A, Barrao ME, Serrano MT. Preservation of the liver graft with Celsior solution. *Transplant Proc* 2006; **38**: 2385-2388 [PMID: 17097942 DOI: 10.1016/j.transproceed.2006.08.032]
- 34 **Uemura T**, Randall HB, Sanchez EQ, Ikegami T, Narasimhan G, McKenna GJ, Chinnakota S, Levy MF, Goldstein RM, Klintmalm GB. Liver retransplantation for primary nonfunction: analysis of a 20-year single-center experience. *Liver Transpl* 2007; **13**: 227-233 [PMID: 17256780 DOI: 10.1002/lt.20992]
- 35 **García-Gil FA**, Serrano MT, Fuentes-Broto L, Arenas J, García JJ, Güemes A, Bernal V, Campillo A, Sostres C, Araiz JJ, Royo P, Simón MA. Celsior versus University of Wisconsin preserving solutions for liver transplantation: postreperfusion syndrome and outcome of a 5-year prospective randomized controlled study. *World J Surg* 2011; **35**: 1598-1607 [PMID: 21487851 DOI: 10.1007/s00268-011-1078-7]
- 36 **Mangus RS**, Kinsella SB, Nobari MM, Fridell JA, Vianna RM, Ward ES, Nobari R, Tector AJ. Predictors of blood product use in orthotopic liver transplantation using the piggyback hepatectomy technique. *Transplant Proc* 2007; **39**: 3207-3213 [PMID: 18089355 DOI: 10.1016/j.transproceed.2007.09.029]
- 37 **Dondé F**, Paugam-Burtz C, Danjou F, Stocco J, Durand F, Belghiti J. A randomized study comparing IGL-1 to the University of Wisconsin preservation solution in liver transplantation. *Ann Transplant* 2010; **15**: 7-14 [PMID: 21183870]
- 38 **Stahl JE**, Kreke JE, Malek FA, Schaefer AJ, Vacanti J. Consequences of cold-ischemia time on primary nonfunction and patient and graft survival in liver transplantation: a meta-analysis. *PLoS One* 2008; **3**: e2468 [PMID: 18575623 DOI: 10.1371/journal.pone.0002468]
- 39 **Belle SH**, Beringer KC, Detre KM. An update on liver transplantation in the United States: recipient characteristics and outcome. *Clin Transpl* 1995; 19-33 [PMID: 8794252]
- 40 **Weismüller TJ**, Fikatas P, Schmidt J, Barreiros AP, Otto G, Beckebaum S, Paul A, Scherer MN, Schmidt HH, Schlitt HJ, Neuhaus P, Klempnauer J, Pratschke J, Manns MP, Strassburg CP. Multicentric evaluation of model for end-stage liver disease-based allocation and survival after liver transplantation in Germany - limitations of the 'sickest first'-concept. *Transpl Int* 2011; **24**: 91-99 [PMID: 20819196 DOI: 10.1111/j.1432-2277.2010.01161.x]
- 41 **Vodkin I**, Kuo A. Extended Criteria Donors in Liver Transplantation. *Clin Liver Dis* 2017; **21**: 289-301 [PMID: 28364814 DOI: 10.1016/j.cld.2016.12.004]
- 42 **Nemes B**, Gámán G, Polak WG, Golley F, Hara T, Ono S, Baimakhanov Z, Piros L, Eguchi S. Extended-criteria donors in liver transplantation Part II: reviewing the impact of extended-criteria donors on the complications and outcomes of liver transplantation. *Expert Rev Gastroenterol Hepatol* 2016; **10**: 841-859 [PMID: 26831547 DOI: 10.1586/17474124.2016.1149062]
- 43 **Zaouali MA**, Mosbah IB, Abdennebi HB, Calvo M, Boncompagni E, Boillot O, Peralta C, Roselló-Catafau J. New insights into fatty liver preservation using Institute Georges Lopez preservation solution. *Transplant Proc* 2010; **42**: 159-161 [PMID: 20172305 DOI: 10.1016/j.transproceed.2009.12.035]
- 44 **Kaltenborn A**, Gwiadas J, Ameling V, Krauth C, Lehner F, Braun F, Klempnauer J, Reichert B, Schem H. Comparable outcome of liver transplantation with histidine-tryptophan-ketoglutarate vs. University of Wisconsin preservation solution: a retrospective observational double-center trial. *BMC Gastroenterol* 2014; **14**: 169 [PMID: 25263587 DOI: 10.1186/1471-230X-14-169]
- 45 **Moray G**, Sevmis S, Karakayali FY, Gorur SK, Haberal M. Comparison of histidine-tryptophan-ketoglutarate and University of Wisconsin in living-donor liver transplantation. *Transplant Proc* 2006; **38**: 3572-3575 [PMID: 17175334 DOI: 10.1016/j.transproce

ed.2006.10.174]

- 46 **Jain A**, Mohanka R, Orloff M, Abt P, Kashyap R, Cullen J, Lansing K, Bozorgzadeh A. University of Wisconsin versus histidine-tryptophan-ketoglutarate for tissue preservation in live-donor liver transplantation. *Exp Clin Transplant* 2006; **4**: 451-457

[PMID: 16827642]

- 47 **Ringe B**, Braun F, Moritz M, Zeldin G, Soriano H, Meyers W. Safety and efficacy of living donor liver preservation with HTK solution. *Transplant Proc* 2005; **37**: 316-319 [PMID: 15808629 DOI: 10.1016/j.transproceed.2004.12.009]

P- Reviewer: Bramhall S, Chiu KW, Inoue K, Rosello-Catafau J, Tsoulfas G
S- Editor: Gong ZM **L- Editor:** A **E- Editor:** Huang Y





Published by **Baishideng Publishing Group Inc**
7901 Stoneridge Drive, Suite 501, Pleasanton, CA 94588, USA
Telephone: +1-925-223-8242
Fax: +1-925-223-8243
E-mail: bpgoffice@wjgnet.com
Help Desk: <http://www.f6publishing.com/helpdesk>
<http://www.wjgnet.com>



ISSN 1007-9327

